

NASA Contractor Report 177413

# Large Deployable Reflector (LDR) System Concept and Technology Definition Study Volume I - Executive Summary, Analyses and Trades, and System Concepts

Donald L. Agnew  
Peter A. Jones

(NASA-CR-177413-Vol-1) LARGE  
DEPLOYABLE REFLECTOR (LDR) SYSTEM  
CONCEPT AND TECHNOLOGY DEFINITION  
STUDY. VOLUME 1: EXECUTIVE SUMMARY,  
ANALYSES AND TRADES, AND SYSTEM  
CONCEPTS Final Technical Report  
(Eastman Kodak Co.) 375 p

N93-12591

Unclass

G3/74 0130688

CONTRACT NAS2-11861  
April 1989



National Aeronautics and  
Space Administration



# **Large Deployable Reflector (LDR) System Concept and Technology Definition Study Volume I - Executive Summary, Analyses and Trades, and System Concepts**

Donald L. Agnew  
Peter A. Jones

Eastman Kodak Company, Rochester, New York

Prepared for  
Ames Research Center  
CONTRACT NAS2-11861  
April 1989



National Aeronautics and  
Space Administration

**Ames Research Center**  
Moffett Field, California 94035



**VOLUME I  
TABLE OF CONTENTS**

<u>Section</u>	<u>Title</u>	<u>Page</u>
	List of Appendices	vii
	List of Figures	viii
	List of Tables	ix
	Foreword	xvi
1.0	EXECUTIVE SUMMARY	1
1.1	Purpose of Report	1
1.2	Study Objectives	1
1.3	Technical Approach	1
1.4	Selected LDR System Concepts	2
1.5	Technology Assessment and Risks	3
1.6	Recommended Technology Development Plan	6
2.0	STUDY APPROACH AND METHODOLOGY	8
2.1	Study Task Flow	8
2.2	Issue Interrelationships	8
2.3	Assumptions	12
2.3.1	Science Instruments	12
2.3.2	Launch Vehicles	13
2.3.3	Space Station	13
2.3.4	Orbital Maneuvering/Transfer Vehicles	13
2.4	Requirements Review	13
2.5	Scientific Instruments Considerations	15
3.0	SYSTEM ANALYSIS AND TRADES	21
3.1	Optical Configuration Trade	21
3.1.1	Task	21
3.1.2	Approach	21
3.1.3	Discussion	21
3.1.3.1	On-Axis Cassegrain Telescope (Circular Aperture)	22
3.1.3.2	Off-Axis Cassegrain	24
3.1.3.3	Radially Degraded Cassegrain	27
3.1.3.4	Slot Cassegrain	29
3.1.3.5	Telescope With Spherical Primary Mirror	33
3.1.3.6	Unfilled Aperture Option	35
3.1.4	Conclusions	40
3.2	Aperture Size Trade	41
3.2.1	Task	41
3.2.2	Approach	41
3.2.3	Discussion	42
3.2.4	Conclusion	44
3.3	Reflector Material Trade	51
3.3.1	Task	51
3.3.2	Approach	51
3.3.4	Conclusions	61
3.4	Segmented Mirror Concepts	64
3.4.1	Task	64
3.4.2	Approach	64

<u>Section</u>	<u>Title</u>	<u>Page</u>
3.4.3	Discussion	64
3.4.3.1	Primary Mirror	67
3.4.3.2	Primary Mirror Control	86
3.4.3.3	Primary Mirror Reaction Structure	88
3.4.3.4	Mirror Surface Processing	92
3.4.4	Conclusions	92
3.5	Optical Subsystem Concepts	94
3.5.1	Task	94
3.5.2	Approach	94
3.5.3	Discussion	94
3.5.3.1	Secondary Mirror	94
3.5.3.2	Secondary Mirror Control	101
3.5.3.3	Secondary Mirror Support Structure	106
3.5.4	Conclusions	110
3.6	Thermal Considerations	111
3.6.1	Task	111
3.6.2	Approach	112
3.6.3.1	Telescope Thermal Control	112
3.6.2.2	Science Instrument and Secondary Mirror Cooling	113
3.6.3	Discussion	114
3.6.3.1	Telescope Thermal Control	114
3.6.3.2	Science Instrument and Secondary Mirror Cooling	132
3.6.4	Conclusions	136
3.6.4.1	Telescope Thermal Control	136
3.6.4.2	Science Instrument and Secondary Mirror Cooling	137
3.7	Pointing and Control	139
3.7.1	Task	139
3.7.2	Approach	139
3.7.3	Discussion	139
3.7.3.1	Pointing Control	143
3.7.3.2	Fine Guidance Sensing	156
3.7.3.3	Chopping	161
3.7.4	Conclusions	166
3.8	Transportation To Orbit (MDAC)	169
3.8.1	Task Approach	169
3.8.2	Requirements	169
3.8.3	Trade and Option Studies	169
3.8.3.1	Launch Vehicle Performance and Constraints	169
3.8.3.2	Orbiter and ACC Environments	174
3.8.3.3	Orbiter Payload Envelope and Center of Gravity	174
3.8.3.4	Orbiter Interface Loads	174
3.8.3.5	Transport Contamination Control	174
3.8.3.6	Transporter Deployment Basing	179
3.8.3.7	Transportation ASE	182
3.9	Structures (MDAC)	184
3.9.1	Task Approach	184
3.9.2	Requirements	184
3.9.3	Trade and Option Studies	184
3.9.3.1	Structural Geometry and Sizing	184
3.9.3.2	Automated Deployment	191
3.9.3.3	Constructed Deployment	191
3.9.3.4	Dimensionally Stable Structures	191

<u>Section</u>	<u>Title</u>	<u>Page</u>
3.9.3.5	Long-Term Dimensional Stability	195
3.9.3.6	Human Factors Influence	196
3.9.3.7	Damage Tolerance	197
3.10	Contamination Control	198
3.10.1	Task	198
3.10.2	Approach	198
3.10.3	Discussion	198
3.10.4	Conclusion	201
3.11	Orbital Parameters (FSC)	203
3.11.1	Task	203
3.11.2	Approach	203
3.11.3	Orbit Decay and Propulsion Requirements	203
3.11.3.1	Discussion	203
3.11.3.2	Conclusions	209
3.11.4	Boost-Decay Operation	209
3.11.4.1	Discussion	209
3.11.4.2	Conclusions	209
3.11.5	Space Station Rendezvous Aspects	212
3.11.5.1	Discussion	212
3.11.5.2	Conclusions	213
3.11.6	Observational Viewing Limits	213
3.11.6.1	Discussion	213
3.11.6.2	Results	213
3.12	Orbital Environment (FSC)	213
3.12.1	Task	213
3.12.2	Approach	217
3.12.3	Radiation Environment	217
3.12.3.1	Discussion	217
3.12.3.2	Results	220
3.12.4	Micrometeoroid Environment and Collision Probability	227
3.12.4.1	Discussion	227
3.13	Spacecraft Functions (FSC)	238
3.13.1	Task	238
3.13.2	Approach	238
3.13.3	Attitude Control; Momentum Storage and Torquing	238
3.13.3.1	Discussion	238
3.13.3.2	Results	243
3.13.4	Spacecraft Power	246
3.13.4.1	Discussion	246
3.13.4.2	Results	248
3.13.5	Spacecraft Configuration	250
4.0	Selected System Concepts	254
4.1	Concept Synthesis Approach	254
4.2	Selection Criteria	256
4.3	Concept 1: Multiple Shuttle Assembly	257
4.3.1	Configuration	257
4.3.2	System and Subsystem Designs	257
4.3.3	Orbital Parameters	258
4.3.4	Assembly Methods and Sequence	261
4.3.5	Launch Vehicle Integration	261
4.3.6	Space Environmental Factors	264

<u>Section</u>	<u>Title</u>	<u>Page</u>
4.3.7	Station Keeping	264
4.3.8	Attitude Control and Pointing Requirements	264
4.3.9	Data Handling	265
4.3.10	Replenishment of Expendibles	265
4.3.11	Refurbishment	265
4.3.12	Typical Instrument Interfaces	265
4.3.13	Mission Analyses	266
4.3.14	Development Risks	266
4.4	Concept 2: Space Station Assembly	266
4.4.1	Configuration	266
4.4.2	System and Subsystem Designs	266
4.4.3	Orbital Parameters	267
4.4.4	Assembly Methods and Sequence	270
4.4.5	Launch Vehicle Integration	272
4.4.6	Space Environmental Factors	274
4.4.7	Station Keeping	276
4.4.8	Attitude Control and Pointing Requirements	277
4.4.9	Data Handling	277
4.4.10	Replenishment of Expendables	277
4.4.11	Refurbishment	277
4.4.12	Typical Instruments Interfaces	278
4.4.13	Mission Analyses	279
4.4.14	Development Risks	279
4.5	Concept 3: Single Shuttle/ACC Assembly	280
4.5.1	Configuration	280
4.5.2	System and Subsystem Designs	283
4.5.3	Orbital Parameters	283
4.5.4	Assembly Methods and Sequences	284
4.5.5	Launch Vehicle Integration	286
4.5.6	Space Environmental Factors	286
4.5.7	Station Keeping	287
4.5.8	Attitude Control and Requirements	287
4.5.9	Data Handling	287
4.5.10	Replenishment of Expendables	287
4.5.11	Refurbishment	287
4.5.12	Typical Instrument Interfaces	288
4.5.13	Mission Analyses	288
4.5.14	Development Risks	288
4.6	Cost Considerations	289
4.7	Analysis Tools Used To Generate the Concepts	295
5.0	CONCLUSIONS AND RECOMMENDATIONS FOR FURTHER STUDY	296
5.1	Highlights of Analyses	296
5.2	Technology Development	297
5.3	Recommendations for Further Study	298



## LIST OF APPENDICES

<u>Appendices</u>	<u>Title</u>	<u>Page</u>
A	Glossary of Terms and Acronyms	A-1
B	Legend of Symbols, Constants, and Numerical Values	B-1
C	List of References	C-1
D	Calculations and Derivations	D1-1
D1	The Correspondence Between Antenna Theory and Optics	D1-1
D2	Issue Interaction Summaries	D2-1
D3	Pointing Trade Study of Optical Configuration and Pointing Techniques	D3-1
D4	Mirror Construction Alternatives - Cost Implications	D4-1
D5	Space Station Rendezvous (FSC)	D5-1

## LIST OF FIGURES

<u>Figure</u>	<u>Title</u>	<u>Page</u>
1.4-1	System Concepts Highlights	2
1.6-1	Summary LDR Technology Development Schedule	7
1.6-2	Technology Development Projected Funding Profile (Cumulative)	7
2.1-1	Study Plan	9
2.1-2	Study Breakdown Structure	10
2.2-1	N <sup>2</sup> LDR System Issues Interrelationships	11
2.2-2	Example of Issue Interaction Summary	12
2.3-1	LDR Science Instruments Subcommittee Report, 26 June 1984	14
2.4-1	Selected LDR System Parameters and Performance Requirements	15
2.5-1	Generic Instrument Categories	16
2.5-2	Summary of Generic Instrument Support Requirements	17
2.5-3	Featron Local Oscillator Features	18
2.5-4	Field Effect Oscillator (Featron) Concept	19
2.5-5	Optical Parametric Oscillator	20
2.5-6	Critical LDR Instrument Development Plan	20
3.1-1	Filled Versus Unfilled Apertures (Stellar Interferometers)	22
3.1-2	Zonal and Meridional Radii for an f/0.5 LDR Mirror	23
3.1-3	LDR Optical Configuration (On-Axis "True" Cassegrain Telescope)	23
3.1-4	SI Interface With Focal Plane	24
3.1-5	Comparison of a "True" Cassegrain With a Ritchey-Chretien Cassegrain	25
3.1-6	Single Shuttle With ACC Optical Configuration	26
3.1-7	LDR Optical Configuration (Off-Axis "True" Cassegrain Telescope)	27
3.1-8	SAG Difference Between Zonal and Meridional Radii Across Tool Diameter For F/0.5 Mirror	28
3.1-9	Aspheric Departure of Outer Annulus With Respect To Best Fit Sphere	28
3.1-10	Radially Degraded Mirror Concepts	29
3.1-11	Radially Degraded Cassegrain Telescope	30
3.1-12	Radially Degraded Primary Mirror	30
3.1-13	Single Shuttle With ACC (Radially Degraded Configuration)	31
3.1-14	Rectangular Aperture Cassegrain Telescope	32
3.1-15	Elongated Aperture (SLOT) Cassegrain Telescope	32
3.1-16	LDR Optical Configuration (SLOT Cassegrain Telescope)	33
3.1-17	Primary Mirror for SLOT Configuration	34
3.1-18	Erectable SLOT Configuration (Primary Mirror Segment Assemblies in ACC)	34
3.1-19	Spherical Primary Mirror Telescope (With Three Mirror Field Corrector)	36
3.1-20	Spherical Primary Mirror Telescope (MMSW)	36
3.1-21	Spherical Primary Mirror Telescope	38
3.1-22	Spherical Primary Mirror Telescope	38
3.1-23	Unfilled Aperture Effect On Encircled Energy	39
3.2-1	Image Diameter For Point Source	41
3.2-2	Light Gathering Capability	41
3.2-3	LDR Primary Mirror Segment Assemblies in Orbiter Bay	42
3.2-4	LDR Elements Stowed in Orbiter Bay	43

<u>Figure</u>	<u>Title</u>	<u>Page</u>
3.2-5	Weight/Diameter Interrelationship (Single Shuttle: H = 150NM; i = 28.5°)	43
3.2-6	Weight/Diameter Interrelationship (Single Shuttle: Polar Orbit)	44
3.2-7	Primary Mirror Segment Size Using ACC	45
3.2-8	Segment Stowage in ACC	45
3.2-9	Weight/Diameter Interrelationship (Shuttle/ACC: H = 150 NM; i = 28.5°)	46
3.2-10	Weight/Diameter Interrelationship (Shuttle/ACC: Polar Orbit)	46
3.2-11	Weight/Diameter Interrelationship (Dual Shuttle: H = 150 NM; i = 20.5°)	47
3.2-12	Weight/Diameter Interrelationship (Dual Shuttle: Polar Orbit)	47
3.2-13	Weight/Diameter Interrelationship (Dual Shuttle/ACC: H = 150 NM; i = 28.5°)	48
3.2-14	Weight/Diameter Interrelationship (Dual Shuttle/ACC: Polar Orbit)	48
3.3-1	Predicted Areal Density (Fusion Welded)	53
3.3-2	Predicted Areal Density (Frit-Bonded)	53
3.3-3	Thermal Expansion Coefficients	56
3.3-4	Thermal Expansion of Corning Fused Silica Glass	56
3.3-5	Lightweight Versus Ultra Lightweight Glass Mirror Technique	57
3.3-6	Selection of Primary Mirror Substrate Material	59
3.3-7	Radii for an f/0.5 Parabolic Mirror	60
3.4-1	Segmented Mirror Concepts Trade Tree	65
3.4-2	LDR Optical Subsystem Operational Performance Prediction	66
3.4-3	RMS Wavefront Error Requirement	67
3.4-4	LDR Optical Subsystem Operational Performance Prediction (Weighted as Before)	68
3.4-5	Primary Mirror Trades	69
3.4-6	Obscuration Effect on Encircled Energy	70
3.4-7	Number of Trapezoidal Segments in Full Mirror	71
3.4-8	Number of Trapezoidal Segments in Single Annulus	72
3.4-9	Number of Trapezoidal Segments in Double Annulus	73
3.4-10	Number of Trapezoidal Segments in Double Annulus	74
3.4-11	Number of Trapezoidal Segments in Triple Annulus	75
3.4-12	Number of Trapezoidal Segments in Triple Annulus	76
3.4-13	Number of Trapezoidal Segments in Triple Annulus	77
3.4-14	Primary Mirror with Hexagonal Segments (20 Meter Diameter)	78
3.4-15	Rigid Body Motions of Segmented Mirror	79
3.4-16	Program Flow for Phased Array Software	79
3.4-17	Simulation of Wavefront from On-Axis Cassegrain Telescope	82
3.4-18	Simulation of Wavefront from On-Axis Cassegrain Telescope	82
3.4-19	Encircled Energy Distributions for Ideal and Aberrated Beams	83
3.4-20	Primary Mirror Wavefront Error Budget	83
3.4-21	Composite Mirror Blank (Passive Design)	84
3.4-22	Composite Mirror Blank (Flexible Design)	84
3.4-23	Typical Segment (20.0 M Mirror)	85
3.4-24	Primary Mirror Control Trades	86
3.4-25	Passive Segment Assembly Options	87
3.4-26	Primary Mirror Control System	88
3.4-27	Passive and Active Segment Assembly Concepts	89
3.4-28	Reaction Structure Trades	90
3.4-29	Candidate LDR Primary Mirror Support Structures	91
3.4-30	LDR Primary Mirror Assembly Sequence in Orbiter Bay	91

<u>Figure</u>	<u>Title</u>	<u>Page</u>
3.4-31	LDR Primary Mirror Segment Manufacture Alternatives	93
3.5-1	Optical Subsystems Concepts Trade Tree	95
3.5-2	LDR Optical Subsystem Operational Performance Prediction	96
3.5-3	LDR Optical Subsystem Operational Performance Prediction (Reallocated To Increase Secondary Mirror Misalignment Allowable Error)	97
3.5-4	Allowable Despace Error	98
3.5-5	Allowable Despace Error	99
3.5-6	Secondary Mirror Trades	100
3.5-7	Instantaneous Thermal Expansion of Fused Silica	101
3.5-8	Secondary Mirror Control Trades	102
3.5-9	Secondary Mirror Wavefront Error Budget	103
3.5-10	Rigid Body Motions of Cassegrain Telescope	103
3.5-11	Secondary Mirror Assembly With Rigid Body Motion Control	104
3.5-12	Location of Sensors For an Internal Decenter and Tilt Sensing Concept	106
3.5-13	Secondary Mirror Support Structure Trades	107
3.5-14	Selection of Secondary Mirror Metering Material	108
3.5-15	Metering Structure Concepts	109
3.6-1	LDR Mirror Thermal Control Approach Schematic	113
3.6-2	Cylindrical Shield Geometry for Primary and Secondary Mirrors	115
3.6-3	Conical Shield Geometry for Primary and Secondary Mirrors	116
3.6-4	Step-Baffled Cylindrical Shield Geometry Primary and Secondary Mirrors	117
3.6-5	Short Cylindrical Maximum Shield Heating Loads at Sub-Solar	117
3.6-6	Long Cylindrical Maximum Shield Heating Loads at Sub-Solar	118
3.6-7	Conical Shield Maximum Heating Loads at Sub-Solar	119
3.6-8	Primary Mirror Maximum Orbital Average Temperature with Adiabatic Shield Walls	120
3.6-9	Primary Mirror Solar Heat Load Distribution at Sub-Solar for 30M Long Cylindrical Shield	121
3.6-10	LDR Mirror and Shield Geometry and Thermal Surface Finishes	122
3.6-11	LDR Thermal Model View Factor/Heat Rate Surface Nodes	123
3.6-12	Maximum Mirror Temperature Versus Backside Thermal Control Plate Temperature	125
3.6-13	Mirror-to-Thermal Control Plate Thermal Coupling Versus Backside Thermal Control Plate Temperature	126
3.6-14	Lateral Mirror Temperature Gradient Versus Backside Thermal Control Plate Temperature	127
3.6-15	Mirror Temperatures for Various Sun Angles and Solar Duty Cycles	128
3.6-16	Thermal Control Plate Heat Flows for Various Sun Angles and Solar Duty Cycles	128
3.6-17	Thermal Control Plate Heat Flows for Maximum and Minimum Earth and Albedo Heat Loads	129
3.6-18	Thermal Control Sensitivity of LDR Mirror	130
3.6-19	Instrument Cooling Passive Radiator Backed Cascaded Cryo-Fluid Cooling Concept	136
3.7-1	Pointing Concepts	140
3.7-2	Line of Sight Error Due to Secondary Mirror Jitter	141
3.7-3	Line of Sight Error With Damping	142
3.7-4	Static Wavefront Error Due to Secondary Mirror Tilt	143
3.7-5	Optical Configurations	145

<u>Figure</u>	<u>Title</u>	<u>Page</u>
3.7-6	LDR Pointing Candidates	146
3.7-7	Basis for MOI Calculation	146
3.7-8	Body Pointing	147
3.7-9	Body Pointing	147
3.7-10	Body Pointing	147
3.7-11	Separate Telescope Pointing	148
3.7-12	Separate Telescope Pointing	148
3.7-13	Separate Telescope Pointing	148
3.7-14	Slew Torque Profile: Body Pointing	151
3.7-15	Slew Torque Profile: Telescope Pointing	151
3.7-16	Slew Torque Profile: Secondary Mirror	152
3.7-17	Scan Torque Profile: Body Pointing	152
3.7-18	Scan Torque Profile: Telescope Pointing	153
3.7-19	Scan Torque Profile: Secondary Mirror	153
3.7-20	Fine Guidance Sensing Options	157
3.7-21	Number of Available Photons	158
3.7-22	Knowledge of Line of Sight Error	159
3.7-23	Two Reimaging Photometer Choppers	162
3.7-24	Fold Mirror Chopping Concepts	163
3.7-25	Secondary Mirror Chopping Concept	163
3.7-26	SM Chopping Mechanism Concepts	164
3.8-1	Transportation to Orbit - Task Summary	170
3.8-2	Transportation to Orbit - Task Approach	170
3.8-3	LDR Transport to Orbiter, Orbiter Performance and Constraints Status	172
3.8-4	SDV Candidates - As of August, 1984	172
3.8-5	SDV to HLLV Evolution for FY 85 Studies	173
3.8-6	LDR Transportation Considerations Transport to Orbit	175
3.8-7	LDR Transport to Orbit SDV Summary	176
3.8-8	LDR Transport to Orbit - Environments	176
3.8-9	LDR Transport to Orbit Orbiter Payload Weight/CG Limits	177
3.8-10	LDR Transport to Orbit Orbiter Vertical (Z) Load Limits	177
3.8-11	Shuttle Orbiter Margins-of-Safety for Module Cargo	178
3.8-12	Shuttle Payload Enclosures by MDAC	180
3.8-13	ACC Deployment Options	180
3.8-14	20 m + DIA Reflector Assembly	181
3.9-1	LDR Structures - Task Summary	185
3.9-2	LDR Structures - Task Approach	185
3.9-3	LDR Structures - Summary	186
3.9-4	Observatory Structural Options	187
3.9-5	Reaction Structure Design Hexagonal Mirror Segment Influence	187
3.9-6	Reaction Structure Design Trapezoidal Mirror Segment Influence	188
3.9-7	Reaction Structure Design Trapezoidal Mirror Segment Influence	189
3.9-8	Reaction Structure Design Trapezoidal Mirror Segment	190
3.9-9	Large Deployable Space Optics	192
3.9-10	Dimensionally Stable Structures	192
3.9-11	LDR Integration Structures Model	193
3.9-12	Interactive Design/Analysis Process	196
3.9-13	LDR Micrometeoroid/Debris Impact Probability	197
3.10-1	Particulate Contamination Control (During Buildup and On-Ground Transportation)	200
3.10-2	Particulate Contamination Control	202

<u>Figure</u>	<u>Title</u>	<u>Page</u>
3.10-3	Particulate Contamination Control	202
3.11-1	Orbit Parameter Field	204
3.11-2	Orbit Decay From 600 KM Initial Altitude (Zero Drag Makeup)	204
3.11-3	Orbit Decay From 700 KM Initial Altitude (Zero Drag Makeup)	205
3.11-4	Orbit Decay From 800 KM Initial Altitude (Zero Drag Makeup)	205
3.11-5	Orbit Decay From 600 KM, High Power LDR (Zero Drag Makeup)	206
3.11-6	Orbit Decay From 700 KM, Polar Orbit, High Power LDR (Zero Drag Makeup)	206
3.11-7	Orbit Decay From 800 KM High Power LDR (Zero Drag Makeup)	207
3.11-8	Incremental Velocity Requirement for Orbit Adjustment	207
3.11-9	LDR Propulsion Requirement for Orbit Adjustment	208
3.11-10	Predicted Solar Flux	210
3.11-11	Spacecraft Concept No. 1, Length = 30M	210
3.11-12	Spacecraft Concept No. 3, Length = 12M	211
3.11-13	Untitled	214
3.11-14	Untitled	215
3.11-15	Untitled	216
3.12-1	Van Allen Trapped Radiation Belts	218
3.12-2	Altitude Variation of Field Strength in the South Atlantic Anomaly (SAA)	218
3.12-3	Proton Isoflux Contours for Energies Above 34 MeV in the South Atlantic Anomaly	219
3.12-4	1976 Distribution of 3866 Satellites Observed by Radar	228
3.12-5	1980 Spatial Density of Observed Objects in Space	228
3.12-6	Size Distribution of Earth Orbiting Satellites	230
3.12-7	Total Area of Satellites in Space	231
3.12-8A	Impacts Expected by Year at 800KM, 1995 Launch Area = 300 M <sup>2</sup>	232
3.12-8B	Impacts Expected by Year at 800KM, 1995 Launch Area = 600 M <sup>2</sup>	232
3.12-9	Penetration Formulas	235
3.12-10	Untitled	236
3.13-1	Untitled	240
3.13-2	Untitled	241
3.13-3	Untitled	242
3.13-4	Untitled	244
3.13-5	Untitled	244
3.13-6	CMG Cluster	245
3.13-7	Configuration of Single Gimbal CMGs	247
3.13-8A	Untitled	252
3.13-8B	Untitled	253
4.1-1	Top-Level "Trade Spaces"	254
4.1-2	Early System Concept Candidates	255
4.3-1	Concept 1: Multiple Shuttle Assembly	257
4.3-2	LDR Observatory	258
4.3-3	Primary Mirror Assembly (Segmented Mirror with Rigid Body Motion Control)	259
4.3-4	Secondary Mirror Assembly (1.3 Meter Convex Hyperbolic Mirror)	260
4.3-5	First Shuttle Load (Rigid Mirror Assemblies in First Annulus)	261
4.3-6	Second Shuttle Load (Mirror Assemblies and Truss Bundles for Rest of Primary Mirror)	252
4.3-7	Third Shuttle Load (Scientific Instruments; Secondary Mirror; Sunshield; Spacecraft Upgrade; FGS)	252

<u>Figure</u>	<u>Title</u>	<u>Page</u>
4.3-8	Assembly/Test Sequence	263
4.3-9	Space Shuttle Flight System	263
4.3-10	LDR Hardware Stowed in Orbiter Bay	264
4.4-1	Concept 2: Space Station Assembly	267
4.4-2	LDR Observatory	267
4.4-3	Primary Mirror Assembly	268
4.4-4	Spherical Primary Mirror Concept	269
4.4-5	First Shuttle Load (Center Seven-Segment Assembly and Spacecraft)	270
4.4-6	Segment Assembly Integration	271
4.4-7	Truss Assembly	271
4.4-8	Sunshield Assembly	272
4.4-9	LDR Observatory Assembly Sequence	273
4.4-10	LDR on Space Station	273
4.4-11	Particulate Contamination Control (Space Station Assembly Concept)	275
4.4-12	LDR Interior Equipment Installation	276
4.4-13	ORU* Exchange Logistics Module (OMV-Based)	279
4.5-1	Concept 3: Single Shuttle/ACC Assembly	281
4.5-2	LDR Observatory	281
4.5-3	Unfilled Aperture Concept	282
4.5-4	LDR Primary Mirror Segment Assemblies in ACC	284
4.5-5	LDR Primary Mirror Assembly Sequence in Orbiter Bay	285
4.5-6	Stowage of Primary mirror Assemblies in ACC	286
4.6-1	Cost Summary Assumptions	290
4.7-1	List of Analysis Tools	295

## LIST OF TABLES

<u>Table</u>	<u>Title</u>	<u>Page</u>
1.4-1	System Concepts Highlights	5
1.4-2	System Concepts Comparison Summary	5
1.5-1	Individual Technology Augmentation Projects Cross Reference	7
3.1-1	Candidate Optical Configurations	21
3.1-2	Radially Degraded Telescope Performance Summary	31
3.1-3	Spherical Versus Aspherical Primary Mirror	35
3.1-4	Spherical Primary Mirror Telescope (MMSW)	37
3.1-5	Aperture Size Comparison	39
3.2-1	Single Shuttle Options	49
3.2-2	Single Shuttle Options	49
3.2-3	Relative Effects of Aperture Size	50
3.3-1	Mirror Material Requirements	51
3.3-2	Reflector Material Trade - Material Properties	52
3.3-3	Glass Mirror Faceplate Weight Estimate	55
3.3-4	Glass Matrix Material	58
3.3-5	Reflector Material Trade Performance Potential	61
3.3-6	Reflector Material Trade Complexity	62
3.3-7	Reflector Materials Trade Replicability	62
3.3-8	Cost	63
3.3-9	Reflector Material Trade Summary	63
3.4-1	Coherently Phased Mirrors	64
3.4-2	Primary Mirror With Trapezoidal Segments	78
3.4-3	Wavefront Propagation Model for a Segmented Mirror	80
3.4-4	Primary Mirror Requirements	81
3.5-1	Secondary Mirror Alignment Sensing Concepts	115
3.5-2	Secondary Mirror Focus Sensing Concepts	115
3.6-1	LDR Telescope Thermal Requirements	111
3.6-2	LDR Scientific Instrument and Secondary Mirror Cooling Thermal Requirements	112
3.6-3	Thermal Modeling Approach	124
3.6-4	Primary Mirror Sensitivity to Surface Heat Flux	131
3.6-5	Primary Mirror Sensitivity to Thermal Coupling	131
3.6-6	Instrument Cooling Cryogenic-Fluid Candidates	133
3.6-7	Instrument Cooling Methods	133
3.6-8	Status of Mechanical Cryogenic Refrigeration Machines	134
3.6-9	Comparison of Cryogenic Cooling Systems for LDR	135
3.7-1	Functional Requirements	143
3.7-2	Body Pointing Technique Summary	148
3.7-3	Separate Telescope Pointing	149
3.7-4	Body Pointing With Fine Pointing Using Secondary Mirror	149
3.7-5	Pointing Trade Study of Optical Configurations and Pointing Techniques Using Jenko Approach	154
3.7-6	Pointing Trade Study of Optical Configurations and Pointing Techniques Using Jenko Approach	155
3.7-7	LDR FGS System Requirements	160
3.7-8	Fine Guidance Sensing Configuration	160
3.7-9	Rotating Versus Push-Pull Tertiary Choppers	164
3.7-10	Secondary Mirror Chopping	166
3.7-11	Chopping Control Mechanism Studies	167



<u>Table</u>	<u>Title</u>	<u>Page</u>
3.7-12	Sensitivity Analysis of Chopping Mode On SM and Tertiary Mirror	168
3.8-1	Transportation Trade and Options Studies	171
3.8-2	Transportation To Orbit - Summary	171
3.8-3	LDR Construction Time Line Orbiter Basing	181
3.9-1	Structures Trade and Options Studies	186
3.10-1	Contamination Concerns and Controls	198
3.12-1	Radiation - 15 Year Dose (KRADS)	220
3.12-2	Solar Cell Degradation Over 10 Years (Radiation Only)	226
3.12-3	Meteoroid Environment	234
3.13-1	Characteristics of Representative Control Moment Gyros	245
3.13-2	Payload Power Requirements	246
3.13-3	Spacecraft Power (Orbit Average) 3 Module Power System 1200 Square Feet Solar Array	249
3.13-4	Mass Properties	251
4.3-1	Technology Risks	266
4.4-1	Technology Risks	280
4.5-1	Technology Risks	288
4.6-1	LDR System Concepts Top-Level Cost Implication	289
4.6-2	Observatory Design and Production Costs	291
4.6-3	Observatory Launch and Deployment Costs	292
4.6-4	Resupply, Refurbish, and Exchange Costs	293
4.6-5	Ranked Cost Drivers In Each Concept	294

## FOREWORD

This volume is one of two volumes that comprise the Final Technical Report. This Volume I includes the Executive Summary for the total study and a report of the systems analysis phase. Topics covered are: study approach and methodology; reports of 13 system analyses and trades tasks; and descriptions of three selected LDR system concepts. Supporting information is contained in appendices.

Volume II contains Technology Assessments and the Technology Development Plan generated during the Technology Definition Phase of the study.

This document is submitted by Eastman Kodak Company to the National Aeronautics and Space Administration (NASA), Ames Research Center in response to Article II, Section C, Paragraph 1, Item i and Article V, Section B, Paragraph 8, of Contract NAS2-11861, Large Deployable Reflector System Concept and Technology Definition Study, as modified.

This document includes inputs and information provided by Kodak's study team members, McDonnell Douglas Astronautics Company-Huntington Beach (MCDAC) and Fairchild Space Company (FSC). Portions of the document prepared by these team members are identified by their company initials following a section or paragraph heading.

Engineers and scientists who contributed to the study are identified below by company affiliation and technical functional role:

### Eastman Kodak Company

Study Manager	Donald L. Agnew
Optical Systems Analysis	Peter A. Jones
Thermal/Cryogenics Analysis	John J. Meyers and Robert D. Grigg
Reflector Materials and Mechanical Analysis	David A. Crowe and Robert R. Brearey
Pointing And Control	Michael J. Clayton, Richard A Kent and Rodney E. Wetterskog
Chopping	Dr. Dennis A. Thompson
Optical Analysis	Randy C. VanVranken and Joseph J. Charles
Structural Analysis	Dr. Vincent J. Piarulli and Dr. Victor L. Genberg
Cost Modeling	Victor F. Vinkey

## 1.0 EXECUTIVE SUMMARY

### 1.1 PURPOSE OF REPORT

This report outlines results of a 12-month "pre-Phase A" study of system concepts and technology needs for the Large Deployable Reflector. LDR is envisioned to be a free-flying astronomical facility which will perform astrophysical studies primarily in the spectral range of 30  $\mu$ m to 1 mm. NASA has included LDR in its planning for a start in the early 1990's with a flight projected by the mid-1990's.

A draft of this report was a major input to the LDR Technology Planning Workshop held March 17-22, 1985, at the Asilomar Conference Center, Pacific Grove, California. The workshop with appropriate scientific and technology experts, organized and managed by NASA, had as an objective the production of a single consensus LDR Technology Development Plan.

### 1.2 STUDY OBJECTIVES

There were two principal objectives. The first (comprising approximately 70% of the study effort) consisted of two steps:

1. Perform engineering studies that provide an understanding of the scientific, technological, and cost implications of each system parameter and subsystem component on a range of systems concepts for LDR.
2. Generate two or more system concepts for LDR, including supporting rationale and cost estimates, based on the tradeoff analyses and performance studies.

The second objective (comprising approximately 30% of the study effort) also involved two steps:

1. Assess the required LDR technologies.
2. Draft a single technology development plan which encompasses the concepts and which provides the desired technology levels by 1991. The time-phased plan is to include an estimate of technology development costs and be consistent with NASA's Master Schedule for LDR implementation.

### 1.3. TECHNICAL APPROACH

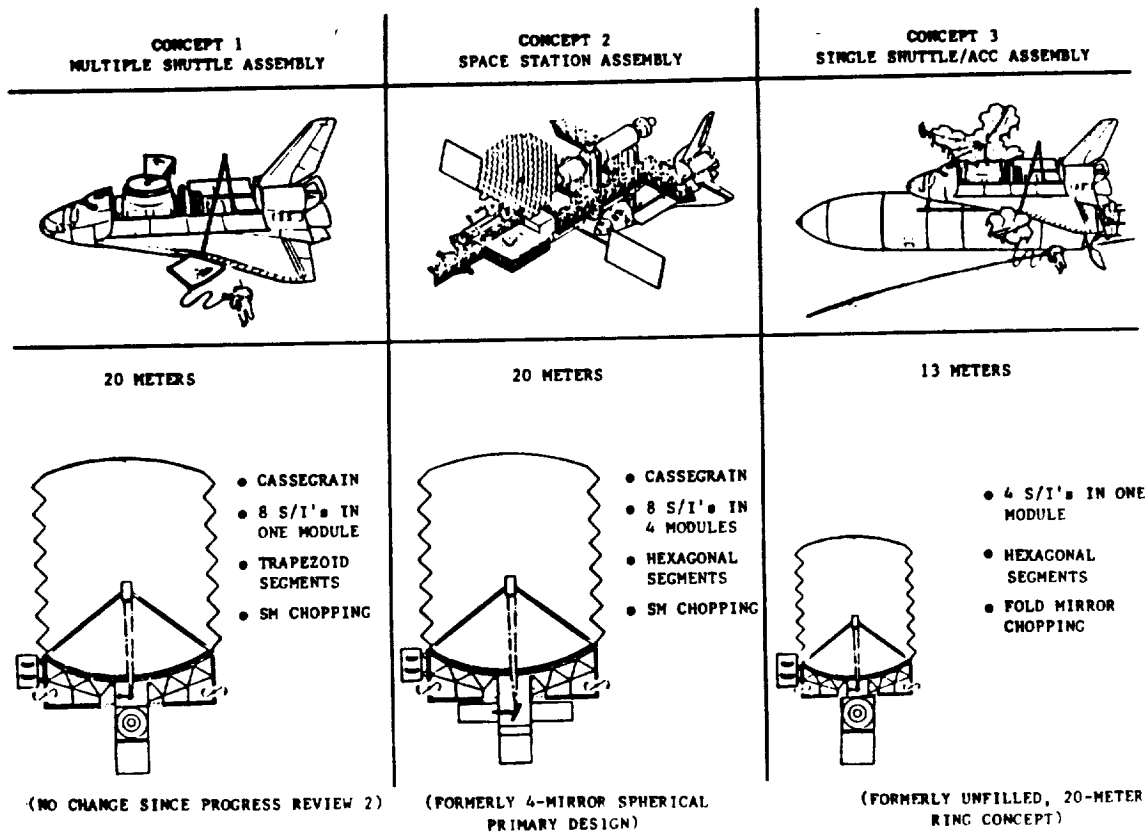
The study objectives were achieved by the following approach (Section 2.0 provides details):

1. Thirteen major system and LDR related issues were examined in order to determine scientific, technical, and cost implications of various alternatives (Section 3).
2. Candidate representative LDR system concepts were synthesized and three selected to aid in the preparation of the technology development plan. (These are highlighted in Paragraph 1.4 following and described in detail in Section 4.)
3. By examining the selected concepts, performance levels of LDR critical technologies were specified and assessed for their degree of readiness by year-end 1991. Technology short falls were identified and technology development plans were prepared for those areas rated most in need of incremental growth or acceleration in order to meet the requirements of LDR. (Summarized in Paragraph 1.5 and discussed in detail in Volume II.)

## 1.4 SELECTED LDR SYSTEM CONCEPTS

The three concepts depicted in Figure 1.4-1 were selected as reasonable and representative LDR system concepts for the purpose of defining the technology plan. The concepts, unoptimized, enable a relative comparison of orbital assembly of 20-meter aperture observatories using only Space Shuttles (Concept 1) or on the manned Space Station (Concept 2).

The 13-meter aperture system concept (Concept 3) was aimed at providing the largest diameter system capable of being deployed/assembled using the proposed Space Shuttle/External Tank with Aft Cargo Compartment transportation system.



SYSTEM CONCEPTS HIGHLIGHTS  
Figure 1.4-1

The triad of system concepts was settled upon following presentation to the NASA review team of three concepts intentionally configured to give visibility to alternative technology candidates. Those featured three different 20 m diameter optical configurations - a Cassegrain, a four-mirror system with a spherical primary, and an unfilled ring aperture concept.

The spherical primary design was discarded (because of the unwieldy size of the secondary and "wild" asphericity of the tertiary and quaternary mirrors) as was the ring concept (high sidelobes and light gathering power equivalent only to that of a 10-meter filled system).

The three agreed-to system concepts all feature "true" Cassegrain formulas with f/0.5 parabolic primaries. Thermal control is accomplished using a step sunshield/louvered aft cavity that permits operation when pointing as close as 60 degrees to the sun and 45 degrees to the Earth's limb. A one-meter aperture visible wavelength fine guidance sensor, co-boresighted to the observatory optical axis, provides input in the fine guidance mode to maintain the LDR absolute pointing requirement of 0.05 arcsec, utilizing the spacecraft control system.

Chopping is accomplished by oscillating the secondary mirror in Concepts 1 and 2. In Concept 3 it's done by moving the fold mirror that directs the incoming beam to the various science instruments.

The two larger diameter concepts are each equipped with eight science instruments. Only four are sized for Concept 3. The shape of primary mirror segments is somewhat arbitrary - trapezoids are identified for Concept 1, while hexagons are featured in Concepts 2 and 3.

All systems featured hybrid (stored cryogenics and mechanical cooler) refrigerators to provide generic cooling for the science instruments. Integral spacecraft provides basic electrical power, propulsion, communications, data processing, attitude control, and other functions.

A top-level comparison of each concept's launch, assembly, insertion into operational orbit, and servicing baseline, and assumptions is shown in Table 1.4-1.

Table 1.4-2 compares overall performance, schedule, and cost implications of the selected system concepts. The influence of the transportation-to-orbit options dominates. The 20-meter LDR assembled at the Space Station appears to have distinct advantages over incremental assembly by a series of Shuttle flights. The multiple Shuttle mode is severely constrained by Shuttle on-orbit loiter time limits. It forces inefficient LDR packaging and introduces complex designs to allow fast assembly. The spacecraft must be able to handle the varying mass properties during the staged buildup and is, in essence, an unmanned platform.

The 13-meter concept fails to satisfy the fundamental aperture requirement, with consequent loss of angular resolution and longer integration times than the 20-meter versions. Fewer science instruments are included as a result of the limited payload weight/volume of the single-Shuttle/ACC. Again, because of loiter time limits on orbit, the 13-meter design would require maximizing automated/modular deployment capability.

## 1.5 TECHNOLOGY ASSESSMENT AND RISKS

Examination of the LDR system concepts reveals technology challenges in many areas. The Kodak-MDAC-FSC team identified more than 30 specific candidate technology issues, prioritized them (with respect to high, medium, low, and non-rated risk criteria), and found 22 which are recommended for supplementary support by NASA to reach levels of readiness deemed necessary for LDR by year-end 1991.

TABLE 1.4-1  
SYSTEM CONCEPTS HIGHLIGHTS

BASELINE	CONCEPT 1 MULTIPLE SHUTTLE ASSEMBLY	CONCEPT 2 SPACE STATION ASSEMBLY	CONCEPT 3 SINGLE SHUTTLE/ACC ASSEMBLY
LAUNCH VEHICLE(S)	≤3 SHUTTLES FOR OBSERVATORY COMPONENTS (DEDICATED) ~3 SHUTTLES FOR ASTRONAUT ASSEMBLY, CHECKOUT (SHARED)	≤3 SHUTTLES FOR OBSERVATORY COMPONENTS, ASSY/CHECKOUT SUPPORT EQUIPMENT	1 SHUTTLE/ACC
ASSEMBLY PLATFORM (28.5° INCLINATION, SHUTTLE/SS ALTITUDE)	SPACECRAFT INTEGRAL TO LDR (ACCOMMODATES VARYING MASS PROPERTIES)	SPACE STATION AND SPACECRAFT INTEGRAL TO LDR	SPACECRAFT INTEGRAL TO LDR (SUPPORTED FROM SHUTTLE PAYLOAD BAY)
INSERTION INTO OPERATIONAL ALTITUDE (>600 KM)	PROPULSION SYSTEM IN INTEGRAL SPACECRAFT	PROPULSION SYSTEM IN INTEGRAL SPACECRAFT	PROPULSION SYSTEM IN INTEGRAL SPACECRAFT
PRIMARY MODE FOR SERVICE/CHANGEOUT (3 YEAR INTERVALS)	OMV FROM SHUTTLE (SMART FRONT END SERVICER)	OMV FROM SPACE STATION (SMART FRONT END SERVICER)	OMV FROM SHUTTLE/ACC (SMART FRONT END SERVICER)
ASSUMPTIONS	SHUTTLE ONLY AVAILABLE (NO SPACE STATION, ACC)	MANNED SPACE STATION AVAILABLE (NO ACC)	SHUTTLE/ACC AVAILABLE (NO SPACE STATION)

TABLE 1.4-2  
SYSTEM CONCEPTS COMPARISON

	CONCEPT 1 MULTIPLE SHUTTLE ASSEMBLY 20M APERTURE	CONCEPT 2 SPACE STATION ASSEMBLY 20M APERTURE	CONCEPT 3 SINGLE SHUTTLE/ACC ASSEMBLY 13M APERTURE
<b>PERFORMANCE</b> ● CONFORMANCE TO STUDY BASELINE REQUIREMENTS FOR LDR OBSERVATORY	POTENTIAL TO MEET ALL REQUIREMENTS	POTENTIAL TO MEET ALL REQUIREMENTS	● DOES NOT MEET APERTURE REQUIREMENT ● LESS RESOLUTION ● LONGER OBSERVATION TIME ● 4 INSTRUMENTS
● TRANSPORTATION TO ORBIT, ASSEMBLY/DEPLOYMENT	● CONSTRAINED BY SHUTTLE LOITER TIME LIMITS ● MAJOR SHUTTLE SCHEDULING IMPACT ● LONG INITIAL ASSY PERIOD ● SPACECRAFT IS "PLATFORM"	● MANNED SPACE STATION MUST BE AVAILABLE ● MORE FLEXIBLE ASSY SEQUENCE, SHUTTLE MANIFEST	● REQUIRES ACC DEVELOPMENT ● ACC CONTAMINATION CONCERNS, RMS ● DIFFICULT AUTOMATION
● IN-ORBIT SERVICING, REPAIR, UPGRADE, REFURBISHMENT	CONSTRAINED BY SHUTTLE LOITER TIME	● ENHANCED OPPORTUNITY FLEXIBILITY	CONSTRAINED BY SHUTTLE LOITER TIME
<b>SCHEDULE</b> ● POTENTIAL FOR ACHIEVING NEEDED LEVEL OF TECHNOLOGY READINESS BY 1991 (FOR LDR)	GOOD	GOOD	BETTER (BASED ON DESCALING ALONE, BUT DEPLOYMENT AUTOMATION MAY OFFSET ADVANTAGES)
<b>COST</b> ● TOTAL COSTS TO LDR IOC	HIGHEST (DEDICATED SHUTTLES)	HIGH	LOWEST (IF ADDITIONAL AUTOMATED DEPLOYMENT DESIGN FEATURES ATTAINABLE)

Five technology areas were assessed as most in need of augmentation because of unique LDR requirements, lack of viable alternatives, high potential payoff, or anticipated long term development effort. These five areas are:

- Cryogenic Cooling                      Demonstration of a hybrid (stored cryogen and closed cycle mechanical cooler) system for the LDR science instruments.
- Human Factors                            Demonstration of astronaut capability to assemble the optical precision LDR in space and to perform other roles.
- Active Primary Mirror                  Demonstration of an LDR-unique segmented mirror design having tilt, piston, and figure control for each panel.
- Dynamic Structural Control            Development of a dynamic simulation model of the LDR that links dispersed structural design and analysis techniques.
- Primary Mirror Contamination Protection    Development of means (such as strippable coatings) to protect the reflector on orbit during deployment/assembly, servicing revisits.

Seventeen other technology assessments were judged to be of "medium" importance. Table 1.5-1 lists the 22 high and medium technology areas by title and provides a cross-reference to their location in Volume II.

TABLE 1.5-1  
INDIVIDUAL TECHNOLOGY AUGMENTATION PROJECTS  
CROSS REFERENCE

OST CATEGORY	TECHNOLOGY PROJECT TITLE	KODAK PROGRAM GROUP	PARAGRAPH LOCATION SECTION 3.C
HIGH PRIORITY (5 PROJECTS)			
B	DYNAMIC STRUCTURAL CONTROL	POINTING & STABILITY	3.2.1
D	HUMAN FACTORS	POINTING & STABILITY	3.4.1
E	HYBRID CRYOGENIC SYSTEM FOR SCIENCE INSTRUMENTS	DETECTABILITY	3.5.1
G	ACTIVE PRIMARY MIRROR	REFLECTOR QUALITY	3.7.1
G	PRIMARY MIRROR CONTAMINATION PROTECTION	DETECTABILITY	3.7.2
MEDIUM PRIORITY (17 PROJECTS)			
A	PRIMARY MIRROR SEGMENT SENSING AND CONTROL APPROACH	REFLECTOR QUALITY	3.1.1
A	FOLD MIRROR CHOPPING	DETECTABILITY	3.1.2
A	SECONDARY MIRROR CHOPPING	DETECTABILITY	3.1.3
A	FINE GUIDANCE SENSING AND CONTROL	POINTING & STABILITY	3.1.4
B	DYNAMIC DIMENSION STABILITY	POINTING & STABILITY	3.2.2
B	DYNAMIC RESPONSE PREDICTION PRECISION	POINTING & STABILITY	3.2.3
B	STRUCTURAL NONLINEARITY	POINTING & STABILITY	3.2.4
B	LOW JITTER AND RAPID SETTLING	POINTING & STABILITY	3.2.5
B	VERIFICATION/ACCEPTANCE GROUND TESTING	POINTING & STABILITY	3.2.6
B	MECHANICAL STABILITY - DAMAGE TOLERANCE	POINTING & STABILITY	3.2.7
B	STEP SUNSHIELD	DETECTABILITY	3.2.8
B	SECONDARY MIRROR TEMPERATURE CONTROL	DETECTABILITY	3.2.9
B	PRIMARY MIRROR TEMPERATURE CONTROL	DETECTABILITY	3.2.10
E	CRYOGENIC SYSTEMS FOR DETECTOR TEMPERATURE LESS THAN 0.3 DEGREES KELVIN	DETECTABILITY	3.5.2
E	ROBOTIC ON-ORBIT CRYOGENIC REPLENISHMENT	DETECTABILITY	3.5.3
G	GLASS MATERIAL FOR PRIMARY MIRROR	REFLECTOR QUALITY	3.7.3
G	COMPOSITE MATERIAL FOR THE PRIMARY MIRROR	REFLECTOR QUALITY	3.7.4

## 1.6 RECOMMENDED TECHNOLOGY DEVELOPMENT PLAN

Kodak has synthesized three broad time-phased, five-year programs from the 22 individual technology issues. This was done to better understand the interrelationships of the projects, so as to identify intermediate decision points where alternatives existed, and to consider the overall funding implications. The three programs are:

- Reflector Quality Program
- Pointing and Stability Program
- Detectability Program

The Reflector Quality Program comprises four interrelated projects concerned with primary mirror (reflector) materials development, selection of a mirror design, and mirror demonstration to meet LDR requirements.

The Pointing and Stability Program combines nine projects. Six are interrelated structural materials, structural design, and test developments. The Dynamic Structure Control simulation modeling is also in this group, as are the Human Factors and Fine Guidance Projects.

The Detectability Program also comprises nine projects. It deals with technologies that principally determine the ability of LDR to achieve its background-limited NEP sensitivity goals. Three projects are concerned with cryogenics, three with thermal control, two with chopping, and one is the Primary Mirror Contamination Protection Project, mentioned above.

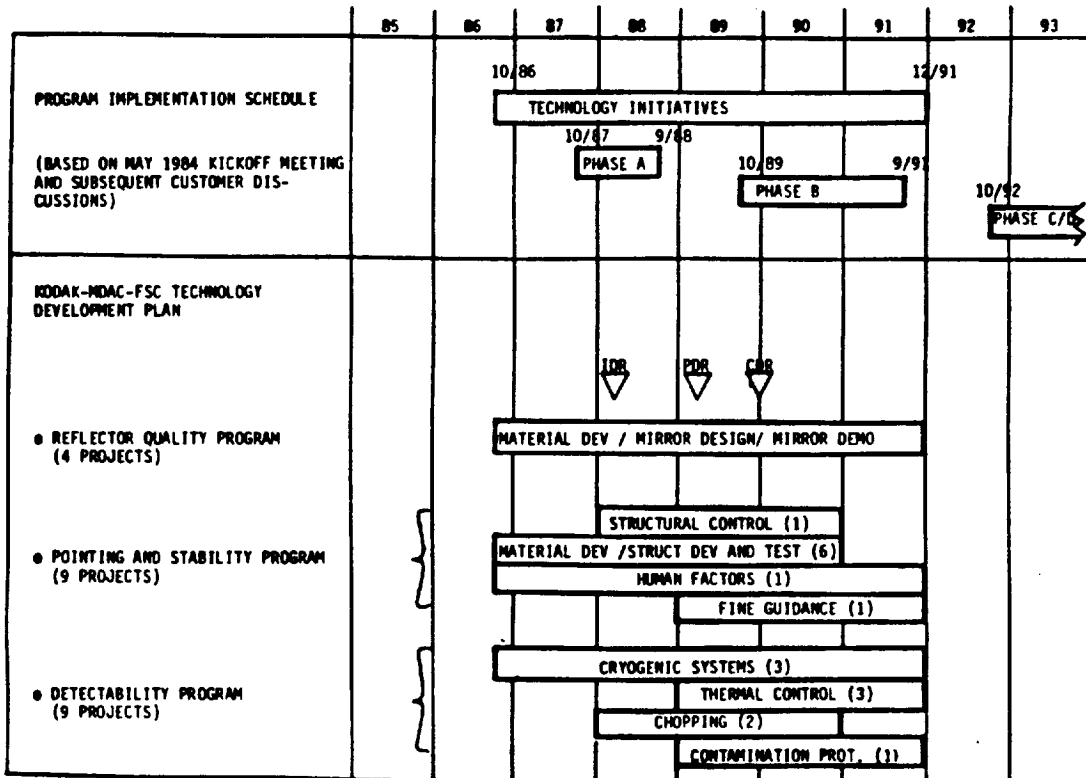
A summary schedule of the Kodak-MDAC-FSC technology development plan is presented in Figure 1.6-1 along with the NASA LDR Master Schedule. Separate, more detailed time-phased plans for each of the three programs are included in Section 4 of Volume II.

The recommended funding for the technology development projects totals \$70.425 million (rough order of magnitude based on 1985 dollars not forward priced). The three component program funding levels are:

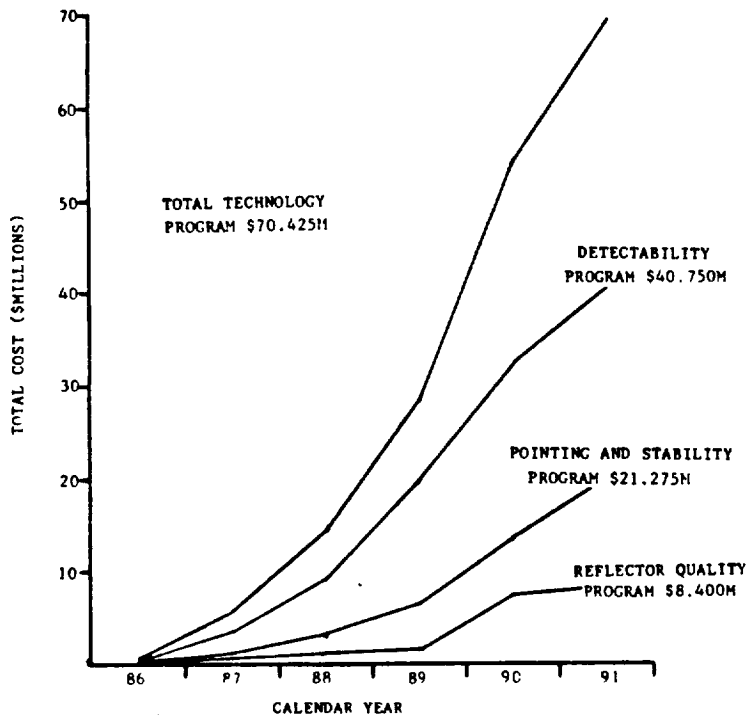
- Detectability Program                   \$40.750 M
- Pointing and Stability Program       \$21.275 M
- Reflector Quality Program           \$ 8.400 M

Time-phased funding details by project and program are also contained in Section 4 of Volume II. The cumulative funding profile is shown below in Figure 1.6-2.





SUMMARY LDR TECHNOLOGY DEVELOPMENT SCHEDULE  
Figure 1.6-1



TECHNOLOGY DEVELOPMENT PROJECTED FUNDING PROFILE (CUMULATIVE)  
Figure 1.6-2

## 2.0 STUDY APPROACH AND METHODOLOGY

### 2.1 STUDY TASK FLOW

The study comprised six major tasks. Figure 2.1-1 is a schematic of the task flow. In general, the study progressed serially from one task to the next, beginning with a review of the baseline requirements and an initial study of optical configurations. Approximately 70% of the total study effort was performed in the study of systems issues and development of systems concepts (blocks above SOW Tasks 3.1 and 3.2 of Figure 2.1-1). Based on the results of systems issue analyses during this phase, three LDR system concepts were synthesized and reported at Technical Progress Review No. 2.

The four ensuing tasks (SOW 3.3 through 3.6) constituted the technology definition phase of the study. Activities and methods employed in this phase are described in detail in Section 1.2.2 of Volume II of this report. The major output of this latter phase was the Technology Assessment and Technology Definition Plan, presented at the Final Briefings at Ames and NASA Headquarters, and at the LDR Technology Workshop.

Contractor team participation in the study tasks and subtasks is indicated in the Work Breakdown Structure shown in Figure 2.1-2.

### 2.2 ISSUE INTERRELATIONSHIPS

A "brute-force" approach was taken at the beginning of the study to identify the interrelationships between system issues. The " $N^2$  chart" systems technique was the method used. This technique involves formally assessing all the possible interrelationships. Figure 2.2-1 presents an  $N^2$  chart for the 14 study subtasks performed in the analysis phase. These are listed as the diagonal elements of the 14 x 14 matrix. The numbered circles at the intersections of horizontal (output) and vertical (input) lines identify a pertinent relationship between the boxes (issues) tied to the two lines.

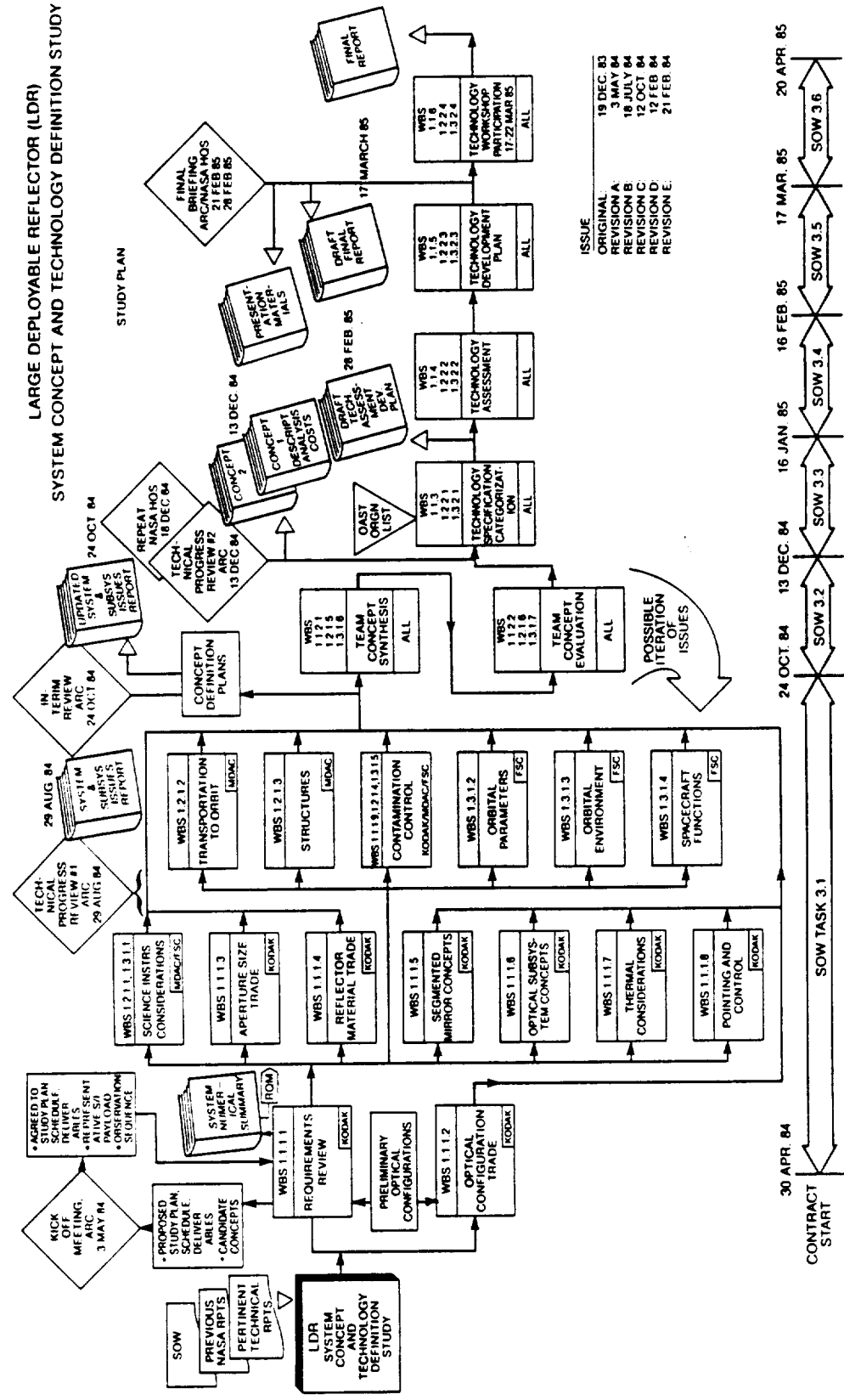
(Because the system issues are comprised of "apples and oranges" to some extent, the designation of a relationship intersection is itself a judgement issue. The generation of an acceptable program  $N^2$  chart is an iterative process, particularly in the conceptual phase.)

The  $N^2$  chart served the purpose of focusing attention on the interactive features of the system issues. Seventy-seven are shown in the figure. Note that "inputs" and "outputs" enter/exit the specified 14 system issues matrix, coming from or going to external items that are not explicitly contained in the system issue tasks. The rightmost list of "external" items encompass components that make up some of the system concept description and system engineering budgets essential to tracking the system concept definition process.

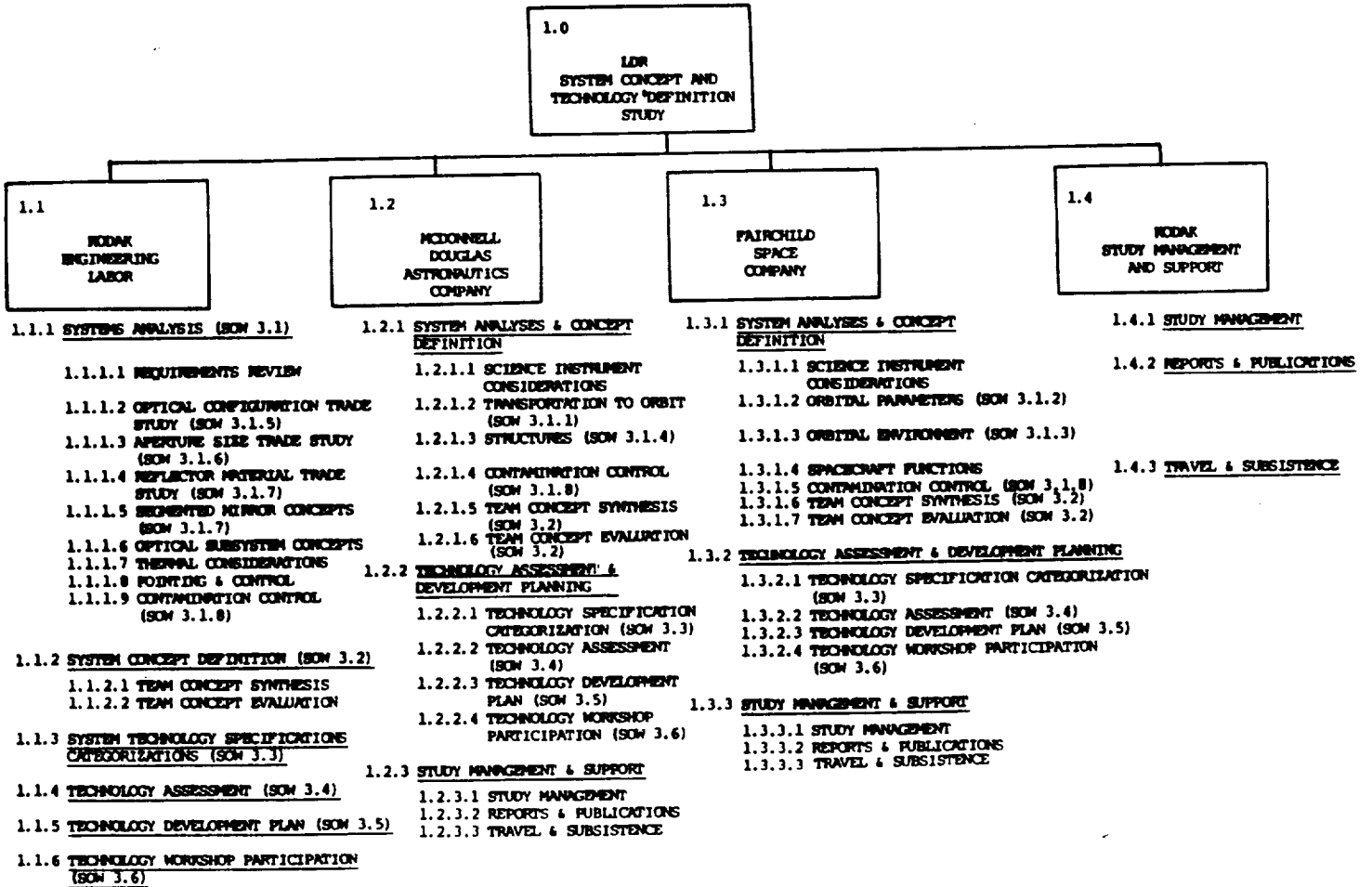
Further understanding of the interrelationships was accomplished by reviewing published LDR and LDR related reports.

Top-level issue interaction summaries were generated for each issue from the  $N^2$  chart analysis. Figure 2.2-2 shows a sample for the structure issue (SOW 3.1.4). Copies of 13 others are contained in Appendix D of this volume.

LARGE DEPLOYABLE REFLECTOR (LDR)  
SYSTEM CONCEPT AND TECHNOLOGY DEFINITION STUDY

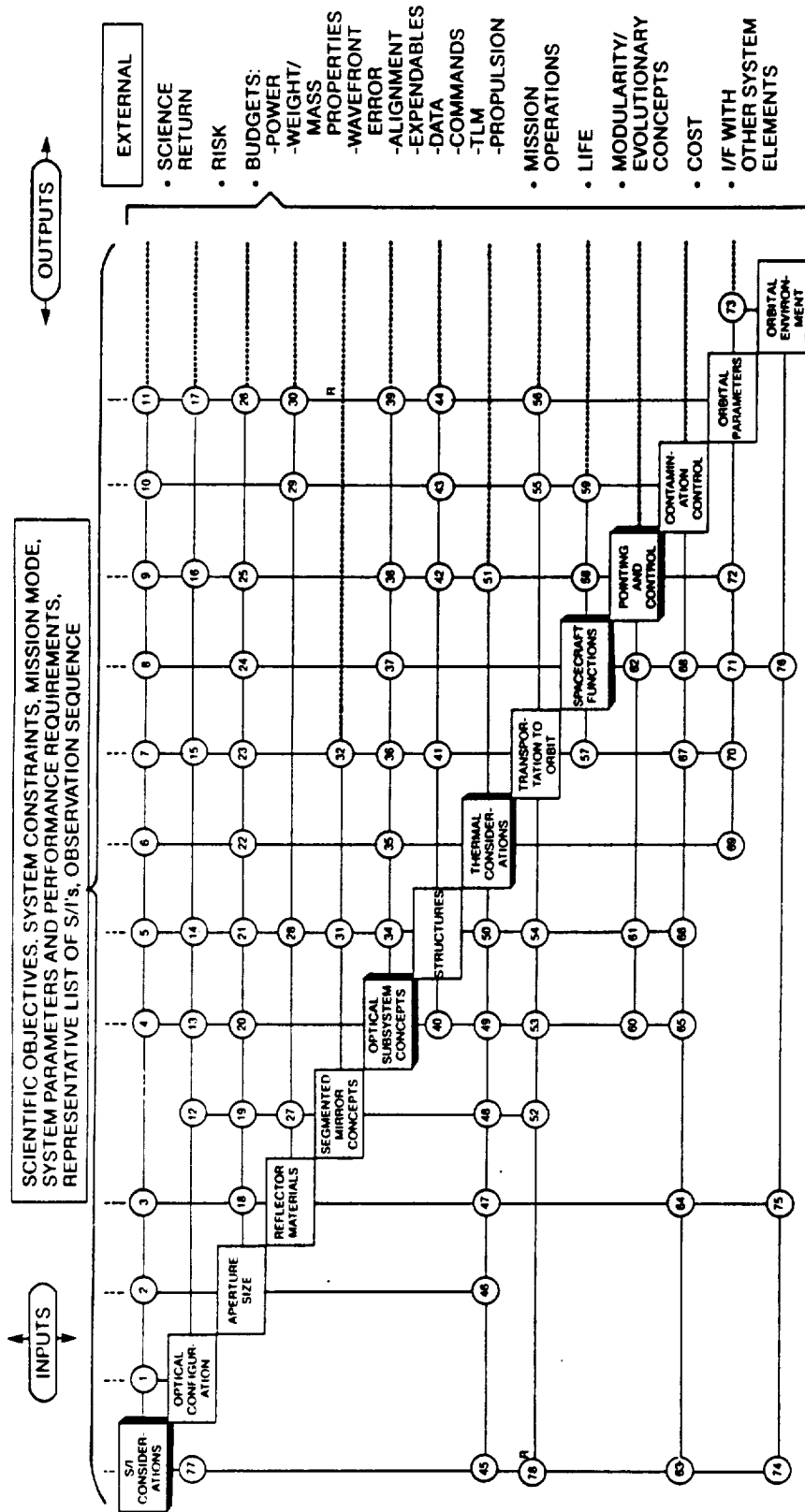


STUDY PLAN  
Figure 2.1-1



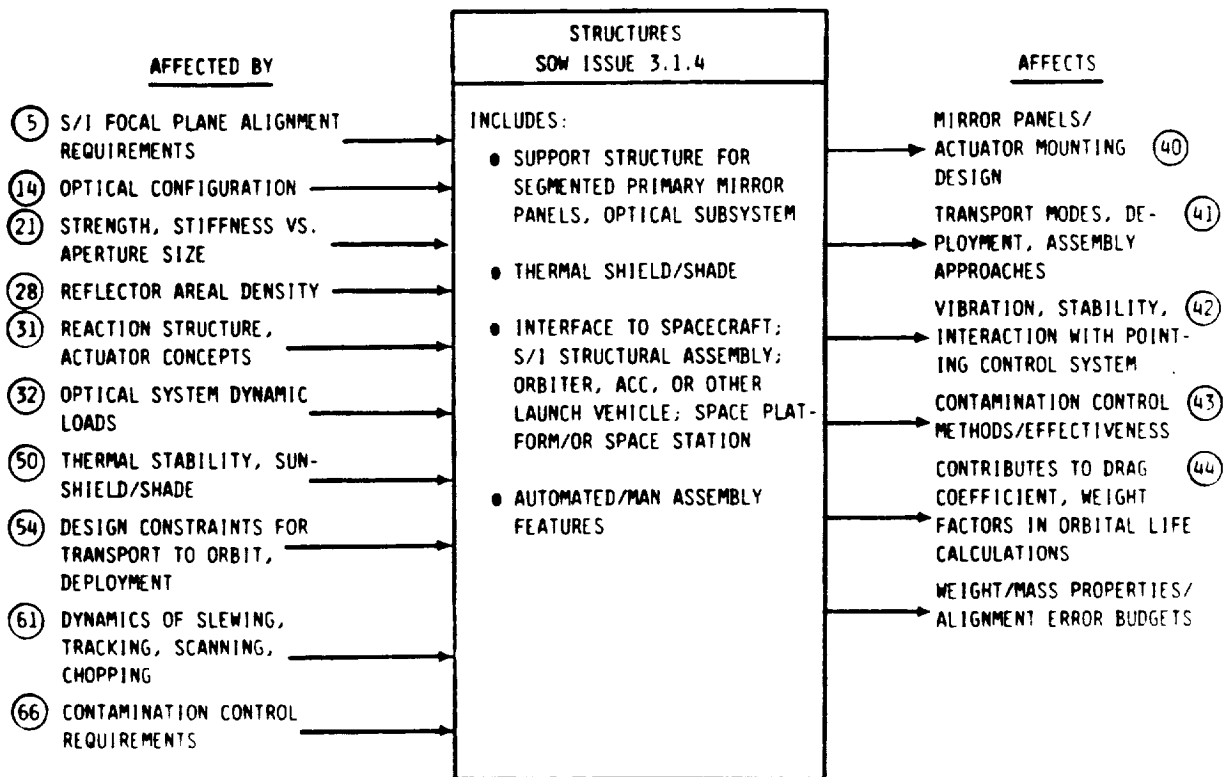
## STUDY WORK BREAKDOWN STRUCTURE

Figure 2.1-2



N<sup>2</sup> LDR SYSTEM ISSUES INTERRELATIONSHIPS

Figure 2.2-1



EXAMPLE OF ISSUE INTERACTION SUMMARY  
Figure 2.2-2

Attention was paid to the issue interrelationships throughout the study. The interaction summary charts were documented in the System Numerical Summary. (See Section 2.4 below).

## 2.3 ASSUMPTIONS

### 2.3.1 Science Instruments

We have assumed for the study that eight focal plane instruments, each contained in an independent module, constitute the baseline science instrument payload. The instrument modules would be capable of being independently changed out in orbit. A generic cryogenic region cooling system would service each of the instruments. A rotating fold mirror would direct the on-axis beam from the telescope optics to the eight instruments (with only one instrument in use during an observation) which are arranged radially about the telescope longitudinal axis.

These general assumptions are based on the provisional configuration and candidate list of instruments presented by the LDR Science Coordination Group at the study kick-off meeting at Ames on 4 May 1984.

Approximate baseline space and mass allocation were assumed to be (instruments only):  
 Total Volume : 2 meters x 3 meters x 3 meters octagonal disk  
 Total Mass: 1,600 Kg

A draft report by the LDR Science Coordination Group, Focal Plane Instrument Subcommittee dated 26 June 1984 provided an updated, provisional list of instruments and their characteristics which was integrated into the baseline interface requirement for the study. A summary is shown in Figure 2.3-1.

Because the science and astronomy issues were outside the specific expertise of the team, an early effort was undertaken to better understand the fundamental technological implications of the science package. This Science Instruments Considerations task is discussed in Section 2.4.

### 2.3.2 Launch Vehicles

For the purpose of this study, it was assumed that the Shuttle orbiter capabilities would remain relatively unchanged with respect to 1985 payload weight and volume capability, other than the proposed mode of operation to orbit the attached External Tank with an Aft Cargo Compartment. This latter mode is basic to our System Concept 3.

An assessment made by MDAC of the viability/availability of proposed shuttle-derived large booster systems (based on current candidate concepts) led us to the baseline assumption to rule out such vehicles, despite their obvious application to LDR.

### 2.3.3 Space Station

An "initial operational capability", manned Space Station was assumed to be a viable baseline study assumption. It is basic to our System Concept 2. Because Space Station capabilities are not yet firm, assumed Space Station accommodation capabilities were based on requirements contained in NASA requests for proposals issued in 1984.

### 2.3.4 Orbital Maneuvering/Transfer Vehicles

It was assumed that an orbital maneuvering vehicle (OMV), a free-flying, remotely piloted vehicle for use with the Shuttle orbiter, and later with the Space Station, to perform LDR servicing would be available in the LDR operational time period. It was also assumed that with an advanced orbital transfer stage and the aid of advanced mission kits ("smart front end") it would be possible to remotely replenish LDR cryogenics and propellants, change out science instruments and orbital repair units, as well as perform other potential LDR roles.

## 2.4 REQUIREMENTS REVIEW

This prelude task was an investigation of each of the study requirements shown in Figure 2.4-1. They were used as the baseline point-of-departure requirements for the LDR system concepts generated during the study.

These baseline requirements represented a consensus of ideas, primarily the result of the LDR Science and Technology Workshop conducted by NASA in June, 1982.

In this task the rationale for each requirement was traced to its scientific technology basis by reviewing reports of predecessor LDR contract concept and technology studies, and published technical reports on LDR.

Number	Instrument	Type	Wavelengths	Mass	Temp. Range	Thermal Load
1	High resolution spectrometer	SIS multichannel heterodyne receiver	3 mm - 400 $\mu$ m	200Kg	2-10K	T <sub>≤</sub> 4K : 50mW T=20K : 300mW
2	High resolution spectrometer	Schottky diode multichannel heterodyne receiver	500 - 200 $\mu$ m	200Kg	~20K	T=20K : 300mW
3	High resolution spectrometer	Photoconductor multichannel heterodyne receiver	200 - 35 $\mu$ m	200Kg	2-20K	T <sub>≤</sub> 4K : 150mW T=20K : 200mW
4	Medium resolution spectrometer	Fabry-Perot interferometers with imaging detector arrays	200 - 35 $\mu$ m	180Kg	4-20K	T <sub>≤</sub> 4K : 150mW T=20K : 200mW
5	Medium-to-low resolution spectrometer	Multichannel grating spectrometers	200 - 35 $\mu$ m	150Kg	2-4K	T < 4K : 100mW T=20K : 300mW
6	Heterodyne array	SIS array	?	200Kg	2-20K	T <sub>≤</sub> 4K : 350mW T=20K : 1,000mW
7	Far-infrared camera	Photoconductor arrays, broadband filters, interference filters	200 - 30 $\mu$ m (5 - 1 $\mu$ m) <sup>a</sup>	150Kg	4-20K	T=20K : 300mW
8	Submillimeter camera	Bolometer arrays, broadband filters, interference filters FTS?	1 mm - 100 $\mu$ m	200Kg	0.3-20K	T < 4K : ? T ≈ 0.3K : ? (Local ADR) T=20K : 200mW

MASS TOTALS

- INSTRUMENT TOTAL 1,480 Kg
- GENERIC ELECTRONICS 300 Kg  
(INCLUDING COMPUTERS)
- MECHANICAL COOLER 400 Kg

ELECTRICAL POWER

- INSTRUMENTS TOTAL ≈ 0.5 KW

\*LDR SCIENCE COORDINATION GROUP, FOCAL PLANE INSTRUMENTS SUBCOMMITTEE REPORT, 26 JUNE 1984

LDR SCIENCE INSTRUMENTS SUMMARY\*  
Figure 2.3-1



The implications of the requirements were assessed with respect to their impact on LDR system concepts. A discussion summarizing the more significant effects is presented in Volume II, Section 1.2.

Results of the review were documented in an "LDR System Numerical Summary", an internal technical guide created for the use of personnel participating in the study. This document provided information on the Scientific Instruments, candidate LDR systems concepts, flowdown functional requirements, the study task interrelationships and interaction summaries, and an extensive LDR bibliography.

Parameters	Requirements
Diameter	20 m primary, 1 m secondary
Field of view	$\geq 3$ arcmin
F/Ratio <sup>b</sup>	System F/10, primary F/0.5
Shortest wavelength of diffraction-limited performance	30-50 $\mu\text{m}$ (aperture efficiency $> 30\%$ at 30 $\mu\text{m}$ )
Light bucket blur circle <sup>a</sup>	2.0 arcsec (at 1-4 $\mu\text{m}$ )
Optics temperature	Primary $\leq 200\text{K}$ ( $\pm 1\text{K}$ uniformity), secondary $\leq 125\text{K}$ ( $\pm 1\text{K}$ uniformity)
Emissivity (system)	0.05
Absolute pointing	0.05 arcsec
Jitter	0.02 arcsec - within 1 min after slew
Slew	20 - 50 $^\circ$ /min
Scan	1 $^\circ$ x 1 $^\circ$ - linear scan at 1 $^\circ$ /min
Track	0.2 $^\circ$ /hr (for comets $\geq 25^\circ$ from Sun)
Chopping <sup>b</sup>	Yes, 2 Hz, 1 arcmin (reactionless)
Sidelobes	Low near sidelobes
Other	Limited cross polarization
Sky exclusion	60 $^\circ$ -90 $^\circ$ from Sun, $\geq 45^\circ$ from Earth
Cryo system	Various temperatures in the range 0.1 K to 50K, 1.5 kW total power required
Lifetime	$> 10$ yr, approximately 3 yr revisit

<sup>a</sup> The tolerances (e.g., rms surface accuracy) needed to achieve a value of 2 arcsec for the light bucket mode are more severe than the tolerances associated with a diffraction limit of 50  $\mu\text{m}$ . This requirement will be studied further.

<sup>b</sup> Approximate. SELECTED LDR SYSTEM PARAMETERS AND PERFORMANCE REQUIREMENTS  
Figure 2.4-1

## 2.5 SCIENTIFIC INSTRUMENTS CONSIDERATIONS

MDAC and FSC conducted surveys of LDR instrumentation in the first month of the study. The object was to review support requirements for the variety of instruments which could utilize the LDR focal plane and represent a broad spectrum of instrument types. The scope of the effort was limited to sampling typical instruments in four generic categories in order to characterize the support requirements. The categories were far infrared imagers, far infrared spectrometers, submillimeter imagers, and submillimeter spectrometers. Potential instruments in these categories are shown in Figure 2.5-1.

Function \ Wavelength Band	FIR (30-200 $\mu\text{m}$ )	SMM (200-3000 $\mu\text{m}$ )
Imaging	<ul style="list-style-type: none"> <li>■ Photoconductor Array Cameras</li> <li>■ Imaging Fabry-Perot</li> </ul>	<ul style="list-style-type: none"> <li>■ Bolometer Array Camera</li> <li>■ Heterodyne Array Radiometer</li> </ul>
Spectrometry	<ul style="list-style-type: none"> <li>■ Photoconductive Mixer Heterodyne</li> <li>■ Fabry-Perot</li> <li>■ Grating</li> </ul>	<ul style="list-style-type: none"> <li>■ Schottky Mixed Het</li> <li>■ SIS Mixer Het</li> </ul>

- Instrumental Differences in  $\lambda$  Coverage and Resolution
- Technology Limits May Prevent Complete  $\lambda$  Coverage at All Resolution Categories in Near Term

GENERIC INSTRUMENT CATEGORIES  
Figure 2.5-1

In this effort, the instruments were presumed to be modular assemblies, having a common folding mirror and on-axis tracker, in accordance with the focal plane configuration concept briefed by the Science Coordination Group at the study kick-off meeting in May 1984.

In the survey, selected astronomers and scientists were contacted by MDAC (on the West Coast) and by FSC (on the East Coast). Consultants who were interviewed or asked to complete written survey requests from each company were:

MDAC

T. Phillips      California Institute of Technology

R. Green        Naval Research Laboratory

FSC

D. Buhl         NASA Goddard Space Flight Center  
(Submillimeter Heterodyne Receiver)

H. Mosely       NASA Goddard Space Flight Center  
(Long Wavelength Survey Spectrometer)

V. Kunde        NASA Goddard Space Flight Center  
(Survey Fourier Transform Spectrometer)

FSC (Cont'd)

- D. Gezari            NASA Goddard Space Flight Center  
                          (Array Camera for Photometric Imaging)
- P. Schwarz            Naval Research Laboratory  
                          (Imaging Far IR Spectrometer)
- D. Harper            Yerkes Observatory  
                          (Bolometer Array)

The summary data were recorded on standardized formats. A summary of the instrument support requirements deduced from survey data is shown in Figure 2.5-2.

Req't Type	Thermal Interface Temp; Load	Mechanical		Electrical Power (W)	Data
		Height (M)	Weight (kg)		
<b>FIR Imager</b>	4° K; 100mW 20° K; 300mW	1.2	250-350	100	16 Bit A/D G.P. Computer 1 kbps Output
<b>SMM Imager</b>	0.1° K; ? 4° K; 100mW 20° K; 200mW	1.2	250-350	100	16 Bit A/D G.P. Computer <1 kbps Output
<b>FIR Spectrometer</b>	4° K; 150mW 20° K; 200mW	2.0	300-400	150	16 Bit A/D, G.P. Computer
<b>SMM Spectrometer</b>	4° K; 50mW 20° K; 300mW	2.0	250-350	300	4000 Channel Analyser, G.P. Computer, 20 Kbps Output

SUMMARY OF GENERIC INSTRUMENT SUPPORT REQUIREMENTS  
Figure 2.5-2

Some findings from the survey, terminated in late May 1984, were:

- Carbon dioxide pumped far infrared laser technology has considerable development risk for LDR use. Issues include complexity (numerous actuators, controls, and adjustments) and lifetime (cross-contamination of laser gasses).
- High local oscillator power is needed for Schottky-diode mixers. The potential application of the featron (field emitter array triode oscillator) and other devices should be investigated.

- The focal plane should be placed near the instrument window.
- Instrument produced data streams require signal processing prior to relay to the ground. Trade studies will be required to optimize instrument/LDR spacecraft subsystem performance.
- Instruments are relatively large (6 to 8m<sup>3</sup>, 250-400 Kg) and complex and extremely sensitive to mechanical, thermal, and radiation disturbances.
- Cryogen supply interface demands are severe. Transfer and resupply of superfluid Helium in the LDR space environment will require technology development.
- Instrument changeout and on-board servicing approaches can affect the overall efficiency of the LDR mission and scientific achievements.

Two oscillator concepts considered by MDAC as potentially beneficial to LDR Science Instruments are the earlier-mentioned featron and the optical parametric oscillator.

The featron concept is suggested as a candidate local oscillator for LDR submillimeter spectrometer application. Its features are depicted in Figure 2.5-3. Figure 2.5-4 is a schematic representation of the featron.

The optical parametric oscillator is a potential replacement for the far infrared laser as the local oscillator. Its main features are depicted in Figure 2.5-5.

■ **Field Emitter Array Triode Oscillator**

- **Microelectronic Vacuum Device**
- **Cathode: Array of Micro-Field Emitters**
- **Gate and Anode Vacuum Deposited Films**
- **No Transit Time Limit at 1000 GHz (0.3 mm)**
- **Cathode-Gate Arrays of 5000 Emitters Produced for TWTAs**
- **High Power Capability (Watts), Low Voltage**

■ **Development Milestones**

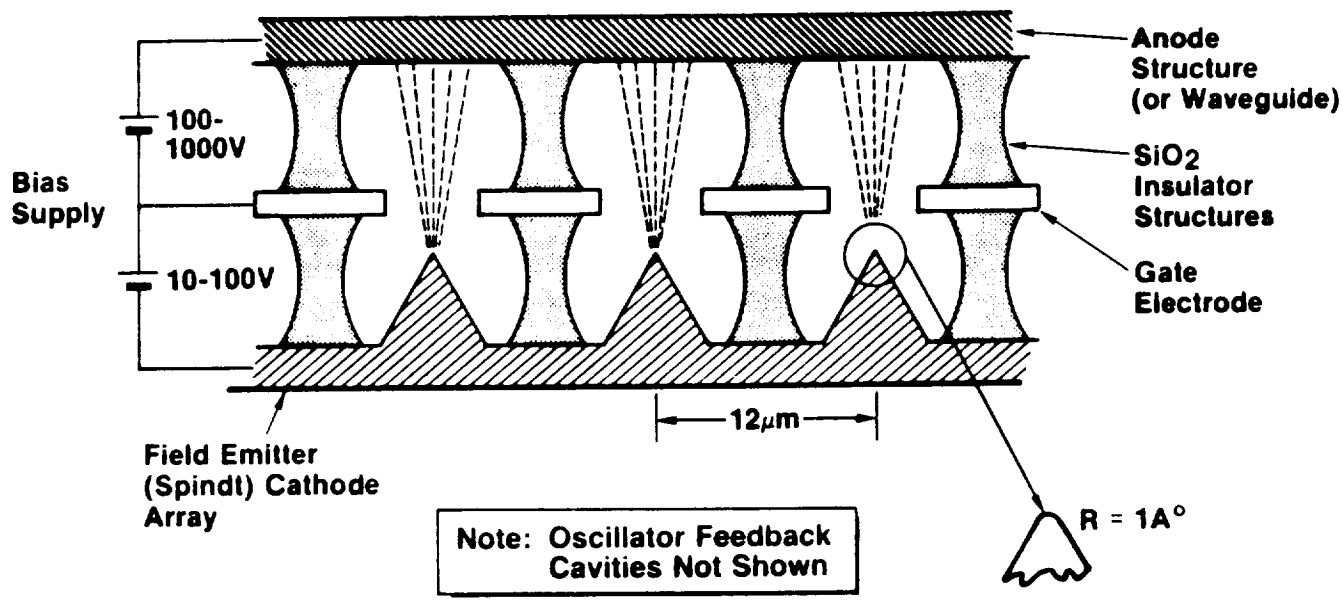
- **Oscillator Design (University of Utah)**
- **Field Emission Cathode Optimization (SRI)**
- **Prototype Production(SRI — Star Microwave)**

■ **General Utility**

- **Reliable EHF Communications Amplifiers (USAF, NASA)**
- **MM, Sub-MM Wave Amplifiers**

FEATRON LOCAL OSCILLATOR FEATURES  
Figure 2.5-3

A flow plan (Figure 2.5-6) to develop and qualify LDR instruments was created by MDAC for submillimeter imagers and spectrometers and far infrared spectrometers.

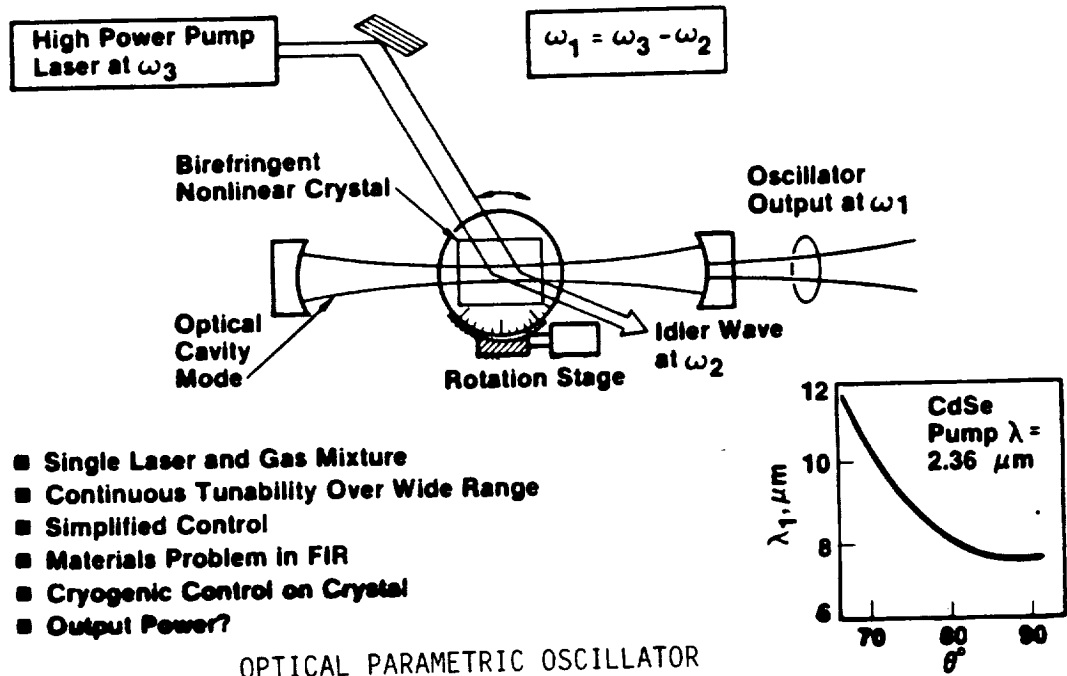


FIELD EFFECT OSCILLATOR (FEATRON) CONCEPT  
Figure 2.5-4

The results of this task were useful in aiding to identify and appreciate instrument interactions within the study of LDR system concepts. However, the definition and development planning for the specific science instruments is being addressed apart from this study by NASA's Science Coordination Group. As indicated in Paragraph 2.3.1, the draft of the report of the Focal Plane Instruments Subcommittee, dated 26 June 1984 was integrated into the baseline interface requirements for the study.

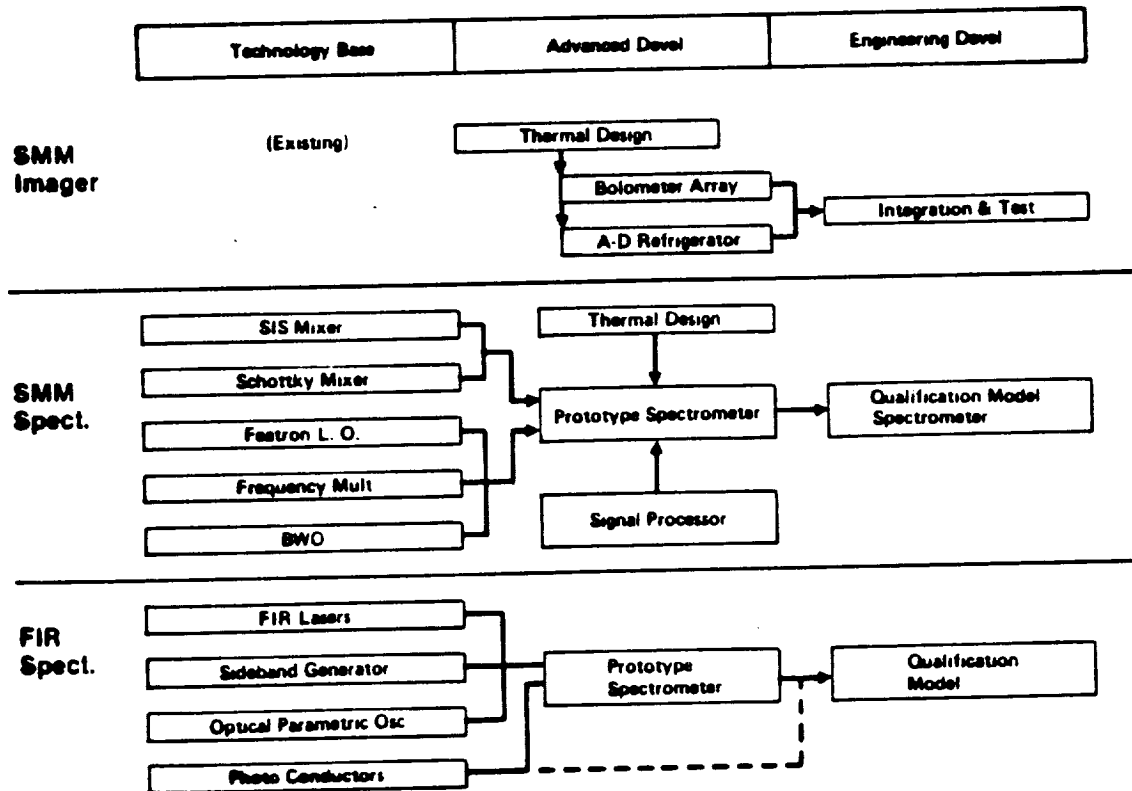
The importance to LDR of the generic cooler for the instruments cannot be understated. Technology issues with respect to the extreme cryogenic cooling needs of LDR were pursued in the Thermal Considerations Task, discussed in Section 3.6.

■ Potential Replacement for FIR Laser as Local Oscillator



- Single Laser and Gas Mixture
- Continuous Tunability Over Wide Range
- Simplified Control
- Materials Problem in FIR
- Cryogenic Control on Crystal
- Output Power?

OPTICAL PARAMETRIC OSCILLATOR  
Figure 2.5-5



CRITICAL LDR INSTRUMENT DEVELOPMENT PLAN  
Figure 2.5-6

### 3.0 SYSTEM ANALYSIS AND TRADES

#### 3.1 OPTICAL CONFIGURATION TRADE

##### 3.1.1 Task

Although considerable progress has been made in the Ames/JPL studies carried out to date, it became clear at the first Asilomar meeting that due to hardware constraints (weight and packaging limitations) further optical configuration definition was required. The purpose of this task was to trade off several candidate configurations.

##### 3.1.2 Approach

Summarized in Table 3.1-1 are the candidate optical systems which were evaluated in this study.

TABLE 3.1-1  
CANDIDATE OPTICAL CONFIGURATIONS

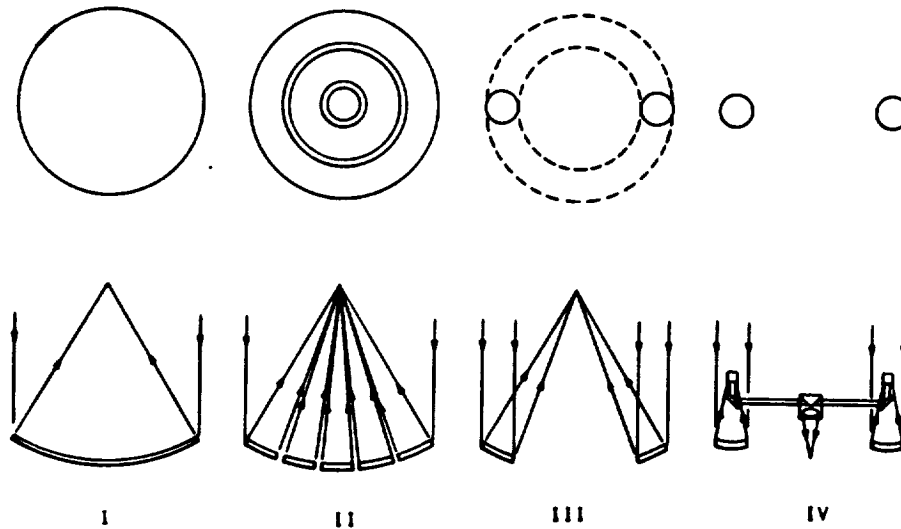
- |  |
|--|
| <ul style="list-style-type: none"><li>● CASSEGRAIN TELESCOPE</li><li>● TRADITIONAL (CIRCULAR APERTURE)</li><li>● RADIALLY DEGRADED PERFORMANCE</li><li>● SLOT (ELONGATED APERTURE)</li><li>● OFF-AXIS VERSION</li><li>● SPHERICAL PRIMARY MIRROR TELESCOPE</li></ul> |
|--|

Also reviewed in this study was an unfilled aperture option. In theory, the light gathering capability is directly proportional to the square of the entrance pupil diameters and the resolution is inversely proportional to the entrance pupil diameter. Therefore, in this option (Figure 3.1-1) the unfilled aperture is utilized to obtain a larger diameter for resolution purposes. Simultaneously it will have less collecting area for light gathering.

##### 3.1.3 Discussion

Candidate configurations included the traditional Cassegrain telescope, the radially degraded Cassegrain telescope which extends the aperture for observations in the submillimeter wavelength region, the slot Cassegrain telescope which allows for an elongated aperture in the Shuttle Orbiter bay, the off-axis Cassegrain which minimizes obscuration, and a telescope with a spherical primary mirror which transfers the complexity factor to the secondary mirror.

In a single mirror telescope, the degrees of freedom available are the radius and conic shape of the mirror. The parabolic mirror has been the mainstay of astronomy ever since the telescope was invented, because the paraboloid is the only conic shape capable of rendering a perfect image definition "on-axis" for an object at infinity;



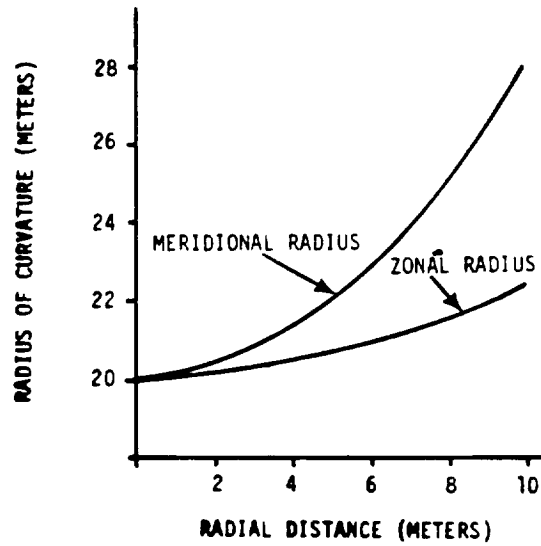
FILLED VERSUS UNFILLED APERTURES (STELLAR INTERFEROMETERS)  
Figure 3.1-1

however, there are not enough degrees of freedom to give any reasonable field of view since there is only one mirror. With only one mirror, the configuration will also be relatively long for a large focal length. Adding a secondary mirror increases the degrees of freedom and the potential for wider fields of view. Astronomical telescopes have evolved from the single mirror parabolic telescope to the two-mirror Cassegrain telescope in which a convex hyperbolic secondary mirror is used with a concave parabolic primary mirror. The true Cassegrain telescope theoretically is corrected for only spherical aberration and is limited by coma.

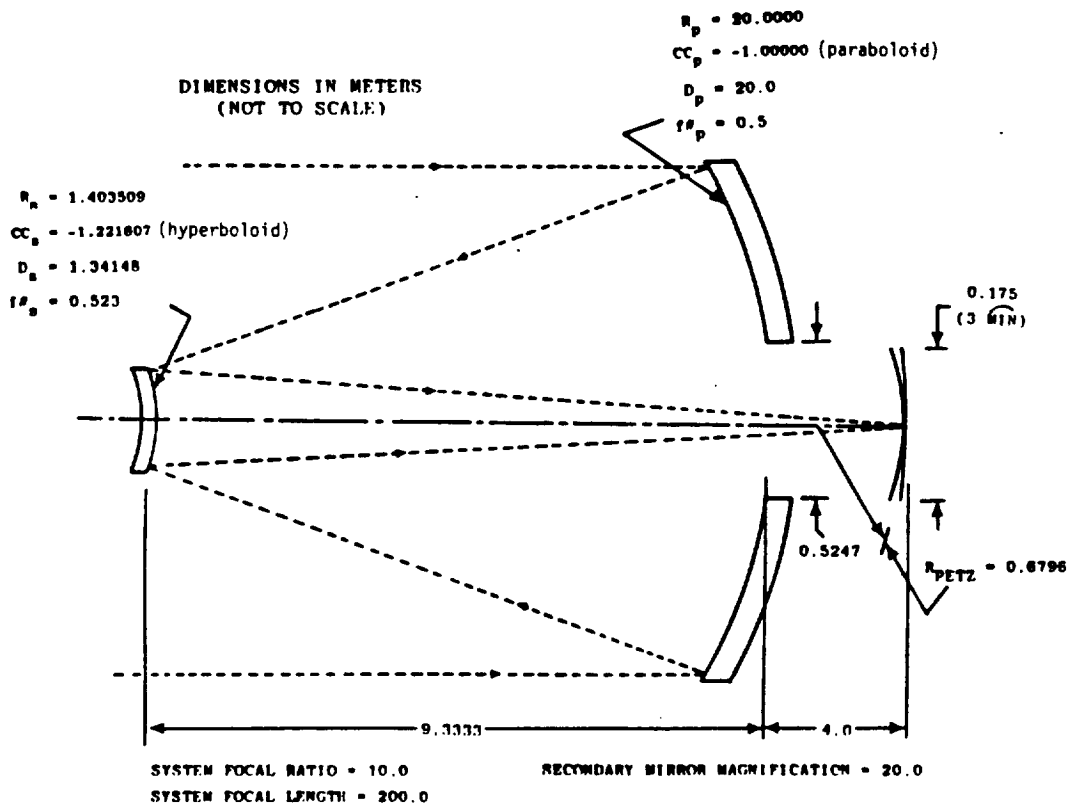
Shown in Figure 3.1-2 are the zonal and meridional radii for an  $f/0.5$  parabolic mirror of a 20-meter diameter Cassegrain telescope. It is the difference in the zonal and meridional radii at any point on the mirror that determines how well a grinding or polishing tool matches the desired asphere. It must be emphasized that this large difference in radii provides a major technical challenge. In comparison, an  $f/0.8$  parabolic mirror of 60-inch diameter was fabricated at Kodak (state-of-the-art in fast aspheres). Alternate telescope designs with a spherical primary mirror were investigated in this study. Obviously a large mirror with a spherical radius (i.e., vertex radius of curvature, zonal radius of curvature and meridional radius of curvature are one and the same) would greatly minimize the manufacturing (fabrication and assembly) complexity and make active radius control an attractive alternative.

**3.1.3.1 On-Axis Cassegrain Telescope (Circular Aperture)** - Shown in Figure 3.1-3 is an optical configuration for a "rotationally symmetric" Cassegrain telescope. The secondary mirror, approximately 9.3 meters from the primary mirror magnifies the primary mirror focal ratio of 0.5 into a system focal ratio of 10. The field of view as specified is 3 arcminutes. Shown in Figure 3.1-4 are two options for locating the scientific instrument entrance apertures onto the focal surface as presented by the optics. The first option is a shared field approach. This arrangement is currently being used on Space Telescope with five scientific instruments. In this approach two or more scientific instruments can be used simultaneously (serpentina mode). In the second option a center folding mirror is indexed to one of the scientific instruments. Only one scientific instrument can be used at a time in this approach.

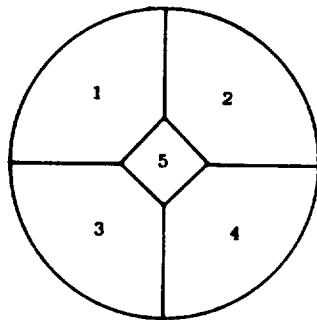




ZONAL AND MERIDIONAL RADII FOR AN f/0.5 LDR MIRROR  
Figure 3.1-2

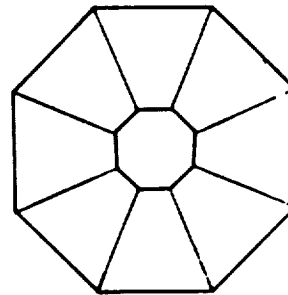


LDR OPTICAL CONFIGURATION (ON-AXIS "TRUE" CASSEGRAIN TELESCOPE)  
Figure 3.1-3



SHARED FIELD

- SIMILAR TO ST ARRANGEMENT
- 4 AXIAL SI'S
- 1 RADIAL SI
- SIMULTANEOUS OPERATION IN "SERENDIPITY" MODE



INDIVIDUAL FIELD

- INDEX CENTERFOLD MIRROR
- 8 RADIAL SI'S
- OPERATION ONE AT A TIME

#### SI INTERFACE WITH FOCAL PLANE

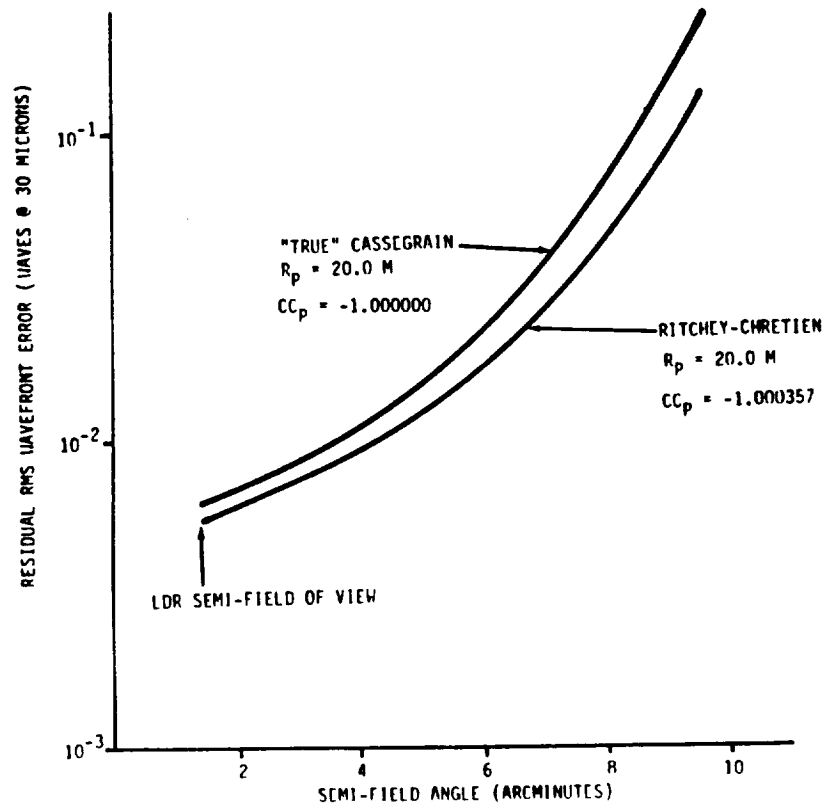
Figure 3.1-4

In order to implement the shared field option a wide field of view will be required. The Space Telescope utilizes a Ritchey-Chretien version of the Cassegrain telescope. It consists of hyperbolic primary and secondary mirrors. (Note: The "true" Cassegrain utilizes a parabolic primary mirror and a hyperbolic secondary mirror.) The conic shapes are chosen to simultaneously correct spherical aberration and coma. The aberrations of astigmatism, field curvature, and distortion are present off-axis in predictable amounts. Shown in Figure 3.1-5 is a comparison of a "true" Cassegrain with a Ritchey-Chretien Cassegrain. For the field of view of 3 arcminutes and utilizing a fold mirror, the "true" Cassegrain with its parabolic mirror is sufficient to meet the requirements.

A smaller Cassegrain telescope is dictated for a single shuttle launch. The optical configuration for this concept is shown in Figure 3.1-6.

In the "rotationally symmetric" Cassegrain the secondary mirror can be designed to be on the order of 1 meter in diameter. This minimizes the central obstruction (necessary from image quality and background noise standpoints). However, the strut obstruction is not optimum. The scientific instruments are, however, symmetrically located around the center line and the optical design is compact. Both these features imply "good" pointing control capability. The "true" Cassegrain was retained in the system concepts for these reasons.

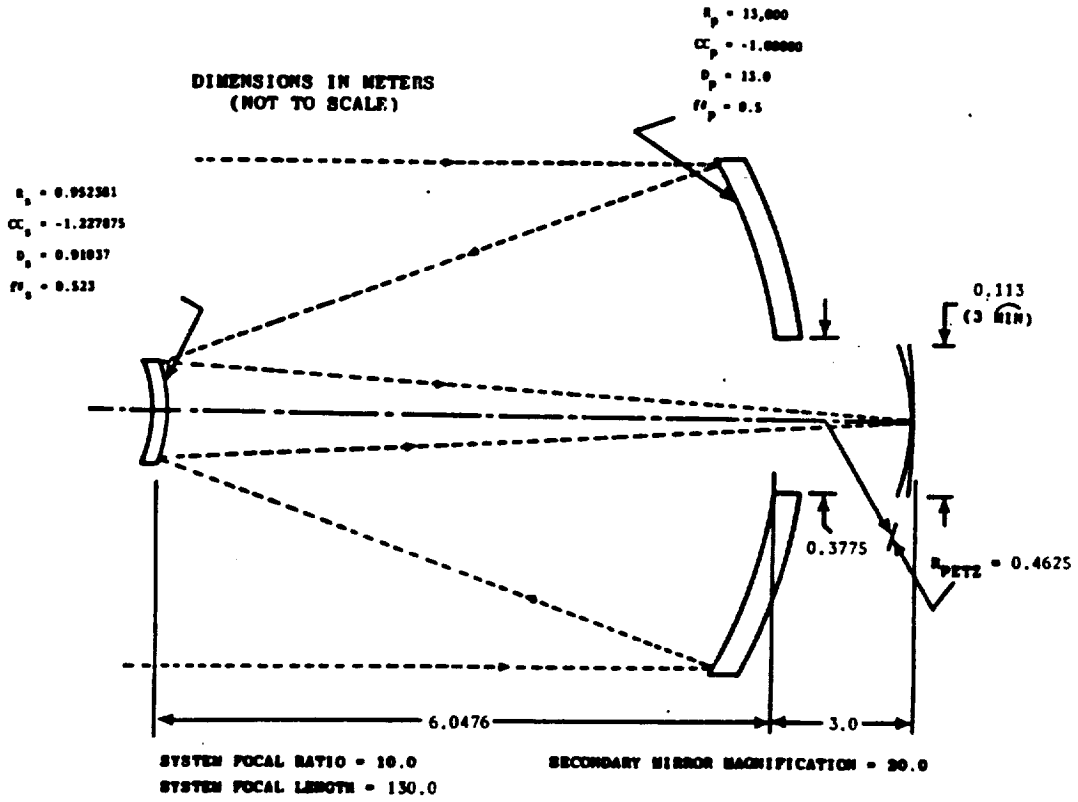
**3.1.3.2 Off-Axis Cassegrain** - Shown in Figure 3.1.7 is an off-axis Cassegrain telescope. In the version chosen here the off-axis primary mirror is a "cut" of a much larger rotationally symmetric primary mirror. The secondary mirror to primary mirror spacing is twice as long as the on-axis Cassegrain. Therefore, static metering and dynamic damping will be more difficult. The central obstruction is minimized. This implies improved performance (S/N; image quality). The scientific



COMPARISON OF A "TRUE" CASSEGRAIN  
 WITH A RITCHEY-CHRETIEN CASSEGRAIN

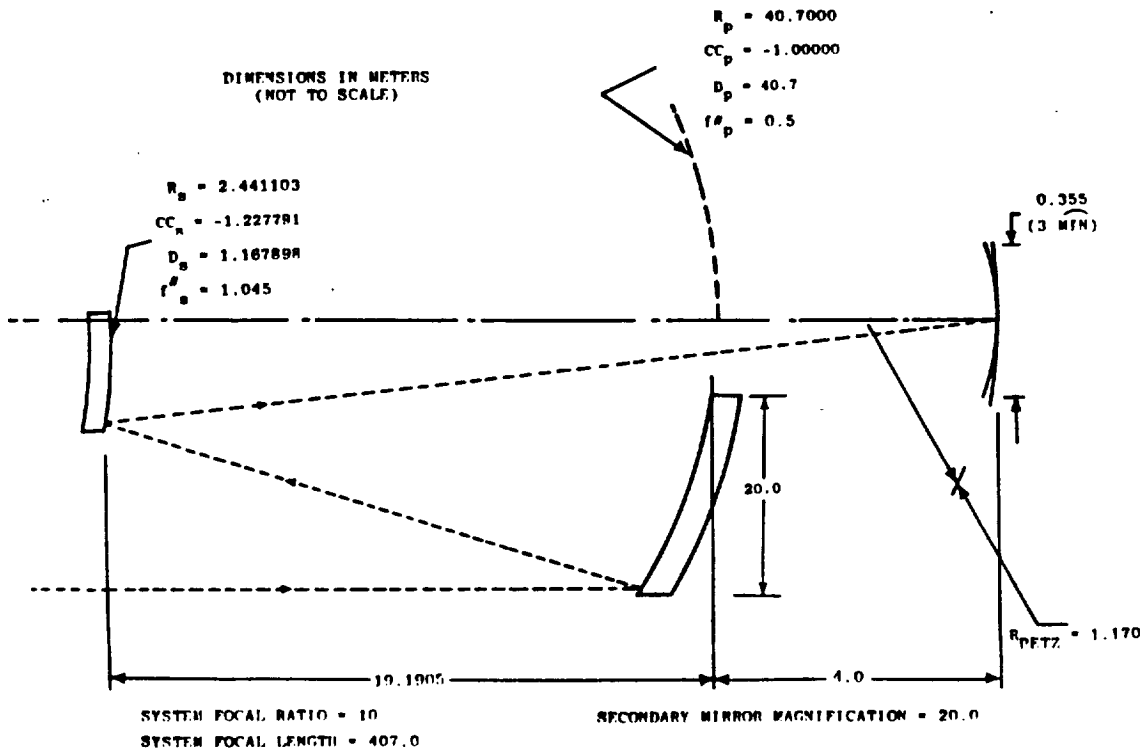
Figure 3.1-5

(On-axis "True" Cassegrain Telescope)



SINGLE SHUTTLE WITH ACC OPTICAL CONFIGURATION

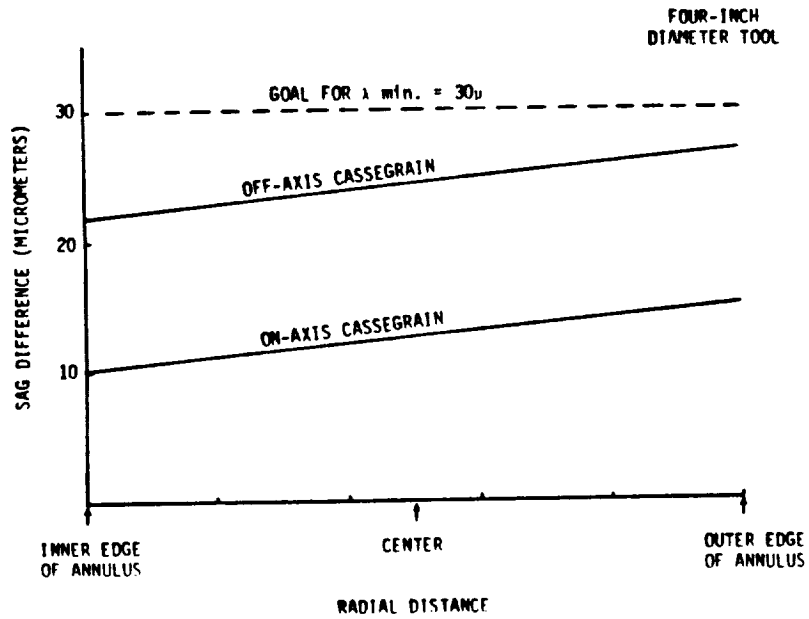
Figure 3.1-6



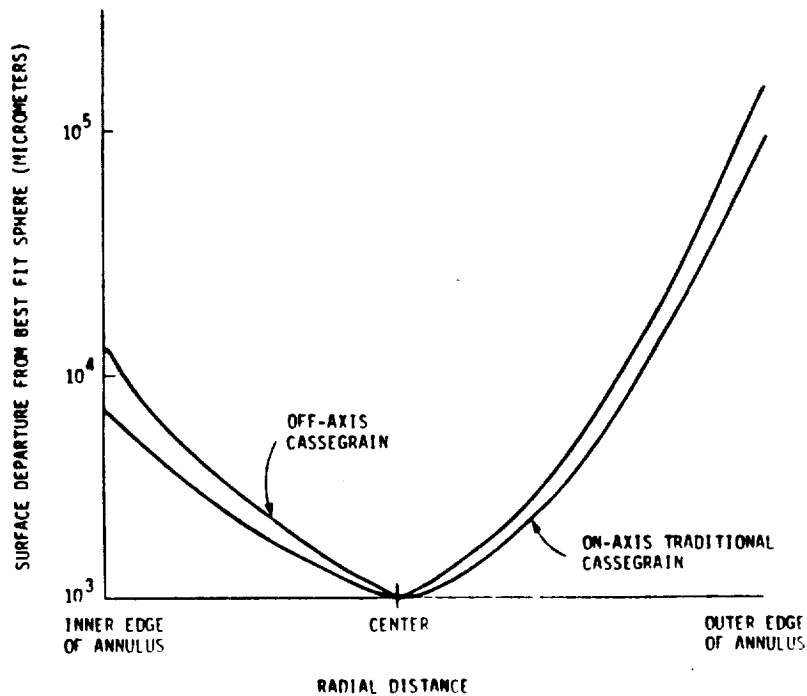
LDR OPTICAL CONFIGURATION  
(OFF-AXIS "TRUE" CASSEGRAIN TELESCOPE)  
Figure 3.1-7

instruments are not symmetrically located around the center line. This implies pointing control could be more difficult. The edge segments of the primary mirror for the off-axis telescope will be more difficult to manufacture. The conventional aspheric generation approach uses loose abrasive grinding. Progression of the polishing task using spherical tools is at the point when the surface is within approximately 1 micrometer of the desired asphere. In the polishing step, the sag difference between the orthogonal radii extremes (zonal and meridional) determines the amount that a spherical polishing tool will "rock" if it fits the shorter of the two radii. The larger the tool diameter, the more the tool will obviously rock. Figure 3.1-8 shows the approximate sag difference for the on-axis and off-axis parabolic mirrors. This value should be less than 1 wave based on current processing approaches. An additional metrology figure of merit is the aspheric departure with respect to the best fit sphere (Figure 3.1-9). The aspheric departure goal is 1000 micrometers. For the outer annulus of the on-axis paraboloid this value is 9,500 micrometers. For the outer annulus of the off-axis paraboloid this value is 15,400 micrometers. For the above reasons the on-axis Cassegrain is preferred over the off-axis Cassegrain.

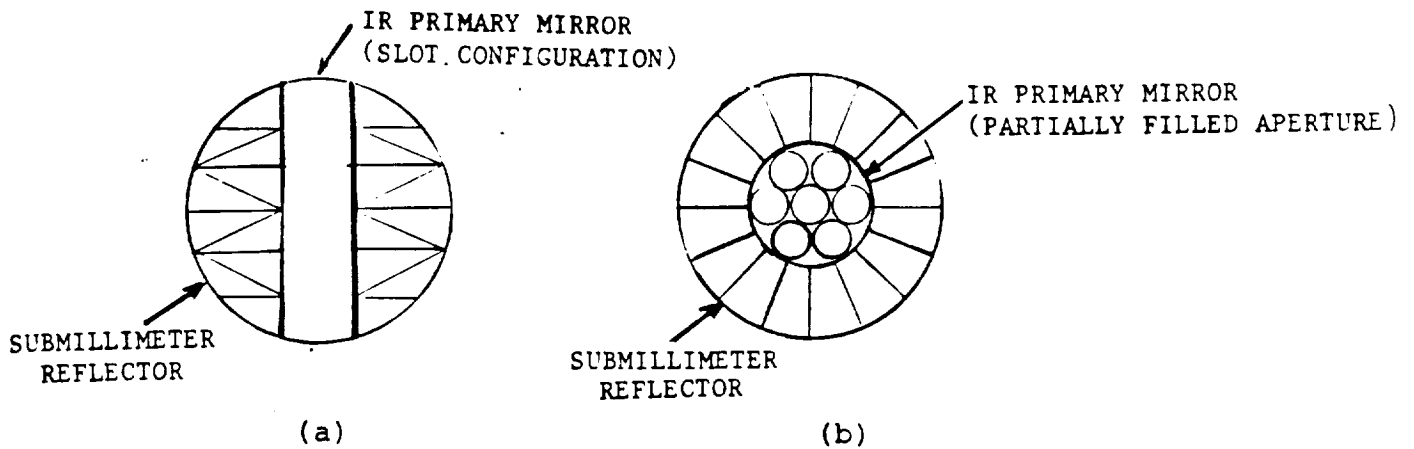
**3.1.3.3 Radially Degraded Cassegrain** - The radially degraded concept takes into account the structural and performance differences imposed by the two distinct wavelength regions. Shown in Figure 3.1-10 are two (of many) radially degraded concepts. In both concepts shown, the outer annulus is optimized for the submillimeter and potentially, since the tolerances are loose, this region might be



SAG DIFFERENCE BETWEEN ZONAL AND MERIDIONAL RADII  
ACROSS TOOL DIAMETER FOR F/0.5 MIRROR  
Figure 3.1-8



ASPHERIC DEPARTURE OF OUTER ANNULUS  
WITH RESPECT TO BEST FIT SPHERE  
Figure 3.1-9



### RADIALLY DEGRADED MIRROR CONCEPTS

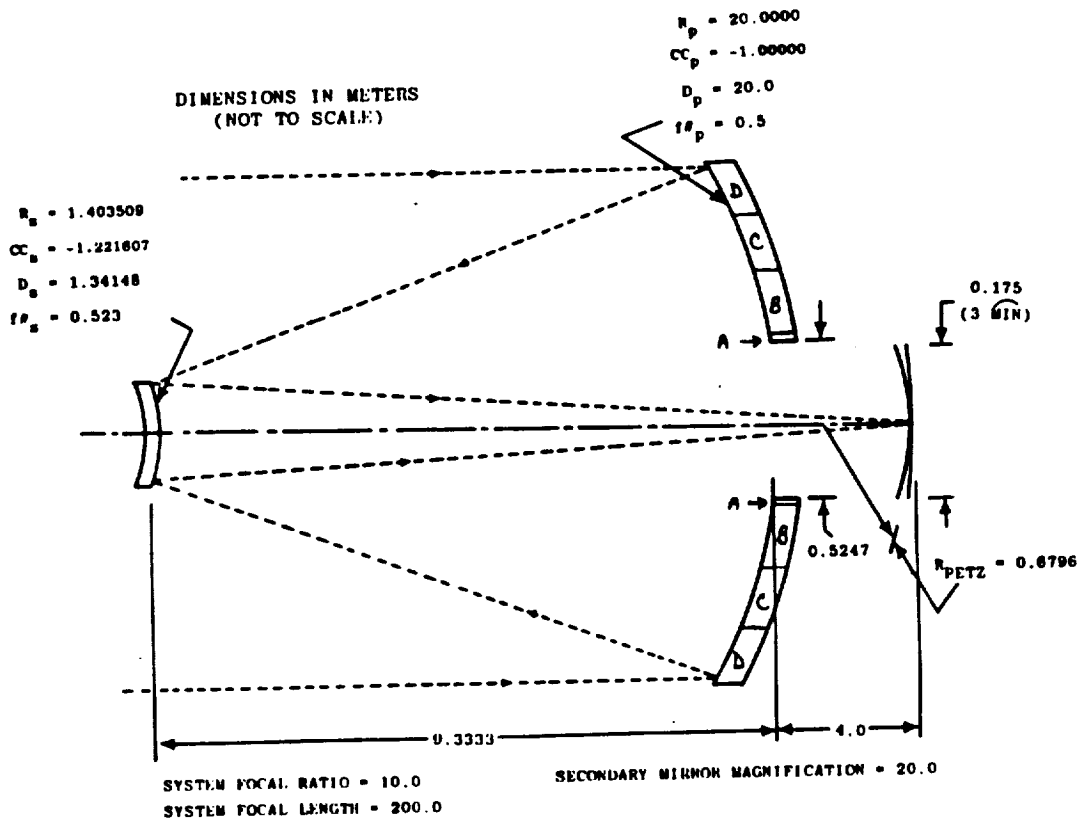
Figure 3.1-10

assembled in space after deployment of the inner zone. It is the inner zone which requires the tighter tolerances and therefore, would benefit from a more traditional ground assembly and verification approach. In concept (a) the inner zone is the slot configuration which could fill the Shuttle bay. In concept (b) the inner zone is shown with partially filled circular apertures.

Shown in Figure 3.1-11 is an optical configuration for the radially degraded concept. The segmented mirror is "laid out" as three annuli about a central mirror. The segments are trapezoidal (Figure 3.1-12). A performance summary is shown in Table 3.1-2. The center mirror with inner annulus ( $D = 9.4$  meters) would operate at wavelengths as low as 50 micrometers. In the mirror region including the center annulus ( $D = 14.8$  meters), the minimum operational wavelength would be 70 micrometers. Using the total mirror ( $D = 20$  meters) the minimum operational wavelength would be 100 micrometers. Therefore, in order to see benefits in material selection and in manufacturing/assembly tolerances the minimum operational wavelength requirement must be relieved to greater than 30 micrometers. It should be noted that the surface roughness required in the polishing step is the same for all segments since the specularity value is set by the light bucket mode at a minimum operational wavelength of 1 micrometer.

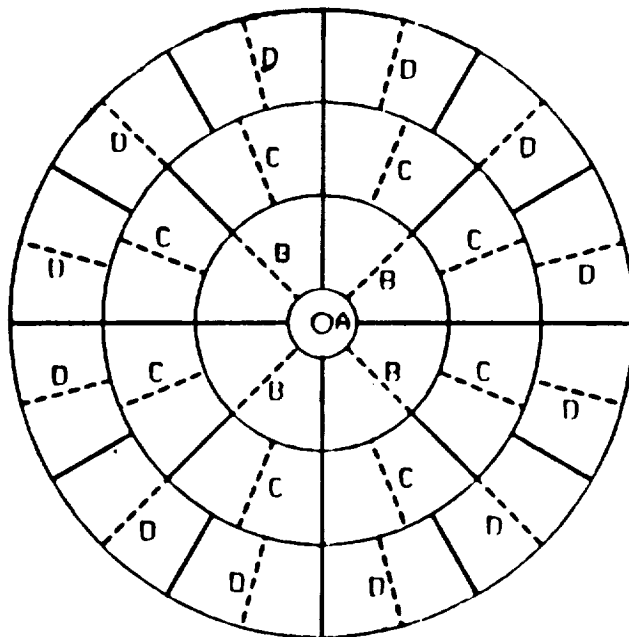
A two annuli radially degraded concept is shown in Figure 3.1-13. The center core with the first annulus is stowed in the Orbiter bay and deployed (i.e., the resultant five meter diameter mirror represents the high quality section). The outer annuli segments are stowed in the ACC and assembled with EVA assistance.

**3.1.3.4 Slot Cassegrain** - Shown in Figure 3.1-14 is a concept for folding a Cassegrain telescope in the Orbiter bay. This concept takes into account that the Shuttle bay length is 18 meters and the Shuttle bay width is 4 meters. By folding the side mirrors with a "door hinge" by  $90^\circ$  in the bay a rectangular mirror with an approximate size of 18 meters by 12 meters could be deployed. In this concept the secondary mirror would be also deployed from a stowed position near the primary mirror. The slot configuration is simply the case without the outer two panels (Figure 3.1-15). This provides the potential that even though the primary mirror



RADIALLY DEGRADED CASSEGRAIN TELESCOPE

Figure 3.1-11



RADIALLY DEGRADED PRIMARY MIRROR

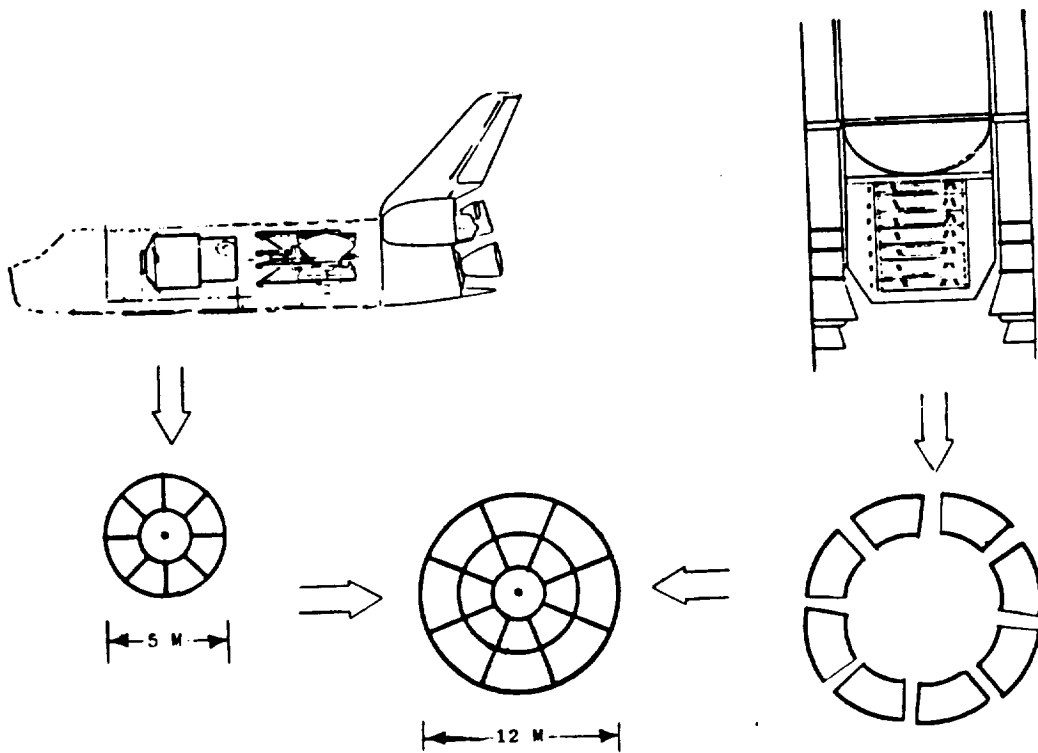
Figure 3.1-12



TABLE 3.1-2  
 RADIALLY DEGRADED TELESCOPE  
 PERFORMANCE SUMMARY

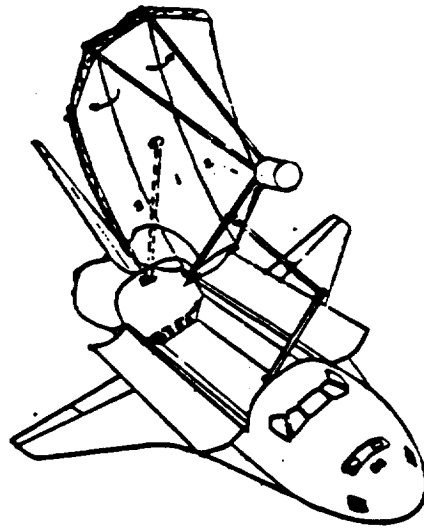
	DIA (M)	$\lambda$ @ $\theta$ ( $\mu$ M)	$\sigma$ ( $\text{\AA}$ )	$\omega$ ( $\mu$ M)	PM SEGMENT RMS SURFACE ERROR ( $\mu$ M)	PM SEGMENT PISTON ERROR ( $\mu$ M)	PM SEGMENT RADIUS MISMATCH (PPM)	SM DESPACED ERROR ( $\mu$ M)
● INNER ANNULUS (B)	9.4	50	250	5.6	1.0	2.0	50	33
● CENTER ANNULUS (C)	14.8	70	250	7.0	1.4	2.8	70	50
● OUTER ANNULUS (D)	20.0	100	250	11.0	2.0	4.0	100	65

\*Set by light bucket mode at  $\lambda = 1.0 \mu\text{M}$



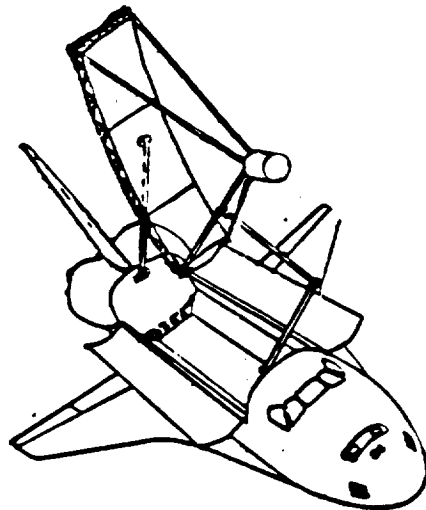
SINGLE SHUTTLE WITH ACC  
 (RADIALLY DEGRADED CONFIGURATION)

Figure 3.1-13



RECTANGULAR APERTURE CASSEGRAIN TELESCOPE

Figure 3.1-14



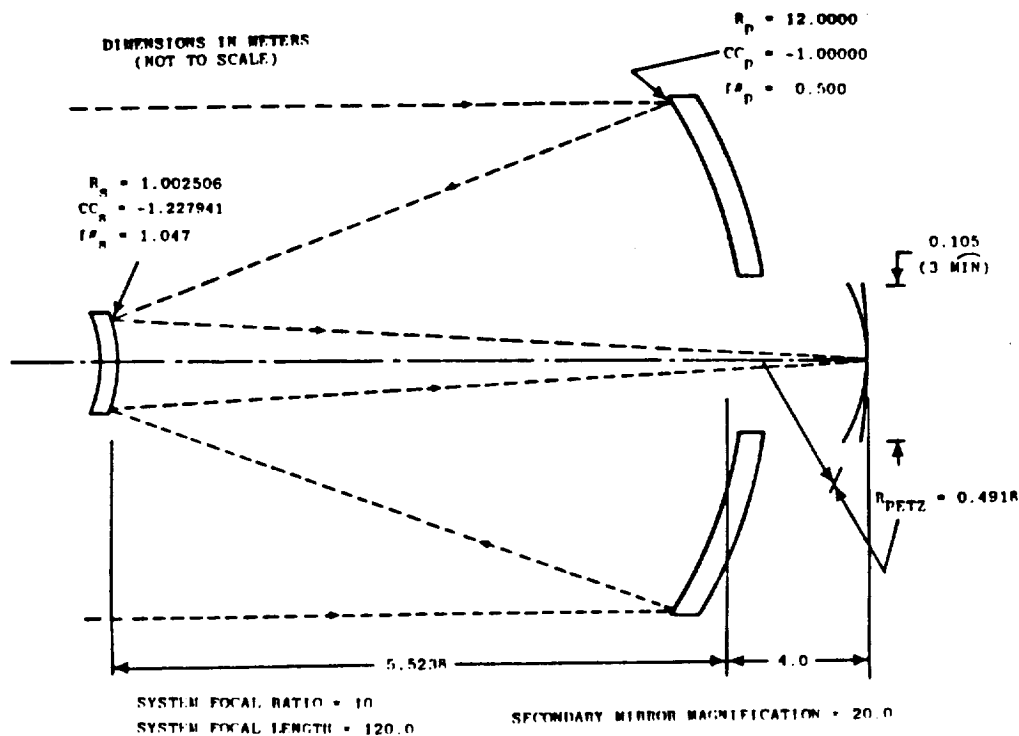
ELONGATED APERTURE (SLOT) CASSEGRAIN TELESCOPE

Figure 3.1-15

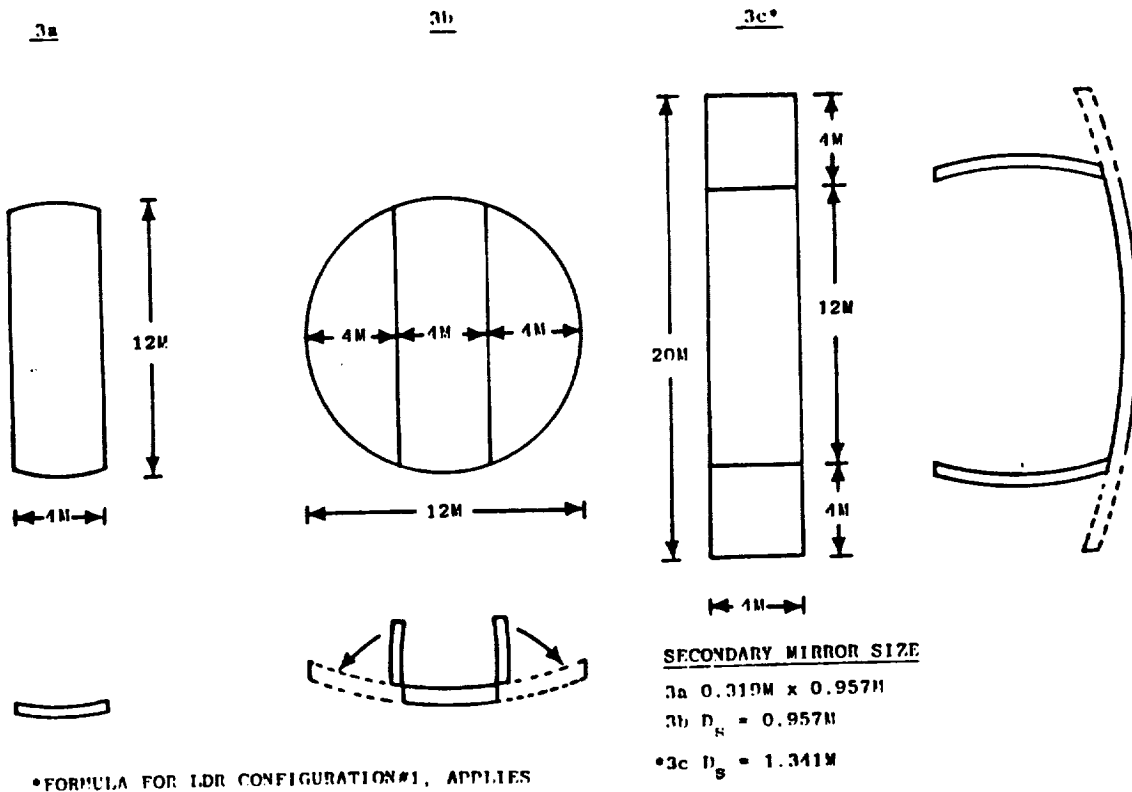
would be made up of segments, the total primary mirror could be assembled, tested, and its performance verified before launch.

Shown in Figure 3.1-16 is an optical configuration for the slot Cassegrain. Three options for the primary mirror are shown in Figure 3.1-17. The length of the primary mirror must be shorter than the Orbiter bay length to allow for stowage of other elements of the observatory and support equipment. Assuming these additional elements are launched separately, a longer slot could be deployed (approximately 20 meters x 4 meters) or a circular aperture could be deployed (approximately 12 meters x 12 meters). Shown in Figure 3.1-18 is a slot configuration using a single Shuttle with an ACC. The primary mirror segment assemblies are stowed in the ACC. Other elements of observatory would be stowed in the Orbiter bay. Total observatory weight limits the length to less than 28 meters for an equatorial orbit. Total observatory weight is not compatible with Shuttle launch capability for polar orbit.

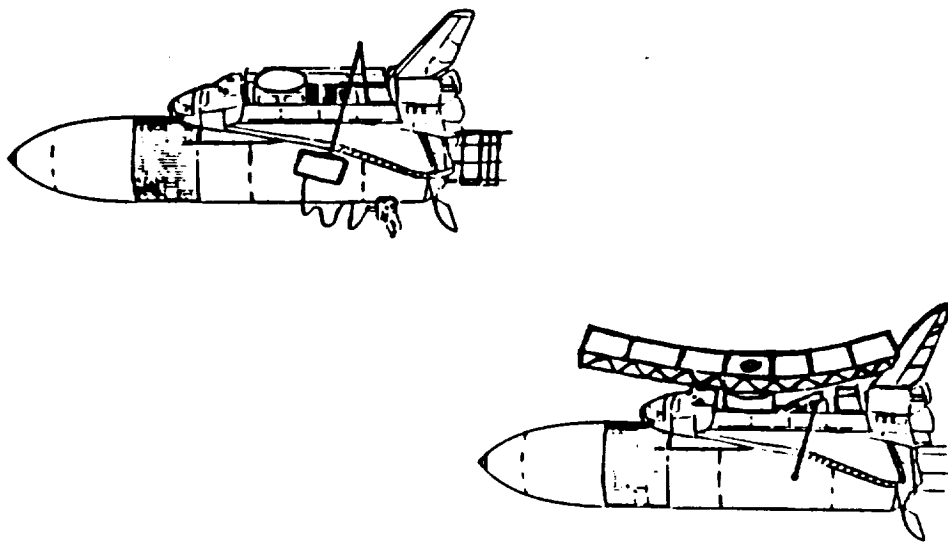
**3.1.3.5 Telescope with Spherical Primary Mirror** - A comparison of the features of a telescope with a spherical primary mirror against an aspherical primary mirror is given in Table 3.1-3. The major advantage is in transferring the hardware complexity from the large segmented primary mirror to the smaller monolithic secondary mirror.



LDR OPTICAL CONFIGURATION  
(SLOT CASSEGRAIN TELESCOPE)  
Figure 3.1-16



PRIMARY MIRROR FOR SLOT CONFIGURATION  
Figure 3.1-17



ERECTABLE SLOT CONFIGURATION  
(PRIMARY MIRROR SEGMENT ASSEMBLIES IN ACC)  
Figure 3.1-18

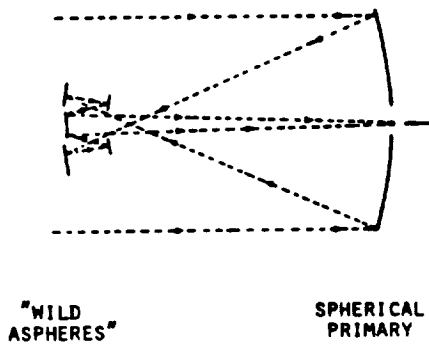
TABLE 3.1-3  
SPHERICAL VERSUS ASPHERICAL PRIMARY MIRROR

	<u>SPHERE</u>	<u>ASPHERE</u>
● RADIUS OF CURVATURE	THE RADIUS OF CURVATURE IS THE SAME FOR ANY SEGMENT	THE RADII OF CURVATURE ARE VARIABLES
● MIRROR MANUFACTURE	SIMPLE	COMPLEX
● TOOLING	SAME FOR ALL SEGMENTS	VARIES
● RAPID FABRICATION	SIMPLE ALTERNATIVES	COMPLEX ALTERNATIVES
● GROWTH POTENTIAL (LARGER DIAMETERS)	ADDING MORE SPHERICAL SEGMENTS DOES NOT INCREASE COMPLEXITY	MANUFACTURING COMPLEXITY INCREASES
● ACTIVE RADIUS CONTROL	RELATIVELY SIMPLE DUE TO SINGLE RADIUS OF CURVATURE	RELATIVELY COMPLEX DUE TO VARYING RADII OF CURVATURE

Shown in Figure 3.1-19 is an optical configuration with a spherical primary mirror. In this example, the secondary mirror assembly is composed of three mirror elements similar to a Gregorian configuration. An alternate spherical primary configuration is shown in Figure 3.1-20 (Reference 1). This configuration was evaluated by Rodgers, Table 3.1-4 (Reference 2). In Concept (a) and Concept (b) an aspheric surface with a 23rd degree power series on the secondary mirror still does not meet the performance requirements. The performance requirements are met, however, in Concept (c) and Concept (d) by the use of general aspheres on the secondary mirror and tertiary mirror. Alternate spherical primary mirror telescopes are shown in Figures 3.1-21 and 3.1-22 (References 3 and 4).

In all cases, the secondary mirror is large (on the order of 5 meters). Consequently, both image quality and background noise level will be compromised unless the secondary mirror elements are reduced to approximately 1 meter (Note: Not considered probable). Also, the goal in this study was to retain the secondary mirror at 125°K. The additional elements will also have to be cooled and their alignment maintained.

**3.1.3.6 Unfilled Aperture Option** - In this option an unfilled aperture is utilized to obtain a larger diameter for resolution purposes. Simultaneously, it will have less collecting area for light gathering. Shown in Table 3.1-5 is a comparison of two filled apertures and a 20 meter diameter unfilled aperture. The annulus has been sized with the same area as the 10 meter filled aperture. It was shown in the study (Concept 3) that a 10 meter category telescope could be launched with a single Shuttle/ACC. The mirrors for the filled aperture would be stowed in the ACC. Therefore, potentially a 20 meter diameter unfilled aperture telescope could be launched using a similar approach. Shown in Figure 3.1-23 is the effect of the large hole in the mirror on the performance (radial energy distribution). This drastic decrease will result in a major increase in the amplitude of the point spread function side lobes.

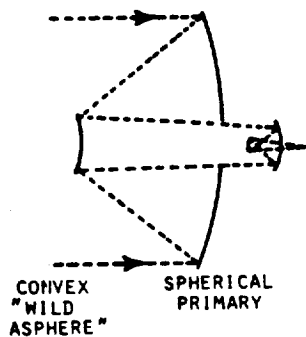


- $D_p = 20$  METERS
- PRIMARY MIRROR TO SECONDARY MIRROR SPACING = 25 METERS
- LINEAR OBSCURATION RATIO (SECONDARY MIRROR) = 0.28
- $D_s = 5.6$  METERS (CONCAVE)

●THESE FEATURES NEGATE ADVANTAGES OF THE SPHERICAL PRIMARY MIRROR FOR THIS CONFIGURATION

### SPHERICAL PRIMARY MIRROR TELESCOPE (WITH THREE MIRROR FIELD CORRECTOR)

Figure 3.1-19



- $D_p = 20$  METERS
- PRIMARY MIRROR TO SECONDARY MIRROR SPACING = 10 METERS
- LINEAR OBSCURATION RATIO (SECONDARY MIRROR) = 0.28
- $D_s = 5.6$  METERS (CONVEX)

●AFTER MEINEL, MEINEL, SU, AND WANG  
●●CONVEX SM IS VERY LARGE AND DIFFICULT TO MANUFACTURE

### SPHERICAL PRIMARY MIRROR TELESCOPE (MMSW)\* (TWO MIRROR CASSEGRAIN WITH TWO MIRROR GREGORIAN FIELD CORRECTOR)

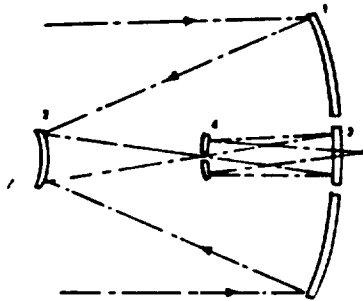
Figure 3.1-20

TABLE 3.1-4

SPHERICAL PRIMARY MIRROR TELESCOPE (MMSW)

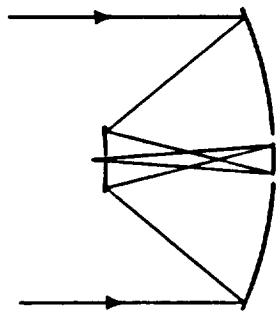
	CONCEPT (a)	CONCEPT (b)	CONCEPT (c)	CONCEPT (d)
● PRIMARY	SPHERE	SPHERE	SPHERE	SPHERE
● SECONDARY	GENERAL ASPHERE 23RD DEGREE POWER SERIES ON BASE SPHERE	GENERAL ASPHERE 23RD DEGREE POWER SERIES ON BASE SPHERE	GENERAL ASPHERE DIFFERENT CURVE FIT CONSISTING OF LOGARITHMS AND SECANTS	GENERAL ASPHERE DIFFERENT CURVE FIT CONSISTING OF POLYNOMIAL SERIES AND HYPERBOLIC COSINES
● TERTIARY	CONIC	GENERAL ASPHERE 23RD DEGREE POWER SERIES ON BASE SPHERE	GENERAL ASPHERE DIFFERENT CURVE FIT CONSISTING OF LOGARITHMS AND SECANTS	GENERAL ASPHERE DIFFERENT CURVE FIT CONSISTING OF POLYNOMIAL SERIES AND HYPERBOLIC COSINES
● QUATERNARY	CONIC	SPHERE	SPHERE	SPHERE



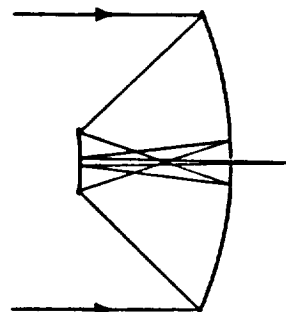


SPHERICAL PRIMARY MIRROR TELESCOPE

Figure 3.1-21



THREE MIRROR CONCEPT




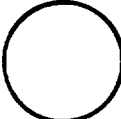
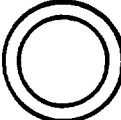
FOUR MIRROR CONCEPT

SPHERICAL PRIMARY MIRROR TELESCOPE

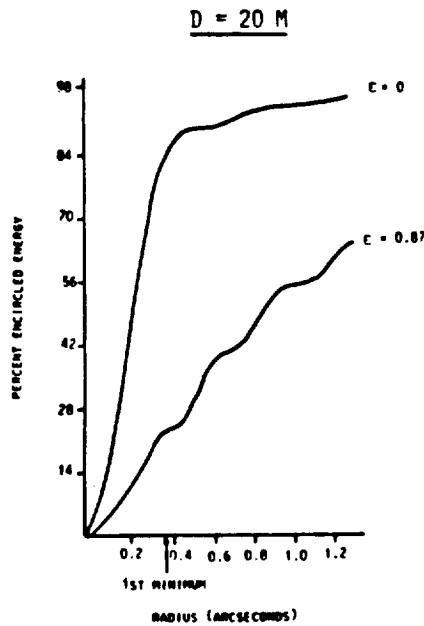
Figure 3.1-22



TABLE 3.1-5  
APERTURE SIZE COMPARISON

APERTURE TYPE/DIAMETER	APPROX. AREA	PERFORMANCE		
		LIMIT OF RESOLUTION (@ 30 μM)	LOW SIDELOBES	RELATIVE SENSITIVITY
 10-METER FILLED	78.5 m <sup>2</sup>	1.5 SEC	YES	1/4
 20-METER FILLED	314 m <sup>2</sup>	0.75 SEC	YES	1
 20-METER UNFILLED (ANNULUS WITH SAME AREA AS 10-METER FILLED)	78.5 m <sup>2</sup>	0.75 SEC	NO	1/4

( $\lambda_{min} = 30 \mu M$ )



UNFILLED APERTURE EFFECT ON ENCIRCLED ENERGY

Figure 3.1-23

### 3.1.4 Conclusions

All five candidate configurations have good and bad features. The traditional Cassegrain was selected for concept synthesis due to its small secondary mirror obscuration and compactness. These features, coupled with symmetry of the scientific instruments about the center line, imply potential for good pointing control.

Notes to Section:

- 1) Meinel, Meinel, Su and Wang, Applied Optics, Vol. 23, No. 17, 1 September 1984
- 2) Rodgers, "Nonstandard Representations of Aspheric Surfaces in a Telescope Design", Applied Optics, Vol. 23, No. 4, 15 February 1984
- 3) Meinel & Meinel, "Large Deployable Reflector (LDR) Configuration Approaches", JPL Contract No. 965017, June 1982
- 4) Korsch Optics Inc., "Highly Corrected Spherical - Primary Telescope Designs Final Report" for George C. Marshall Space Flight Center, October 1984

### 3.2 APERTURE SIZE TRADE

#### 3.2.1 Task

The scientific requirements for high resolution and high light gathering capability with the hardware constraints of weight and packaging limitations strongly affect the selection of an optimum LDR aperture. The purpose of this task was to evaluate relative effect of aperture size on system performance, complexity, and cost.

#### 3.2.2 Approach

Shown in Figure 3.2-1 is the effect of aperture diameter on image diameter (resolution  $\propto 1/\text{aperture diameter}$ ). Shown in Figure 3.2-2 is the effect of aperture

diameter on light gathering power (throughput  $\propto (\text{aperture diameter})^2$ ). The scientific need for larger diameters must be evaluated against hardware considerations (i.e., manufacturing and operational constraints).

The option of significantly reducing the LDR aperture does not satisfy the astronomical requirements in the IR to submillimeter wavelength region. Therefore, the baseline LDR aperture size (20 meters) was retained as a goal. The system trade study addressed the hardware considerations of weight and packaging to meet this goal.

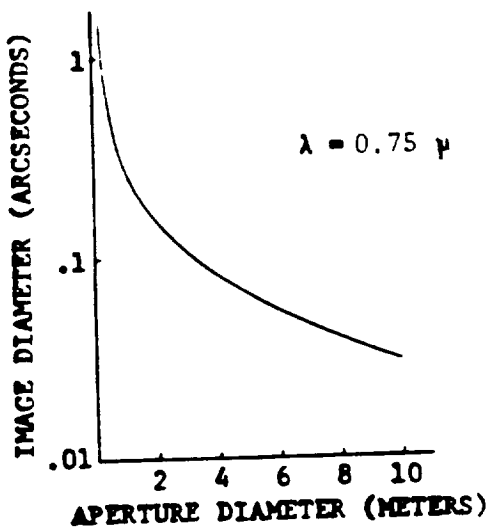
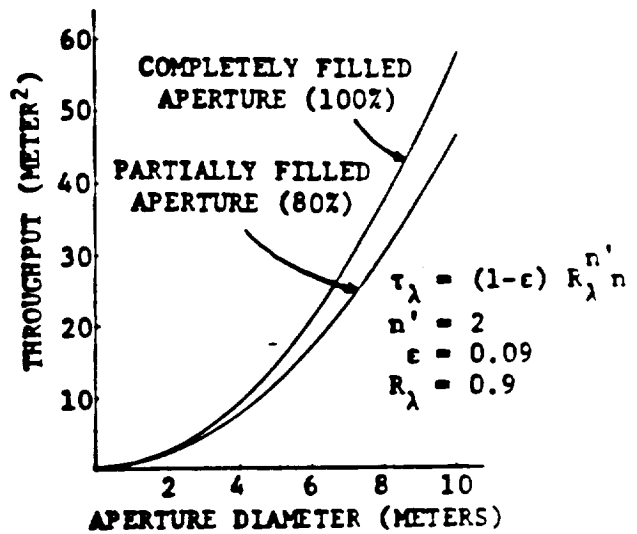


IMAGE DIAMETER FOR POINT SOURCE

Figure 3.2-1



LIGHT GATHERING CAPABILITY

Figure 3.2-2

### 3.2.3 Discussion

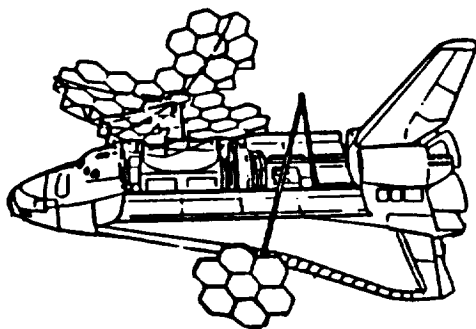
The first major issue is packaging limitations. In the Shuttle era, the Orbiter Bay imposes the basic payload size constraint. A circular mirror larger than four meters in diameter would have to be segmented and folded to meet the width allocation of the Shuttle Orbiter Bay.

The second major hardware constraint is payload weight. The end orbit as well as the number of launches is affected by this basic parameter.

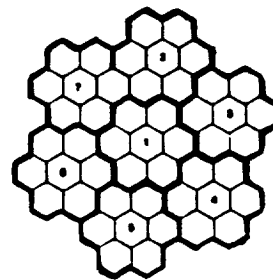
Shown in Figure 3.2-3 is a concept whereby the LDR primary mirror segment assemblies are stowed in the Orbiter Bay. The arrangement of seven seven-mirror assemblies was chosen for evaluation. In addition to the mirror assemblies the remaining elements of the observatory (spacecraft, scientific instruments, thermal shroud, etc.) and support equipment must also be stowed in the Orbiter Bay (Figure 3.2-4).

Shown in Figure 3.2-5 is a weight estimate for this concept. Such a graph can be used to visualize aperture size effects. For example, from this graph three choices are possible for a single STS equatorial launch (assuming packaging density is compatible with STS volume allocation): (1) a 20-meter diameter primary mirror assembly could be launched; (2) a 18-meter diameter optical subsystem could be launched (primary mirror with secondary mirror); or (3) a 13-meter observatory could be launched. Therefore, primary mirror segment assemblies stowed in Orbiter Bay limits aperture diameter to approximately 13 meters. However, there is not enough available space for all elements of the observatory (i.e., solar panels and shroud). Shown in Figure 3.2-6 is a weight estimate for a single Shuttle polar orbit. It can be seen from this figure that the total observatory weight is not compatible with Shuttle launch capability for polar orbit.

(ERECTABLE CONCEPT, III: 1.5-METER SEGMENTS)



SEVEN SEVEN-MIRROR  
ASSEMBLIES

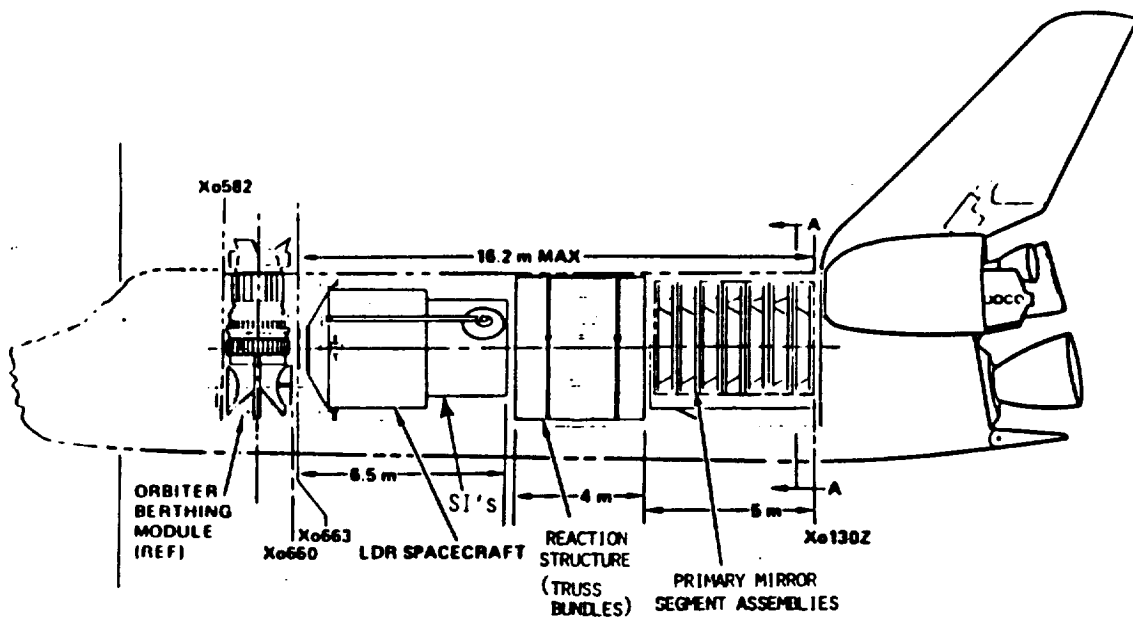


10 m

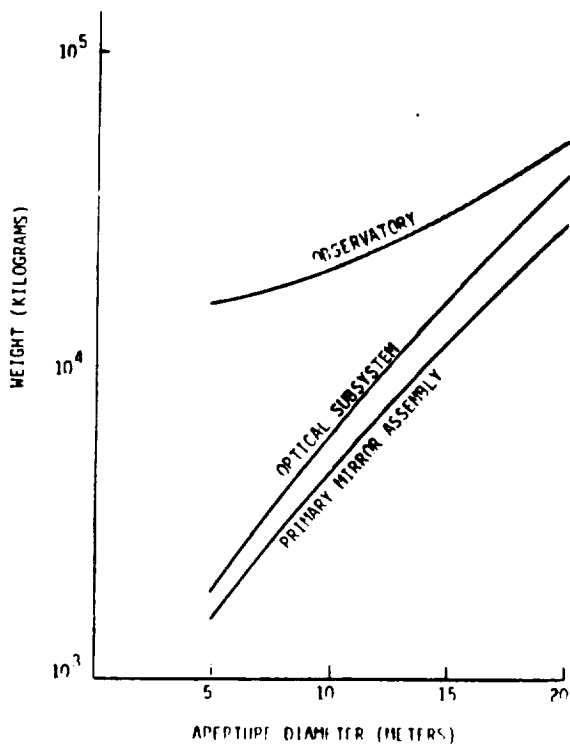
LDR PRIMARY MIRROR SEGMENT ASSEMBLIES IN ORBITER BAY

Figure 3.2-3

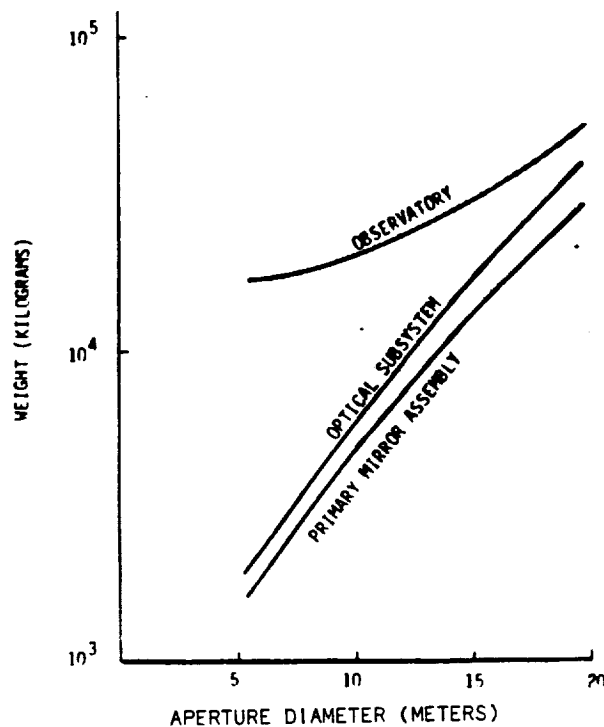
(“DECK OF CARDS” CONCEPT)



LDR ELEMENTS STOWED IN ORBITER BAY  
Figure 3.2-4



WEIGHT/DIAMETER INTERRELATIONSHIP  
(SINGLE SHUTTLE:  $H = 150\text{NM}$ ;  $i = 28.5^\circ$ )  
Figure 3.2-5



WEIGHT/DIAMETER INTERRELATIONSHIP  
(SINGLE SHUTTLE: POLAR ORBIT)

Figure 3.2-6

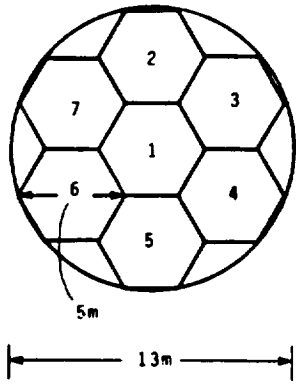
An approach utilizing a single Shuttle with ACC was also studied. The primary mirror segments (Figure 3.2-7) would be stowed in the ACC (Figure 3.2-8). Shown in Figures 3.2-9 and 3.2-10 are the weight/diameter interrelationship graphs. The total observatory diameter is limited to approximately 13 meters. The total observatory weight is compatible with Shuttle launch capability for equatorial orbit. The Orbiter Bay would be used for all other elements of the observatory (support structure, spacecraft, scientific instruments, solar panels and shroud). The total observatory weight is not compatible with Shuttle launch capability for polar orbit.

Shown in Figures 3.2-11 to 3.2-14 are the weight/diameter interrelationship graphs for a dual Shuttle launch. A 20-meter diameter observatory weight allocation "appears to be compatible" with two Shuttle loads. However, packing density will force more than two Shuttle loads. (Goal: 20-meter diameter observatory in three Shuttle loads).

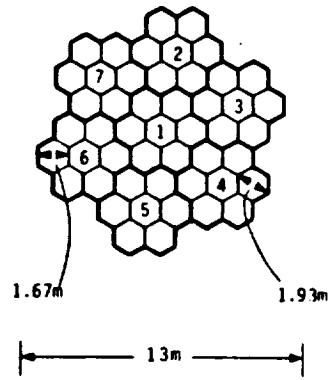
#### 3.2.4 Conclusion

Shown in Table 3.2-1 and Table 3.2-2 is a summary of the aperture trade results for a single Shuttle launch. The LDR observatory is limited to approximately 13 meters. Multiple Shuttles (> 3) will be required for an LDR observatory of 20-meter aperture diameter. Summarized in Table 3.2-3 are the relative effects of aperture size.

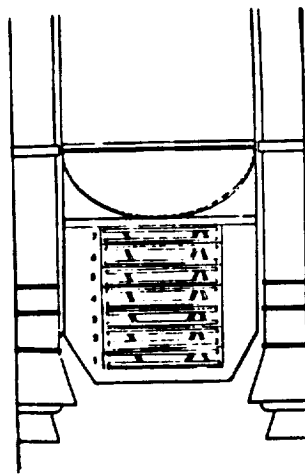
OPTION I



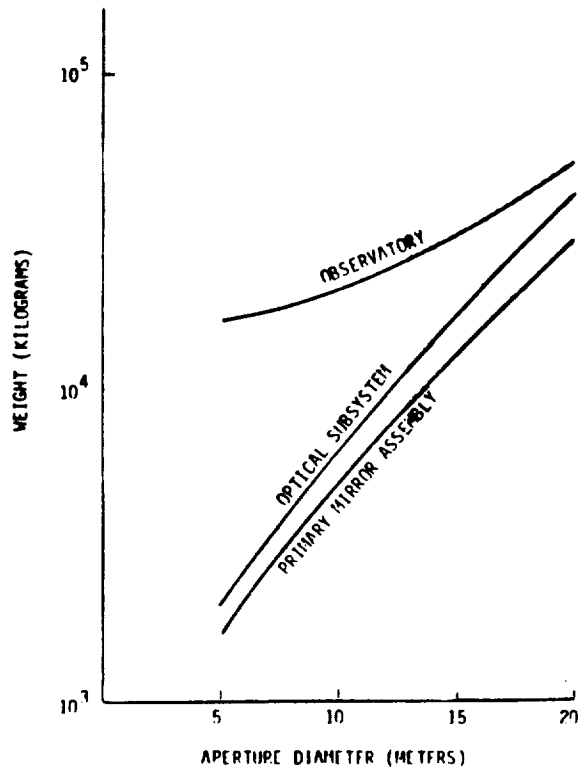
OPTION II



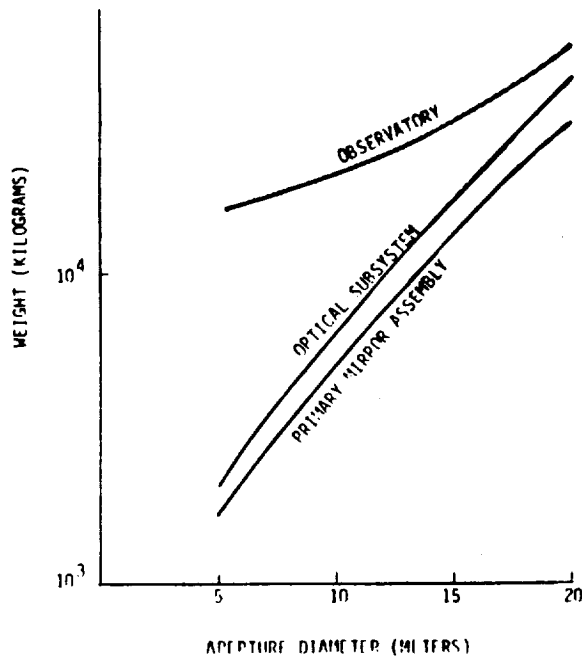
PRIMARY MIRROR SEGMENT SIZE USING ACC  
Figure 3.2-7



SEGMENT STOWAGE IN ACC  
Figure 3.2-8

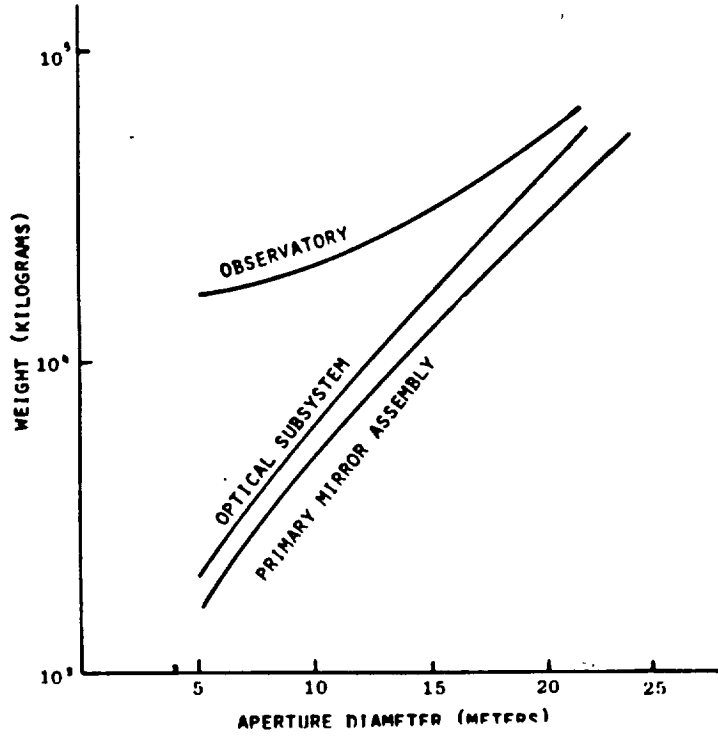


WEIGHT/DIAMETER INTERRELATIONSHIP  
 (SHUTTLE/ACC: H = 150 NM; i = 28.5°)  
 Figure 3.2-9



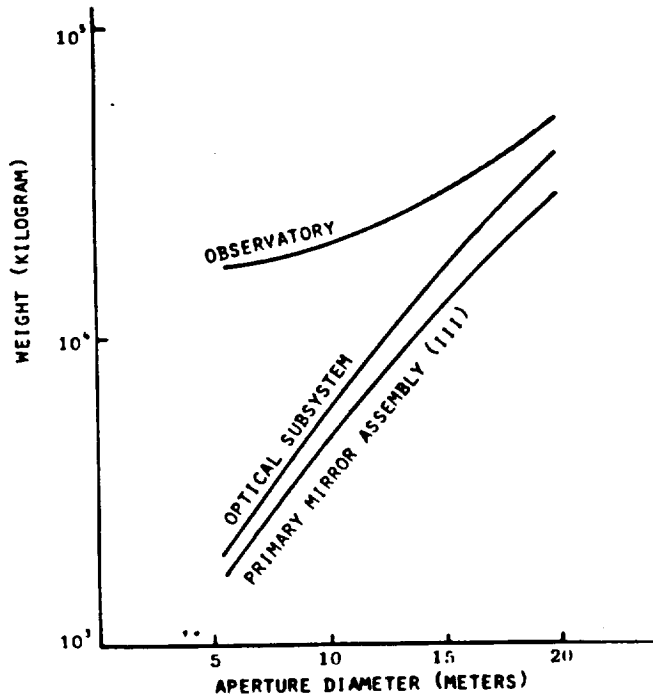
WEIGHT/DIAMETER INTERRELATIONSHIP  
 (SHUTTLE/ACC: POLAR ORBIT)  
 Figure 3.2-10





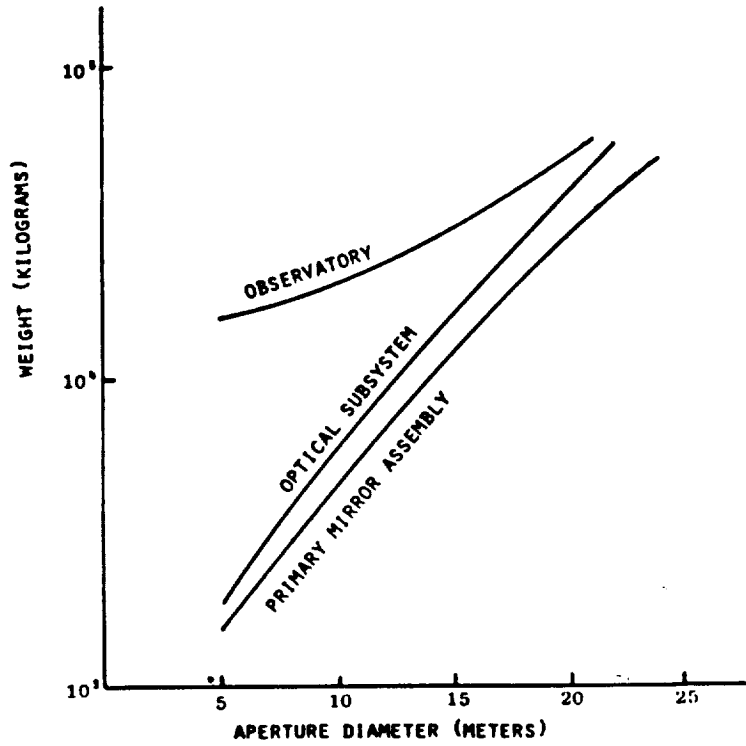
WEIGHT/DIAMETER INTERRELATIONSHIP  
 (DUAL SHUTTLE:  $H = 150 \text{ NM}$ ;  $i = 20.5^\circ$ )

Figure 3.2-11

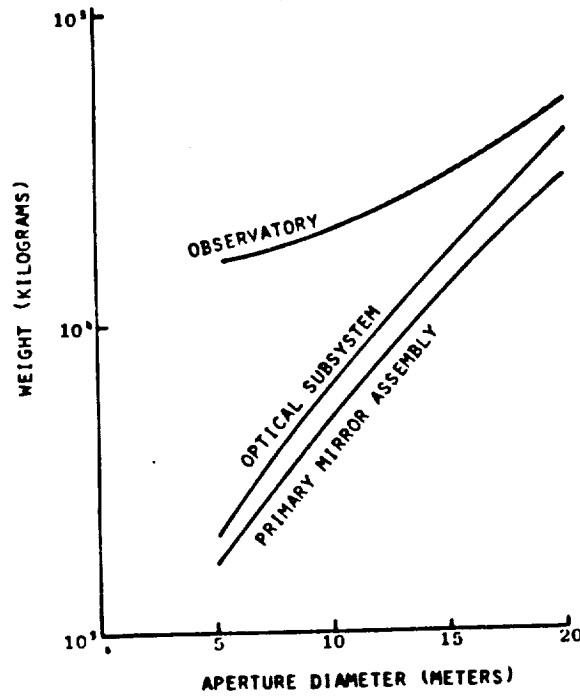


WEIGHT/DIAMETER INTERRELATIONSHIP  
 (DUAL SHUTTLE: POLAR ORBIT)

Figure 3.2-12



WEIGHT/DIAMETER INTERRELATIONSHIP  
 (DUAL SHUTTLE/ACC:  $H = 150 \text{ NM}$ ;  $i = 28.5^\circ$ )  
 Figure 3.2-13



WEIGHT/DIAMETER INTERRELATIONSHIP  
 (DUAL SHUTTLE/ACC: POLAR ORBIT)  
 Figure 3.2-14

TABLE 3.2-1  
SINGLE SHUTTLE OPTIONS

GOAL: TO GET TOTAL OBSERVATORY INTO ORBIT WITH SINGLE LAUNCH



	CIRCULAR APERTURE WITH SHUTTLE ONLY	CIRCULAR APERTURE WITH SHUTTLE AND ACC
		
<b>TRADE PARAMETERS</b>		
● WEIGHT	● COMPATIBLE WITH EQUATORIAL LAUNCH ● INCOMPATIBLE WITH POLAR LAUNCH	● COMPATIBLE WITH EQUATORIAL LAUNCH ● INCOMPATIBLE WITH POLAR LAUNCH
● DIAMETER	● CLEAR APERTURE LIMITED TO APPROXIMATELY 10 METERS	● CLEAR APERTURE LIMITED TO APPROXIMATELY 13 METERS
● VOLUME	● ORBITER BAY	● ORBITER BAY WITH ACC (ADDS 60% VOLUME CAPABILITY)
<b>CONCLUSION</b>	● NOT ENOUGH AVAILABLE SPACE FOR ALL ELEMENTS OF OBSERVATORY ● WILL REQUIRE SECOND SHUTTLE EVEN FOR 10 METERS	● ALL ELEMENTS OF OBSERVATORY "MIGHT BE" LAUNCHED IN SINGLE SHUTTLE

TABLE 3.2-2  
SINGLE SHUTTLE OPTIONS

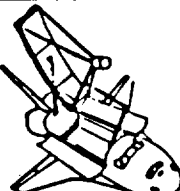
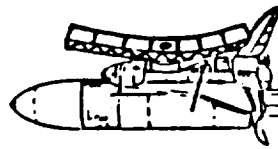
	RECTANGULAR APERTURE (SLOT) WITH SHUTTLE ONLY	RECTANGULAR APERTURE (SLOT) WITH SHUTTLE AND ACC
		
<b>TRADE PARAMETERS</b>		
● WEIGHT	● COMPATIBLE WITH EQUATORIAL LAUNCH ● INCOMPATIBLE WITH POLAR LAUNCH	● COMPATIBLE WITH EQUATORIAL LAUNCH ● INCOMPATIBLE WITH POLAR LAUNCH
● DIAMETER	● APERTURE LENGTHS $\leq 12$ METERS (STOWED) ● APERTURE LENGTHS $\leq 20$ METERS (DEPLOYED)	● APERTURE LENGTHS $\leq 28$ METERS
● VOLUME	● ORBITER BAY	● ORBITER BAY WITH ACC (ADDS 60% VOLUME CAPABILITY)
<b>CONCLUSION</b>	● NOT ENOUGH AVAILABLE SPACE FOR ALL ELEMENTS OF OBSERVATORY ● REQUIRES SECOND SHUTTLE WHICH NEGATES ADVANTAGE OF SLOT	● ALL ELEMENTS OF OBSERVATORY "MIGHT BE" LAUNCHED IN SINGLE SHUTTLE

TABLE 3.2-3  
RELATIVE EFFECTS OF APERTURE SIZE

(ASSUME F/0.5 CASSEGRAIN, FIXED MIRROR SEGMENT SIZE)

APERTURE SIZE DIAMETER, M	SYSTEM PERFORMANCE		COMPLEXITY ● NUMBER OF MIRROR SEGMENTS, STRUTS, ACTUATORS, JOINTS ● SUNSHIELD AREA ● CONTROL REQUIREMENTS ● DEPLOYMENT	COST ● DEVELOPMENT ● DESIGN ● MANUFACTURE ● TEST ● DEPLOYMENT
	INTEGRATION TIME	SPATIAL RESOLUTION		
D	$\propto D^2$	$\propto D$	$\propto D^2$	$\propto D^3$
10	1/4	1/2	1/4	1/8
20	1	1	1	1
30	2 1/4	1 1/2	2 1/4	3 3/8
40	4	2	4	8

### 3.3 REFLECTOR MATERIAL TRADE

#### 3.3.1 Task

The purpose of this task was to compare potential LDR reflector materials based on cost, replicability, complexity and performance in both the diffraction limited mode and the light bucket mode.

#### 3.3.2 Approach

A glass material has been used for applications such as LDR because of its low CTE and low CTE variability. For applications where the dimensional change can be tolerated metals offer an attractive alternative. Therefore, in a concept such as the radially degraded telescope, metals may have potential application in the sub-millimeter region. Carbon/carbon materials offer the potential of a nearly zero coefficient of thermal expansion as well as meeting the requirements for stiffness, strength, freedom from outgassing, and relatively short cycle time production.

In this study three categories of materials (metals, glass/ceramics, and composites) were evaluated and compared for the LDR primary mirror.

The properties of various candidate mirror materials are extremely important in determining their applicability to the design of the LDR mirror (Table 3.3-1).

TABLE 3.3-1  
MIRROR MATERIAL REQUIREMENTS

#### REQUIREMENTS

- MANUFACTURABLE TO DESIRED OPTICAL FIGURE
- MINIMUM STRESSES AND DEFORMATIONS IN "1-g" TESTING
- LAUNCH SURVIVAL
- MINIMUM THERMAL DISTORTIONS IN OPERATION
- LONG-TERM DIMENSIONAL STABILITY
- COMPATIBILITY WITH OPTICAL COATING
- COMPATIBILITY WITH MOUNTING ARRANGEMENT
- COMPATIBILITY WITH FIGURE AND/OR ALIGNMENT CONTROL ARRANGEMENT

A high degree of thermal stability is required to minimize figure changes due to variations in thermal environment. High strength and low density are both important in minimizing the mirror weight. This takes on increased importance in a large aperture system such as the LDR. A high degree of long-term dimensional stability is also a requirement, primarily for the same reasons as discussed for thermal stability. The material must also allow for fabrication of components to design specifications. A material having extremely attractive intrinsic properties is of little value if it is unable to withstand the fabrication loads or cannot be assembled with precision. The material must also have the capability of being polished to required specifications of asphericity (low frequency error) and surface roughness (high frequency error) with a sufficient level of adhesion to accept optical coatings. In the design of a passive segment (assuming only piston and tilt control) it will be required to have minimal deflections throughout the range of

normal operating temperatures. A mirror substrate, such as the LDR primary mirror, must, therefore, have a coefficient of thermal expansion (CTE) as close to zero as possible.

A list of candidate mirror materials and their associated properties are given in Table 3.3-2.

TABLE 3.3-2  
REFLECTOR MATERIAL TRADE - MATERIAL PROPERTIES

MATERIALS	$\alpha @ 200^{\circ}\text{K}$ $\mu\text{M}/\text{M}^{\circ}\text{K}$	$\Delta\alpha$ $\mu\text{M}/\text{M}^{\circ}\text{K}$ PART/PART	E GPa	$\rho$ GM/CM <sup>3</sup>	k WATT/M <sup>2</sup> °K	C <sub>p</sub> J/KG <sup>2</sup> °K	FIGURES OF MERIT			
							E/ $\rho$ SPEC. STIFF	D = k/ $\rho c$ DIFFUSIVITY	$\alpha/D$ THERMAL DISTORTION	
<b>METALS</b>										
ALUMINUM/FOAM	19.		69.	2.7	233	920	25.6	0.094	202	
BERYLLIUM	8.2	±0.3	290.	2.4	159	1880	121.0	0.035	233	
<b>GLASS/CERAMICS</b>										
FUSED SILICA (3% TiO <sub>2</sub> )	0	±0.03	76.	2.2	1.4	740	34.5	8.6x10 <sup>-4</sup>	35	
ZERODUR	0.16	±0.05	94.	2.5	1.6	821	37.6	7.8x10 <sup>-4</sup>	256.	
PYREX	2.9		65.	2.2	1.1	753	29.5	6.6x10 <sup>-4</sup>	4395.	
MAXALLOY (αSiC)	3.9 (RT)	±0.3	410.	3.1	125	1420	132	0.028	139. (RT)	
<b>COMPOSITES</b>										
GLASS/GRAPHITE TSC-1 (0/90)	∥ ⊥	-0.1 4.0	±0.1*	90.	2.0	27.3 2.25	837	45	0.016 0.0013	6.2 2976.
GRAPHITE MAGNESIUM (0/90)		1.5	±0.5*	210	1.8	26	962	117	0.015	100
GRAPHITE/EPOXY (GY70/CODEB7)	∥ ⊥	0.1	±0.1*	100	2.0	23 8	960	50	0.012	8.4

\*Orientation Variation (Estimated)

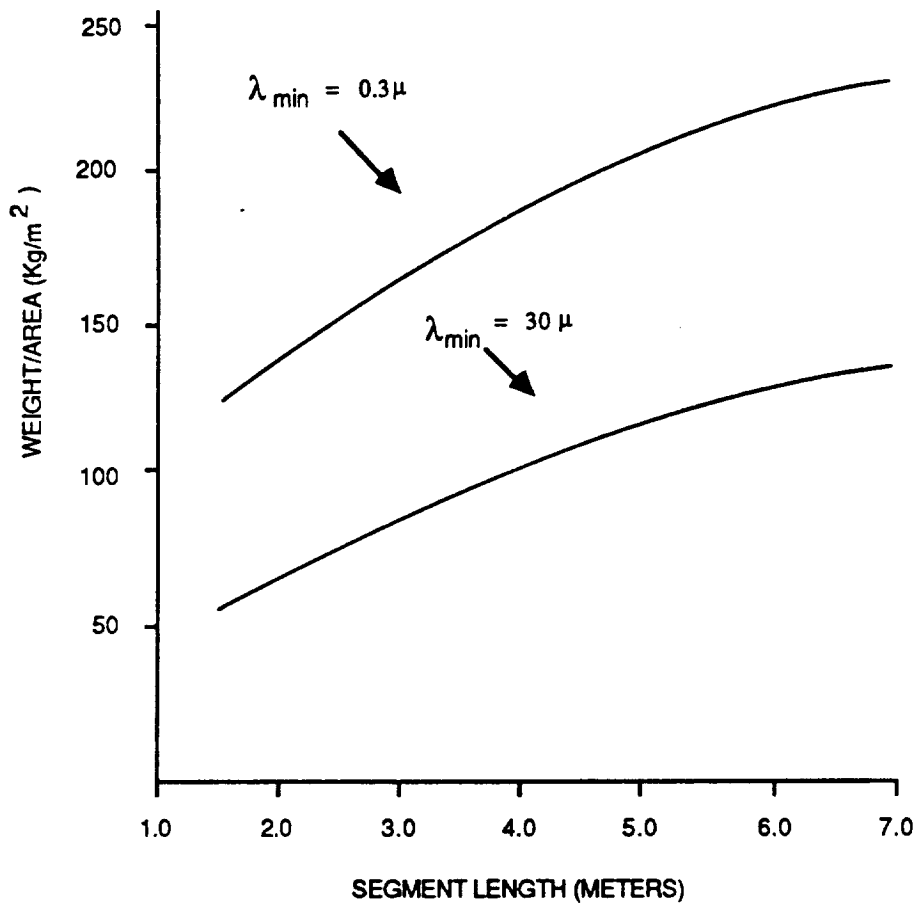
Included are materials in categories such as metals, glasses, glass ceramics, and composites. The properties listed are Young's Modulus (E), density (ρ), thermal expansion coefficient (α), conductivity (k), and heat capacity (c). Also shown in the table are three "figures of merit".

The ability of a material to athermalize can be described by the second figure of merit called thermal diffusivity: (conductivity/ (density x heat capacity)). A material with a high diffusivity value will athermalize quickly. Most materials with low CTE, such as glass, have low conductivity and low specific heat. These materials athermalize (reach equilibrium) very slowly. This means that mirrors made of glass or glass ceramic materials (operating above 100°K) are more stable under thermal transients or gradients; however, they will take a very long time to reach thermal equilibrium. For applications where the dimensional change and thermal distortion can be tolerated and rapid athermalization is required, a low CTE metal such as beryllium should be considered.

Predicted mirror areal densities for lightweight glass mirrors are shown in Figures 3.3-1 and 3.3-2.

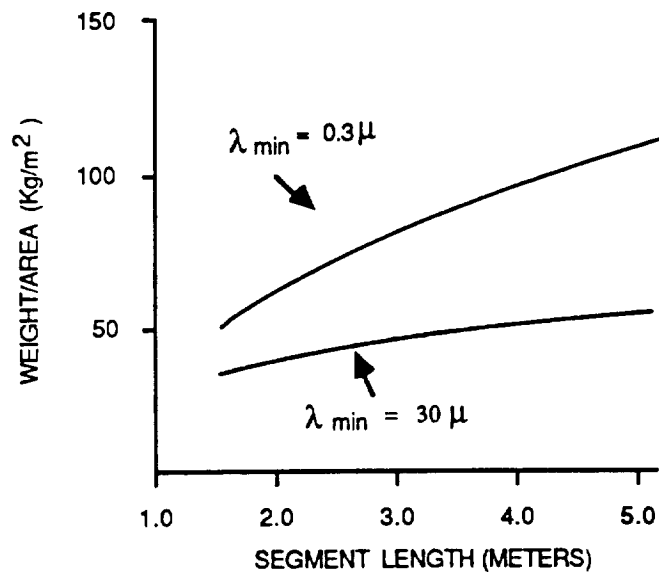
Based on preliminary analyses of a simply supported, "unmounted" mirror design, the technology associated with a segmented, frit bonded mirror is approaching a mirror

goal of 25 kg/m<sup>2</sup>.



PREDICTED AREAL DENSITY (FUSION WELDED)

Figure 3.3-1



PREDICTED AREAL DENSITY (FRIT-BONDED)

Figure 3.3-2

In both cases the top curve shows a design optimized for visible light applications with an aspect ratio of 7 to 1 and a rigidity of a few waves. The lower curve was calculated for an aspect ratio of 20 to 1, reducing the weight at the expense of the inherent structural rigidity. The basic assumption is that larger deflections can be tolerated at far infrared and submillimeter operational wavelengths.

A comparison of the total weight of the 20 meter primary mirror for fusion welding and frit bonding is shown in Table 3.3-3.

Shown in Figure 3.3-3 is a comparison of candidate mirror material CTE's. There is no "ideal" material for optical components that will perform over the entire range of thermal environments because the CTE of all materials changes with temperature. In general, all metal materials approach "zero expansion" properties at low cryogenic temperatures. The low expansion glass materials (ULE, Zerodur, and Cervit) have negligible thermal expansion near room temperature (300°K). Fused silica has a zero coefficient at about 140°K. At very low cryogenic temperatures (50°K), metals also approach low CTE values, particularly beryllium. The glass materials may no longer have a thermal advantage because the metals have a low CTE and a high diffusivity at these low temperatures.

Shown in Figure 3.3-4 is the instantaneous coefficient of expansion for Corning's fused silica material. Corning's ULE material is fused silica doped with 7.5 percent titanium dioxide. From the figure it can be seen that this biases the point where the instantaneous CTE is zero at approximately 300°K (room temperature). From the figure, if the LDR secondary mirror is retained at 125°K the instantaneous CTE is closer to zero using basic fused silica with no doping. In a similar manner a new ultra low expansion glass could be envisioned for the primary mirror at 200°K by using fused silica with 3 percent doping. The next issue which must be addressed is the temperature variation from the set point. Assuming the real material selected does have the instantaneous CTE curve shown, a variation in the operating temperature will result in an "optical power" error, which can be backed out by refocusing. However, CTE inhomogeneities, which can occur in buildup of a lightweight mirror blank, will result in higher order figure error.

Glass and glassy-ceramic materials have reached a level of maturity for space optical mirrors. The ability to lightweight, polish to excellent optical quality, and retain this figure has been demonstrated on programs such as Space Telescope.

Lightweight glass mirror blanks are currently manufactured for high reliability, diffraction-limited optics using a high temperature, fusion welding process. A "honeycomb" core, a faceplate, and a backplate are separately fabricated; the faceplate is bonded to the plano-plano core, and the whole assembly is inverted and slumped over a form to the desired curvature. In this process, distortions are inevitably introduced into the faceplate, backplate, and core struts. Such distortions can be reduced by preshaping the core and plates before fusion bonding. Since the core and plates must be heated to the softening point, some distortion is unavoidable. The mirror blank must be designed with the mirror blank manufacturing constraints in mind.

The high temperature process to achieve plate-to-core bonding in the fusion-welded mirror places a constraint on the mirror design and, in effect, limits the amount of lightweighting than can be achieved. A manufacturing process called frit bonding



avoids the high temperature, fusion-welding technique, thus relieving the mirror blank manufacturing weight constraint. In frit bonding the glass mirror blank is manufactured by using a glass adhesive system eliminating the high temperature fusion step while retaining the balance of the conventional mirror manufacturing process.

Based on a preliminary analysis of a simply supported, unmounted mirror design, the technology associated with a segmented, frit bonded mirror is approaching a mirror goal of 25 kg/m<sup>2</sup>.

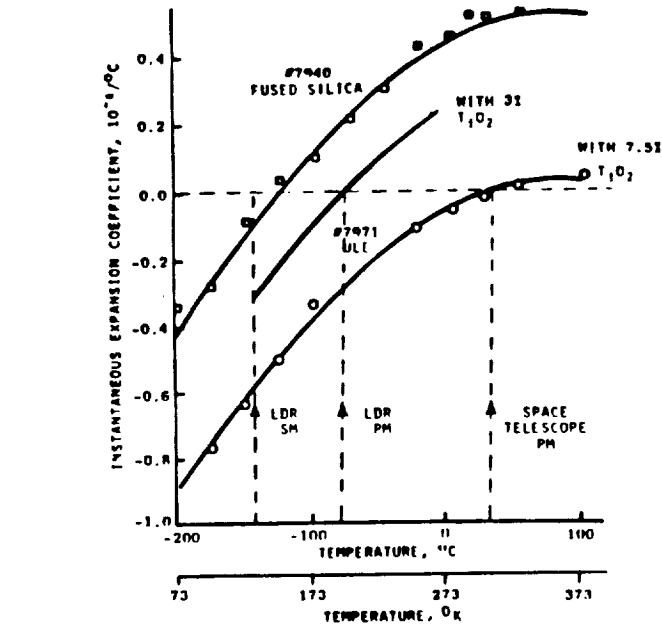
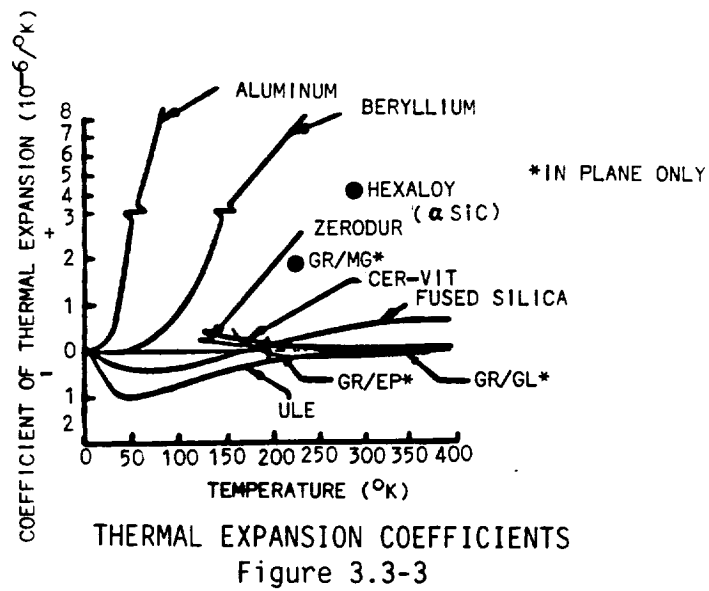
TABLE 3.3-3  
GLASS MIRROR FACEPLATE WEIGHT ESTIMATE

OPTION I

	FUSION WELDED			FRIT BONDED		
	AREAL DENSITY (KG/M <sup>2</sup> )	NUMBER	WEIGHT (KG)	AREAL DENSITY (KG/M <sup>2</sup> )	NUMBER	WEIGHT (KG)
CENTER CORE	104	1	1.307	48	1	603
INNER ANNULUS	134	4	6.737	56	4	2.816
MIDDLE ANNULUS	125	8	12.570	54	8	5.430
OUTER ANNULUS	<u>120</u>	<u>12</u>	<u>18.101</u>	52	<u>12</u>	<u>7.844</u>
TOTAL	123	25	38.715	53	25	16.693

OPTION II

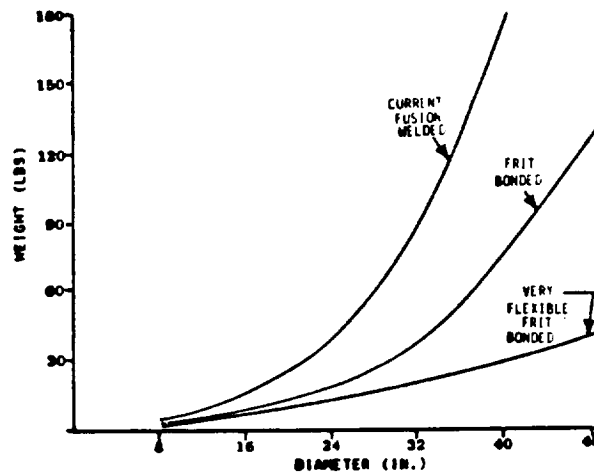
	FUSION WELDED			FRIT BONDED		
	AREAL DENSITY (KG/M <sup>2</sup> )	NUMBER	WEIGHT (KG)	AREAL DENSITY (KG/M <sup>2</sup> )	NUMBER	WEIGHT (KG)
CENTER CORE	104	1	1.307	48	1	603
INNER ANNULUS	94	8	4.723	45	8	2.261
MIDDLE ANNULUS	85	16	8.541	44	16	4.421
OUTER ANNULUS	<u>80</u>	<u>24</u>	<u>12.058</u>	<u>42</u>	<u>24</u>	<u>6.330</u>
TOTAL	85	49	26.629	43	49	13.615



THERMAL EXPANSION OF CORNING FUSED SILICA GLASS  
Figure 3.3-4

Further lightweighting can be achieved by removing the back plate and contouring the core.

Shown in Figure 3.3-5 is a weight comparison of glass mirrors. The technology for a very flexible frit-bonded mirror is approaching 10 kg/m<sup>2</sup>.



LIGHTWEIGHT VERSUS ULTRA LIGHTWEIGHT GLASS MIRROR TECHNIQUE  
Figure 3.3-5

Kodak is investigating advanced structural materials for high precision optics and optical support structures in space applications. For example, Kodak with Corning is investigating the use of glass matrix materials. When coupled with glass optics the potential for extremely high metering performance is suggested. This is especially important in a reaction structure where the mirror surface figure must be retained to fractions of the wavelength of light. The state-of the art and goals for the material are shown in Table 3.3-4. Note the anisotropic CTE which is currently a problem with composite materials. This includes resin matrix composites (graphite/epoxy) and metal matrix composites; (graphite/aluminum; graphite/magnesium). Other inherent technology problems which have to be addressed for either a mirror substrate or a support structure are structural joints and outgassing. The latter is extremely important in a cooled telescope.

The radius mismatch issue is the most difficult parameter in coherently phasing a segmented mirror. The inability to manufacture an optical element to a designed meridional and zonal radii, directly affects the lens focal length and can contribute to spherical aberration. For a monolithic aspheric mirror, the radius is manufactured during the contour generation step and measured to the final known accuracy in an interferometric test configuration using a null corrector. An additional metrology issue is imposed on a segmented, phased array telescope. A mismatch between radii of the segments in the array and the design radius of the overall mirror will also result in a wave front error.

In this study a radius mismatch requirement of 50 parts per million was established for operation at wavelengths as low as 30 micrometers.

TABLE 3.3-4  
GLASS MATRIX MATERIAL

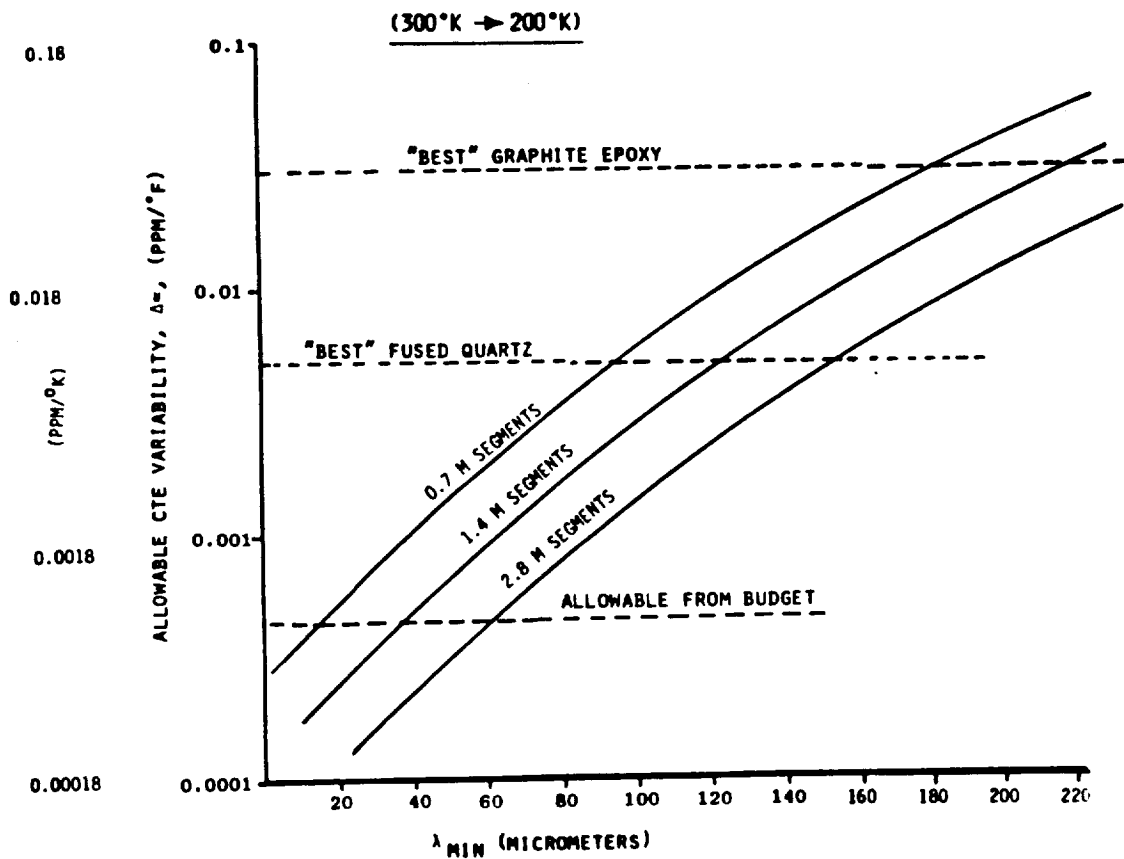
<u>STATE-OF-THE-ART</u>	<u>MATERIAL GOALS</u>
<ul style="list-style-type: none"> <li>● FIBER: CARBON OR SILICON CARBIDE</li> <li>● FIBER VOLUME: 25 PERCENT TO 50 PERCENT</li> <li>● MODULUS: 20,000 PSI TO 30,000 PSI</li> <li>● DENSITY: 0.07 LBS/IN<sup>3</sup> TO 0.09 LBS/IN<sup>3</sup></li> <li>● CTE: -0.6 IN/IN/°C TO 4.5 IN/IN/°C (-200°C) TO 25°C)</li> <li>● SHAPE: FLAT SHEET</li> </ul>	<ul style="list-style-type: none"> <li>● ELASTIC MODULUS: 30 x 10<sup>6</sup> PSI (IN THE PLANE OF THE LAMINATE)</li> <li>● DENSITY: 0.07 LBS/IN<sup>3</sup></li> <li>● CTE: 0 ±0.1 x 10<sup>-6</sup> IN/IN/°C</li> <li>● ULTIMATE STRESS: 25,000 PSI</li> </ul>

Anisotropic CTE is currently a problem with composite materials for mirrors. Shown in Figure 3.3-6 is the allowable CTE variability as a function of minimum operational wavelength. As can be seen from this figure there are four options. The first is the utilization of smaller segments. The second is operation at longer minimum wavelengths. The third is the development of a composite material that meets CTE goal of

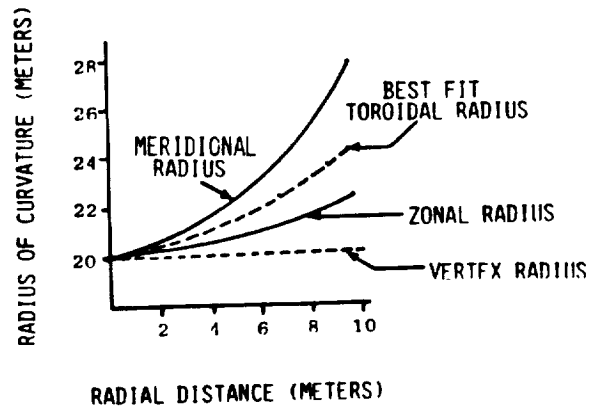
$0 \pm 0.03 \times 10^{-6}$  per °K and low CTE variability, and the fourth is active radius control to compensate for the inherent radius mismatch.

The first three options enable a passive (piston, tilt actuation only) segmented mirror concept. The fourth option is an active (figure, piston and tilt actuation) segmented mirror concept. If this latter concept is required the shape of the primary mirror is of concern. In a telescope with a spherical primary mirror, active radius control can be controlled with a single central linear actuator on the back of the mirror (note: this changes optical power). In a telescope with an aspheric primary mirror, active radius control is more complex. Shown in Figure 3.3-7 are the radii on the f/0.5 parabolic primary mirror. Active figure control (note: higher order aberration correction) will be required to maintain parabolic shape (match meridional and zonal radii simultaneously).

LDR will be operated in two modes (diffraction limited and light bucket). Requirements on the mirror surface can be defined by three spatial frequency domains. The low spatial frequency domain is quantified by the surface figure error. This value was established at 1.5 micrometers rms and is set by the lowest operational wavelength (30 micrometers) in the diffraction limited mode. The mid spatial frequency domain is quantified by the autocorrelation length to pupil diameter ratio. For both modes it has been set at a value of 0.125. The high spatial frequency domain is quantified by the surface roughness. This specularity value was established at 250 angstroms rms and is set by the lowest operational wavelength (1 micrometer) in the light bucket mode. Glass can readily be polished to this specularity requirement (the Space Telescope primary mirror was polished to 20 angstroms rms). Metals also can be made highly specular. Composite materials due to the layup are not directly polishable to the LDR requirements. One option is a top optical facesheet. Kodak is experienced in an alternative in which ULE™ is deposited on top of a carbon/carbon substrate via a sputtering process, to accomplish this purpose. It has been shown to be polishable to a specular surface with an rms surface roughness of 20 angstroms.



SELECTION OF PRIMARY MIRROR SUBSTRATE MATERIAL  
Figure 3.3-6



RADII FOR AN  $f/0.5$  PARABOLIC MIRROR  
 Figure 3.3-7

### 3.3.4 Conclusions

Three categories of materials were evaluated (metals, glass/ceramics and composites). The results are summarized in Tables 3.3-5 through 3.3-9. Metals will not meet the performance requirements at operational wavelengths as low as 30 micrometers. Glass/ceramics should meet the performance requirements utilizing only rigid body motion (piston and tilt) control of the mirror segments. Composite materials have potential in a concept utilizing rigid body motion control with radius control of the mirror segments.

TABLE 3.3-5  
REFLECTOR MATERIAL TRADE  
PERFORMANCE POTENTIAL

	<u>PERFORMANCE POTENTIAL</u>	<u>PERFORMANCE DRAWBACKS</u>	<u>PERFORMANCE BENEFITS</u>
<b>METAL</b>			
ALUMINUM/FOAM	POOR	HIGH CTE, LOW E/ $\rho$	HIGH DIFFUSIVITY
BERYLLIUM	GOOD	UNIFORMITY	HIGH E/ $\rho$ & DIFFUSIVITY
<b>GLASS/CERAMIC</b>			
FUSED SILICA (3% TiO <sub>2</sub> )	EXCELLENT	LOW DIFFUSIVITY	VERY LOW CTE, UNIFORMITY
ZERODUR	EXCELLENT	LOW DIFFUSIVITY	VERY LOW CTE, UNIFORMITY
PYREX	GOOD	UNIFORMITY, LOW DIFFUSIVITY	LOW CTE
HEXALLOY ( $\alpha$ SIC)	GOOD	UNIFORMITY	HIGH E/ $\rho$ & DIFFUSIVITY
<b>COMPOSITES</b>			
GRAPHITE/GLASS	GOOD	ISOTROPY	LOW CTE
GRAPHITE/MAGNESIUM	FAIR	ISOTROPY, HYSTERISIS	HIGH E/ $\rho$
GRAPHITE/EPOXY	FAIR	ISOTROPY, HYGRO- SCOPICITY	LOW CTE

TABLE 3.3-6  
REFLECTOR MATERIAL TRADE COMPLEXITY

	<u>COMPLEXITY</u>	<u>IMPORTANT CONSIDERATIONS</u>
<b>METALS</b>		
ALUMINUM/FOAM	LOW	ROOM TEMPERATURE FORMING, BRAZING
BERYLLIUM	HIGH	HIGH FORMING PRESSURE, TOXICITY
<b>GLASS/CERAMIC</b>		
FUSED SILICA (3% TiO <sub>2</sub> )	MEDIUM	HIGH TEMPERATURE - GOOD FORM CONTROL
ZERODUR	MEDIUM	MEDIUM TEMPERATURE - CERAMING CAUSES DISTORTION
PYREX	MEDIUM	MEDIUM TEMPERATURE - SOME DISTORTION
HEXALLOY (α-SiC)	HIGH	POOR FORMING CONTROL, VERY DIFFICULT TO GRIND
<b>COMPOSITES</b>		
GRAPHITE/GLASS	HIGH	ISOTROPY CONTROL, CRYO CYCLE FOR STABILITY
GRAPHITE/MAGNESIUM	HIGH	ISOTROPY CONTROL, CRYO CYCLE FOR STABILITY
GRAPHITE/EPOXY	MEDIUM	ISOTROPY CONTROL, LOW TEMPERATURE CURE

RATING SYSTEM: HIGH IMPLIES VERY COMPLEX  
LOW IMPLIES NOT COMPLEX

TABLE 3.3-7  
REFLECTOR MATERIALS TRADE REPLICABILITY

	<u>REPLICABILITY</u>	<u>MATERIAL/PROCESSING ADVANTAGES</u>	<u>MATERIAL/PROCESSING DISADVANTAGES</u>
<b>METALS</b>			
ALUMINUM/FOAM	MEDIUM	ROOM TEMP. FORMING	HIGH CTE, POOR UNIFORMITY
BERYLLIUM	MEDIUM	MEDIUM PROCESS TEMP	HIGH CTE, POOR UNIFORMITY
<b>GLASS/CERAMIC</b>			
FUSED SILICA (3% TiO <sub>2</sub> )	MEDIUM	LOW CTE, UNIFORMITY	HIGH FORMING TEMPERATURE
ZERODUR	LOW	LOW CTE	CERAMING CYCLE DISTORTS UNIFORMITY
PYREX	MEDIUM	MEDIUM PROCESS TEMP.	UNIFORMITY
HEXALLOY (α-SiC)	LOW	COLD PRESSING	HIGH PROCESS TEMPERATURE
<b>COMPOSITES</b>			
GRAPHITE/GLASS	MEDIUM	LOW CTE	ANISOTROPY
GRAPHITE/MAGNESIUM	LOW	LOW CTE	ANISOTROPY, HYSTERISIS
GRAPHITE/EPOXY	MEDIUM	LOW TEMP. PROCESSING	ANISOTROPY, HYGROSCOPICITY

RATING SYSTEM: HIGH IMPLIES VERY REPLICABLE  
LOW IMPLIES NOT REPLICABLE



TABLE 3.3-8  
COST

	<u>COST</u>	<u>CONSIDERATIONS</u>
<b>METALS</b>		
ALUMINUM/FOAM	LOW	EXISTING TECHNOLOGY
BERYLLIUM	MEDIUM	TOXICITY, MATERIAL AND MANUFACTURING DEV. REQUIRED
<b>GLASS/CERAMIC</b>		
FUSED SILICA (3% TiO <sub>2</sub> )	HIGH	HIGH COST MATERIAL AND MANUFACTURING
ZERODUR	HIGH	HIGH COST MATERIAL AND MANUFACTURING
PYREX	MEDIUM	LOW COST MATERIAL
HEXALLOY (αSIC)	MEDIUM	LOW COST MATERIAL, MANUFACTURING DEV. REQUIRED
<b>COMPOSITES</b>		
GRAPHITE/GLASS	HIGH	MEDIUM MATERIAL COSTS, MANUFACTURING DEV. REQUIRED
GRAPHITE/MAGNESIUM	HIGH	MEDIUM MATERIAL COSTS, MANUFACTURING DEV. REQUIRED
GRAPHITE/EPOXY	MEDIUM	LOW MATERIAL COSTS, MANUFACTURING DEV. REQUIRED

RATING SYSTEM: HIGH IMPLIES HIGH COST  
LOW IMPLIES LOW COST

TABLE 3.3-9  
REFLECTOR MATERIAL TRADE SUMMARY

<u>METALS</u>	<u>PERFORMANCE</u>	<u>COMPLEXITY</u>	<u>REPLICABILITY</u>	<u>COST</u>
● ALUMINUM/FOAM	LOW	LOW	MEDIUM	LOW
● BERYLLIUM	MEDIUM	HIGH	MEDIUM	MEDIUM
<b>GLASS/CERAMICS</b>				
● FUSED SILICA (3% TiO <sub>2</sub> )	HIGH	MEDIUM	MEDIUM	HIGH
● ZERODUR	HIGH	MEDIUM	LOW	HIGH
● PYREX	MEDIUM	MEDIUM	MEDIUM	MEDIUM
● HEXALLOY (αSIC)	MEDIUM	HIGH	LOW	MEDIUM
<b>COMPOSITES</b>				
● GRAPHITE/GLASS	MEDIUM	HIGH	MEDIUM	HIGH
● GRAPHITE/MAGNESIUM	LOW	HIGH	LOW	HIGH
● GRAPHITE/EPOXY	LOW	MEDIUM	MEDIUM	MEDIUM
DESIRED	HIGH	LOW	HIGH	LOW

### 3.4 SEGMENTED MIRROR CONCEPTS

#### 3.4.1 Task

The purpose of this task was to evaluate alternate concepts for the primary mirror. Parameters considered include mirror segment shape and segment control approach. Alternative approaches to mirror manufacture were also evaluated.

#### 3.4.2 Approach

Shown in Figure 3.4-1 is the segmented mirror concept trade tree used in this study. Trades were performed in three areas: mirror, mirror control, and mirror reaction structure.

#### 3.4.3 Discussion

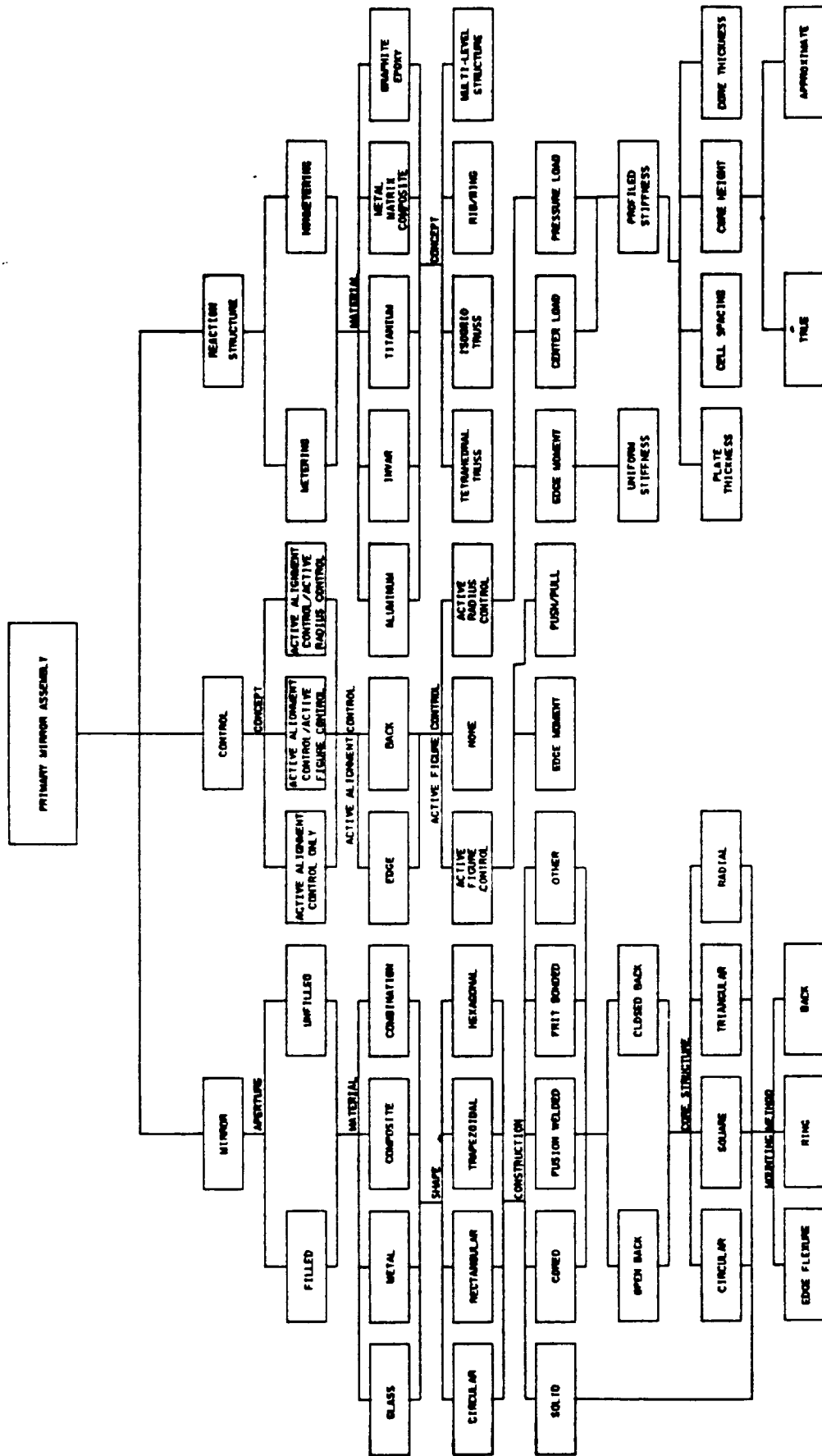
In manufacturing a coherently phased mirror made up of segments, the technical issues can be divided into two types. The first involves the issues of fabricating the mirror segments themselves, and the second involves assembly issues of initializing in "1-g" and retaining in "0-g" an aggregate segmented mirror in which coherent phasing between segments is required.

The diameter (aperture) of an optical system has two important limiting effects: light-gathering capability and resolution. In a light-bucket mode using a segmented mirror, no attempt is made to match the phases of the wave fronts reflected from the individual elements. The size of the final image is governed by the size and quality of the individual small segment apertures, while its intensity is equal to the sum of the individual image intensities. In the other case, for coherently phased imaging system, the size of the final image is governed by the size of the single large aperture, while its intensity is equal to the sum of the individual image intensities. In this study, concepts were evaluated for diffraction-limited performance at wavelengths as low as 30 micrometers and the potential of a light-bucket mode of operation at wavelengths as low as 1 micrometer.

Four possible concepts for coherent phasing are shown in Table 3.4-1. In this study the last two types of mirrors were emphasized.

TABLE 3.4-1  
COHERENTLY PHASED MIRRORS

<u>TYPE</u>	<u>CHARACTERISTICS</u>
PASSIVE MONOLITHIC	● NO ACTIVE FIGURE CONTROL ● NO ACTIVE SEGMENT ALIGNMENT CONTROL
ACTIVE MONOLITHIC	● ACTIVE FIGURE CONTROL ● NO ACTIVE SEGMENT ALIGNMENT CONTROL
PASSIVE SEGMENTED	● NO ACTIVE FIGURE CONTROL ● ACTIVE SEGMENT ALIGNMENT CONTROL
ACTIVE SEGMENTED	● ACTIVE FIGURE CONTROL ● ACTIVE SEGMENT ALIGNMENT CONTROL



SEGMENTED MIRROR CONCEPTS TRADE TREE

Figure 3.4-1

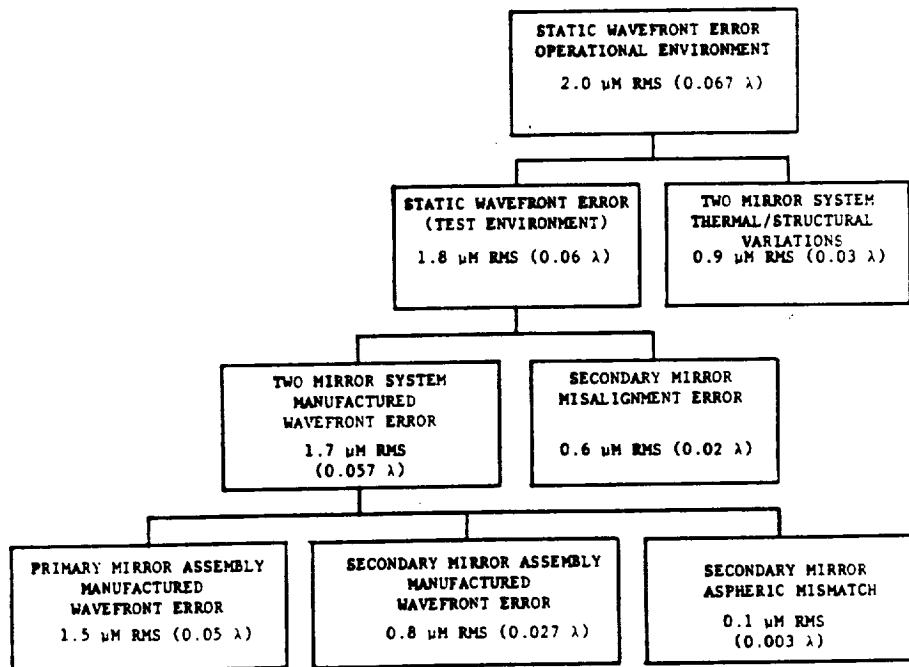
In the change from manufacturing a one-piece monolithic mirror to a mirror made up of segments, the additional technical issues can be divided into two types. The first involves the issues of manufacturing the mirror segments themselves (coherent phasing of a segment), and the second involves assembly issues of making an aggregate segmented mirror in which coherent phasing between segments is required. The figuring (polishing) of each segment should be addressed first since it affects the degree of active figure control required during operation. Each point on an aspheric surface has orthogonal radii (zonal and meridional) at any point on the surface. The sag difference between the radii extremes is a measure of the amount that a spherical tool will "rock" if it fits the shorter of the two radii. The sag difference between the two orthogonal radii at the edge of the mirror surface is, therefore, related to the "degree of difficulty" in the manufacture of the mirror surface.

The second figure of merit which represents a "metrology degree of difficulty" is the aspheric departure from the best fit sphere. The aspheric departure value is the starting point in the contour generation of the mirror surface.

The third figure of merit is the mirror segment surface error. It represents how well each off-axis segment is in itself coherently phased.

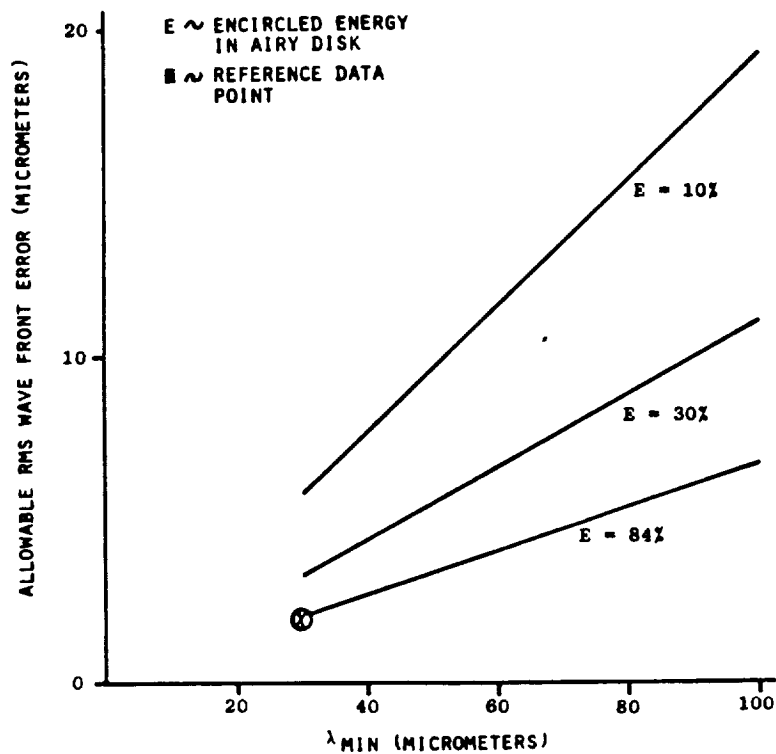
Based on an optical tolerance budgeting approach in which manufacturing errors, alignment errors, and assembly errors are allocated portions of a budget, the mirror segment surface error becomes one of the contributors.

Shown in Figure 3.4-2 is the baseline wave front budget established in this study.



LDR OPTICAL SUBSYSTEM  
 OPERATIONAL PERFORMANCE PREDICTION  
 ( $\lambda$  MIN = 30  $\mu$ M; E = 84%; D = 20 M)  
 Figure 3.4-2

A wave front error of 1.5 micrometers rms was set for the primary mirror assembly. This budget assumes the "classic" definition of diffraction limit with 84% of the energy in the central disk. In Figure 3.4-3 is shown the effect of reducing this encircled energy requirement.

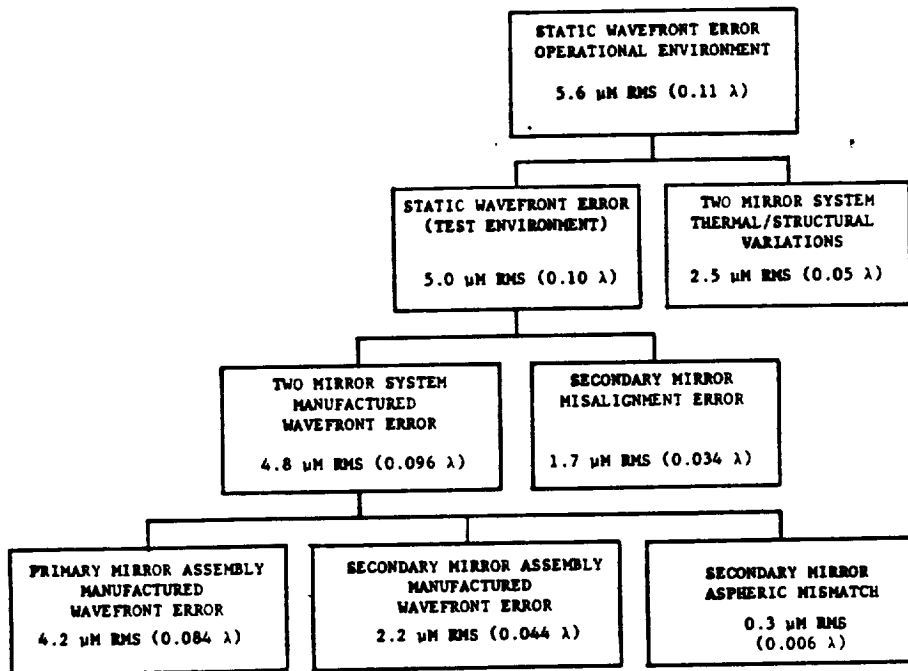


RMS WAVEFRONT ERROR REQUIREMENT  
Figure 3.4-3

Shown in Figure 3.4-4 is a different budget which "loosens" the tolerances by increasing the minimum operational wavelength and reducing the encircled energy in the central disk. It should be noted that there can be many variations in the wave front allocations. One version (see Section 3.5) reallocates the budget to maximize the allowable secondary mirror misalignment error. Further refinements should be evaluated before the budget is "frozen".

**3.4.3.1 Primary Mirror** - The primary mirror trade tree is shown in Figure 3.4-5. The obscuration effect on encircled energy is shown in Figure 3.4-6. The scientific concerns for the best imaging resolution over the largest area possible and the thermal emissivity of a large central obscuration dictate a filled aperture.

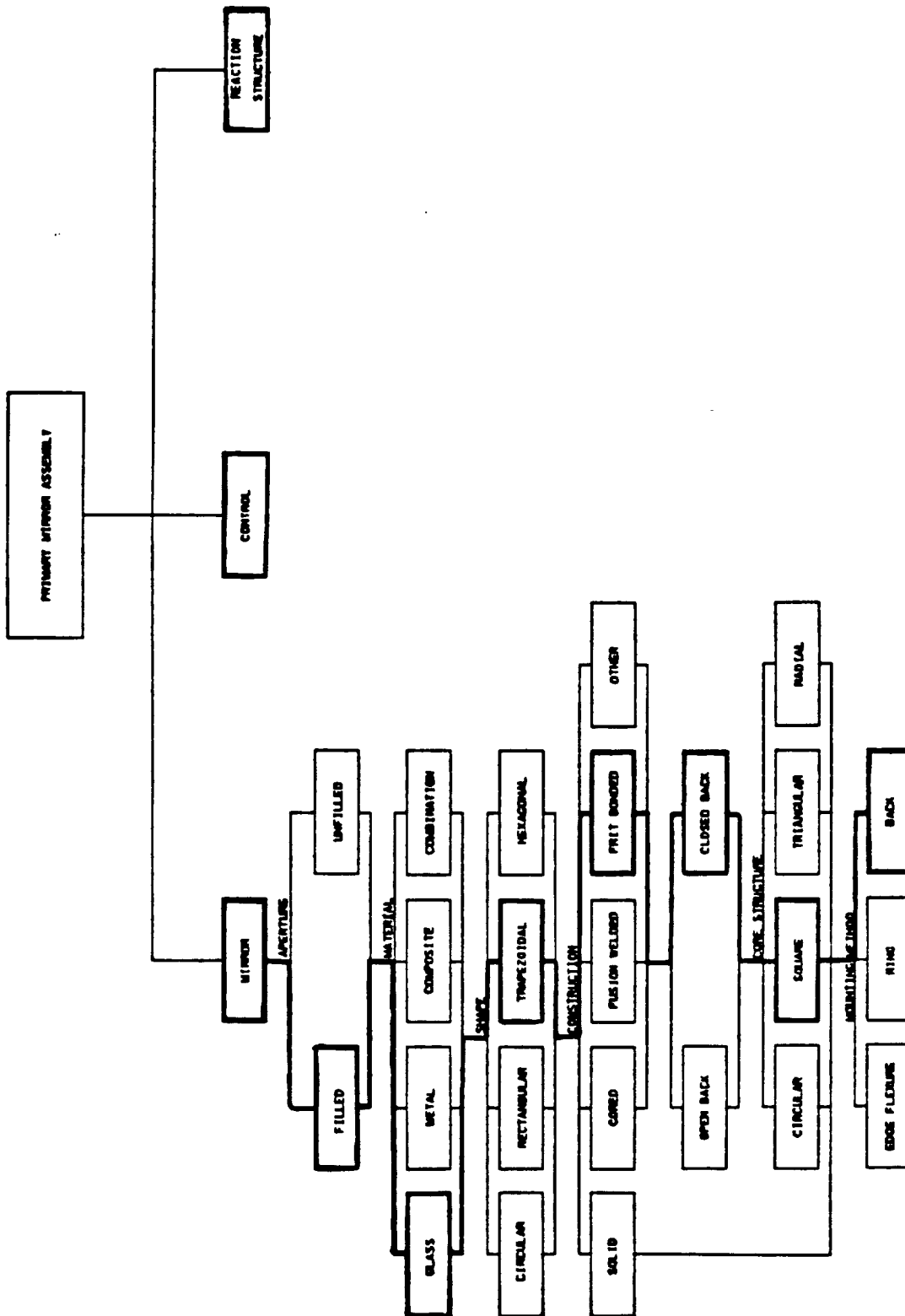
Two shapes were evaluated: trapezoidal and hexagonal. Trapezoidal segments are "slightly" preferred over hexagonal segments. There are two reasons: (1) radial symmetry minimizes the number of different processing tools and (2) more structural options available. However, it is concluded it is still "too early" to make a shape selection. The two shapes have been arbitrarily included in the system concepts to insure alternative choices are given visibility.



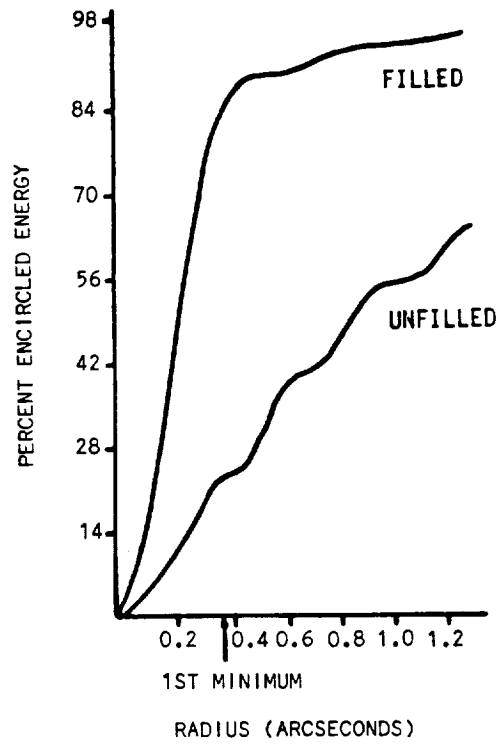
LDR OPTICAL SUBSYSTEM  
 OPERATIONAL PERFORMANCE PREDICTION (WEIGHTED AS BEFORE)  
 ( $\lambda$  MIN = 50  $\mu$ M; E = 30%; D = 20 M)  
 Figure 3.4-4

The selection of size of the segment and the number of segments was based on the preferred area of the segment. The area of the segment impacts processing time, handling/transportation and facility modifications. It also was concluded that a circular central core was considered desirable for alignment. Shown in Figures 3.4-7 to 3.4-13 are alternative arrangements for trapezoidal segments. Based on the preferred area of the segment, a mirror made up of three annuli and a central mirror was selected. This mirror arrangement is summarized in Table 3.4-2. Shown in Figure 3.4-14 are alternative arrangements for hexagonal segments. A mirror made up of a seven segment center core and six seven-segment sets located in a single annulus was selected (Concept b).

Shown in Figure 3.4-15 are the rigid body motions of concern in a Cassegrain telescope with a segmented primary mirror. The sensitivity analysis establishes the metering structure and the secondary mirror rigid body motion actuator requirements. The additional rigid body motions of the mirror segments and radius matching between segments are also of concern. Kodak, under IR&D, has developed a specialized wave front propagation model for segmented mirror evaluation. Shown in Figure 3.4-16 is the program flow for this software. The capability of the software is summarized in Table 3.4-3.



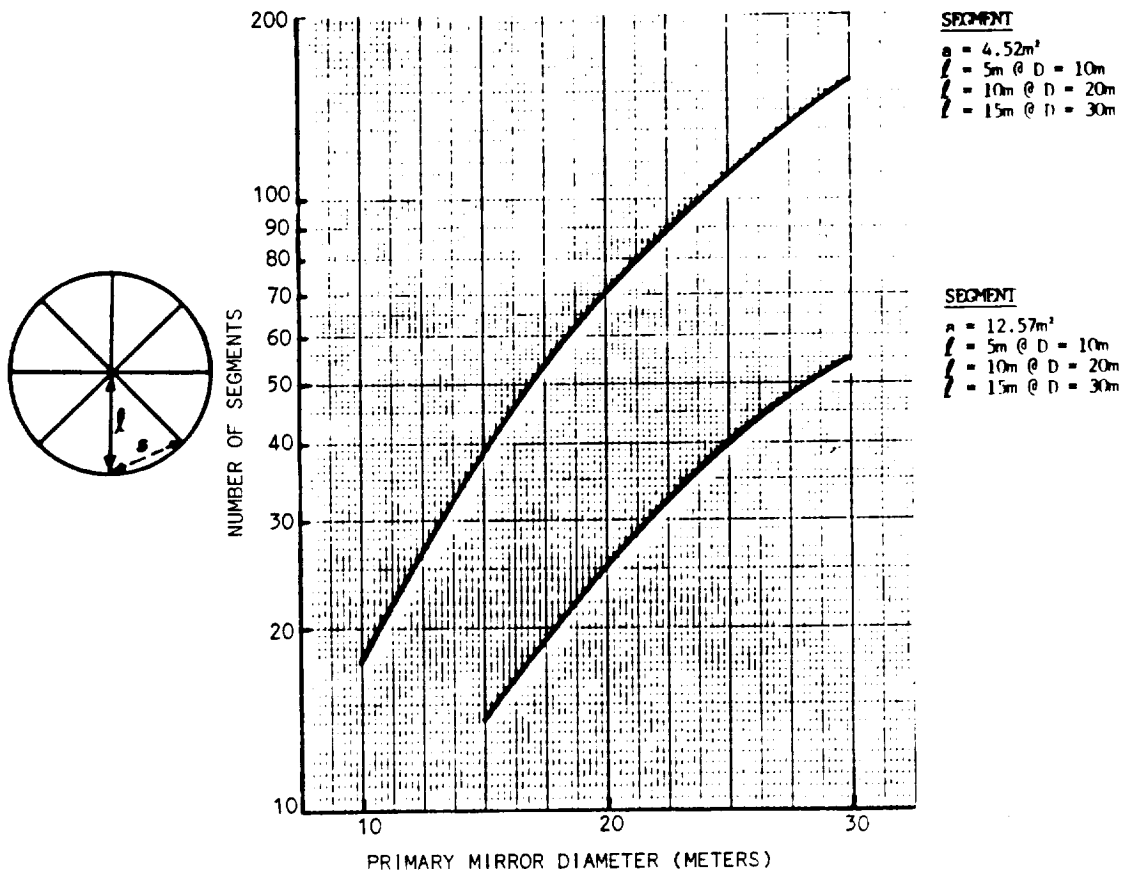
PRIMARY MIRROR TRADES  
Figure 3.4-5



OBSCURATION EFFECT ON ENCIRCLED ENERGY  
 (D = 20 M;  $\lambda$  MIN = 30  $\mu$ M)

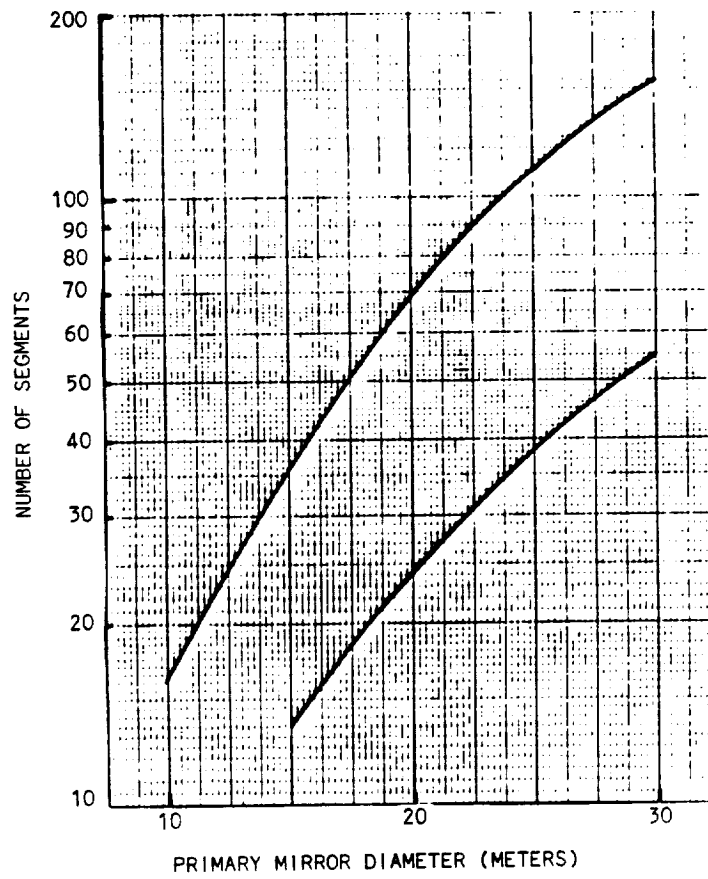
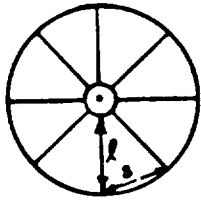
Figure 3.4-6





NUMBER OF TRAPEZOIDAL SEGMENTS IN FULL MIRROR

Figure 3.4-7



**CENTER MIRROR**  
 $D = 2.4m$

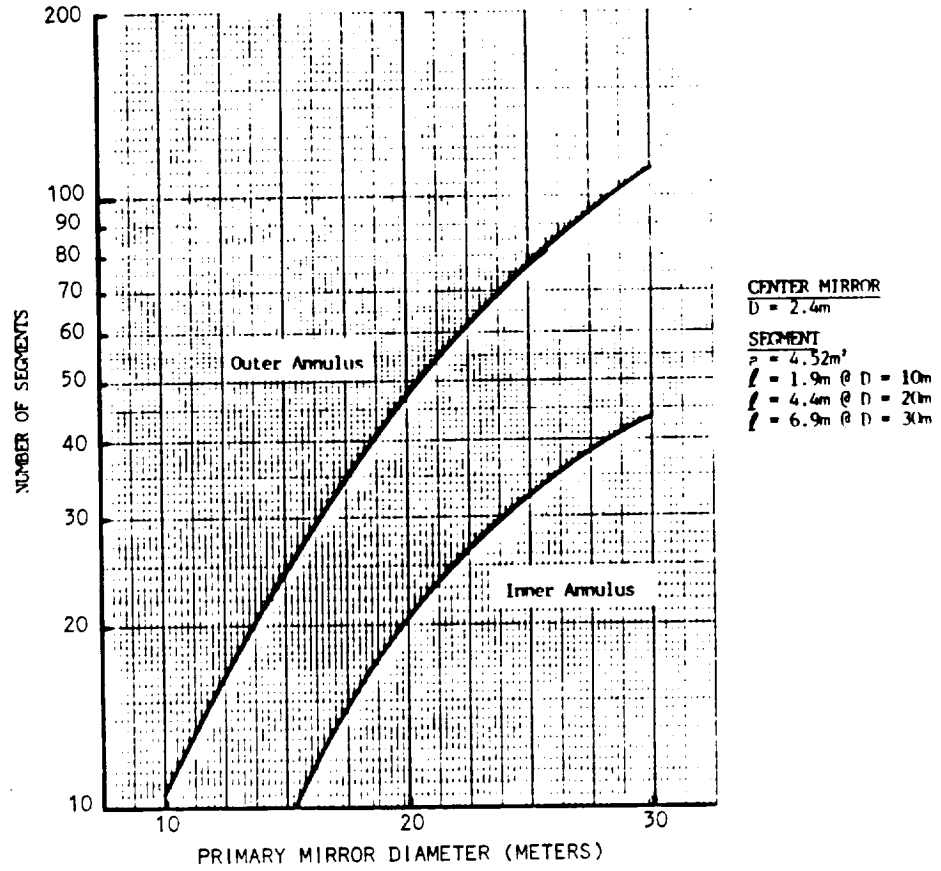
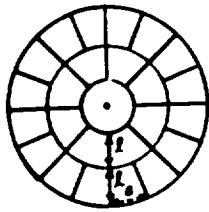
**SEGMENT**  
 $A = 4.52m^2$   
 $l = 3.8m @ D = 10m$   
 $l = 8.8m @ D = 20m$   
 $l = 13.8m @ D = 30m$

**CENTER MIRROR**  
 $D = 4.0m$

**SEGMENT**  
 $A = 12.57m^2$   
 $l = 3.0m @ D = 10m$   
 $l = 8.0m @ D = 20m$   
 $l = 13.0m @ D = 30m$

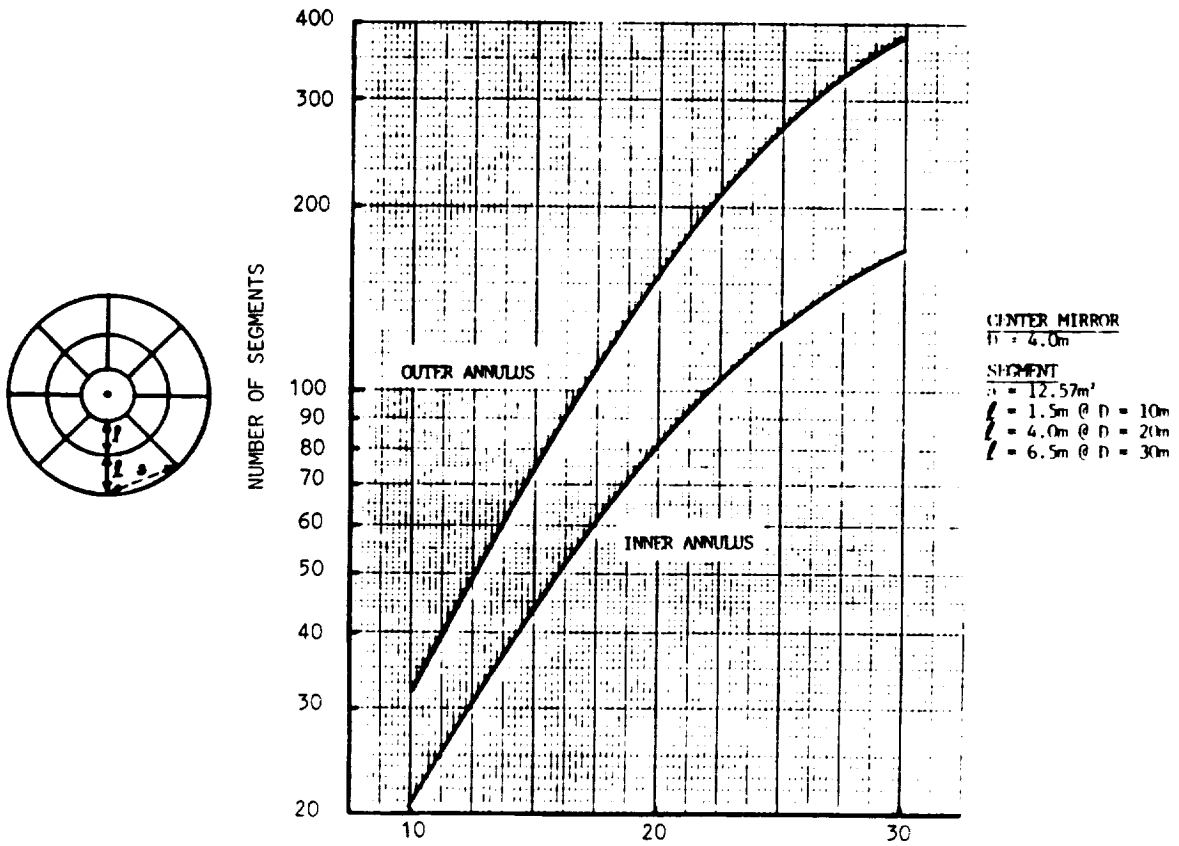
NUMBER OF TRAPEZOIDAL SEGMENTS IN SINGLE ANNULUS

Figure 3.4-8



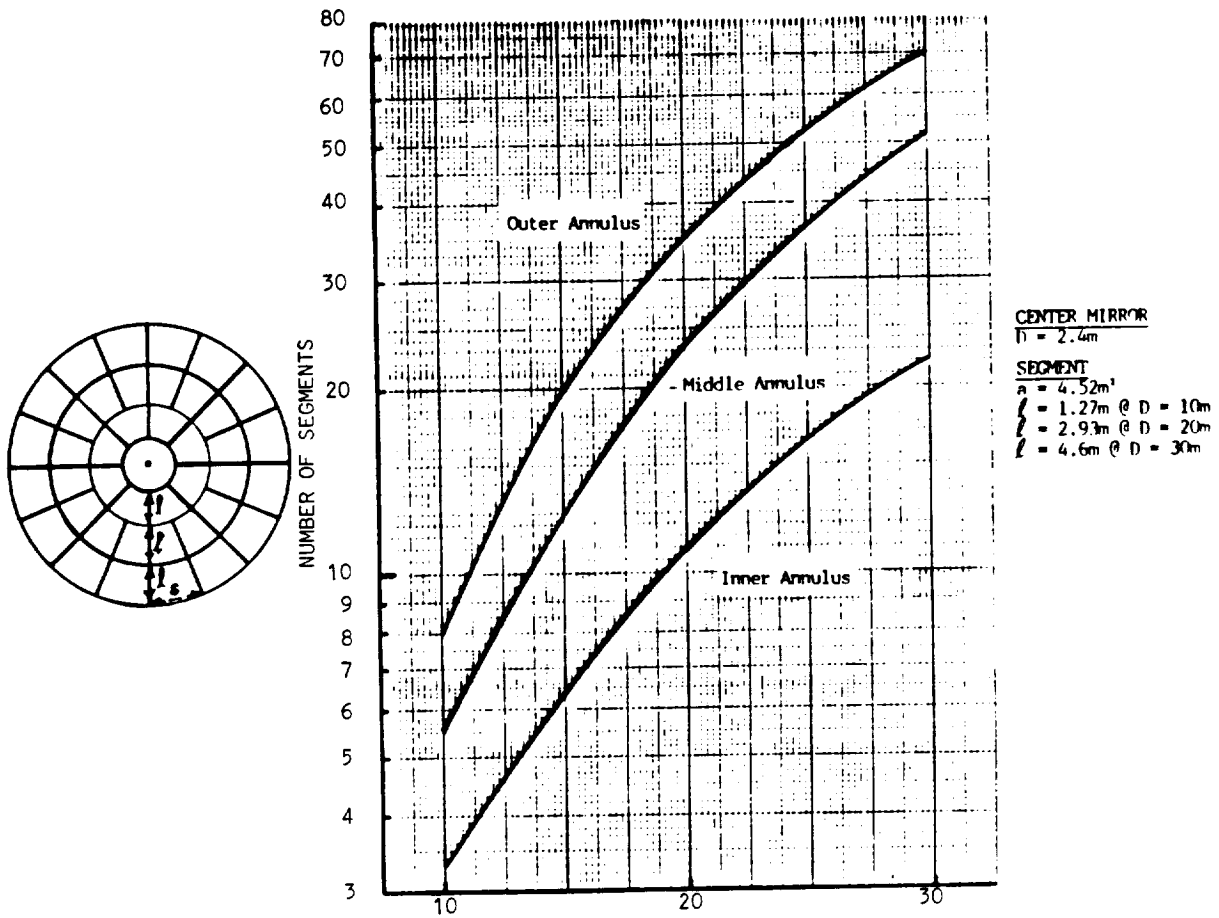
NUMBER OF TRAPEZOIDAL SEGMENTS IN DOUBLE ANNULUS

Figure 3.4-9



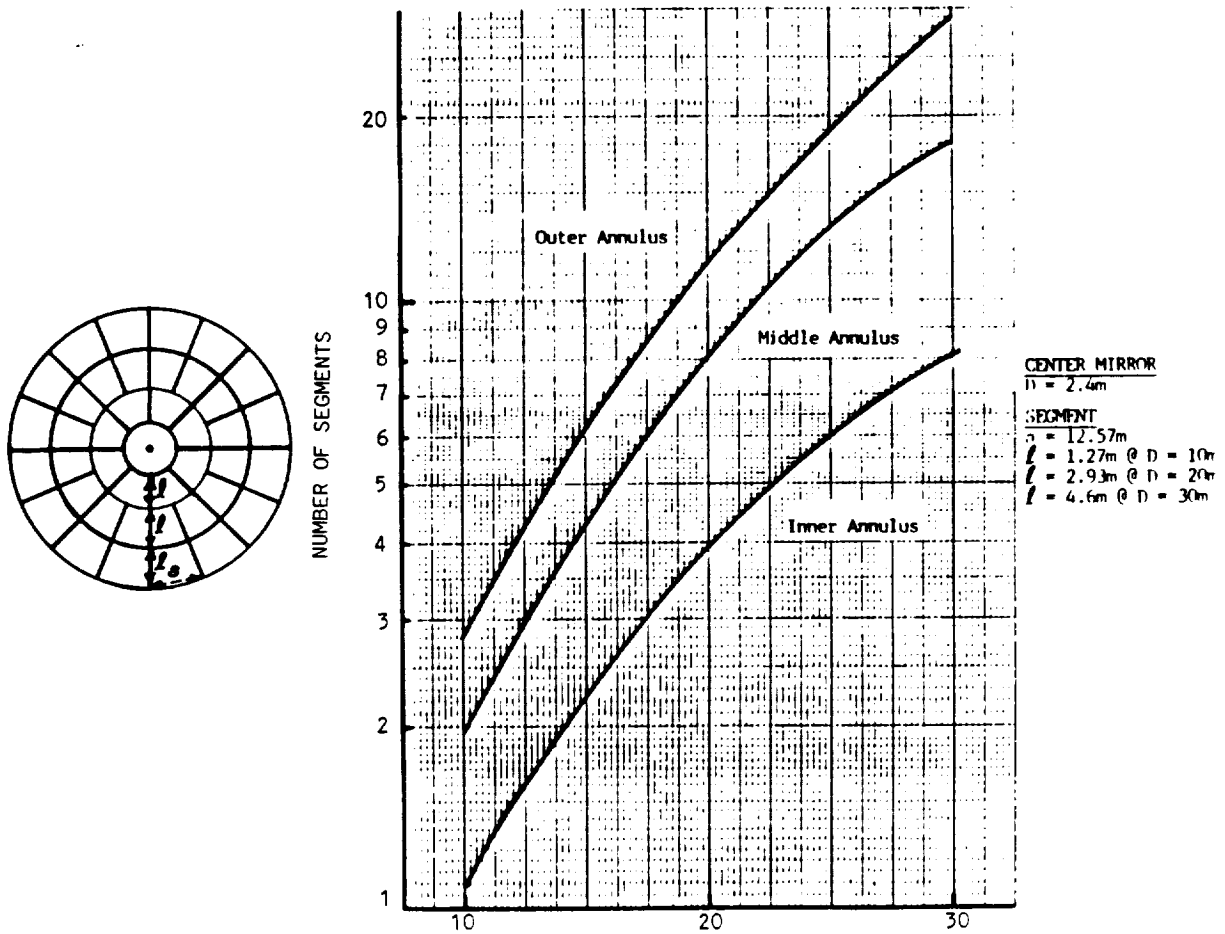
NUMBER OF TRAPEZOIDAL SEGMENTS IN DOUBLE ANNULUS

Figure 3.4-10



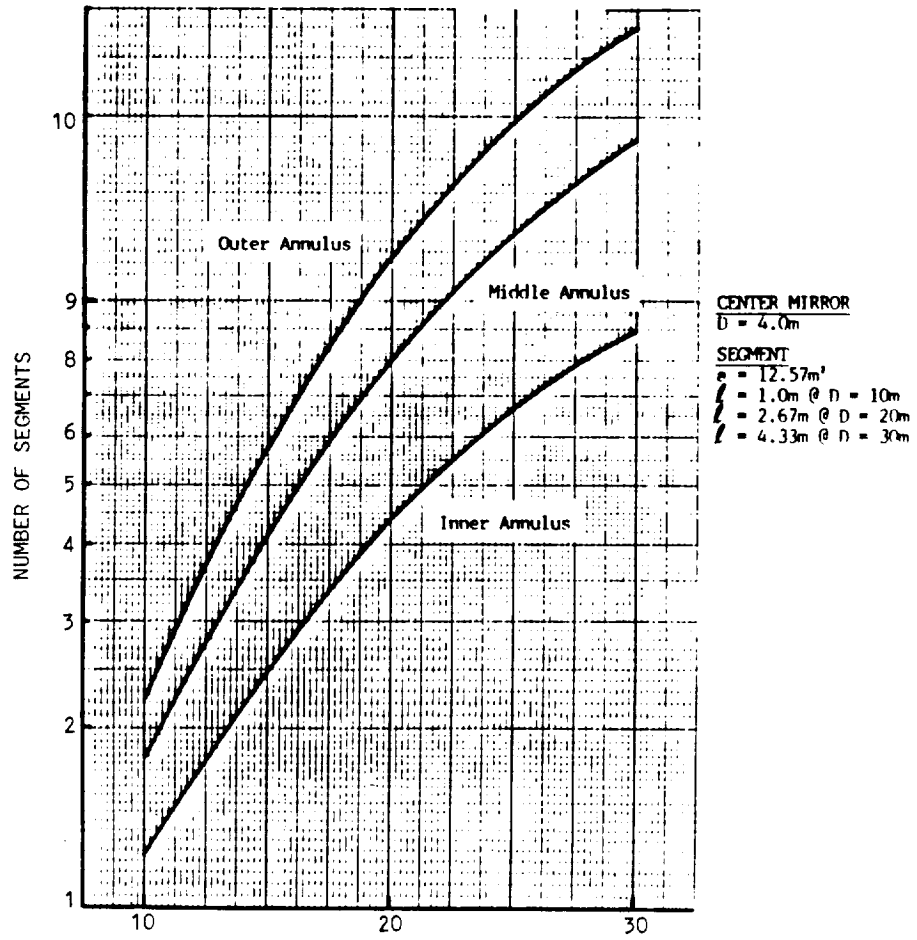
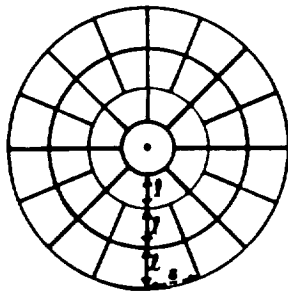
NUMBER OF TRAPEZOIDAL SEGMENTS IN TRIPLE ANNULUS

Figure 3.4-11



NUMBER OF TRAPEZOIDAL SEGMENTS IN TRIPLE ANNULUS

Figure 3.4-12



NUMBER OF TRAPEZOIDAL SEGMENTS IN TRIPLE ANNULUS

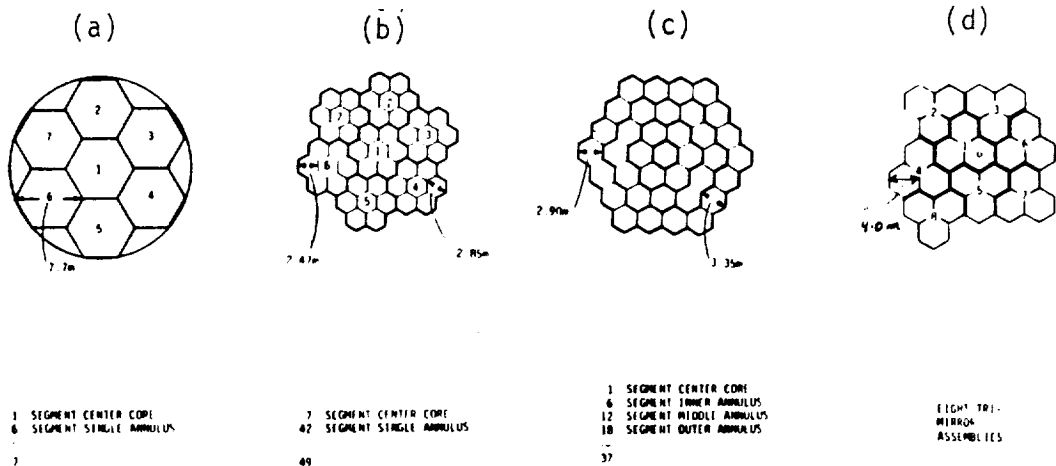
Figure 3.4-13

TABLE 3.4-2  
 PRIMARY MIRROR WITH TRAPEZOIDAL SEGMENTS  
 (DIAMETER = 20 METERS)

<u>Option I</u>	<u>Number of Segments</u>	<u>Radial Length (m)</u>	<u>Chord Length (m)</u>
Center Core	1	2.0	
Inner Annulus	4	2.7	6.6
Middle Annulus	8	2.7	5.7
Outer Annulus	12	2.7	5.2
<b>TOTAL</b>	<b>25</b>		

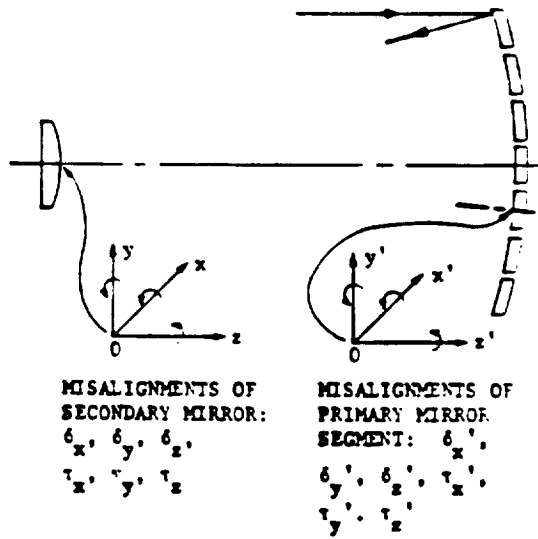
<u>Option II</u>	<u>Number of Segments</u>	<u>Radial Length (m)</u>	<u>Chord Length (m)</u>
Center Core	1	2.0	
Inner Annulus	8	2.7	3.3
Middle Annulus	16	2.7	2.85
Outer Annulus	24	2.7	2.6
<b>TOTAL</b>	<b>49</b>		



PRIMARY MIRROR WITH HEXAGONAL SEGMENTS  
 (20 METER DIAMETER)

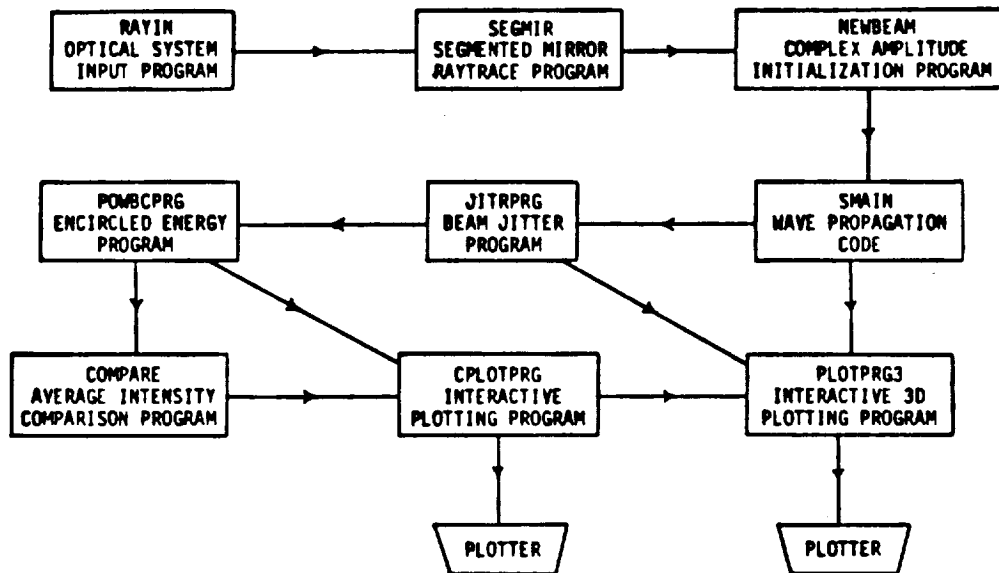
Figure 3.4-14





RIGID BODY MOTIONS OF SEGMENTED MIRROR

Figure 3.4-15



PROGRAM FLOW FOR PHASED ARRAY SOFTWARE

Figure 3.4-16

TABLE 3.4-3  
WAVEFRONT PROPAGATION MODEL FOR A SEGMENTED MIRROR

- OPTIMUM OPTICAL SYSTEM CONFIGURATION
  - Reflective Versus Refractive Elements
  - Conic Surfaces or Rotationally Symmetric General Aspheres
  - Elliptical or Multisided Apertures, Obscurations, and Surface Boundaries
  - Off-Axis Elements
- DEVELOP BUDGETS FROM PERFORMANCE SPECIFICATIONS
  - Segment Tilt
  - Segment Piston
  - Segment Radius of Curvature
  - Segment Surface Figure
- OPTIMUM NUMBER OF SEGMENTS
  - Function of Primary Mirror F-Number
  - Function of Alignment Accuracy
  - Function of Surface Figure Manufacturing Accuracy
  - Function of Edge Length Per Unit Area
- OPTIMUM SHAPE (TRAPEZOIDAL VERSUS HEXAGONAL)
  - Far-Field Diffraction Pattern
  - Edge Length Per Unit Area
  - Aspheric Departure within Segment

The wave front propagation model can be used in the selection of important parameters for LDR.

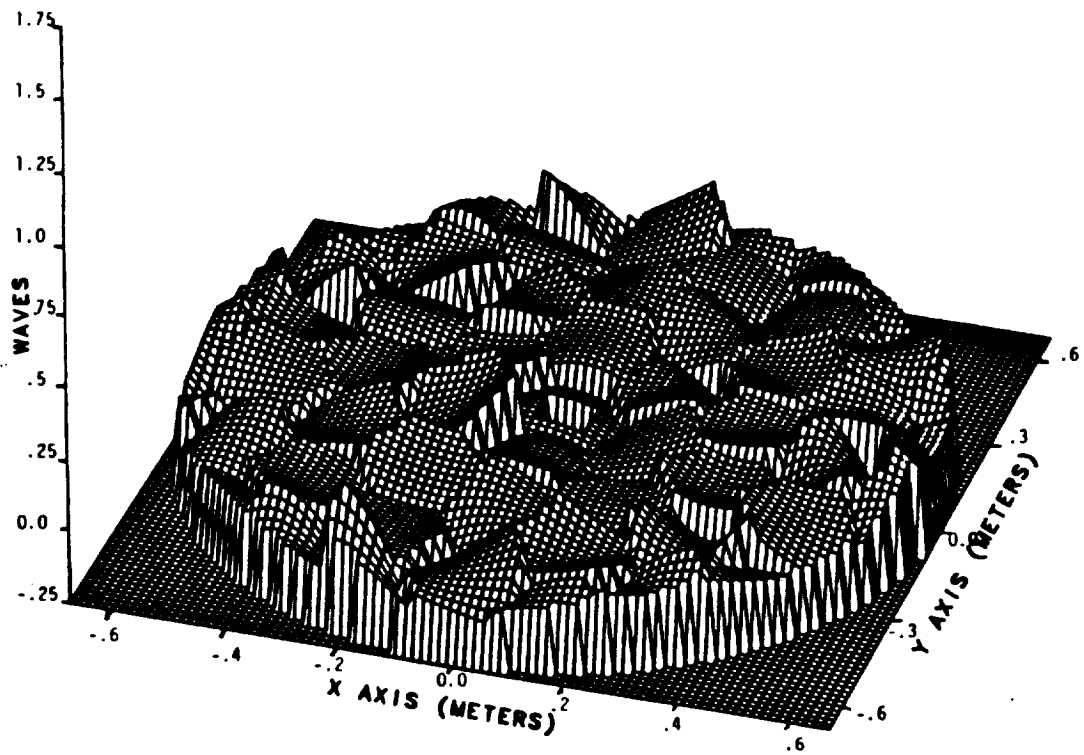
Shown in Figures 3.4-17 and 3.4-18 are the wave front maps for the trapezoidal and hexagonal segmented primary mirrors. The resultant radial energy distributions for varying wave front errors is shown in Figure 3.4-19. From this analysis the requirements on the primary mirror segment were established (Table 3.4-4). The primary mirror wave front error budget established in this study is shown in Figure 3.4-20.

TABLE 3.4-4  
PRIMARY MIRROR REQUIREMENTS

- Segment Surface Quality	0.45 Micrometer RMS
- Radius Mismatch	50 RPM
- Piston Error	1.3 Micrometers
- Tilt Error	0.6 Microradian

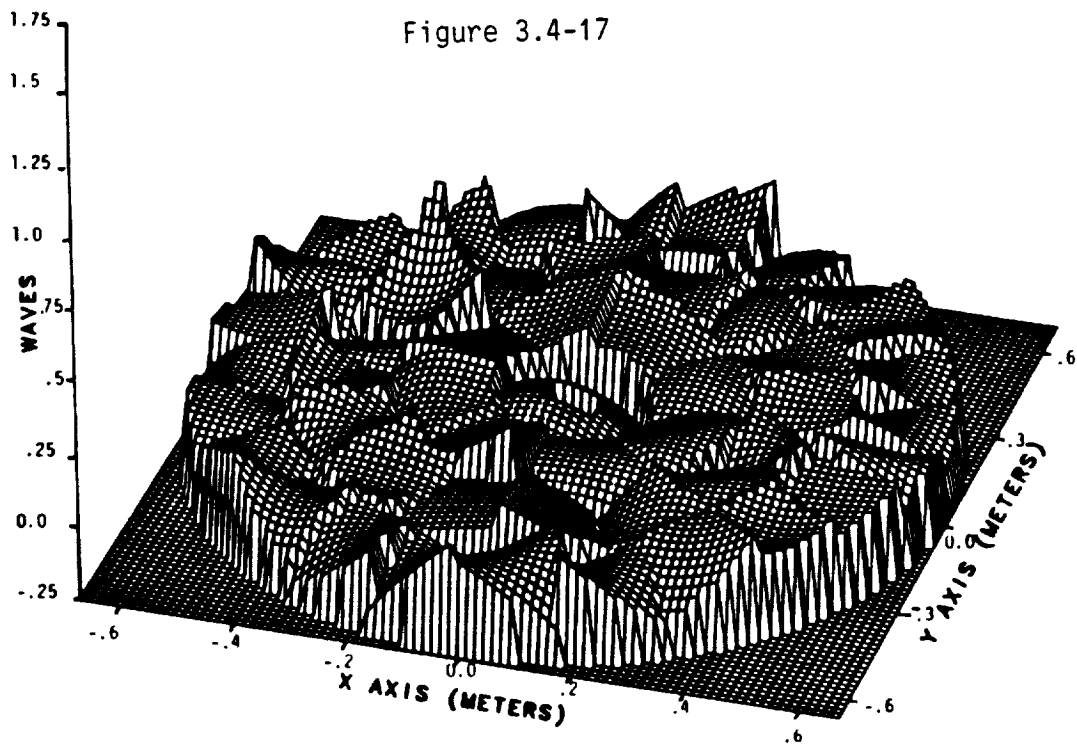
With segment surface quality, radius matching, and rigid body motion requirements known, two versions of a segmented mirror can be addressed. If the surface quality of the off-axis segment and the radius matching requirement can be manufactured and retained during on-the-ground testing, then we have a case in which only segment alignment (that is, segment tilt and segment piston error) need be sensed and controlled during operation in orbit. This case we call a passive segmented mirror. However, if the quality and/or the radius matching requirements cannot be manufactured and retained during on-ground testing, then the figure and/or radius must be sensed and controlled during operation in orbit. In addition, the rigid body motions of segment tilt and piston error must also be sensed and controlled. This latter case is what we call an active segmented mirror.

Two candidate materials (glass and composite) are being considered for use in a passive segmented mirror concept. For diffraction limited performance at wavelengths as low as 30 micrometers and operation at 200 K a material with low CTE and homogeneity is required. The technology development plan suggests investigating a new glass for LDR. An early evaluation indicates fused silica doped with approximately 3% titanium dioxide should meet the requirements. Anisotropic CTE is currently a problem with composite materials for mirrors. Can a new composite material be developed to maintain the surface figure quality passively? Shown in Figure 3.4-21 is a preliminary concept for a passive segment using a composite material. In Figure 3.4-22 is a similar concept for an active segment. A comparison of the mirror segment designs is shown in Figure 3.4-23.



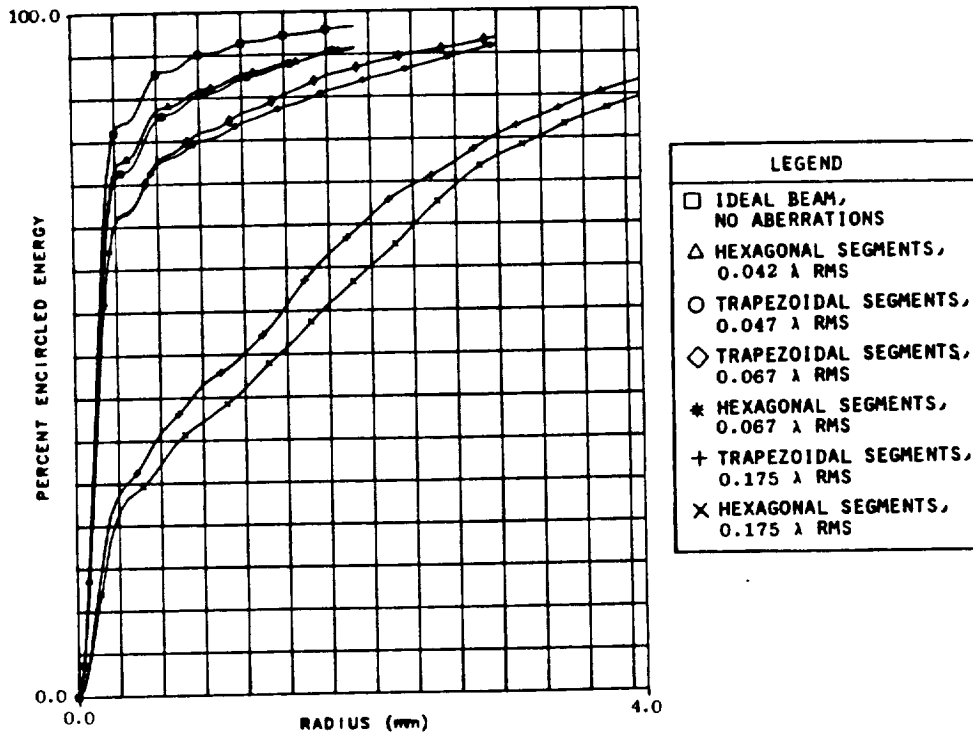
SIMULATION OF WAVEFRONT FROM ON-AXIS CASSEGRAIN TELESCOPE  
(HEXAGONAL SEGMENTS)

Figure 3.4-17

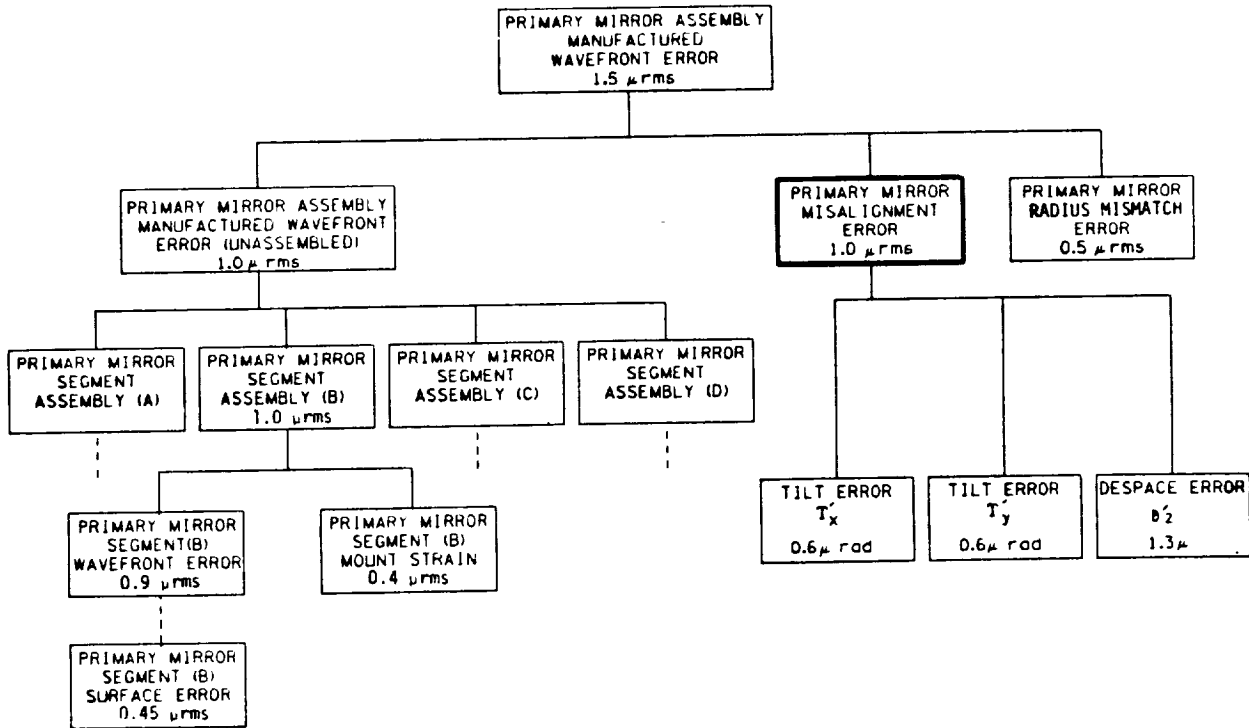


SIMULATION OF WAVEFRONT FROM ON-AXIS CASSEGRAIN TELESCOPE  
(TRAPEZOIDAL SEGMENTS)

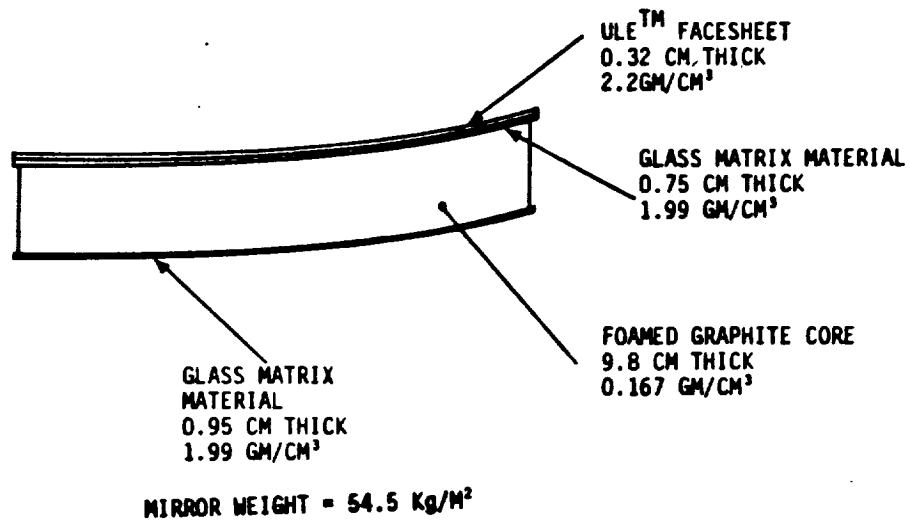
Figure 3.4-18



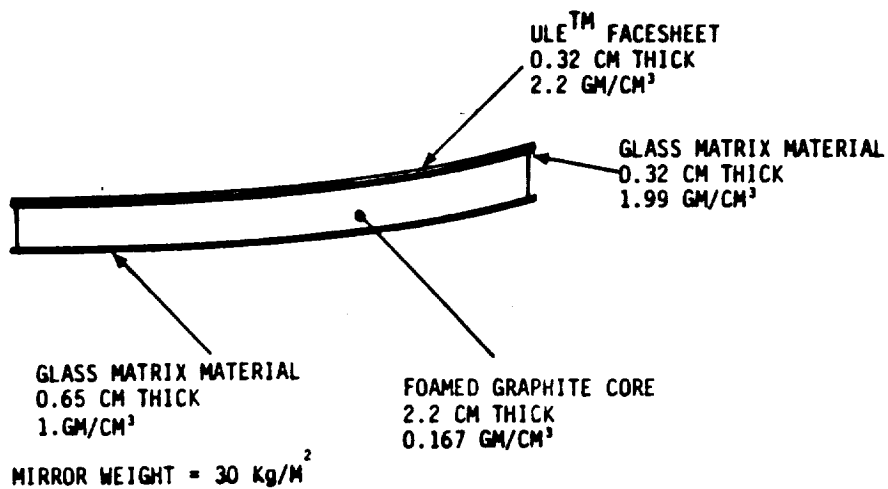
ENCIRCLED ENERGY DISTRIBUTIONS FOR IDEAL AND ABERRATED BEAMS  
Figure 3.4-19



PRIMARY MIRROR WAVEFRONT ERROR BUDGET  
Figure 3.4-20



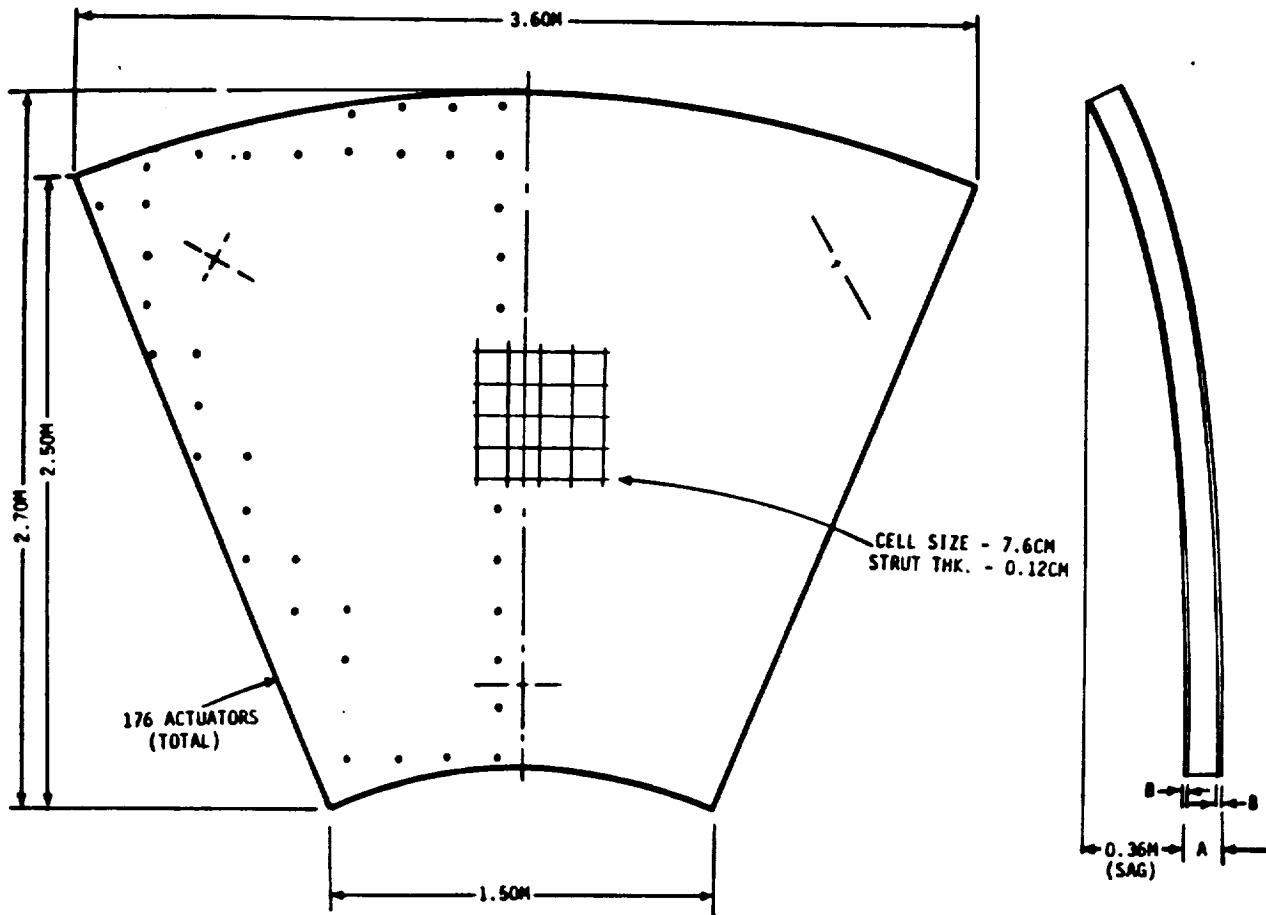
COMPOSITE MIRROR BLANK  
(PASSIVE DESIGN)  
Figure 3.4-21



COMPOSITE MIRROR BLANK  
(FLEXIBLE DESIGN)  
Figure 3.4-22

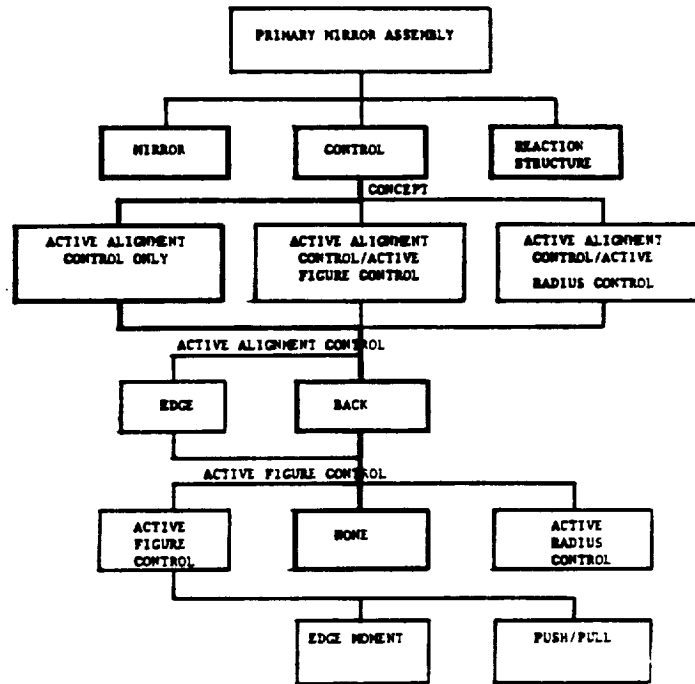
ULE™ MIRROR

	FLEXIBLE	PASSIVE
A	3.8CM	10.2CM
B	0.65CM	0.95CM
WT	28.8kg/M <sup>2</sup>	42.7kg/M <sup>2</sup>



TYPICAL SEGMENT  
 (20.0 M MIRROR)  
 Figure 3.4-23

3.4.3.2 Primary Mirror Control - The primary mirror control trade tree is shown in Figure 3.4-24. Since the mirror segments "butt" together, it can be assumed two translational degrees of freedom of segment centration and one rotational degree of freedom are constrained by adjacent segments. The unconstrained degrees of freedom of concern, are therefore, the two remaining rotations (segment tilt) and one translation (segment piston error).



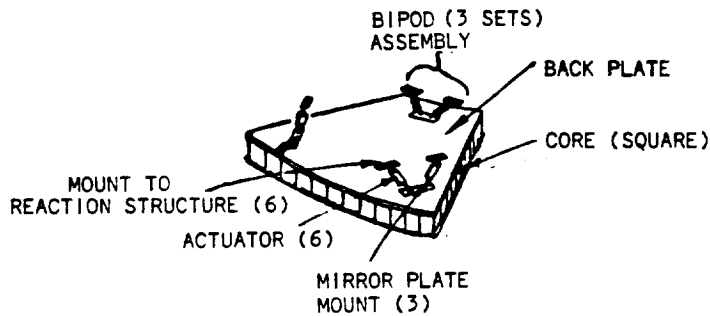
PRIMARY MIRROR CONTROL TRADES  
Figure 3.4-24

The rigid body misalignments, which must be sensed, are the unconstrained degrees of freedom of segment tilt and segment piston error. Two choices are possible. The first uses an external star source to monitor wave front error at system focus. The rigid body misalignments have to be implied from the wave front error. The second and preferred method is to monitor the rigid body motions directly using an internal sensing concept.

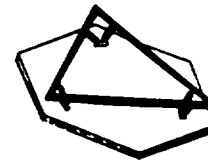
A capacitive sensing concept using capacitance changes to imply small displacements is currently preferred over concepts such as optical triangulation. The concept can retain long-term stability, large dynamic range, and sensitivity to a few nanometers under severe environmental conditions.

The three remaining "unconstrained" rigid body motions (two tilts and one piston) would be retained within the budgeted allocation via three sets of bipods with linear actuators. These bipods would be mounted to a delta frame reaction structure. These three tiers (mirror, rigid body actuators and delta frame) form a segment assembly. This concept is shown in Figure 3.4-25 for trapezoidal and hexagonal segments.





TRAPEZOIDAL FACEPLATE



HEXAGONAL FACEPLATE

- 3 BIPOD MOUNTS
- DELTA FRAME REACTION STRUCTURE

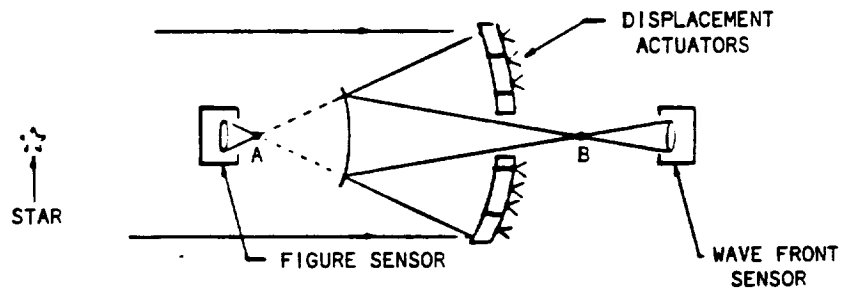
### PASSIVE SEGMENT ASSEMBLY OPTIONS

Figure 3.4-25

Radius matching between segments imposes a critical requirement on a coherently phased segmented mirror. If the radius matching requirement cannot be established and retained during on-ground testing, then the radius must be sensed and controlled during operation in orbit.

Representative of current technology is a concept derived from the SLCSAT program. A linear actuator could be mounted on the central hub of the reaction structure on the center of the mirror. This produces a change in the wave front error at the lowest spatial frequency (i.e., optical power). This change in power is directly related to a change in the radius of curvature.

Figure 3.4-26 illustrates a primary mirror control system representative of current technology for an active segmented mirror. The primary mirror figure control subsystem consists of push/pull or moment-type actuators on the primary mirror which are used to reduce the manufactured mirror surface error to lie within the allocated budget. In order to control the figure, the state of the figure is sensed via the primary mirror wave front sensing system (either closed-loop or open-loop). A figure sensor installed at the prime focus is, in practice, obstructed by the secondary mirror. A wave front sensor installed at the Cassegrain focus will monitor the total wave front error. In the active segmented case the total wave front error will be due to the rigid body misalignments of the secondary mirror, rigid body misalignments of the primary mirror segments, and the figure changes in the primary mirror.



- PRIMARY MIRROR FIGURE CONTROL SUBSYSTEM
  - PUSH/PULL OR MOMENT ACTUATORS ON PRIMARY MIRROR
- PRIMARY MIRROR WAVE FRONT SENSING SUBSYSTEM
  - WAVEFRONT SENSOR AT SYSTEM FOCUS MEASURING SYSTEM WAVE FRONT ERROR

### PRIMARY MIRROR CONTROL SYSTEM

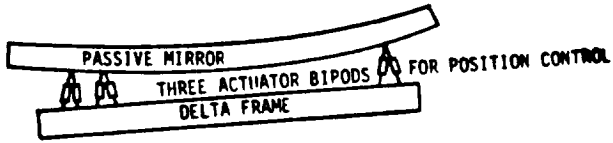
Figure 3.4-26

Shown in Figure 3.4-27 are concepts, established in this study, for a passive segment assembly and an active segment assembly.

**3.4.3.3 Primary Mirror Reaction Structure** - The primary mirror reaction structure trade tree is shown in Figure 3.4-28. The reaction structure must retain the mirror surface figure to fractions of the operational wavelength. A "true" metering structure philosophy allows the reaction structure to be the stable reference platform for the entire observatory. Graphite/epoxy is the state-of-the-art material for a "true" metering structure due to its excellent dimensional stability (CTE). Potential trouble areas are: structural joints, built in stresses, assembly variations, stress redistribution during repeat actuation, and outgassing. Metal matrix has tremendous potential but is an immature material relative to graphite/epoxy.

Candidate LDR primary mirror lightweight support structure concepts based on current technology are shown in Figure 3.4-29. Included are: a near isotropic tetrahedral truss, a deep isogrid truss, rib/ring and a multi-level structure.

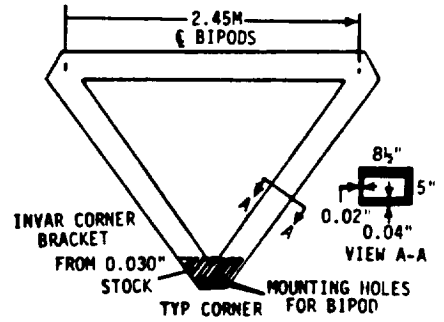
The tetrahedral truss was selected in this study. Trapezoidal aspect ratios near 1.0 yield the best truss geometry. Ground and orbital assembly operations will be simplest if the truss forward face segments have sufficient flexural stiffness to support the segments independent of the backup truss members. Shown in Figure 3.4-30 is a representative primary mirror assembly sequence. In this approach the tetrahedral truss is installed after the segment assemblies (mirror, actuators and delta frame).



TOTAL AREAL DENSITY  
(INCLUDES MIRROR, Δ FRAME,  
ACTUATORS)

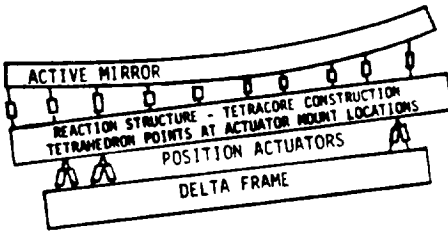
GLASS - 50 Kg/M<sup>2</sup>  
GL/GR - 61 Kg/M<sup>2</sup>

PASSIVE SEGMENT ASSEMBLY



TOTAL WEIGHT = 30 POUNDS  
INVAR WEIGHT = 15 POUNDS  
GR/EP WEIGHT = 15 POUNDS

DELTA FRAME



176 FIGURE ACTUATORS  
8" x 8" PATTERN

TOTAL AREAL DENSITY

GLASS - 85 Kg/M<sup>2</sup>  
GR/GL - 86 Kg/M<sup>2</sup>

ACTIVE SEGMENT ASSEMBLY

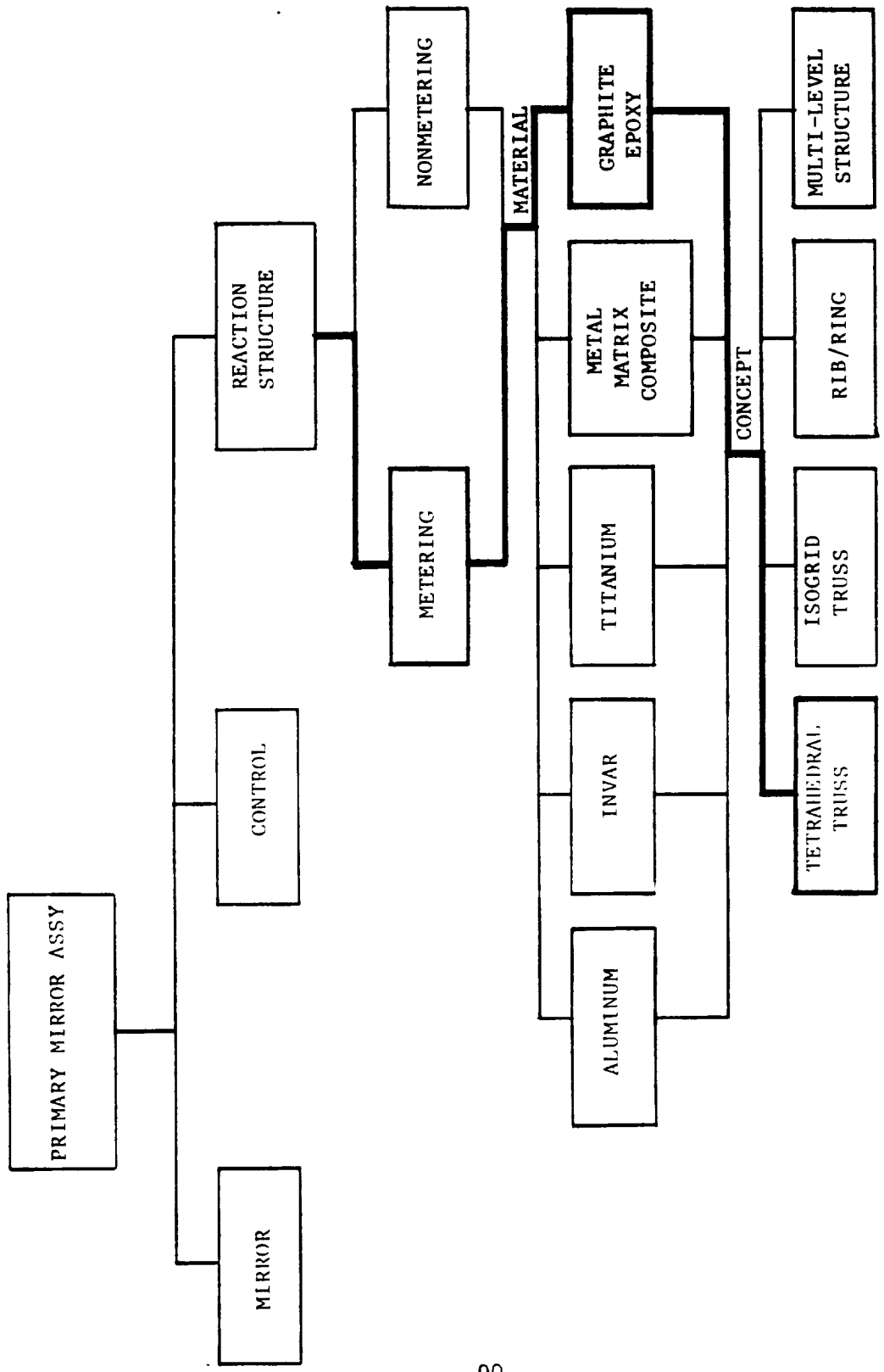


SAME SHAPE AS MIRROR BLANK  
TOTAL WEIGHT = 89 POUNDS (41 Kg)

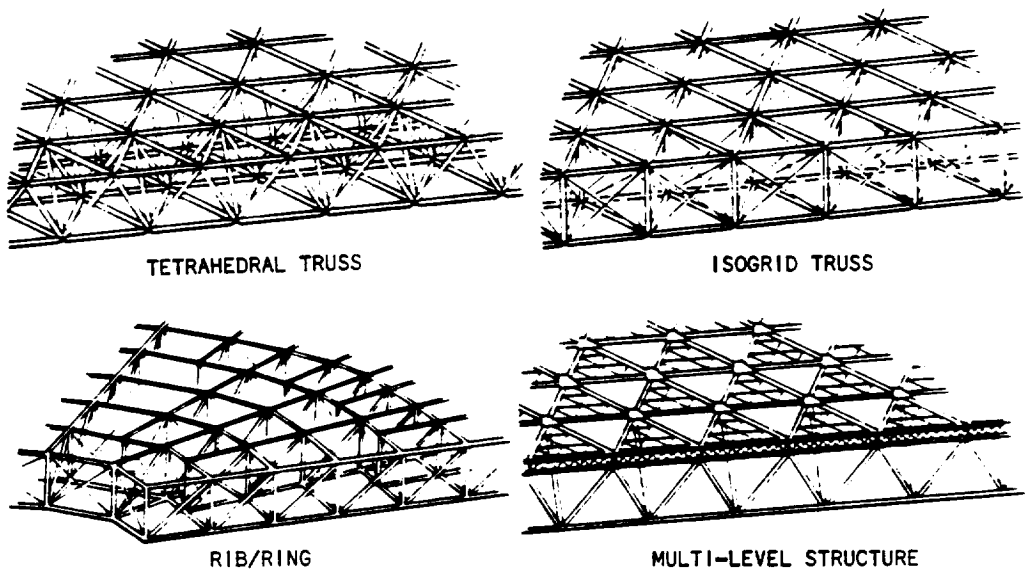
REACTION STRUCTURE

PASSIVE AND ACTIVE SEGMENT ASSEMBLY CONCEPTS

Figure 3.4-27

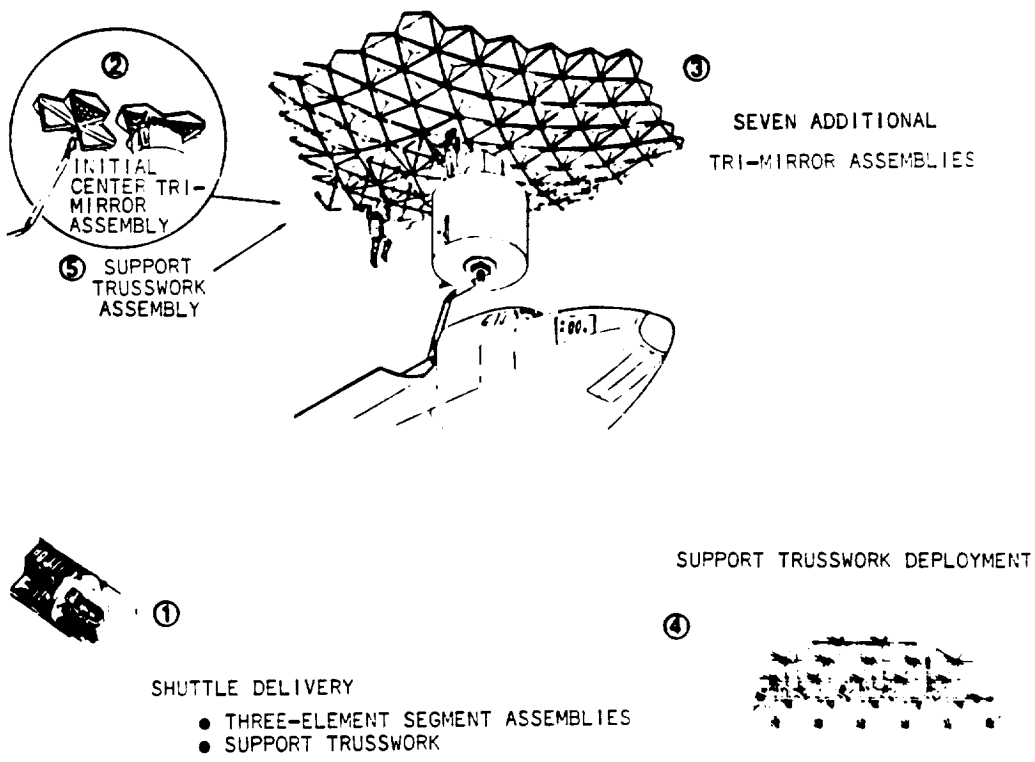


REACTION STRUCTURE TRADES  
Figure 3.4-28



CANDIDATE LDR PRIMARY MIRROR SUPPORT STRUCTURES

Figure 3.4-29



LDR PRIMARY MIRROR ASSEMBLY SEQUENCE IN ORBITER BAY

Figure 3.4-30

3.4.3.4 Mirror Surface Processing - Alternate surface processing methods are available in today's technology. The traditional method is in two steps: contour generation and polishing. The conventional aspheric generation approach uses loose abrasive grinding. Progression to the polishing task using spherical tools is at the point when the surface is within approximately one micrometer of the desired asphere. In the polishing step, the sag difference ( $\Delta$ sag) between the orthogonal radii extremes (zonal and meridional) determines the amount that a spherical polishing tool will "rock" if it fits the shorter of the two radii. The larger the tool diameter, the more the tool will obviously "rock".

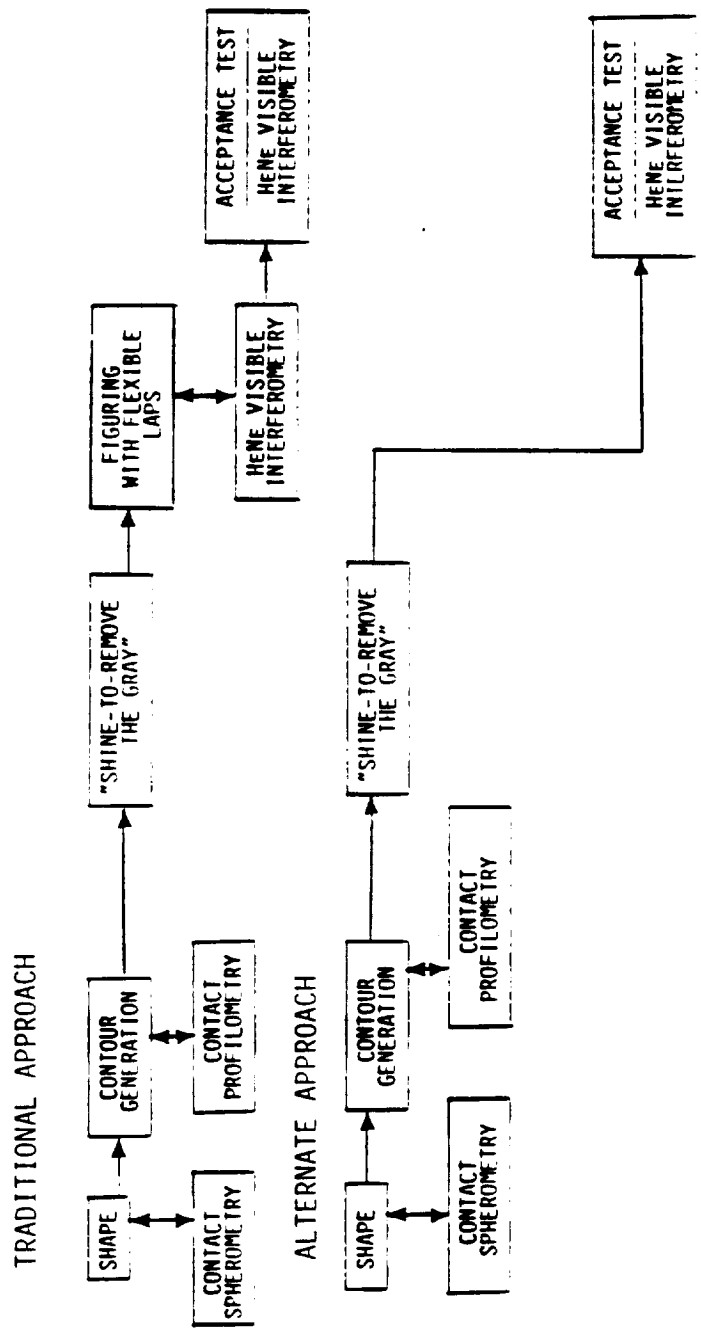
The wave front error maps, generated interferometrically, are separated into symmetrical and asymmetrical errors. Separate full aperture tools are fabricated which address the symmetrical and the asymmetrical errors.

Many mirror segments must be produced for the LDR primary reflector. The large aperture tooling approach at Kodak minimizes the mirror processing time (amount of time the tool is actually on the mirror). This allows parallel processing of mirror segments, thus reducing the need for a large number of machines. This will aid the replicability issue for LDR and is an attractive approach.

An alternate approach could eliminate the need for polishing. This alternate approach would extend the contour generation step past the traditional hand-off point of one micrometer to as close to the final desired asphere as possible. This maximizes the major material removal step (contour generation) and minimizes the polishing step. If the contour generation step (grinding) could reach the desired asphere, no formal polishing step would be required. The segment would require only a "shine to remove the grey" to meet the specularly requirement. Kodak has investigated and built a "proof-of-concept" contour generator under IR&D. It has been used successfully to generate large optics to tolerances similar to those of LDR. The two alternatives are shown in Figure 3.4-31.

#### 3.4.4 Conclusions

There are minor advantages (process tooling and structural options) of trapezoidal shaped segment over hexagonal shaped segment. To identify technology shortfalls, both options have been included in the system concepts. Glass/ceramics materials should meet the performance requirements utilizing only rigid body motion control of the mirror segments. Composite materials have potential in a concept utilizing rigid body motion control with radius/figure control of the mirror segments.



LDR PRIMARY MIRROR SEGMENT MANUFACTURE ALTERNATIVES

Figure 3.4-31

## 3.5 OPTICAL SUBSYSTEM CONCEPTS

### 3.5.1 Task

The fast primary mirror focal ratio ( $f/0.5$ ) implies extremely tight tolerances of secondary mirror metering. The purpose of this task was to evaluate options to meet the performance requirements.

### 3.5.2 Approach

In this study trade offs were evaluated in three areas affecting performance: secondary mirror, secondary mirror control, and the secondary mirror support structure. The optical subsystem concepts trade tree is shown in Figure 3.5.1.

### 3.5.3 Discussion

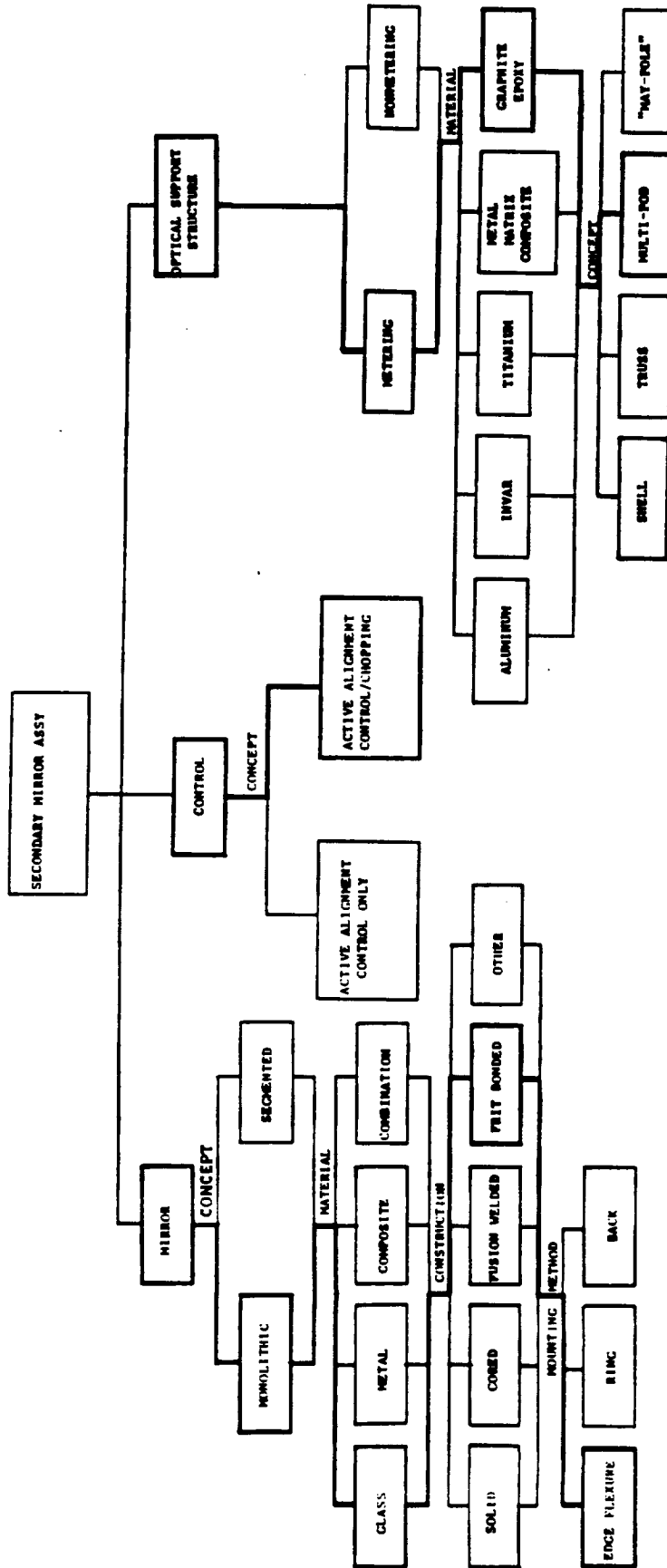
Because of the high asphericity of the LDR primary mirror ( $f/0.5$ ), the misalignments of the secondary mirror must be controlled to accuracy levels consistent with the allocated tolerances using rigid body actuators with a "true-metering" structure.

If the primary mirror can be coherently phased and isolated from mechanical and thermal stresses during assembly, launch, and operation, it can be established as the fixed reference for the telescope. Optical performance degradation will, therefore, be due to rigid body misalignments of the passive monolithic secondary mirror and rigid body misalignments of the focal plane structure relative to the focal surface.

Shown in Figure 3.5-2 is the baseline LDR wave front budget established in this study. Highlighted is the wave front allocation for secondary mirror misalignment (root sum square of the rms wave front errors due to tilt, decentration and despace of the secondary mirror). The change in the secondary mirror-to-primary mirror spacing imposes the tightest requirement. This is due to the fast aspheric secondary mirror which magnifies the primary mirror focal ratio of 0.5 into a Cassegrain system focal ratio of 10. This spacing change is magnified by the secondary mirror into a large focus error at the scientific instrument detector surface. Shown in Figure 3.5-3 is a wave front budget reallocated to increase the allowable error for secondary mirror misalignment. The minimum operational wavelength has been increased from 30 micrometers to 50 micrometers. The allowable encircled energy in the central disk of the point spread function has been reduced from 84% to 30%. The resultant allowable physical despace error is shown in Figure 3.5-4. As can be seen in Figure 3.5-5 this stringent requirement can also be relieved by increasing the minimum operational wavelength.

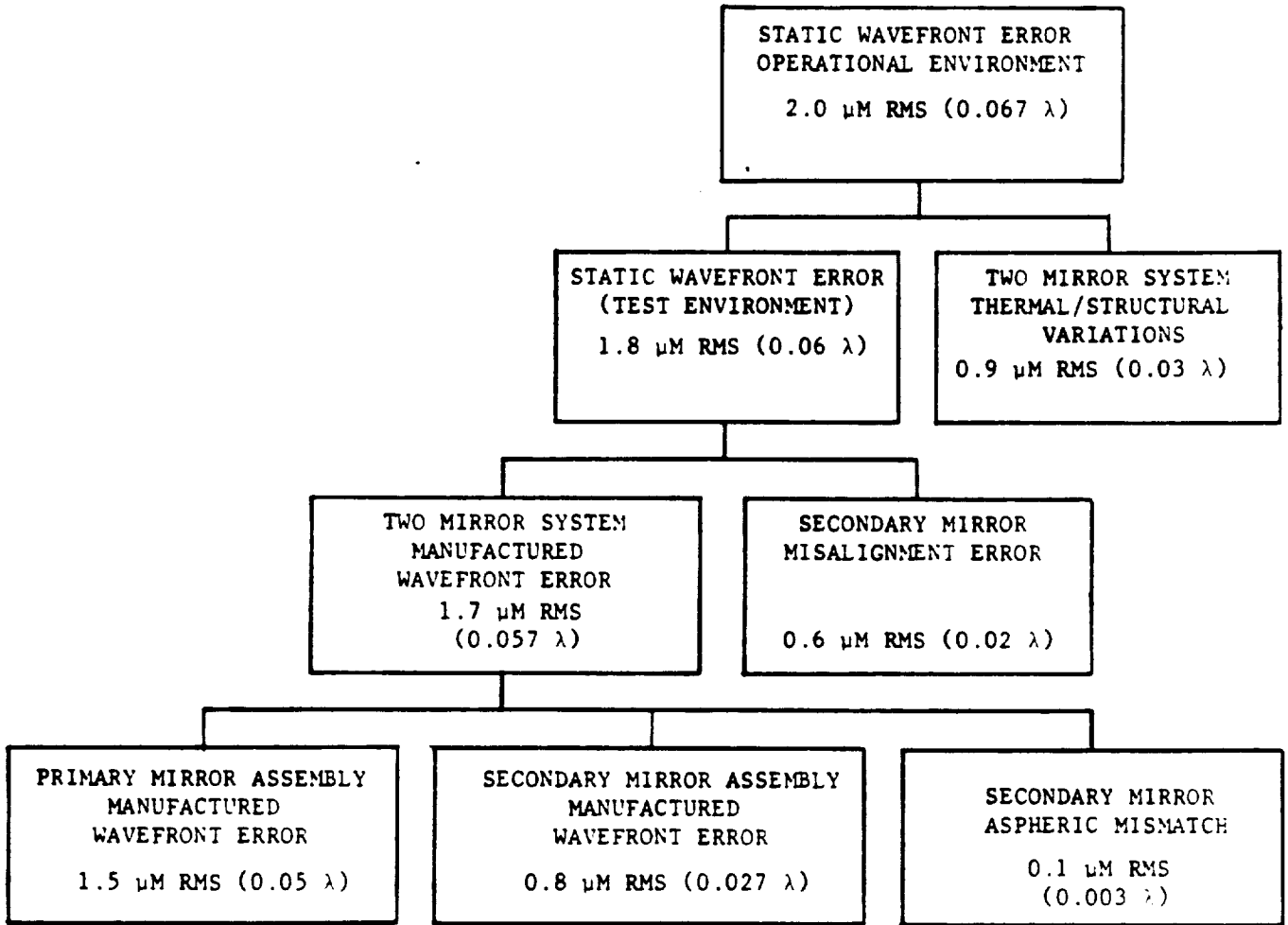
**3.5.3.1 Secondary Mirror** - The trade tree for the secondary mirror is shown in Figure 3.5-6. The secondary mirror in the Cassegrain optical configuration has a clear aperture of 1.3 meters. A monolithic (one-piece) mirror is an obvious choice over a segmented mirror in this size domain. Shown in Figure 3.5-7 is the instantaneous CTE of Corning fused silica materials. The CTE of fused silica (without doping) is near zero at the secondary mirror operational temperature of 125°K. State-of-the-art lightweighting techniques (such as fusion welding and frit bonding) can be readily applied to glass mirrors of this size. Therefore, a frit-bonded, fused silica secondary was established as the baseline for LDR.





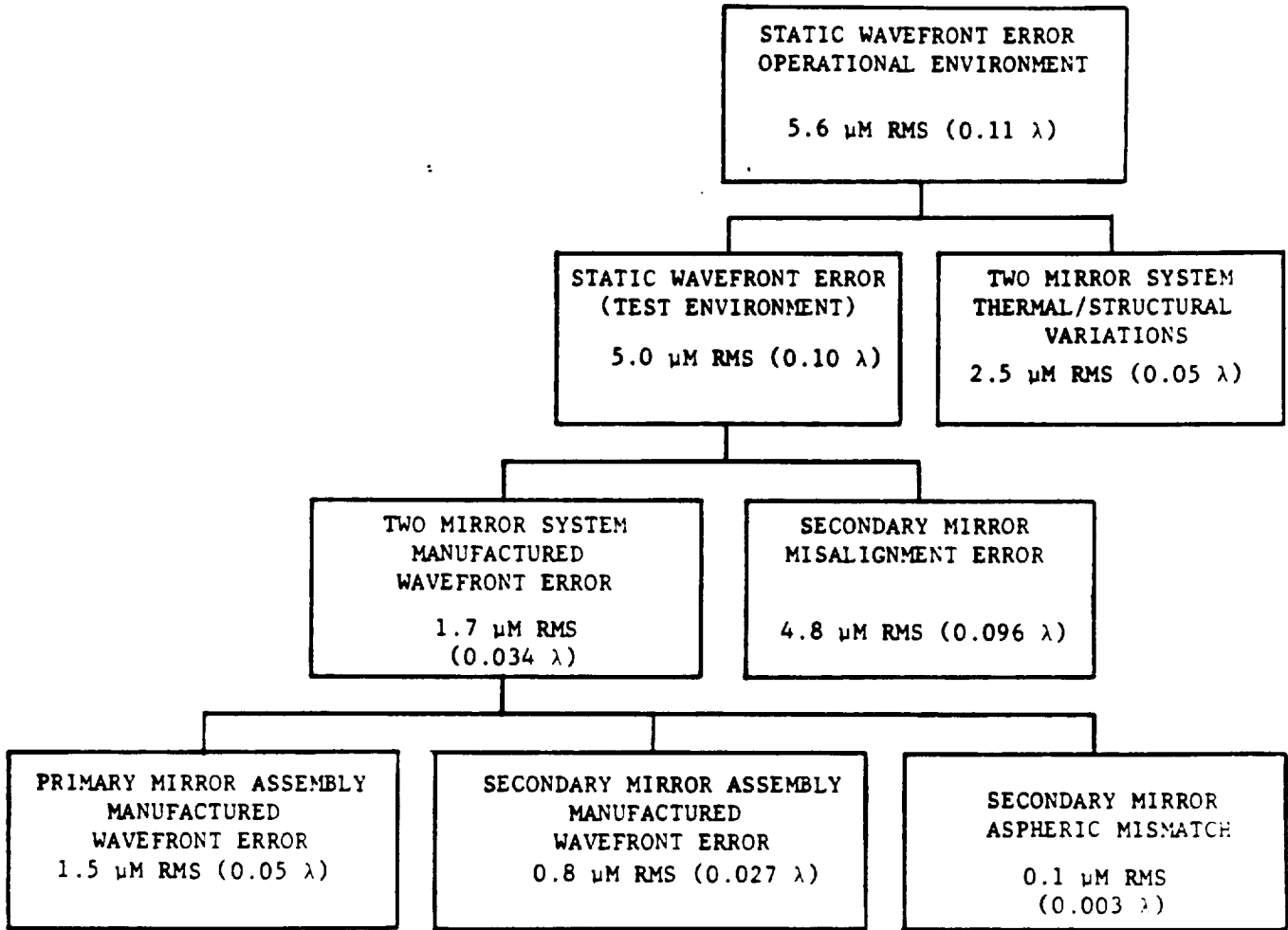
OPTICAL SUBSYSTEMS CONCEPTS TRADE TREE

Figure 3.5-1



LDR OPTICAL SUBSYSTEM  
 OPERATIONAL PERFORMANCE PREDICTION  
 ( $\lambda$  MIN = 30  $\mu$ M; E = 84%; D = 20 M)

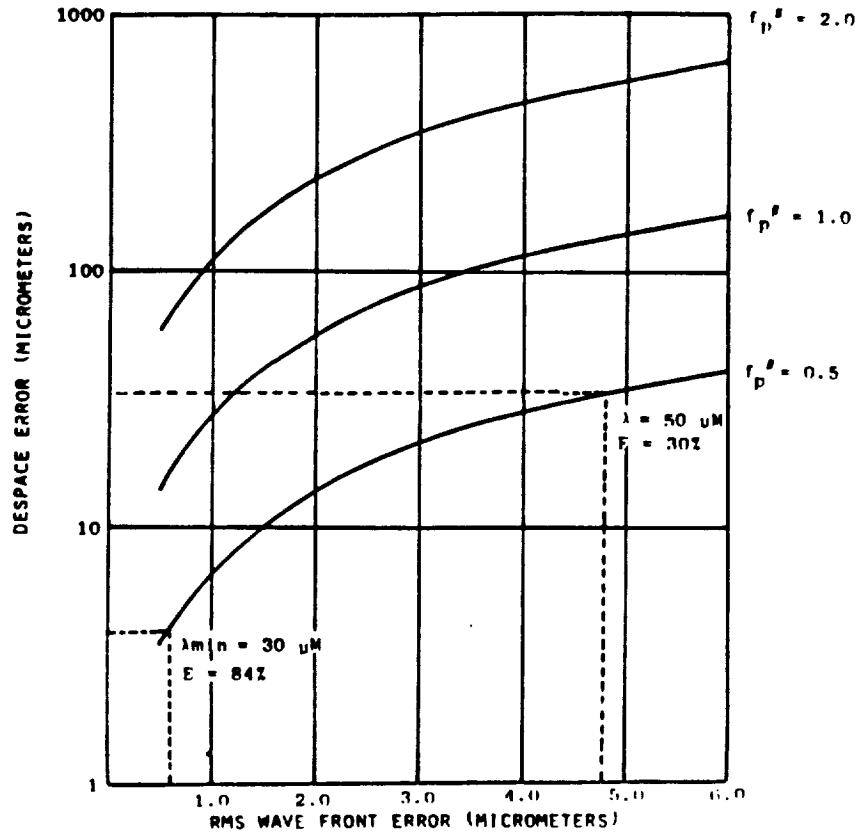
Figure 3.5-2



\*WORST CASE (ASSUMES SM MISALIGNMENT ERROR GETS TOTAL INCREASE)

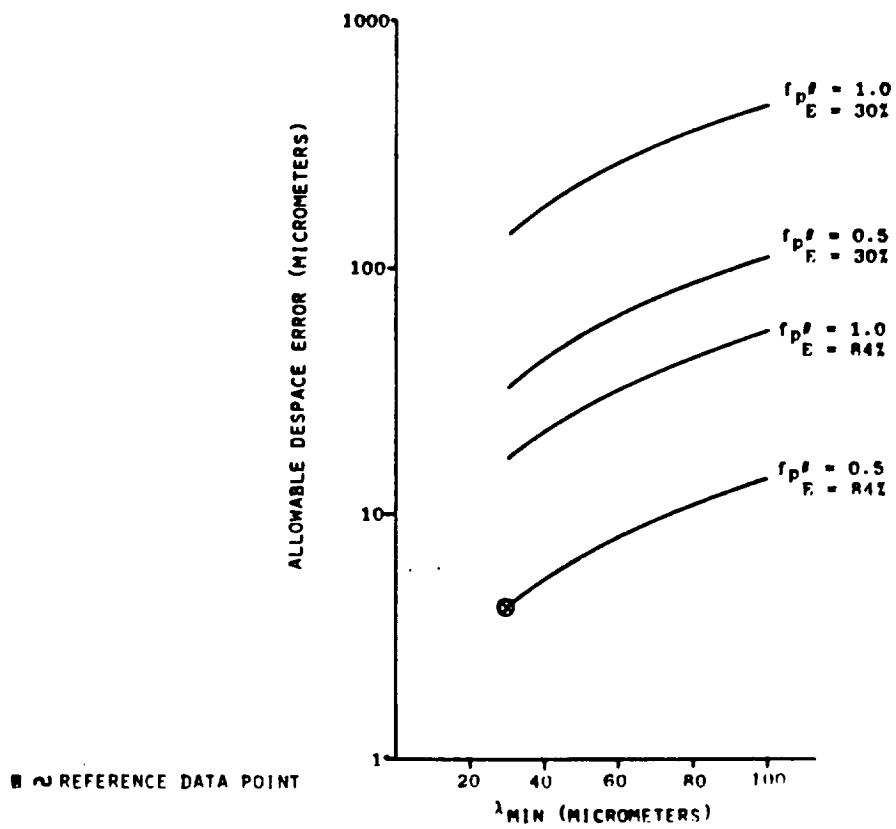
LDR OPTICAL SUBSYSTEM  
 OPERATIONAL PERFORMANCE PREDICTION (REALLOCATED TO INCREASE  
 SECONDARY MIRROR MISALIGNMENT ALLOWABLE ERROR)\*  
 (λ MIN = 50 μM; E = 30%; D = 20 M)

Figure 3.5-3



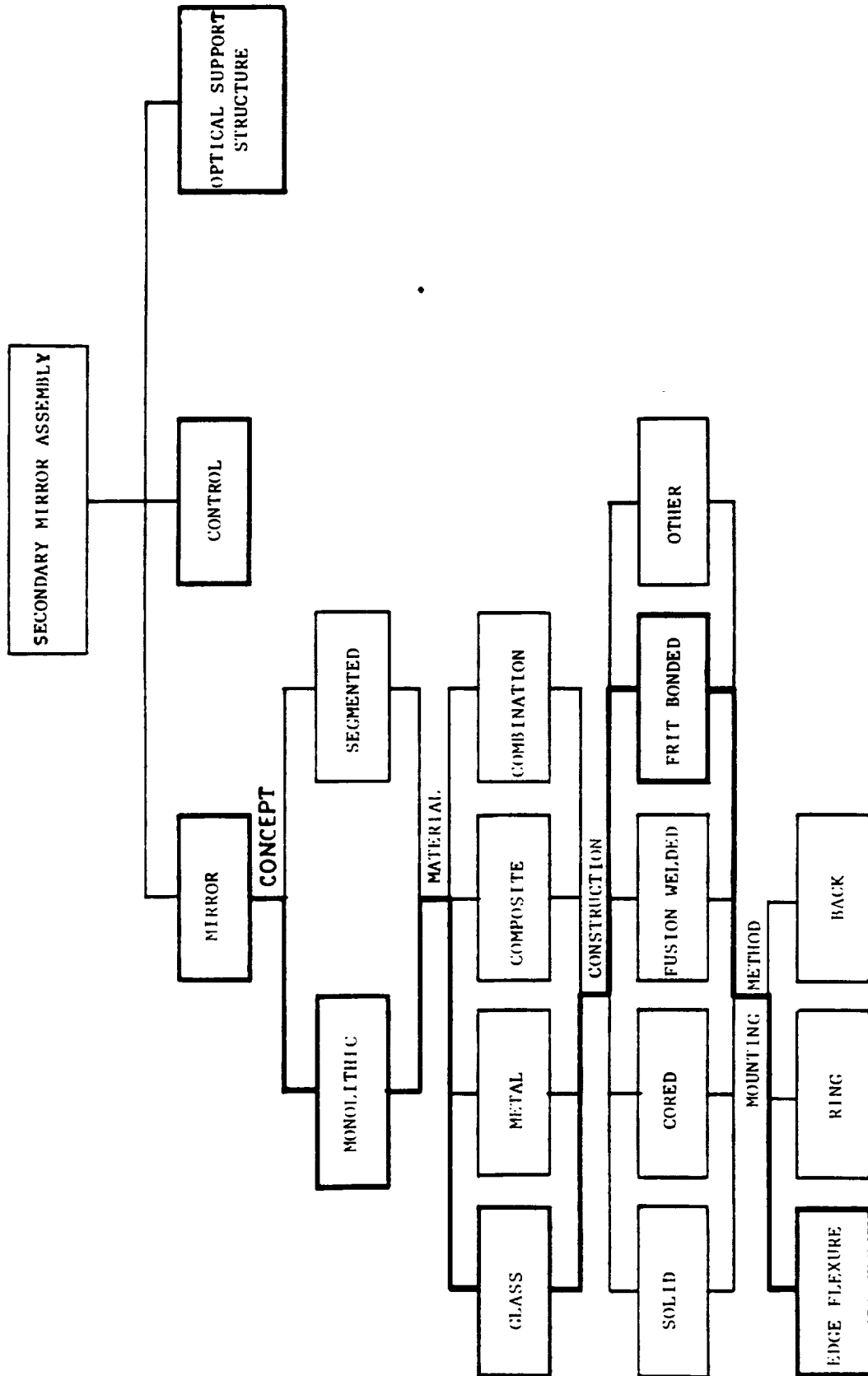
ALLOWABLE DESPACE ERROR

Figure 3.5-4



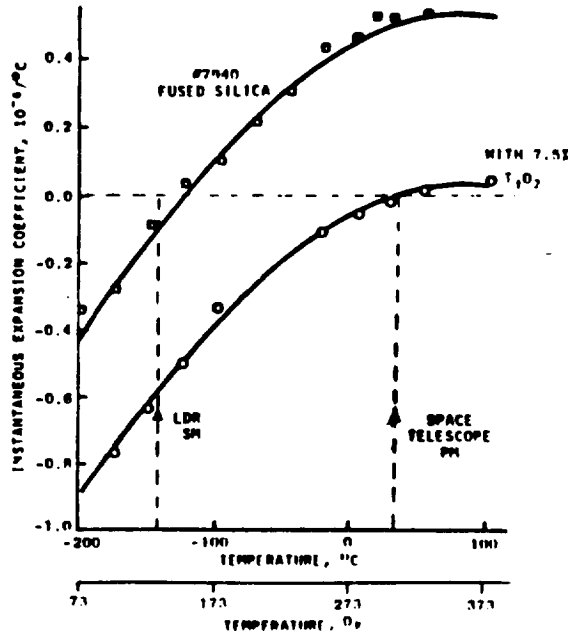
ALLOWABLE DESPACE ERROR

Figure 3.5-5



SECONDARY MIRROR TRADES

Figure 3.5-6

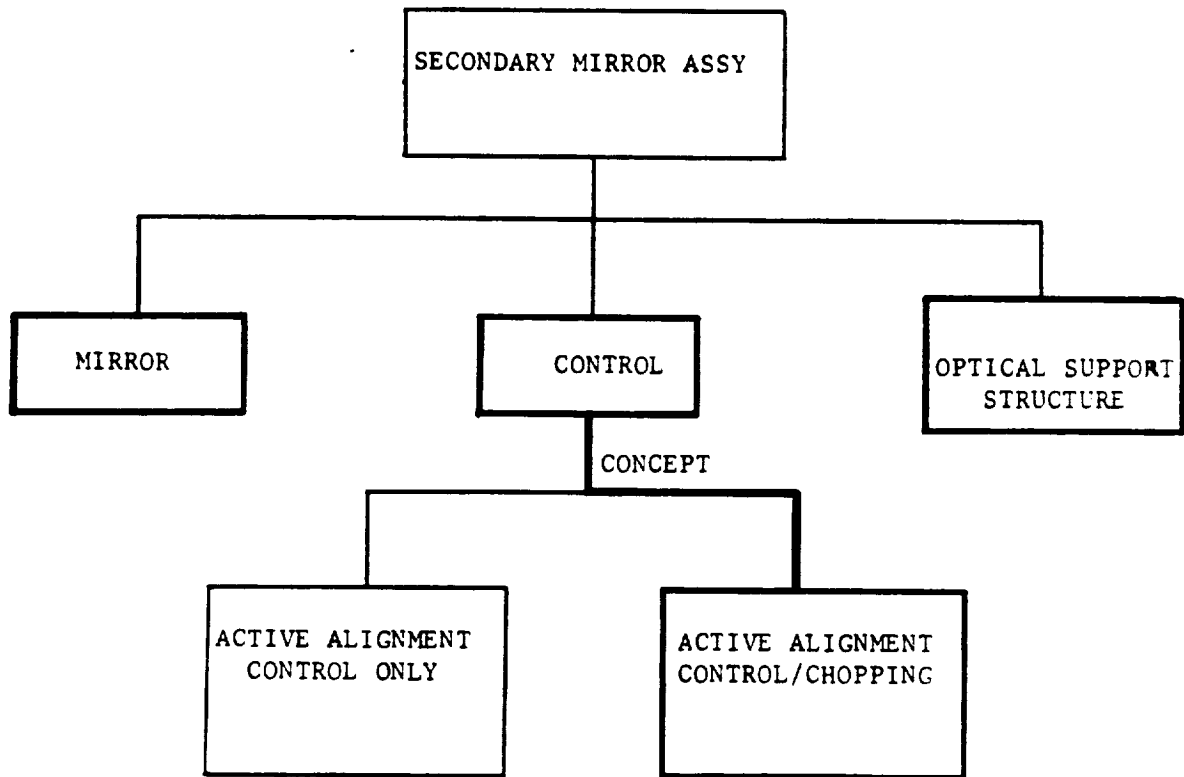


INSTANTANEOUS THERMAL EXPANSION OF FUSED SILICA  
Figure 3.5-7

3.5.3.2 Secondary Mirror Control - The trade tree for secondary mirror control is shown in Figure 3.5-8. The baseline secondary mirror wave front error budget is shown in Figure 3.5-9. The rigid body motions of concern are referenced to the secondary mirror vertex (Figure 3.5-10).

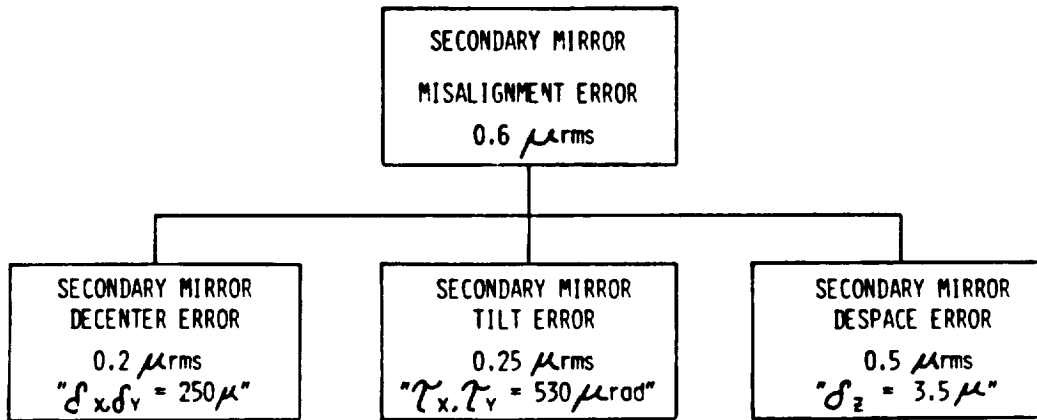
The functions of the secondary mirror control subsystem are to:

- (1) Sense the condition of secondary mirror optical axis to primary mirror optical axis misalignment ( $\delta_x, \delta_y, \tau_x, \tau_y$ ).
- (2) Sense the condition of focus ( $\delta_z$ ).
- (3) Define the relative positions of the focal surface(s) with respect to reference mounting surfaces on the focal plane structure.
- (4) Provide the means by which alignment and focus can be adjusted (between operational sequences).
- (5) Provide the means for chopping (during operational sequence). Alternate locations are also being considered.



SECONDARY MIRROR CONTROL TRADES  
Figure 3.5-8

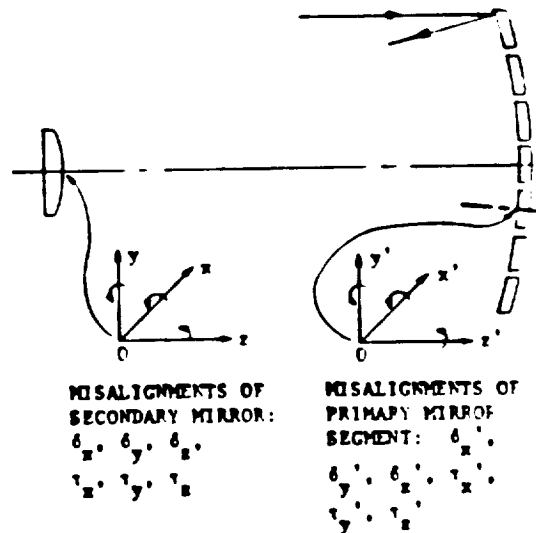




SECONDARY MIRROR WAVEFRONT ERROR BUDGET

( $\lambda$  MIN = 30  $\mu$ M; E = 84%)

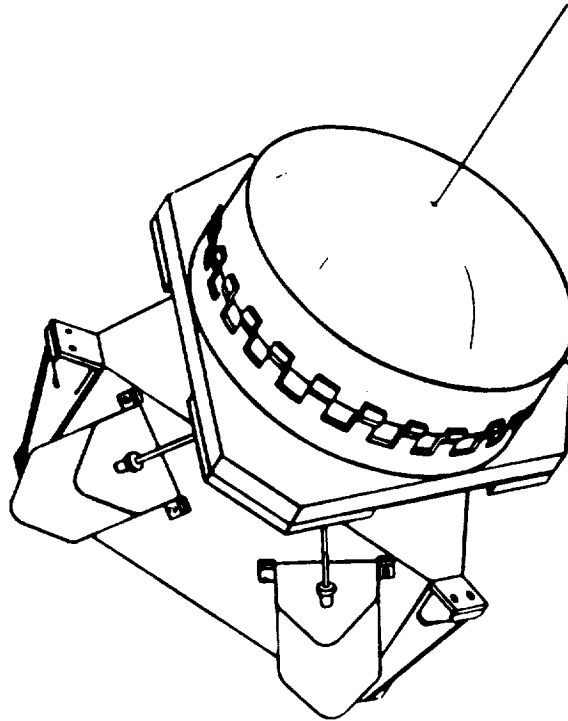
Figure 3.5-9



RIGID BODY MOTIONS OF CASSEGRAIN TELESCOPE

Figure 3.5-10

Shown in Figure 3.5-11 is a sketch of a breadboard control concept consisting of six linear actuators to control secondary mirror misalignment with respect to the fixed primary mirror (two decenters, two tilts, and despace). Only five linear actuators are actually needed, but the sixth actuator would be provided for redundancy.



SECONDARY MIRROR ASSEMBLY WITH RIGID BODY MOTION CONTROL  
Figure 3.5-11

Secondary mirror alignment and focus sensing options are summarized in Tables 3.5-1 and 3.5-2. The approach that directly monitors the rigid body motions of the secondary mirror ( $\delta_x$ ,  $\delta_y$ ,  $\delta_z$ ,  $\tau_x$ ,  $\tau_y$ ) is preferred in most cases for a space telescope, since it can be conceptually demonstrated via on-ground measurement/verification techniques that on-orbit alignment of the secondary mirror to the primary mirror axes can be accomplished. The focal surface topography can also be determined on the ground with a focal surface reference fixture (FSRF). Direct rigid body motion monitoring, therefore, conceptually permits complete alignment to the designed performance under simulated zero-g conditions. The telescope's secondary mirror would be realigned and focused to the primary mirror after launch using the secondary mirror control system to restore factory-level optical performance. After initialization on-orbit, the telescope would not require focus or alignment adjustments during extended operation. (NOTE: This assumes true-metering structure philosophy with an active thermal control system.)

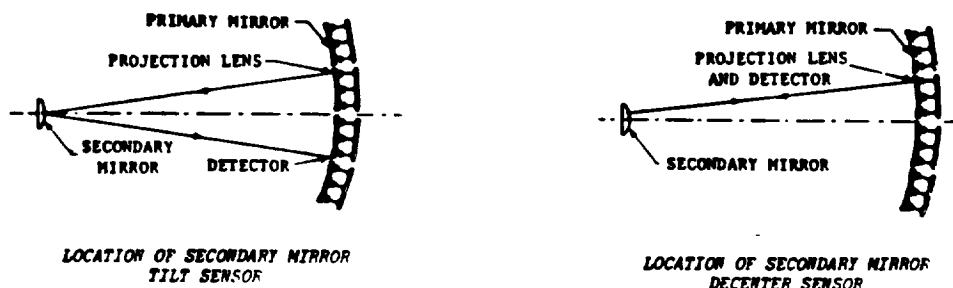
TABLE 3.5-1  
SECONDARY MIRROR ALIGNMENT SENSING CONCEPTS

- INTERNAL ALIGNMENT SENSING (SELF-ILLUMINATED)
  - MEASURE MISALIGNMENTS DIRECTLY USING SEPARATE TILT ( $\tau_x, \tau_y$ ) AND DECENTER ( $\delta_x, \delta_y$ ) SENSORS
  - CALCULATE OPTICAL DEGRADATION INDIRECTLY
  - INTEGRAL WITH THE PRIMARY AND SECONDARY MIRRORS
  - INDEPENDENT OF FOCUS CONDITION
- EXTERNAL ALIGNMENT SENSING (STAR FIELD)
  - MEASURE OPTICAL DEGRADATION DUE TO MISALIGNMENTS DIRECTLY WITH WAVEFRONT SENSORS
  - CALCULATE MAGNITUDE AND DIRECTION OF TILTS AND DECENTERS INDIRECTLY
  - NOT INTEGRAL WITH THE PRIMARY AND SECONDARY MIRRORS
  - HIGHLY DEPENDENT ON FOCUS CONDITION

TABLE 3.5-2  
SECONDARY MIRROR FOCUS SENSING CONCEPTS

- INTERNAL FOCUS SENSING (SELF - ILLUMINATED)
  - LINEAR RELATIONSHIP BETWEEN CHANGE IN MIRROR SPACING ( $\delta_x$ ) AND CHANGE IN FOCAL POSITION ( $\delta_{x_1}$ )
  - MEASURE CHANGE IN SPACING VIA RANGING DEVICE
  - CALCULATE CHANGE IN FOCAL POSITION INDIRECTLY
- EXTERNAL FOCUS SENSING (STAR FIELD)
  - UTILIZE IMAGING PROPERTIES (POINT SPREAD FUNCTION, MODULATION TRANSFER FUNCTION, ETC.) OF SCIENTIFIC INSTRUMENT OR SEPARATE FOCUS SENSOR TO DETERMINE CHANGE IN FOCAL POSITION DIRECTLY.
  - THREE FOCUS SENSORS IN FIELD CAN MONITOR MISALIGNMENTS OF THE FOCAL PLANE STRUCTURE RELATIVE TO THE FOCAL SURFACE.

Figure 3.5-12 shows the locations of sensors for an internal decenter and tilt sensing concept. The sources and detectors would be attached to the primary mirror fixed reference. The amount of rigid body motion of secondary mirror misalignment (tilt and decenter) would be measured directly.



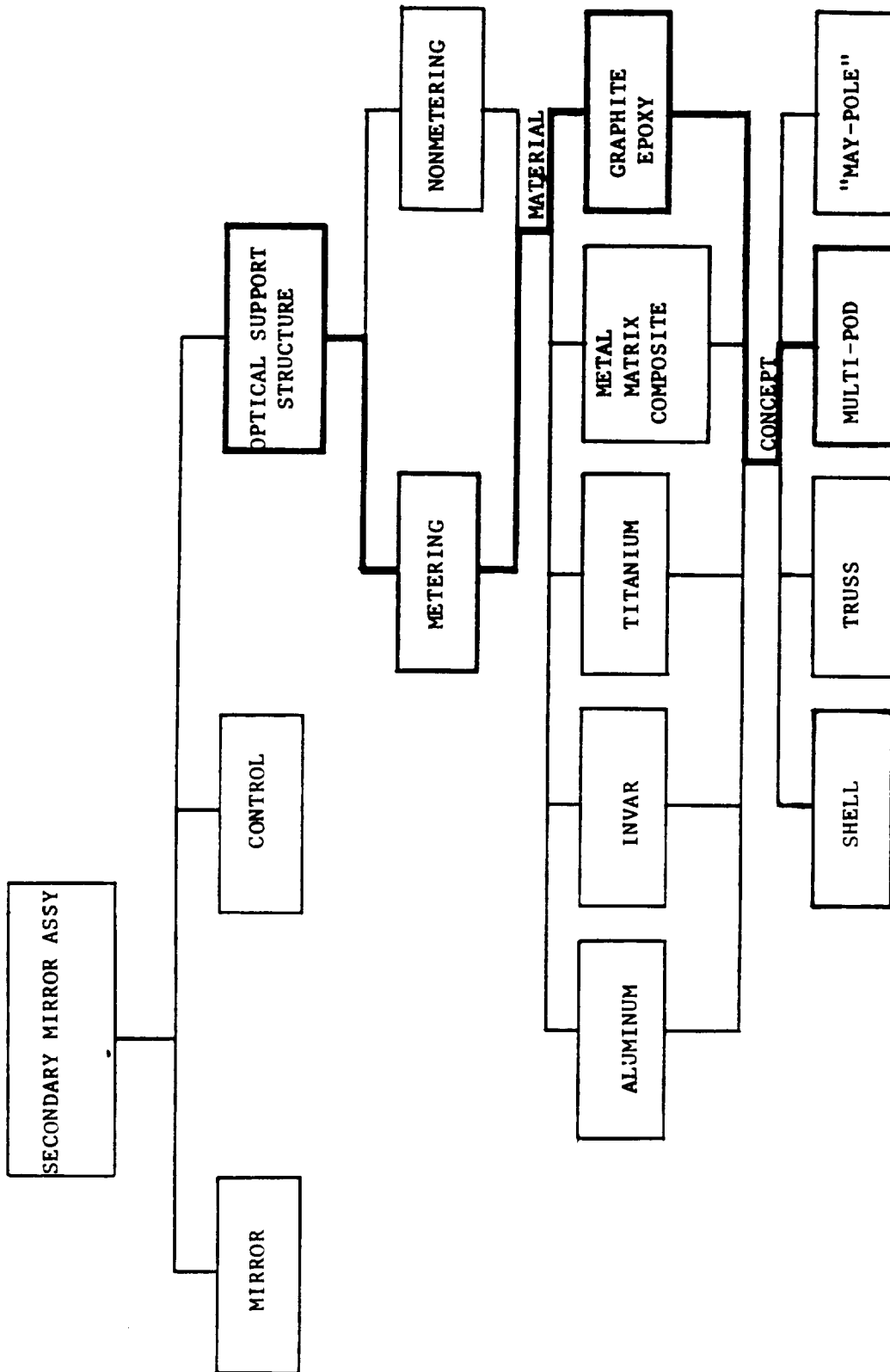
LOCATION OF SENSORS FOR AN INTERNAL DECENTER AND TILT SENSING CONCEPT  
Figure 3.5-12

**3.5.3.3 Secondary Mirror Support Structure** - The trade tree for the secondary mirror support structure is shown in Figure 3.5-13. If mechanical and thermal stresses during operation are small (i.e., true-metering structure with active thermal control), then an open-loop versus a closed-loop optical sensing and control system can be used between operations instead of during operations. Therefore, a "true" metering structure philosophy should be a design goal since it allows for rigid body motion control of wave front degradation between observational periods and chopping during observations.

Key design requirements for the secondary mirror support structure are, therefore, minimum obtainable structural distortion with long term environmental stability. The three basic elements of this are: structural geometries which minimize deflection components in critical directions; materials which have the necessary properties of high specific stiffness, near zero CTE and high conductivity; and high levels of internal material damping and/or damping devices.

Performance degradation produced by mechanical and thermal loading environments can be minimized by the use of structural materials which possess high specific stiffness and strength and self-damping characteristics. Dimensional stability of the LDR structure will also be significantly enhanced by the use of materials with near zero coefficient of thermal expansion (CTE) and which possess high thermal conductivity in order to minimize thermal gradients and stresses.

Beryllium is an excellent structural material. However, it rates low for use in a highly stable metering structure due to its high CTE. Kodak adapted with Universal Cyclops a low expansion version of Invar for use in metering structures with ULE optics. However, it probably will be "too heavy" for LDR. Graphite/epoxy is currently the "state-of-the-art" metering material due to its excellent CTE. A major critical issue in the use of composite structures in a metering application is the joint between subsections. The isotropic properties can affect the dimensional

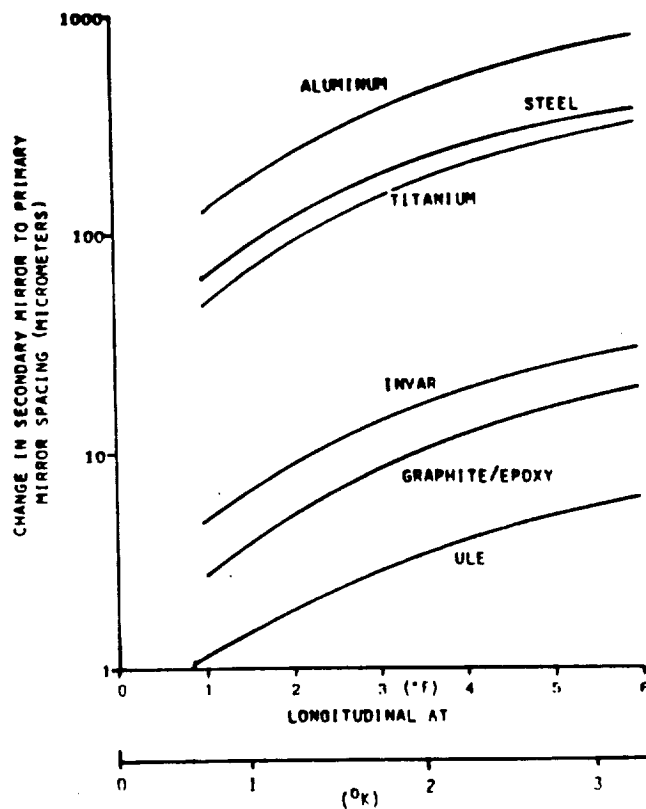


SECONDARY MIRROR SUPPORT STRUCTURE TRADES

Figure 3.5-13

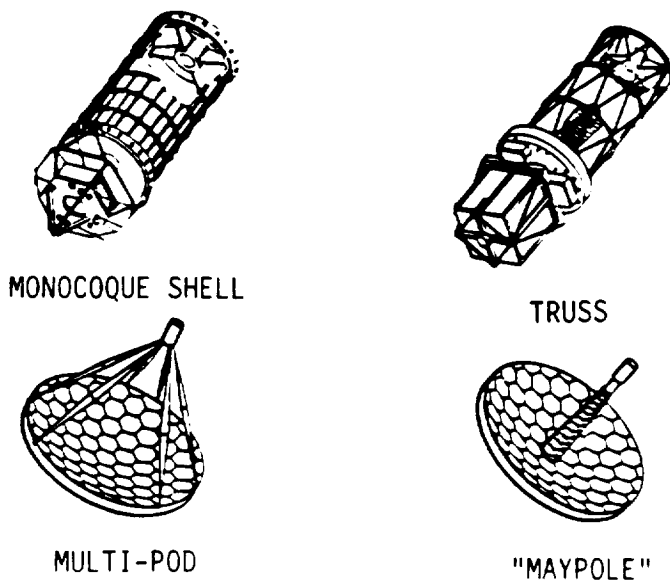
properties and, therefore, affect metering. Potential trouble areas include: built-in stresses, assembly variations, stress redistribution during repeat actuation, and material response to the operational environment (outgassing). The metal matrix materials (graphite/aluminum and graphite/magnesium) offer tremendous potential as a metering structure material: However, they are immature materials relative to graphite/epoxy. Another attractive approach is a hybrid structure utilizing a material such as glass for metering and an outer layer of a material such as aluminum for strength. Such an approach has already been used by the United States Naval Observatory in their astrometric telescope.

Shown in Figure 3.5-14 is a summary for selection of the secondary mirror metering material. For despace requirements of less than 40 micrometers, it can be seen that the preferred choice is graphite/epoxy.



SELECTION OF SECONDARY MIRROR METERING MATERIAL  
Figure 3.5-14

Shown in Figure 3.5-15 are four metering structure concepts. The monocoque shell provides the best metering; however, since it is an enclosed cylinder, it is relatively heavy. In this concept stray light control and metering are provided by the same structure. The shell was eliminated due to the hardware constraints of weight and volume. The truss can provide excellent metering; however, a nonstructural thermal shroud must be added. The other concepts shown (multi-pod and "maypole") do not provide as good metering as the monocoque shell or truss. The "maypole" has stiffness limitations. This affects the capability to point in operation and will interact with the launch dynamics.



METERING STRUCTURE CONCEPTS  
Figure 3.5-15

The multi-pod was selected for its metering structure properties. A separate non-structural shroud will also have to be used for thermal/straylight control. The multi-pod selected in the study was a triple bipod; six struts in three triangulated pairs. This imposes a relatively low obscuration. The struts can be tuned for first mode frequency tailoring. The secondary mirror assembly (mirror with mounts) could be preassembled to the struts on the ground. The primary mirror attachment points would then be the only on-orbit assembly interfaces.

#### 3.5.4 Conclusions

- The secondary mirror should be made from a high dimensionally stable material such as glass.
- "Adequate" metering can be provided by a triple bipod support made from a material such as graphite/epoxy.
- Five degrees of rigid body motion control are required (two tilts, two decenters, and one despace) on the secondary mirror for wave front control between observations.
- Modifying the "diffraction limited" performance requirement from 85% encircled energy to 30% encircled energy improves the despace tolerance. Nevertheless, an "excellent" metering material such as graphite/epoxy coupled with 5 degrees of rigid body motion control will still be required.



## 3.6 THERMAL CONSIDERATIONS

### 3.6.1 Task

The LDR thermal task involved an investigation and study for providing thermal control to the telescope assembly and for providing cryogenic cooling to the science instruments and the secondary mirror. The major thermal control requirements which were specified for the LDR are listed in Table 3.6-1 for the telescope assembly and are listed in Table 3.6-2 for the science instruments and secondary mirror. The 10 year life expectancy implies that all considered design approaches have the potential for extremely high reliability.

A major objective for the telescope thermal control approach was to meet the specified requirements on any given day, at all positions in the orbit, and to simultaneously accept both the solar and earth heating loads over the entire range of specified "earth/sun" telescope exclusion angles. The objective for furnishing cryogenic cooling to the science instruments was to provide a system approach which will not require servicing or replenishment more frequently than every three years.

TABLE 3.6-1  
LDR TELESCOPE THERMAL REQUIREMENTS

#### ORBIT AND EARTH/SUN TELESCOPE EXCLUSION

ORBIT: 700 - 1,100 KM ALTITUDE; 28.5° INCLINATION

TELESCOPE EXCLUSION:  $\geq 45^\circ$  EARTH/ALBEDO;  $60^\circ - 90^\circ$  SUN

#### TEMPERATURES

20M DIAMETER PRIMARY MIRROR:  $T \leq 200 \pm 1^\circ \text{K}$

1.34M DIAMETER SECONDARY MIRROR:  $T \leq 125 \pm 1^\circ \text{K}$

#### OTHER

0.05 OVERALL SYSTEM EMITTANCE

REASONABLE COOL-DOWN TIMES

10-YEAR LIFE

3-YEAR SERVICE INTERVAL

Considering the large size of LDR, it becomes important that all thermal control concepts and designs be compatible to packaging within the space Shuttle and be either capable of orbital deployment or of reasonable assembly, by astronauts, on the Space Station.

All elements of the thermal control must be stable, in a space environment, and must not outgas water and solvents, or generate particles, which will degrade thermal control finishes and optical surfaces. Weight is also an important parameter and the thermal design must consider means by which weight, particularly stored cryogenics, can be minimized.

TABLE 3.6-2  
LDR SCIENTIFIC INSTRUMENT AND SECONDARY MIRROR COOLING THERMAL REQUIREMENTS

PROVIDE A CRYO-COOLING SYSTEM HAVING A THREE-YEAR LIFE BETWEEN SERVICING INTERVAL FOR SCIENTIFIC INSTRUMENTS. THE "CONTINUOUS-BASIS-AVERAGE" INSTRUMENT COOLING LOADS, INCLUDING INSTRUMENT PARASITICS, ARE DEFINED AS:

2 WATTS AT 77°K  
1 WATT AT 20°K  
0.25 WATT AT 4°K

CONSIDER MEANS FOR PROVIDING CRYO-COOLING TO 0.1°K FOR SPECIAL SCIENTIFIC INSTRUMENTS WITH SMALL (150MW) COOLING LOAD DEMAND

PROVIDE A CRYO-COOLING SYSTEM HAVING A THREE-YEAR LIFE BETWEEN SERVICING INTERVAL TO HOLD SECONDARY MIRROR AT A TEMPERATURE OF 125  $\pm$ 1°K.

FIVE (5) WATT MAXIMUM HEAT GAIN OBTAINED FROM MIRROR TEMPERATURE CONTROL TASK ANALYSIS.

Initial temperature control cool-down and stabilization must be factored into the design; in the case of the very cold cryogenic temperatures of the science instruments this involves a large cooling capacity.

While no limits were specified for operational electrical power the thermal control considered this important and identified only concepts which will require reasonable levels of electrical power; this conserves total LDR system weight and contributes to improved reliability.

### 3.6.2 Approach

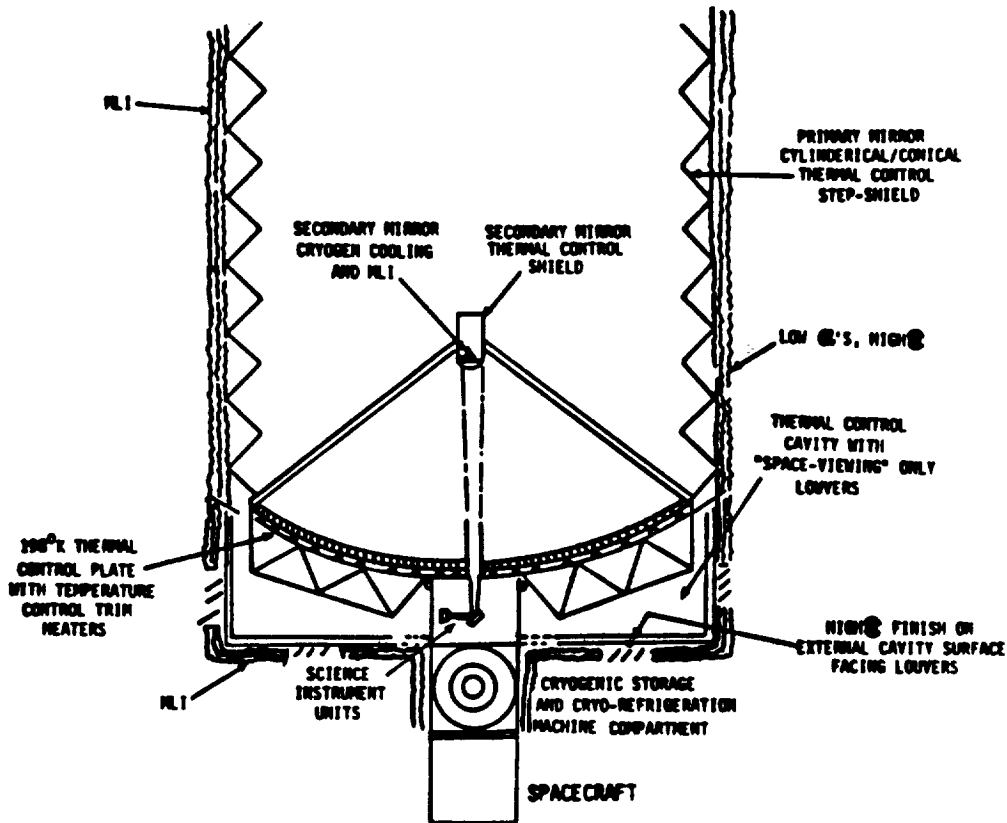
3.6.2.1 Telescope Thermal Control - A semi-passive thermal control concept has been preliminarily analyzed for meeting the LDR telescope thermal control requirements. The concept is shown in Figure 3.6-1.

To reduce solar and earth/albedo heat loads falling on the telescope mirrors and to achieve fairly uniform environmental heating loads over the mirror surfaces a step-baffled cylindrical shield will be placed around the telescope assembly. This will enable the specified primary mirror base temperature, 200°K, to be achieved.

To fine-tune the mirror temperature and provide the specified  $\pm$ 1°K "point-to-point" lateral temperature control, the mirror temperature will be modulated by means of a thermal control plate, equipped with trim heaters, that faces the rear surface of the mirror. The temperature control plate, in turn, views a thermal control cavity, from its backside, which is equipped with "space-viewing louvers". The louvers are opened to discharge heat at times when excess thermal energy falls onto the mirror.

The system is described as semi-passive because it employs active but highly reliable electrical trim heaters for temperature control. The reliability will be further enhanced by using separate heaters and controls for each mirror segment. The moving

louvers will use bi-metal control elements with over-riding electrical motor drives.



LDR MIRROR THERMAL CONTROL APPROACH SCHEMATIC  
Figure 3.6-1

To achieve the colder, 125°K, secondary mirror temperature, this mirror will be cooled with LN<sub>2</sub> cryogen. A cryogen supply system can be either located at the mirror or cryogen can be plumbed to the mirror from a remote LN<sub>2</sub> storage system; this is an important design issue to be addressed in future studies.

A thermal model of the concept was prepared and analyzed using the NEVADA and SINDA thermal analysis computer programs. Early thermal investigations involved with selection of the primary mirror shield geometry and thermal finishes employed the NEVADA and Kodak SATAN computer programs. Other individualized thermal analysis studies were conducted using either hand calculations to solve the equations or somewhat less sophisticated computer programs (e.g., simultaneous solutions of multi-equation networks).

**3.6.2.2 Science Instrument And Secondary Mirror Cooling** - The cold temperatures specified for all of the science instruments requires cryogenic cooling. The temperature range from 41°K to 77°K can be provided with stored LHe, LH<sub>2</sub>, and LN<sub>2</sub>

while superfluid Helium can achieve 2°K. Closed-cycle mechanical or chemical absorption pumps can be reasonably built to reach temperatures over the range of about 10°K to 77°K and with added difficulty they can achieve about 4°K (e.g. with Joule Thomson expansion). To obtain the lower temperatures specified, to 0.1°K, will require exotic active cryogenic refrigeration systems. Such systems are He<sup>3</sup> evaporation, for 0.3°K, and Adiabatic Demagnetization (ADR) or He<sup>3</sup>-H<sup>4</sup> Dilution Refrigeration (difficult in zero-g) for achieving 0.1°K.

A heat balance thermal model considering the initial cool-down heat loads, the operational refrigeration loads, and the parasitic heat leakage into storage vessels, piping, and instrument assemblies, was prepared in order to estimate the cryogenic refrigeration demands at 4°K, 20°K, and 77°K over a three year period. The average continuous operational loads used were 0.25W at 4°K, 1 watt at 20°K, and 7 watts (2W instruments, 5W secondary mirror) at 77°K.

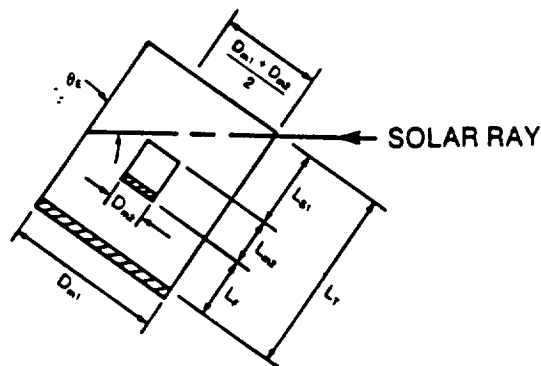
It was determined unlikely that an active mechanical or chemical pump could meet the requirements alone, particularly for cool-down, and that the overall LDR system reliability would be greatly compromised. Likewise, a system employing only stored cryogens would be exceptionally large and impractical. This study indicated a "hybrid system" consisting of stored cryogens together with active closed-cycle mechanical or chemical refrigeration machines could meet the LDR science instrument cooling, from 4°K-77°K, and provide a reliable practical system; systems such as He evaporation and ADR are needed for temperatures below 2°K (superfluid Helium).

### 3.6.3 Discussion

3.6.3.1 Telescope Thermal Control - To provide the specified cold (200°K) primary mirror and cold (<125°K) secondary mirror over the specified range of telescope pointing requirements (60°-90° to sun and >45° to the earth) it is necessary to employ a thermal shield for reducing thermal loading into the mirrors; otherwise, the heat gains would be enormous for a 20M diameter mirror and the ±1°K temperature uniformity, "point-to-point" over the entire surface, would become unachievable. The thermal shielding technique also enables the passive thermal control approach to be used which provides the needed high system reliability. Furthermore, active cooling systems, even in conjunction with shields, would be very large, create vibrations, require momentum compensation, consume large amounts of power which in turn requires thermal cooling, are costly, difficult to test, and offer minimal flexibility to design and system operational parameter changes.

Three types of thermal shielding geometry were considered: A cylindrical shield as shown in Figure 3.6-2, a cylindrical/conical shield as shown in Figure 3.6-3, and a step-baffled cylindrical shield as shown in Figure 3.6-4.

The cylindrical shield is the simplest design but results in the highest heating loads. This is shown in Figure 3.6-5 for a short cylinder and in Figure 3.6-6 for a long cylinder. The cylindrical/conical shield becomes very large, but significantly reduces the mirror heat loads as shown in Figure 3.6-7. The maximum orbital average temperature achievable with these two configurations is given in Figure 3.6-8 and indicates the 200°K goal would likely not be reached with a straight cylindrical shield. Also, as shown in Figure 3.6-9, these two configurations result in a very non-uniform heat distribution over the primary mirror unless a thermally black shield



$$L_{S1} = \frac{D_{m1} + D_{m2}}{2} \tan(90 - \theta_E)$$

$$L_T = L_{S1} + L_{m2} + L_p$$

For: $\theta_E = 60^\circ$	$L_{m2} = 1.5 \text{ m}$	$L_p = 10 \text{ m}$	$D_{m1} = 20 \text{ m}$
	$D_{m2} = 1.7 \text{ m}$		
$L_T = 17.76 \text{ m}$	$22.35 \text{ m For } \theta_E = 45^\circ$		

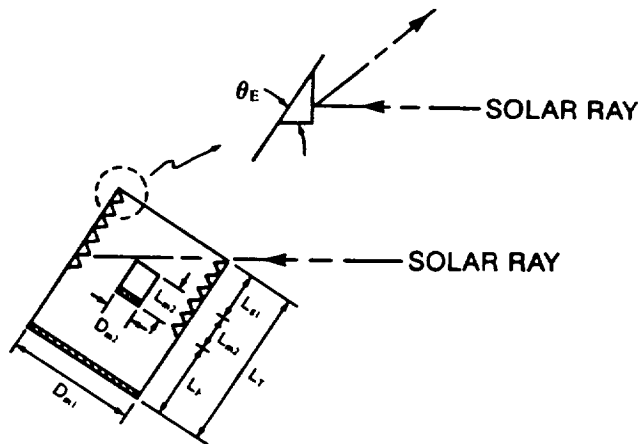
**CYLINDRICAL SHIELD GEOMETRY  
FOR  
PRIMARY AND SECONDARY MIRRORS  
Figure 3.6-2**

finish is employed and such a finish violates the 0.05 maximum system emittance constraint. The results presented in these figures were derived by employing the Turner Assoc. NEVADA and Kodak SATAN thermal model computer programs.

By examination of the results obtained for the cylindrical and cylindrical/conical shield geometries it was determined that a step-baffled cylindrical shield geometry could be tailored to meet the telescope thermal control requirements of LDR; the selected configuration is shown in Figure 3.6-10. The thermal control finishes will be specular with low solar absorption and high emittance on the top sides of the steps and diffuse with high solar absorption and low emittance on the bottom sides of the steps. This surface finish combination together with the step-geometry configuration directly reflects a majority of the incoming solar and albedo energy from the shield cavity. Next, it "scavenges" most of the internally bounced specular solar wavelength energy and reduces the direct IR wavelength energy radiated to the mirror from the underside shield surfaces viewing the mirror. In addition to the shield thermal finishes, the surfaces of all optics (primary and secondary mirrors) will be highly specular with low solar absorption and low emittance coatings (polished silver).

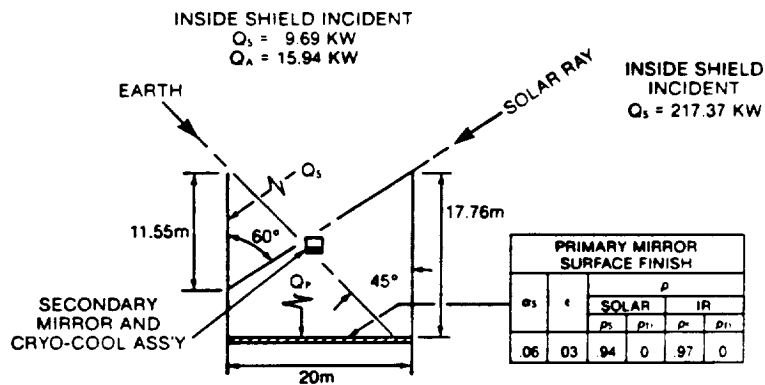
Complementing the large step-baffled cylindrical shield a small polished silver cylindrical shield will be incorporated at the backside of the secondary mirror. This will further reduce the cooling load on the cryogenics needed to cool the secondary mirror to 125°K.





FOR:  $\theta_E = 60^\circ$   $L_{m2} = 1.5m$   $L_F = 10m$   $D_{m1} = 20m$   $D_{m2} = 1.7m$   
 $L_{s1} = 6.56m$   $L_T = 17.76m$   
 FOR  $\theta_E = 45^\circ$  (EARTH CASE) -  $L_T = 22.35m$

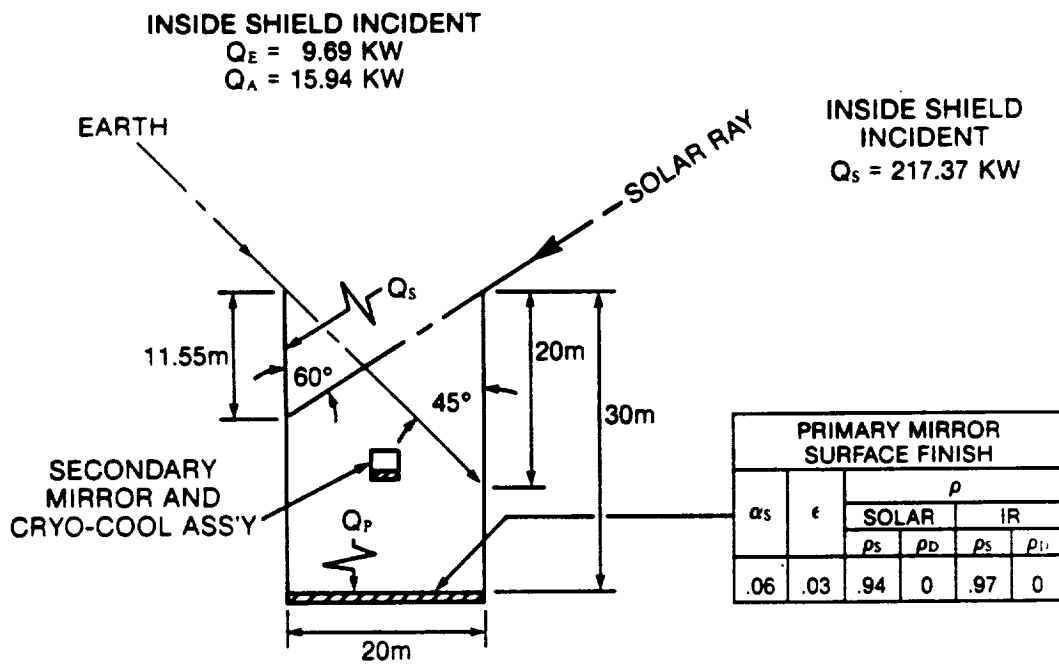
STEP-BAFFLED CYLINDRICAL SHIELD GEOMETRY FOR PRIMARY AND SECONDARY MIRRORS  
 Figure 3.6-4



PRIMARY MIRROR SURFACE FINISH						
$\alpha_s$	$\epsilon$	$\rho$				
		SOLAR		IR		
		$\rho_s$	$\rho_i$	$\rho_e$	$\rho_r$	$\rho_{tr}$
06	03	94	0	97	0	

TYPE	SURFACE FINISH						HEAT LOADS (KW)					
	$\alpha_s$	$\epsilon$	$\rho$				SOLAR		ALBEDO		EARTHSHINE	
			$\rho_s$	$\rho_i$	$\rho_e$	$\rho_r$	$Q_s$	$Q_r$	$Q_a$	$Q_e$	$Q_i$	$Q_{tr}$
A	1	8	72	18	16	04	75.9	10	6.1	0.62	9.0	0.012
B	15	05	68	17	76	19	102	8.7	8.0	0.54	2.2	0.22
C	80	80	02	18	02	18	202	0.48	14.7	0.033	9.0	0.012

SHORT CYLINDRICAL MAXIMUM SHIELD HEATING LOADS AT SUB-SOLAR  
 Figure 3.6-5



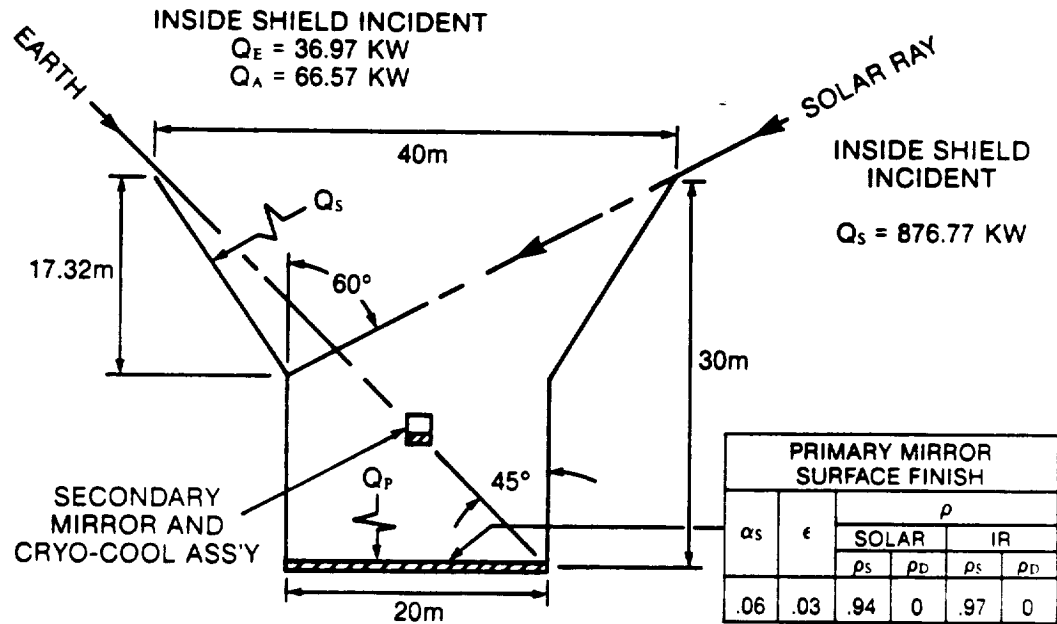
SURFACE FINISH		HEAT LOADS (KW)										
TYPE	$\alpha_s$	$\epsilon$	$\rho$				SOLAR		ALBEDO		EARTHSHINE	
			SOLAR		IR		$Q_S$	$Q_P$	$Q_S$	$Q_P$	$Q_S$	$Q_P$
			$\rho_s$	$\rho_D$	$\rho_s$	$\rho_D$						
A	.1	.8	.72	.18	.16	.04	107	8.0	8.2	0.54	9.5	0.004
B	.15	.05	.68	.17	.76	.19	135	6.5	10.2	0.43	3.1	0.21
C	.80	.80	.02	.18	.02	.18	203	0.13	15.0	0.01	9.5	0.004

COMMENT: FINISH "C" (BLACK PAINT) PROVIDES LOWEST HEAT LOAD TO MIRROR BUT DEPARTS FROM 0.05 SYSTEM EMISSANCE SPECIFICATION.

LONG CYLINDRICAL MAXIMUM SHIELD HEATING LOADS AT SUB-SOLAR

Figure 3.6-6



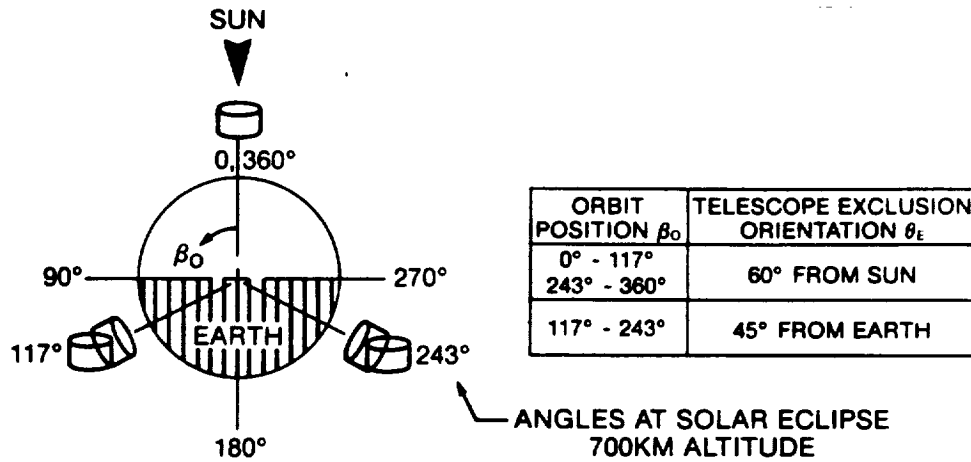


SURFACE FINISH				HEAT LOADS (KW)								
TYPE	$\alpha_s$	$\epsilon$	$\rho$				SOLAR		ALBEDO		EARTHSHINE	
			SOLAR		IR		$Q_s$	$Q_p$	$Q_s$	$Q_p$	$Q_s$	$Q_p$
			$\rho_s$	$\rho_D$	$\rho_s$	$\rho_D$						
A	.1	.8	.72	.18	.16	.04	124	0.70	9.3	0.12	32.1	0.004
B	.15	.05	.68	.17	.76	.19	181	0.61	13.6	0.11	2.7	0.041
C	.80	.80	.02	.18	.02	.18	763	0.088	57.6	0.013	32.1	0.004

COMMENT: THE FINISH "C" (BLACK PAINT) IS STILL BEST, BUT FINISH "B" IS FAIRLY COMPARABLE TO FINISH "C" FOR A LONG CYLINDER AND MEETS 0.05 SYSTEM EMITTANCE SPECIFICATION.

CONICAL SHIELD MAXIMUM HEATING LOADS AT SUB-SOLAR

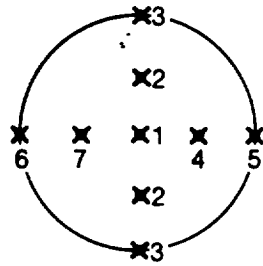
Figure 3.6-7



SHIELD INSIDE SURFACE FINISH TYPE	AVERAGE MIRROR TEMPERATURE (°K)		
	30M CYLINDRICAL	17.76M CYLINDRICAL	30M CONICAL/CYLIND'RL
A	230	233	146
B	222	225	156
C	213	211	204

PRIMARY MIRROR MAXIMUM ORBITAL AVERAGE TEMPERATURE  
WITH ADIABATIC SHIELD WALLS

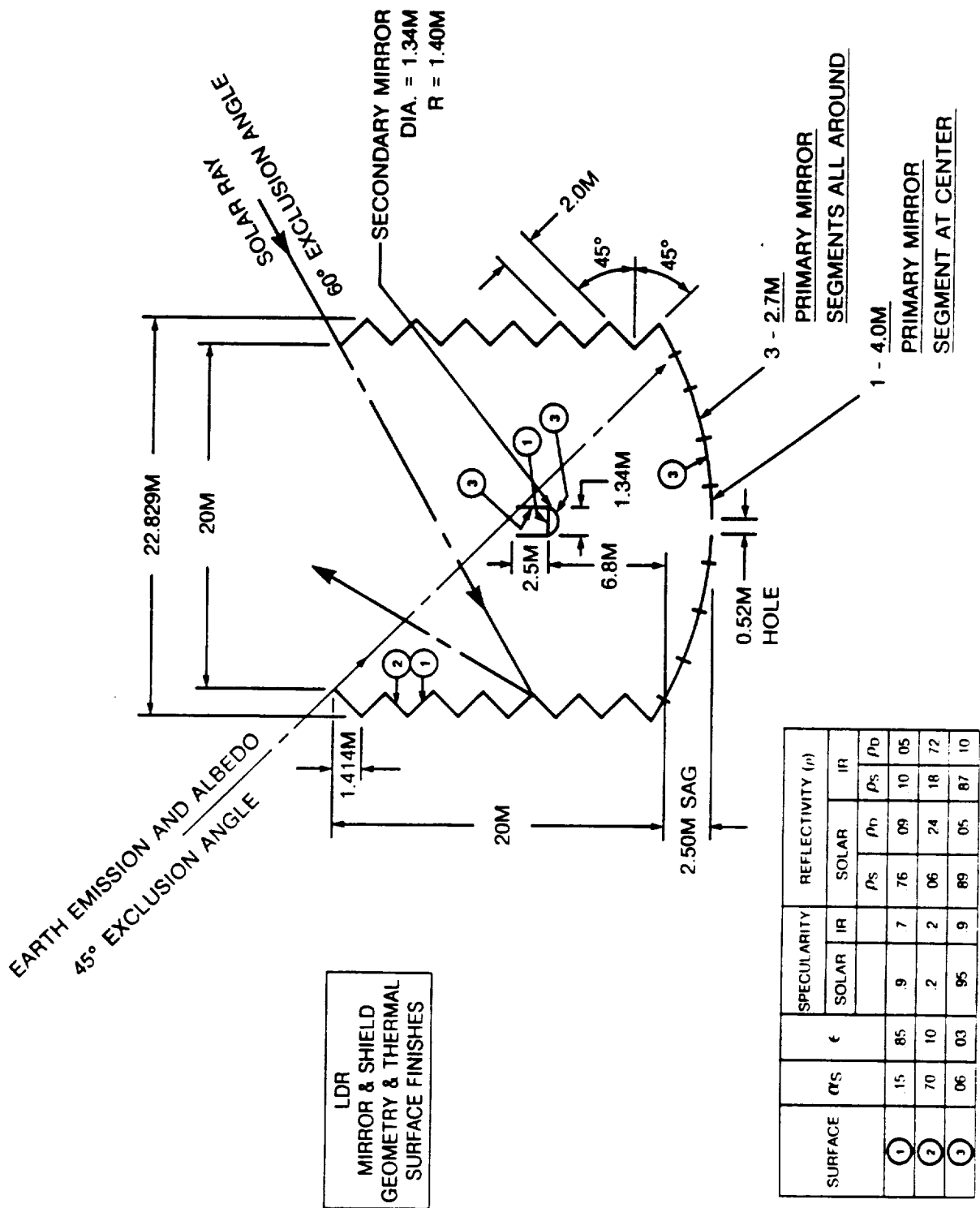
Figure 3.6-8



SHIELD INSIDE SURFACE FINISH	$\alpha_s$	$\epsilon$	$\rho$			
			SOLAR		IR	
			$\rho_s$	$\rho_D$	$\rho_s$	$\rho_D$
A	.1	.8	.72	.18	.16	.04
B	.15	.05	.68	.17	.76	.19
C	.80	.80	.02	.18	.02	.18

POINT	HEAT LOAD (WATTS)		
	FINISH A	FINISH B	FINISH C
1	94	75	~ 6
2	124	102	~ 6
3	98	79	~ 6
4	41	33	~ 6
5	38	28	~ 6
6	74	61	~ 6
7	135	113	~ 6

PRIMARY MIRROR SOLAR HEAT LOAD  
DISTRIBUTION AT SUB-SOLAR FOR 30M LONG CYLINDRICAL SHIELD  
Figure 3.6-9



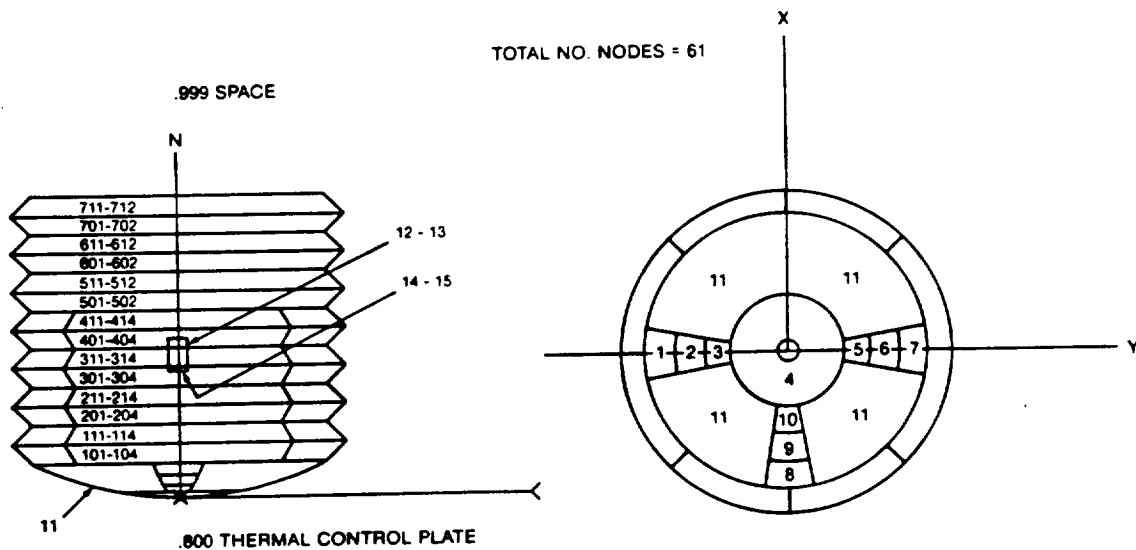
LDR MIRROR AND SHIELD GEOMETRY AND THERMAL SURFACE FINISHES

Figure 3.6-10

To analyze the telescope thermal control concept a thermal model was prepared which described the step-baffle shield, primary mirror, and secondary mirror. The model consisted of 61 nodes (including space and thermal control plate) as shown in Figure 3.6-11. A 1,100 KM altitude, 28.5° inclined orbit and simultaneous heat inputs from 60° sun and 45° earth/albedo was analyzed to obtain a worst-hot case; this orbit placed the telescope in sunlight for 82% (maximum possible) of the orbit period. The model considered both specular and diffuse radiation between all nodes but conservatively no allowance was made for conduction between nodes in the mirror material.

The analysis was conducted using the Turner Associates "NEVADA" computer program for determining all specular and diffuse radiation exchange between nodes as well as absorbed earth albedo and earth IR heat loads. The SINDA computer program was employed to solve all heat balances and to compute the nodal temperatures based on the NEVADA inputs; this program also calculated the needed trim-heater thermal control power. An outline and description of the thermal modeling approach and the major functions of the various computer programs employed in solving the model is shown in Table 3.6-3.

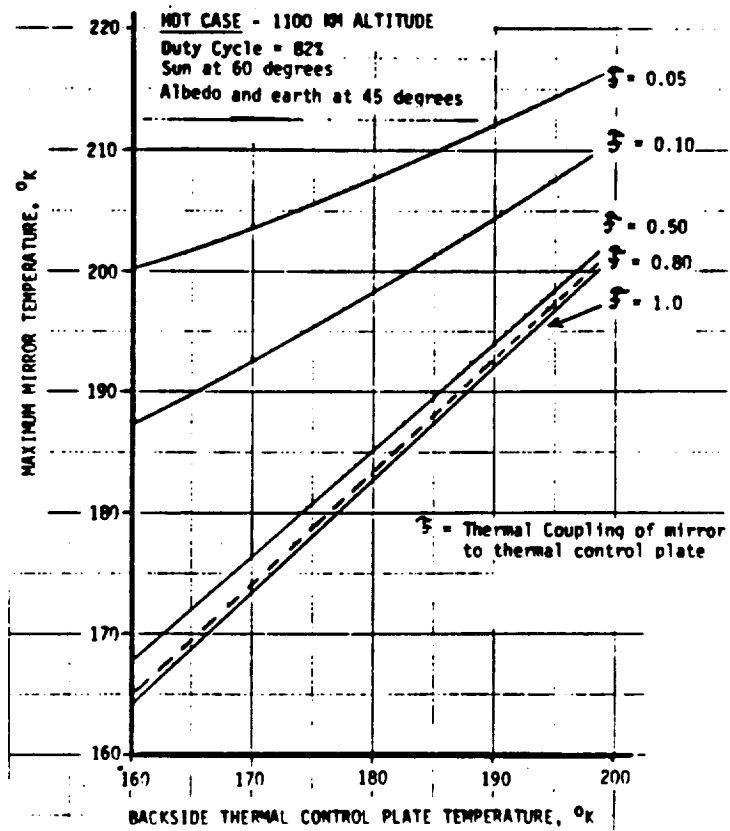
Results from this analysis are shown in Figures 3.6-12 through 3.6-17. In Figures 3.6-12 and 3.6-13 primary mirror temperature is shown as a function of thermal control plate temperature and thermal coupling between the mirror and the thermal control plate. In Figure 3.6-14 the effect of mirror lateral temperature gradient is shown as a function of thermal control plate temperature and thermal coupling between the mirror and the thermal control plate. These figures indicate that a



LDR THERMAL MODEL  
VIEW FACTOR/HEAT RATE SURFACE NODES  
Figure 3.6-11

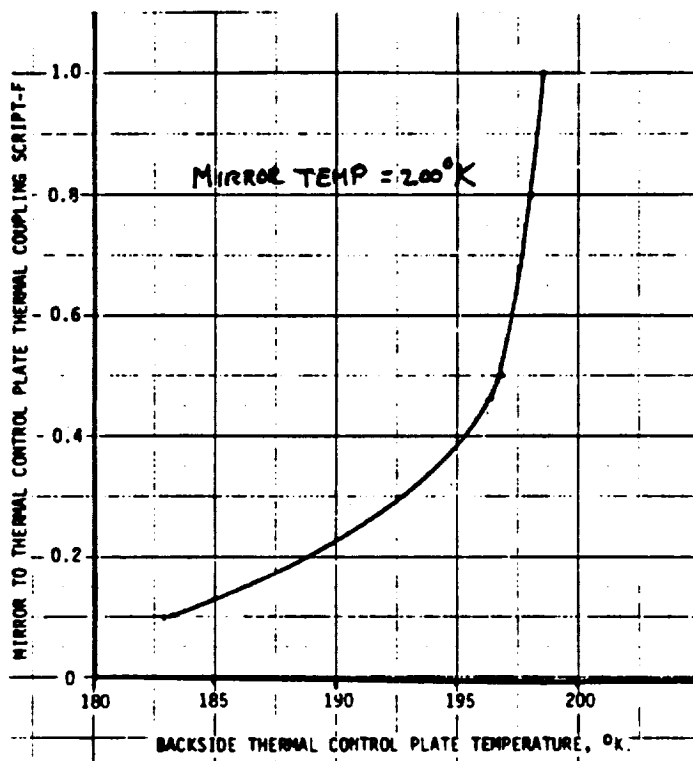
TABLE 3.6-3  
THERMAL MODELING APPROACH

- REPRESENT DESIGN CONCEPT BY APPROPRIATE NODES
- HAND COMPUTE NODE THERMAL CAPACITANCES
- HAND COMPUTE SOLID THERMAL CONDUCTION BETWEEN NODES
- EMPLOY "NEVADA" COMPUTER PROGRAM (7TH EDITION, 1980 TURNER ASSOC., BREA, CA)
  - RENO SECTION: GEOMETRIC VIEW FACTORS ( $F_{i-j}$ )  
(DETERMINES) RADIATION EXCHANGE ( $B_{i-j}$ ) BOTH DIFFUSE AND SPECULAR  
SCRIPT - "F" FACTOR ( $B_{i-j} \epsilon_i$ ) AND SURFACE AREA. NOTE: A  
KODAK PROGRAM CONVERTS THIS NEVADA OUTPUT TO RADIATION  
THERMAL TRANSFER CONDUCTANCE BETWEEN NODES (SCRIPT - "F" X  
AREA)
  - VEGAS SECTION: DIFFUSE PLUS SPECULAR EXTERNAL HEAT LOADS VERSUS ORBIT POSITION  
(COMPUTES) (SOLAR AND SURFACE REFLECTION AND EMISSION.)
  - SPLOT SECTION: CONSTRUCTS COMPUTER DRAWING OF BOTH CONFIGURATION AND ORBIT  
GEOMETRY
- EMPLOY SINDA COMPUTER PROGRAM FOR DETAILED NODAL TEMPERATURE AND CONTROL POWER  
ANALYSIS IN ORBIT
  - SOLVES ALL HEAT BALANCES BETWEEN NODES WITH INPUT CAPACITANCES CONDUCTANCES  
(SOLID PLUS RADIATION), BOUNDARY TEMPERATURES, EXTERNAL DIFFUSE PLUS SPECULAR  
HEAT LOADS, AND OPERATIONAL POWER PROFILES.



MAXIMUM MIRROR TEMPERATURE VERSUS  
 BACKSIDE THERMAL CONTROL PLATE TEMPERATURE

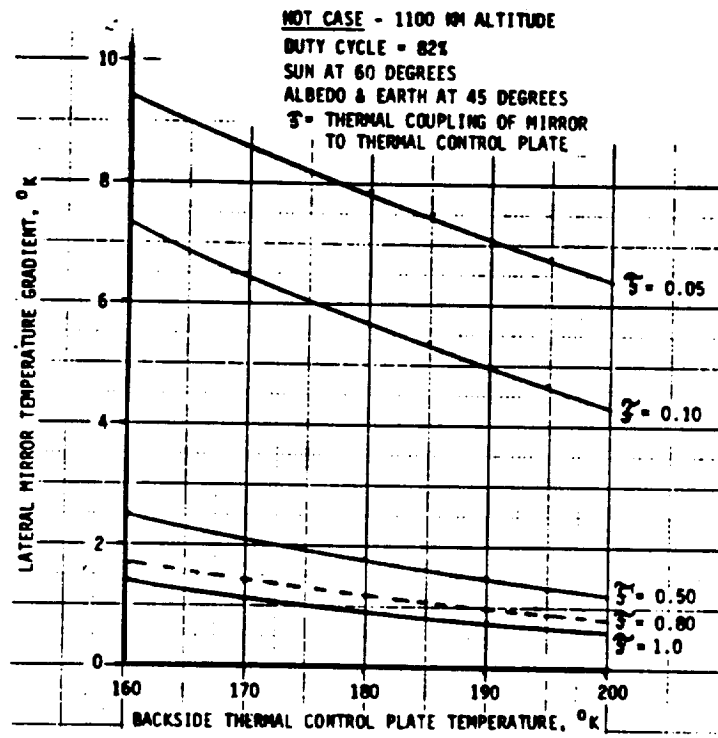
Figure 3.6-12



MIRROR-TO-THERMAL CONTROL PLATE THERMAL COUPLING VERSUS  
BACKSIDE THERMAL CONTROL PLATE TEMPERATURE

Figure 3.6-13

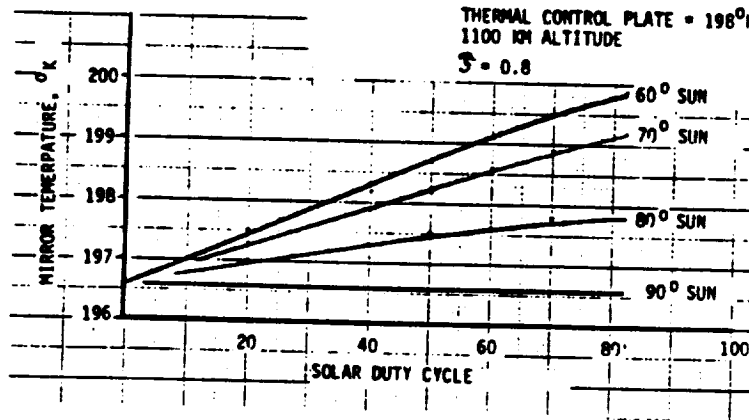




LATERAL MIRROR TEMPERATURE GRADIENT VERSUS  
 BACKSIDE THERMAL CONTROL PLATE TEMPERATURE

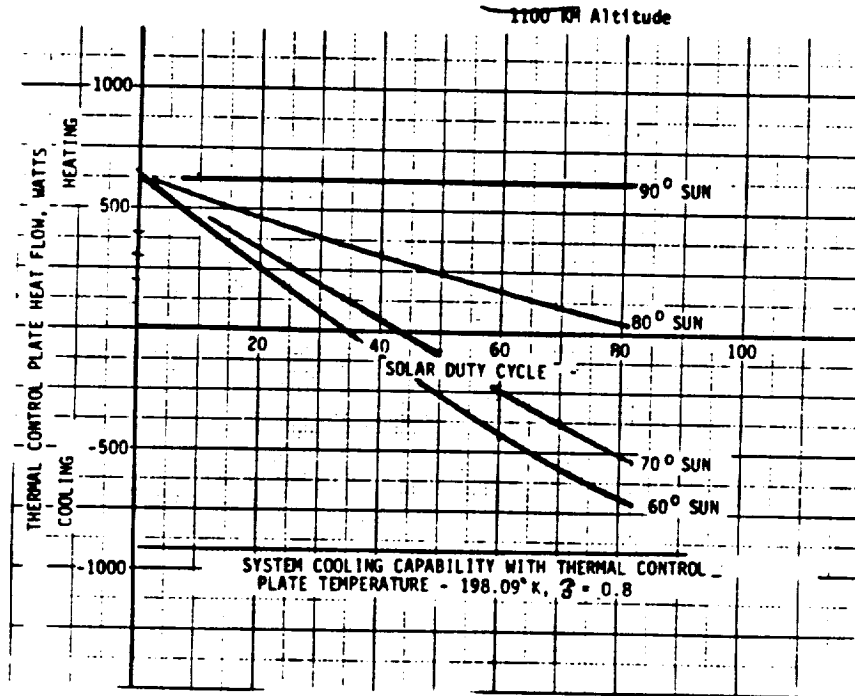
Figure 3.6-14

EARTH AND ALBEDO AT 45 DEGREES

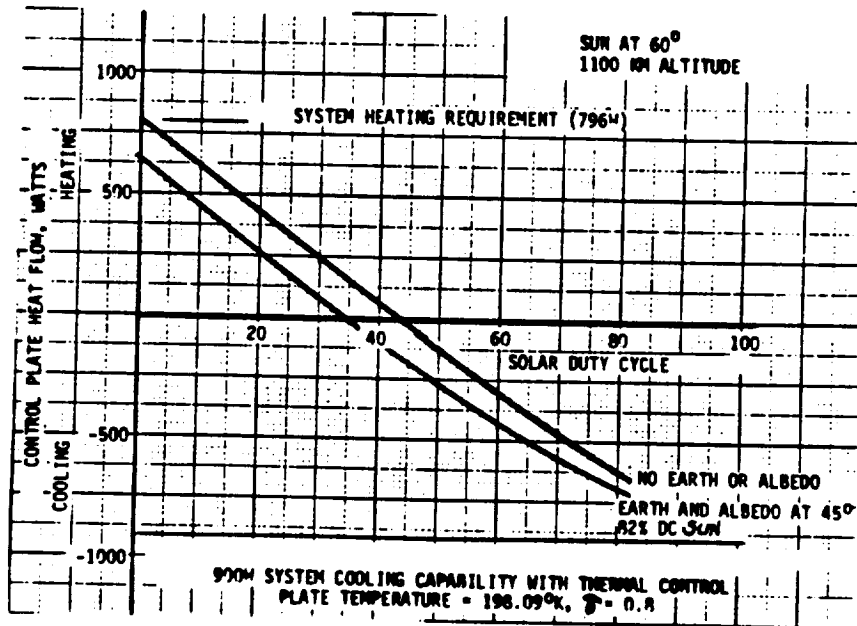


MIRROR TEMPERATURES FOR VARIOUS SUN ANGLES AND SOLAR DUTY CYCLES  
Figure 3.6-15

Earth and Albedo at 45°



THERMAL CONTROL PLATE HEAT FLOWS FOR VARIOUS SUN ANGLES AND SOLAR DUTY CYCLES  
Figure 3.6-16



THERMAL CONTROL PLATE HEAT FLOWS  
FOR MAXIMUM AND MINIMUM  
EARTH AND ALBEDO HEAT LOADS  
Figure 3.6-17

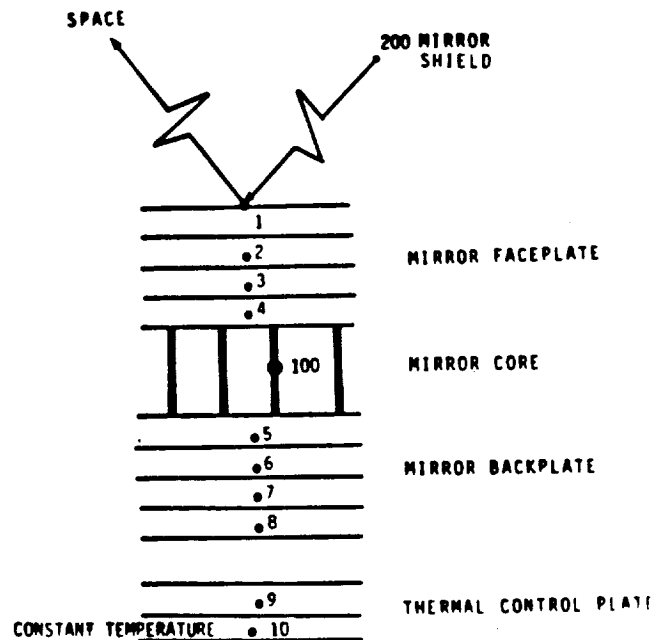
"point-to-point" lateral temperature gradient of 1°K can be maintained with a minimum coupling of roughly 0.68 and with a thermal control plate temperature maintained at 194°K - 198°K; under these conditions the maximum primary mirror temperature will range from 197°K to 200°K. A separate radiation analysis showed that a coupling of 0.68 can be achieved when applying a thermal emittance of 0.95 to both the backside of the mirror faceplate and to the thermal control plate in addition to providing 50% open area in the mirror backplate for defining the radiation coupling between mirror faceplate and thermal control plate; these parameters are obtainable. Relaxation of the +1°K gradient to just +1.5°K will provide a much wider design margin and can further lower the primary mirror temperature. For instance, a 0.5 coupling and 190°K thermal control plate lowers the primary mirror temperature to 194°K with a maximum lateral gradient of 1.5°K.

Figure 3.6-15 shows how the base temperature of the mirror is influenced by the solar exclusion angle for a control plate temperature held at 198°K and a coupling of 0.8. It indicates the mirror temperature will range between the stated 200°K at 60° solar exclusion angle and 196.5°K at a 90° solar exclusion angle. If it were desired to hold the mirror 200°K for the 90° solar exclusion angle about 600 watts of heater power is needed as given by Figure 3.6-16. Further, as indicated by Figure 3.6-15 and Figure 3.6-16 when the altitude is lowered and the solar duty cycle (fraction of orbit period pointing at the sun) decreases, some heater power will be needed if it is desired to hold the primary mirror temperature at 200°K; however, the maximum never exceeds about 600 watts. The results in Figure 3.6-16 also show the amount of cooling load which must be dumped to space through the thermal control cavity louvers as a function of solar angle and solar duty cycle. The influence on heating and cooling loads from the earth/albedo loads is presented in Figure 3.6-17.

To determine the sensitivity of the mirror temperature to heat flux and to its thermal coupling with the shield a detailed nodal model of the mirror (faceplate, core, backplate) was prepared as shown in Figure 3.6-18. Results from the solution of this model are given in Table 3.6-4 and Table 3.6-5. This data indicates a change in the mirror base temperature of only 0.4°K with 50% of the expected maximum heat flux, and only 0.8°K for doubling the expected maximum heat flux. The data further shows a mirror base temperature range of only -0.09°K to +0.42°K for +20% variations in mirror-to-thermal shield coupling, and only +0.21°K to +0.60°K for +20% variations in mirror coupling to space. Again, these small temperature changes represent changes to the average mirror base temperature and are not "point-to-point" lateral temperature gradients along the mirror surface; thus, the mirror has a desired low sensitivity to its thermal coupling with both the shield and to space.

An analysis was also conducted for the thermal control cavity and "space-view" louvers. A nodal model describing the thermal control plate, the thermal control cavity, the louvers, and space was written in terms of an Oppenheim Radiation Network involving nine (9) equations. Heater control power as well as heat load from the mirror to the thermal control plate was included in the model. A simultaneous solution of the resulting equations showed that the maximum expected mirror heat load

of about 902 watts can be dumped to space through 27.87 m<sup>2</sup> of louver area with an emittance of 0.9 on all surfaces (control plate, cavity, louvers). The corresponding system temperatures will be: 198°K control plate, 196.73°K cavity, and 165.32°K exposed louver area. In addition, a heater control power of 164 watts is needed to hold the control plate at 198°K. This analysis showed that the thermal control



THERMAL CONTROL SENSITIVITY OF LDR MIRROR  
Figure 3.6-18

TABLE 3.6-4  
PRIMARY MIRROR SENSITIVITY TO SURFACE HEAT FLUX

AT 60° SUN ANGLE, 45° EARTH AND ALBEDO ANGLE,  
AND SCRIPT-F = 0.8

4-METER DIAMETER CENTER SEGMENT

FLUX (WATTS/M <sup>2</sup> )	MIRROR SURFACE TEMPERATURE (°K) FOR 198°K CONTROL PLATE
0.5	199.0
1.0 (EXPECTED MAX)	199.4
2.0	200.2

2.7-METER SEGMENT AT EDGE

FLUX (WATTS/M <sup>2</sup> )	MIRROR SURFACE TEMPERATURE (°K) FOR 198°K CONTROL PLATE
0.25	198.01
0.5 (EXPECTED MAX)	198.4
1.0	199.2

TABLE 3.6-5  
PRIMARY MIRROR SENSITIVITY TO THERMAL COUPLING

SENSITIVITY OF LDR PRIMARY MIRROR SURFACE TEMPERATURE TO THERMAL COUPLING  
("SCRIPT-F") BETWEEN MIRROR SURFACE AND SHIELD AND BETWEEN MIRROR SURFACE  
AND SPACE-AT EXPECTED MAXIMUM HEAT FLUX ON EDGE SEGMENT

<u>% CHANGE IN <math>\Phi</math></u> <u>MIRROR TO SHIELD STEP</u> <u>SURFACE FACING DOWN</u>	<u>% CHANGE IN <math>\Phi</math></u> <u>MIRROR-TO-SHIELD STEP</u> <u>SURFACE FACING UP</u>	<u>% CHANGE IN <math>\Phi</math></u> <u>MIRROR-TO-SPACE</u>	<u>MIRROR SURFACE</u> <u>TEMPERATURE (°K)</u>
NOMINAL (N)	N	N	200.41
+20%	N	N	200.52
-20%	N	N	200.09
N	+20%	N	200.42
N	-20%	N	200.41
N	N	+20%	200.21
N	N	-20%	200.60

NOTE: THE THERMAL CONTROL PLATE TEMPERATURE WAS 200°K. FOR A 198°K PLATE,  
SUBTRACT 2°K FROM THE ABOVE MIRROR SURFACE TEMPERATURES.

cavity and louvers will accommodate the highest expected heat loads with a practical design. Other combinations of louver areas and temperatures will also work and future design studies would optimize the system.

**3.6.3.2 Science Instrument And Secondary Mirror Cooling** - A study was conducted to determine the merits of various cryogenic fluids. A summary of the properties and achievable temperatures for a number of fluids is presented in Table 3.6-6; it was decided to select LN<sub>2</sub> at 77°K, LH<sub>2</sub> at 20°K and LHe at 4.2°K for further

investigations. It also appears that some superfluid Helium at 2°K will be needed.

Another study was conducted to determine the current status and technology of active mechanical or chemical closed-loop cryogenic refrigeration machines. The candidate machines are listed in Table 3.6-7 and a current status and performance summary is presented in Table 3.6-8.

Using the refrigeration load requirements listed in Table 3.6-2, and when considering the needed system cool-down capacity it appeared unlikely that requirements can be met with completely active refrigeration machines; also reliability is greatly compromised. Further, to consider only the use of stored cryogenes would also result in a large, heavy, and impractical cryogen storage system. However, a combination, or "hybrid system", of active refrigeration and stored cryogen appears attractive. This is shown in Table 3.6-9. The table data indicates that a stored cryogen system alone would require a concentric cascaded spherical vessel with an outer diameter of 5.86 meters and contain 43325 Kg of cryogenes but that the requirements can be reduced to a 3.00 meter diameter vessel containing only 7516 Kg of cryogen when used in combination with active refrigeration of 0.67 watt at 4°K, 20 watts at 20°K, and 13.5 watts at 77°K. A system comprised of multiple units of the cascaded vessels is also possible and may be more attractive for packaging and would improve reliability. The 1.50 meter diameter LHe vessel shown in this comparison is considered about minimum since analysis indicates that the equivalent LHe volume in a 1.18 meter diameter spherical vessel is needed for cool-down assuming all cool-down is furnished using stored LHe cryogen. However, the necessary cool-down capacity can be better serviced with somewhat smaller vessels if LN<sub>2</sub> is first used to lower the temperature of the

LH<sub>2</sub> equipment and if LN<sub>2</sub> followed by LH<sub>2</sub> is initially used to lower the temperature

of the LHe cooled equipment. A separate set of stored cryogenes may also be more attractive for the purpose of initial system cool-down. A study showed that a cascaded (LHe, LH<sub>2</sub>, LN<sub>2</sub>) stored cryogen vessel with an outer diameter of about 1

meter can satisfy the needed cool-down refrigeration. This also fits the philosophy of multi-unit storage vessels. Further, the parasitic heat leaks can be reduced by employing space radiator cooled shields as indicated on the conceptual cascaded cryo-fluid storage system sketch, Figure 3.6-19. An even more interesting and attractive "hybrid system" comparison would result if larger mechanical pumps can be developed and used to supplement cool-down. These are all trades which can be made in future design studies.

TABLE 3.6-6  
INSTRUMENT COOLING CRYOGENIC-FLUID CANDIDATES

GAS	P NBP PRES (PSIA)	T NBP TEMP		$\rho$ NBP LIQUID DENSITY (LB/FT <sup>3</sup> )	$\Delta H_v$ NBP LATENT HEAT OF VAPORIZATION BTU/LBm	$V_g = \frac{1}{\Delta H_v \rho}$ FT <sup>3</sup> BTU	COMMENTS
		°F	°K				
He	14.7	-452.1	4.216	7.798	8.72	0.01471	
SUPER-FLUID He	0.73	-455.8	2				
H <sub>2</sub>	14.7	-423.2	20.28	4.42	193	0.0011723	
N <sub>2</sub>	14.7	-320.4	77.4	50.46	85.7	0.000231245	
O <sub>2</sub>	14.7	-297.3	90.19	71.27	91.7	0.000153	POSSIBLE SUBSTITUTE FOR LN <sub>2</sub>
AIR	14.7	-317.8 -312.4	78.67 81.67	54.56	88.2	0.00020781	POSSIBLE SUBSTITUTE FOR LN <sub>2</sub>
Ar	14.7	-302.6	87.29	86.98	70.2	0.00016377	POSSIBLE SUBSTITUTE FOR LN <sub>2</sub>
Ne	14.7	-410.9	27.16	75.35	37	0.00035869	USE IF H <sub>2</sub> VOL IS PROBLEM
CH <sub>4</sub>	14.7	-258.7	111.7	26.5	219	0.0001723	

TABLE 3.6-7  
INSTRUMENT COOLING METHODS

- CASCADED STORED CRYOGENIC FLUIDS BACKED WITH PASSIVE RADIATOR-COOLER
  - LN<sub>2</sub> (77°K)
  - LH<sub>2</sub> (20°K)
  - LHe (4°K)
  - SUPERFLUID LHe (2°K)
- MECHANICAL CRYOGENIC REFRIGERATION MACHINES: STIRLING, BRAYTON, ROTARY RECIPROCATING, VUILLEMIER
- CHEMICAL CRYOGENIC REFRIGERATION SYSTEMS
  - NEGATIVE HEATS OF ABSORPTION/DESORPTION
  - JPL APPROACH EMPLOYING LONi<sub>5</sub> HYDRIDE/HYDROGEN
- HYBRID STORED CRYOGENIC/MECHANICAL/CHEMICAL REFRIGERATION SYSTEMS
- JOULE THOMSON EXPANSION
- VERY LOW TEMPERATURE TECHNIQUES
  - ADIABATIC DEMAGNETIZATION
  - HELIUM DILUTION (DIFFICULT IN ZERO-G)

TABLE 3.6-8  
STATUS OF MECHANICAL CRYOGENIC REFRIGERATION MACHINES

STATUS OF MECHANICAL CRYOGENIC REFRIGERATION MACHINES (1)													
Mfg.	Type	Weight (lb) (2)		Machine Size (ft) Dia. Length	Input Power Watts	Refrigeration Output (units)					Comments		
		Machine	Electronics			10°K	12°K	25°K	38°K	60°K		75°K	
Hughes (Phillips)	Sterling Cycle Magnetic Dry. (NASA Cooler) 2 stage	180	7 very complex	0.92	4.7	700	--	--	0	5	--	10	<ul style="list-style-type: none"> <li>Developed</li> <li>5 yr. life</li> <li>Projected</li> <li>Vibration</li> <li>Complicated</li> <li>Expensive</li> </ul>
Phillips	Sterling Cycle Magnetic Dry. 3 stage	468	220 very complex	0.9	6.5	2285	1.0	--	10	--	--	15	<ul style="list-style-type: none"> <li>Under development</li> <li>Vibration</li> <li>Complicated</li> <li>Expensive</li> </ul>
Garrett	Brayton Cycle Turbo Refrig. 3 stage	200	7 very complex	1.0	4.5	1300	1.0	--	10	--	--	15	<ul style="list-style-type: none"> <li>Complicated</li> <li>Very expensive</li> <li>Noisy</li> <li>Vibration</li> </ul>
A. D. Little	Rotary Recip- rocating refrig. 2 stage	450	2 large cansels very complex 70 lb.	?	?	2700	1.5	--	--	--	40	--	<ul style="list-style-type: none"> <li>20 yrs. under development</li> <li>5 yr. life</li> <li>Projected</li> <li>Complicated</li> </ul>
A. D. Little	Rotary Recip- rocating refrig. 3 stage	400	7 very complex	1.0	4.0	1500	1.0	--	10	--	--	15	<ul style="list-style-type: none"> <li>Under development</li> <li>Vibration</li> <li>Expensive</li> </ul>
Hughes	Willomer (W) cycle 3 stage	468	220	0.83	5.0		0.15	--	2	--	5	--	<ul style="list-style-type: none"> <li>Models built</li> <li>5 yr. life</li> <li>Projected</li> <li>Min. vibration</li> <li>Very expensive</li> <li>Semi-complicated</li> </ul>

(1) Data obtained at SBSS Technology Review to Industry Sponsored by Air Force Space Technology Center at Kirtland AFB, Albuquerque, NM, on Sept. 19, 1983.  
(2) Does not include heat rejection radiator.

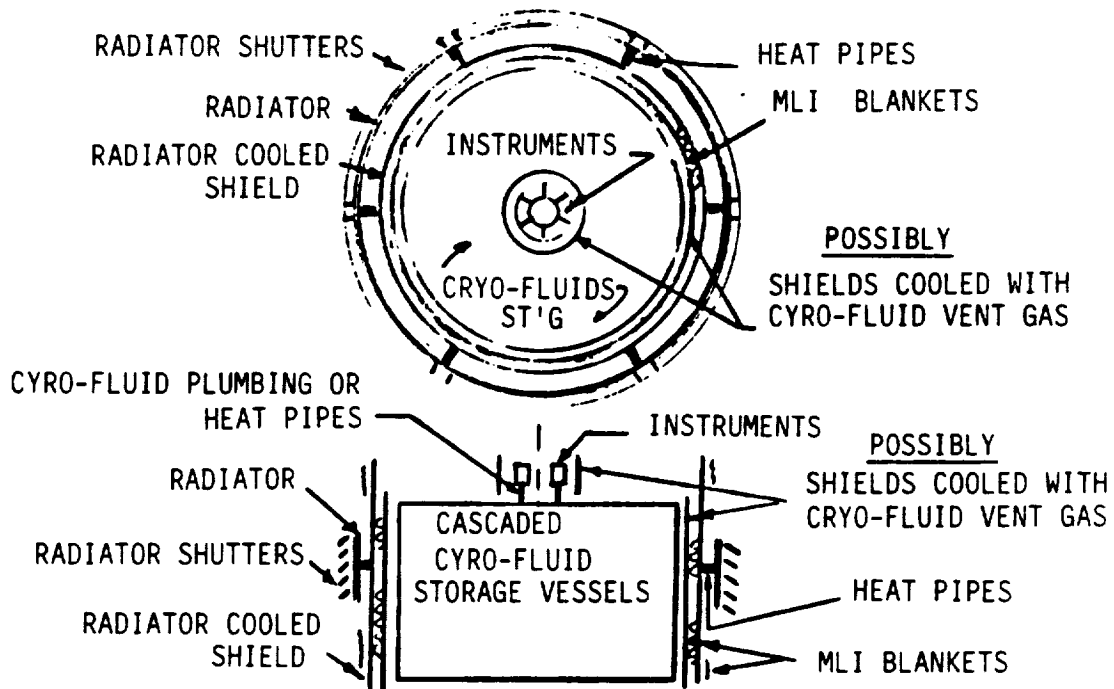


TABLE 3.6-9  
COMPARISON OF CRYOGENIC COOLING SYSTEMS FOR LDR

**Basis: - 3 year life**

- continuous operational loads: 0.25 watt at 4°K (LHe)  
1.00 watt at 20°K (LH<sub>2</sub>)  
7.00 watts at 77°K (LN<sub>2</sub>)
- parasitic heat leakage for concentric spherical storage vessels and 0.08M vacuum/insulation jackets on each vessel
- cool-down loads for 10Kg at 4°K, 30Kg at 20°K, 78Kg at 77°K

STORED CRYOGEN	ACTIVE MECHANICAL REFRIGERATION CAPACITY		
	NONE	0 W at 4°K 2.4 W at 20°K 14.0 W at 77°K	0.67 W at 4°K 2.0 W at 20°K 13.5 W at 77°K
VESSEL INSIDE DIA (M)			
LHe	3.74	3.74	1.50
LH <sub>2</sub>	4.64	4.30	2.00
LN <sub>2</sub>	5.86	5.30	3.00
CRYOGEN VOLUME (M <sup>3</sup> )			
LHe	27.39	27.39	1.77
LH <sub>2</sub>	21.25	11.52	1.79
LN <sub>2</sub>	47.46	31.50	8.86
CRYOGEN WEIGHT (Kg)			
LHe	3425	3425	221
LH <sub>2</sub>	1506	816	127
LN <sub>2</sub>	38394	25484	7168
TOTAL CRYOGEN	43325	29725	7516



**INSTRUMENT COOLING  
PASSIVE RADIATOR BACKED CASCADED CRYO-FLUID  
COOLING CONCEPT  
Figure 3.6-19**

The stored cryogen<sub>3</sub> must also be employed to serve other functions in conjunction with the ADR and He<sup>3</sup> evaporation machines that are needed for temperatures between 0.1°K and 0.3°K. In the case of ADR the cryo-fluids are needed to provide a desired superconductivity in the machine magnet and to act as a heat sink during isothermal magnetization of the paramagnetic salt. In the case of He<sup>3</sup> evaporation a cryogenic heat sink, below about 10°K, is needed during absorption of evaporated He<sup>3</sup> (in the absorption pump) and a heat sink, below 2°K, is needed to condense the returned He<sup>3</sup> gas (in the cooling chamber) when it is desorbed from the absorption pump prior to its re-evaporation in the cooling chamber to produce refrigeration at 0.3°K.

### 3.6.4 Conclusions

**3.6.4.1 Telescope Thermal Control** - The described thermal control concept and its preliminary analysis shows that the specified LDR telescope thermal requirements can be met with a reliable, weight and power economical, and practical system.

The selected temperature control approach will provide a primary mirror temperature range of  $197 \pm 1^\circ\text{K}$  to  $200 \pm 1^\circ\text{K}$  and a secondary mirror temperature of  $125 \pm 1^\circ\text{K}$ . When considering the average pointing orientation and the system thermal inertia, it is expected that the primary mirror temperature will operate at an average of about  $198 \pm 1^\circ\text{K}$ .

The primary mirror design is semi-passive requiring only a shield around the front face, and temperature control trim-heaters plus "space-viewing" active louvers at the near face. For reliability, separate heaters will be used for each mirror segment and the louvers will be operated with bi-metallic drives backed-up with electrical drives.

The secondary mirror requires cryogen cooling to achieve a temperature of 125°K. The cooling load is reasonable (worst-case max. is 5 watts; average is likely 1 watt or less). Further effort is needed to determine the best technique for adapting cryogen cooling to this mirror (e.g., stored cryogen system packaged at the mirror or cryogen fluid plumbed to the mirror from remote storage).

The design approach entails no operating time constraints at any orbit position, and will accommodate simultaneous sun and earth/albedo exposures at their maximum specified heat load exclusion angles (60° sun, 45° earth).

Providing thermal finishes that are stable in a space environment over a 10 year period is an important issue. The surface of the finishes must not be contaminated with organics such as those generated by rocket propellants or by composite materials outgassing. Further, the coatings must not be seriously eroded by meteorites and accordingly, coated thin plastic membranes which meteorites can penetrate are judged unacceptable.

The design must consider packaging within the space Shuttle in addition to means for on-orbit deployment and/or assembly at the Space Station. The shield can also serve as a work-tent to protect the telescope from Space Station contamination sources during the LDR assembly period.

Areas of critical technology and the suggested technology effort to be completed by 1991 are addressed in the Technology Assessment Report, Volume II.

3.6.4.2 Science Instrument And Secondary Mirror Cooling - The described "hybrid" cryo-fluid storage and active closed-loop refrigeration system will meet the specified LDR instrument and secondary mirror cryo-cooling requirements and the system will be reliable and weight economical. Redundant active refrigeration machines are suggested and the system must be serviced and cryogens replenished at three year intervals; refrigeration machine life should be aimed at 10 years but module replacement, at three years, will not be impractical. Attention should be given to multi-compartmentalized cryogen storage vessels or to multi-unit storage vessels to guard against total cryogen leakage loss from causes such as wall penetration by large meteorite impacts; meteorite guard walls should also be considered.

Both mechanical and chemical absorption active refrigeration machines are potential candidates with a likely preference toward using a chemical system (e.g., JPL Lanthanum Pentanickel Hydride). Temperatures to 4°K will likely require compressor/Joule Thomson expansion cycle machines and temperatures between 0.1°K and

0.3°K will require Adiabatic Demagnetization and He<sup>3</sup> Evaporation machines. A He<sup>3</sup> -

He<sup>4</sup> Dilution Refrigeration system is another possible candidate but will require many technology advances to enable it to operate in a zero-g space environment. Current effort is underway for all of the needed active cryogenic cooling machines but

considerably more effort is needed (particularly to 4°K and lower) to meet the needs for LDR. For instance, just 0.10 watt of mechanical refrigeration at 4°K over a three year period is equivalent to 3.74 cubic meters of stored LHe. Also, the volume ratio of stored LHe to LN<sub>2</sub> is nearly 64:1 for equal cooling capacity.

The refrigeration capacity needed for initial cool-down of LDR equipment cannot be met using a practical sized active closed loop refrigeration machine. The cool-down will demand a supply of stored cryogen, and this was included in the capacity analysis of the suggested "hybrid" cryogenic cooling system; however, a separate cool-down cryogen supply vessel may be more attractive. For example, a calculation showed that a "hybrid" system employing a 2-meter outside diameter cascaded cryogen vessel, containing 3270 Kg of stored cryogens, is possible without considering initial cool-down, and another smaller vessel (about 1 meter diameter) would service cool-down.

Servicing and replenishment of the "hybrid" cryogenic refrigeration system is needed and will require currently non-existing on-orbit robotic implementation techniques. It appears, both from the standpoint of cost and the risks of losing LDR, that it is better to provide servicing for the cryogenic refrigeration system at the operational orbit position of LDR rather than bringing LDR back to the Space Station for servicing. Also, this will minimize contamination risks to the thermal and optical surfaces on LDR.

To reduce vibration to a minimum, at the telescope and science instrument focal planes, it may become necessary to consider split-cycle active refrigeration machines; this will increase parasitic heat leakage and further complicate the system design. The efficiency of active refrigeration machines must be increased. Work is needed on designing highly efficient and compact (large area to volume ratio) heat exchangers for use with these machines, and more effective thermal radiators are needed to reject the mechanical power heat loads. An improvement is needed in the implementation of cryogen-cooled thermal insulation shielding, using spent cryogen, and to the recycle (i.e., recover) of this cryogen. The simultaneous and continuous management of cryogen liquid and vapor within a common storage vessel, in a zero-g environment, presents many engineering challenges.

Avoiding contamination of the instrument detector surfaces is a very critical design issue since these surfaces must be maintained pristine clean to preserve the required detector sensitivities. At those very low cryogenic temperatures almost all materials can act as a source of contamination; very inert metals such as gold and platinum may be needed immediately surrounding the detector assemblies. The immediate optical path should be provided with vapor diffusion channels and cold-stops and it may become necessary to employ shutters that are closed except during the operation period.

Areas of critical technology and the suggested technology efforts to be completed by 1991 are addressed in the Technology Assessment Report, Volume II.

## 3.7 POINTING AND CONTROL

### 3.7.1 TASK

The purpose of this task was to evaluate alternate pointing control, fine guidance sensing and chopping concepts.

### 3.7.2 Approach

Movement of the large LDR observatory will induce line of sight errors into the LDR telescope. Alternate control concepts (body pointing, separate telescope pointing, additional smaller optics) and dynamic control via damping of high strain elements were considered to minimize jitter.

Kodak recently completed a contract to NASA/MSFC to investigate Space Telescope fine guidance sensing concepts with no moving parts. A similar concept for LDR was investigated in this study. Chopping alternatives (secondary mirror, fold plane mirror, and re-imaging optics) were also investigated.

### 3.7.3 Discussion

The pointing and control concept will consist of sensors, control actuators and control algorithms. The control elements of concern include deployment stabilization; attitude reference acquisition; maneuvering; guide star acquisition; fine pointing stability, and control to a passive attitude for servicing. Depending upon operating modes, LDR attitude would be obtained from either sun sensor, star tracker, magnetometer or fine guidance sensor information. Control torque commands would be generated by processing sensor signals in the onboard processor according to programmed momentum management, reaction wheel, and magnetic steering laws.

The pointing requirements imposed on the LDR are of two types, initialization and dynamic. For initialization, the pointing accuracy is traditionally set at one-tenth the Airy disk diameter.

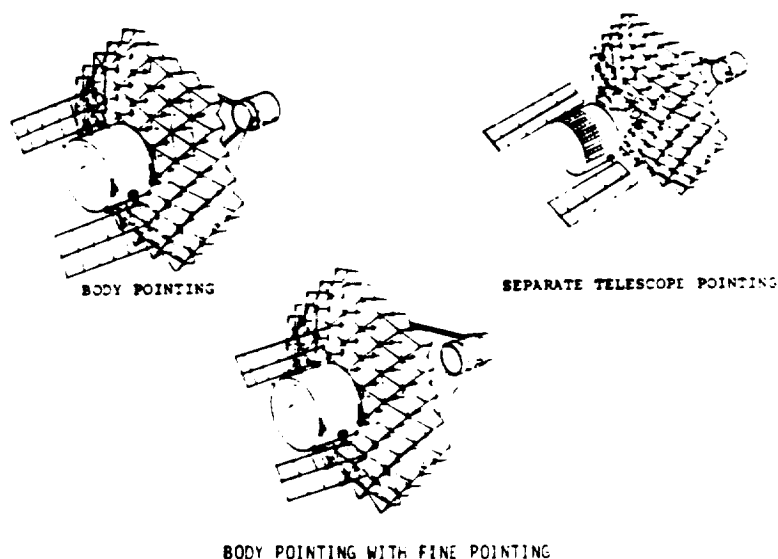
For LDR initialization the calibration focal plane accuracy must be such that any scientific instrument aperture can be positioned with respect to a guide star to 0.05 arcsecond.

For dynamic control, the pointing stability error is traditionally set at one-thirtieth the Airy disk diameter. A slightly more lenient LDR requirement of 0.02 arcsecond was set at the 1982 Asilomar workshop. Under LDR operation excitation during fine pointing (due to relative motion of LDR structure to spacecraft or between optical elements), the relative dynamic displacement between the LDR image and any scientific instrument aperture must therefore not exceed 0.02 arcsecond.

In its on-orbit state, LDR will have structural characteristics that could seriously degrade the system's optical performance. The improper selection of a control concept could increase the mechanical disturbances which produce pointing errors.

In this study three passive pointing concepts were evaluated: (1) body pointing, (2) separate telescope pointing, and (3) fine pointing. These concepts are shown in Figure 3.7-1. In the body pointing concept the spacecraft (aft end); primary mirror and secondary mirror are rigidly coupled. The roll, pitch and yaw of the vehicle are slewed about the moment of inertia of the entire LDR observatory. In the second concept the spacecraft is decoupled from the LDR optical subsystem (primary mirror and secondary mirror). A three degree of freedom gimbal (pitch, roll and yaw) would be provided at the interface. The LDR optical subsystem would be moved separately. An alternative is the use of a tertiary mirror, which in addition to a base stabilization system (body pointing) requires a vernier control system to achieve fine pointing.

There is an interrelationship between the spacecraft control system and the telescope control system (figure control and rigid body control). The degree of dynamic structural control required influences the structural design approach.

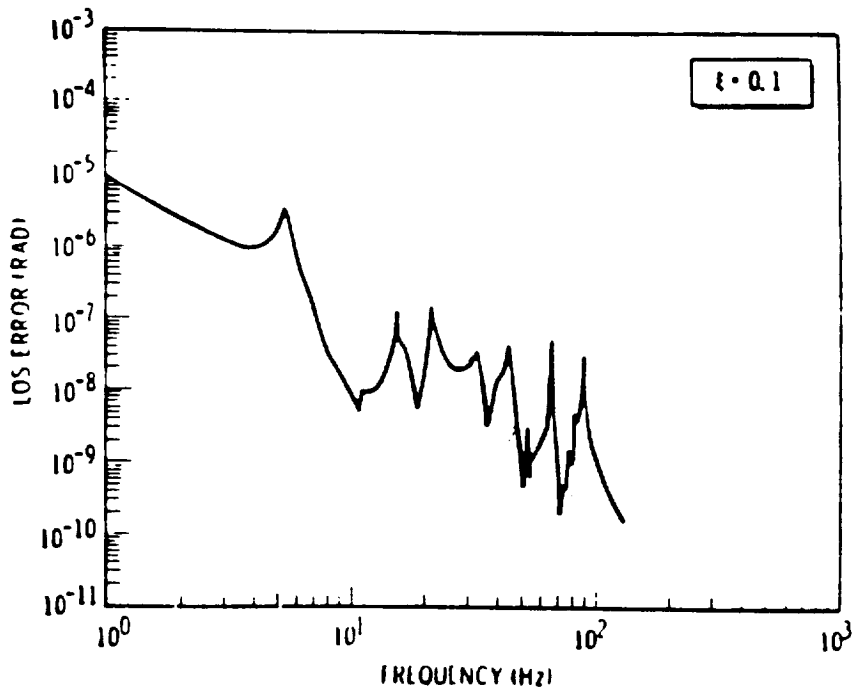


POINTING CONCEPTS  
Figure 3.7-1

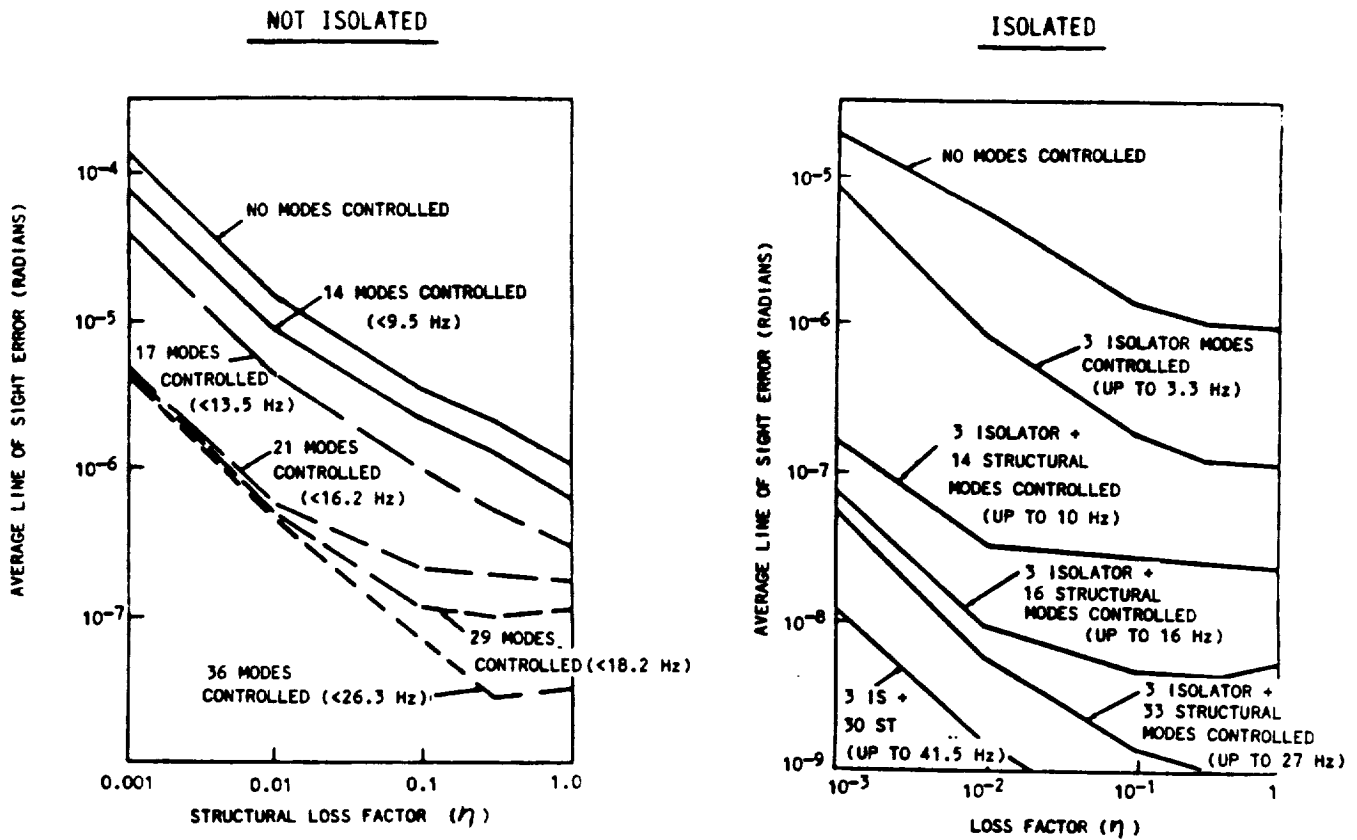
An all-deployable structure would have many joints which tend to introduce an unknown degree of flexibility into the structure. The joints introduce an error into the dynamic model because their stiffness characteristics are not well defined. This error will result in a degradation of optical performance possibly to the extent that an active control system could not compensate. A preloaded joint design may eliminate this problem. An LDR will have high modal density which may aggravate the pointing control task. Material degradation of structural members due to the space environment may cause the structural frequencies to shift. The use of viscoelastic

materials (VEM) may be of benefit for reducing optical error. Unfortunately, they too are subject to degradation. Their structural characteristics are not well defined and they are highly temperature-dependent. Realistic VEM hardware suitable for LDR applications is just now being developed. The potential benefits of such devices have been studied to some degree in the DARPA sponsored ACOSS (Active Control of Space Structures) program. In their concept (two mirror Cassegrain telescope) most of the strain energy was in the secondary mirror support struts below 20 Hz. If damping is applied to these high strain members a reduction in the line of sight error is achieved as shown in Figure 3.7-2. In addition, damping makes isolation more effective as illustrated in Figure 3.7-3.

Effective isolation of vibratory equipment on the LDR will be necessary to obtain adequate optical performance. Maintaining the dimensional stability of the support structure will be essential. The distortions caused by vibratory equipment and thermal cycling will have to be studied.



LINE OF SIGHT ERROR DUE TO SECONDARY MIRROR JITTER  
Figure 3.7-2



LINE OF SIGHT ERROR WITH DAMPING

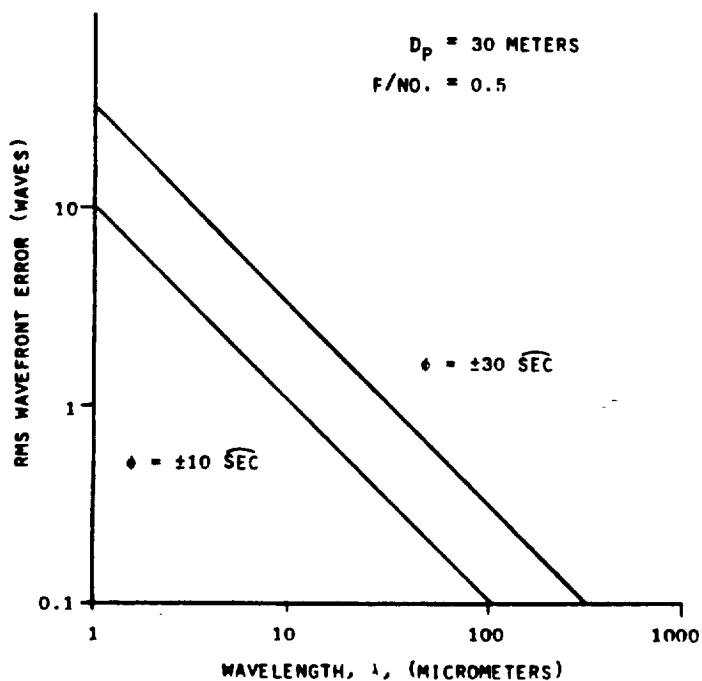
Figure 3.7-3

Field of view scanning by chopping (possibly by oscillating the secondary mirror) is an LDR requirement. Through this process, weak IR sources can be detected in a region of comparable background IR radiation.

With respect to using the secondary mirror chopping technique, note that in a static sense, misalignment of the secondary mirror optical axis with respect to the primary mirror optical axis increases the telescope wave front error (mainly coma).

Shown in Figure 3.7-4 is a graph of wave front degradation introduced by misaligning the secondary mirror axis. Obviously the scan FOV must be larger than the image diameter. A scan FOV of 60 arcseconds is about five times the spot diameter at the operational wavelength of 800 micrometers. At the longer wavelengths (greater than approximately 100 micrometers), the coma due to secondary mirror misalignment has negligible effect on telescope performance. However, the scan amplitude is so large that at the lower operational wavelengths, misalignment coma is unacceptable if the scan is accomplished by secondary mirror tilting.





STATIC WAVEFRONT ERROR DUE SECONDARY MIRROR TILT  
 Figure 3.7-4

Oscillating the secondary mirror may excite intolerable resonances in the rest of the structure. These vibrations could be controlled by isolating the disturbance sources or by application of viscoelastic damping treatments.

Due to these hardware concerns, alternate approaches may be preferable. One approach may be to oscillate a small tertiary mirror near the focal plane. This reflector might also serve as a fast steering mirror for small pointing corrections.

3.7.3.1 Pointing Control - This study effort was based on the functional requirements presented in Table 3.7-1.

TABLE 3.7-1  
 FUNCTIONAL REQUIREMENTS

Absolute Pointing	0.05 $\overline{\text{sec}}$
Jitter	0.02 $\overline{\text{sec}}$ - within 1 minute after slew
Slew	20-50°/minute
Scan	1° x 1° - Linear scan at 1°/minute
Track	0.2°/hour (for comets $\geq 25^\circ$ from sun)

The first three specifications (pointing, jitter, and slew) present the most problems using existing technology. Improvements in technology to meet these specifications are discussed. In addition, trade-offs between mechanism weight, complexity, availability, and desired fast slew rate may be necessary (although not addressed in this study). A detailed targeting sequence profile study might determine that slower slew rates could be accepted.

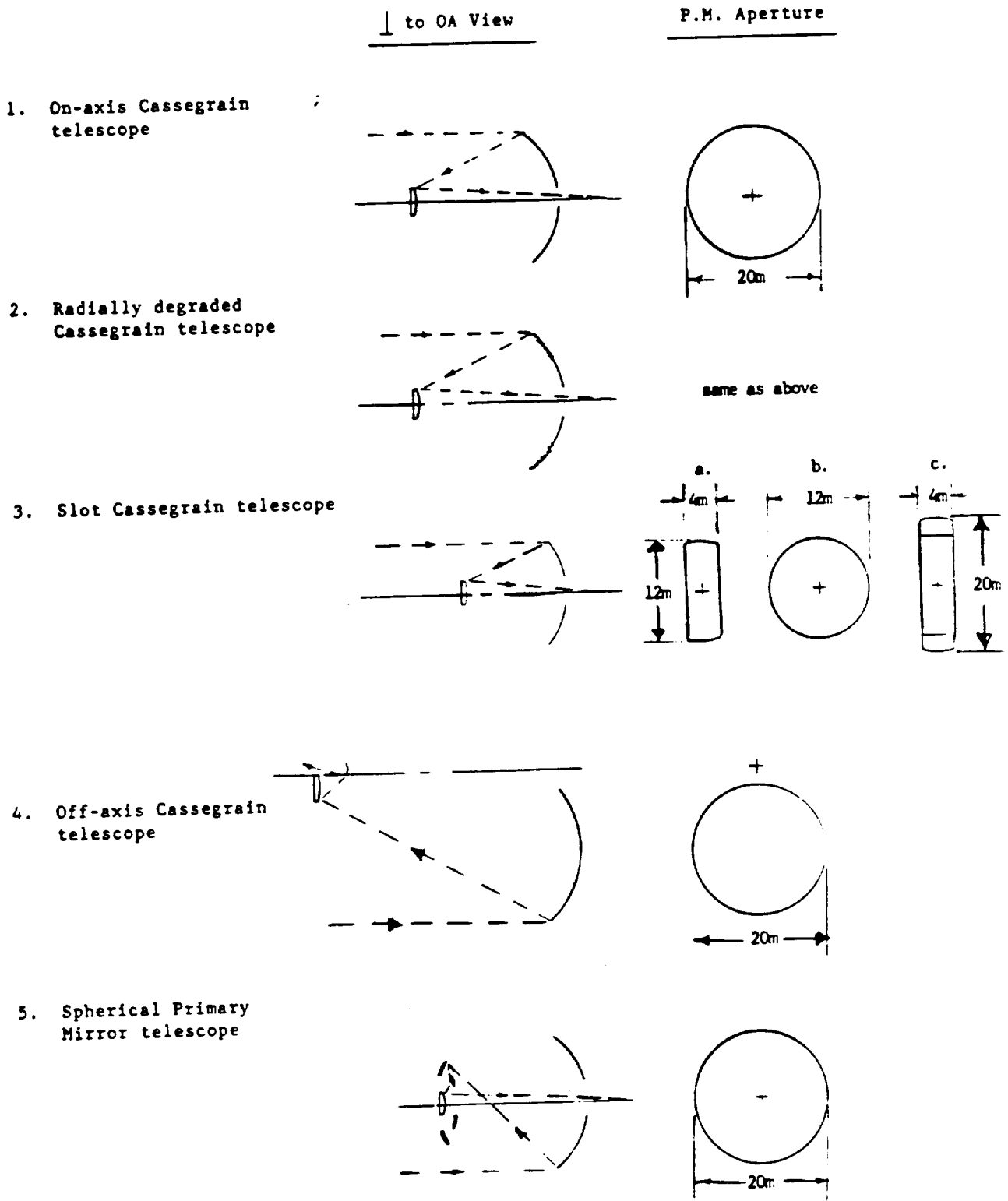
Figure 3.7-5 illustrates the optical configurations evaluated in this study. Views looking both down the optical axis and perpendicular to the optical axis are depicted.

Configurations 1-4 have aspheric primaries and secondaries. Configuration 5 has a spherical primary, but a compound secondary with potentially two or three aspheric surfaces.

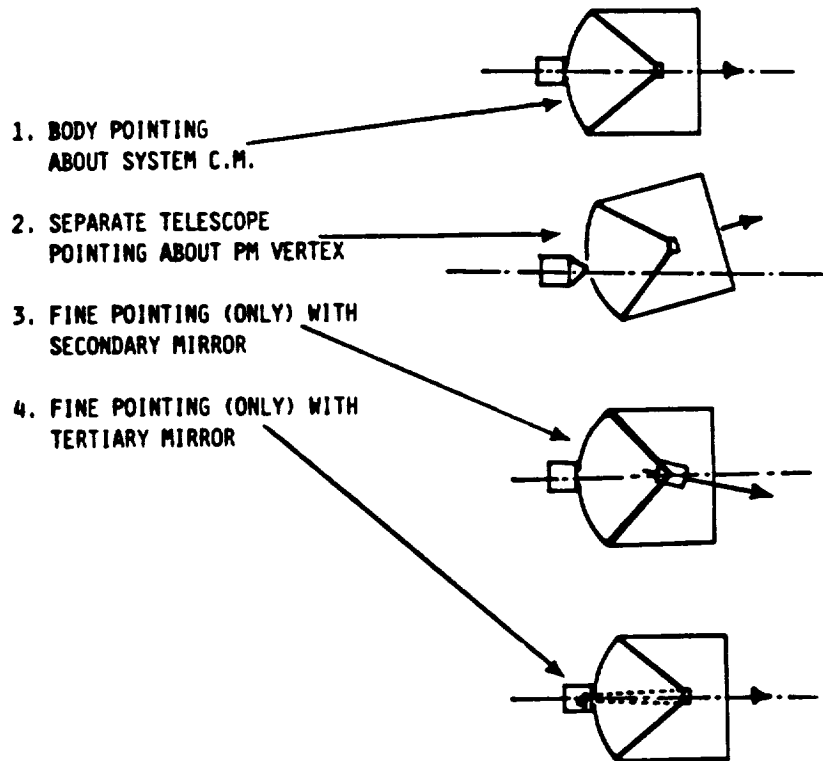
Figure 3.7-6 illustrates the pointing candidates. Fine pointing techniques (or image motion compensation) were investigated using either a secondary mirror or tertiary mirror. Either fine pointing method could be coupled to either coarse pointing technique - body pointing or separate telescope pointing. Fine pointing utilizing the secondary mirror concept requires a larger, more stable platform for the secondary. Fine pointing using either method would be complicated if the same technique were also used as the method for chopping (i.e., secondary mirror chopping and secondary mirror fine pointing).

3.7.3.1.1 Moments of Inertia - The basic assumptions used in moments of inertia (MOI) calculations were:

- A. Thermal Shield - MOI standard equation for a hollow cylinder was used, with a length 7.76m longer than the primary to secondary mirror spacing, constructed to fit the shape of the primary mirror, and an areal density of  $0.645 \text{ Kg/m}^2$ .
- B. Scientific Instruments Package - MOI standard equation for a solid cylinder was used, with a 4.5m diameter by 4.0m long package, with a mass of 4500 kg.

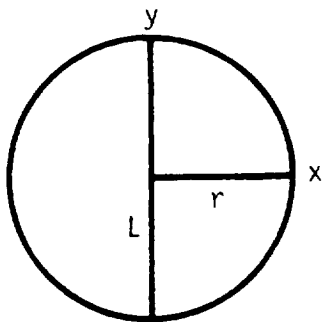


OPTICAL CONFIGURATIONS  
Figure 3.7-5



LDR POINTING CANDIDATES  
Figure 3.7-6

- C. Spacecraft - MOI standard equation for a solid cylinder, 4.5m diameter by 4.0m long, with a mass of 5000 kg.
- D. Secondary Mirror Support - (Refer to Figure 3.7-7). The following approximation was used:



a tripod having legs with  
a mass of 200kg each

$$I = 2I_{\perp} + \frac{1}{3} mr^2$$

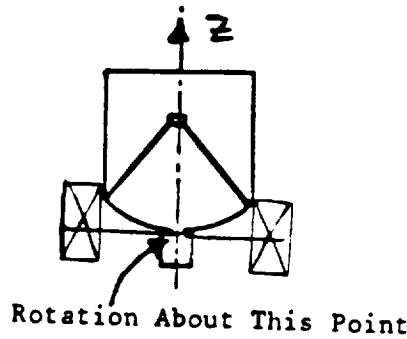
$$= m\left(\frac{2}{3}L^2 + \frac{1}{3}r^2\right)$$

BASIS FOR MOI CALCULATION  
Figure 3.7-7

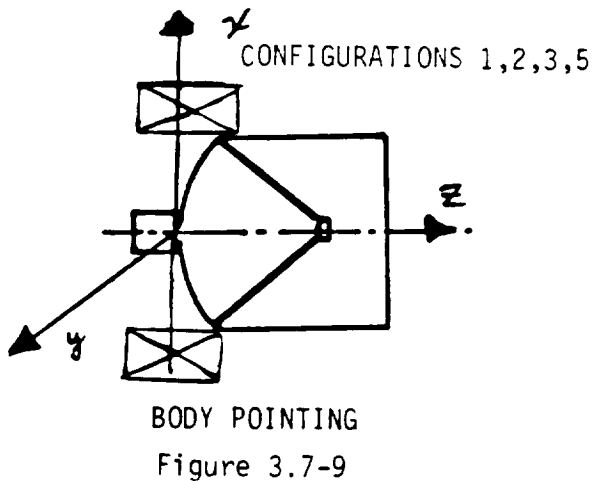
- E. Solar Cells - MOI for a solid rectangle, with two 5m wide by 10m long solar panels of 500 kg mass each.
- F. Primary Mirror Assembly - MOI depends upon configuration, with a 7400 kg mass for Configuration 1, and proportionally scaled to other configurations.
- G. Primary Mirror Integrating System - 3000 kg mass for Configuration 1, and proportionally scaled to other configurations.
- H. Secondary Mirror Assembly - 250 kg mass for pointing Technique 1.

All five configurations were evaluated for each of the three pointing techniques.

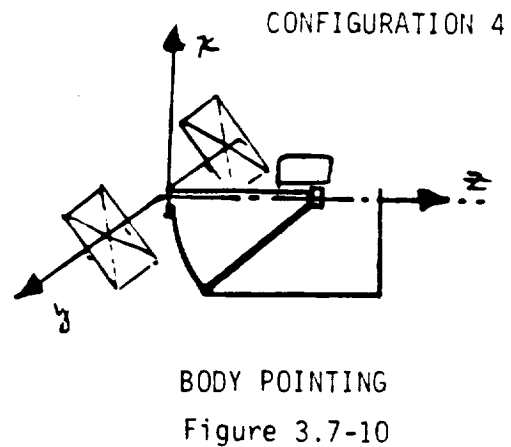
3.7.3.1.1.1 Body Pointing - The entire unit is considered to be rigid and the axis of rotation is about the y-axis with the origin at the hole in the scientific instrument package (Figure 3.7-8). Note the difference when comparing Configurations 1, 2, 3, and 5 to Configuration 4 (Figures 3.7-9 and 3.7-10).



BODY POINTING  
Figure 3.7-8



BODY POINTING  
Figure 3.7-9



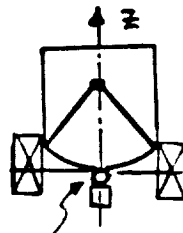
BODY POINTING  
Figure 3.7-10

The body pointing technique results are presented in Table 3.7-2.

TABLE 3.7-2  
BODY POINTING TECHNIQUE SUMMARY

CONFIGURATION	PROPERTY OF INERTIA ( $10^3 \text{ kg-m}^2$ )		
	X	Y	Z
ON-AXIS RADIALLY DEGRADED	698	930	872
SLOT	a.	340	495
	b.	372	434
	c.	515	698
OFF-AXIS	1.241	992	1.038
SPHERICAL PRIMARY	791	1.022	873

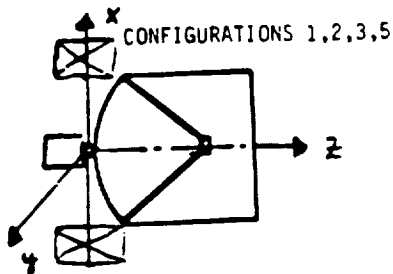
3.7.3.1.1.2 Separate Telescope Pointing - A gimbal is placed between the primary mirror integrating structure and the scientific instruments (Figure 3.7-11). This permits movement about the axis at the same origin; however, when determining MOI, the instruments and spacecraft are ignored.



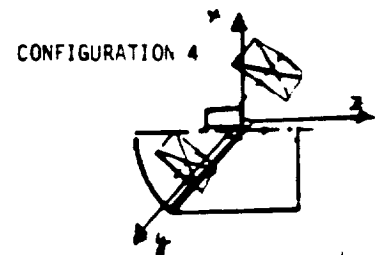
Gimbal is New Pivot Point

SEPARATE TELESCOPE POINTING  
Figure 3.7-11

Again, note the difference between Configuration 4 and the others: (Figures 3.7-12 and 3.7-13)



SEPARATE TELESCOPE POINTING  
Figure 3.7-12



SEPARATE TELESCOPE POINTING  
Figure 3.7-13

For all configurations but 4, the MOI is less than for body pointing, since the spacecraft and instrument package may be ignored. Configuration 4 is more because the pivot point is no longer at the center of mass (around the vertex of the primary mirror), but is located at the scientific instrument package so that as the package subtends an angle with respect to the telescope, the range may just be pivoted about the origin.

The results of this technique are presented in Table 3.7-3.

TABLE 3.7-3  
SEPARATE TELESCOPE POINTING

CONFIGURATION	MOMENT OF INERTIA ( $10^3 \text{ kg-m}^2$ )		
	X	Y	Z
ON-AXIS RADIALLY DEGRADED }	412	412	623
SLOT {	a.	59	87
	b.	91	91
	c.	234	406
OFF-AXIS	4,346	4,316	731
SPHERICAL PRIMARY	510	510	613

3.7.3.1.1.3 Body Pointing with Secondary Mirror as a Fine Pointer - Same as Configuration 1, except the secondary mirror will be doing more functions; therefore, its mass will be greater (340 kg). Also, the mass of the scientific instrument package increases to 4750 kg to accommodate the increased mass of wiring and electronics for the new secondary mirror assembly.

Table 3.7-4 summarizes the results of body pointing using the secondary mirror to fine point.

TABLE 3.7-4  
BODY POINTING WITH FINE POINTING USING SECONDARY MIRROR

CONFIGURATION	MOMENT OF INERTIA ( $10^3 \text{ kg-m}^2$ )		
	X	Y	Z
ON-AXIS RADIALLY DEGRADED }	722	953	872
SLOT {	a.	345	500
	b.	376	439
	c.	525	708
OFF-AXIS	1,331	1,083	1,038
SPHERICAL PRIMARY	803	1,035	874

**3.7.3.1.2 Torque Profile** - Torque profiles (slew and scan) were determined using the MOI calculations for the 15 combinations of configurations and pointing techniques. Figures 3.7-14 to 3.7-16 show the slew torque profiles for the three pointing techniques. Using the secondary mirror for fine pointing implies that a larger slew torque is required (i.e., the secondary mirror assembly has a longer mass). Figures 3.7-17 to 3.7-19 show the scan torque profiles.

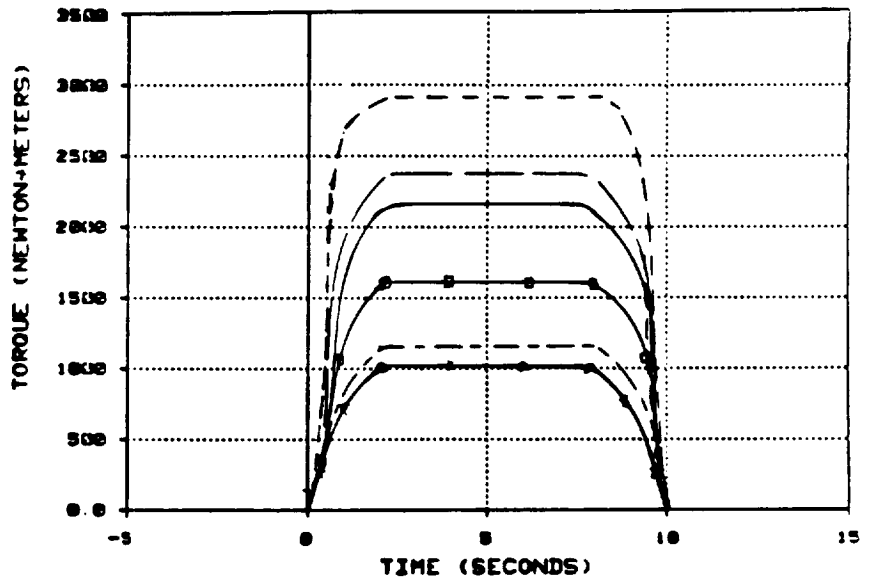
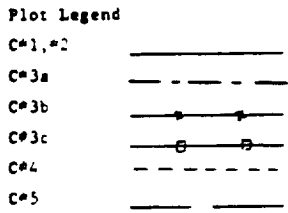
**3.7.3.1.3 Pointing Trades** - A trade study of the optical configurations and the pointing techniques was performed using the Jenko (Perado) approach. This approach arrives at a numerical evaluation of the systems while removing subjective bias on the part of the evaluator. The method consists of rating each contributing parameter for each system, multiplying these ratings by a weighting system based on degree of concern, and summing the results. The results were then normalized to arrive at a relative rating system. Table 3.7-5 shows the rating for each influencing parameter and the total score for each system. The normalized ratings are presented in Table 3.7-6. Data was unavailable on several of the contributing parameters, two of which have high weights. Thus, this data could possibly change the order of the top five rated configurations. It should also be noted that the same tabulated weights were used for rating both the configurations and pointing techniques, when in reality, different weights may be desired (e.g., moment-of-inertia and torque are the two determining factors for pointing and should probably be rated high. However, the order of rating would not change).

The following conclusions can be drawn from Tables 3.7-5 and 3.7-6. Even though the tabulation is incomplete, the on-axis Cassegrain configuration should outrate the radially degraded Cassegrain. (An anticipated  $\Delta$  weighting in favor of Configuration 1 of 2 for optical quality and at least 1 for spec. would have to be balanced by at least 4.3 in favor of Configuration 2 for cost - which is unlikely). Therefore, there appears to be little reason to continue the radially degraded configuration. By similar reasoning, the off-axis, spherical primary, and slot configuration of 20 x 4 m can be deleted. Thus, by a process of elimination, the on-axis Cassegrain and the 12 x 4 m and 12 m dia slot configurations are the preferred choices. If the program is transportation-limited (i.e., delivery to orbit), the slot configurations would be preferred. Note, however, that the information gathering capability as defined by the system aperture is in an inverse ratio when compared to the final ratings of these three configurations.

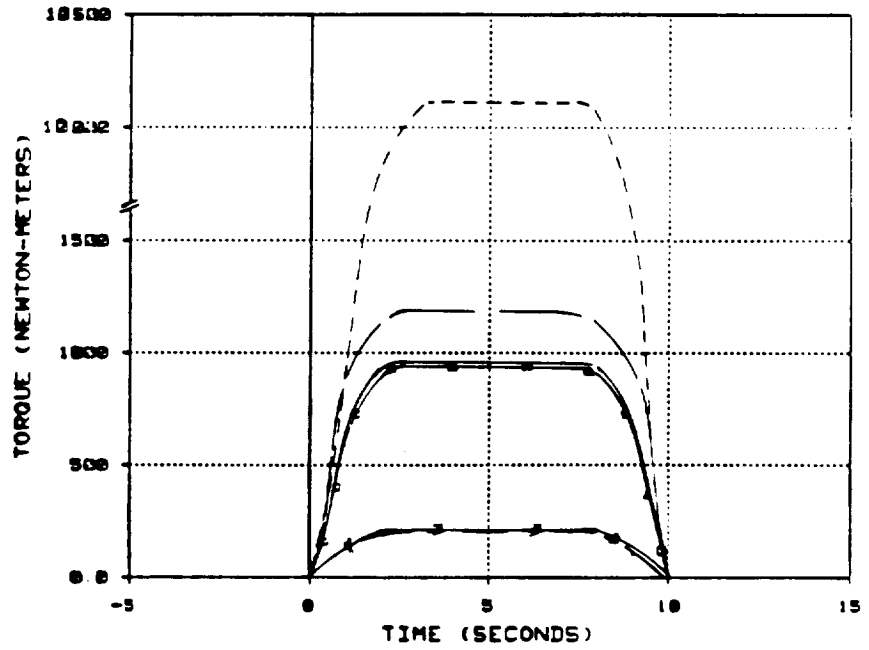
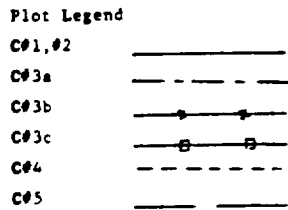
Since there is no significant advantage between body pointing and separate telescope pointing the preferred coarse pointing method is body pointing. In separate telescope pointing a control gimbal would have to be installed between the telescope and the spacecraft. This implies increased complexity and increased cost. Fine pointing using the tertiary mirror concept is the preferred method; however, the effect of using the same technique for fine pointing and chopping has not been thoroughly evaluated, and may not be recommended.

The Space Telescope utilizes body pointing for both coarse pointing and fine pointing. Reduction in CMG jitter may allow a similar philosophy for LDR, thereby eliminating the need for a separate fine pointing subsystem.

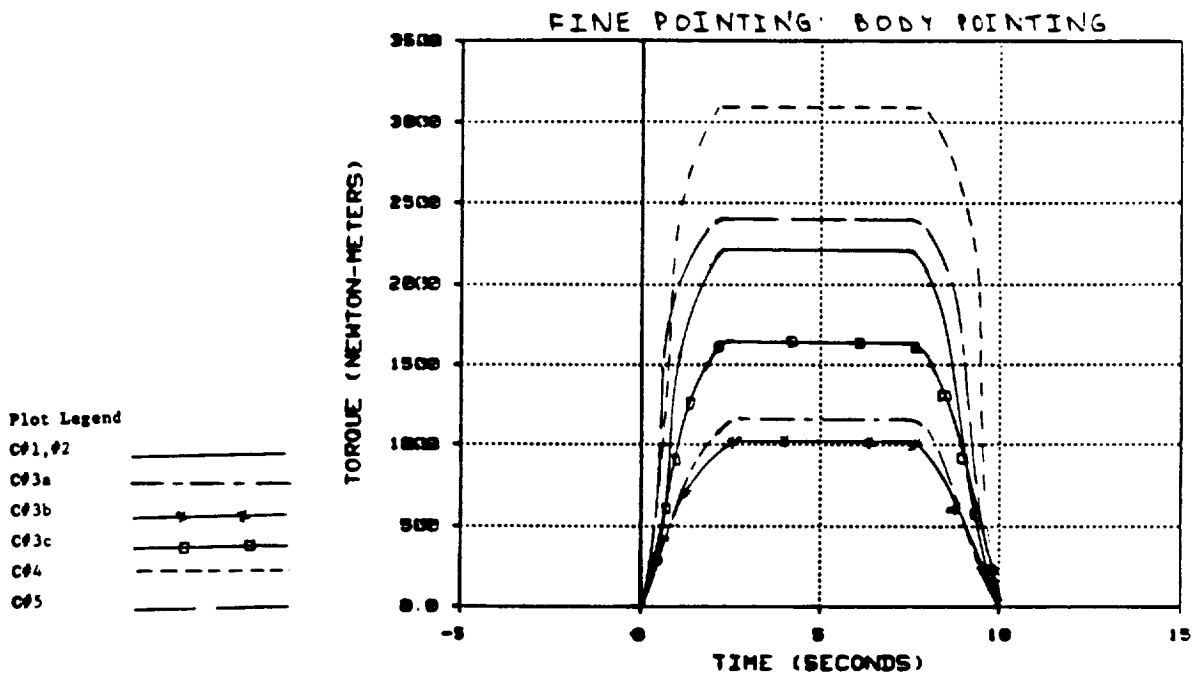




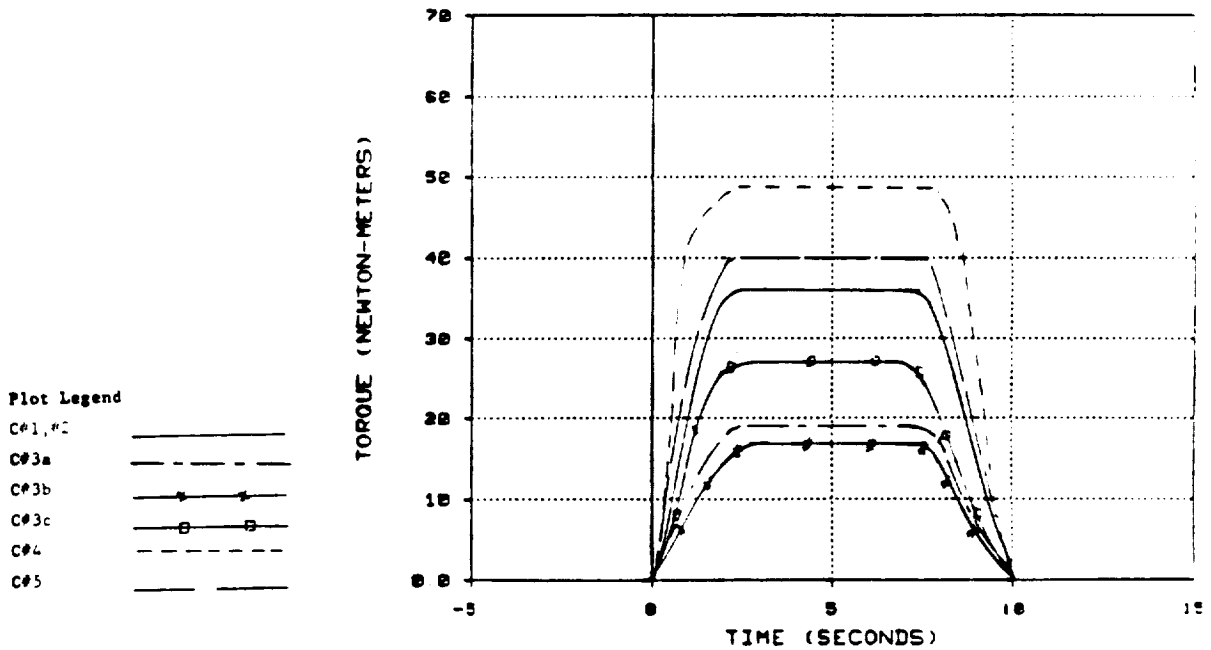
SLEW TORQUE PROFILE: BODY POINTING  
Figure 3.7-14



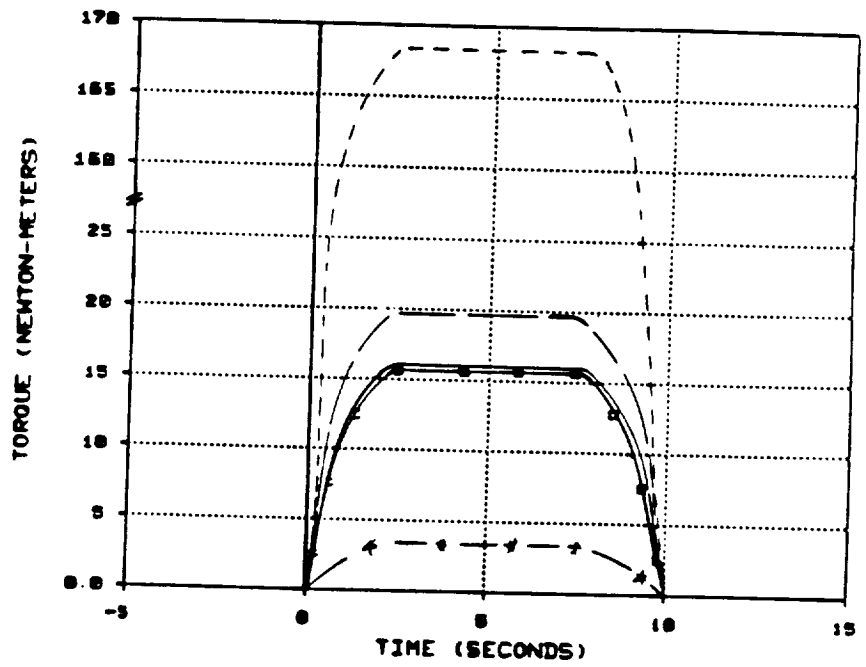
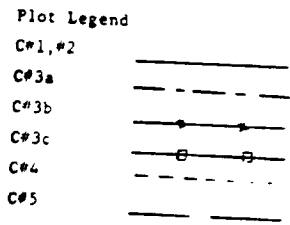
SLEW TORQUE PROFILE: TELESCOPE POINTING  
Figure 3.7-15



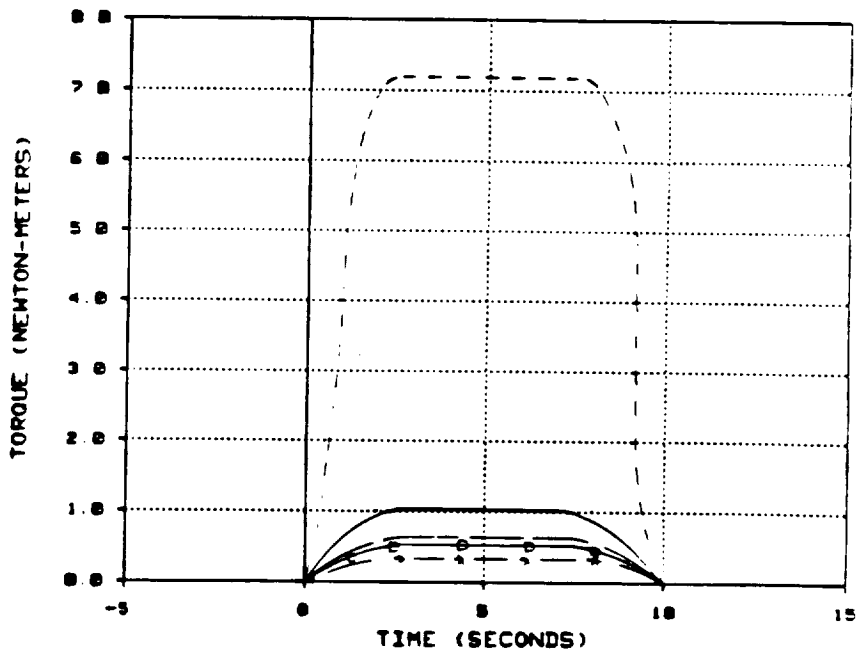
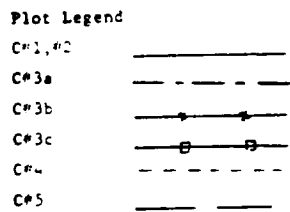
SLEW TORQUE PROFILE: SECONDARY MIRROR  
Figure 3.7-16



SCAN TORQUE PROFILE: BODY POINTING  
Figure 3.7-17



SCAN TORQUE PROFILE: TELESCOPE POINTING  
Figure 3.7-18



SCAN TORQUE PROFILE: SECONDARY MIRROR  
Figure 3.7-19

TABLE 3.7-5  
 POINTING TRADE STUDY OF OPTICAL CONFIGURATIONS  
 AND POINTING TECHNIQUES USING JENKO APPROACH

<u>Configuration</u>	<u>Energy Mof I Torque</u>	<u>Optical Quality</u>	<u>Align- ment</u>	<u>Manu- facture</u>	<u>Stability/ Control</u>	<u>Meet Spec.</u>	<u>Complexity</u>	<u>Reliability</u>	<u>Technology</u>	<u>Weight</u>	<u>Cost</u>	<u>Weighted Total</u>
1. On-axis	6.1	8.73	7.5	6.5	8	TPO	8	9	(1)*	7.2	TPO	522.5
2. Radially Dep.	6.1	8.73	7.5	7	8	TPO	7	8		7.2		510.5
3. Slot												
a. 12 x 4	10	9.86	8.5	6	8.5		9	10		10		612.2
b. 12 dia.	9.9	9.86	8.5	6	9		8	9		8.8		590.8
c. 20 x 4	7.4	8.86	8	5	7		8	7		8.9		510.1
4. Off-axis	1.0	3	1.5	4.5	5		4	5		7		264.5
5. SPH PH	5.6	8.7	7	7	6		7	7		7.1		470.9
WEIGHTING	8	9	9	8	10	10	6	10	5	8	7	
<u>Techniques</u>												
<u>Coarse</u>												
Body	7	8	9	9	8	9	9	8	8	10	TPO	705
Telescope	9	9	8	8.5	10	8	8	9	8	9		723
<u>Fine</u>												
SH	-	-	9	7.7	9	8	9	7	7	8		535.6
TH	-	-	10	8	10	10	10	10	6	10		624

\* SEE APPENDIX

TABLE 3.7-6  
 POINTING TRADE STUDY OF OPTICAL  
 CONFIGURATIONS AND POINTING TECHNIQUES  
 USING JENKO APPROACH\*

<u>Configuration</u>	<u>Normalized Weighted Score</u>	<u>Concerns/Comments</u>
1. On-axis	.85	- Insufficient data available to evaluate: optical quality, satisfying specs, or cost. These values could have a significant impact on conf. 1-3 standing (conf. 4 and 5 are not expected to change positions). - Conf. 3 may be the best choice if the system is transportation limited, i.e., delivery to orbit (which was not considered in this analysis).
2. Radially Degraded	.83	
3. Slot		
a. 12 x 4 m	1.0	
b. 12 m dia.	.97	
c. 20 x 4 m	.83	
4. Off-axis	.43	
5. Spherical PM	.77	
<u>Techniques</u>		
Body } Coarse Pointing	.98	
Telescope }	1.0	
SM } Fine Pointing	.86	
TM }	1.0	

\*Higher number indicates better rating

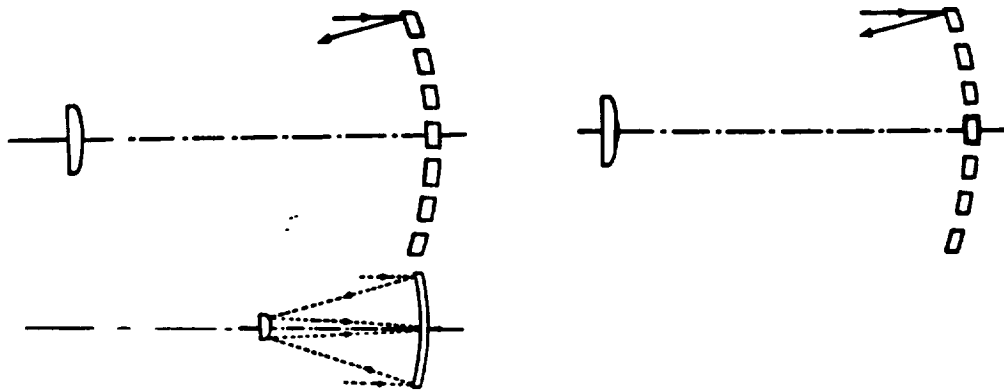
**3.7.3.2 Fine Guidance Sensing** - A fine guidance sensor has several functions. In the Space Telescope its primary function is to detect misalignment of the line of sight (LOS) vector by measuring the positions of auxiliary or guide star images in the telescope focal plane. (Note: To a pointing stability requirement of 0.007 arcsecond and to a pointing accuracy requirement of 0.01 arcsecond.) The measurement is converted to an electrical error signal for use of the Support System Module (SSM) in correcting the pointing direction. Depending on the application in some cases, knowledge of the condition of focus of a telescope, as well as the value of the focal length, can be determined from the fine guidance sensor.

The LDR must be designed so that the motion of target star images due to thermal/mechanical effects in the LDR during observation periods will be less than 0.02 arcsecond, or approximately 19 micrometers in image space. The LDR stability requirement, therefore, essentially defines the image motion of a target star relative to an SI aperture during an observation, with ideal pointing and no mechanical disturbances. For the above conditions, there are three primary image motion error sources: motion of the target star image relative to the guide star image; motion of the fine guidance sensor (FGS) effective aperture relative to the SI mount; and motion of the SI aperture relative to the SI mount.

Even though the LDR pointing stability requirement (0.02 arcsecond) is approximately three times the Space Telescope pointing stability requirement (0.007 arcsecond) it is still difficult by today's standards. A value of 0.2 arcsecond can be achieved with current technology and extreme care. The major hardware concern is dimensional stability of the sensor itself. Optics and any moving mechanisms in the sensor can produce large rather than small error contributions to the end result line of sight error. Therefore, the pointing requirements, even though less stringent than those imposed on Space Telescope, must be considered critical issues until further pointing and control definition is established for LDR.

One option for implementing fine guidance sensing would be to utilize the LDR telescope for fine guidance sensing (i.e., the Space Telescope approach). However, visible fine guidance sensing is not compatible with the LDR operational wavelength region from the far IR to the submillimeter region. Two alternate approaches were evaluated in the study (Figure 3.7-20). The first approach utilizes a section(s) of the LDR optical subsystem for fine guidance sensing. The visible quality section(s) could be an inner annulus, an outer annulus, or patches. The concept has the advantages of (1) the same line of sight and (2) the focal length of the fine guidance sensor is the same as the focal length of LDR allowing relatively small pointing errors to be sensed. It has the disadvantage of (1) fabricating and maintaining visible quality on sections of a large segmented mirror and (2) maintaining visible quality on section(s) of the secondary mirror.

The selected concept was to utilize a separate visible telescope for fine guidance sensing.



OFF-SET POINTING

CO-BORESIGHT POINTING

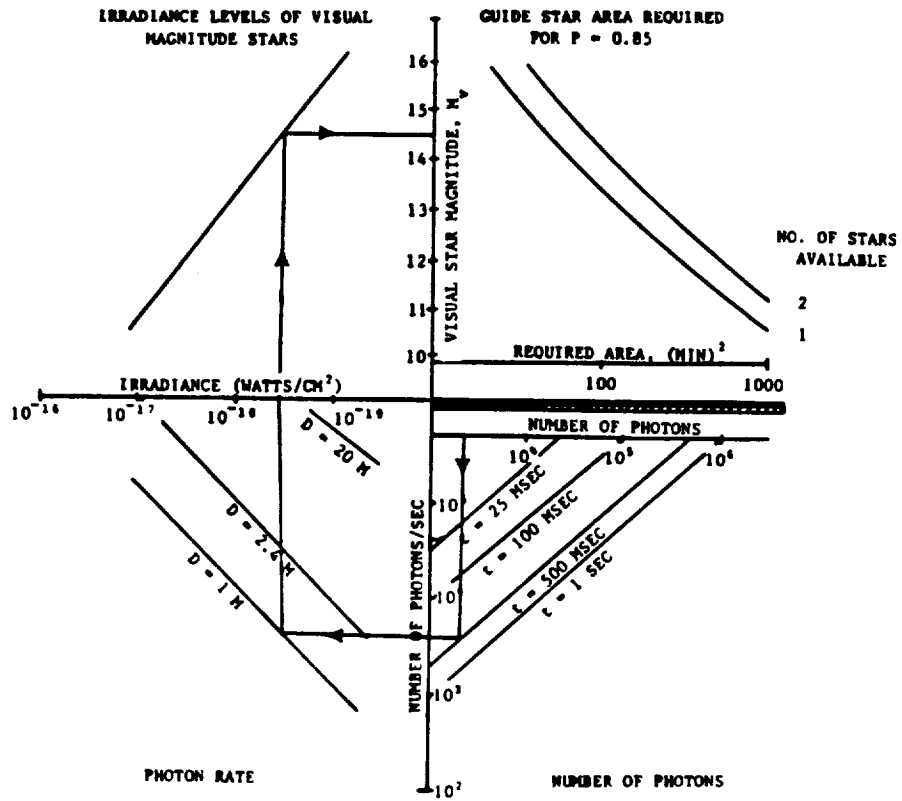
### FINE GUIDANCE SENSING OPTIONS

Figure 3.7-20

In order to first understand the fine guidance sensing problem (an angular error of 0.02 arcsecond is analogous to hitting a dime at 75 miles) a four quadrant system engineering approach was utilized. In this approach all parameters are first considered variables. Secondly, the fixed parameters are identified, thereby identifying the "real" variables. It is these variables which establish the options which can be used to solve the problem. Shown in Figure 3.7-21 is the first four quadrant diagram. The parameters in the four quadrants are guide star area, visual star magnitude, irradiance, aperture diameter, number of photons per second, integration time and the number of photons. The fixed parameters are visual star magnitude, aperture diameter and integration time. The "route-of-the-arrow" indicates the number of available photons. Shown in Figure 3.7-22 is the second four quadrant diagram (eight quadrants were required to completely define all the parameters). The parameters in the four quadrants are available photons, signal to noise ratio, subimage resolution, system focal ratio, knowledge of image location, system focal length and knowledge of line of sight error. The fixed parameters are system focal ratio and system focal length. Starting with the number of available photons from the previous four quadrant diagram the "route-of-the-arrow" indicates the line of sight error that could be achieved under these conditions. Summarized in Table 3.7-7 are the requirements imposed on the fine guidance sensor to meet the 0.02 arcsecond pointing stability requirement.

Solid State Sensors (CCD's, CID's, PDA's) have become increasingly attractive for astronomical imaging. This is due to low readout noise, high quantum efficiency, high dynamic range, linearity, and stability. The predominance of red stars near the galactic pole (poorest star density region) when combined with a solid state sensor leads to more available stars for a given threshold magnitude than with either the eye or a photomultiplier tube as a detector. Technical improvements and availability (yield) make solid state sensors ready for serious consideration in a 1980's fine guidance sensor.

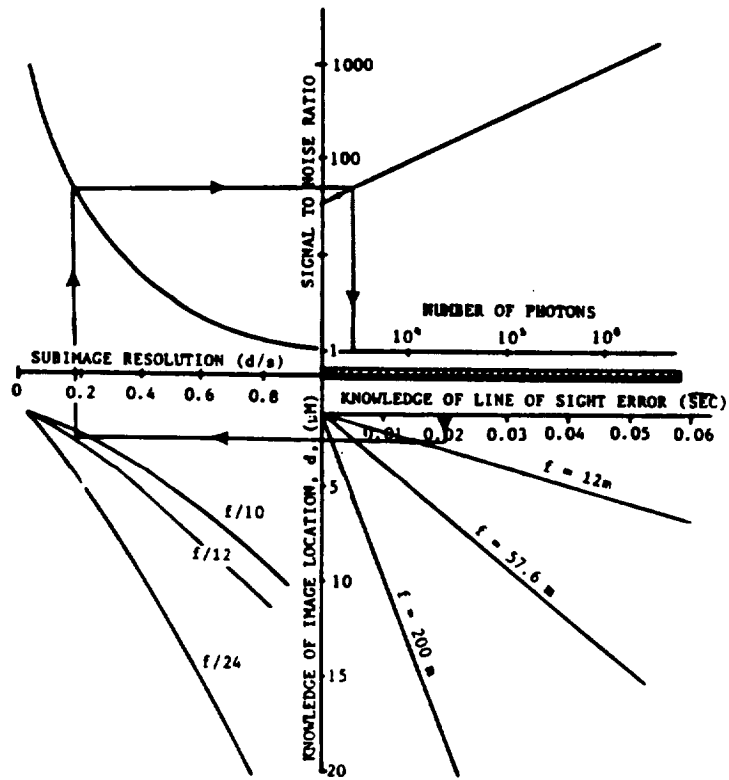
In the concept reviewed in this study the visible telescope would have an aperture of approximately 1 meter. The detectors would be installed directly onto the focal surface presented by the optics. This would maximize throughput and minimize



NUMBER OF AVAILABLE PHOTONS

Figure 3.7-21





KNOWLEDGE OF LINE OF SIGHT ERROR

Figure 3.7-22

pointing stability error by not incorporating any additional optical elements. The features of this fine guidance sensing configuration are summarized in Table 3.7-8.

TABLE 3.7-7  
LDR FGS SYSTEM REQUIREMENTS

● SPACE TELESCOPE FGS GUIDE STAR CATALOG	
● THRESHOLD VISUAL MAGNITUDE	≤15.0
● PROBABILITY OF TWO OR MORE GUIDE STARS IN GUIDE FIELD AREA	85%
● GUIDE FIELD AREA	33 SQUARE ARCMINUTES
● INTEGRATION TIME	500 MILLISECONDS

TABLE 3.7-8  
FINE GUIDANCE SENSING CONFIGURATION  
(OFF-SET POINTING)

OPTICAL SUBSYSTEM

- CATADIOPTRIC CASSEGRAIN TELESCOPE
  - DIAMETER = 1.0 METERS
  - FOCAL LENGTH = 12.0 METERS
  - SPOT SIZE = 60 MICROMETERS

DETECTOR SUBSYSTEM

- CCD SOLID STATE SENSOR
  - PIXEL SIZE = 30 MICROMETERS
  - NO. OF PIXELS/ARRAY = 312 x 520
  - NO. OF ARRAYS = 128

3.7.3.3 Chopping - The baseline requirements for chopping in the LDR system may be summarized by stating that the system should be reactionless with a 1 hertz chop frequency and a 1 arcminute chop throw. Selectability of chop axis is also desirable. In addition, the chopping system must be capable of serving up to eight separate science instrument packages, one at a time. Cryogenic cooling is required in any chopping system, since in the LDR all "optical" elements except the primary mirror require cooling. The chopping throw, coupled in the resolution and background subtraction, must yield an image displacement equivalent to five times the diameter of the Airy disk.

Chopping in an astronomical observation system is conceptually simple. It is utilized when either the signal emitted by the astronomical object under observation is very close in level to that of background sources, and the background contributions to total signal must be removed, or when the detector system under use exhibits fatigue or decay characteristics in output when looking at a constant input signal.<sup>(1)</sup> Chopping causes the detector to see two alternating fields in the sky. The signal from the observed object is thus the difference in radiation detected in the two orientations. Chopping permits removal of uniformly distributed background and foreground radiation from the detector signal.

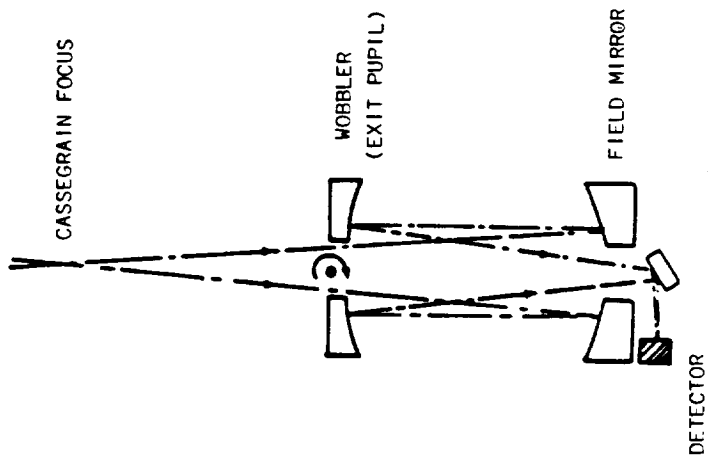
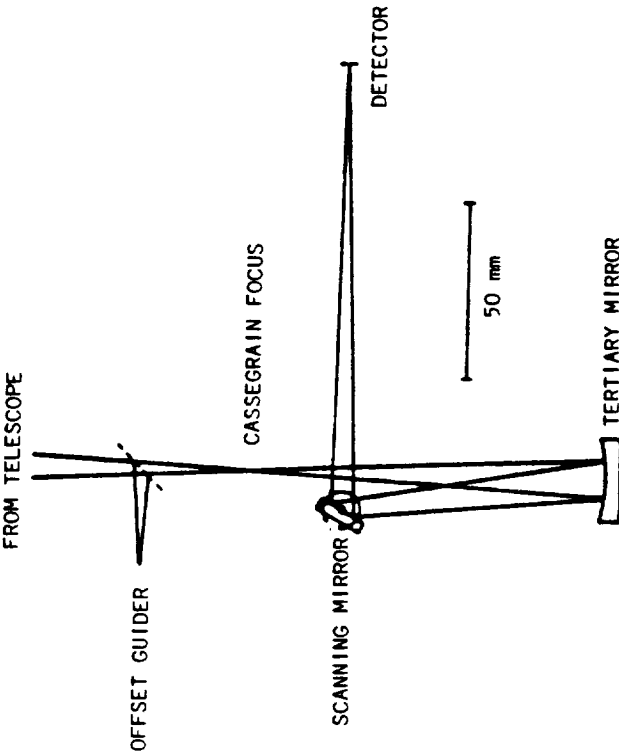
Chopping techniques can be separated into three main categories for LDR considerations. First is the reimaging photometer technique, two forms of which are shown in Figure 3.7-23. Next is tertiary or fold mirror chopping utilizing either a rotating or vibrating mirror approach (Figure 3.7-24). Finally, is secondary mirror chopping about either the vertex or the neutral (zero coma) points of the secondary mirror (Figures 3.7-25 and 3.7-26).

The reimaging photometer essentially places another optical system behind a telescope looking at its focus. "Optically," this approach would require at least two more elements in the system past the secondary mirror, introducing another source of background/instrument radiation into the detector as well as increasing the complexity of the image forming system. Mechanical complexity would also greatly increase, especially considering the two directions of rotation mandated by the chopping itself and the selectable chopping orientation as well as the cooling requirement placed on such a system. For these reasons, the reimaging photometer has been tentatively eliminated from consideration as a viable chopping alternative.

A discussion of the two tertiary mirror chopping methods is presented in Table 3.7-9.

This summary of the relative advantages and disadvantages of each technique<sup>(1,2)</sup> led to the tentative selection of the push/pull method for further consideration, if the tertiary mirror approach were selected.

From a conceptual standpoint, chopping with the secondary mirror presents some distinct advantages. This method would have the most commonality between ray paths, since all portions of the path behind the secondary mirror would be identical. Hence, all background/foreground contributed by the hardware beyond the secondary mirror would also be the same. However, it is physically the largest of these systems since the secondary is so large. Designing such a system must also allow for rigid body control for both chopping and active alignment of the secondary mirror as well as being cryogenically cooled. Mechanical implementation may be a major problem.

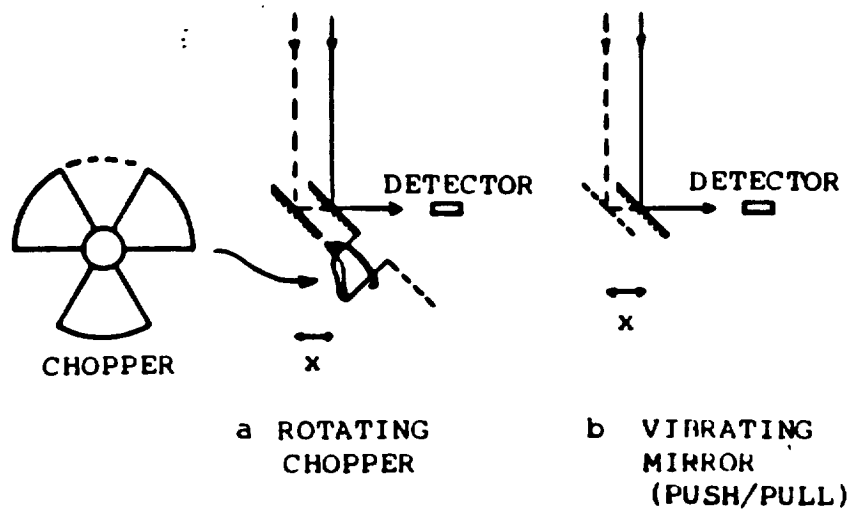


JEROME APT, et al, APPLIED OPTICS, VOL. 19, NO. 10  
15 MAY 1980

LDR SCIENCE AND TECHNOLOGY WORKSHOP  
ASILOMAR, 1982

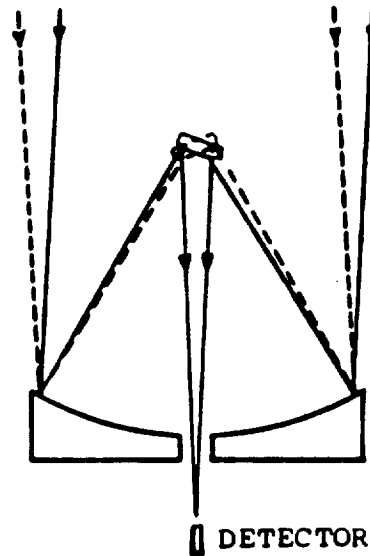
TWO REIMAGING PHOTOMETER CHOPPERS

Figure 3.7-23



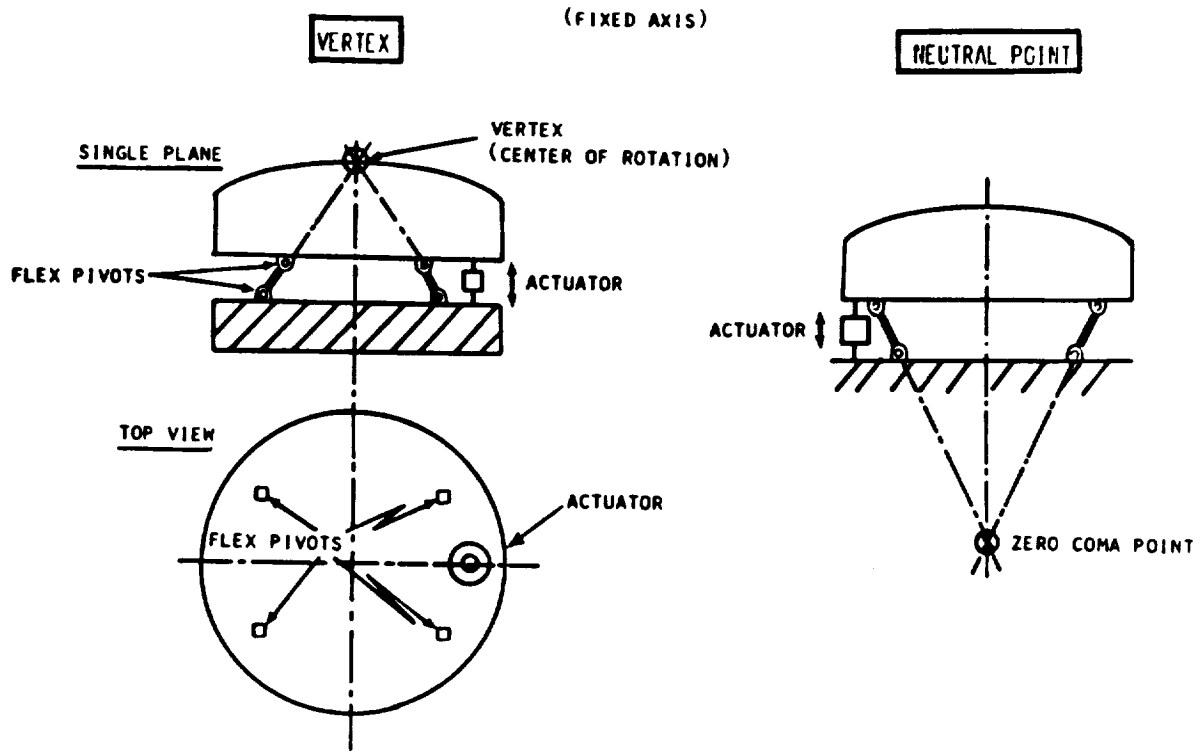
FOLD MIRROR CHOPPING CONCEPTS

Figure 3.7-24



SECONDARY MIRROR CHOPPING CONCEPT

Figure 3.7-25



SM CHOPPING MECHANISM CONCEPTS  
Figure 3.7-26

TABLE 3.7-9  
ROTATING VERSUS PUSH-PULL TERTIARY CHOPPERS

	<u>DISADVANTAGES</u>	<u>ADVANTAGES</u>
<b>ROTATING</b>	<p>TWO MIRRORS MAY BE AT DIFFERENT TEMPERATURES</p> <p>EDGES MAY REFLECT WARM OBJECTS</p> <p>HARD TO CHANGE PLANE OF ROTATION</p> <p>BEAMS MAY NOT FOLLOW EQUIVALENT PATHS</p>	<p>UNIFORM MOTION EASIER TO SYNCHRONIZE AND CONTROL</p> <p>LESS WASTED TIME BETWEEN POSITIONS</p>
✓ <b>PUSH-PULL</b>	<p>MORE TIME REQUIRED BETWEEN POSITIONS</p> <p>MECHANICAL VIBRATION</p>	<p>SINGLE MIRROR-NO TEMPERATURE DIFFERENTIAL</p> <p>MINIMIZE EDGE EFFECTS</p> <p>LOWER OFFSET</p> <p>SMALLER MODULATION NOISE</p> <p>EASIER TO ROTATE MIRROR PLANE</p>

The satellite programs which do utilize chopping are, with respect to LDR, small telescope systems. For example, SIRTf has a primary mirror approximately the same size as the secondary for LDR. Chopping with the secondary is therefore well beyond anything done or planned for space before. Also, few telescope systems have to operate over the 30-1000  $\mu\text{m}$  wavelength range of LDR. Requirements which can be met at the long wavelength end of this range may not be met at the short wavelength end.

There is an inadequate data base upon which to make a chopping method selection at this time. There are some indicators, however; optical diffraction limited performance traditionally means that 84% of the incident energy must be received within the first Airy ring. Another possible criteria presented is that 30% of this energy must be so enclosed. Both criteria are addressed in Table 3.7-10. Secondary mirror chopping is addressed for both cases at the 30  $\mu\text{m}$  and 1000  $\mu\text{m}$  end points of LDR performance, for both vertex and neutral point chopping approaches. Since chopping amplitude is required to be five times the diameter of the Airy disk, it can be seen that the + 30 arcsecond (1 arcminute) chopping requirement cannot be met over the entire spectral range for either encircled energy value. If the chop amplitude is restricted to three Airy disk diameters, and the 30% encircled energy value is used, vertex chopping may be allowed but not otherwise.

Further comparisons can be made. Table 3.7-11 shows the control mechanisms, stability, and advantages for the two chopping methods. Preliminary ray trace data indicates that the tripod supported secondary mirror (for the on-axis Cassegrain configuration) when decentered by 0.2 mm, will change the focal position by 4 micrometers. This is over 80% of the secondary mirror misalignment error budget. The 0.2 mm decenter is an equivalent lateral shift at the secondary for the required 1 arcminute chopping effect. This indicates that some form of focus adjustment is required; no such effect occurs for the tertiary mirror. It is also interesting to note that the jitter specification of 0.02 arcsecond equates to a decenter of the secondary of  $< 0.05$  mm. Hence, the stability control requirement for jitter is four times more stringent than that for the image quality focus budget.

Table 3.7-12 compares the effects of the two chopping methods of image quality. The equations for image quality effects caused by secondary mirror perturbations were

obtained from a paper by A.B. and M.P. Meinel.<sup>(3)</sup> Note this data again shows that neutral point chopping to be the preferred secondary mirror technique although it is more difficult to mechanically implement.

The arguments about background noise rejection may prove to be the deciding factor.<sup>(4-7)</sup> It may be that the background elimination characteristics of the secondary and tertiary chopping techniques prove to be the dominant decision criteria. However, the mechanical (structural and vibratory) and cryogenic constraints coupled together will still be major considerations. The possibility of using the secondary mirror for both pointing and chopping also can increase the system complexity.

It may be more advantageous to chop using one method, and fine point using the other. The secondary mirror may be better suited to fine pointing, while the tertiary could handle either function with far less complication than the secondary. This aspect of fine pointing and chopping with the same element should be investigated in further study. The decision about secondary or tertiary chopping should also be made after further study. Each technique has a presently preferred configuration; tertiary chopping a push/pull system and secondary chopping being a neutral point system.

### 3.7.4 Conclusions

Body pointing about system center of mass is the preferred pointing approach. However, additional fine pointing may be required using a small optical element. Off-set sensing with a separate visible telescope is the preferred fine guidance sensing approach. Two chopping alternatives show promise for LDR: (1) neutral point chopping of the secondary mirror and (2) push/pull chopping of the fold mirror. If fine pointing is required it probably should not be implemented by the chopping mirror.

TABLE 3.7-10  
SECONDARY MIRROR CHOPPING

<u>OPERATIONAL WAVELENGTH (μm)</u>	<u>ENCIRCLED ENERGY (%)</u>	<u>AIRY DISK DIA. (SEC)</u>	<u>VERTEX * CHOPPING FOV (SEC)</u>	<u>NEUTRAL ** POINT CHOPPING FOV (SEC)</u>
30	84	1	± 0.5	± 2
30	30	1	± 2.8	± 12
1000	84	33	± 16	± 64
1000	30	33	± 100	± 400

- THE ± 30 SEC CHOPPING REQUIREMENTS CANNOT BE MET OVER THE ENTIRE SPECTRAL RANGE, BASED ON EITHER 84% OR 30% ENCIRCLED ENERGY ALLOCATION.
- RELIEF TO 30% ENCIRCLED ENERGY ALLOCATION WILL ALLOW VERTEX CHOPPING FOV OF ± 3 AIRY DISK DIAMETERS.
- HOW SMALL A CHOPPING FIELD OF VIEW IS ACCEPTABLE (I. E., HOW MANY AIRY DISK DIAMETERS) AND STILL DO NECESSARY BACKGROUND SUBTRACTION?

\* ALLOWABLE THROW LIMITED BY COMA

\*\* ALLOWABLE THROW LIMITED BY ASTIGMATISM (APPROXIMATE CALCULATION)



TABLE 3.7-11

CHOPPING CONTROL MECHANISM STUDIES

- Guidelines: 1. Body or telescope pointing will be employed for coarse pointing control.  
 2. Fine pointing will be accomplished by either the secondary mirror (SM) or tertiary mirror (TM) concept.

<u>Concept</u>	<u>Mechanism</u>	<u>Torque Req</u>	<u>Pointing Stability</u>	<u>Advantages ( Left Shifted)</u> <u>Disadvantages ( Right Shifted)</u>
SM	Roller Bearings	Moderate	Fair-moderate (dependent on configuration)	- Heritage - Chopping w/SM requires strict pointing controls to maintain sensitive S <sub>1</sub> spacing. - Requires lateral stability of SM mount within .05 mm while still performing chopping w/SM to meet jitter requirement.
TM	Flexures	Small	Excellent	- Lowest torque requirements. - Permits static platform for SM mount insuring better lateral and longitudinal control for S <sub>1</sub> spacing and jitter.

Note: The stability control requirement of jitter is more stringent than the image quality focus budget requirement on the S<sub>1</sub> spacing.

TABLE 3.7-12  
SENSITIVITY ANALYSIS OF CHOPPING MODE  
ON SM AND TERTIARY MIRROR

A. Secondary Mirror\*

- Comatic image dimensions when chopping by tilting around the vertex of SM
  - along chop direction = 21.5 arcseconds
  - across chop direction = 14.3 arcseconds
- Astigmatic image dimensions negligible in comparison to coma
- Chopping by pivoting the SM about its zero-coma point
  - along chop direction = 0.19 arcsecond
  - across chop direction = 0.14 arcsecond
- See Table A2-3 for relative pointing stability control

B. Tertiary Mirror (TM)

- Lateral or longitudinal shifts of TM produce a corresponding shift of the beam at the focal plane but no wave front effect
- Tilts of the TM chop the scene but have no effect on wave front
- Pointing stability control to TM much easier to achieve than with SM

SECTION REFERENCES

1. Allen, D.A. Infrared The New Astronomy, (Keith Reid Ltd., Devan), 27-39 (1975).
2. Low, F.J. and Ricke, G.H. in Methods of Experimental Physics, N Carleton, ed., (Academic, New York) 12, 415-462 (1974).
3. Meinel, A.B., and Meinel, M.P., Aberrations of an IR Chopping Secondary, App. Opt., 23 (16), 2675 (1984).
4. Wright, E., LDR Study Kickoff Meeting, NASA Ames Research Center, May 4, 1984.
5. Baum, W.A., in Astronomical Techniques, W.A. Hiltner, ed., (The University of Chicago Press), 6-13 (1962).
6. Papoular, P., The Processing of Infrared Sky Noise by Chopping, Nodding and Filtering, Astron Astrophys., 117, 46 (1983).
7. Kleinmann, D.E., The Use of a Large Telescope in the Infrared, in Far Infrared Astronomy, M. Rowan-Robinson, ed., (Pergamon Press, Oxford) 33 (1976).

## 3.8 TRANSPORTATION TO ORBIT (MDAC)

LDR could be transported to orbit by single or multiple shuttle launches, including the ACC as an option, and could advantageously use an SDI/SDV launch vehicle if it develops on a timely basis. The task highlights are summarized in Figure 3.8-1.

### 3.8.1 Task Approach

The approach to assessing capabilities, options, constraints, and future needs for transporting LDR to orbit was to establish a limited set of objectives, identify the critical issues and perform studies to resolve the issues. These are summarized in Figure 3.8-2.

### 3.8.2 Requirements

Preliminary launch phase assessment identified the following lead-in requirements:

- Minimize total launch costs
- Constrain LDR transport packaging to Shuttle limitations with or without benefit of ACC
- Provide a benign launch phase environment
- Provide a 100,000 class clean transport environment for all LDR critical components.

### 3.8.3 Trade and Option Studies

The trade and option studies listed in Table 3.8-1 and discussed below were performed to accomplish the task objectives and resolve the critical issues. The general conclusions are shown in Table 3.8-2.

**3.8.3.1 Launch Vehicle Performance and Constraints** - The Space Shuttle System Payload Accommodations document, JSC 07700, Vol. XIV, Rev. H, Change 48, dated 25 Oct. 1984 and its attachment ICD 2-19001 Shuttle Orbiter/Cargo Standard Interfaces, were used to define the general performance, accommodations, interfaces and constraints for packaging and transporting LDR to orbit. At the time this study was underway, the Space Station proposal efforts were initiated and undocumented orbiter constraints were defined to the proposal team by C. H. Lambert, Shuttle Payload Integration Office in August of 1984. The LDR effort reviewed the data and concluded it should be accounted for in the LDR studies. It now appears that some of these constraints may not be as severe as stated. Those constraints and policy positions are summarized in Figure 3.8-3.

The STS assumptions for ACC and the accommodations it provides the payload are based on the ACC Model 101 as defined in the Mid-Term Review Dec., 1983 "General Purpose Aft Cargo Carrier Study" and the Final Review Nov., 1983 "Ground OPS Study - Advanced Space Transportation System (ASIS)."

The Shuttle Derived Vehicles (SDV) which have been studied would provide a notable increase in delivery performance over the orbiter and would offer additional options to LDR. The advent of the Strategic Defense Initiative (SDI) has made the possibility of SDV configurations in the LDR time frame a consideration. These studied vehicles and their potential FY85 concepts were examined for cost, performance and payload accommodation and are summarized in Figures 3.8-4 and 3.8-5.

**SOW task (3.1.1): Investigate single and multiple shuttle launches and alternate payload integration methods**

**Key Issues:**

- Useful payload and operational constraints of single launch
- LDR assembly/deployment basing mode – orbiter/free flyer, space station
- Packaging and stowage in orbiter bay
- Launch/delivery environment acceptability – contamination protection
- Assembly/deployment aids

**Major Conclusions:**

- Filled aperture LDR in excess of 10 to 13-m diameter unlikely in a single shuttle launch
- ACC Benefit is limited, and LDR may be only near-term customer
- Significant benefit of SDV options appear limited to advanced versions
- ASE and assembly/deployment aids will be a substantial effort
- Other than for single-launch concept, transportation does not drive design
- Orbiter deployment basing may drive subsystem changes for orbiter

**TRANSPORTATION TO ORBIT - TASK SUMMARY**

Figure 3.8-1

- Objectives:**
- Assess launch vehicle weight/volume performance
  - Assess LDR packaging/integration options
  - Determine LDR launch vehicle related requirements
  - Determine ASE requirements

<u>Key Issues</u>	<u>Approach and Products</u>
Launch Vehicle Options	<ul style="list-style-type: none"><li>■ Identified orbiter volumes and intrusions for EVA egress, EVA equipment, HPA/PIDA equipment, RMS manipulation limitations, and orbiter shadowing concerns</li><li>■ Identified real orbiter payload weight constraints for structural landed limits – shuttle PIO statements as given to MDAC space station proposal team</li><li>■ Identified ACC 101 characteristics</li><li>■ Identified SDV characteristics as defined and as forecast for Fy85 study</li></ul>
LDR Packaging/ Integration Options	<ul style="list-style-type: none"><li>■ Assessed:<ul style="list-style-type: none"><li>● Packaging integration techniques and potential reqs</li><li>● LV environments</li><li>● Packaging influence on LDR component sizing</li><li>● Companion payload options</li></ul></li></ul>
Launch Vehicle Related Requirements	<ul style="list-style-type: none"><li>■ Assessed:<ul style="list-style-type: none"><li>● Regimes where LV constraints may drive LDR</li><li>● Orbiter for deployment basing</li></ul></li></ul>
ASE Requirements	<ul style="list-style-type: none"><li>■ Assessed:<ul style="list-style-type: none"><li>● The need for pallets and the problems associated with them</li><li>● The need for subsystem interfaces with orbiter</li><li>● The manipulative problems and where equipment aids are likely</li><li>● The impacts of EVA on LDR and LDR on EVA</li></ul></li></ul>

**TRANSPORTATION TO ORBIT - TASK APPROACH**

Figure 3.8-2

TABLE 3.8-1

VHA378

## TRANSPORTATION TRADE AND OPTIONS STUDIES

Study Issue	Concerns
■ Launch vehicle (LV) performance and constraints	<ul style="list-style-type: none"> <li>● What the realistic orbiter delivery performance may be constrained to</li> <li>● How the ACC could benefit LDR and whether LDR would share its funding/development</li> <li>● Whether SDV configuration would benefit LDR and appear on a timely basis</li> </ul>
■ Orbiter and ACC environments	<ul style="list-style-type: none"> <li>● Whether the ACC and Orbiter payload environments are effectively the same</li> <li>● Whether the Orbiter/ACC environment is more of a design driver than other LV options</li> </ul>
■ Orbiter payload envelope and center of gravity	<ul style="list-style-type: none"> <li>● Whether the Orbiter envelope would drive the design of LDR elements</li> <li>● The extent that Orbiter center of gravity limits will constrain LDR packaging</li> </ul>
■ Orbiter interface loads	<ul style="list-style-type: none"> <li>● The extent to which Orbiter interface load limits may constrain LDR package size and in-bay locations</li> </ul>
■ Transport contamination control	<ul style="list-style-type: none"> <li>● The need and techniques for LDR contamination control in the Orbiter bay</li> </ul>
■ Transporter deployment basing	<ul style="list-style-type: none"> <li>● Compatibility of LDR deployment time and the available Orbiter loiter time and EVA time</li> <li>● The ability and desirability of Orbiter attitude control during buildup and other means to accomplish it</li> <li>● The methods for achieving contamination free revisit acquisition of LDR during interim construction phases</li> </ul>
■ Transportation ASE	<ul style="list-style-type: none"> <li>● The extent and identity of major transport, delivery, transport-related manipulation aids, and monitor/control/checkout equipment</li> </ul>

TABLE 3.8-2

## TRANSPORTATION TO ORBIT - SUMMARY

VGY058

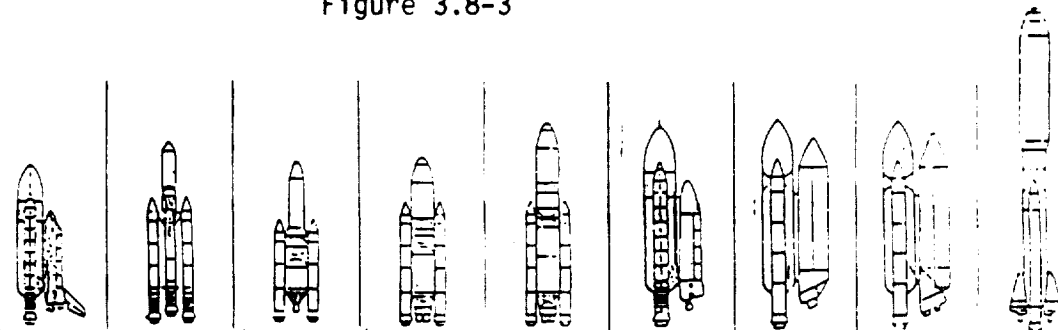
- STS orbiter should be planned for LV at this time.
- ACC can provide complexity/cost reduction for single launch concept if LDR is not prime development source of ACC.
- Planning for SDV would be high risk unless SDI is given early go-ahead.
- Multilaunch LDR concepts do not appear to be driven by LV.
- Single-launch LDR would be a severely limited, filled-aperture observatory of less than 12 m or an unfilled aperture up to 20 m with severe constraints on science instrument accommodations.
- Substantial LV integration, deployment support, and assembly aids are anticipated.
- Contamination will be the driving transportation environment.
- Orbiter deployment basing will require in-depth study of orbiter operating constraints such as propulsion inhibits, attitude control with berthed LDR and orbiter radiator shadowing, as well as investigation of effluent inhibiting

Source: C. H. Lambert (Payload Integration Office)  
 Basis: Clarifications To MDAC Space Station Group, Aug, 1984

- NASA Is Admant About Payload Design Being Orbiter S/N Independent
- Based On Orbiter OV-099/102 (Structural Limitation) Limits Landed (Abort) Weight To 42k lbs (Ref: 50k lbs For OV-103/104)
- If Shuttle Mods Were To Occur They Would Not Appear Before Mid To Late 1990s — Mod Funding Is Not Listed In '85, '86, '87 OR '88 Budget
- If OV-105 Is Completed It Will Be The Same As OV-104
- Revisit: S/S Wants A 90 Day Resupply — PIO Cannot Agree To This S/S Wants A 22 Day Rescue Notification — PIO Feels Even 45 Days Is Questionable, Current Planned "Launch On Need" Is 4 Months
- Orbiter Concern: Shadowing By A Companion Berthed System
  - Orbiter Cannot Go Dormant And Has Power Consumption Requirements Which Translates Into Radiator Thermal Rejection Requirements.

LDR TRANSPORT TO ORBITER, ORBITER  
 PERFORMANCE AND CONSTRAINTS STATUS

Figure 3.8-3

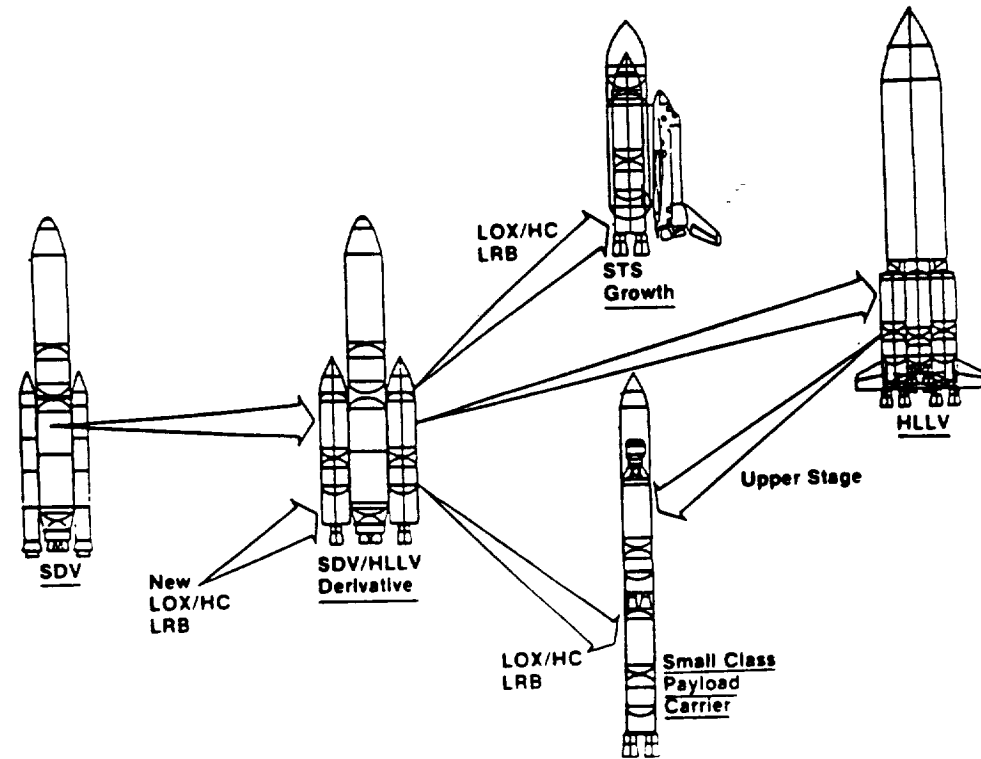


	ORBITER	SRB-X 3-SEG SRB TITAN STAGE 2 CENTAUR	1 X SSME	2 X SSME LARGE CARGO COMP.	3 X SSME LARGE CARGO COMP.	2 X SSME ORBITER DERIVATIVE	2 X SSME LARGE CARGO COMP.	3 X SSME LARGE CARGO COMP.	HLLV
Payload Envelope	150 x 60	150 X 69	250 x 60	250 x 60	250 x 90	150 x 60	250 x 90	250 x 90	
Payload Lift Mt. (LEO)	65K (40K)	445.9-54.6K	78.2K	123.1K	174.6K		83.2K	136.8K	
Payload Support Mode	Cradle	Cantilever	Cantilever	Cantilever	Cantilever	Cradle	Cradle	Cradle	Cantilever
Cost/FLT (Millions) 1984 \$	108	116	184/-	-/105			288/-	-/133	
First Launch Lead Time*		2.8	3.7/4.8				3.7/-	-/5.0	

\* From Phase C/D ATP Years Code = Expendable/Reusable

SDV CANDIDATES - AS OF AUGUST, 1984

Figure 3.8-4



SDV TO HLLV EVOLUTION FOR FY 85 STUDIES  
Figure 3.8-5

The merits of the orbiter and the ACC are compared in Figure 3.8-6 and the SDV in Figure 3.8-7.

**3.8.3.2 Orbiter and ACC Environments** - The STS orbiter has a fundamentally more benign payload environment than any launch vehicle to date. The question of the anticipated ACC environment was assessed by comparing the orbiter data and the data contained in "Design Requirements Document 809-3300, PAM Class/Aft Cargo Carrier" dated 5 Nov. 1983 by Martin Marietta, Denver Aerospace, Michoud Div., which was prepared for MDAC under contract. The comparison, as seen in Figure 3.8-8, indicates that the ACC internal environment is essentially the same as the orbiter's.

**3.8.3.3 Orbiter Payload Envelope and Center of Gravity** - The orbiter payload envelope and center-of-gravity limits were assessed for impact on LDR transport packaging. The orbiter payload envelope is essentially a 4.57m-diameter cylinder 18.27m long with minor intrusions along its length. An orbiter Cabin EVA ingress/egress path and access/storage space for one or two MMUs may decrease the usable length of the payload envelope to 16.8m. For orbiter construction basing a work platform of some kind will be required and one similar to postulated HPA would further reduce the usable payload envelope length to about 15m. The presence of an ACC will add a volume approximately 7.62m diameter and 5 to 5.5m long. The ACC volume is beneficial, especially in permitting the option of selected LDR components to be transported in an uncompacted form. The penalty for ACC use is the loss of that part of the payload in the event of an abort which will not achieve orbit.

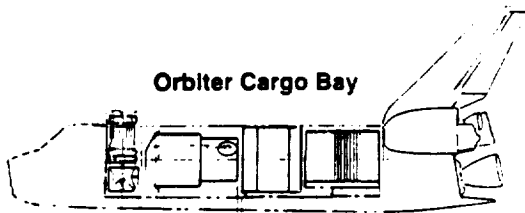
When viewed in conjunction with weight limits, timeline scenarios and orbiter loiter limits, the payload envelope does not appear to be more constraining than other launch vehicle options.

The orbiter has center-of-gravity limits which are applicable to reentry return or abort modes involving atmospheric flight with a payload. Various orbiter loading arrangements of LDR packaged increments were examined for center-of-gravity constraints. These included all LDR payloads and shared mission payloads with a typical spacecraft delivery such as a PAM-DII payload. The assessment indicated the major weight elements need to be in the aft third of the payload bay but no dramatic constraints are identified. The worst potential situation, typified in Figure 3.8-9, appears to be where part of the payload (such as a companion payload) cannot be delivered and must be returned to earth. If it is inopportune, because of ASE constraints or other reasons, to relocate the returned payload, center of gravity limits may be violated. In general, meeting orbiter center-of-gravity limits does not appear to be a challenge.

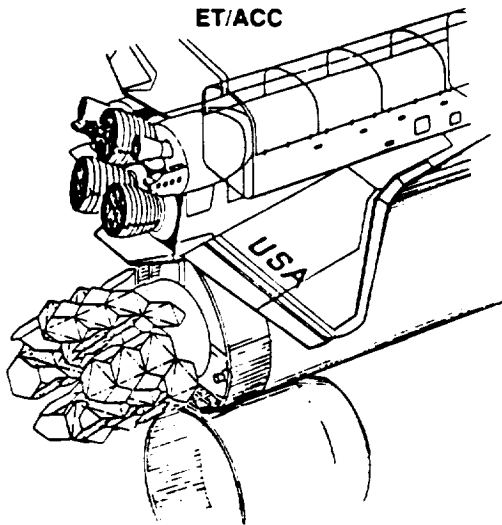
**3.8.3.4 Orbiter Interface Loads** - The orbiter provides an array of structural interface options for payload elements. The allowable limit interface loads will constrain payload integration options more often than the center-of-gravity limits. The various LDR package arrangements were examined for this limitation, typified in Figure 3.8-10. Since the spacecraft part of LDR or a palletized primary mirror group may be a substantially large single element, the orbiter margin of safety was examined for sensitivity variations, weight distribution and structural interface location, shown in Figure 3.8-11. This assessment indicates that sufficient options exist for LDR transport packaging to preclude other than normal program design issues.

**3.8.3.5 Transport Contamination Control** - It was determined that much of LDR includes either optical or thermal control surfaces and a need for 100,000-class





- Any Performance Level Orbiter
- Will Require Multiple Launches For Mirror Diameters Greater Than 15 Meters
- Mass Distribution Constraints
- Limited to 15 ft Dia Elements
- Design all LDR Elements to Orbiter Environment
- May Present Complex Contamination Control
- Multiple Launches May Provide Possible Orbiter Payload Sharing



- Based on ACC Model 101
- Requires High Performance Orbiter
- May Permit Single Launch Delivery
- Permits Payload Element ~ 25 ft Dia x 18 ft L
- LDR Segment Weights Less Constrained by Orbiter/ACC Load Limits
- ACC Segment May Have Lower Peak Acceleration Loads
- Requires More Manipulation Hardware
- Simpler Contamination Control
- Acoustic Environment Similar To Orbiter
- Thermal Environment Similar to Orbiter Bay
- ACC Payload Loss in Launch Abort
- Possibility for Shared Payload

LDR TRANSPORTATION CONSIDERATIONS TRANSPORT TO ORBIT

Figure 3.8-6

**Shuttle Derived Launch Vehicles (SDV)**

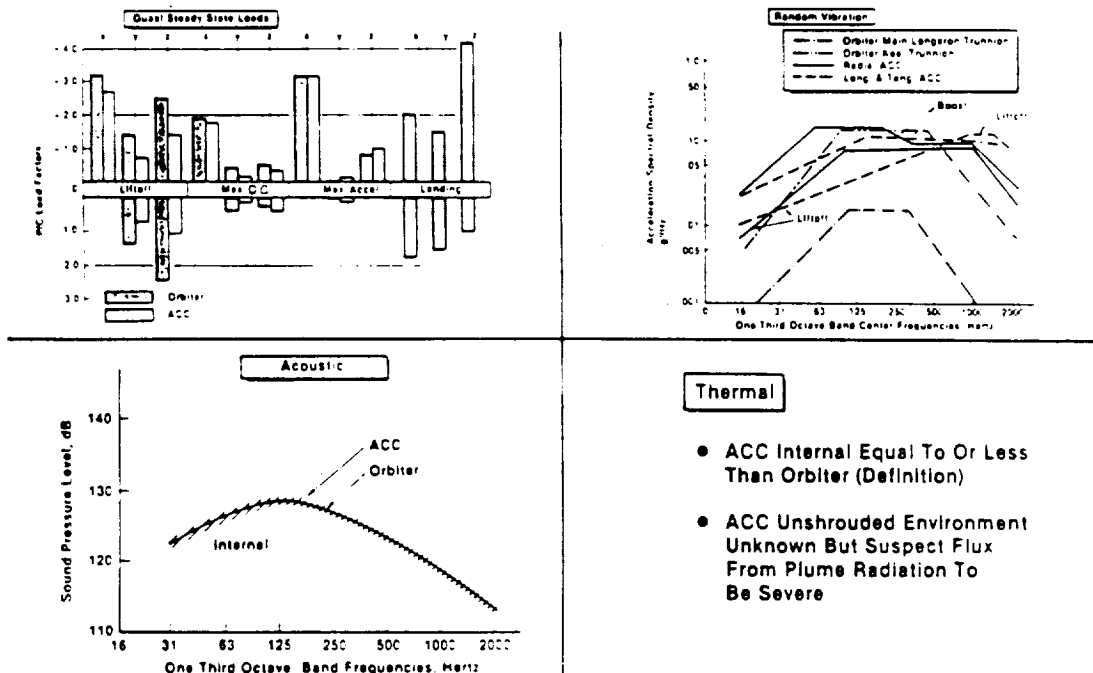
- SDV Maturity Prior to End of 1990's Requires Early SDI Go-Ahead and SDV Selection
- SDV Sizing Posture at This Time Is Generic
- Candidate Payload Envelopes Are 4.6, 7.6, and 15.3 m Diameters and 18.3-27.4 m Length
- Leo Delivery Weight Range: From Shuttle Capability to 175,000 lbs for In-Line Staging or 138,000 lbs for Sidemount Staging
- HLLV Delivery Is Stated at 300,000 lbs to 1000 km Polar Orbit

**LDR Implications**

- Single Launch LDR Delivery Is Possible With Any of the Higher Performance SDVs
- Single SDV Plus Advanced Orbiter Appears to Give Feasibility for LDR Construction/Deployment Independent of Space Station
- Large Preassembled Segments Are Possible
- HLLV Would Permit a Single LDR Launch With Minimal On-Orbit Assembly or Deployment (Possible Automated Deployment)

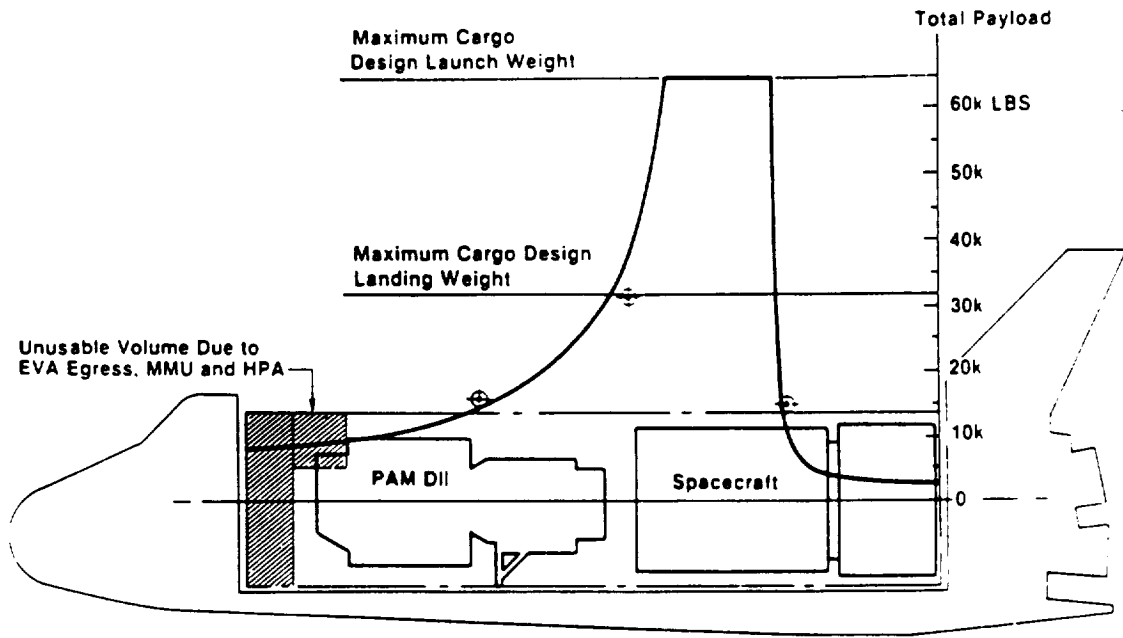
**LDR TRANSPORT TO ORBIT SDV SUMMARY**

Figure 3.8-7



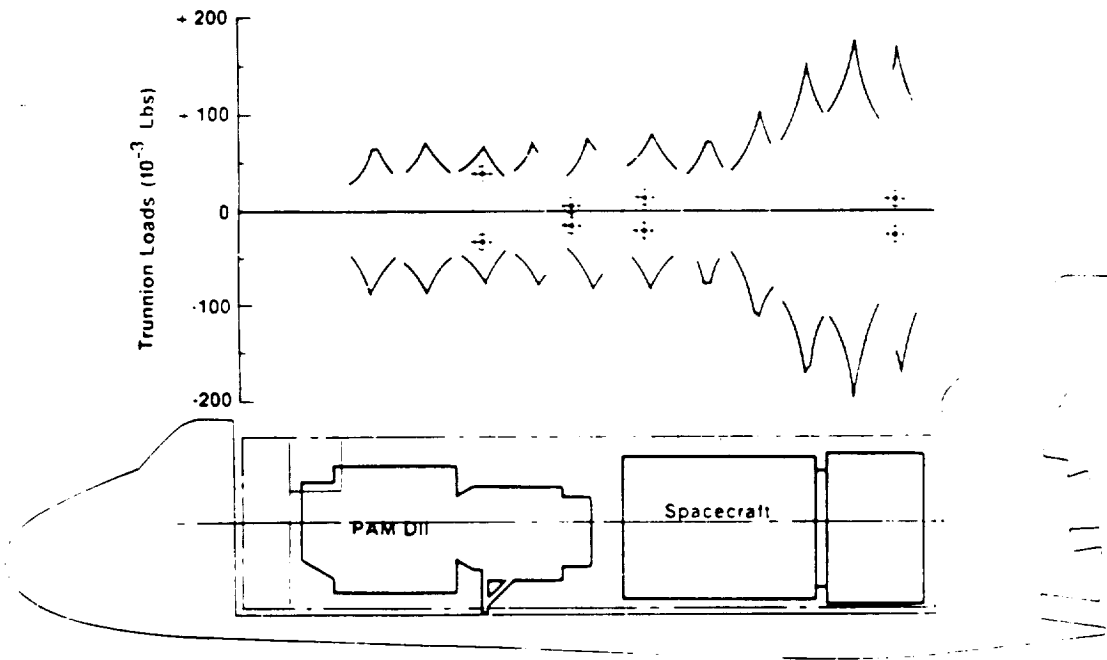
**LDR TRANSPORT TO ORBIT - ENVIRONMENTS**

Figure 3.8-8



LDR TRANSPORT TO ORBIT  
ORBITER PAYLOAD WEIGHT/CG LIMITS

Figure 3.8-9



LDR TRANSPORT TO ORBIT  
ORBITER VERTICAL (Z) LOAD LIMITS

Figure 3.8-10

**Objectives**

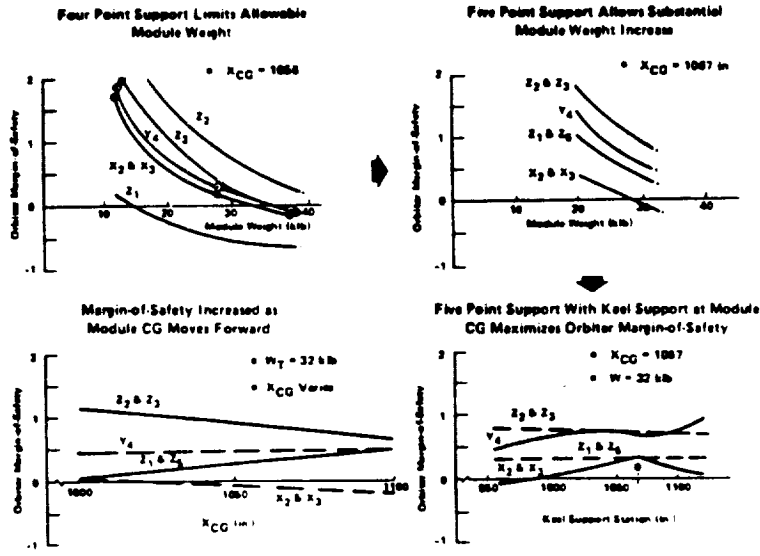
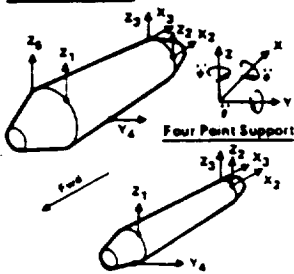
- Is Module Weight Limited by Orbiter Structural Capability?
- How Many Supports Are Required?
- What Are Favorable Locations of Keel Support?
- What Are Loads on Module During STS Transportation?

**Methods**

- MSFC Orbit Code
- Several Runs Using JEC Plung Code
- Sensitivity to Parameters
- Limit Load Factor Combinations

	$\alpha_x$	$\alpha_y$	$\alpha_z$	$\phi$	$\theta$	$\psi$
Min	-1.0	-1.0	-0.2	-0.8	-1.0	-0.8
Max	2.0	1.0	1.0	0.8	11.0	0.8

**Five Point Support**



SHUTTLE ORBITER MARGINS-OF-SAFETY FOR MODULE CARGO

Figure 3.8-11

03

clean conditions identified. The orbiter, as with most launch vehicle accommodations, is relatively "dirty" and schemes for contamination control of LDR during boost are necessary. Previous MDAC studies for DoD spacecraft having second surface mirror passive thermal control surfaces, IR optical systems and special thermal control coatings were reviewed for contamination control concepts. Delta and PAM programs were also reviewed for payload contamination control techniques. These are typified in Figure 3.8-12.

The study/review concluded that contamination control containers for boost phase environments are well within the state-of-the-art and present little penalty other than weight and payload envelope diameter.

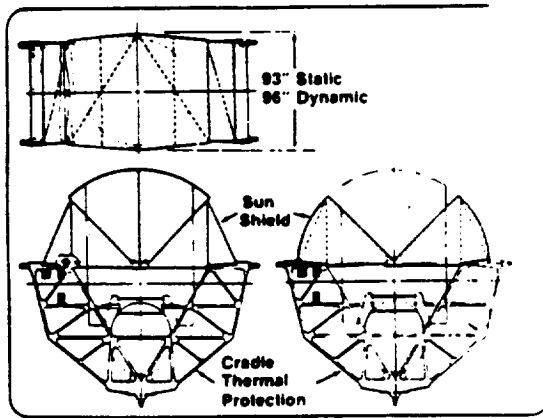
**3.8.3.6 Transporter Deployment Basing** - For the option of deploying or constructing LDR from the orbiter, the key issues are: orbiter time on station and available EVA time, attitude control during deployment, and LDR/Shuttle interactive environments. The basic deployment scenarios are to: deploy from orbiter only; deploy from orbiter and ACC. Both cases have essentially the same work platform requirements and concerns but the ACC case has three possible ways of deploying the ACC portion of the LDR. These are: to maneuver the elements by EVA/MMU motive control; to utilize a "new" orbiter RMS of extended reach and degrees of freedom; to eject the ACC payload intact and then to do a rendezvous maneuver to grapple and stow that part of the payload in an appropriate manner. The last two modes are illustrated in Figure 3.8-13.

The deployment/construction on the orbiter requires some kind of work platform for the LDR, such as the proposed Handling and Positioning Adapter (HPA). The basic buildup environment is illustrated in Figure 3.8-14. The key issues identified previously were assessed within the above mode of operation.

The significant issues for orbiter deployment basing, whether for single or multiple launches, is the amount of time the orbiter has on-station in direct support of the deployment operation and the amount of available EVA crew time also available. The orbiter has a nominal seven-day stay time capability. With no other mission requirements, the bulk of the crew time is available for LDR deployment. A 200-plus line item timeline was generated for a construction intensive LDR concept and is shown in condensed form in Table 3.8-3. Not shown is the time for unplanned contingencies or problems and the time necessary for LDR to temperature stabilize prior to first mirror alignment. The indications are that delivery capability (weight and volume) is more program constraining than the deployment scenario.

The two key issues of attitude control are for (1) the control mode of the LDR/orbiter composite vehicle during deployment operations, and (2) attitude control between orbiter visits. These were assessed and are summarized below.

The LDR at even intermediate deployment status is nearly as large as the orbiter in terms of area and moment of inertia and will result in a common center of gravity outside of the nominal orbiter control capability. Two basic options are available to resolve this. The first is the use of a special ASE work platform structure which contains sufficient CMG capacity to provide contamination-free control forces along with an independent sense and control system or a means of interfacing the orbiter's sense and control system. The second is to alter the orbiter software and if necessary supplement the orbiter's own force system. There is also a third option and that is to allow the total system to free drift in some sort of a gravity gradient mode if there is a reasonable expectation of a near stable attitude.



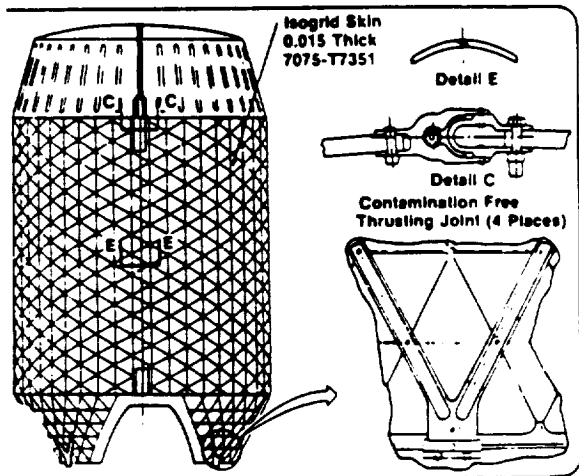
PAM-D thermal control system

Soft Goods System For Communications Satellites

Aluminum System For Extremely Sensitive Spacecraft Surfaces

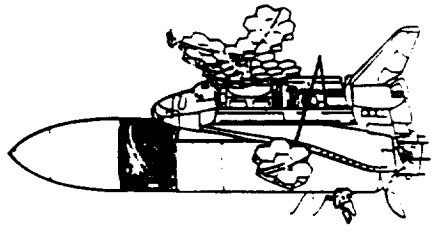
Design for spacecraft contamination cover

- LDR May Utilize Both Kinds of Shrouds for Different Packaged Elements
- 100,000 Class Clean Shrouds Will Require Purge Gas Interface With Orbiter for Ground Supply Source

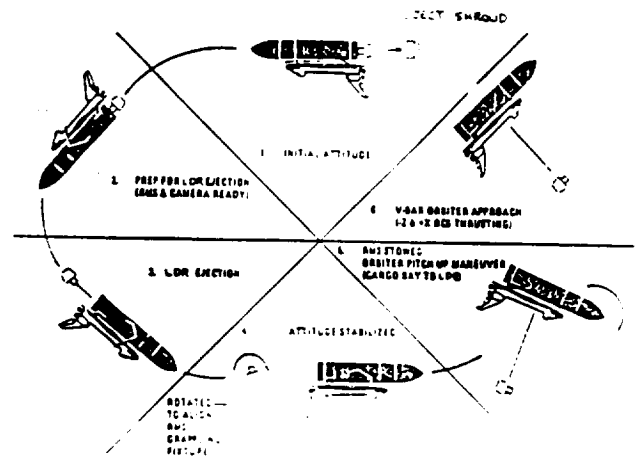


SHUTTLE PAYLOAD ENCLOSURES BY MDAC  
Figure 3.8-12

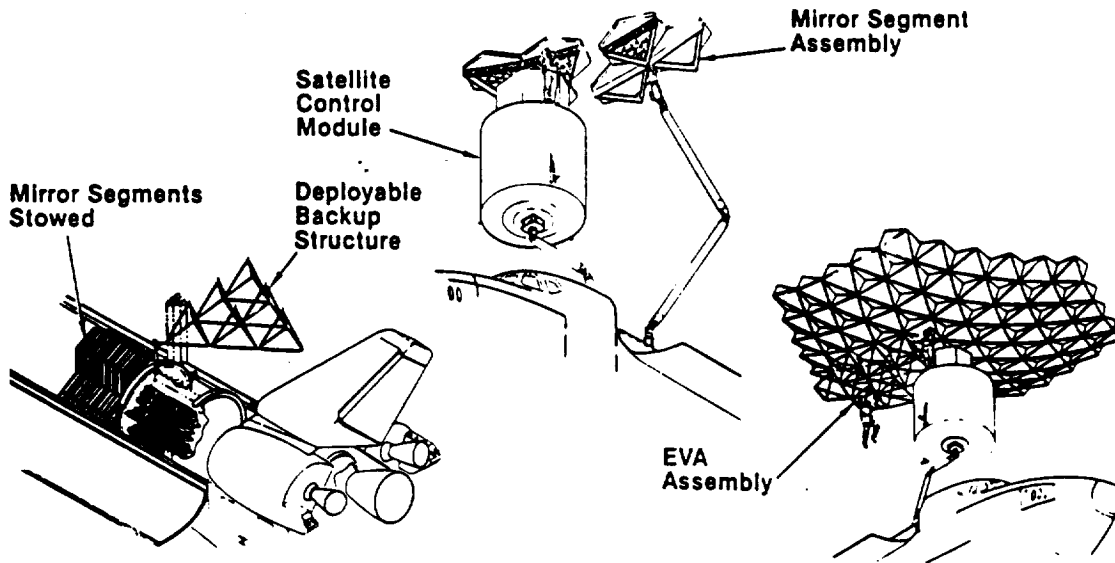
**Large Deployable Reflector**



**LDR Ejection Operations**



ACC DEPLOYMENT OPTIONS  
Figure 3.8-13



20 m + DIA REFLECTOR ASSEMBLY  
Figure 3.8-14

TABLE 3.8-3  
LDR CONSTRUCTION TIME LINE ORBITER BASING

■ Ascent Rendezvous	4-26 Hours
■ Orbiter/Crew Preparations	4-8
■ LDR S/C Status Check, Orbiter EVA/RMS Preparation, Deploy HPA, Deploy S/C	5
■ Crew Rest/Personal Care	12
■ EVA Preparations	2
■ Deploy Mirror Modules	9-30
• Inspect, Unstow Manipulate/Translate, Inspect Mounting, Mount (0.7 hr/Module)	
■ Crew Rest/Personal Care/10 hr Shift	12-36
■ Deploy Primary Mirror Truss Modules	6
• Inspect, Unstow, Manipulate, Expand Joint Inspect/Lock (2 hr/Module)	
■ Install/Attach Truss to Primary	10-25
• EVA Travel, Inspect, Attach (0.1 hr/Attachment)	
■ Crew Rest/Personal Care/10 hr Shift	12-24
■ Deploy Secondary Mirror Assembly	2
• Checkout, Unstow, Manipulate, Expand Spider Truss, Attach	
■ Deploy Sunshield	5-8
• Inspect, Unstow, Manipulate, Install (0.8 hr/Segment)	
■ Deploy Primary Mirror Truss Thermal Blanket	4
■ Final Inspection	2
■ Vehicle Checkout	2
■ Mirror Alignment	6
■ Spacecraft Initialization	1
■ Spacecraft Release/OPS Checkout	2

Nominal Orbiter Limit 100-200 Hours  
~ 170 Hours

Between orbiter visits to LDR during buildup, the LDR must be maintained under reasonable control (active or passive) and be a friendly target for orbiter rendezvous docking or grappling. The issues with respect to the orbiter RCS plume interaction for both forces and contaminants. The least interactive approach is for the orbiter to perform a sortie rendezvous and then for the LDR to accomplish the terminal maneuver with a cold gas system while the orbiter is in a thruster inhibit condition.

The third key issue is the interactive LDR/orbiter environment. It includes contamination control, which is discussed in 3.10, and thermal interaction. The two aspects of the thermal issue are the impact on LDR of the orbiter as a source and the degree to which the LDR may obscure the orbiter radiator heat rejection. An analysis was not performed and it is not clear at this time that the orbiter heat load on LDR during construction is unacceptable. There is real concern that the LDR will obscure the orbiter's ability to reject its own heat through its radiators. Even with the orbiter in a quiescent mode, there is a considerable parasitic power consumption base and a comparable heat rejection requirement. This suggests a firm requirement that LDR be constructed on a work platform which will place LDR essentially above and forward of the cabin. This will require a fixture more substantial than the proposed HPA.

**3.8.3.7 Transportation ASE** - Airborne Support Equipment (ASE) will be required to support both the transporting of LDR to orbit and deployment/construction of LDR. These include: carrier pallets, containment structures, manipulation devices, a work platform, LDR-peculiar monitor/control/checkout equipment at least part of which will be located at the orbiter's mission specialist station. The various phases in which the orbiter will require associated or supplemental equipment were evaluated and the major equipment needs are summarized below.

The LDR spacecraft body (instrument and housekeeping systems modules) can be configured to be self-supporting in the orbiter payload bay. LDR-peculiar carrier pallets specially configured to support, contain, and protect the other LDR components will be required. These will incorporate the features to provide the required level of environmental and contamination control. They may include loose components to provide interstitial support between components in a package, either for inertial loads or vibration loads.

For orbiter deployment basing, manipulative devices will be required for or related to the orbiter. The orbiter rms will probably be adequate for general construction; however, as previously noted, where an ACC is used in conjunction with the orbiter, a new longer reach rms with more degrees of freedom (primarily rotation between the shoulder and the elbow) would be required. As has been demonstrated by orbiter/EVA retrieval of two satellites last year, EVA manipulation could be used. However, unless great improvement in EVA bulk mobility and control is developed, the time constraints for today's level of performance would be prohibitive.



The various issues previously discussed point to a need for either an HPA or more likely a substantially large work platform on which to construct the LDR at a position above and sufficiently forward of the cabin to uncover the orbiter radiators. This would also likely be necessary to provide a more effective reach envelope for the baseline RMS. As in previous discussion, this platform may contain, in addition to a rotatable berthing interface for LDR support, CMGs, a cold gas RCS system, and a modicum of intelligent subsystems. For multiple orbiter mission deployment, this platform would most effectively remain with LDR until final completion of deployment/construction.

LDR-peculiar monitor/control/checkout equipment is an expected requirement throughout the LDR deployment phase. The ultimate extent of this will determine whether it can all be contained in the orbiter's mission specialist station or whether some must be remotely located on a carrier pallet in the payload bay.

In summary, it appears that substantial ASE requirements peculiar to the LDR program will evolve.

### 3.9 STRUCTURES (MDAC)

This study examined a wide range of LDR construction and deployment structural concepts, Orbiter and Space Station deployment basing, and the characteristics affecting extreme dimensional stability in the support structure for the optical elements as a basis for determining future technology needs for LDR. The task highlights are summarized in Figure 3.9-1.

#### 3.9.1 Task Approach

The approach to assessing acceptable structural characteristics was to examine options to structural geometry, form and sizing; deployment/assembly mode influences; dynamic parameters and processes; and material influences. These are summarized in Figure 3.9-2.

#### 3.9.2 Requirements

The initial structural requirements comprise both generic and specific goals including:

- Structural dynamic dimensional stability to approximately 1 micron limit
- Short post-maneuver settling times
- Low jitter or vibration propagation
- Automated and/or constructed deployment
- Orbiter or Space Station deployment basing

Requirements that were derived from other systems and operations assessment include:

- Long-term dimensional stability
- Space environment damage tolerant structure
- Predominate ground testing

#### 3.9.3 Trade and Option Studies

The trade, option and assessment studies listed in Table 3.9-1 and discussed below were performed to accomplish the task objectives and resolve the critical issues. The general conclusions are shown in Figure 3.9-3. It should be noted that the study level of effort did not support any analytical modeling or computer analyses. Hand calculations were used for the geometry and structural parameters examined. Unigraphics 3D point/line modeling was used to examine various truss arrangements.

**3.9.3.1 Structural Geometry and Sizing** - Structural concepts were examined at both the observatory level and the individual mirror-support structure level.

The merits of the observatory structural arrangements shown in Figure 3.9-4 were assessed and are summarized in Table 3.9-2. Concept D is probably the best structurally in terms of minimizing disturbances to the optical system and isolating probable subsystem vibration sources. However, Concept A was selected for the trade studies reference or point of departure as a good compromise between disturbance control and deployment/construction simplicity.

Structural concepts were examined for axisymmetric dishes and near rectangular slot reflectors and for both hexagonal and trapezoidal mirror segments. These are typified respectively in Figures 3.9-5, 3.9-6, 3.9-7, and 3.9-8. The general

**SOW Task (3.1.4): Investigate a range of construction concepts and configurations from totally autonomous deployment to astronaut assembly, including space platform or space station basing**

**Key Issues**

- Observatory, component, and mirror segment sizing
- Total available launch volume and weight
- Orbital assembly time constraints and equipment aids
- Observatory configuration and thermal-critical structural dimensions
- Deployment basing design options

**Major Conclusions**

- Single-launch concepts would be limited to >12 m for filled aperture, while up to 20 m unfilled may be feasible for astronaut-assembled concepts
- Favorable primary mirror support structure proportions result best from mirror segments of near 1.0 aspect ratios and 2.5-m<sup>2</sup> to 5.0-m<sup>2</sup> area
- Trapezoidal mirror segments permit support structures with the fewest number of differing parts – lowest development and recurring costs
- Extensive deployment automation would result in poor packaging density, high risk levels of complexity, and expensive development test programs
- A thermally shielded structure will reduce the importance of the material CTE and more readily achieve required thermodynamic distortion stability

LDR STRUCTURES – TASK SUMMARY

Figure 3.9-1

- Objective to Assess:**
- Primary mirror support structure and mirror segment relationship
  - Secondary mirror module support options
  - Sun-shield design options
  - Deployment basing impact on design

<u>Key Issues</u>	<u>Approach and Product</u>
Mirror Segment Size and Shape Influence	<ul style="list-style-type: none"> <li>■ Defined structural geometry options for various-sized trapezoidal and hexagonal candidates</li> <li>■ Assessed relative structural-thermal dynamic merits of options</li> <li>■ Assessed packaging and assembly concepts for options</li> <li>■ Assessed options for automation impacts</li> <li>■ Assessed options for manipulation and assembly impacts</li> <li>■ Assessed manufacturing merits of options</li> </ul>
Secondary Mirror Module Support	<ul style="list-style-type: none"> <li>■ Defined multipod, cylinder-beam and maypole concepts characteristics of options</li> <li>■ Assessed relative optical field shadowing</li> </ul>
Sun-Shield Options	<ul style="list-style-type: none"> <li>■ Defined sun-shield geometry, support, and construction for both cylinder and cylinder-cone options</li> <li>■ Assessed potential passive, active, and semiactive mechanizations, including incorporation of spacecraft bulk heat-rejection radiators</li> <li>■ Considered implications of use as contamination shroud</li> </ul>
Structural-Thermal Dynamic Stability	<ul style="list-style-type: none"> <li>■ Defined structural-thermal dynamic rationale for control design options</li> <li>■ Assessed complexity, risk, mechanization of options</li> </ul>
Deployment Basing Impacts	<ul style="list-style-type: none"> <li>■ Defined deployment assembly scenarios for basing options</li> <li>■ Assessed design options for scenarios</li> <li>■ Assessed interface impacts of ASE/EVA aids or available basing equipment</li> <li>■ Assessed environments for design implications</li> </ul>

LDR STRUCTURES – TASK APPROACH

Figure 3.9.2

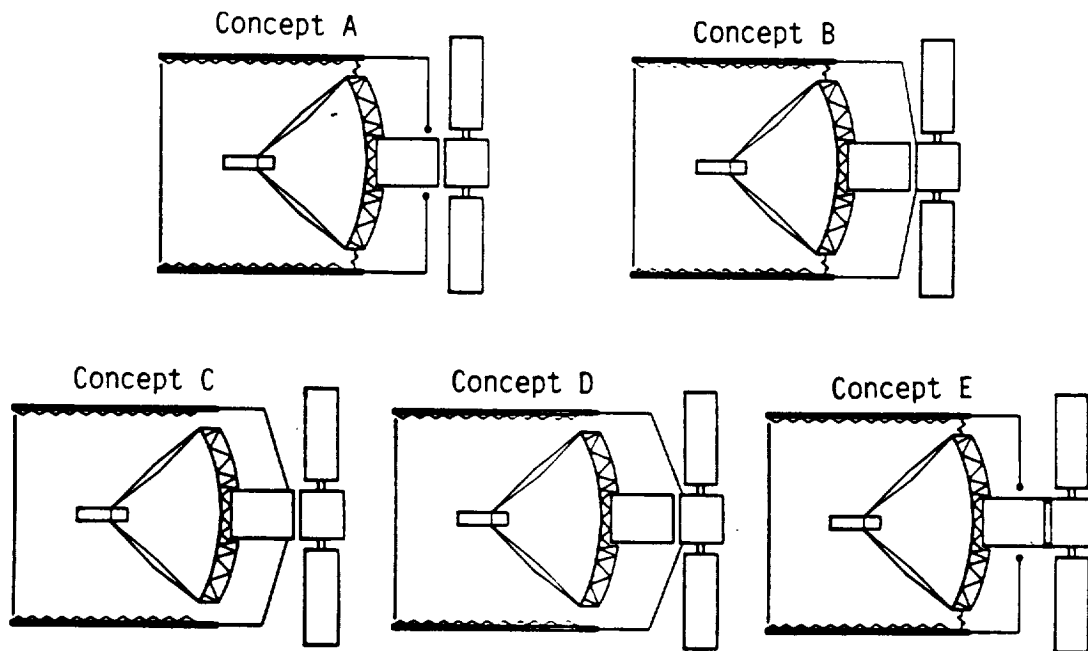
TABLE 3.9-1  
STRUCTURES TRADE AND OPTIONS STUDIES

STUDY ISSUE	CONCERNS
<ul style="list-style-type: none"> <li>● STRUCTURAL GEOMETRY AND SIZING</li> </ul>	<ul style="list-style-type: none"> <li>● WHETHER MIRROR SEGMENT SIZE AND GEOMETRY SIGNIFICANTLY CONSTRAINS STRUCTURAL DESIGN OPTIONS, DEPLOYMENT MODES, AUTOMATION LEVELS OR ANALYTICAL MODELING.</li> <li>● WHETHER THERE IS AN OBVIOUS PREFERENCE BETWEEN HEXAGONAL AND TRAPEZOIDAL SEGMENT SHAPES FOR STRUCTURES</li> </ul>
<ul style="list-style-type: none"> <li>● AUTOMATED DEPLOYMENT</li> </ul>	<ul style="list-style-type: none"> <li>● WHETHER A FULLY-AUTOMATED (SINGLE LAUNCH) LDR OF REASONABLE PERFORMANCE IS FEASIBLE AND AT WHAT SIZE.</li> <li>● WHETHER AUTOMATION IS BENEFICIAL AT THE SUBASSEMBLY LEVEL.</li> </ul>
<ul style="list-style-type: none"> <li>● CONSTRUCTED DEPLOYMENT</li> </ul>	<ul style="list-style-type: none"> <li>● WHAT THE EFFECT OF ORBITER VS. SPACE STATION BASING WILL SHOW IN LDR DESIGN.</li> <li>● THE EXTENT MAN'S INVOLVEMENT WILL PRODUCE IN LDR DESIGN FEATURES.</li> <li>● WHAT KINDS OF ASE AND TOOLS MAY BE REQUIRED.</li> </ul>
<ul style="list-style-type: none"> <li>● DIMENSIONALLY STABLE STRUCTURES</li> </ul>	<ul style="list-style-type: none"> <li>● WHAT THE KEY STABILITY ISSUES ARE AND WHETHER OTHER SYSTEMS CAN ALLEVIATE THE REQUIREMENT</li> <li>● WHETHER THE THERMAL TRANSIENT RESPONSE WILL DRIVE LDR TO EXOTIC MATERIALS OR PROCESSES.</li> <li>● WHETHER PASSIVE OR ACTIVE DAMPING WOULD BE REQUIRED FOR SHORT SETTLING TIMES.</li> <li>● WHETHER ANALYTICAL MODELING, SIMULATIONS AND TESTING TECHNIQUES ARE ADEQUATE.</li> <li>● THE EXTENT THAT NON-LINEAR FEATURES AFFECT LDR.</li> </ul>
<ul style="list-style-type: none"> <li>● DAMAGE TOLERANCE</li> </ul>	<ul style="list-style-type: none"> <li>● WHETHER LDR CAN INCLUDE A DAMAGE-TOLERANT STRUCTURE AND WHAT IS REQUIRED FOR ITS DESIGN CRITERIA.</li> </ul>

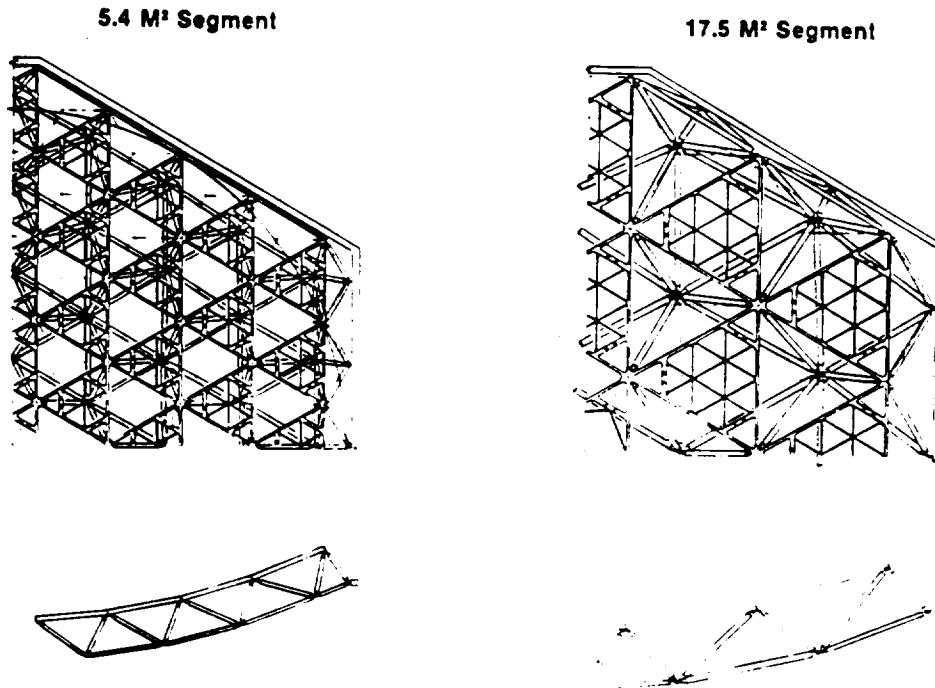
- Limited-capability, high-risk, fully automated, single-launch, ~10-m filled aperture observatory may still be feasible
- Limited-capability, low-risk, constructed, single-launch (with ACC) ~20-m unfilled ring mirror appears very achievable
- Full-capability, medium-risk, constructed, multilaunch, orbiter or space station based ~20-m filled aperture appears very achievable
- For multilaunch concepts, launch vehicle payload weight and volume does not appear to be a design driver
- For parabolic primary mirror, trapezoidal mirror segments will show most optimal support structures
- A fully containing thermal shroud should minimize importance of structural CTE and result in broader material options
- Planned EVA construction will provide complexity/cost benefits
- Extensive ASE will be both necessary and beneficial to design
- Space station basing will reduce concern for construction time, interrupts, and interim configuration controllability
- Assessment of structural precision stability will require more extensive modeling and analysis than that provided by this task-level of effort

LDR STRUCTURES - SUMMARY

Figure 3.9-3



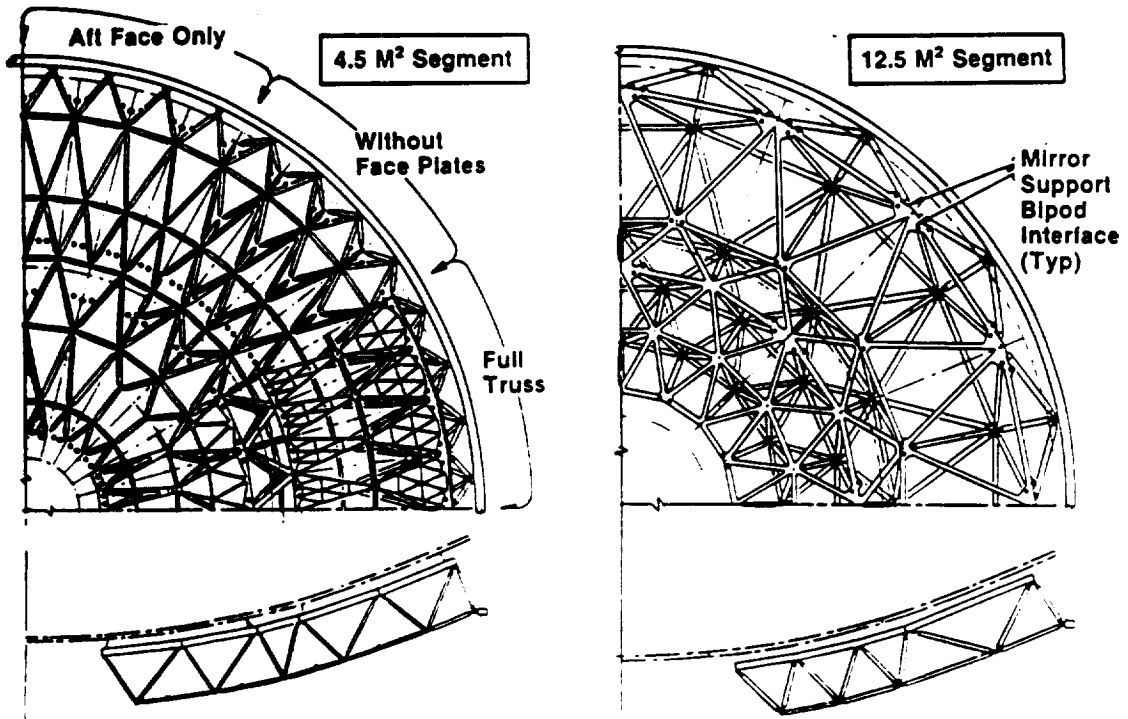
OBSERVATORY STRUCTURAL OPTIONS  
Figure 3.9-4



REACTION STRUCTURE DESIGN  
HEXAGONAL MIRROR  
SEGMENT INFLUENCE

Figure 3.9-5

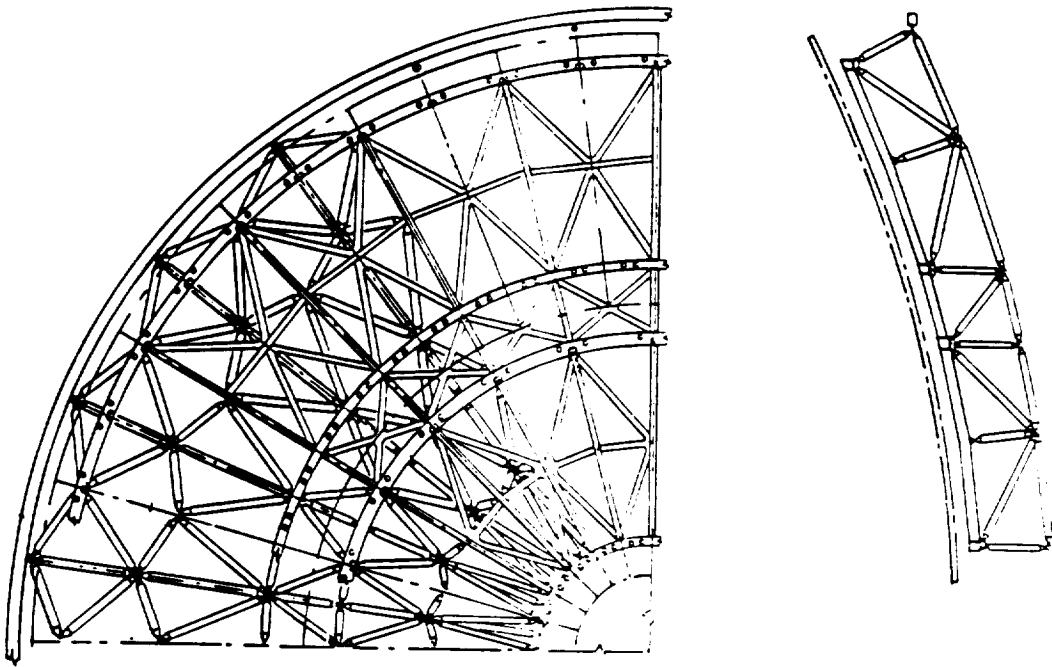
### TETRAHEDRAL TRUSS



### REACTION STRUCTURE DESIGN TRAPEZOIDAL MIRROR SEGMENT INFLUENCE

Figure 3.9-6

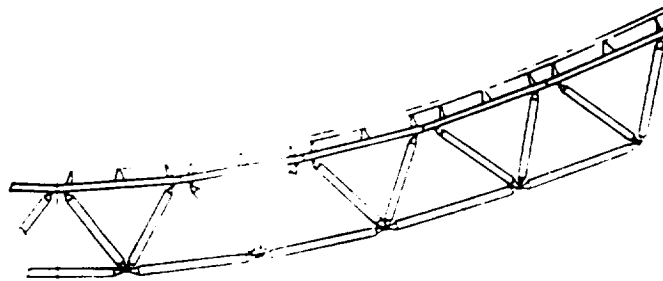
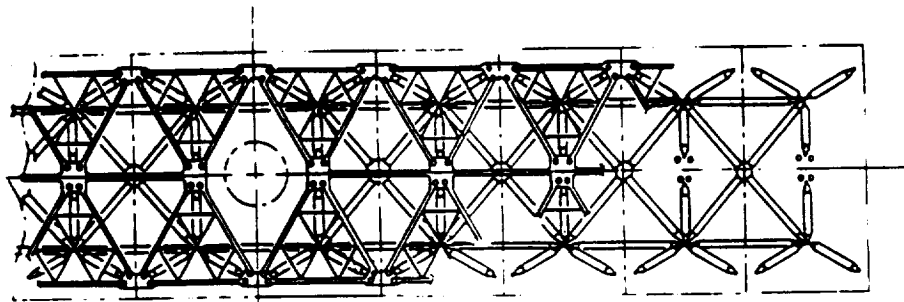
Rib/Ring Concept



REACTION STRUCTURE DESIGN  
TRAPEZOIDAL MIRROR SEGMENT INFLUENCE

Figure 3.9-7

**Slot Configuration - Tetrahedral Truss**



REACTION STRUCTURE DESIGN  
TRAPEZOIDAL MIRROR SEGMENT

Figure 3.9-8



conclusion was that there were no concept option related issues that would drive the technology requirements or development.

**3.9.3.2 Automated Deployment** - Observatory configurations were examined for the possibility of a fully automated single-launch LDR. Concepts offered by previous studies and authors were examined since there have been some ingenious suggestions. New concepts were developed in the study. These were all examined with the following general conclusions:

- Concepts should have the least number of field joints to be made at deployment.
- Concepts should minimize the use of segments which need to be translated rather than hinged.
- Concepts should use segment folding schemes that minimize the number of connectors and large angle folds to the wiring runs for mirror actuators and other electrical equipment serviced across the primary mirror truss.
- The thermal shield will be limited to soft membrane structures.

A concept was developed that reflected these conclusions. Fan or umbrella style fold methods fit the single launch constraints. It appears that with a 4 m diameter 6 m long spacecraft body the mirror diameter would be limited to about 13 m. This concept is depicted in Figure 3.9-9 which shows the deployment.

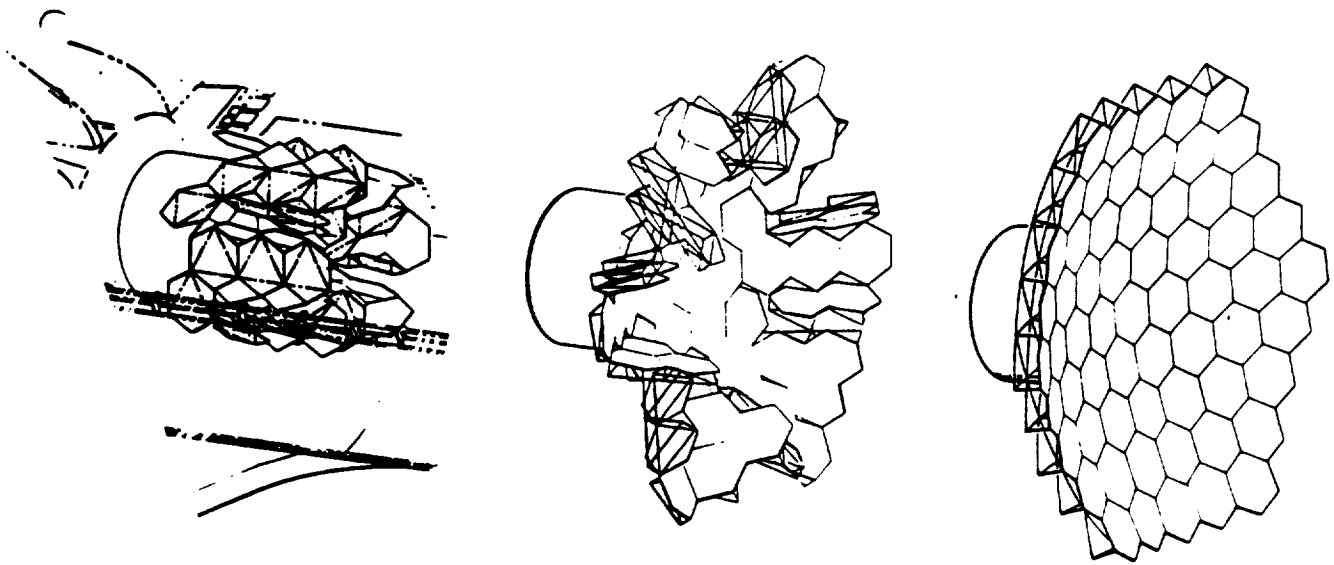
**3.9.3.3 Constructed Deployment** - Observatory configurations were examined for a full range of construction options and basings with the 20 m diameter primary mirror as the size example. The assessment generally concluded:

- That a good compromise between stowage complexity and launch cost results in a deployment with 3 Orbiter launches or more.
- That symmetry during buildup would be desirable for Orbiter basing but is immaterial for Space Station basing.
- That the reach and manipulation envelopes would favor the assembly of the mirror/ reaction frame part of the dish first and then assembly of the truss to that.
- That structural designs need to reflect the requirements or accommodation of EVA crew limitations.

The aspects of a constructed LDR are reflected by Figure 3.8-14.

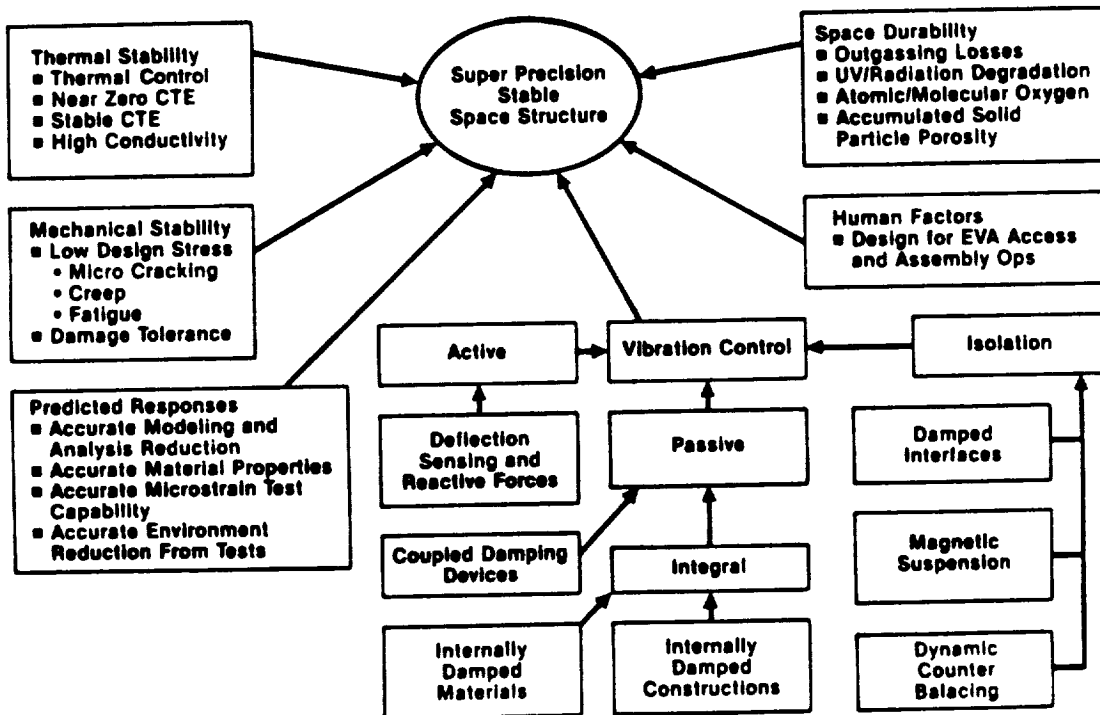
**3.9.3.4 Dimensionally Stable Structures** - The single most significant structural issue is to design, produce, test, and deploy/construct in orbit an optical system support structure which will maintain the optical reflector elements to approximately one micron deflection error budget from dynamic structural distortions during observation periods which may occur two or more times per orbit. The generalized issues which influence a super precision stable space structure may be seen in Figure 3.9-10. The typified structural model used for the various assessments is shown in Figure 3.9-11. Some issues are discussed in other sections, but most are discussed below. These issues are, in fact, interactive but were assessed somewhat independently.

**3.9.3.4.1 Dynamic Dimensional Stability** - Two key dynamic issues assessed in this study were vibration and thermal transient responses. Vibration includes two basic issues: modal vibration from major disturbances such as targeting maneuvers and higher frequency propagations from vibrating equipment such as CMG's or refrigerant pumps. The main issue for the modal vibration is damping time which is discussed in the following section. Equipment vibration isolation as an issue depends entirely on



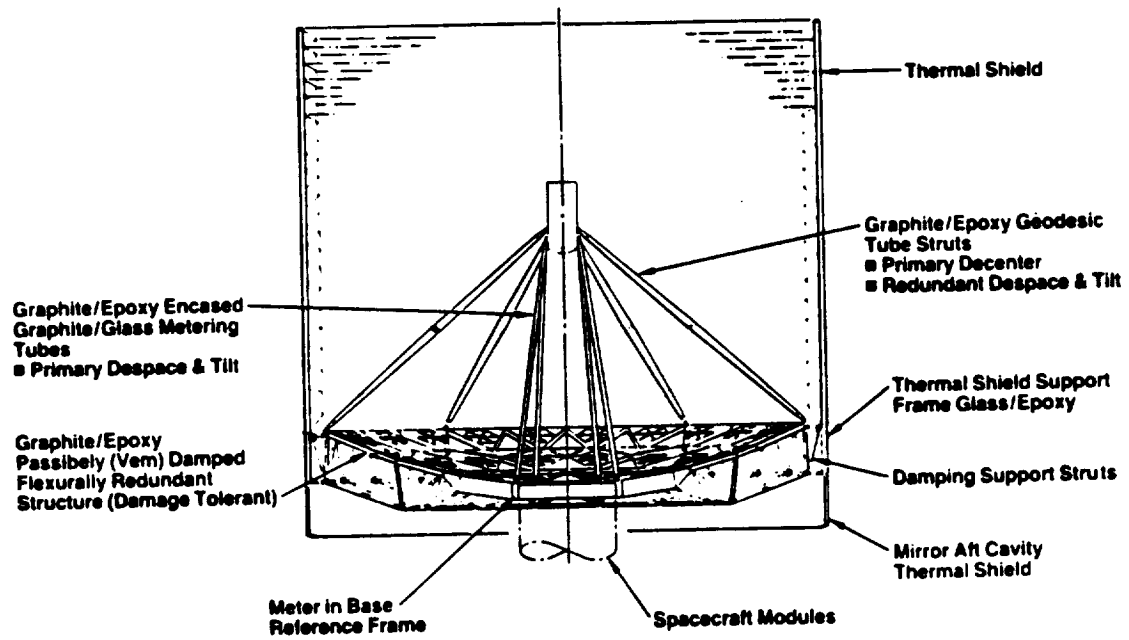
LARGE DEPLOYABLE SPACE OPTICS

Figure 3.9-9



DIMENSIONALLY STABLE STRUCTURES

Figure 3.9-10



LDR INTEGRATION STRUCTURES MODEL

Figure 3.9-11

the potential equipment vibration signatures and the extent to which design configurations aid in physically separating it from the critical structure. In the LDR case most equipment of concern can be located in a spacecraft module which can be dynamically isolated by highly damped interfaces, which may include magnetic suspensions. Further, the use of high damping interfaces in the structural arrangement, i.e., Visco Elastic Materials (VEM), a candidate for modal damping, can suppress the propagation of higher frequency vibrations through the structural elements.

The principal dynamic concern examined in the trade study is thermal transient responses. First, there is a tradeoff between the performance of structural thermal control techniques and the inherent thermal strain stability of the structural materials (the better the structural thermal control the less important is a near zero CTE). Initially it was argued that the primary mirror would need an aft face thermal shield which could also enclose its supporting structure. This would provide essentially the same thermal load on the support structure as the reflector aft face. Also initially, the target for the primary mirror was  $200^{\circ}\text{K} \pm 1^{\circ}\text{K}$ . If this were

maintained by common control in the structure then CTE's in the  $10^{-5}$  to  $10^{-6}$  range might be acceptable. However, during the study it was argued that the nominal mirror temperature could be allowed to range perhaps as much as  $\pm 20^{\circ}\text{K}$ , although maintaining the  $1^{\circ}\text{K}$  temperature dispersion.

With this possibility, a material would be needed which could exhibit a CTE in the  $10^{-6}$  to  $10^{-7}$  range or better. Examination of candidate materials resulted in a preference for graphite fiber resin matrix material. It is rapidly becoming a well understood material with a fair range of properties tailoring possible. The main deficiency at this time appears not in designing a laminate of specific properties, but in manufacturing, testing and demonstrating super precision properties on a repeatable low rejection rate basis.

The same general rationale is applicable to the structure supporting the secondary mirror module within the primary thermal shield. The configuration used for assessment, however, adds the full radius dynamic deflections of the primary mirror support structure to the deflections of the secondary mirror supports. Subject to a precision analysis this was resolved by considering the use of metering rods between the secondary mirror module and the primary mirror reference plane frame. These would be the primary despace control. The material candidate considered for this was graphite fiber/glass matrix tubes contained, with a visco elastic material interface, within a graphite/epoxy tubular housing for a thin highly damped metering rod.

**3.9.3.4.2 Low Jitter and Short Settling Time** - The issue assessed here was the maximization of observation times which are inherently limited by the need to avoid exposure angle limits for the sun and the earth albedo. Target dwell times are limited to about 35-40 minutes maximum. A settling time goal of 300 seconds was considered. No dynamic modeling or analyses were performed for this task. Previous efforts such as ACOSS, which used a somewhat similar size and arrangement structure, was re-examined and that in conjunction with engineering judgement, indicated a definite need for effective damping aids to the basic structure. Subject to a precision analytical model analysis, a passive damping approach is targeted.

Visco Elastic Material (VEM) devices show strong promise. There are state-of-the-art techniques to incorporate them into structure; however, most tend to be excessively heavy for LDR. Lightweight concepts are currently under study by AFOSR (MDAC is the contractor). Continued development of this damping approach could provide the necessary resolution for LDR.

**3.9.3.4.3 Dynamic Response Predictive Precision** - In order to commit to an LDR program with its extreme dynamic deflection limits, there must be strong assurance that the analytical techniques and processes will predict such precision accurately. Without this confidence it would be necessary to build and flight test comparably large prototype structures with the potential for numerous test flights to achieve the required goals. The only valid way to assess these analytical processes is to perform sample analyses with parametric sensitivities and demonstrate correlation testing. This study supported neither. This was an introspective assessment only.

It was first concluded that the key analytical issues must be performed interactively. This is reflected in condensed form in Figure 3.9-12. The process appears to be adequate. The concerns are for the analytical program capacities (DOF, etc.), the database precision (E, CTE, etc.), scaling, eigenvalue and other factors, the modeling accuracy of nonlinear elements, the accuracy of nonlinear time domain solutions, and correlation testing.

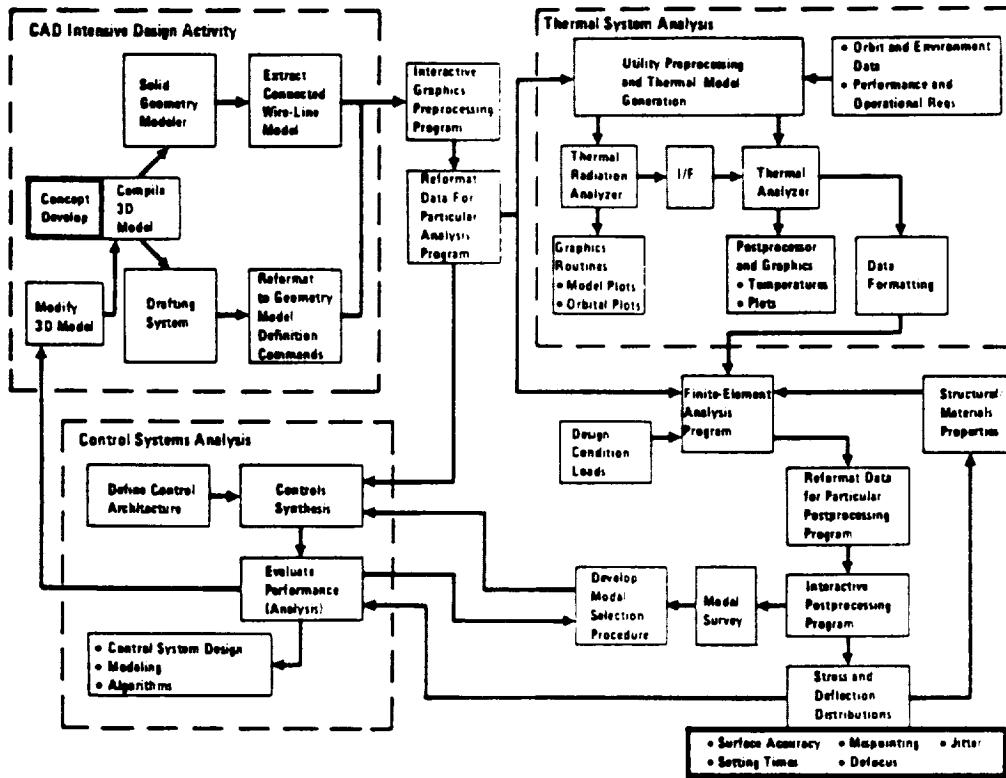
To reduce the modeling burden the design concepts should be simple, have the fewest possible nodes and members, the highest possible component commonality and should strive to minimize nonlinear features. In summary, for the predictive process, NASA should continue to push the development of precision damping modeling, test data, and design criteria; to evolve the analytical tools for super precision very large DOF models having complex modal distributions, complex nonlinear features and time-varying characteristics. There is a parallel need for testing and simulations with environments of sufficient fidelity to provide the necessary confidence in the analytical predictions.

**3.9.3.4.4 Structural Nonlinearity** - An integral part of the foregoing and one of the more significant uncertainties is the issue of nonlinearity in various structural members such as joints with hinges and other fasteners. Two areas assessed are strongly influenced by this issue: the amount of computer intensive nonlinear dynamic analyses; and the architectural concepts for the vehicle control system. Extensive nonlinear model programs can be relatively expensive. Most classical spacecraft control systems are based on the assumption of linear structural responses and a spacecraft exhibiting appreciable nonlinear responses may require the development of new control system concepts.

There is a need, then, to develop high fidelity analytical modeling techniques for the joints and to develop design criteria to minimize nonlinear features by design.

**3.9.3.5 Long-Term Dimensional Stability** - The key issues include: changes to material length through mass loss (i.e., water from resin matrix composites), micro-cracking, creep, fatigue yield, changes to material properties (i.e., E modulus and CTE).

These were assessed from the standpoint of materials, space environments, and design philosophies. Their control generally was considered to be near-term state-of-the-art by: designing for low stresses; preconditioning materials; sealing or protectively coating materials; use of environmental barrier or shield structures. If resin matrix composites are selected, then development/demonstration of pre-conditioning and coatings are advised.



INTERACTIVE DESIGN/ANALYSIS PROCESS  
Figure 3.9-12

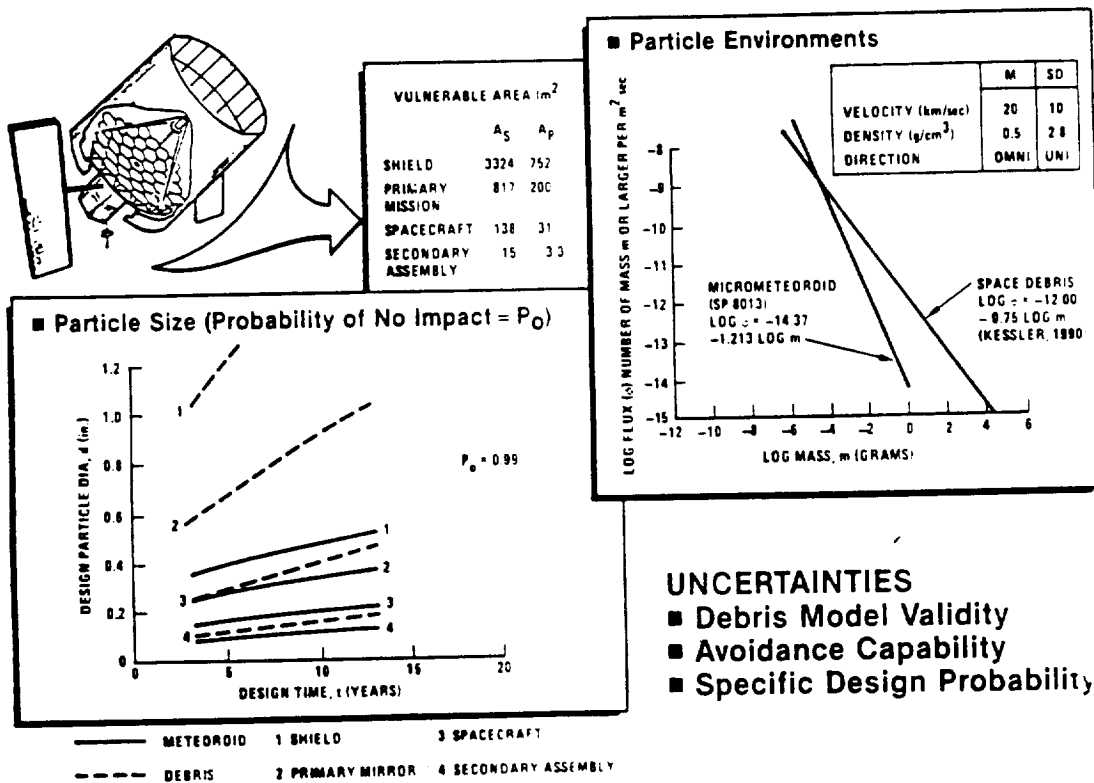
**3.9.3.6 Human Factors Influence** - As part of the Human Factors influence discussion in Volume II, the need to include design features in the constructed LDR concept structure to accommodate and take advantage of the EVA role in deployment was assessed.

The assessment established primary considerations including: structural bluntness for crew safety; access paths of adequate size for all interfaces needing crew contact or close proximity viewing; hand tools for manipulating, locating, preload leveraging and fastening mechanical joints. Joint designs, attachment concepts, electrical network interfaces, etc., should be based on demonstrated EVA simulations. It can be noted that tetrahedral truss concepts work well for all of these considerations.

3.9.3.7 Damage Tolerance - The primary issue assessed in this study was with respect to micrometeoroid and space debris object damage sources. A worst case probable impact analysis was performed with the following assumptions.

- Component shielding of other components was not accounted for
- Average Profile Areas are based on random exposure direction and are the average of minimum profile to maximum profile
- Use of 500 km altitude data

Due to the various uncertainties of the debris model its data suggests it rather than the micrometeoroid environment will be the driving influence. Therefore, this analysis was performed to reflect the probable importance of the impact damage issue rather than to provide realistic values. As indicated in the analysis summary, Figure 3.9-13, even the primary mirror support structure with its low effective porosity at some view angles (a vulnerable area slightly less than the spacecraft) may anticipate impact by particles up to 5 mm in diameter during the ten-year life of LDR. It is vital then that damage modes and residual integrity of LDR specific members be well understood in order to be able to predict the degree and manner of impact survivability and the potential refurbishment requirements.



LDR MICROMETEOROID/DEBRIS  
IMPACT PROBABILITY  
Figure 3.9-13

### 3.10 CONTAMINATION CONTROL

#### 3.10.1 Task

The purpose of this task was to evaluate contamination protection alternatives during buildup, transportation to orbit, and during operation.

#### 3.10.2 Approach

Contamination control was considered in all phases of the LDR buildup and end use; in the design and selection of materials and coatings; in manufacture, assembly, and testing by defining facility and hardware cleanliness requirements; and in subsequent transportation, integration, prelaunch testing, deployment, and telescope operation.

A summary of contamination concerns and control methods for various transitional phases from prelaunch to operation on orbit is shown in Table 3.10-1.

TABLE 3.10-1  
CONTAMINATION CONCERNS AND CONTROLS

<u>Mission Phase</u>	<u>Concern</u>	<u>Control Measures</u>
Prelaunch	Cleanliness Maintenance During Handling, Installation and Checkout	● Protable Clean RM ● Protective Pkging ● Purging
Boost/Delivery	In-Bay/Out-Bay Deposition, Outgas, Offgas, Vent, RCS	● Protective Pkging ● Inhibited Orbiter Vent and RCS OPS
Assembly/Revisit	Orbiter Effluents Docking, Separation, EVA	● Docking Location ● Mirror/Detector Covering During Assembly
Boost to Operating Orbit Operations	Transfer Phase Effluents RCS Thrusters Self-Contamination	● Fences ● Duty Cycle Control ● Selected Material ● Detector Purge ● Periodic Detector Warmup

#### 3.10.3 Discussion

The requirements for control of primary mirror contamination can best be stated in terms of performance. When chopping a source, it is important to obtain a uniform background signal. The presence of particulate contamination on the primary mirror will produce scattered radiation, contributing to a reduction in ability to remove background radiation.



If molecular monolayers are deposited on the primary mirror, these may produce unwanted spectral absorption lines which will produce unknown effects on the radiometric performance of the instrument. In addition to these effects, the overall throughput of the instrument will be reduced because of reduced mirror reflectance. The presence of contamination may also alter the thermal performance of the optics by changing the emissivity and absorptance.

In the later stages of program development (usually in Phase B or C), a contamination control plan must be developed which will establish standards and requirements. The plan must specify contamination control in the design by selection of materials and coatings; in manufacture, assembly, and testing by defining facility and hardware cleanliness requirements and testing procedures; and in subsequent transportation, integration, prelaunch testing, deployment, and operation.

Material implications are given by the example of selecting a material for the secondary mirror support structure. A stiff, lightweight, thermally insensitive structure is required. The state-of-the-art mature metering structure material is graphite-epoxy. Data has shown that untreated laminates using epoxy cause optically significant changes: 1) change in primary mirror to secondary mirror spacing results in a wave front error, 2) water vapor deposits on the coolest surfaces--mirrors and detector--severely degrading performance. Some attempts have been made to encapsulate the material in a moisture barrier to minimize the dimensional instability and outgassing; however, more work needs to be done.

Particle size distribution curves can be used to establish the "degree of cleanliness" required in each step of LDR buildup. During the early stages of mirror segment fabrication, a Class 100,000 environment is probably adequate.

However, once the mirror surface is coated, cleanliness becomes a major factor--Class 300 levels are typically required. In the later stages of LDR buildup, it will be difficult to maintain these types of levels on the large primary mirror.

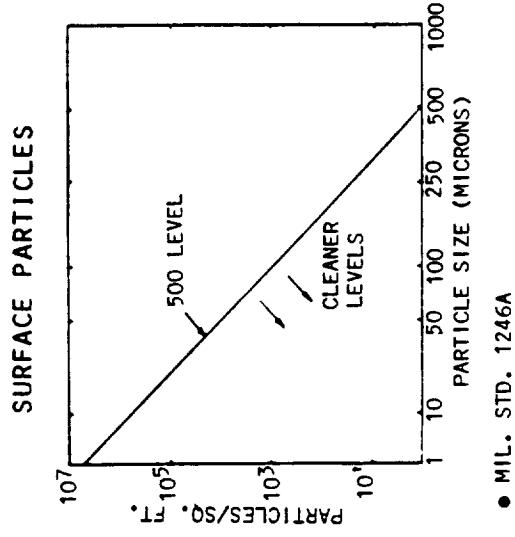
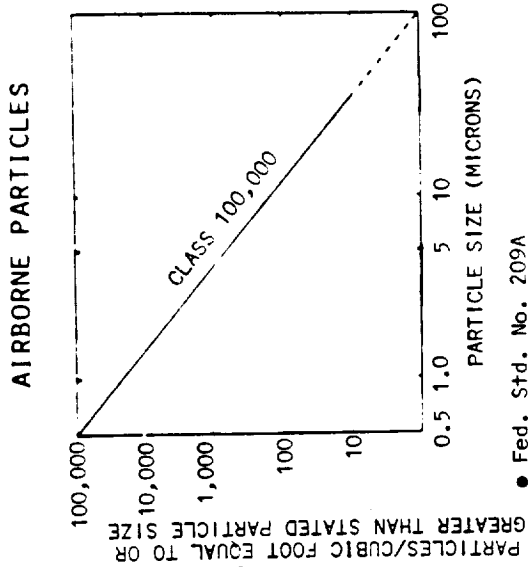
A summary of the particulate contamination concerns and control approaches for the LDR primary mirrors during buildup and on-ground transportation is shown in Figure 3.10-1. Contamination control in these stages is implemented by the use of "clean" rooms and packaging.

Major phases of later concern are the in-Orbiter prelaunch, boost, and on-orbit deployment environment. Also of concern is the revisit maintenance phase in the presence of the Orbiter or Space Station/Space Platform facility.

A major concern in the boost, deployment, operation, and revisit/maintenance phases is contamination due to propulsion effluents. Basic propulsion capabilities are well developed and divided into monopropellant and bipropellant systems. Spacecraft contamination is a concern with both types. Payloads launched with the STS must endure a contaminating environment which require contamination protection. Sensitive surfaces which can be protected from the Shuttle environment should be able to use the same protection for infrequent integral propulsion burns. If spacecraft propulsion is required frequently, a contamination-free system will require development; i.e., hydrogen-oxygen bipropellant or resister jets.

- STEP
- CONTOUR GENERATION OF PRIMARY MIRROR SEGMENTS
- FIGURING OF PRIMARY MIRROR SEGMENTS
- COATING OF PRIMARY MIRROR SEGMENTS
- INTEGRATION OF PRIMARY MIRROR SEGMENT ASSEMBLIES
- ON-GROUND TRANSPORTATION OF PRIMARY MIRROR SEGMENT ASSEMBLIES

- CLEANLINESS REQUIREMENTS
- CONTAMINATION CONTROL
- "CLEAN ROOM ENVIRONMENT"
- "CLEAN PACKAGING"



PARTICULATE CONTAMINATION CONTROL  
(DURING BUILDUP AND ON-GROUND TRANSPORTATION)  
Figure 3.10-1

Shown in Figure 3.10-2 are two particulate contamination control concepts which could be used during in-orbit assembly and Shuttle revisit. In the first concept a moveable panel can be reinserted at appropriate times to protect only the mirror. In the second concept the shroud folds to protect the entire "front end" of the observatory (primary mirror, secondary mirror and secondary mirror support structure).

The range of control options, therefore, go from total LDR containment on one extreme to specific patches, port covers, and local "baggies" on the other extreme. One might expect LDR control to optimize in hybrid form; for instance, total containment of the stacked mirror elements; removable/retractable, or blowoff port covers for the scientific instruments and spacecraft and little or no control for various structural packages. One potential control aid for the mirror surfaces is a strippable film. Depending on the environments and surface sensitivities, such a film may be beneficial not only for the transport mode but also for the environment of the deployment/construction area. This would be especially likely if the assembly platform is the Orbiter. It may, however, prove to be very difficult to handle and dispose of a strippable film in orbit.

Revisiting LDR by the Shuttle for refurbishment and maintenance is of major concern. The collapsible sunshield concept is an attractive option, which could be closed between telescope operations and during Orbiter rendezvous.

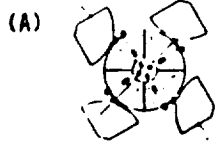
If LDR is assembled on the Space Station some type of LDR protection will be required against the environment around the Space Station. This could be due to reaction control system effluents from Shuttles, Space Station atmosphere leakage and a variety of other contaminants from the Space Station and payloads. Also, independent of the contamination issue, the incidence of sunlight on the LDR mirrors and structures during construction may counter the high accuracy optical figure and position measurements envisioned. Therefore, there may be a requirement for some sort of environmental shielding, either fully or fractionally enclosing the LDR. Such a "lightweight" covered structure is shown in Figure 3.10-3. In view of the expense involved in such a unique accessory, a study of the needs of other environmentally sensitive payloads or payload servicing functions should be analyzed before a design is selected. In the traditional buildup of a Cassegrain telescope, the secondary mirror is attached to the primary mirror and then the shroud is installed. An interesting LDR unique variation could be to install the thermal shroud first and build up the telescope. This would allow the thermal shroud to be the construction "hanger".

#### 3.10.4 Conclusión

The cleanliness requirements for particulate contamination are set by the specular requirement in the light bucket mode. Contamination control during on-ground buildup should be maintained by using "clean" rooms and packaging. During in-orbit assembly the primary mirror and secondary mirror should be protected by a "strippable" coating. Some type of collapsible shroud might be needed during Shuttle revisiting for refurbishment and maintenance. Some type of clean room environment might also be needed for Space Station assembly.

(DURING IN-ORBIT ASSEMBLY AND SHUTTLE REVISIT)

PRIMARY MIRROR  
PROTECTION DURING  
IN-ORBIT ASSEMBLY



MOVEABLE PROTECTION

(B) STRIPPABLE COATING

OPTICAL SUBSYSTEM PROTECTION  
FOR SHUTTLE REVISIT

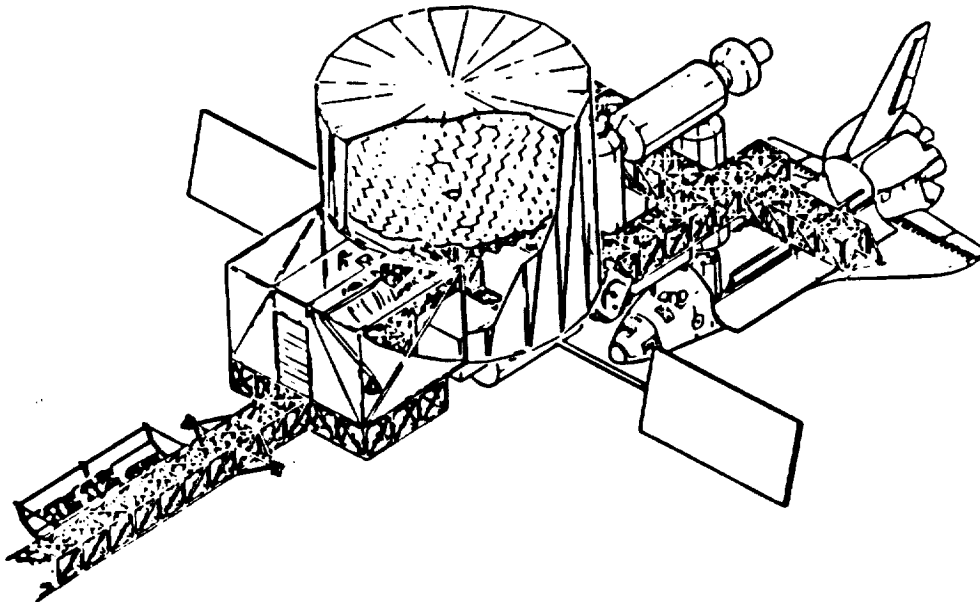


MDAC SUNSHIELD SHROUD  
COMBINATION

PARTICULATE CONTAMINATION CONTROL

Figure 3.10-2

(SPACE STATION ASSEMBLY CONCEPT)



PARTICULATE CONTAMINATION CONTROL

Figure 3.10.3

### 3.11 ORBITAL PARAMETERS (FSC)

#### 3.11.1 Task

The objective of this task was to determine the orbital parameters for LDR in order to permit the trade-off of various orbital parameters against conceptual designs. Various orbit altitudes and inclinations were analyzed to establish the orbit environment for LDR.

#### 3.11.2 Approach

The work performed within this task required the utilization of orbital models, atmospheric models, and development of models which factor in the sky availability due to earth and sun avoidance requirements.

The factors considered in the analysis were:

- a) Spacecraft lifetime as function of: altitude, drag characteristics, solar activity, solar cycle.
- b) Delta-velocity evaluation; fuel requirements
- c) Rendezvous delta-velocity evaluation; phase and nodal error corrections for Space Station servicing.
- d) Solar and earth avoidance angles leading to spacecraft slew requirements.

#### 3.11.3 Orbit Decay and Propulsion Requirements

3.11.3.1 Discussion - The orbit parameter evaluations were based initially on the spacecraft parameters shown in Figure 3.11-1. The case of 550 square meters effective drag area represents a case which requires cryo-refrigerator power, resulting in an increase in deployed solar-array area.

In this series of analyses, lifetime evaluations were based on a +2 sigma sun and do not reflect exact launch dates since the majority of the lifetime values are large multiples of the nominal 11-year solar cycle.

The results of this analysis are shown in Figures 3.11-2 through 3.11-7.

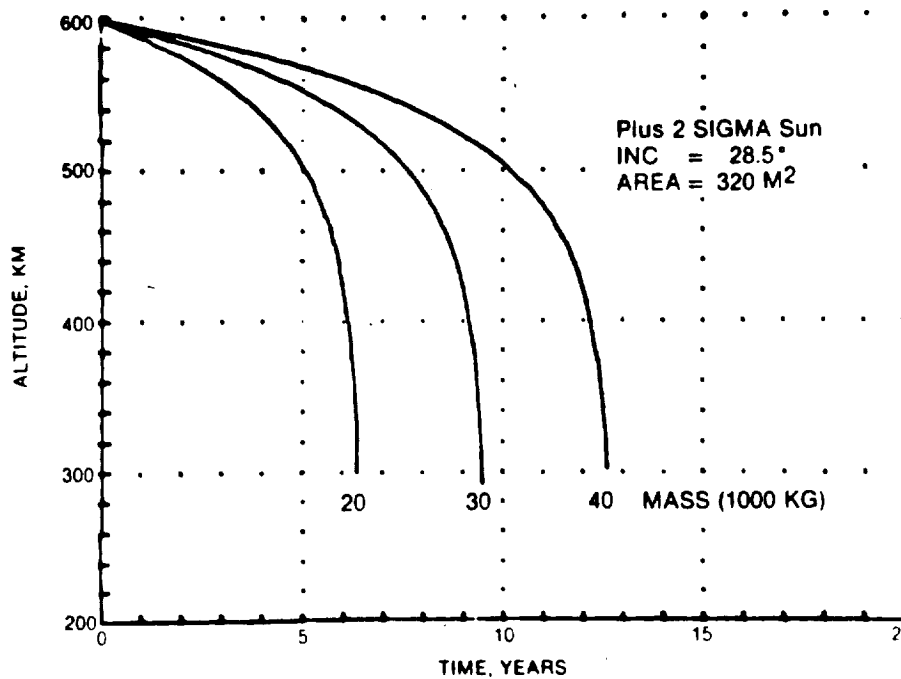
Total delta-v required for round trip of LDR from a 300 km start altitude to a variable fixed cruise altitude and thence to a 480 km rendezvous altitude is presented in Figure 3.11-8. No drag makeup at cruise is assumed. This translates to the propellant mass parameters shown in Figure 3.11-9, based on specific impulse of 300 sec, typical of a bi-propellant system.

Mass (KG)	Area (M <sup>2</sup> )	Ballistic Coefficient @ Cd = 3.42
40,000	320	17.218
30,000	320	12.913
20,000	320	8.609
40,000	550	10.019

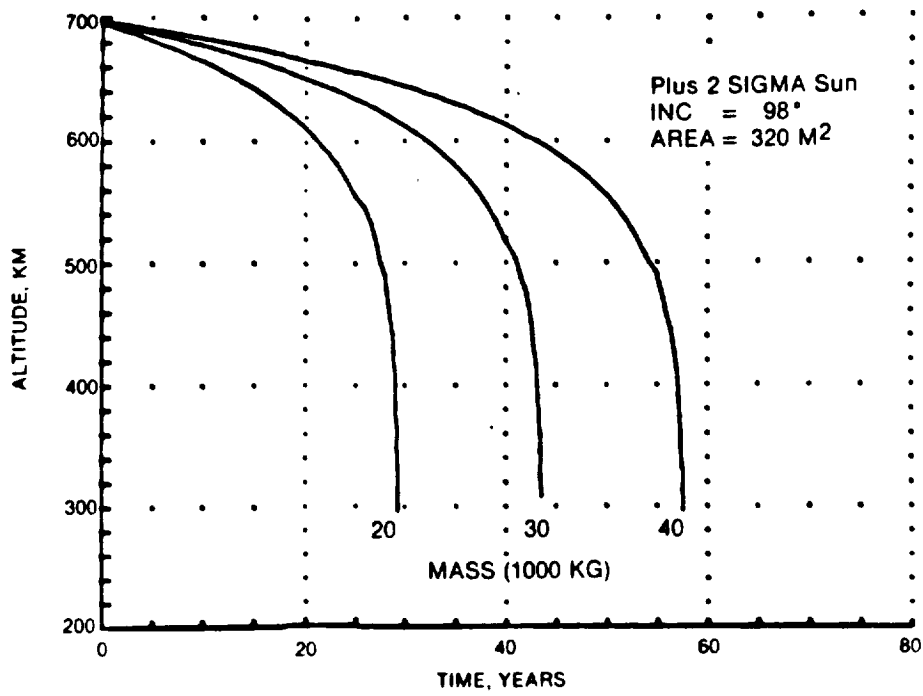
Average F<sub>10.7</sub> cm (solar flux) = 160.7

+ 2 sigma T<sub>sun</sub> = 916.52

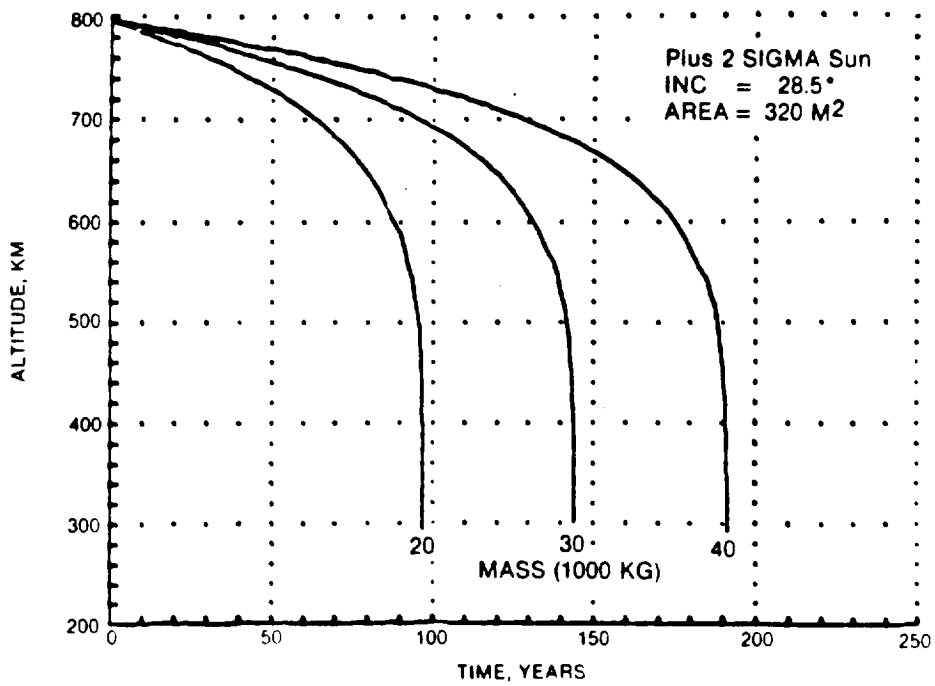
ORBIT PARAMETER FIELD  
Figure 3.11-1



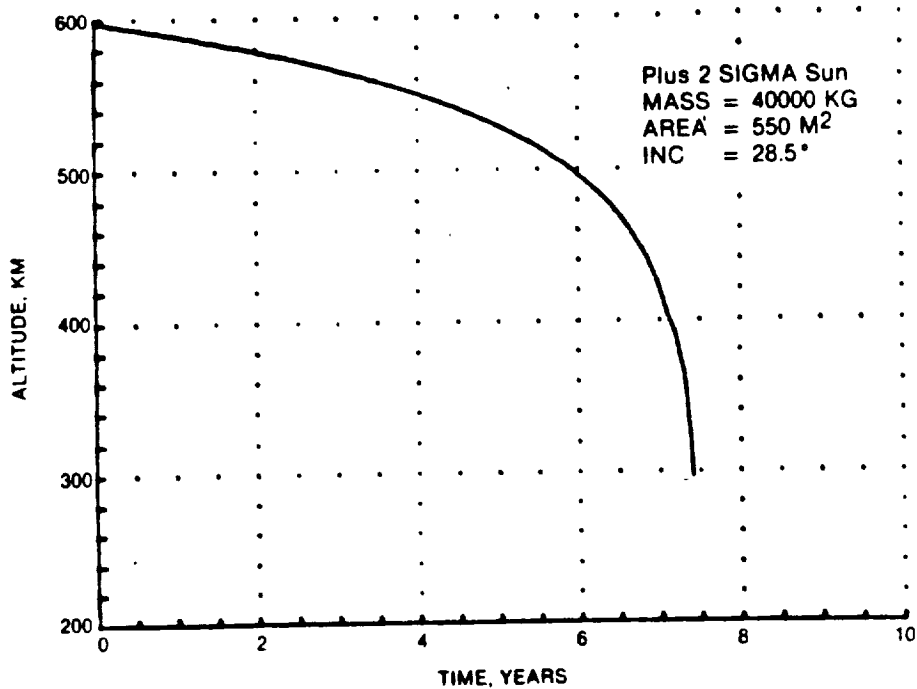
ORBIT DECAY FROM 600 KM INITIAL ALTITUDE  
(ZERO DRAG MAKEUP)  
Figure 3.11-2



ORBIT DECAY FROM 700 KM INITIAL ALTITUDE  
(ZERO DRAG MAKEUP)  
Figure 3.11-3

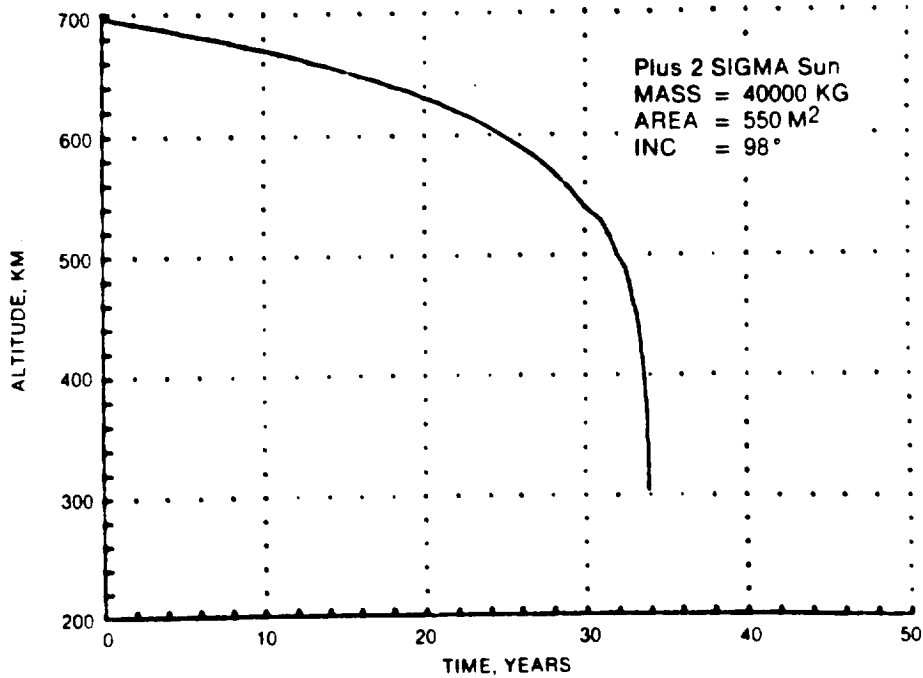


ORBIT DECAY FROM 800 KM INITIAL ALTITUDE  
(ZERO DRAG MAKEUP)  
Figure 3.11-4



ORBIT DECAY FROM 600 KM, HIGH POWER LDR  
 (ZERO DRAG MAKEUP)

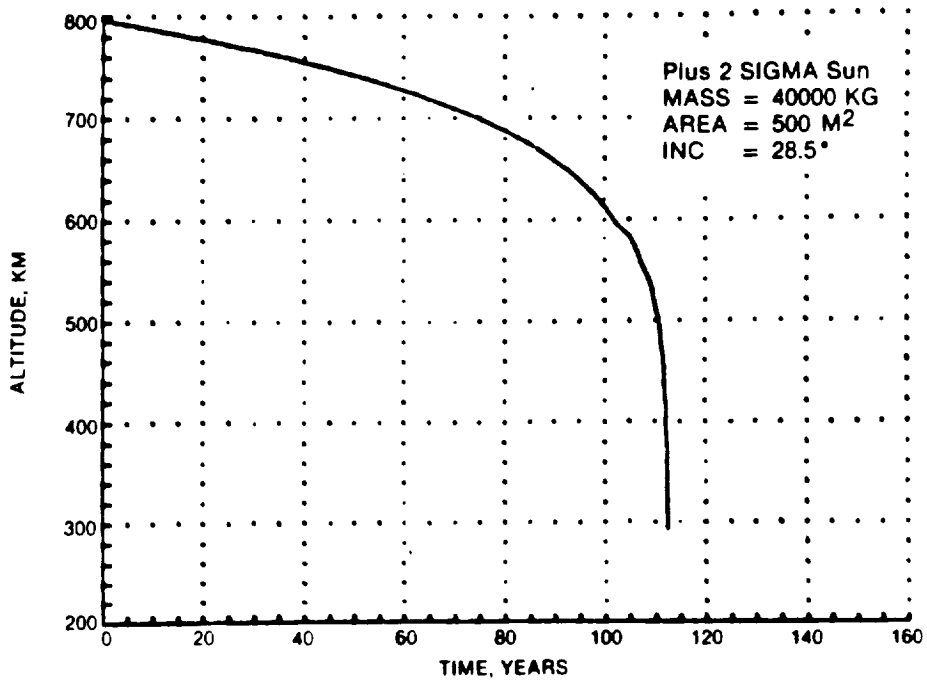
Figure 3.11-5



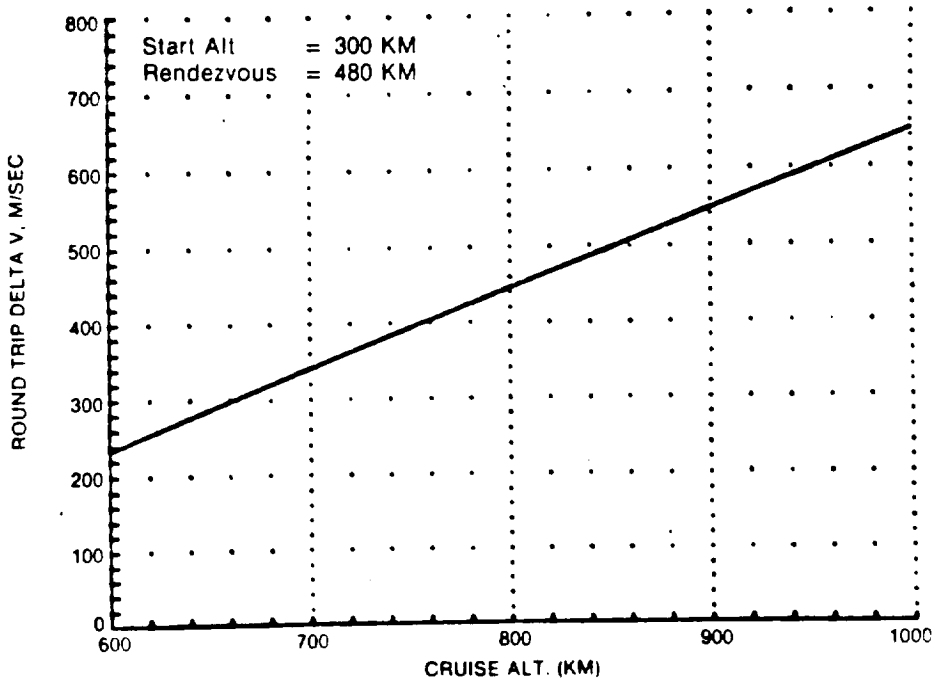
ORBIT DECAY FROM 700 KM, POLAR ORBIT,  
 HIGH POWER LDR (ZERO DRAG MAKEUP)

Figure 3.11-6

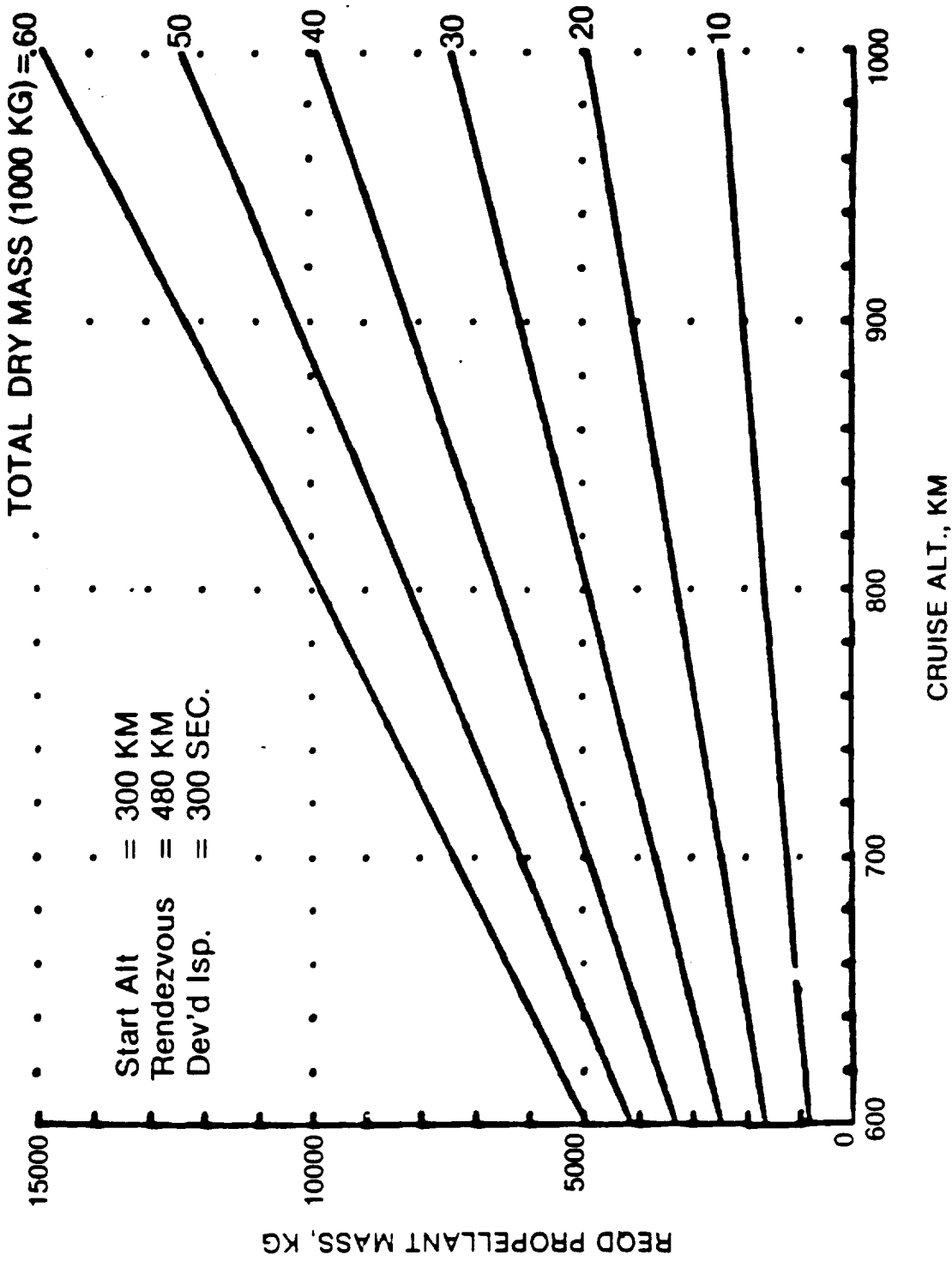




ORBIT DECAY FROM 800 KM HIGH POWER LDR  
 (ZERO DRAG MAKEUP)  
 Figure 3.11-7



INCREMENTAL VELOCITY REQUIREMENT  
 FOR ORBIT ADJUSTMENT  
 Figure 3.11-8



LDR PROPULSION REQUIREMENT  
 FOR ORBIT ADJUSTMENT

Figure 3.11-9

This analysis assumes that a complete cycle is accomplished in a time period short compared to the decay time of the LDR, as shown in Figures 3.11-2 through 3.11-7.

### 3.11.3.2 Conclusions

In order to avoid a need for drag makeup during a nominal three-year mission cycle, operational altitude should be greater than 600 km. However, in order to avoid excessive propellant requirements, operational altitude should be less than 800 to 1000 km.

An alternative mode of operations could be a boost-decay mode, as discussed below.

### 3.11.4 Boost-Decay Operation

#### 3.11.4.1 Discussion

In order to limit fuel consumption of LDR, a "boost-decay" operating mode may be postulated. This is based on a prediction of solar activity for the next operating period, e.g., three years. The spacecraft is boosted to that altitude at which, according to the prediction, atmospheric drag would bring it back to the standard Shuttle service altitude (assumed to be 482 km) at the end of the period.

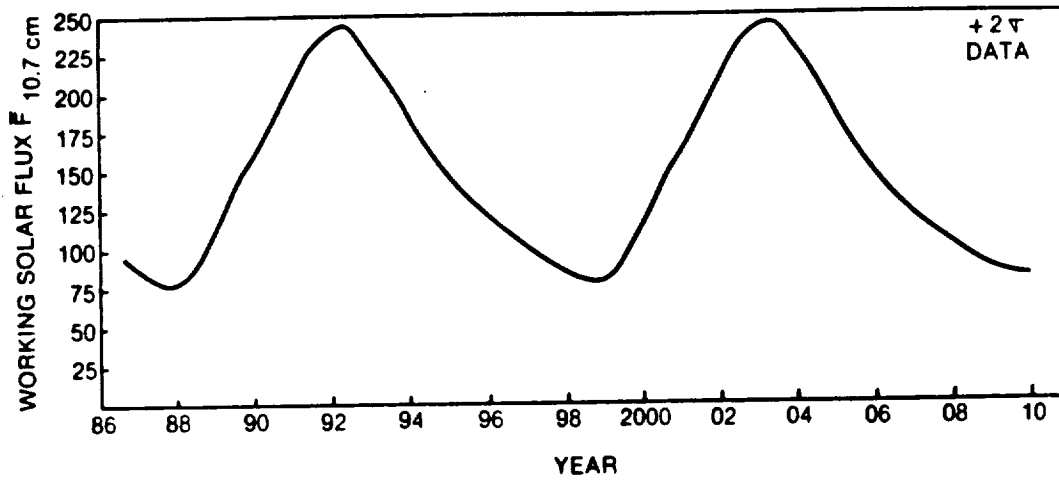
Figure 3.11-10 shows the currently predicted solar activity variation for the period 1987 through 2010. Figure 3.11-11 illustrates a boost-decay operation mode through three 3-year cycles, based on concept No. 1 with LDR length = 30 meters and mass = 42,000 kg.

A similar analysis is shown in Figure 3.11-12 for an unfilled aperture LDR concept (No. 3), with the parameters as shown.

#### 3.11.4.2 Conclusions

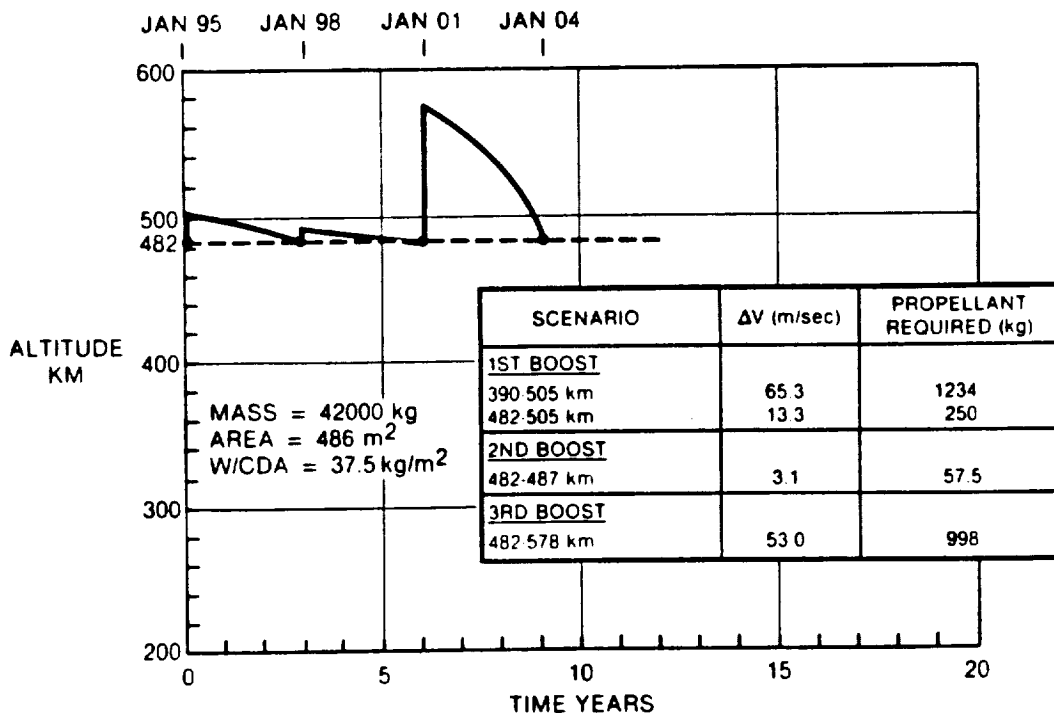
From the viewpoint of orbit decay parameters, the boost-decay mode of operation results in a very modest propulsion requirement, if Shuttle servicing is postulated. Since solar activity, and hence the rate of orbit decay, cannot be predicted with certainty, a certain amount of flexibility will be required of mission operations: shutting down operations whenever the rendezvous altitude is approached, and performing altitude hold maneuvers while awaiting Shuttle rendezvous. This mode may also lead to a requirement for dedicated service flights since the observatory will have little ability to adjust its orbital node or phase. For an observatory of LDR's size and importance, however, this is likely to be the case in any event.

Since 482 km is also to be the nominal altitude of Space Station operation, a similar cycle may be envisioned for servicing by the Space Station. This is generally not feasible, however, as a result of the effect of differential nodal regression experienced between a station at a relatively fixed altitude and a co-orbiting platform at a varying altitude. The results of this constraint are discussed below.



PREDICTED SOLAR FLUX

Figure 3.11-10



SPACECRAFT CONCEPT NO. 1, LENGTH = 30M

Figure 3.11-11

$\text{DRAG AREA} = 3287.12 \text{ FT}^2 = 306.55 \text{ m}^2$

$\text{W/CDA} = 12.25 \text{ \#/FT}^2 = 59.57 \text{ kg/m}^2$

SCENARIO	$\Delta V$ m/sec	PROPELLANT (kg) REQUIRED
1ST BOOST 390-495 km 482-495 km	59.1 7.2	1116 134
2ND BOOST 482-485 km	1.1	19
3RD BOOST 482-555 km	40.7	767

SPACECRAFT CONCEPT NO. 3, LENGTH = 12M

Figure 3.11-12

### 3.11.5 Space Station Rendezvous Aspects

#### 3.11.5.1 Discussion

LDR design concept No. 2 is based on Space Station servicing. A preliminary orbital/rendezvous analysis for an LDR having a spherical primary mirror configuration is based on the following assumptions:

1. Nominal 3 year mission cycles with the Space Station as service base [Altitude = 482 km, Inclination = 28.45 degrees]
2. No propellant utilized during a 3 year mission cycle
3. Observatory Electrical Power = 10 kw
4. Observatory mass = 65,000 kg
5. Primary Reflector Diameter = 20 m
6. Operating Mode: inertial pointing
7. Propulsion System is refuelable

Outputs are parametric in nature. The detailed analysis, which is contained in Appendix D.5, proceeds by a consideration of the following factors:

1. Drag area and ballistic coefficient
2. LDR orbital/rendezvous considerations
3. Orbital decay rates
4. Altitude/Nodal error sensitivity
5. Nodal errors due to solar activity excursions from nominal + 2- sigma value
6. Propellant requirements
7. Phase make-up

3.11.5.2 Conclusions - From the analysis, the following conclusions can be drawn:

1. Because of differential nodal regression, operating altitude will be a strong determinant of possible service frequency. At 800 km operating altitude, only one service period per annum is possible. Thus, some provision for system survival for up to one year in the event of subsystem failure should be considered. Even at 1000 km altitude, service opportunities will occur at only 9-to-10 month intervals.
2. For a nominal three-year mission interval, available altitudes become quantized; e.g., 580, 684, 800 km, for 1-to-3 rendezvous opportunities respectively.
3. At 800 km, relative nodal regression is approximately 1 degree/day. Thus, for an OMV-type of retrieval operation, a very brief window is available to effect the round trip. For every day spent by an OMV at 800 km, approximately three days at 400 km will be required to correct for the nodal shift introduced, before final rendezvous with the station at 480 km may be effected.
4. To correct for a misprediction of solar activity, a slightly higher-than-nominal altitude is recommended. Thus a nominal or higher-than-anticipated solar activity will result in a slightly earlier-than-anticipated shutdown for service, while a less-active sun will not extend the mission period excessively, thus avoiding the possible danger to the sensors which could result from an extended period without cooling.

### 3.11.6 Observational Viewing Limits

3.11.6.1 Discussion - A limited analysis of viewing limits due to solar and earth exclusion zones was performed. Figures 3.11-13, 14, 15 cover the near extremes of solar latitude variation for an observatory at 28.5 degrees inclination and for earth and sun avoidance angles of 45 and 60 degrees respectively.

3.11.6.2 Results - Maximum potential continual viewing of a single target is seen to occur over 140 degrees of observatory orbital motion, or 38.3 minutes of time. Total time between target observations, which is comprised of slew time and settling time, should be minimized. Because LDR's line of sight is roughly on the target during the settling time, some of the potential viewing time (38.3 minutes) must be lost if the exclusion limits are to be considered inviolate. (Image motion compensation in LDR could reduce or eliminate this loss.)

This result is used to determine the slewing requirement for the observatory (see Spacecraft Functions, Section 3.13.).

## 3.12 ORBITAL ENVIRONMENT (FSC)

### 3.12.1 Task

The objective of this task was to define the orbital environment of interest to LDR; in particular, the South Atlantic anomaly was included.

**BOUNDARIES OF EXCLUDED REGIONS FOR S/C LOS WITH**

**EARTH AVOIDANCE ANGLE (DEG) = 45**

**SUN AVOIDANCE ANGLE (DEG) = 60**  
**WITH S/C ORBIT ANGLE AS PARAMETER**

**ORBIT ALTITUDE (KM) = 700**

**LATITUDE IS ANGLE ABOVE ORBIT PLANE**

**LONGITUDE IS ANGLE IN ORBIT PLANE MEASURED FROM ORBIT NOON**

**SUN IS AT 0 DEG LONGITUDE AND LATITUDE (DEG) = 0**

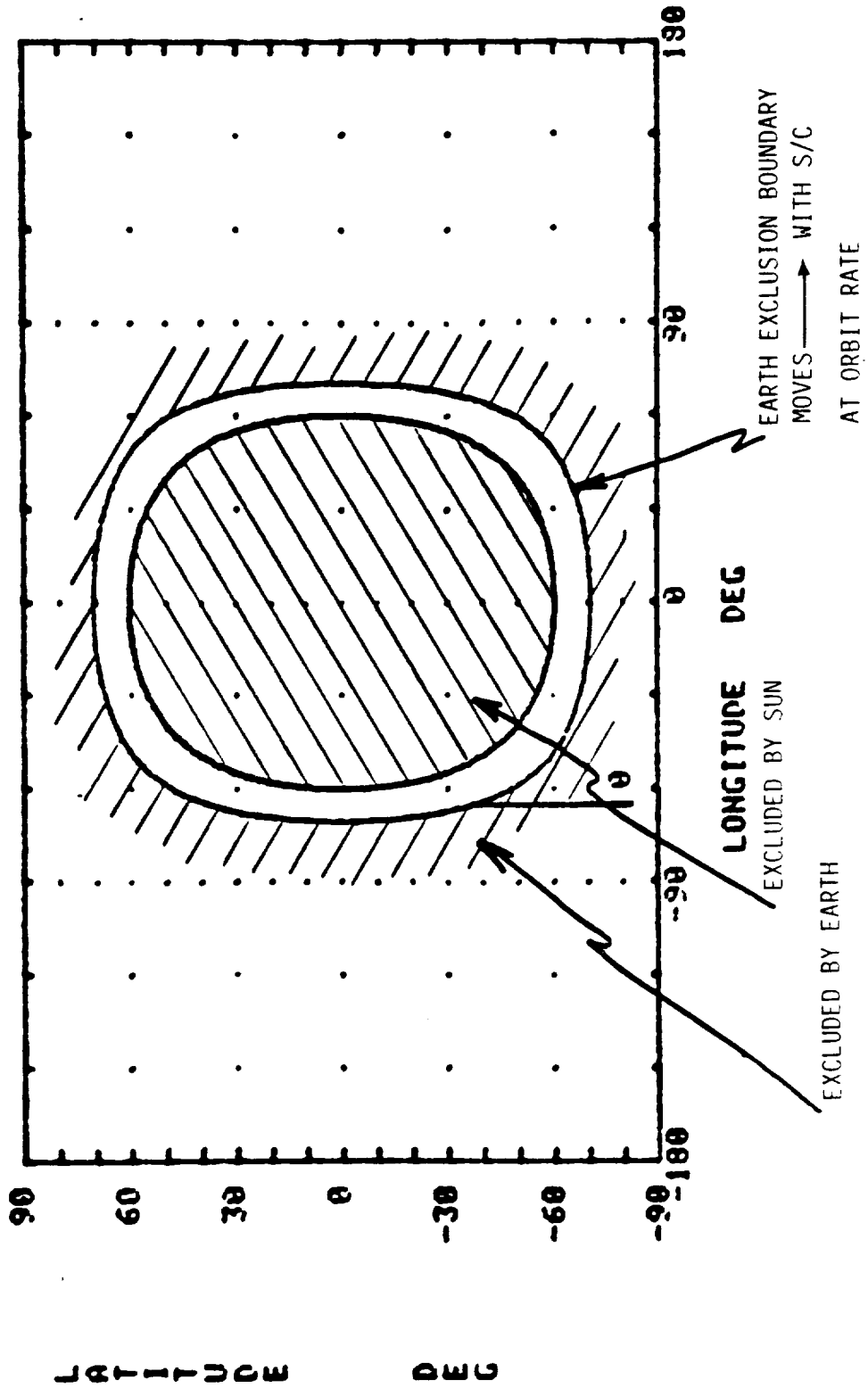


Figure 3.11-13



**BOUNDARIES OF EXCLUDED REGIONS FOR S/C LOS WITH**

**EARTH AVOIDANCE ANGLE (DEG) = 45**

**SUN AVOIDANCE ANGLE (DEG) = 60**

**WITH S/C ORBIT ANGLE AS PARAMETER**

**ORBIT ALTITUDE (KM) = 700**

**LATITUDE IS ANGLE ABOVE ORBIT PLANE**

**LONGITUDE IS ANGLE IN ORBIT PLANE MEASURED FROM ORBIT MOON**

**SUN IS AT 0 DEG LONGITUDE AND LATITUDE (DEG) = -26**

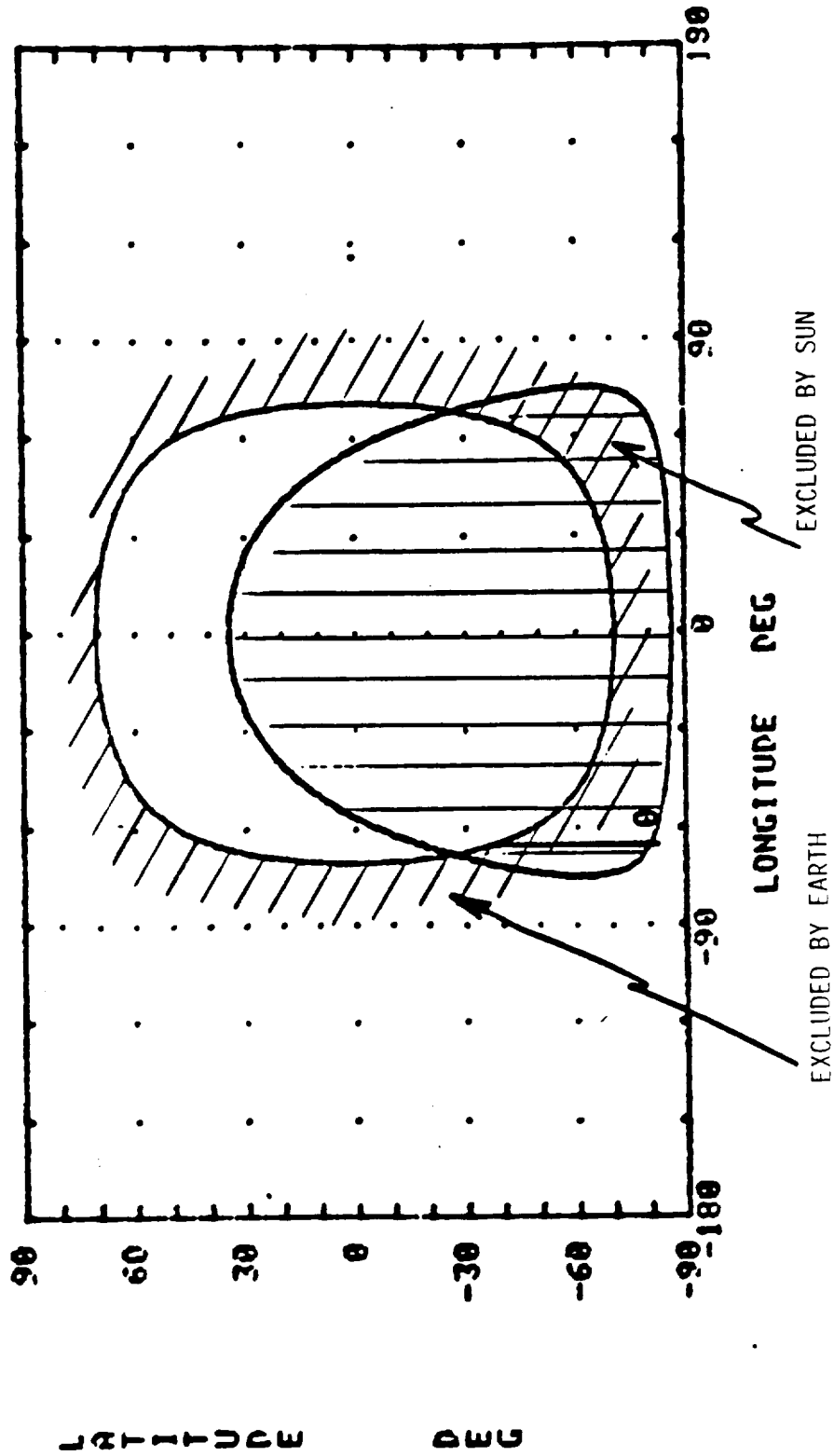


Figure 3.11-14

**BOUNDARIES OF EXCLUDED REGIONS FOR S/C LOS WITH**

**EARTH AVOIDANCE ANGLE (DEG) = 43**

**SUN AVOIDANCE ANGLE (DEG) = 60**

**WITH S/C ORBIT ANGLE AS PARAMETER**

**ORBIT ALTITUDE (KM) = 700**

**LATITUDE IS ANGLE ABOVE ORBIT PLANE**

**LONGITUDE IS ANGLE IN ORBIT PLANE MEASURED FROM ORBIT NOON**

**SUN IS AT  $\theta$  DEG LONGITUDE AND LATITUDE (DEG) = -52**

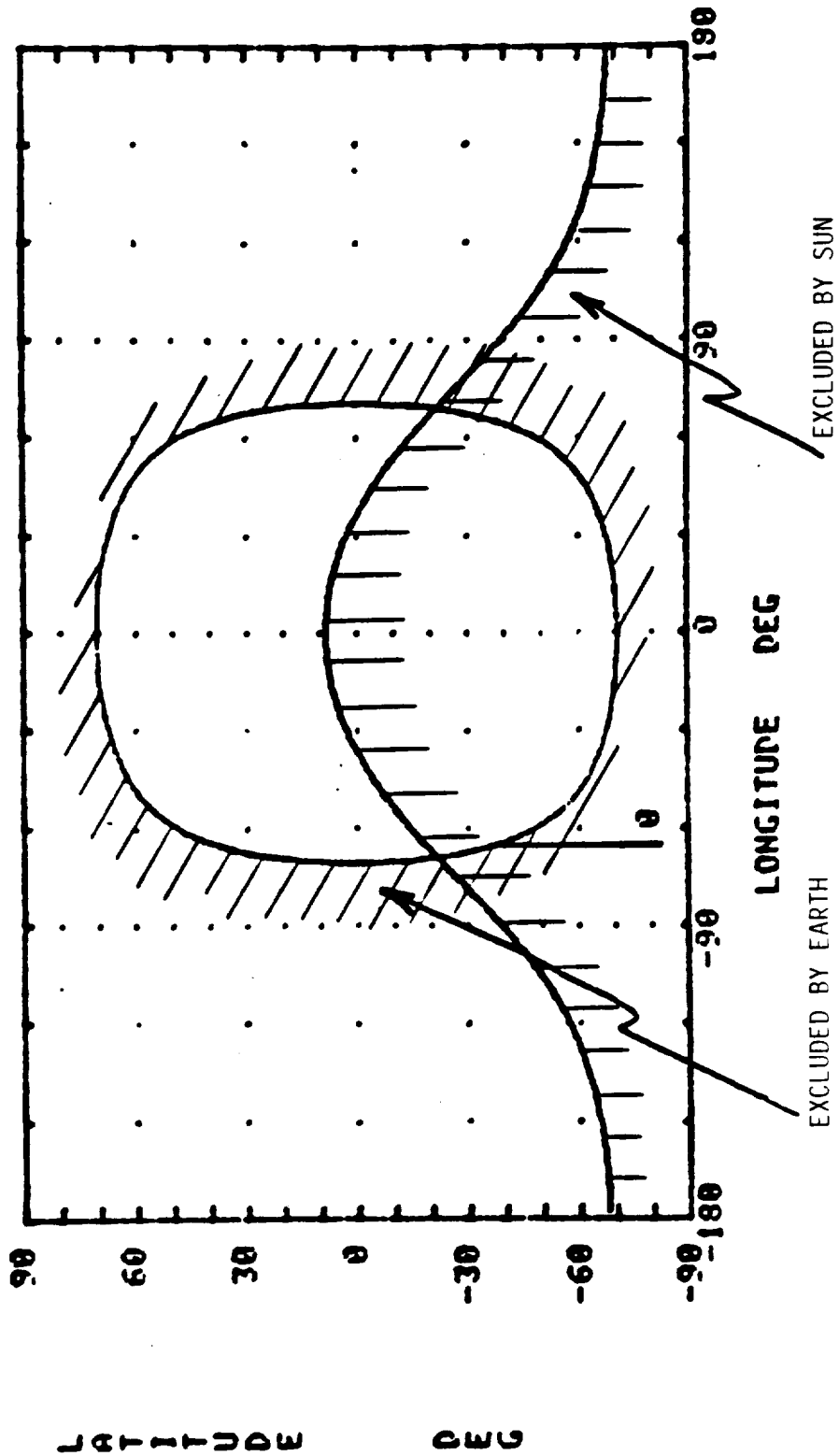


Figure 3.11-15

### 3.12.2 Approach

The work performed under this task established the radiation and micrometeoroid environment, based on a literature survey for a range of orbits provided under the Orbital Parameters task.

The tools used included existing radiation models and micrometeorite models.

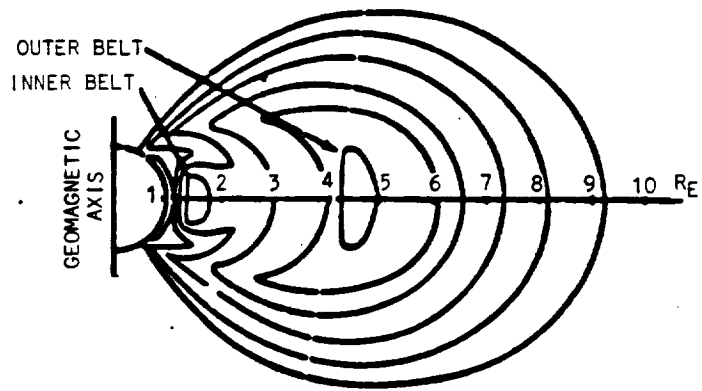
The output of this task were the environmental models for LDR design criteria, and an estimate of solar array degradation over 10 years at the various altitudes and inclinations of interest.

### 3.12.3 Radiation Environment

3.12.3.1 Discussion - There are two belts of geomagnetically trapped radiation around the Earth (the Van Allen Belts). The Earth's magnetic field constitutes a trap for high energy electrons and protons - the geomagnetic field ensures such an interaction. The directionality of the electrons and protons is related to the orientation of the Earth's magnetic field. Because the orientation of a spacecraft or a Space Station varies with respect to the Earth's magnetic field during the course of a mission, particle fluxes are usually considered to be isotropic. Because of different trapped particle flux and energy characteristics there are, as previously noted, two radiation belts: an inner belt at 1.2 to 3.2 Earth radii, and an outer belt at 3 to 7 Earth radii, as shown in Figure 3.12-1. High energy electrons and protons are contained in the inner belt, whereas high energy electrons and lower energy protons are found in the outer belt. The relatively high fluxes and energies associated with these trapped particles make them the primary source of radiation damage for spacecraft or platforms operating in orbits all the way from 200 km to geosynchronous orbit.

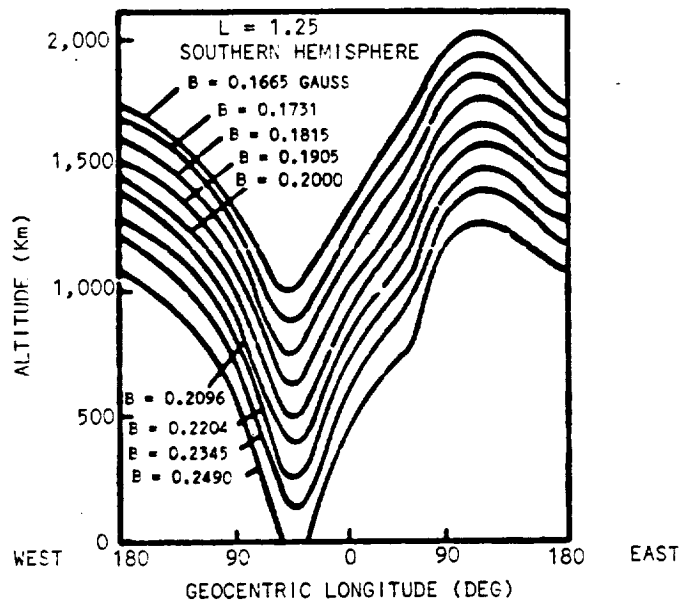
The Van Allen radiation belts are not entirely symmetrical, however. In the South Atlantic anomaly, extending from 0 to 60 degrees west longitude and 20 to 50 degrees south latitude, the trapped proton intensity for energies more than 30 MeV is the equivalent at an altitude of 100 to 200 miles, to that at 800 miles altitude elsewhere. This is due to a perturbation of the Earth's geomagnetic field. For flight paths of LEO space platforms of 30 degrees or greater inclinations there will be approximately five traverses through this anomalous area each day. Experience with orbital missions shows that a major portion of the accumulative radiation has been attributable to passage through this geomagnetic anomaly.

In South Atlantic anomaly region, the magnetic flux lines reach to a low point at about 30 degrees latitude, which manifests itself as a dip in the inner radiation belt. Figure 3.12-2 shows the altitude variation of field strength (flux density) in the SAA. The consequence of this field anomaly is an anomalously high flux of energy particles at low altitudes in the SAA region. This is illustrated in Figure 3.12-3 which shows for an altitude of 240n mi that proton fluxes are two orders of magnitude higher at the center of the anomaly than, for example, a location only 20 degrees to the south at the same longitude.



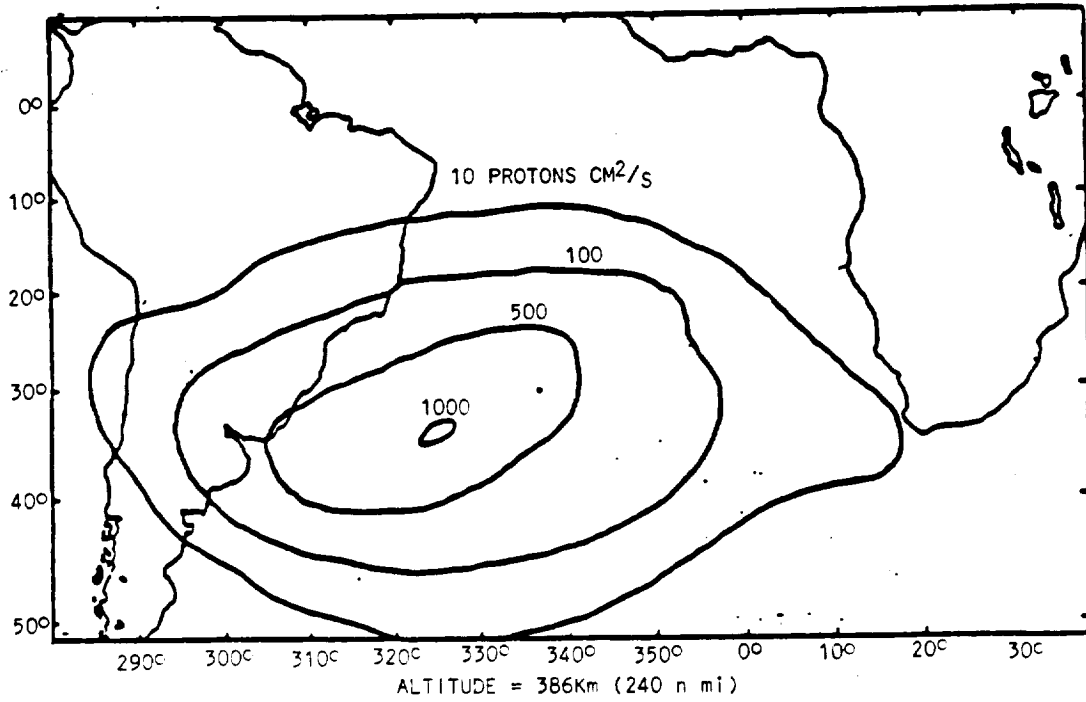
VAN ALLEN TRAPPED RADIATION BELTS

Figure 3.12-1



ALTITUDE VARIATION OF FIELD STRENGTH IN THE SOUTH ATLANTIC ANOMALY (SAA)

Figure 3.12-2



PROTON ISOFLUX CONTOURS FOR ENERGIES ABOVE 34 MeV  
IN THE SOUTH ATLANTIC ANOMALY

Figure 3.12-3

### 3.12.3.2 Results

#### 3.12.3.2.1 Radiation Dose

Charged particle radiation dosages, including the South Atlantic Anomaly, for a spacecraft in various orbits for 15-year missions for 50 mil Aluminum (Al) shielding and 200 mil Al shielding are given in Table 3.12-1.

TABLE 3.12-1

RADIATION - 15 YEAR DOSE (KRADS)

ORBIT	SHIELD THICKNESS	
	50 mil Al.	100 mil Al.
400 km @ 28.5 degrees	33.0 - 67.5	21.0 - 33.0
500 km @ 28.5 degrees	57.0 - 228.5	37.5 - 58.5
600 km @ 28.5 degrees	112.5 - 234.0	73.5 - 117.0

Note: Data for South Atlantic Anomaly for altitudes of 500 km and 600 km is not available. However, as the tendency is to increase in the magnitude of dose as the altitude increases, an assumption is made that the dose at 500 km will be two times and the dose at 600 km will be four times the dose at 400 km. The ranges result from inherent uncertainties in the method of estimation utilized.

The method in arriving at this estimate is as follows: First a measure of the radiation level that would exist at the outside surface of a spacecraft in this orbit was estimated. Formally, this step should be accomplished by models which utilize measured instantaneous proton and electron fluences (in particles/cm/sec) at each position in an orbit. Secondly, these spectra are then utilized as inputs to a second model which calculates the amount of this energy that would be deposited in various thicknesses of the shield. The amount of the incident charged particle energy over the mission lifetime that is not deposited in the shield, i.e., that which penetrates, is then reported as the charged particle radiation dose.

Historically, models for two shield geometries have been developed. One computes the radiation penetrating to the center of a spherical shell of thickness  $t$ . The second computes the radiation which penetrates a semi-infinite slab (i.e., incident radiation only from one side) of the same thickness. The slab geometry, obviously, predicts dosages several times lower than the spherical shell geometry.

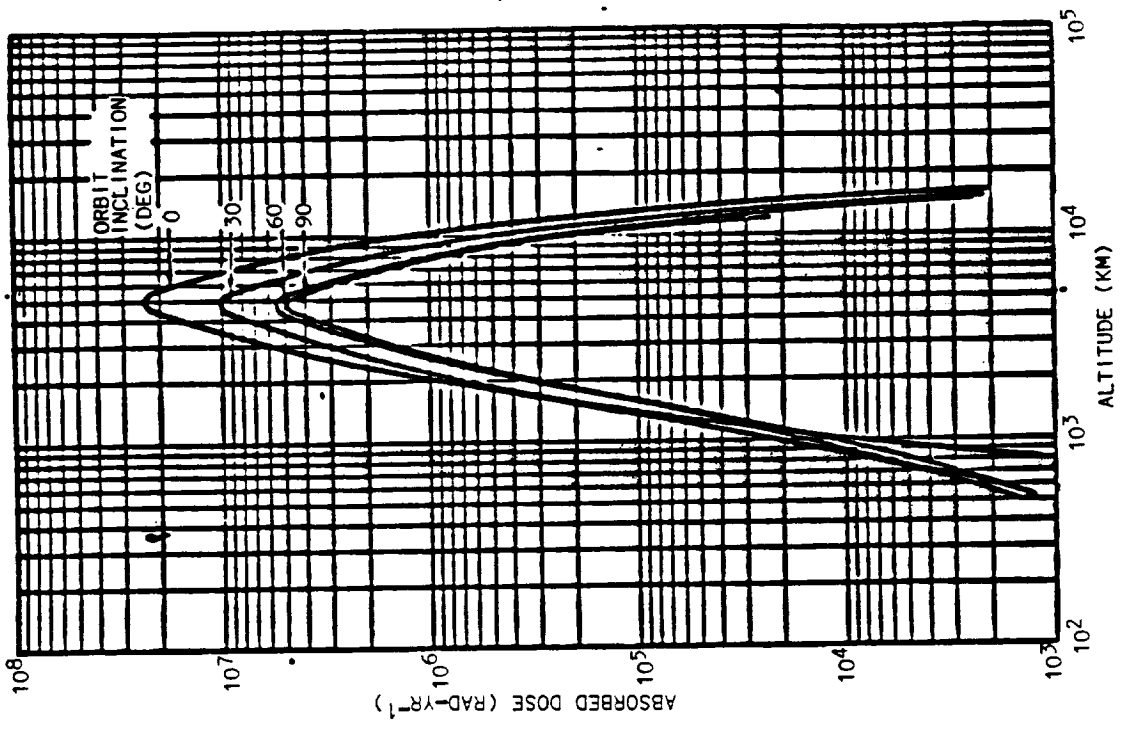
This information is approximated, using attached Figures 2.5-6 and 2.5-7 from Reference (1) (See end of this Section for reference). The ordinates are the doses deposited in solar cell glass cover slides of 0.15 mm in rads/year. From these curves one obtains radiation doses for one year for the above mentioned orbits for electrons and protons. The relative dose at this depth in aluminum to that penetrating thicker shields can be estimated from the data plotted from Table I (attached) from Reference (2). For example, a shield thickness of 130 mil reduces approximately 97% of the dose transmitted to the 5.9 mil depth.

Figure 2.5-6 gives dose in fused silica glass. However, silicon and aluminum are almost identical absorbers of fast charged particles, as they are adjacent on the periodic table. (A reference for this is Solar Cell Radiation Handbook, Third Edition, NASA/JPL, Nov. 1, 1982, P. 3-3).

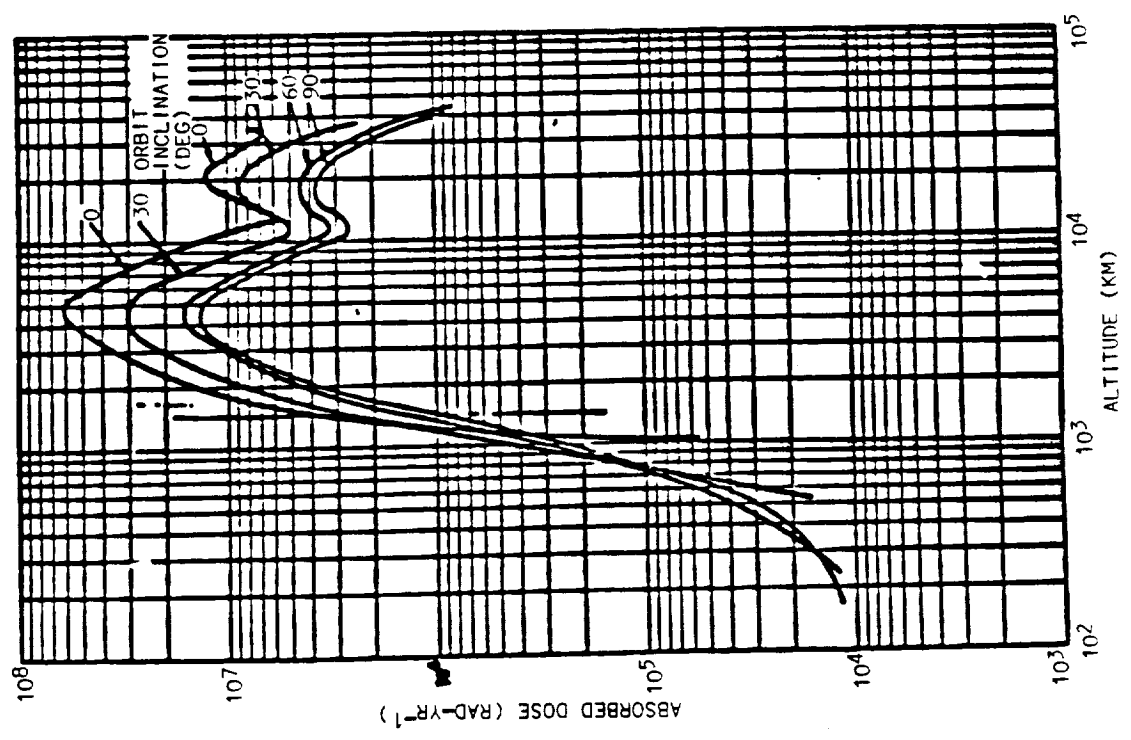
This method must be used with caution, however. Actual energy absorptions in aluminum depend on the details of the incident fluence-energy spectrum, which in turn are orbit specific. Data gathered from several sources (3), (4), (5) and summarized in Table II indicate that aluminum slabs may absorb between 95 and 99% of incident energy at a 100 mil thickness and 97-99% of incident energy at 250 mil thickness.

Taking these variabilities into account and scaling up to a 10-year mission, the radiation dose inside aluminum slabs of the thickness indicated would fall into the ranges as given in Table 3.12-1.

These results are tied to the use of the slab geometry. This geometry is utilized because the baseline data from Figure 2.5-6 of Reference (1), are for cover slides effectively receiving radiation from only one side (2-pi steradians) and because the slab geometry is probably closer to the actual geometry of a practical spacecraft.



AVERAGE ABSORBED DOSE IN 0.15-MM THICK COVERS  
IN CIRCULAR EARTH ORBITS DUE TO TRAPPED PROTONS  
(Figure 2.5-7)



AVERAGE ABSORBED DOSE IN 0.15-MM THICK COVERS  
IN CIRCULAR EARTH ORBITS DUE TO TRAPPED ELECTRONS  
(Figure 2.5-6)



TABLE 1  
 APPROXIMATE WORST CASE TOTAL DOSES<sup>1</sup> FOR 1 YEAR  
 (SOURCE: E. G. STASSINOPOULAS, NASA GSFC, 1980)

SHIELD THICKNESS (ALUMINUM)		DOSE AT TRANSMISSION SURFACE OF ALUMINUM SLAB SHIELDS <sup>2</sup>	DOSE IN SEMI-INFINITE ALUMINUM MEDIUM <sup>3</sup>	DOSE AT CENTER OF ALUMINUM SPHERES <sup>4</sup>
S gm/cm <sup>2</sup>	T (mm)			
	T			
	(mils)			
0.10	0.37	4.750E 06	6.198E 06	2.423E 07
0.20	0.74	2.287E 06	2.951E 06	1.298E 07
0.30	1.11	1.351E 06	1.730E 06	8.496E 06
0.40	1.48	8.668E 05	1.099E 06	5.953E 06
0.50	1.85	5.874E 05	7.240E 05	4.251E 06
0.80	2.96	2.399E 05	2.859E 05	1.740E 06
1.00	3.70	1.567E 05	1.815E 05	1.105E 06
1.25	4.63	1.018E 05	1.136E 05	7.195E 05
1.50	5.56	7.164E 04	7.679E 04	4.692E 05
1.75	6.48	5.546E 04	5.749E 04	3.089E 05
2.00	7.41	4.625E 04	4.701E 04	2.175E 05
2.50	9.26	3.696E 04	3.715E 04	1.397E 05
3.00	11.11	3.187E 04	3.197E 04	1.139E 05
3.50	12.96	2.800E 04	2.845E 04	9.891E 04
4.00	14.81	2.568E 04	2.580E 04	8.972E 04
5.00	18.52	2.168E 04	2.178E 04	7.806E 04
6.00	22.22	1.873E 04	1.882E 04	7.023E 04
7.00	25.93	1.642E 04	1.650E 04	6.315E 04
8.00	29.63	1.450E 04	1.458E 04	5.699E 04
10.00	37.04	1.164E 04	1.170E 04	4.676E 04

<sup>1</sup>DOSE CONTRIBUTIONS: Obtained from surface incident, integral omnidirectional, isotropic fluxes.

MODELS

Trapped Electrons : AE17-L0 for L=4.0 Earth radii  
 Bremsstrahlung : from above electrons  
 Trapped Protons : AP8 for L=1.5 Earth radii  
 Solar Flare Protons: SOLPRO - 1 Anomalously Large Event

- No Geomagnetic Shielding Applied

<sup>2</sup>Absorbed dose in a thin aluminum detector at the transmission surface of an aluminum plane slab of Thickness S. Irradiation is from one side only. (2 π steradian incidence, cosine θ distribution).

<sup>3</sup>Absorbed dose in a thin aluminum detector at Depth S in a semi-infinite plane aluminum medium. Irradiation is from one side only. (2 π steradian incidence, Cosine θ distribution).

<sup>4</sup>Absorbed dose in an aluminum detector of small volume at the center of a solid aluminum sphere of Radius S. Irradiation is from all directions.

TABLE II  
 ALUMINUM ABSORPTION OF ORBITAL CHARGED PARTICLES  
 ENERGIES FROM SELECTED REFERENCES

ORBIT	INFORMATION SOURCE	Al SKIN THICKNESS (MILS)	ESTIMATED PERCENTAGE REDUCTIONS OF INCIDENT RADIATION	
			<u>SPHERICAL GEOMETRY</u>	<u>SLAB GEOMETRY</u>
M <sup>3</sup> Unspecified 3 year LEO Orbit Mission	MMC (5)	100	98.8%	94.0%
		150	99.9%	97.2%
GRO 130- 2224 km, circular	TRW (6)	100	99.2%	96.0
		150	99.7%	98.2
GPS (19,200 km, 63° circular)	Grumman (7) Aerospace	100	99.4	96.9
		150	99.8	99.1

References:

- (1) Solar Array Design Handbook, Vol. 1, Oct. 1976, P. 2.5-9.
- (2) NASA Environmental Engineering Standards for STS Payload, Part IV Charged Particle Radiation, NASA, Oct. 14, 1981.
- (3) Data acquired from a curve of three year radiation doses in the M3S orbit supplied by customer.
- (4) Environmental Specification, Design and Test Requirements for GRO Component A, Assemblies and Models, GRO-82-235, Jan. 1982, P. 14.
- (5) From Fairchild Technical Note prepared from raw data supplied by Grumman Aerospace Company, August 1982.
- (6) E. G. Stasslinopoulos, "World Maps of Constant B, L, and Flux Contours". NASA-SP-3054, 1970.

3.12.3.2.2 Solar Cell Degradation - Based on the radiation environment noted, the predicted solar cell degradation is shown in Table 3.12-2 for the assumption noted. The substantial penalty for operations at higher altitudes are noted. This can be ameliorated by an increase in cover glass and backside shielding thickness, at the penalty of increased system mass.

TABLE 3.12-2  
SOLAR CELL DEGRADATION OVER 10 YEARS  
(RADIATION ONLY)

ORBIT	DEGRADATION FACTOR
600 km @ 28.5 degrees	0.84
800 km @ 28.5 degrees	0.755
1000 km @ 28.5 degrees	0.665
700 km @ 98 degrees	0.80
900 km @ 98 degrees	0.735

**Assumptions**

Silicon solar cells  
10 ohm-cm, 8 mils thick  
back surface field (BSF)  
dual anti-reflection (DAR) coating

back surface reflector (BSR)  
backside shielding: 30 mils equivalent  
6 mils, fused silica cover glass

### 3.12.4 Micrometeoroid Environment and Collision Probability

3.12.4.1 Discussion - As a result of the increasing numbers of orbiting objects, the probability of in-orbit collision with LDR must be considered. These questions are pertinent:

1. What is the probability of impact with a man-made orbiting body?
2. What is the probability of impact with meteroids?
3. What is the effect of such collisions?

Question 3 is not addressed here. However, a set of pertinent references is included, for its potential value, in the references list. Questions 1 and 2 are discussed in the following two sections.

3.12.4.1.1 Collisions with Man-Made Objects - Although evaluation of in-orbit collisions for specific satellites with the present known population is possible using known characteristics of individuals in that population, changes in the population make appropriate the estimation of future collisions by probability methods.

Reference (1), (see end of this section) provides such a method by assuming a uniform volumetric distribution of orbiting objects at any one altitude. The probability of impact of any single satellite with those objects during any time interval is determined by calculating the probability that any part of any orbiting objects will lie within the volume swept out during that time interval by the single satellite of interest.

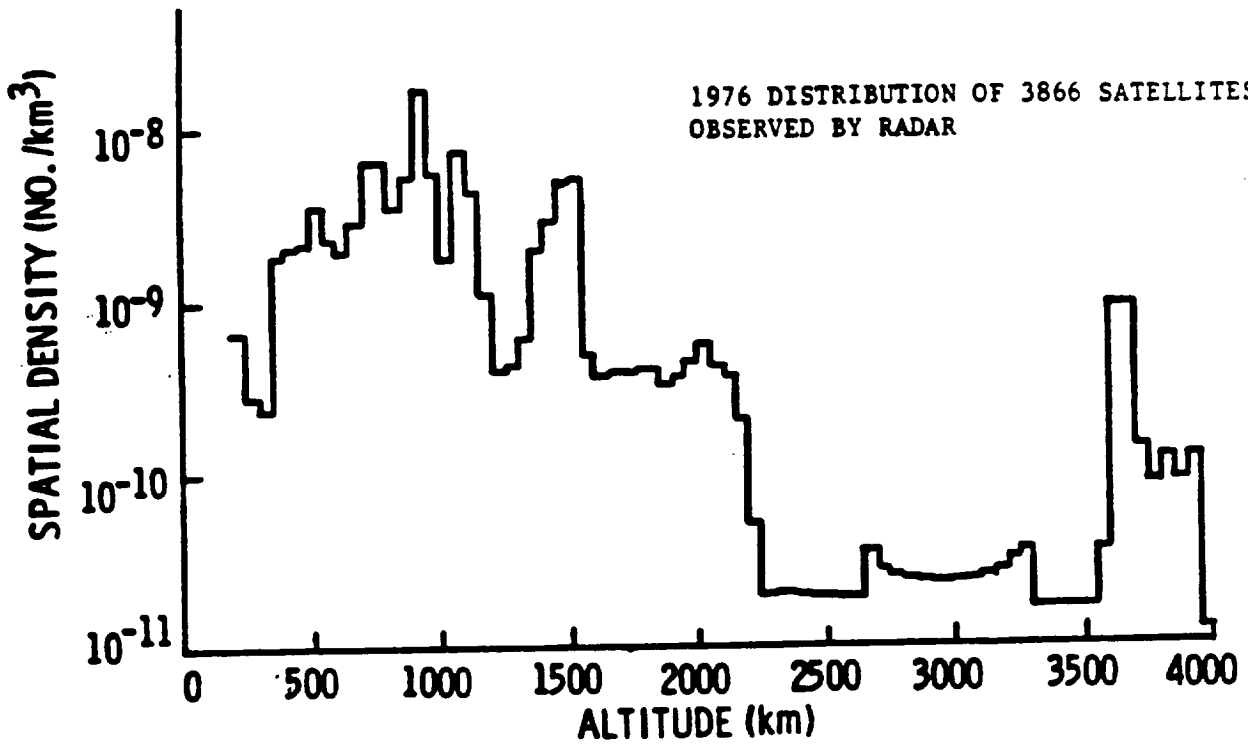
The question equivalent to that statement is:

$$dI/dt=S*V*A \tag{1}$$

Where

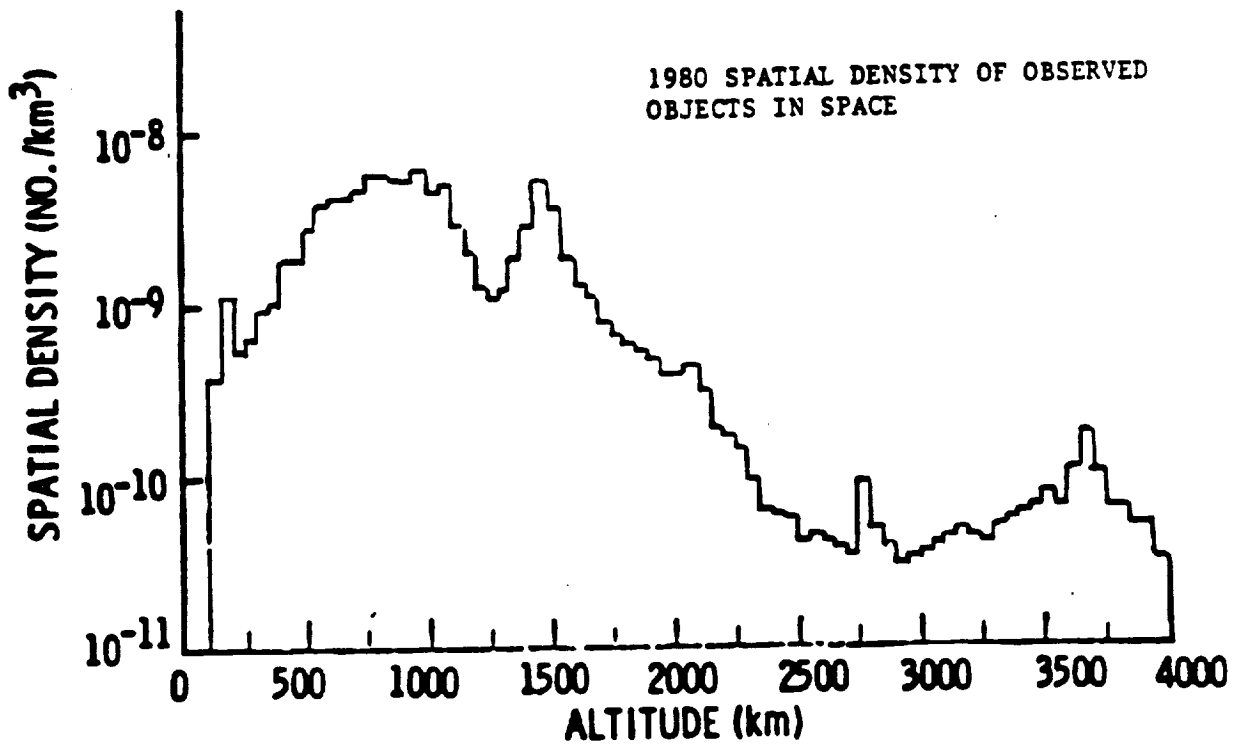
S is the spatial (volumetric) density of the orbiting population at the altitude of the object of interest, V is the mean velocity of the object of interest relative to the neighboring orbiting population, A is the possible collision area.

The spatial density has increased rapidly since the initial orbiting of man-made objects. Figures 3.12-4 and 3.12-5 are indicative of the change (primarily maintenance of relative density) as a function of altitude. Estimates of future densities are speculative at best. In the late 1960's, the rate of increase was about 15% per year; in the 1970's the rate of increase was about 10% per year. Equation (1) shows that the rates of importance in collision estimation are collisional area rates.



SOURCE: REF. 1

Figure 3.12-4



SOURCE: REF. 2

Figure 3.12-5

Radar measurements were used by Reference (1) to determine the 1976 distribution of areas (greater than 0.001 square meter) shown in Figure 3.12-6. No distribution of areal distribution with altitude is indicated; we assume, as does Reference (1), the distribution is independent of altitude and invariant with time, even though the advent of the Space Shuttle will almost undoubtedly mean the launching of relatively larger satellites in the future than in the past.

Here, we present predictions based upon geometric annual rates (5%, 10%, 15%) of increase of total area as well as arithmetic increases or multiples (1X, 2X, 3X) of Shuttle Bay cross-sectional area (15 ft x 60 ft). Twenty Shuttle launches per year are postulated.

Based upon the observed persistence of the relative density with altitude, we assume future persistence and use Figure 3.12-5 as the prototype relation.

Collisional areas may be estimated by assuming all bodies as spherical, thereby obtaining collision when the distance between centers of the two bodies is less than the sum of their radii.

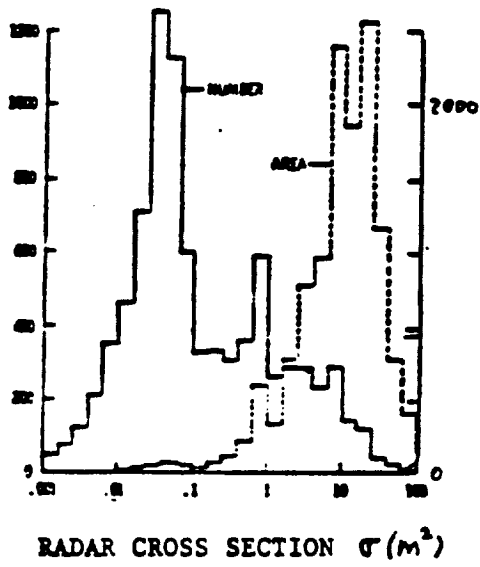
Evaluation of mean relative velocity  $V$  was made by Reference (1) by averaging the results obtained using a random sample of the 1976 population.  $V$  was evaluated to be 7 Km/sec. Also obtained was the mean collisional velocity which, at 10 Km/sec differs from, and is higher than, the mean relative velocity because objects with higher velocities sweep out more volume per unit time and are, therefore, more likely to collide with the resident population than a body with the mean relative velocity.

Evaluation of expected total impacts as a function of future dates has been made by integrating equation (1) and using the conditions of April 1976: total objects (with significant areas) in orbit, 3866; total area in orbit, 5480 square meters. The altitude of the LDR will be in the range of 600 to 1000 km, the region of maximum spatial density. For calculational purposes, 800 km altitude was assumed, although the results would apply to any altitude in the 600-to-1000 km range.

With geometric and arithmetic rates of increase per year as parameters, Figure 3.12-7 indicates projected area in space and Figures 3.12-8a, b indicate impacts expected by the LDR over time. Figure 3.12-8a assumes that the total spacecraft area is dominated by the primary reflector area. Figure 3.12-8b assumes a solar array of equivalent size, as could occur if spacecraft orbit average power is in the range of 15 kilowatts.

It should be explicitly noted that extremely large areas are projected:  $10E6$  meters is equivalent to a square more than one-half mile on a side. Twenty Shuttle flights a year, each delivering 900 square feet, increase the area by more than 1600 square meters each year.

NUMBER OF OBJECTS TRACKED WITH CROSS SECTIONS  
BETWEEN  $1\sigma$  AND  $1.58\sigma$

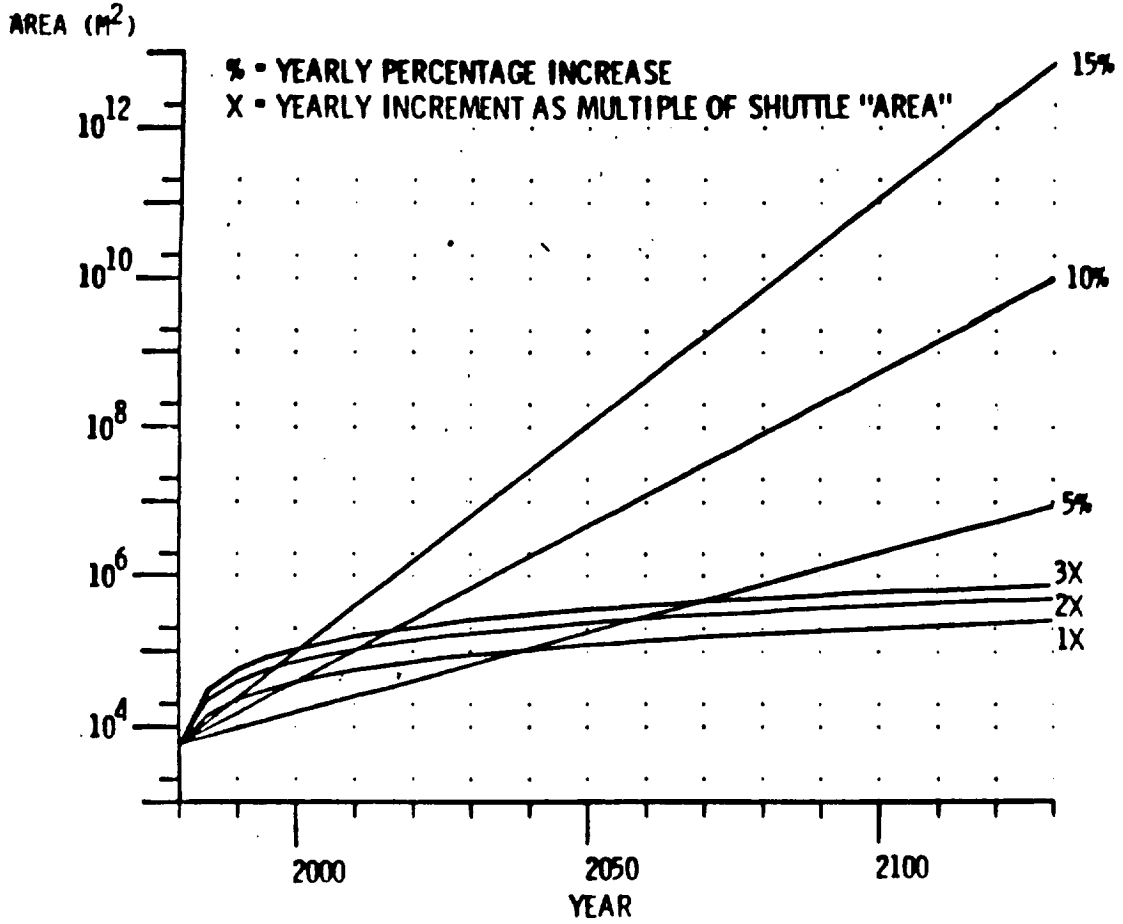


TOTAL AREAS  $m^2$  WITH INDIVIDUAL AREAS  
AREAS BETWEEN  $1\sigma$  AND  $1.58\sigma$

SIZE DISTRIBUTION OF EARTH ORBITING SATELLITES

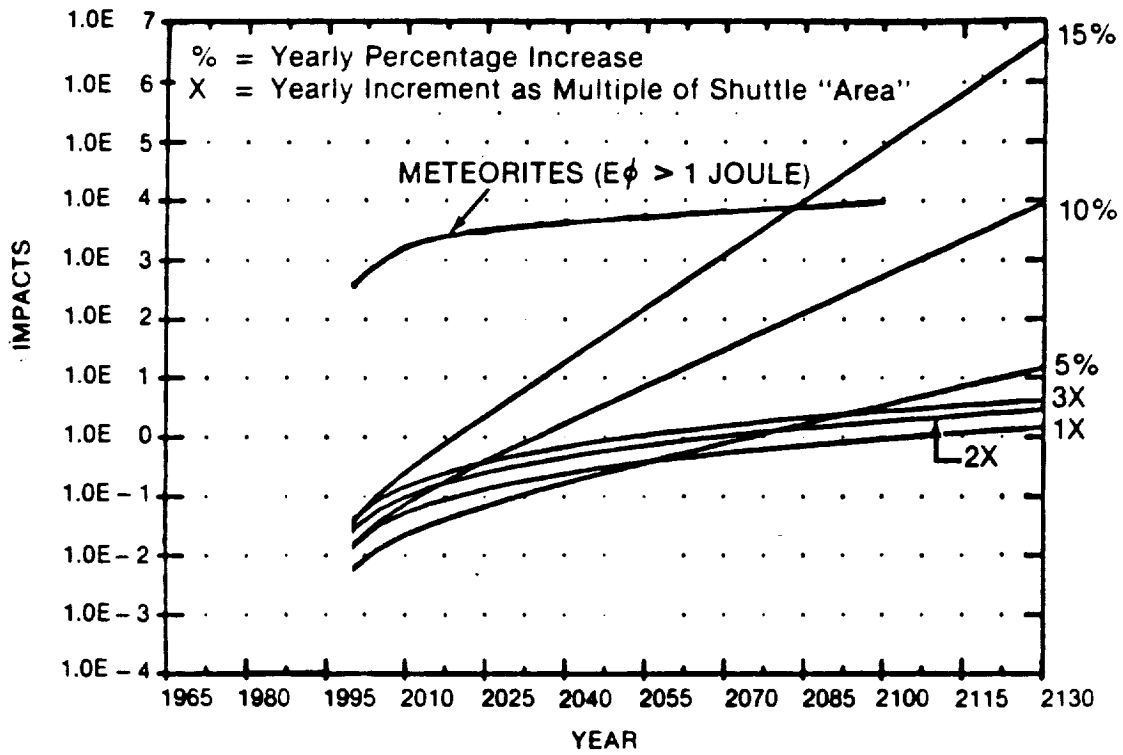
Figure 3.12-6





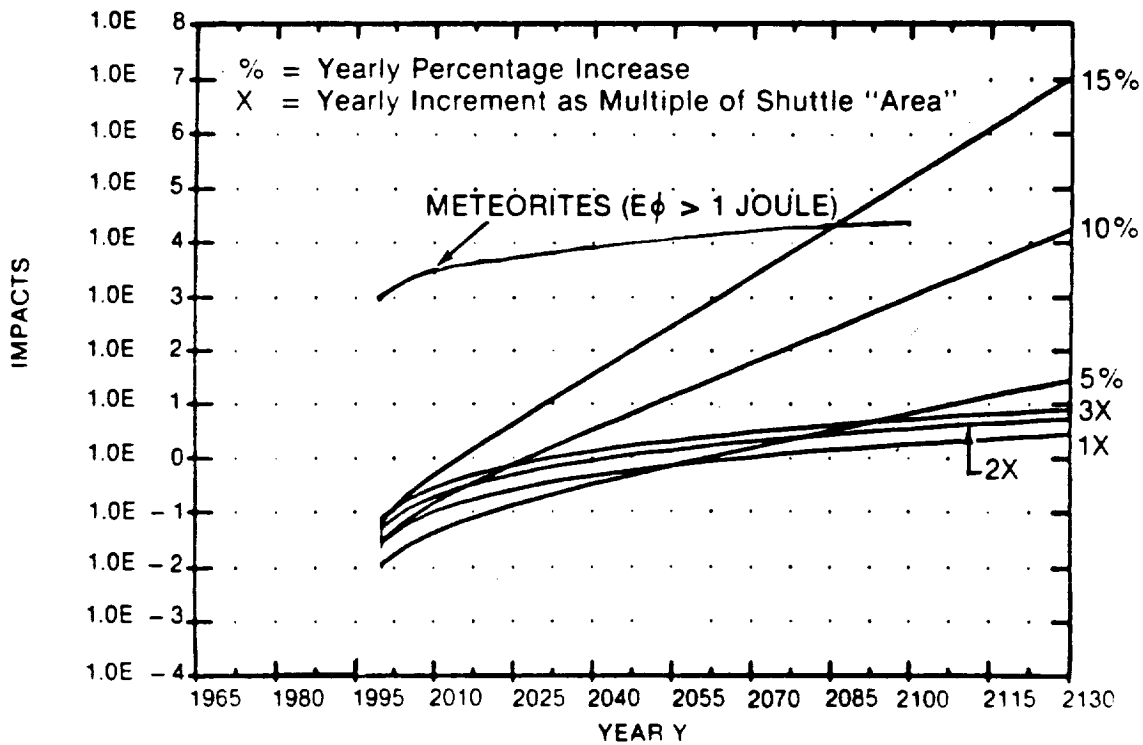
TOTAL AREA OF SATELLITES IN SPACE

Figure 3.12-7



IMPACTS EXPECTED BY YEAR AT 800KM, 1995 LAUNCH AREA = 300 M<sup>2</sup>

Figure 3.12-8A



IMPACTS EXPECTED BY YEAR AT 800KM, 1995 LAUNCH AREA = 600 M<sup>2</sup>

Figure 3.12-8B

The calculations yielding Figures 3.12-7 and 3.12-8, the area and impact curves, do not take into account area increases due to impacts between any two bodies already in space. Such impacts often result in bodies with smaller linear dimensions than the parent bodies. Ground testing to date has primarily been concerned with the hypervelocity impact of small bodies with large solids, either metals or rock. Impact under these conditions can result in a large number of smaller bodies; resultant areas have not been a concern in these experiments. Impacts between orbiting bodies with large areas are more likely to be impacts between "thin" surfaces such as solar arrays rather than between "solid" bodies with all dimensions large. If the surface thickness is near the smallest linear dimension of the resultant bodies, hardly any increase in area will occur. Even the break-up of a sphere into N spheres results at most in increasing the area by a factor of the cube root of N over the original area. But the total area permitting collision has increased with N because the collisional area depends upon the dimensions of both impacting areas and the total number of areas available for impact. As an example, consider the collisional area for two spheres, one with radius  $R_0$ , the other with radius  $R_1$ .

The collisional area is  $\pi (R_0 + R_1)^2$ . Let the sphere with radius  $R_0$  be broken into N equal spheres, each with radius  $R_0/N^{1/3}$ .

The total collisional area of the intact and split sphere's parts is now  $N\pi (R_1 + R_0/N^{1/3})^2$ .  $R_1$  is small compared to  $R_0$ , the new collisional area is approximately  $\pi R_0^2 N^{1/3}$  modest increase; if  $R_1$  is large compared to  $R_0$ , the new collisional area is approximately  $N\pi R_1^2$ , a large increase. Thus,

although it can be expected that the areal increase of the impactable bodies will not be large, nor will the total impacting bodies be involved in the collision, there will be a large increase in the total collisional area due to the large increase in the number of particles.

3.12.4.1.2 Collisions With Meteoroids - The meteoroid environment for LDR is noted in Reference (6) and is repeated here in Table 3.12-3. For convenience, Reference (6)'s penetration formulas for high velocity particles are reproduced in Figure 3.12-9.

TABLE 3.12-3  
METEROID ENVIRONMENT

ITEM	Units	Design Value
Particle Density	g/cm	0.59
Particle Velocity	km/sec	20.0

Notes:

1. Flux mass models: for  $10E-6 \leq M \leq 10E 0$   
 $\text{Log Nt} = 14.37 - 1.213 \text{ Log N.}$   
for  $10E-12 < M < 10E-6$   
 $\text{Log Nt} = 14.399 - 1.584 \text{ Log M} - 0.63 (\text{Log M})^2$
2. M = mass in grams
3. Nt = number of particles of mass M per meter squared per second

Meteoroid velocities range from about 10 Km/sec to about 70 Km/sec; Reference (6) uses 20 Km/sec as its design value. With this velocity assumed, Figure 3.12-10 shows the cumulative impacts on LDR per year over the range of meteorite masses (hence kinetic energies).

3.12.4.1.3 Conclusions - With these considerations and uncertainties in mind it may reasonably be concluded that for radar-observable particles, within twenty-five years after a 1995 launch, there will be about a one-in-ten chance of collision involving a  $300 \text{ m}^2$  LDR with a man-made orbiting object and a one in seven chance for a  $600 \text{ m}^2$  LDR with a man-made orbiting object. Radical changes in number of particles at the altitude of LDR due to collision of other in-orbit bodies could increase these estimates sharply. Estimates of on-orbit areas as illustrated in Figure 3.12-7 over much longer periods are so unreliable as to be worthless.

Impacts with micrometeoroids of low mass will be frequent and essentially continuous. However, there will be a high probability of one impact per year with a particle of energy greater than 100 joules for an LDR of deployed area =  $600 \text{ m}^2$ .

Three formulas were found for high velocity particle depth of penetration; one from JPL based on the Brinell hardness of the material being penetrated and the others from NASA based on the penetrated material percent elongation or the meteoroid mass. They are as follows:

JPL

$$t \text{ (cm)} = \frac{2.48 \times P_m^{1/2} V_m^{2/3} D_m^{1.06}}{P_t^{1/6} H_t^{1/4}}$$

- D<sub>m</sub> = meteoroid diameter, cm
- P<sub>m</sub> = meteoroid density, g/cc
- P<sub>t</sub> = sheet density, g/cc
- H<sub>t</sub> = sheet Brinell Hardness
- V = relative velocity in Km/sec

NASA E

$$t \text{ (cm)} = 0.65 (P_m/P_t)^{1/2} V_m^{7/8} D_m^{19/18} / E_t^{1/8}$$

E<sub>t</sub> = sheet % elongation

NASA M

	K	Al	Sst
t (cm) = K M <sub>m</sub> <sup>0.351</sup> P <sub>m</sub> <sup>1/6</sup> V <sub>m</sub> <sup>2/3</sup> infinite solid	0.42		0.25
t (cm) = K M <sub>m</sub> <sup>0.352</sup> P <sub>m</sub> <sup>1/8</sup> V <sub>m</sub> <sup>0.875</sup> thin ductile plate	0.57		0.38

M<sub>m</sub> = Meteoroid mass, grams

PENETRATION FORMULAS

Figure 3.12-9

IMPACTS PER YEAR ON LDR BY METEORITES  
 WITH ENERGY GREATER THAN  $E_0$   
 as a function of  
 LDR MIRROR DISC AREA

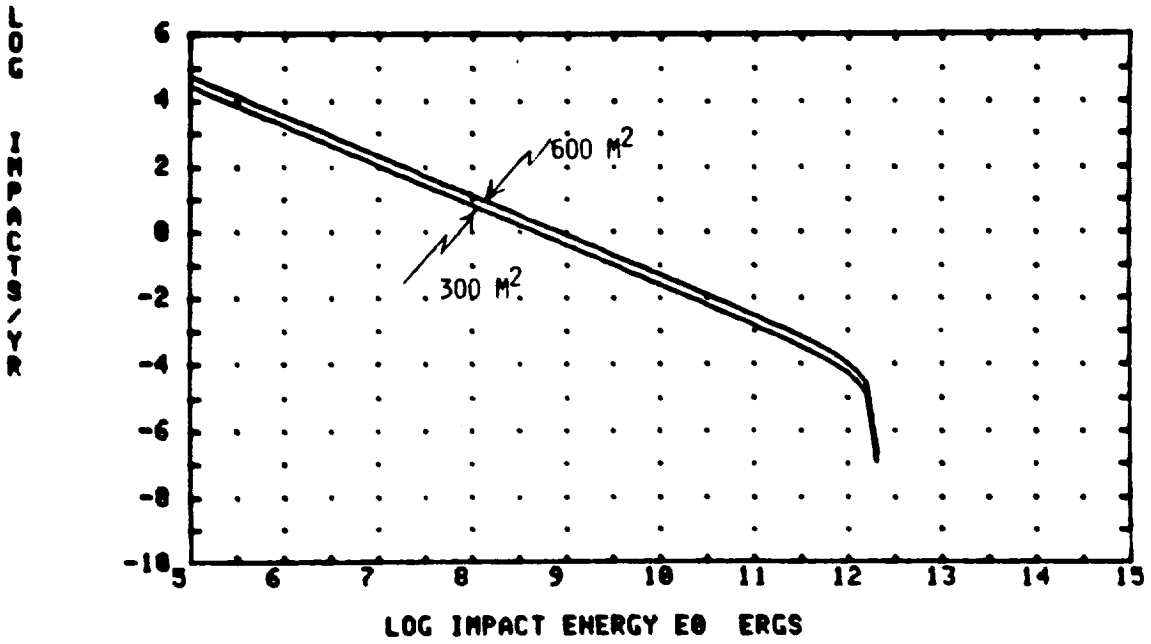


Figure 3.12-10

## References

1. Kessler, Donald J. and Cour-Palais, Burton G. (1970). "Collision Frequency of Artificial Satellites: The Creation of a Debris Belt." *Journal of Geophysical Research*. Vol. 83, No. A6 June 1, 1978.
2. Chobotov, V.A. (1981). "Collision Hazard in Space." The Aerospace Corporation Report TR-0081, February 1961.
3. Blanco, V.M, and McCuskey, S.W., "Basic Physics of the Solar System." Addison-Wesley Publication Company, Reading, Mass.
4. Fujiwara, A., Kamemoto, G., and Tsukamoto, A. (1977). "Destruction of Basaltic Boxes by High-Velocity Impact." *Icarus*. 31, 277-288 (1977).
5. Jaffe, L.D. and Rittenhouse, J.B. "Behavior of Materials in Space Environments." Technical Report #32-150. Jet Propulsion Lab, Pasadena, California, Nov 1, 1961.
6. "SLD Trade Study, Impact of Meteoroid Criteria on Reaction Control Subsystem." Date 23 September 1981. No. SSD-D-SD018, Naval Research Laboratory, 455 Overlook Ave. S. W. Washington, D.C.
7. Wolfe, M., Chobotov, V., Kessler, D., and Reynolds, R. "Man-made Space Debris - Does it Restrict Free Access to Space?" AIAA-81-256.

### 3.13 SPACECRAFT FUNCTIONS (FSC)

#### 3.13.1 Task

The objective of this task was to first define the current envelope of spacecraft performance that is available for LDR; then to assess which elements can be reasonably expected to be improved or could be improved at a reasonable cost in order to enable LDR system options.

#### 3.13.2 Approach

Based on inputs in terms of overall optical system design, size, and power requirements, the basic requirements on spacecraft subsystems were derived. Straightforward analytical tools of Newtonian mechanics were applied for the derivation of attitude control and propulsion requirements.

Spacecraft power requirements were estimated from the derived attitude control requirements, from the input payload power requirements, and from the estimated return-link data transmission requirement. Other subsystem power requirements were estimated from experience with similar systems.

Spacecraft data system requirements were assumed to be satisfied by the NASA standard telemetry command and communications (STACC) components, as embodied in the NASA standard Communication and Data Handling (C&DH) module, with power added to accommodate a maximum data return link rate of 3 Mbps.

#### 3.13.3 Attitude Control; Momentum Storage and Torquing

3.13.3.1 Discussion - Angular momentum storage magnitude requirements are set by the requirements to store the integrated torques of the external environment and/or the slew torques. Torque capability must be adequate to counter external torques and, for slew, be large enough to utilize the requisite angular momentum in times short compared to the total slew times.

For the purpose of establishing the basic order of magnitude of the requirements, the following input information for observatory moments of inertia was used:

$$I_{\text{boresight axis}} = 6 \times 10^5 \text{ kg-m}^2 = (4.43 \times 10^5 \text{ slug ft.}^2)$$

$$I_{\text{lateral axes}} = 8 \times 10^5 \text{ kg-m}^2 = (5.90 \times 10^5 \text{ slug-ft.}^2)$$



3.13.3.1.1 Inertial Hold; Storage and Torque Requirements - At the operational altitudes of interest (700 km and higher) aerodynamic torques are small and gravity gradient torques dominate over all other environmental torques. For inertially fixed orientation spacecraft the maximum gravity gradient torques (Tmax), maximum cyclic accumulated angular momentum (Hmaxcyc) and angular momentum accumulation (Hmaxacc) over a single orbit are:

$$\begin{aligned} T_{\max} &= 3/2 W_o (\Delta I_{\max} W_o) \\ H_{\max\text{cyc}} &= 3/4 (\Delta I_{\max} W_o) \\ H_{\max\text{acc}} &= (3/2)\pi (\Delta I_{\max} W_o) \end{aligned}$$

where  $W_o$  = orbital rate  
 $\Delta I_{\max}$  = maximum principal axis moment of inertia (MOI) difference

Therefore, for the assumed moments of inertia, at 700 km where  $W_o = 1.06 \times 10^{-2}$  rad/sec:

$$\begin{aligned} T_{\max} &= 0.25 \text{ ft-lb} \\ H_{\max\text{cyc}} &= 117 \text{ ft-lb-sec} \\ H_{\max\text{acc}} &= 734 \text{ ft-lb-sec} \end{aligned}$$

The accumulating angular momentum must be unloaded -- propellant expulsion and magnetic torquing against the earth's field are the usual techniques. Assuming only the latter is acceptable, storage for approximately half an orbit's accumulation may be accomplished by torquer bars with per axis dipole magnitudes of 85,000 Am (2). Torquer bars of this magnitude may be readily implemented.

3.13.3.1.2 Slew Requirements - Observatory slew is required between target viewings to acquire new targets and to avoid regions of exclusion for heating or brightness reasons. Figures 3.13-1,-2,-3, indicate potential boundaries of sun and earth exclusion regions. Maximum potential continuous viewing of a single target is shown as occurring over 140 degrees of Observatory orbital motion or 38.3 minutes of time. Total time between target observations, which is comprised of slew time and settling time, should be minimized. Because LDR's line of sight is roughly on the target during the settling time, some of the potential viewing time (38.3 minutes) must be lost if the exclusion limits are to be considered inviolate. (Image motion compensation in LDR will reduce or eliminate this loss).

**BOUNDARIES OF EXCLUDED REGIONS FOR S/C LOS WITH**

**EARTH AVOIDANCE ANGLE (DEG) = 45**

**SUN AVOIDANCE ANGLE (DEG) = 60**

**WITH S/C ORBIT ANGLE AS PARAMETER**

**ORBIT ALTITUDE (KM) = 700**

**LATITUDE IS ANGLE ABOVE ORBIT PLANE**

**LONGITUDE IS ANGLE IN ORBIT PLANE MEASURED FROM ORBIT NOON**

**SUN IS AT 0 DEG LONGITUDE AND LATITUDE (DEG) = 0**

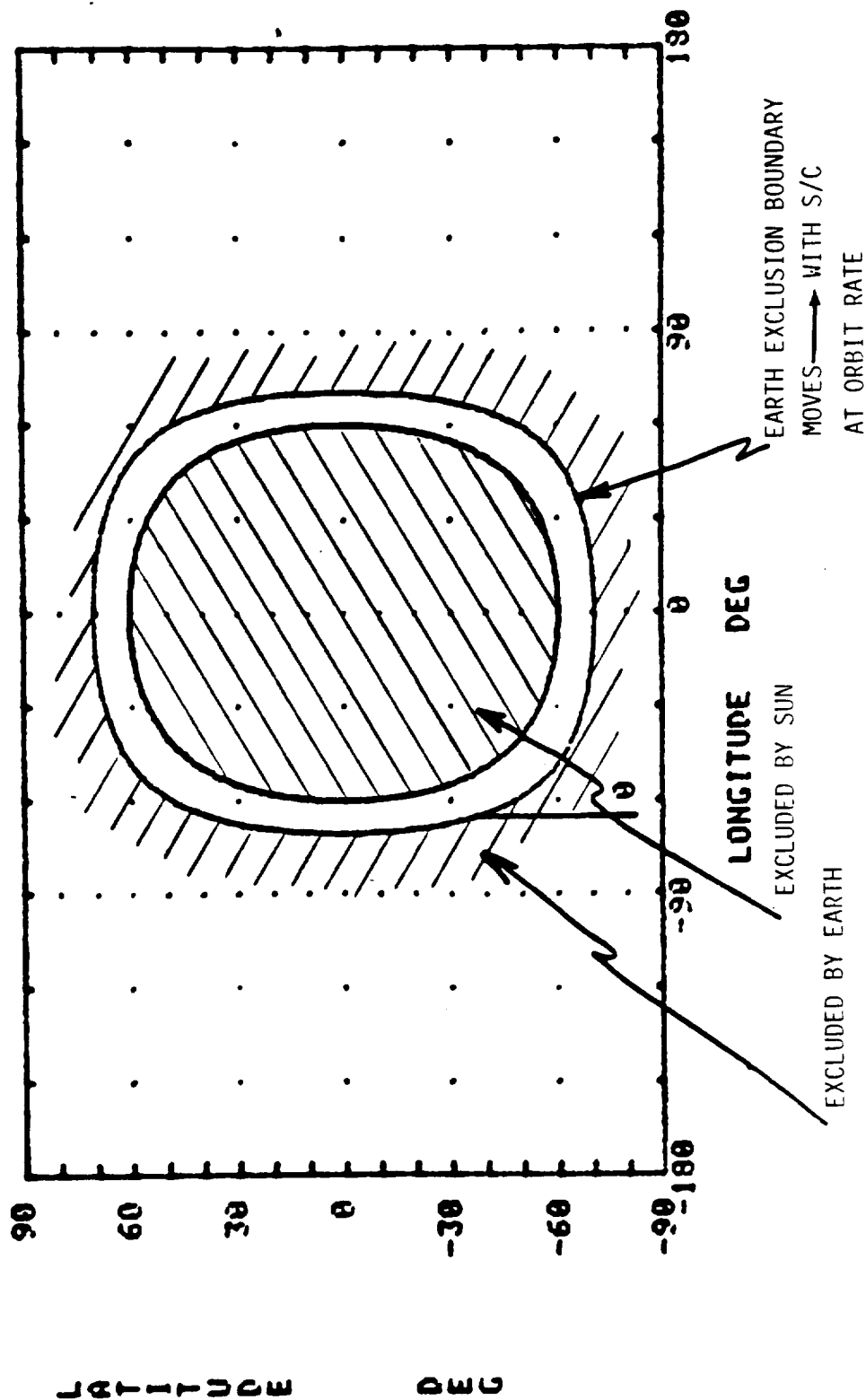


Figure 3.13-1

**BOUNDARIES OF EXCLUDED REGIONS FOR S/C LOS WITH**  
**EARTH AVOIDANCE ANGLE (DEG) = 45**  
**SUN AVOIDANCE ANGLE (DEG) = 60**  
**WITH S/C ORBIT ANGLE AS PARAMETER**  
**ORBIT ALTITUDE (KM) = 700**  
**LATITUDE IS ANGLE ABOVE ORBIT PLANE**  
**LONGITUDE IS ANGLE IN ORBIT PLANE MEASURED FROM ORBIT NOON**  
**SUN IS AT 0 DEG LONGITUDE AND LATITUDE (DEG) = -26**

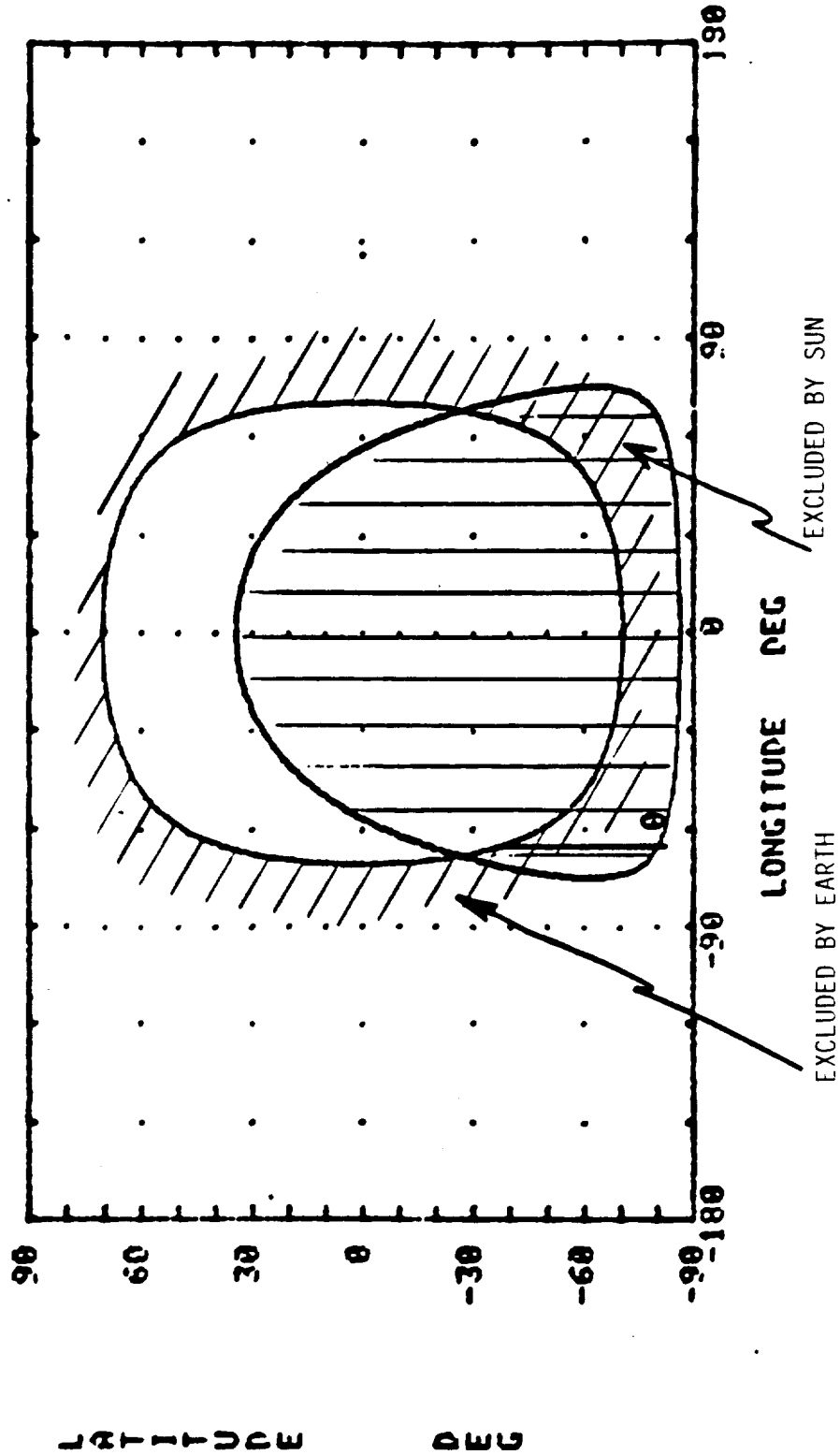


Figure 3.13-2

**BOUNDARIES OF EXCLUDED REGIONS FOR S/C LOS WITH**

**EARTH AVOIDANCE ANGLE (DEG) = 43**

**SUN AVOIDANCE ANGLE (DEG) = 68**

**WITH S/C ORBIT ANGLE AS PARAMETER**

**ORBIT ALTITUDE (KM) = 700**

**LATITUDE IS ANGLE ABOVE ORBIT PLANE**

**LONGITUDE IS ANGLE IN ORBIT PLANE MEASURED FROM ORBIT NOON**

**SUN IS AT  $\theta$  DEG LONGITUDE AND LATITUDE (DEG) = -52**

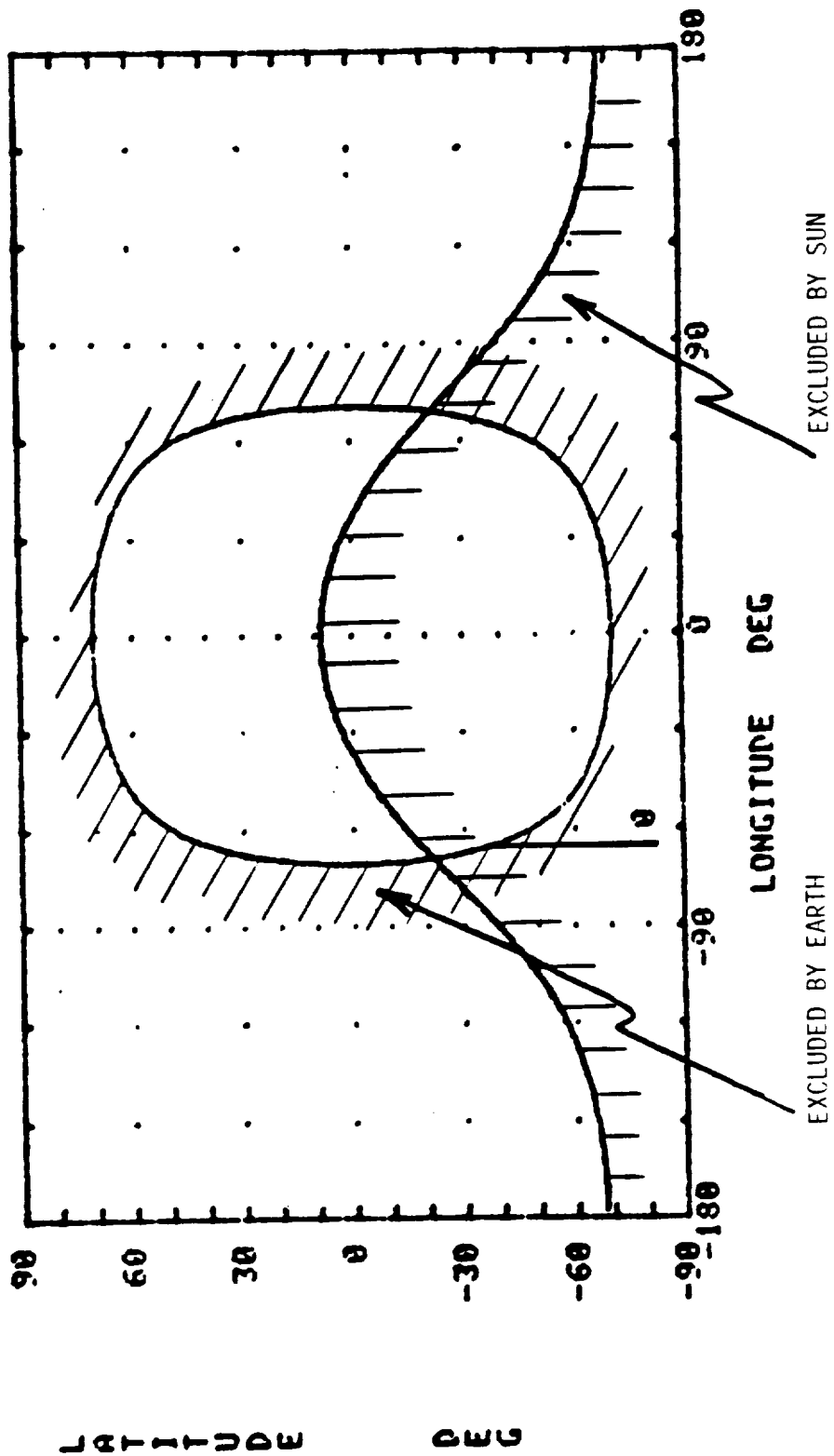


Figure 3.13-3

Figure 3.13-4 shows the relation between slew torque and time, with control angular momentum as parameter. The slew is achieved by maximum torque for acceleration. If maximum rate is reached, drift at maximum speed follows. Then, deceleration at maximum torque follows until the rate is nulled. The reductions in slew times achievable by raising the torque level above 100 ft-lb are small, so that 100 ft-lb appears to be a reasonable maximum torque requirement. Angular momentum availability should be as large as possible, possibly in the range of 5000 to 6000 ft-lb-sec.

3.13.3.2 Results

3.13.3.2.1 Requirements - The results for 180-degree slews are illustrated in Figure 3.12-5. Total requirements are summarized below:

MODE	ANGULAR MOMENTUM (ft-lb-sec)	TORQUE (ft-lb)
Slew	3000 - 6000	100
Gravity Gradient	370	0.25
Total	3370 -6370	100*

\* Resolution on torque depends upon the control scheme; a control capability of levels below 0.01 ft-lb would be desirable.

3.13.3.2.2 Alternative Angular Momentum Configurations - Two generic configurations may be considered: those using double-gimballed control moment gyros (DCMG) and those using single-gimballed control moment gyros (SCMG).

DCMG Configurations

Figure 3.13-6 depicts the three DCMG configuration used on Skylab. All units are alike: two DCMGs are adequate for the torquing function and the third is a redundant unit. Using two DCMGs over 3000 ft-lb-sec of angular momentum, capability is available for slew about all axes. LDR requirements are primarily about axes normal to the boresight so that increased capability can be obtained by some rearrangement of the DCMGs. Characteristics of the Skylab DCMG are given in Table 3.13-1.

**180 DEGREE SLEW TIME FOR LDR AS FUNCTION OF SLEW TORQUE  
 WITH SLEW ANGULAR MOMENTUM H AS PARAMETER  
 SLEW MOMENT OF INERTIA (SLUG FT<sup>2</sup>) = 443888**

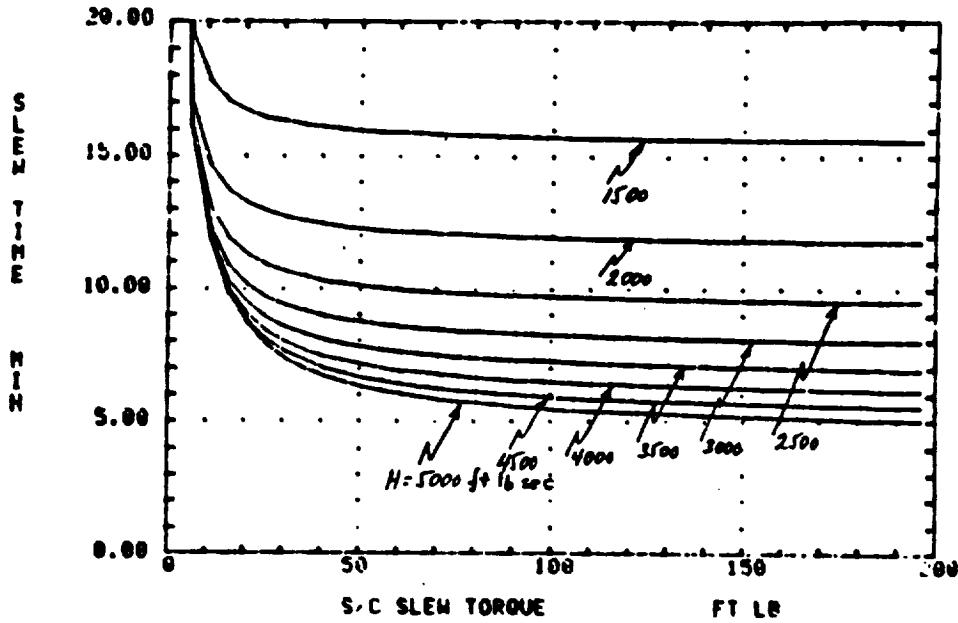


Figure 3.13-4

**180 DEGREE SLEW TIME FOR LDR AS FUNCTION OF SLEW TORQUE  
 WITH SLEW ANGULAR MOMENTUM H AS PARAMETER  
 SLEW MOMENT OF INERTIA (SLUG FT<sup>2</sup>) = 701000**

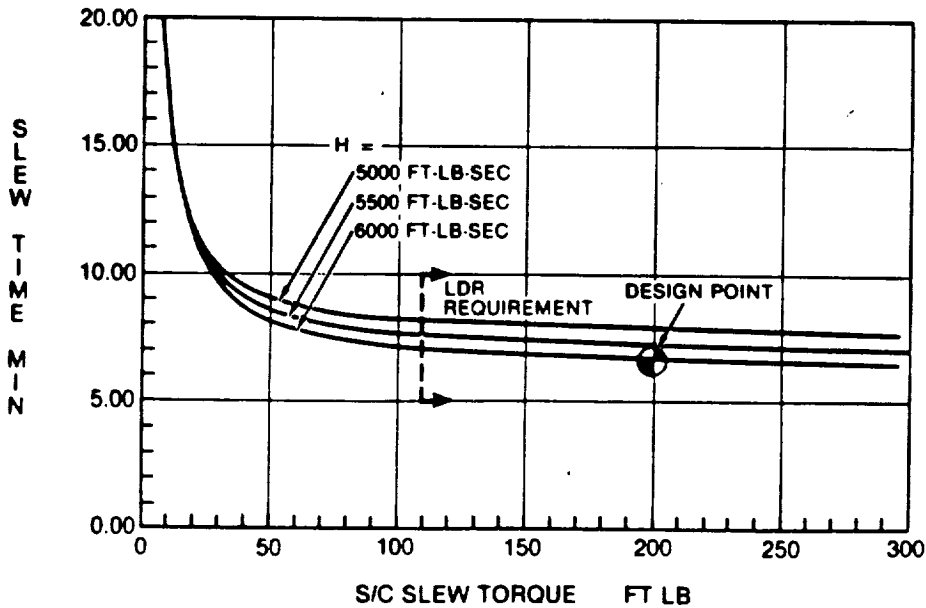
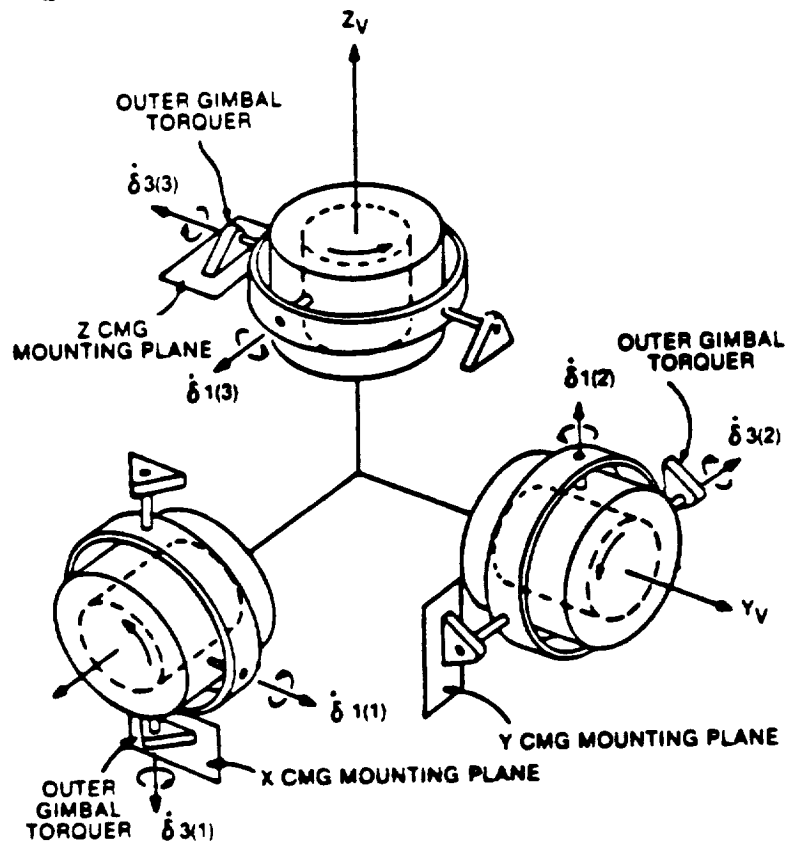


Figure 3.13-5



CMG CLUSTER  
Figure 3.13-6

TABLE 3.13-1  
CHARACTERISTICS OF REPRESENTATIVE CONTROL MOMENT GYROS  
(SOURCE: BENDIX CORPORATION)

MODEL	WEIGHT (KG)	ROTOR SPEED (RPM)	ANGULAR MOMENTUM (KG M <sup>2</sup> /S)	MAXIMUM OUTPUT TORQUE (N M)	GIMBAL FREEDOM (DEG)	MAXIMUM GIMBAL RATE (DEG/SEC)	APPROXIMATE SIZE
BENDIX DOUBLE GIMBAL MA-2000	253	4,000 TO 12,000	1400-4100	237	UNLIMITED	5 30	1.1 M DIA. SPHERE
BENDIX DOUBLE GIMBAL MA-2300 FOR SKYLAB	190	9,000	3100	165	$\pm 80$ $\pm 175$	4 7	1.0 M DIA. SPHERE
BENDIX SINGLE GIMBAL MA-500 AC	66	7,850	340-1000	680	: 170	57.3	CYLINDER 0.51 M DIAM X 0.81 M LONG
BENDIX SINGLE GIMBAL MA-5-100-1	17	8,000	7	140	UNLIMITED	1146	CYLINDER 0.25 M DIAM X 0.25 M LONG

## SCMG Configuration

Figure 3.13-7 depicts a four SCMG configuration, all units alike, which may be used by LDR. The control law for this approach is simple but there is no redundancy unless three SCMGs are adequate for slew (3000 ft-lb-sec), i.e., each SCMG with about 1200 ft-lb-sec.

Redundancy, with smaller SCMG size, can be obtained by using arrangements with six SCMGs similar to that of Figure 3.13-7. One arrangement would place one additional SCMG's gimbal axis along the Z axis and one additional SCMG's gimbal axis along the X axis and one additional SCMG's gimbal axis along the Y axis. An alternate arrangement has gimbal axes of all six SCMGs with orientations normal to the non-base sides of a six-similar-sided pyramid with hexagonal base. 750 ft-lb-sec SCMGs would probably be adequate with either of these six unit configurations.

### 3.13.4 Spacecraft Power

3.13.4.1 Discussion - Overall spacecraft power requirements were estimated based on the early estimate of payload power requirements summarized in Table 3.13-2.

TABLE 3.13-2  
PAYLOAD POWER REQUIREMENTS

---

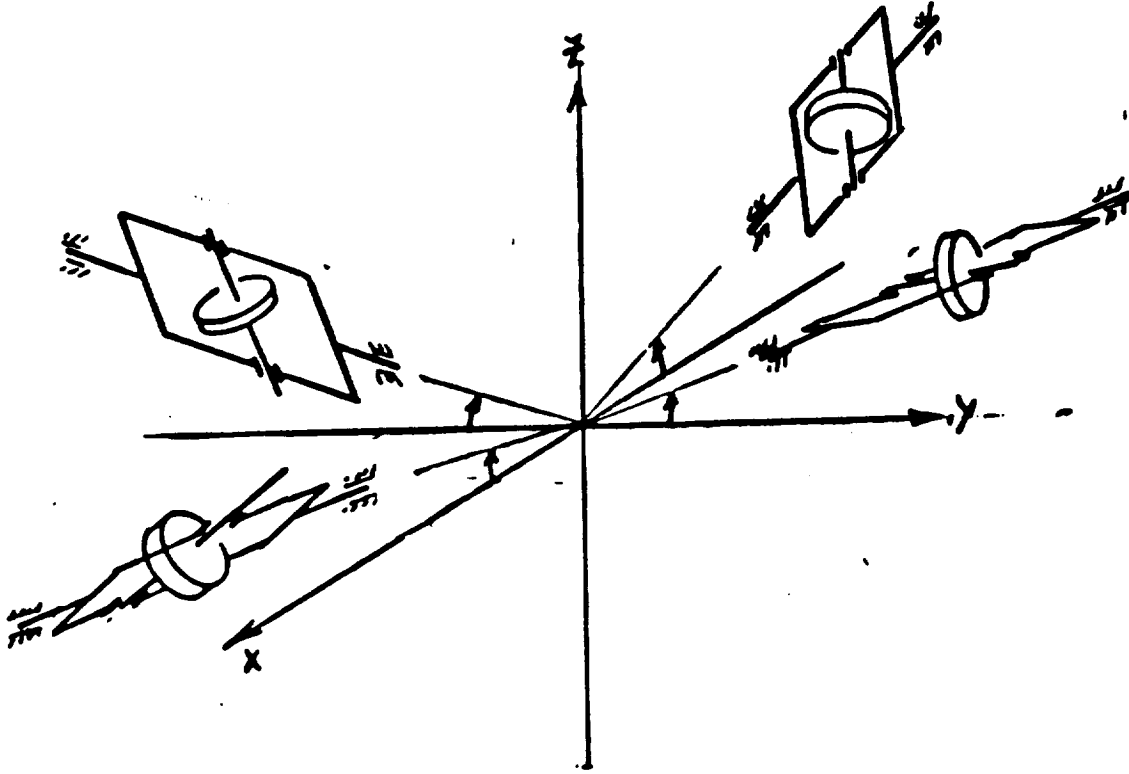
Cryo System	1500W
Thermal	250W
Mechanisms	100W
Control	100W
Instrumentation	50W
Scientific Inst.	300W
Deployment Mechs.	500W
(In't Load)	
Total	<u>2800W</u>

---

Based on this requirement, a Leasecraft platform with three power modules (NASA-Standard Module Power Subsystems) was postulated.

The two conditions of interest are: slewing periods, and periods of data acquisition. For the latter, continuous operation of the 20-watt RF amplifier was assumed. This provides adequate link margin for a 3 Mbps transmission rate through TDRSS, assuming a 4-foot diameter antenna on the spacecraft.





CONFIGURATION OF SINGLE GIMBAL CMGs

Figure 3.13-7

In order to estimate the slew power requirement for the two gimbal/CMG configurations discussed above, the following conditions apply:

1. Double-Gimbal CMG (Based on Bendix unit MA 2300)

Quiescent power = 80 w/unit  
Incremental power when both gimbals deliver 122 ft-lb = 170w  
LDR requirement = 200/3 ft-lb (torquing)  
+ 40 ft-lb (for bucking WxH)  
= 110 ft-lb (max s/c rate = 0.52 rad/sec)  
Estimated gimbal power = 110/122 x 170 = 153 w  
Total power/CMG when slew torquing = 80 + 153 = 223 w  
Total set power when slew torquing = 3(223) = 669 W  
Estimated control power/CMG = 20 w  
Total set power during normal operations = 3(80 + 20) = 300 w

2. Single-Gimbal CMG  
(Based on Sperry Unit M1300)

Quiescent power = 50 w/unit  
Power at max torque (2200 ft-lb) = 700 w  
  
Peak gimbal rate (estimated) = 1/4 rad/sec  
Resultant peak torque = 1/4 x 1300 = 325 ft-lb  
Estimated power/unit = 325/2200 x 700 = 103 w  
  
Total set power when slewing = 6 x 103 = 618w  
Total set power during normal operations = 6 x 50 = 300w

(Power increment above quiescent for normal operations = 0.)

Thus, the power estimates for the two approaches are quite close, since the Bendix units are the relatively inefficient AC-driven Skylab units. The Sperry units are DC-driven and are of more recent vintage.

3.13.4.2 Results - The overall results are summarized in Table 3.13-3. Additional payload power may be produced in increments of roughly 1600 watts by adding power modules and 400 square-foot solar array sections.

TABLE 3.13-3

SPACECRAFT POWER (ORBIT AVERAGE)  
 3 MODULE POWER SYSTEM  
 1200 SQUARE FEET SOLAR ARRAY

	POWER (WATTS)	
	SLEW	NORMAL CONTROL
POWER (3 MODULES)	150	150
C&DH	200	340*
ACS	840	470
PROPULSION	200	200
SPECIAL FUNCTION MODULE	40	40
SOLAR ARRAY DRIVE	25	25
HARNESSES	50	50
THERMAL CONTROL	100	100
TOTAL POWER FOR SPACECRAFT	1,605	1,375
TOTAL POWER PRODUCED	4,950	4,950
AVAILABLE FOR PAYLOAD	3,345	3,575

\*ASSUMES CONTINUOUS USE OF 20 W RF AMPLIFIER

### 3.13.5 Spacecraft Configuration

Figure 3.13-8 depicts a spacecraft configuration which is consistent with the power and data requirements estimated in the previous section. It carries the following complement of NASA-standard modules:

- 1 - Communications and Data Handling (C&DH)
- 2 - Modular Power Subsystem (MPS)
- 3 - Modular Attitude Control Subsystem (MACS)

The last-mentioned is intended to represent the equivalent mass and power of the CMG complement required for LDR.

The mass properties of this configuration are shown in Table 3.13-4.

TABLE 3.13-4  
MASS PROPERTIES

Mass Properties Program            10-19-84            Full Fuel, 1200 S/A Stow, No P/L

SUMMARY OF MASS PROPERTIES

Weight	16039.90 LBS.	7275.58 KG.	
CGX	61.48 IN.	156.16 CM.	
CGY	1.53 IN.	3.89 CM.	
CGZ	-27.79 IN.	-70.59 CM.	
KXX	54.63 IN.	138.77 CM.	
KYY	66.70 IN.	169.41 CM.	
KZZ	68.06 IN.	172.88 CM.	
IXX	10333.58 SLUG-FT2	14010.45 KG-M2	1428.67 K-M-S2
IYY	15401.02 SLUG-FT2	20880.97 KG-M2	2129.27 K-M-S2
IZZ	16037.75 SLUG-FT2	21744.27 KG-M2	2217.30 K-M-S2
PXY	-370.84 SLUG-FT2	-502.79 KG-M2	-51.27 K-M-S2
PXZ	-114.39 SLUG-FT2	-155.09 KG-M2	-15.82 K-M-S2
PYZ	178.90 SLUG-FT2	242.55 KG-M2	24.73 K-M-S2

PRINCIPAL INERTIAS AND AXES (STRUCTURAL COORD. SYSTEM)

\*\*\*111            10304.80 SLUG-FT2            13971.44 KG-M2            1424.69 K-M-S2

ALONG UNIT VECTOR (0.99725, 0.07195, 0.01765)

WHICH MAKES            4.24842 DEGREES WITH X-AXIS  
85.87411 DEGREES WITH Y-AXIS  
88.98849 DEGREES WITH Z-AXIS

\*\*\*122            15375.52 SLUG-FT2            20846.40 KG-M2            2125.74 K-M-S2

ALONG UNIT VECTOR (-0.06451, 0.96052, -0.27062)

WHICH MAKES            93.69860 DEGREES WITH X-AXIS  
16.15291 DEGREES WITH Y-AXIS  
105.70114 DEGREES WITH Z-AXIS

\*\*\*133            16092.03 SLUG-FT2            21817.85 KG-M2            2224.80 K-M-S2

ALONG UNIT VECTOR (-0.03643, 0.26874, 0.96252)

WHICH MAKES            92.08758 DEGREES WITH X-AXIS  
74.41087 DEGREES WITH Y-AXIS  
15.73538 DEGREES WITH Z-AXIS

**NOTES**

- ▲ ADDED MODULE MAY BE ANY OF THE FOLLOWING
  - POWER MODULE
  - SS (SECONDARY PAYLOAD MODULE)
  - REACTION WHEEL MODULE
- ▲ THE MODULE, ALONG WITH ITS WEDGE STRUCTURAL SUPPORT BASE, MAY BE ROTATED EITHER 90° CW OR 90° CCW AS INDICATED BY THE PHANTOM LINES.
- ▲ THIS IS THE MACS MODULE LOCATION WHEN THE STAR TRACKERS ARE NOT INSTALLED IN IT.
- ▲ THIS IS THE MACS MODULE LOCATION WHEN THE STAR TRACKERS ARE INSTALLED IN IT.
- ▲ MAGNETIC TORQUERS ARE INSTALLED IN THE LOWER STRUCTURE.
- ▲ THE UPPER STRUCTURE CONTAINS PROVISIONS FOR THE REACTION WHEEL INSTALLATION.
- ▲ THE LOWER STRUCTURE CONTAINS THE MAGNETIC INSTALLATION.
- ▲ THE PAYLOAD COULD BE ROTATED TO VIEW THE EARTH ALONG THE LEASCREFT -Y AXIS. THIS WOULD REQUIRE THE TDSR ANTENNA TO BE ALONG THE +X AXIS.

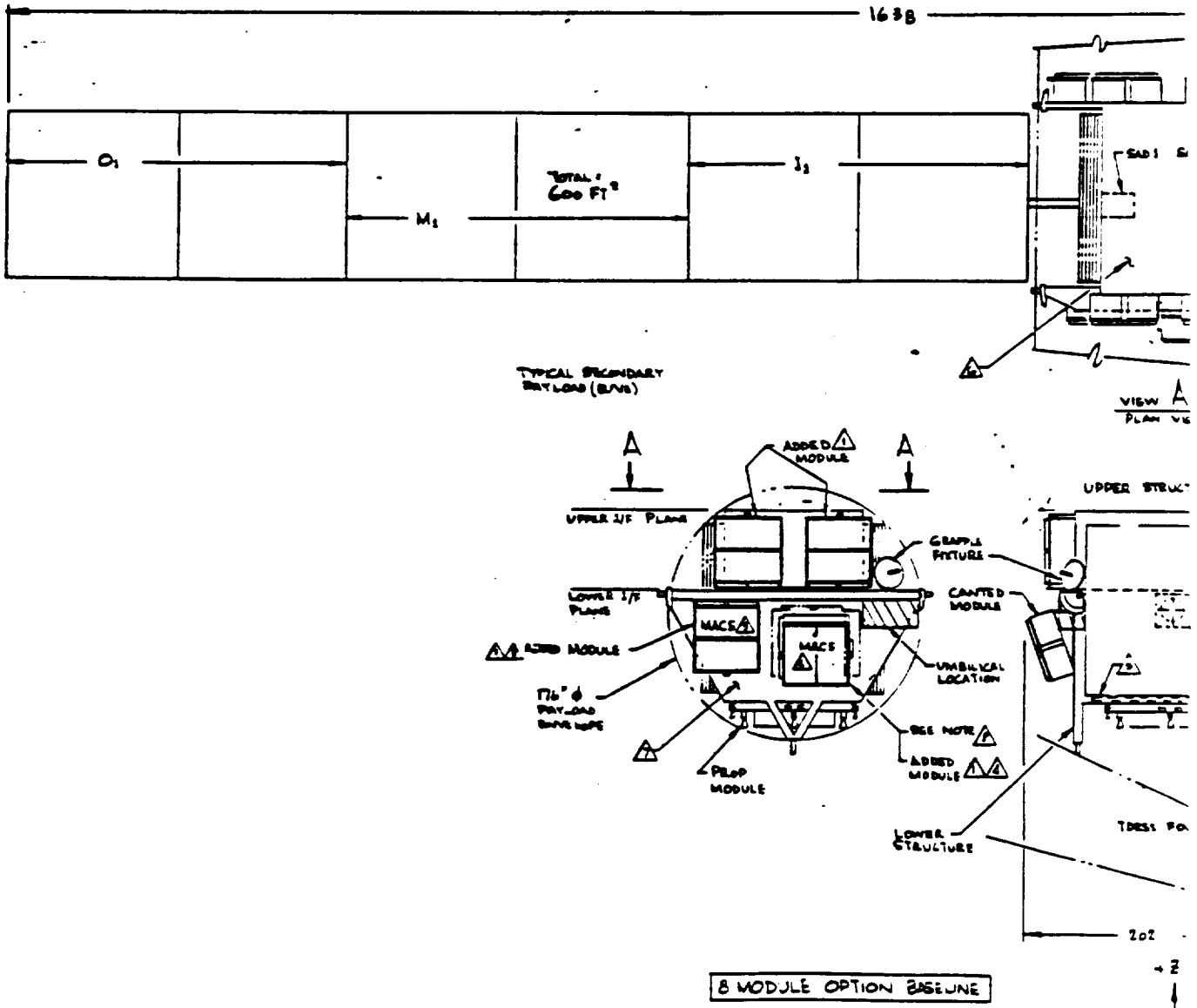
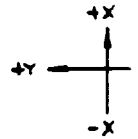
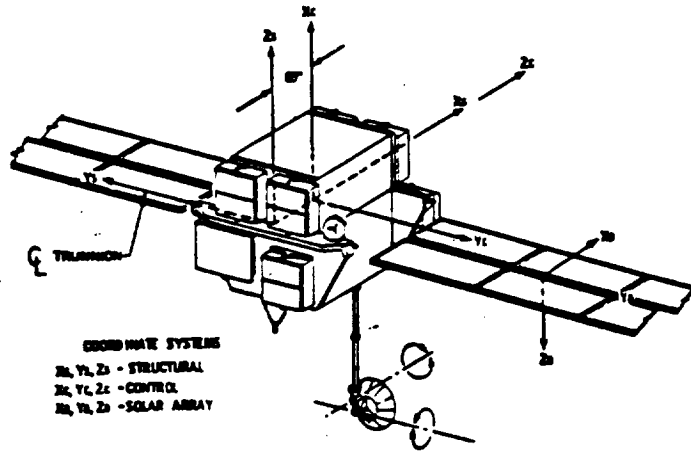
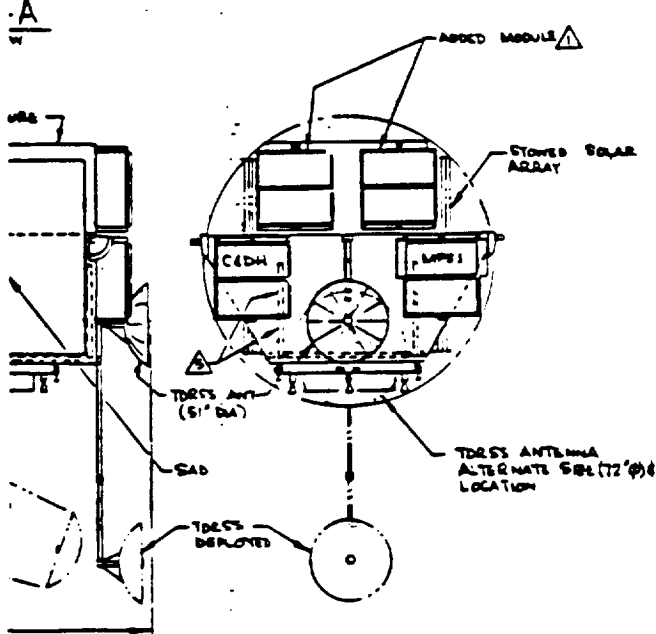
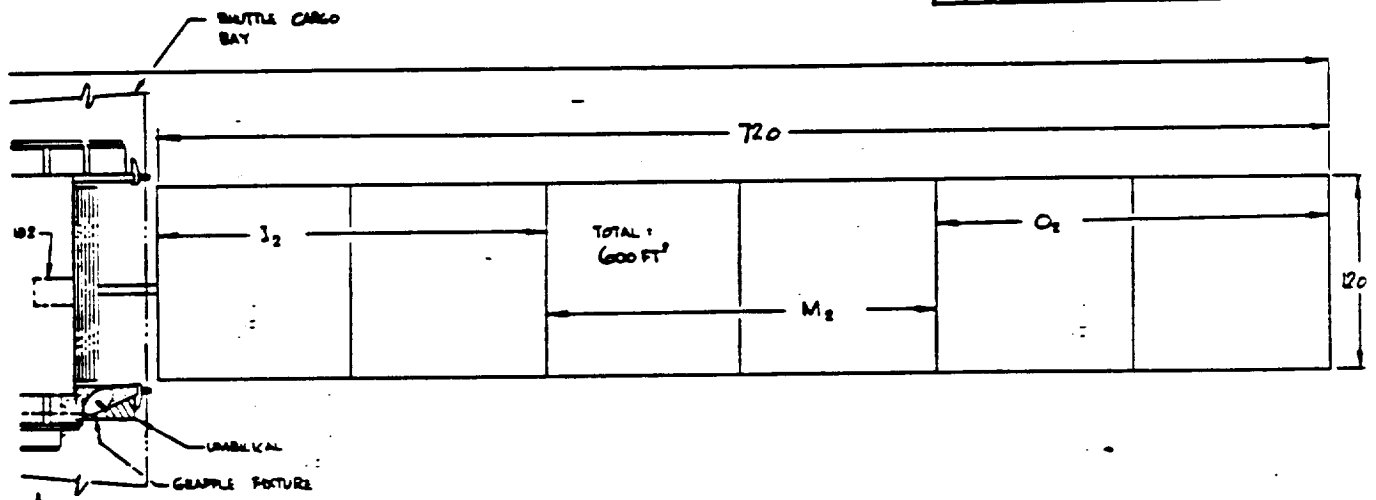


Figure 3.13-8A



COORDINATE SYSTEM

-Y



REV	DESCRIPTION	DATE	APPROVED
1	FIRST RELEASE	11/18/78	T. L. HANE
A	1) CANTED & ROTATED MACS MODULE TO IMPROVE FIELD OF VIEW 2) ADDED NOMENCLATURE & Δ 3) ADDED DIMENSIONS 4) ADDED DEPLOYED TDS ANT. & 5) LOCATED STOWED TDS		
B	1) COMPLETELY REDESIGNED & REBUILT 2) REWORKED TYPICAL CARGO PATTERNS INTO THE TOP STRUCTURE IN ORDER TO REDUCE THE OVERALL LC LENGTH. 3) ADDED TDS ANT TO FRONT BULKHEAD. 4) ADDED VPS & ADDED MODS, VPS CUTTER TO PROVIDE ROOM FOR POSSIBLE TDS ANTENNA. 5) CUT SCREW PLATES IN HALF. (6) ADDED UNRAILICAL LOCATION 7) ADDED STOWED ARRAY 8) ADDED SHT #2 TO DWG SHOWING BOTTOM HALF ONLY LC CONTR. & SMALL ARRAY		
C	ON SHT #1 1) THIS SHT COMPLETELY REDRAWN WITH CHANGES. (2) ADDED Δ THE Δ 2) DWG TITLE WAS PLACED BASELINE 3) ADDED COORDINATE AXES 4) ADDED GRAPPLE MODULE 5) ADDED SHTS 5 THRU 7 TO DWG.		
D	REVISED SHT #5		
E	REVISED SHT #5		
F	SHT 1, ADDED COORDINATE SYSTEM SHT 5, MOVED SHT 5 TO REAR BULKHEAD & DELETED CANTED MODULE ADDED SHT 6 SHT 5, EXTENSIVE CHANGES - SOLAR ARRAY CHANGED SIDES - TITLE WAS LAMPAT'S CONFIG - PAYLOAD VOLUME CHANGED - LACH MOD WAS MACS MOD		

ORIGINAL PAGE IS OF POOR QUALITY

Figure 3.13-8B

## 4.0 SELECTED SYSTEM CONCEPTS

The concept selection methodology, selection criteria, concept descriptions, cost implications, and analysis tools are presented.

### 4.1 CONCEPT SYNTHESIS APPROACH

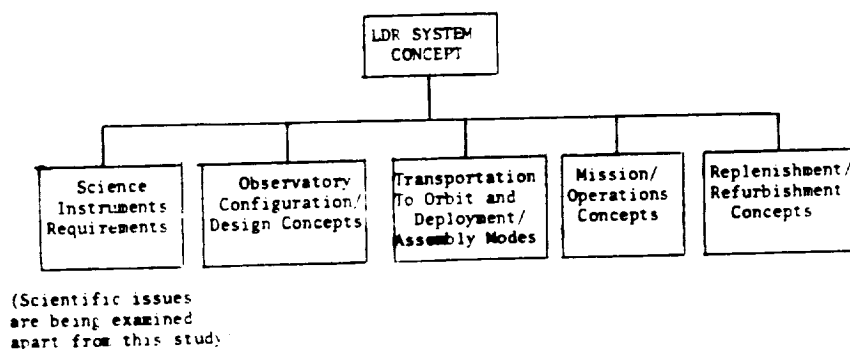
Generation of the two or more system concepts (required by the study) was an interactive process.

There were at least five broad "trade spaces" that lent themselves to developing "trade trees" and thus establishing system concepts. These are shown schematically in Figure 4.1-1. These top-level "trade spaces" are:

1. Science Instruments Requirements
2. Observatory Configuration/Design Concepts
3. Transportation to Orbit and Deployment/Assembly Modes
4. Mission/Operations Concepts
5. Replenishment/Refurbishment Concepts

Since science issues are being examined outside of this study, "Trade Space" 1 was limited to addressing a number of basic considerations (number of SI's, their weight, space, power, refrigeration needs, etc.) and picking a scientific package compatible with each scenario.

Also, since this is not a Phase A study, the candidate system concepts were not optimized. The purpose of specifying the system concepts was to help guide the technology development plans to be delivered at the end of the study.



TOP-LEVEL "TRADE SPACES"  
Figure 4.1-1

Candidate system concepts were proposed at the start of the study and capsule descriptions documented in the System Numerical Summary study guide. Figure 4.1-2 presents four such preliminary system concepts. These were selected on the basis of



emphasizing a range of differences in science return, technology impact, transportation-to-orbit impact, and life cycle cost.

#### CANDIDATE SYSTEM CONCEPTS

##### 1. SINGLE LAUNCH CANDIDATE

This approach features a 4m by 20m slot optical configuration (rectangular section of on-axis Cassegrain) and assumes use of both the ACC and Shuttle payload bay of one launch to deploy the LDR observatory (telescope, SI's, Spacecraft, thermal shield, etc.). A major goal is minimum astronaut involvement to assemble the primary mirror. Observational limitations may be impacted by aperture size, number of scientific instruments, rotation of system to obtain high resolution in orthogonal directions, long primary mirror reaction structure stiffness, and others.

##### 2. DUAL SHUTTLE LAUNCH, ASTRONAUT ASSEMBLY CANDIDATE

In this concept, a 20m on-axis Cassegrain telescope is carried aloft in one Shuttle launch and remaining subsystem elements in a second Shuttle. The segmented primary mirror, made of high quality glass is assembled in low earth orbit. The observatory is boosted to operational altitude by a dedicated S/C. The S/l complement is maximized and allows for changeout on future visits. A heavy-duty, long duration cryogenic support unit is included. This concept is selected to satisfy all the study baseline requirements and emphasizes modularity aspects to ease EVA time for assembly/deployment and checkout.

##### 3. EVOLUTIONARY, GROWTH CANDIDATE

In this concept, a complete telescope featuring a reduced-sized central core primary mirror of high quality is carried to orbit in a single Shuttle/ACC launch. The deployed system is designed to be gainfully used for scientific observation (but at reduced spatial resolution) for an interim period. The diameter can later be increased by adding additional ring(s) of panels, in-orbit by astronaut, or by returning it to Earth. A so-called "radially-degraded" design is a possibility. The mirror panels could be replaced by higher surface quality panels. As better detectors evolve or scientific interests change, they can be accommodated by the evolutionary design.

##### 4. SPACE STATION CANDIDATE

An LDR compatible with manned Space Station assembly requirements is the driving consideration in this system concept. An aperture greater than 20 meters diameter can be considered as baseline (or a planned performance improvement) since on-orbit assembly time becomes much less constrained than with Shuttle-based astronaut assembly. Thus, this concept features increased spatial resolution opportunity, provision for ease of servicing at operating orbit from the Space Station, and excellent instrument change out/modularity aspects.

#### EARLY SYSTEM CONCEPT CANDIDATES

Figure 4.1-2

As the analysis phase evolved, the slot optical configuration was found to have serious deficiencies with respect to science return, operational limitations, and pointing control impact; therefore, it was dropped. The dual Shuttle launch was found to be too optimistic for 20-meter aperture and evolved into a multiple Shuttle assembled concept (Concept 1 of the final three selected).

The evolutionary, growth candidate was eliminated based on cost benefit considerations. Design compatibility requirements imposed on the initial sub-scale primary mirror (in order to accommodate an eventual 20-meter aperture) were expensive when compared to starting with a 20-meter design at the outset. On-orbit conversion to larger aperture is particularly complicated by thermal control (sun shield) needs and efforts to upgrade the spacecraft pointing and control. On-orbit reassembly, deemed potentially possible with a manned Space Station, would, nevertheless, require a great deal of planning and be relatively expensive. Return-to-earth for upgrading and reassembly also appears to be cost inefficient.

The early Space Station candidate evolved into the final selected Concept 2, with a 20-meter aperture based on cost to satisfy, but not exceed, the baseline aperture size requirement.

Results of the 13 system analysis tasks were reviewed and several additional concepts considered.

Three system concepts were then synthesized (based on the criteria discussed in Paragraph 4.2 following) and presented to the NASA review team at Technical Progress Review No. 2 in August 1984. Two of these were extensively modified, based on review inputs. The three final, selected concepts are:

Concept 1 - Multiple Shuttle Assembled 20-Meter Cassegrain

Concept 2 - Space Station Assembled 20-Meter Cassegrain

Concept 3 - Single Shuttle/ACC Assembled 13-Meter Cassegrain.

These are detailed in Paragraphs 4.3, 4.4, and 4.5 respectively.

#### 4.2 SELECTION CRITERIA

Selection factors included considerations of cost, complexity, system performance, and relative risk associated with the required technology development.

The selection of three concepts was driven by the objective of developing representative (but unoptimized) LDR systems that would enable the various candidate subsystem technologies to be given visibility. Using this approach, it was thought that the technology development plan, the final output of the study, would have broad end-use potential.

Consequently, three system concepts were selected for presentation at the Technical Progress Review No. 2. These somewhat were arbitrarily configured with respect to subsystem elements. The three were:

Concept 1 - Multiple Shuttle Assembled 20-Meter Cassegrain

Concept 2 - Space Station Assembled 20-Meter Optical System Having a Spherical Primary

Concept 3 - Single Shuttle/ACC Assembled 20-Meter Diameter Ring Mirror Configuration

The second concept, featuring a spherical primary mirror and comprising four-mirror elements, was deleted because of its very large diameter secondary and highly aspheric surfaces on the tertiary and quaternary mirrors. The same Cassegrain optical design of Concept 1 was adopted for the final Concept 2. The unfilled, 20-meter aperture ring mirror concept was eliminated. This concept had only the light-gathering capability of a 10-meter filled aperture, and exhibited high side lobes. It was coupled to a single Shuttle/ACC transportation-to-orbit mode. At the request of the review team, this concept was deleted, and an alternate approach taken: a configuration having the largest filled aperture Cassegrain that could be fitted into a single Shuttle/ACC was developed for Concept 3. This gave rise to the 13-meter aperture concept described in Section 4.5.

### 4.3 CONCEPT 1: MULTIPLE SHUTTLE ASSEMBLY

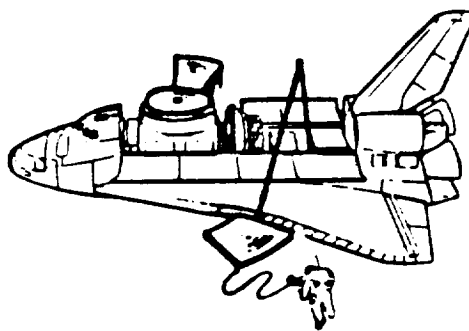
#### 4.3.1 Configuration

Concept 1 incorporates an assembly concept utilizing the Shuttle orbiter only (Figure 4.3-1). The goal is to get the LDR up in three Shuttle loads. However, as many as three additional Shuttles for astronaut assembly may be required. In this concept, EVA time must be minimized. This could be accomplished by: (1) maximizing and testing on the ground, (2) complete LDR observatory checkout on the ground, (3) transporting to orbit finished assemblies where possible, (4) utilizing RMS device(s) with EVA assist and (5) utilizing "simple" latching mechanisms. The LDR observatory concept (Figure 4.3-2) is a "true" Cassegrain telescope with trapezoidal primary mirror segments. Chopping would be performed with the secondary mirror.

#### 4.3.2 System And Subsystem Designs

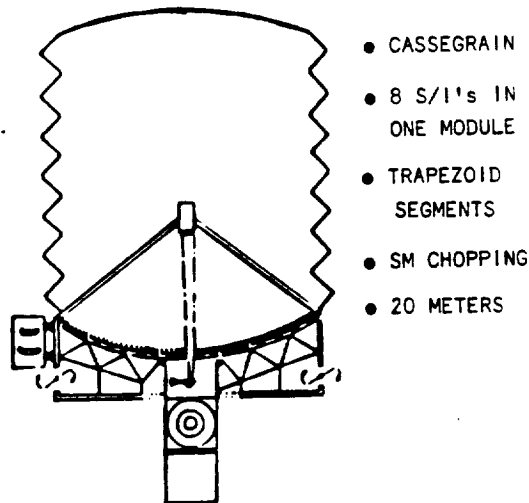
Shown in Figure 4.3-3 are the features of the primary mirror assembly. The elements of the primary mirror assembly are the mirror, control sensing mechanisms and the reaction structure. The primary mirror is glass. The coefficient of thermal expansion has been set at zero for operation at 200°K. Preliminary analysis indicates that fused silica doped with 3% titanium dioxide will have this feature as well as excellent homogeneity. This should enable a passive segmented mirror concept to be implemented. The mirror substrate is assumed to be frit bonded. The aspect ratio (segment diameter/thickness) was set at 20 to 1. This reduces the weight at the expense of the inherent structural rigidity. The basic assumption is that larger deflections can be tolerated at far infrared and submillimeter operational wavelengths.

The mirror is made up of three annuli of trapezoidal segments about a central core mirror. The central core mirror is necessary for alignment reference purposes. Three annuli were selected to optimize the segment area. This approach is preferred from processing and handling/transportation standpoints. Since there is a radial symmetry with a trapezoidal shape, the number of processing tools is minimized.



CONCEPT 1: MULTIPLE SHUTTLE ASSEMBLY

Figure 4.3-1



LDR OBSERVATORY  
Figure 4.3-2

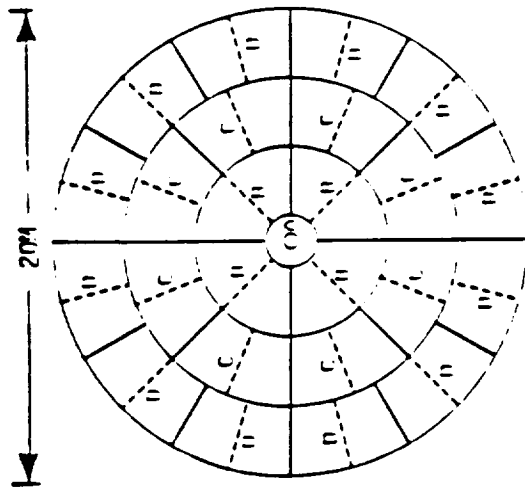
There are also more structural options. To implement the passive segmented mirror concept three linear actuated bipods are mounted on the back of each segment. This controls the three degrees of unconstrained motion (2 orthogonal tilts, and 1 translational piston).

The secondary mirror assembly is shown in Figure 4.3-4. The secondary mirror is glass. The CTE of fused silica (undoped) is approximately zero at the operational temperature of 125°K. Due to the large magnification the tightest tolerance is the allowable spacing change between the primary mirror and the secondary mirror. To minimize obstruction (image quality and background noise concerns) the secondary mirror is metered with six struts in three triangular pairs. The secondary mirror has six linear actuators for wave front error control. With a "true" metering structure philosophy this control system would be used infrequently between observations. A linear actuator would be used for chopping at 2 hertz. This device is used for background noise subtraction during observations. Two secondary mirror chopping concepts were evaluated (vertex and neutral point). In this system concept neutral point chopping was chosen to allow a greater chopping throw without compromising wave front error. The thermal shroud concept is a step sunshield in which geometry and surface finishes are used to control the primary mirror uniformity.

Since more than one Shuttle launch is needed the spacecraft will provide the space platform capability throughout the LDR observatory assembly period.

#### 4.3.3 Orbital Parameters

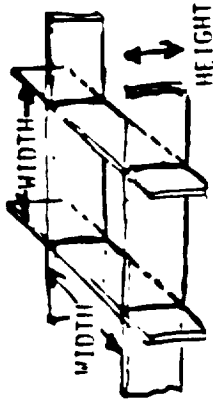
LDR will be assembled in orbit using Shuttle launches from KSC. For assembly an inclination of 28.5° and an altitude of 300 km has been assumed. The LDR spacecraft would insert LDR into its operational orbit with an inclination of 28.5° and an altitude greater than 600 km. Natural orbit decay to a lower orbit would then occur. Enough propulsion would be provided for a Shuttle revisit in three years.



(CORE NOT TO SCALE)

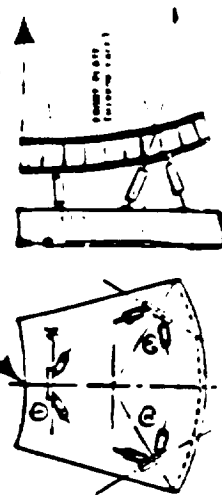
f/0.5 PARABOLLOID

	RADIAL LENGTH (M)	LENGTH (M)	DENSITY (KG/M <sup>3</sup> )	NUMBER	WEIGHT (KG)
CENTER CORE	2.0	---	48	1	603
INNER ANNULUS	2.7	3.3	45	8	2,261
MIDDLE ANNULUS	2.7	2.85	44	16	4,421
OUTER ANNULUS	2.7	2.6	42	24	6,330
			43	49	13,615



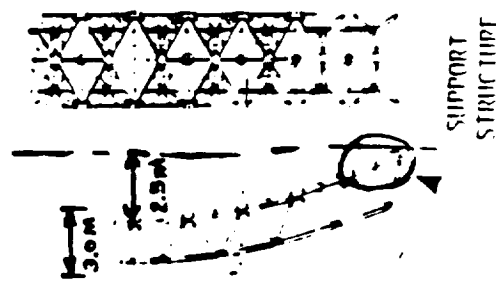
- FRONT PLATE THICKNESS 1.3 CM
- CORE HEIGHT 10.2 CM
- CORE WIDTH 10.2 CM
- BACK PLATE THICKNESS 1.3 CM

POSITION ACTUATORS (3 BIPODS)



WEIGHT
(FUSED SILICA) 13,615
300
200
100

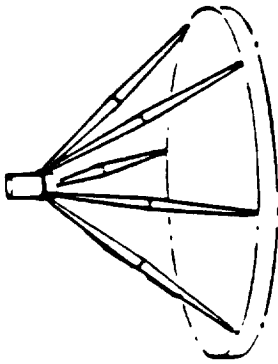
- PRIMARY MIRROR
- POSITION ACTUATORS
- POSITION SENSORS
- POSITION ACTUATOR/SENSOR ELECTRONICS
- REACTION { DELTA FRAMES } GRAPHITE/EPOXY
- STRUCTURE { SUPPORT STRUCTURE }



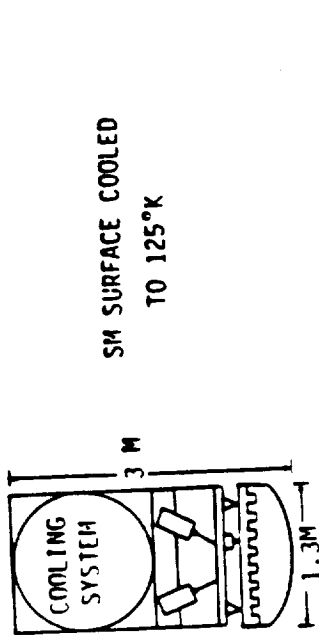
SUPPORT STRUCTURE

PRIMARY MIRROR ASSEMBLY  
(SEGMENTED MIRROR WITH RIGID BODY MOTION CONTROL)

Figure 4.3-3



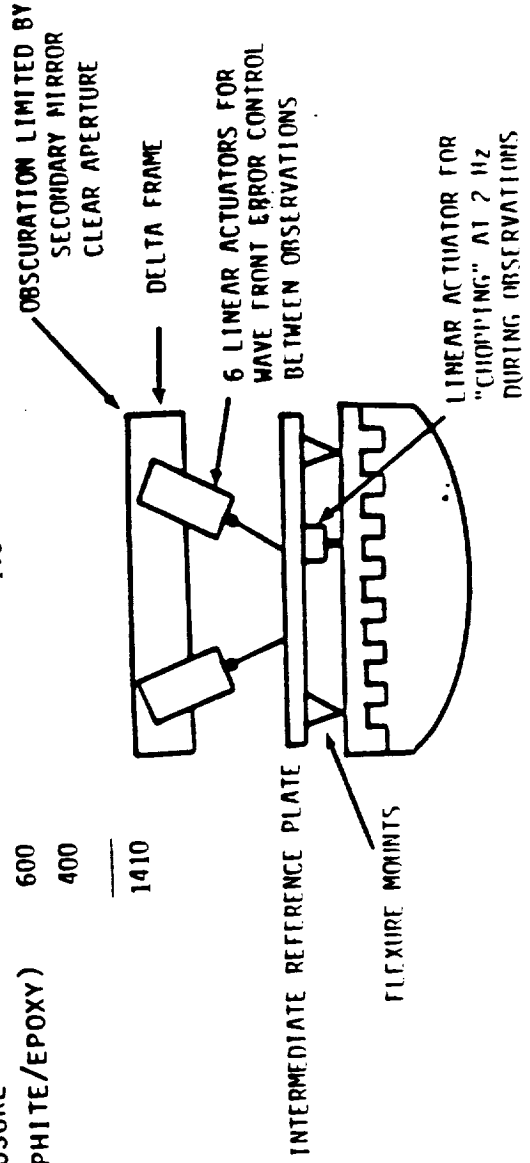
- SIX STRUTS IN THREE TRIANGULATED PAIRS
- SUPPORT POINTS AT PRIMARY MIRROR PERIMETER
- PRIMARY MIRROR TO SECONDARY MIRROR SPACING: 9.33 M



WEIGHT (KG)

- 200
- 50
- 10
- 100
- 50
- 600
- 400
- 
- 1410

- SECONDARY MIRROR (FUSED SILICA)
- POSITION ACTUATORS/CHOPPING MECHANISM
- POSITION SENSORS
- ELECTRONICS
- REACTION STRUCTURE/ENCLOSURE
- METERING STRUCTURE (GRAPHITE/EPOXY)
- COOLING SYSTEM



SECONDARY MIRROR ASSEMBLY  
(1.3 METER CONVEX HYPERBOLIC MIRROR)

Figure 4.3-4

#### 4.3.4 Assembly Methods And Sequence

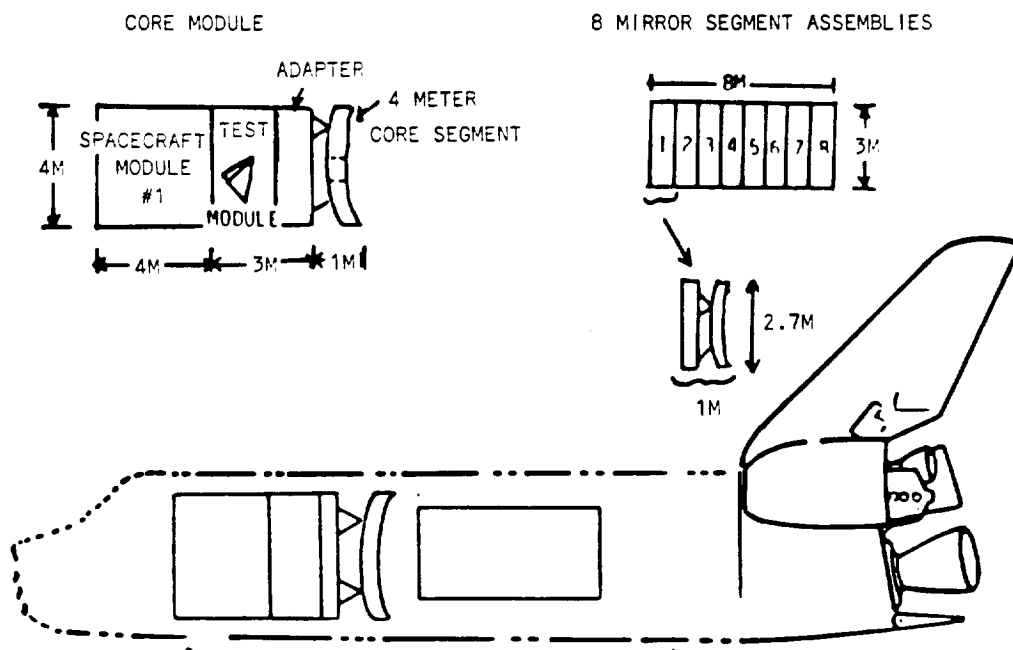
The goal is to get the LDR up in three Shuttle loads. Shown in Figure 4.3-5 to 4.3-7 is the sequence for each of the three Shuttle launches. The assembly sequence is summarized in Figure 4.3-8. As can be seen there is a lot to do in each Shuttle launch. Due to the time limitations in orbit (approximately 1 week), as many as three additional Shuttles for astronaut assembly may be required.

#### 4.3.5 Launch Vehicle Integration

Payload weight and packing density will be prime configuration drivers for LDR. The Orbiter bay is assumed capable of carrying a cylindrical payload with a maximum diameter of 4.6 meters (Figure 4.3-9). The length of the cylinder is 18.3 meters. This implies an allowable Orbiter bay volume of 304 cubic meters.

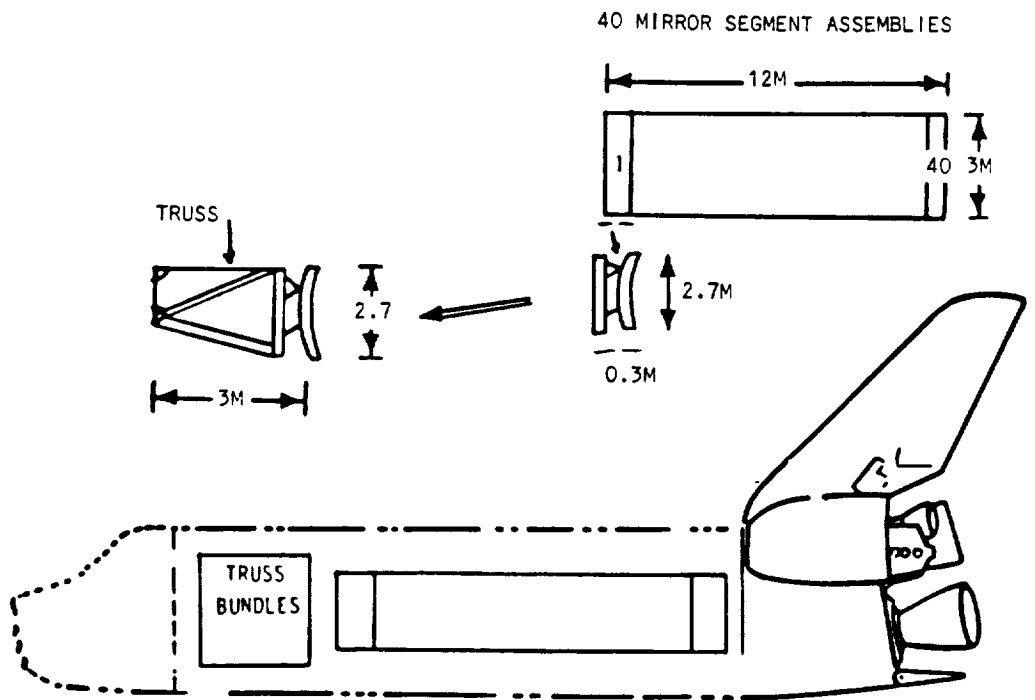
Distributed payloads up to 29,484 kg (65,000 pounds), without CG limits, have a density of  $96.9 \text{ kg/m}^3$  ( $6.6 \text{ lbs/ft}^3$ ). However, strict adherence of cargo CG limits for a given orbit and inclination will vary payload dimensional characteristics and the density from approximately  $3 \text{ lb/ft}^3$  to  $8 \text{ lb/ft}^3$ . NASA believes it can achieve the 65,000-pound payload capability for the Space Shuttle from Kennedy Space Center by early 1986 when lightweight tank, lighter and improved solid rocket booster, and 109 percent engine power will be available. Polar orbiting payload capabilities from Vandenberg AFB, California, are calculated at 22,000 pounds in the Orbiter Columbia and 28,000 pounds in Challenger and Discovery (AVIATION WEEK AND SPACE TECHNOLOGY, May 23, 1983). A polar orbit was excluded for LDR due to this weight limitation.

In addition to "prime" LDR hardware stowed in the Orbiter bay, space must be allocated for support equipment. For example, shown in Figure 4.3-10 is the Orbiter berthing module, which would be stowed close to the aft flight deck.

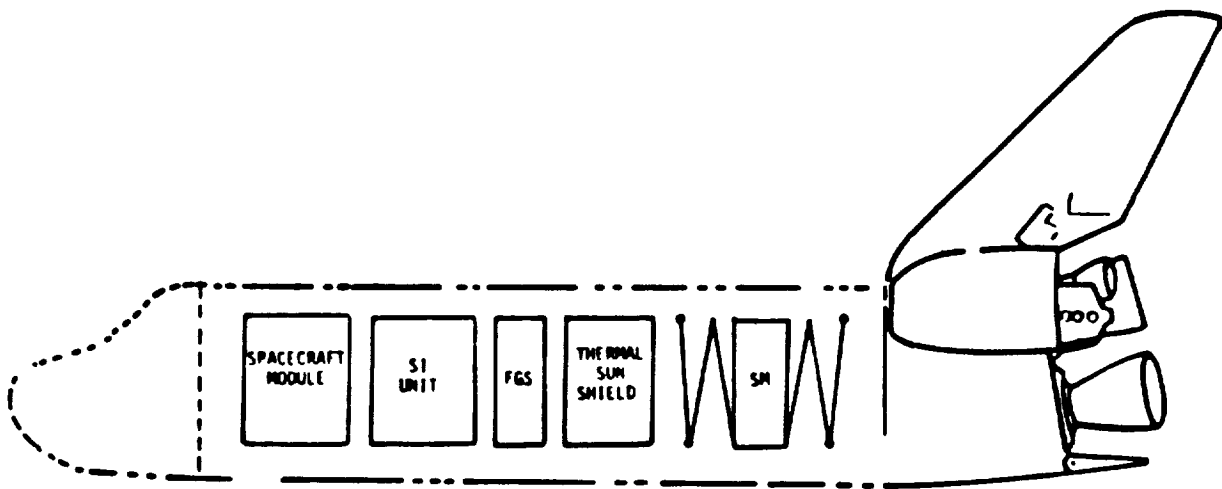


FIRST SHUTTLE LOAD  
(RIGID MIRROR ASSEMBLIES IN FIRST ANNULUS)

Figure 4.3-5



SECOND SHUTTLE LOAD  
 (MIRROR ASSEMBLIES AND TRUSS BUNDLES FOR REST OF PRIMARY MIRROR)  
 Figure 4.3-6



THIRD SHUTTLE LOAD (SCIENTIFIC INSTRUMENTS; SECONDARY MIRROR; SUNSHIELD;  
 SPACECRAFT UPGRADE; FGS)  
 Figure 4.3-7



### FIRST SHUTTLE LOAD

1. DEPLOY CORE MODULE WITH RMS
- 2 → 9 DEPLOY MIRROR SEGMENT ASSEMBLY WITH RMS AND LATCH (EVA ASSIST) TO ADAPTER ON CORE MODULE

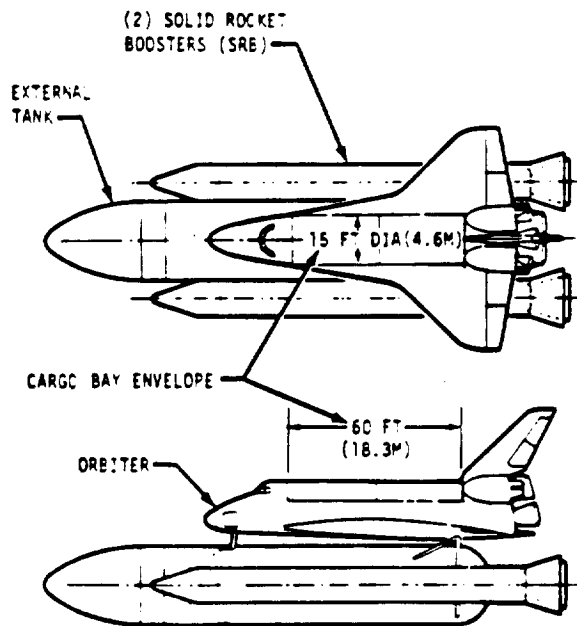
### SECOND SHUTTLE LOAD

- 1 → 40 DEPLOY MIRROR SEGMENT ASSEMBLY WITH RMS AND LATCH (EVA ASSIST) TO INNER ANNULUS
- 41 DEPLOY AND INSTALL REACTION STRUCTURE (TRUSS)

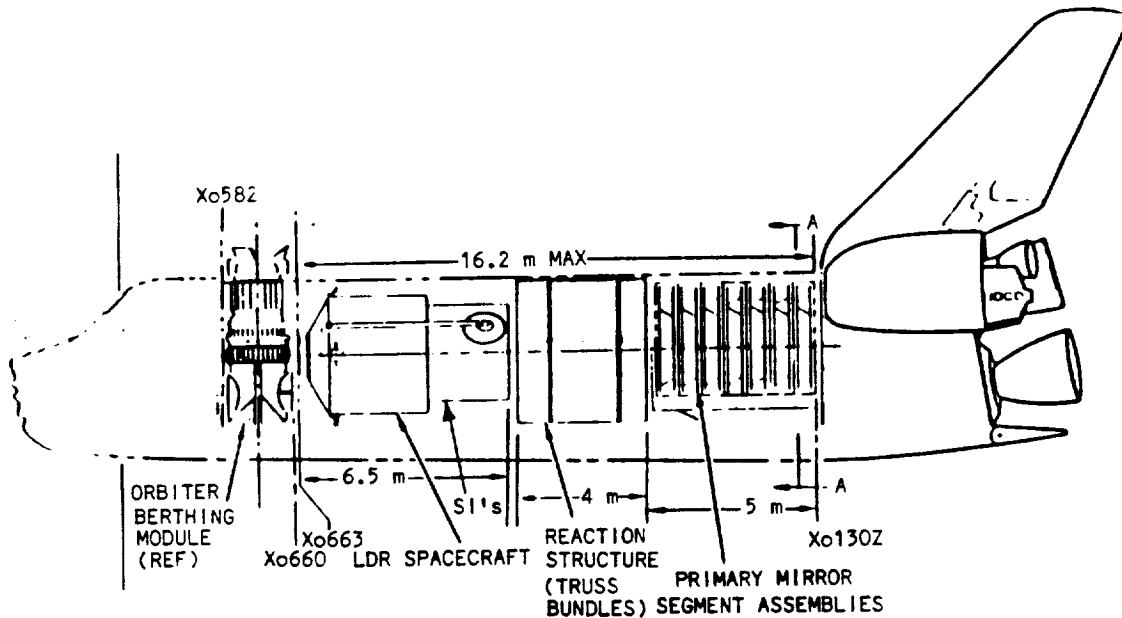
### THIRD SHUTTLE LOAD (+?)

1. DEPLOY AND INSTALL THERMAL SHROUD
2. DEPLOY SECONDARY MIRROR MODULE (WITH TRIPLE BIPOD ALREADY ON) AND LATCH TO PRIMARY MIRROR
3. DEPLOY FINE GUIDANCE SENSOR AND LATCH TO REACTION STRUCTURE
4. CHECK-OUT CASSEGRAIN WITH TEST MODULE IN CORE MODULE (CONTROLLED FROM SHUTTLE)
5. REMOVE SPACECRAFT MODULE NO. 1 AND TEST MODULE FROM CORE ADAPTER
6. DEPLOY AND INSTALL SCIENTIFIC INSTRUMENT UNIT TO CORE ADAPTER
7. DEPLOY AND INSTALL SPACECRAFT MODULE NO. 2 TO SPACECRAFT MODULE NO. 1
8. REMOVE TEST MODULE
9. INSTALL UPDATED SPACECRAFT MODULE TO SCIENTIFIC INSTRUMENT UNIT

ASSEMBLY/TEST SEQUENCE  
Figure 4.3-8



SPACE SHUTTLE FLIGHT SYSTEM  
Figure 4.3-9



LDR HARDWARE STOWED IN ORBITER BAY  
Figure 4.3-10

#### 4.3.6 Space Environmental Factors

The LDR mirrors are sensitive to particulate and gas film deposition, therefore some protection will be required against the Shuttle reaction control system effluents. A "strippable" coating on the primary mirror and secondary mirror has been suggested as a possible means for minimizing this problem. The coating would be removed after LDR buildup.

#### 4.3.7 Station Keeping

Assembly, checkout and launch of the LDR into its final operational orbit will require many months. As many as three Shuttle loads will be required to transport the LDR elements to orbit. As many as three additional Shuttles may be required for assembly support. During the periods between Shuttle visits the spacecraft will provide space platform capability. Station keeping during these "down" periods should be by JSC. During Shuttle visits a combined station keeping philosophy between the Shuttle and JSC may be required. Complete handoff to JSC should occur after final assembly but before insertion into operational orbit.

#### 4.3.8 Attitude Control And Pointing Requirements

The system concept utilizes body pointing about the center of mass for coarse pointing. Two options for fine pointing are suggested. The first utilizes the fold mirror. The secondary mirror is not recommended since chopping is performed here. The second option and the one shown in this concept is body pointing to the fine pointing level. This will require improvement in the level of CMG noise. The sensing concept is a separate visual telescope. The information from this sensor would be fed directly back to the CMG's if the second option is implemented. In order to cobe-sight this telescope to the LDR line of sight the primary mirror reaction structure is assumed to be the stable reference platform.

#### 4.3.9 Data Handling

Within the proposed science instrument complement, some instruments have the potential for requiring autonomous science data handling and storage. The requirement for high rate data and readout is driven by heavy government and commercial interest and is unlikely to be impacted directly by LDR.

#### 4.3.10 Replenishment of Expendibles

The total life requirements for LDR are at least 10 years with a goal of 15 years. The large demand for cryogenic cooling over this long period becomes unmanageable in terms of stored cryogens, and the reliability demands on active closed-cycle mechanical cryogenic refrigeration equipment would be totally unrealistic. Studies shown that a "hybrid" system composed of stored cryogen and active closed-cycle mechanical or chemical absorption refrigeration systems are possible and practical over a three year life period. Accordingly, it will be necessary to reservice the cryogenic cooling systems from three to four times over the lifetime of LDR. Two approaches are possible: return the LDR to the Shuttle or conduct a robotic controlled service operation (OMV) at the operational orbit position of LDR. The first option is probably preferred since refurbishment will also be required. (See Section 4.3.11) At the refurbishment times cryogens and spacecraft propellants would be replenished.

#### 4.3.11 Refurbishment

The LDR subsystems and science instruments should be designed for on-orbit replacement at the Shuttle. The first step will be to bring back LDR to the Shuttle orbit using the LDR spacecraft. The modules would be designed to interface using "simple" latching mechanisms. This would allow removal of the entire unit and reinstallation of a different unit. For example this could be a new scientific instrument. Since this approach requires a change in the LDR orbit, careful schedule planning of the Shuttle launch is required.

#### 4.3.12 Typical Instrument Interfaces

The science instrument unit consists of eight scientific instruments (SI's) in a single module. A fold mirror indexes to one of the eight instruments. There is no serendipity mode (simultaneous operation). Access would be provided to remove an SI.

The design philosophy of the scientific instrument should be to introduce the least possible degradation to the image provided by the Cassegrain telescope. Ideally, all of the scientific instruments would be designed with their detector surfaces at the LDR surface. However there are three basic reasons for optics in the scientific instrument. The first is to correct the coma and astigmatism in the field. LDR has a relatively small field of view (approximately 3 arcminutes). Therefore, this should not be a problem. The second reason is to change the system focal ratio (f/10). This will change the angular resolution and the field of view. The third reason is to relay the image to a different location for ease of access.

The scientific instruments will be mounted to the focal plane structure and initialized to tight alignment tolerances using shims and then latched. In order to remove and reinstall a scientific instrument "simple" latching mechanisms meeting precision tolerances will be required. Due to the stringent temperature control requirements "cool down" before installation may be required.

#### 4.3.13 Mission Analyses

Because no science scenario was provided no mission analyses were performed.

#### 4.3.14 Development Risks

The preliminary list of development risks is shown in Table 4.3-1. All items except latching mechanisms have been included in the LDR technology plan. Due to the time limitations in orbit "simple" latching mechanisms will be required. Until further definition this is considered an engineering problem and not a technology problem.

TABLE 4.3-1  
TECHNOLOGY RISKS

- OFF-AXIS PARABOLIC PRIMARY MIRROR SEGMENTS
- THERMAL SHROUD ("STEP SHIELD")
- CRYO-FLUID STORAGE AND ACTIVE REFRIGERATION SYSTEM FOR SCIENTIFIC INSTRUMENTS AND SECONDARY MIRROR
- SECONDARY MIRROR CHOPPING MECHANISM
- "SIMPLE" LATCHING MECHANISMS
- REACTION STRUCTURE JOINTS
- STRIPPABLE COATING
- RIGID BODY CONTROL MECHANISMS

### 4.4 CONCEPT 2: SPACE STATION ASSEMBLY

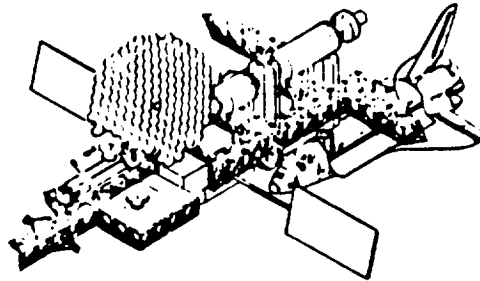
#### 4.4.1 Configuration

Concept 2 is a space station assembly concept utilizing three Shuttles to transport the observatory components and the support equipment (Figure 4.4-1). The LDR observatory concept (Figure 4.4-2) is a "true" Cassegrain telescope with hexagonal primary mirror segments. Chopping would be performed with the secondary mirror.

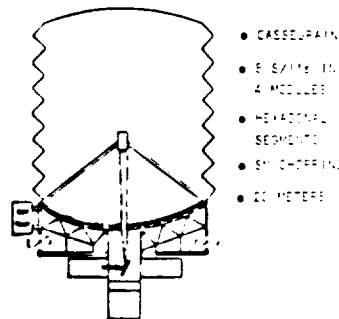
#### 4.4.2 System And Subsystem Designs

Shown in Figure 4.4-3 are the features of the primary mirror assembly. The elements of the primary mirror assembly are the mirror, control/sensing mechanisms and the reaction structure. The primary mirror is glass. The coefficient of thermal expansion has been set at zero for operation at 200°K. Preliminary analysis indicates that fused silica doped with 3% titanium dioxide will have this feature as well as excellent CTE homogeneity. This should enable a passive segmented mirror concept to be implemented. The aspect ratio (segment diameter/thickness) was set at 20 to 1. This reduces the weight at the expense of the inherent structural rigidity. The basic assumption is that large deflections can be tolerated at far infrared and sub-millimeter operational wavelengths. The mirror is made of six seven-segment hexagonal assemblies in a single annulus about a central seven segment hexagonal assembly. This central core assembly is necessary for alignment reference purposes. To implement the passive segmented mirror concept three linear actuated bipods are mounted on the back of each segment. This provides the necessary control for the three degrees of unconstrained motion (two orthogonal tilts, and one translational piston).

The selection of a passive or active mirror will determine the degree of figure control required and the approach for coherent phasing of a segment and radius matching between segments. The "true" Cassegrain telescope utilizes a parabolic mirror. This aspheric shape can be defined by orthogonal meridional and zonal radii. If the mirror cannot be coherently phased using a passive segmented concept, active figure control will be required to maintain these orthogonal radii. Concepts utilizing a spherical primary mirror were investigated in this study. Shown in Figure 4.4-4 is one of these concepts as envisioned for Space Station assembly.



CONCEPT 2: SPACE STATION ASSEMBLY  
Figure 4.4-1



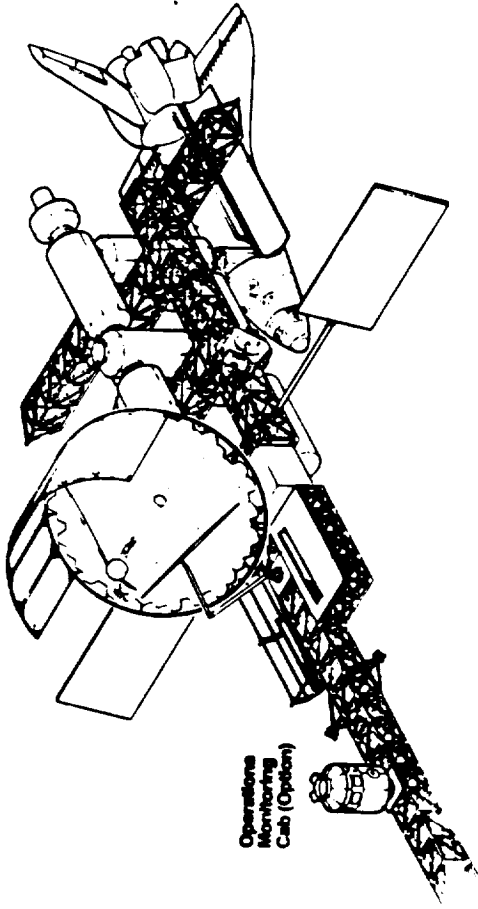
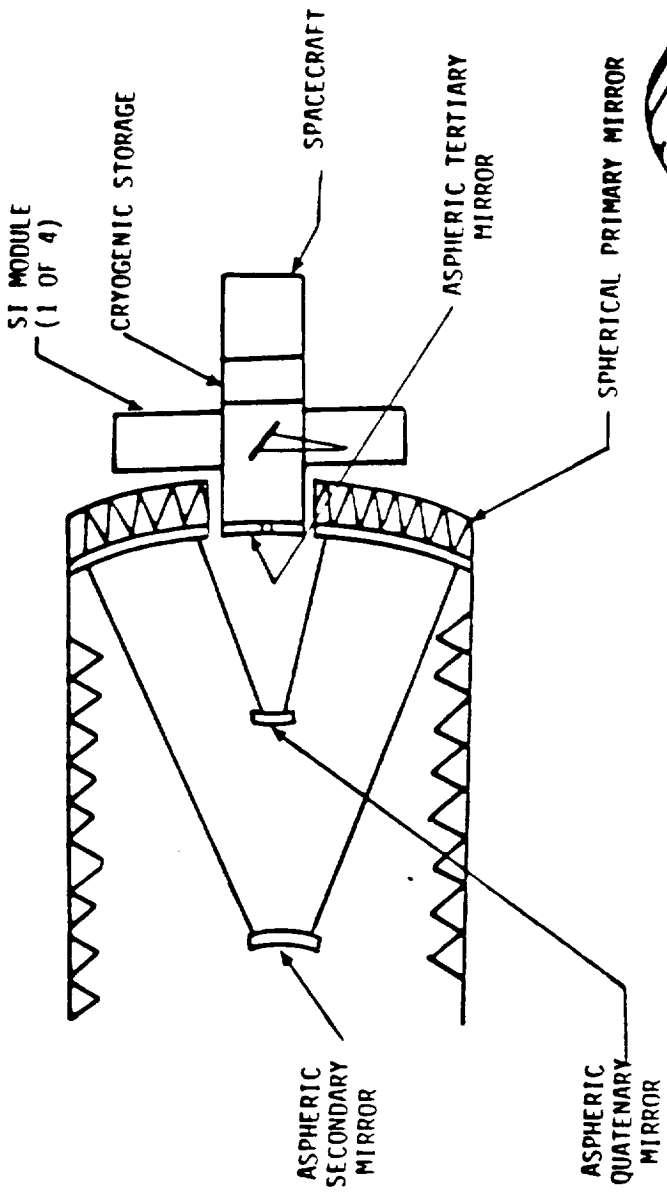
LDR OBSERVATORY  
Figure 4.4-2

Since the primary mirror is spherical the physical radii are the same at all locations on the mirror surface. Active figure control could be implemented by changing optical power only (called active radius control). This concept has been used successfully using a central linear actuator. However the spherical primary mirror concept was rejected early in this study due to the other optical elements. They are large (image quality and background noise concerns) and must be maintained to tight alignment tolerances and cooled. It should also be noted that the thermal shroud would be about twice as long as the shroud used on the Cassegrain telescope.

#### 4.4.3 Orbital Parameters

LDR will be assembled in orbit on the Space Station. The LDR spacecraft would insert LDR into its operational orbit with an inclination of  $28.5^\circ$  and an altitude greater than 600 km. Natural orbit decay to a lower orbit would then occur. Enough propulsion would be provided for a Space Station revisit in three years.





SPHERICAL PRIMARY MIRROR CONCEPT

Figure 4.4-4

#### 4.4.4 Assembly Methods And Sequence

The LDR flight system elements will be delivered to the Space Station for assembly in three or four Shuttle cargo loads. The first load will consist of the LDR spacecraft, the science instrument unit and the core mirror segments pre-assembled as a set into their flight configuration (Figure 4.4-5). This pre-assembled set will be extracted from the Shuttle cargo bay and moved along the Space Station keel structure (9 foot x 9 foot truss work) with a movable remote manipulator and installed on a two tier cube truss which features a rotating tilt-table head.

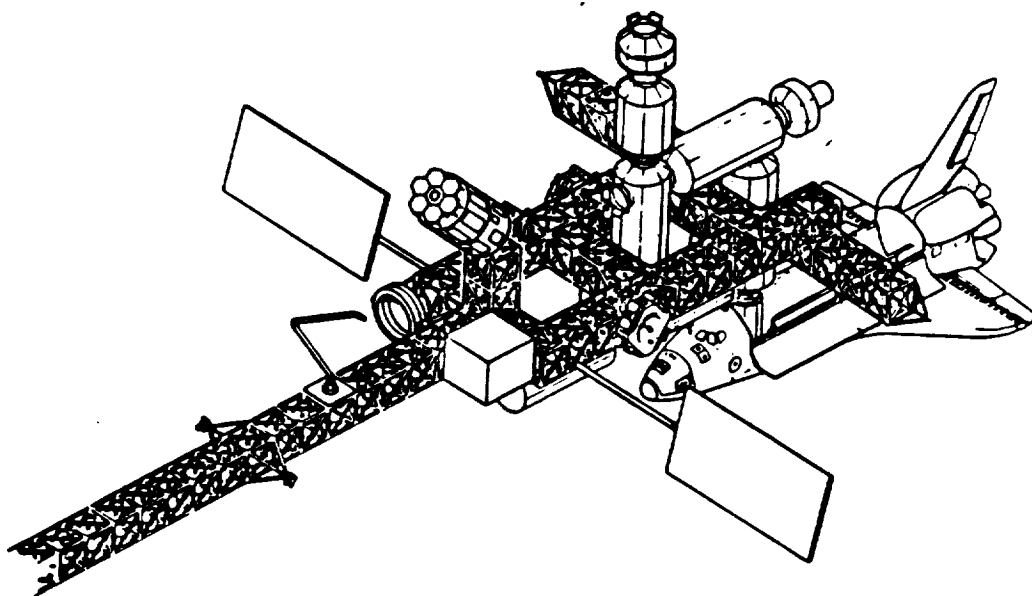
The LDR assembly control and checkout equipment will be delivered inside of the Space Station logistics module (which is delivered/replaced every 90 days). That interior LDR equipment will be transferred by the crew through the Space Station hatch at one end of the habitation module, and finally installed in the vertical racks of Lab Module #1 where astrophysics activities are broadly assigned.

Individual mirror segments will be transported to orbit in a special stowage rack in the Orbiter cargo bay, and shrouded in same fashion to prevent contamination.

At the Station the rack of mirrors will be removed from the cargo bay, transferred to and installed in a position near the assembly location accessible to the assembly manipulator (Figure 4.4-6). Here, the contamination shroud will be removed and the mirrors extracted and assembled edge-to-edge at their support frames. Each mirror is actually mounted on three "piston and tilt positioning actuators" which are mounted on the support frame.

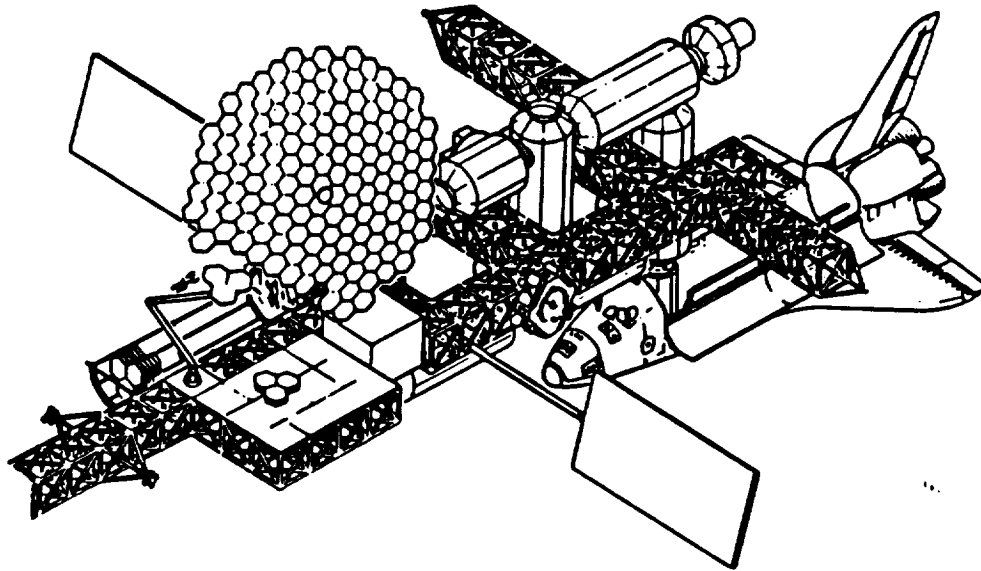
The movable remote manipulator is controlled by one EVA astronaut, while another assists in the actual latching or perhaps even bolting together of the mirror support frames.

Portable, temporary fixtures are used to support progressive checks and adjustments of the mirror positions and inter-mirror relationships.



FIRST SHUTTLE LOAD (CENTER SEVEN-SEGMENT ASSEMBLY AND SPACECRAFT)  
Figure 4.4-5



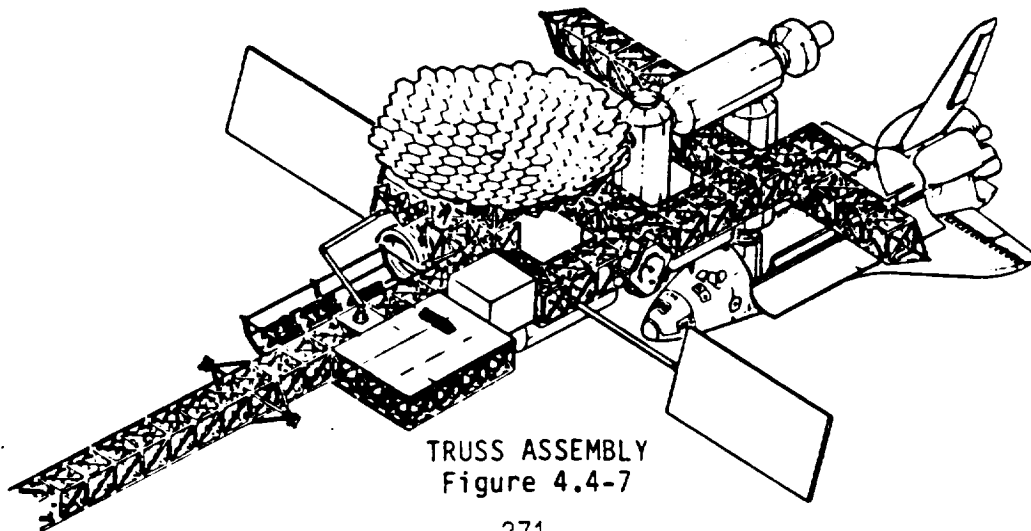


SEGMENT ASSEMBLY INTEGRATION  
Figure 4.4-6

A complex trusswork provides the reaction structure for the mirror assemblage. This 20 meter diameter structure is divided into numerous orbit-assemblable segments for compaction and delivery in the Shuttle cargo bay. Its struts (which number in the hundreds) are graphite-epoxy tubes connected by a variety of simple and complex joints.

The trusswork segments are "bundled" and stored in a carrier-cradle during Shuttle transport, and on orbit, the cradle is transferred to a location accessible to the assembly area/manipulator (Figure 4.4-7). Here it may be necessary to provide an auxiliary platform or fixture for intermediate truss deployment/rigidization prior to attaching each truss segment to the back of the mirror sets.

EVA support will probably be required for (1) the interim truss deployment/rigidization function as well as (2) the truss-to-mirror-set attachment, which may be a simple bolting function for optimum high-load/low-cost joining. Structural dynamics requirements call for high-load joints which are difficult to achieve with reasonable-cost, automated latch mechanisms.



TRUSS ASSEMBLY  
Figure 4.4-7

Once the primary mirror segments are all assembled and a peripheral structural ring is added, assembly/erection of the sunshield and secondary mirror can begin.

The sunshield will probably consist of around 20 vertical sections of multi-layer insulation stretched between solid or deployable verticals, each erected individually. Another peripheral stiffening ring may have to be installed at the forward end (opening) of sunshield to suppress dynamics. This ring, as well as a lower one, would be brought to orbit in sections, in an orbiter bay cradle.

The secondary mirror unit and its supporting tripod would be assembled before or during the sunshield assembly, Figure 4.4-8. This unit is a complex assemblage of movable optics, a cryogenic dewar, electronics and thermal control. The tripod would be delivered folded or disassembled. The complexity of LDR and other mirror assembly jobs may call for an operations monitoring cab as shown for various on-site support functions.

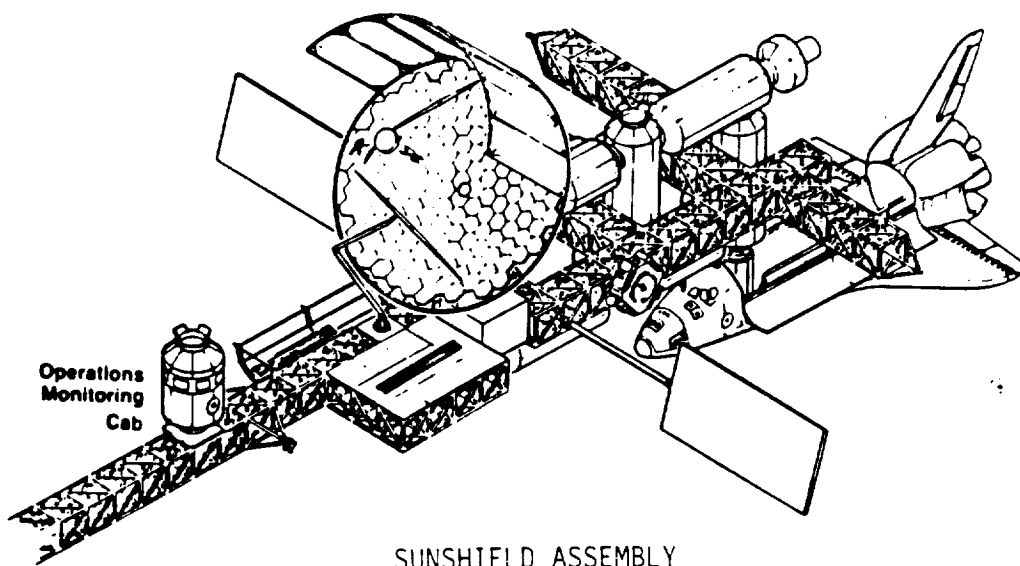
The preliminary assembly approach is summarized in Figure 4.4-9.

#### 4.4.5 Launch Vehicle Integration

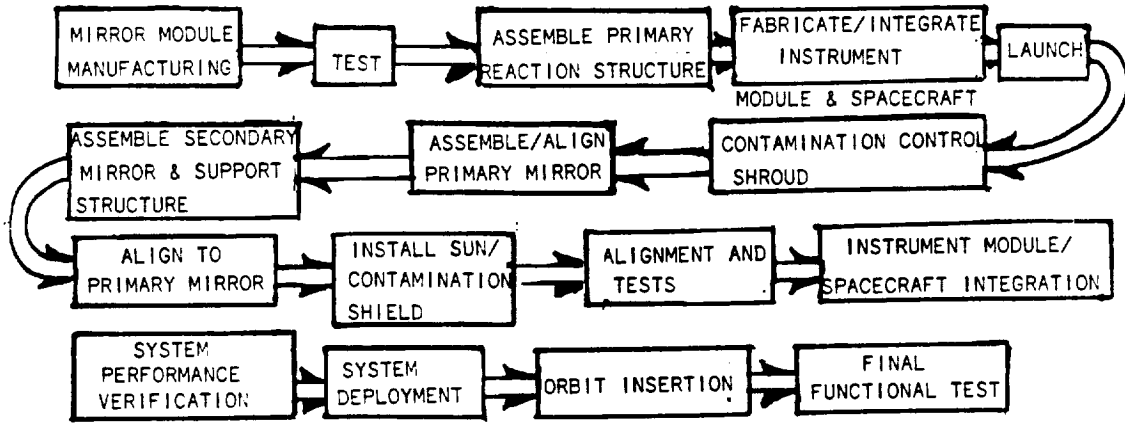
The flight system may require three or four Shuttle cargo loads to orbit the total assemblage.

The LDR flight system will be assembled at a particular position on the back of the lower keel of the Space Station (Figure 4.4-10). This exterior position is assigned for large structure assembly in general and suits the LDR in particular.

LDR specialists as well as assembly control and checkout equipment will be located in one of the LAB modules at the lower portion of the Space Station.

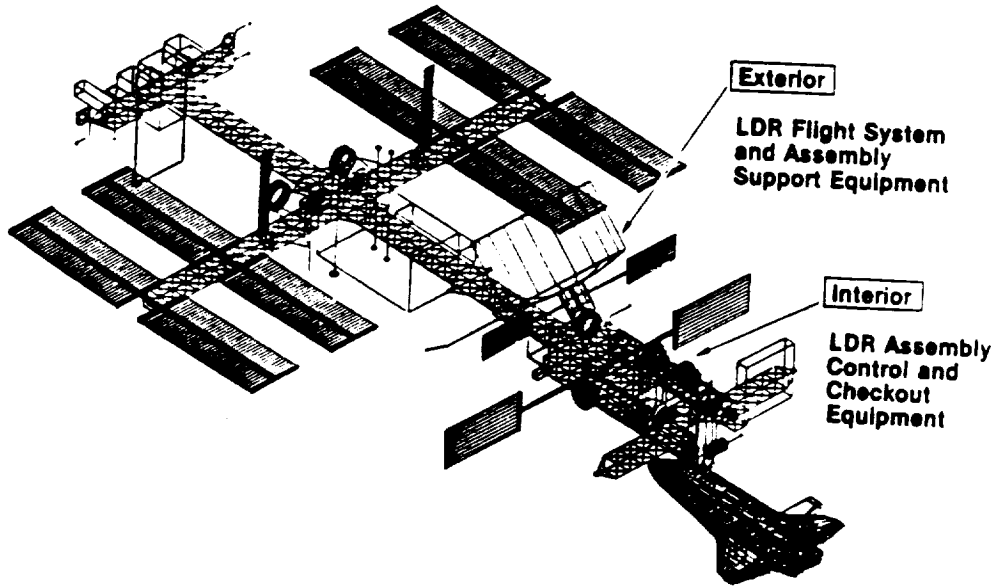


SUNSHIELD ASSEMBLY  
Figure 4.4-8



LDR OBSERVATORY ASSEMBLY SEQUENCE

Figure 4.4-9



LDR ON SPACE STATION

Figure 4.4-10

LDR specialists as well as assembly control and checkout equipment will be located in one of the LAB modules at the lower portion of the Space Station.

Two LAB modules and two HAB, or habitation modules, make up the IOC pressurized modules. In addition to Astrophysics activities in the LAB modules, there will be Life Science, Earth Science, Materials Processing, Spacecraft Servicing, Vehicle Launching, Technology Development Test and a variety of other activities in a constantly changing customer scenario throughout the life of the Space Station. Shuttle visits to the Station are planned to be every 90 days.

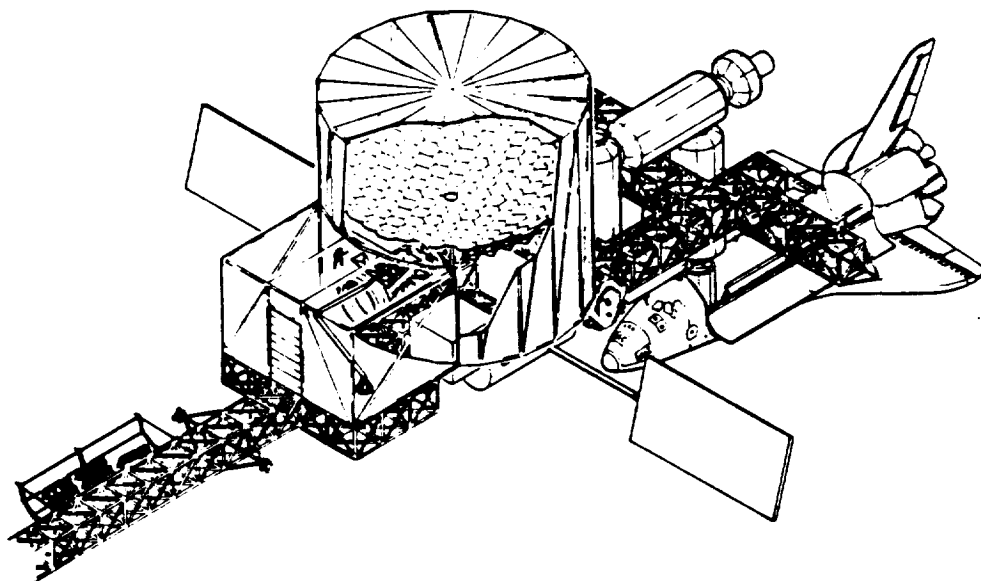
LDR elements will be delivered by the Shuttle and integrated with Space Station in a variety of ways. LDR flight system elements will be packaged (and in some cases, protected against contamination) in the Shuttle cargo bay and removed and stowed on the Station by the combined use of the Shuttle and Station remote manipulator. LDR equipment which ends up installed in the LAB module is delivered in the Space Station logistics module and crew-transferred through one end of the habitat modules to its destination in LAB #1. Construction viewing is provided by a combination of Station TV coverage, EVA astronaut on-site witnessing and LAB #1 window utilization. Logistics of the entire LDR operation, covering all parts and procedures, will utilize the Space Station logistics system which begins with pre-launch ground preparations, tracks all orbit transfer/stowage/disposition and ends with return to earth of any LDR elements.

#### 4.4.6 Space Environmental Factors

The LDR mirrors are sensitive to particulate and gas-film deposition; therefore, some LDR protection will be required against the environment around the Space Station due to visiting Shuttle reaction control system effluents, Station atmosphere leakage and a variety of other contaminants from Space Station and payloads.

Also, the incidence of sunlight on the LDR mirrors and structures during construction may counter the high-accuracy optical figure and element position measurements envisioned.

Therefore, there may be a requirement for some sort of environmental shielding, either fully or fractionally enclosing the LDR (Figure 4.4-11). In view of the expense involved in such a unique accessory, a study of the needs of other environmentally sensitive payloads or payload servicing functions should be analyzed before a design is selected.



PARTICULATE CONTAMINATION CONTROL (SPACE STATION ASSEMBLY CONCEPT)  
Figure 4.4-11

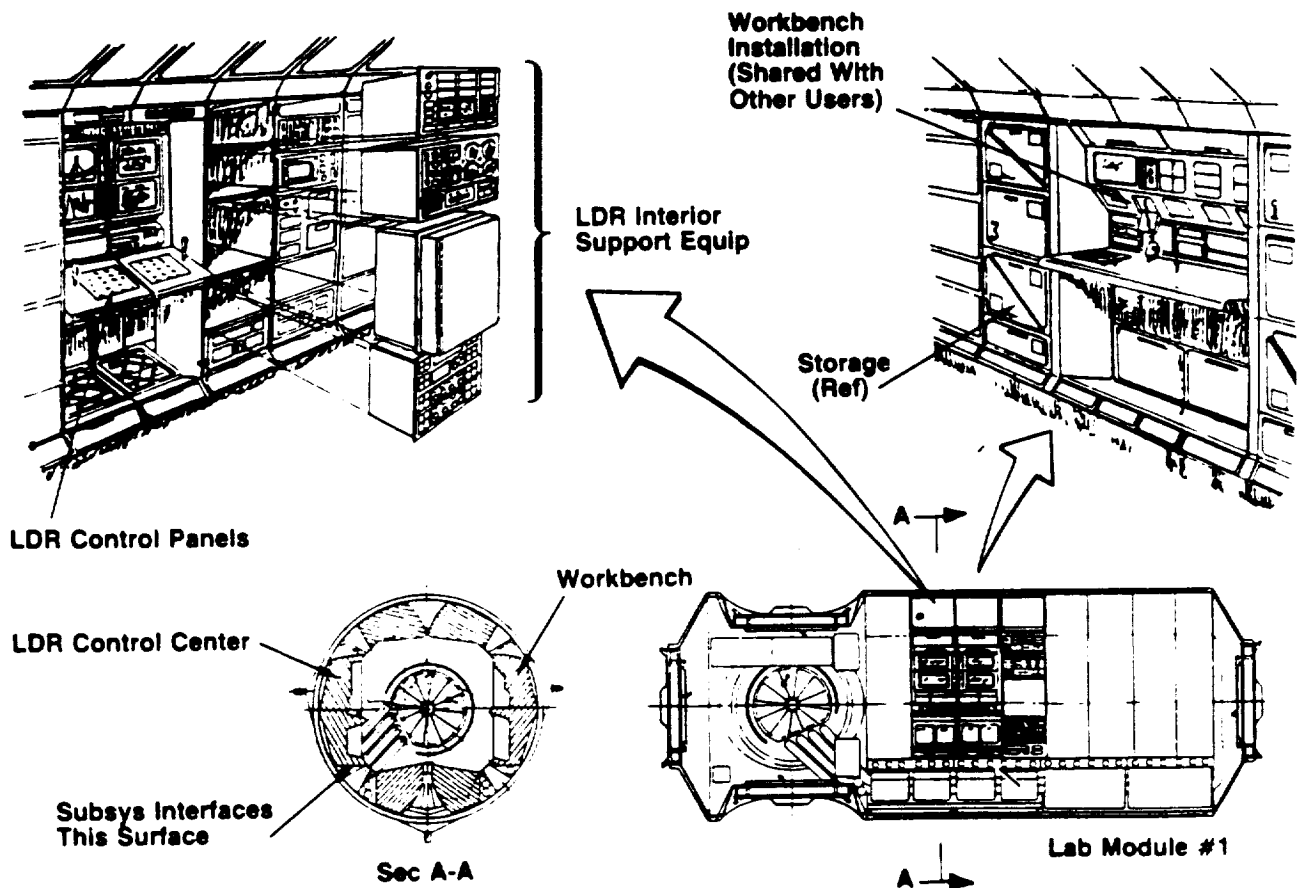
#### 4.4.7 Station Keeping

Assembly checkout and launch of the LDR on Space Station will be complex and perhaps long in duration (weeks, maybe months). The on-site control, monitoring, diagnosis and corrective action (when required) will be concentrated in LDR specialists and equipment located inside of LAB #1 on the Space Station.

The LDR specialists and equipment will have been involved in LDR pre-flight testing on earth as will certain of the Space Station crew members who are assigned and trained specifically to support LDR activities.

The interior equipment (delivered in the Space Station Logistics module) is used to activate, control, plus record and diagnose data related to the entire LDR activity on Space Station.

Since the LDR will be brought up in "pieces," the checkout functions will involve a long series of progressively integrated steps. Some will involve temporarily "rigged" checkout fixtures, some fraction of subsystems, and finally an "all-up" integrated test, countdown and launch. This spectrum of activities is envisioned to require approximately the family of interior support equipment shown in Figure 4.4-12.



LDR INTERIOR EQUIPMENT INSTALLATION  
Figure 4.4-12

#### 4.4.8 Attitude Control And Pointing Requirements

The system concept utilizes body pointing about the center of mass for course pointing. Two options for fine pointing are suggested. The first utilizes the fold mirror. The secondary mirror is not recommended since chopping is performed here. The second option and the one shown in this concept is body pointing to the fine pointing level. This will require improvement in the level of CMG noise. The sensing concept is a separate visual telescope. The information from the sensor would be fed directly back to the CMG's if Option 2 is implemented. In order to cobeersight this telescope to the LDR line of light the primary mirror reaction structure is assumed to be the stable reference platform.

#### 4.4.9 Data Handling

Within the proposed science instrument complement, some instruments have the potential for requiring autonomous science data handling and storage. In the area of data management a major effort at developing fault tolerant software and a more autonomous operating system is planned for Space Station. LDR is unlikely to require greater capability in these areas. The requirement for high rate data storage and readout is driven by heavy government and commercial interest and is unlikely to be impacted directly by LDR.

#### 4.4.10 Replenishment of Expendables

The total life requirements for LDR are at least 10 years with a goal of 15 years. The large demand for cryogenic cooling over this long period, becomes unmanageable in terms of stored cryogen, and the reliability demands on active closed-cycle mechanical cryogenic refrigeration equipment would be totally unrealistic. Studies show that a "hybrid" system composed of stored cryogen and active closed-cycle mechanical or chemical absorption refrigeration systems are possible and practical over a three year life period. Accordingly, it will be necessary to reservice the cryogenic cooling systems from three to four times over the lifetime of LDR. Two approaches are possible: return LDR to the Space Station or conduct a robotic controlled service operation (OMV) at the operational orbit position of LDR. The best technical judgement indicates servicing the cryogenic systems at the on-orbit location of LDR is feasible and that this approach will be the most economical and cost effective. Also, protection of the LDR optical telescope system from contamination at all times is mandatory, and this can be more realistically accomplished by OMV cryogenic system servicing.

#### 4.4.11 Refurbishment

The LDR subsystems and science instruments should be designed for on-orbit replacement, either remotely via OMV, or under a major service need situation, back at the Space Station. The latter return to Space Station is only planned for a six-year cycle for major refurbishment/overhaul/update and also replenishment. In that cycle length, it is anticipated the technology of detectors and science interests will have advanced to a degree which merits science instrument replacement. In the interim some malfunctions may require earlier servicing. One approach is to provide a "smart kit" on the front end of the OMV (i.e., module exchange or manipulator).

The Space Station will also provide a highly-useful, broad-service base for not only LDR assembly but subsequent checkout, malfunction correction, launch to operational orbit with an OMV, bi-annual remote servicing with the OMV and some TBD module exchanges and also, every six years a return to the Space Station for major refurbishment, overhaul, modifications and replenishment.

#### 4.4.12 Typical Instrument Interfaces

The science instrument unit consists of four scientific instrument modules. There are two scientific instruments (SI's) in each module. A fold mirror indexes, to one of the eight instruments. There is no serendipity mode (simultaneous operation). Access would be provided to remove an SI module.

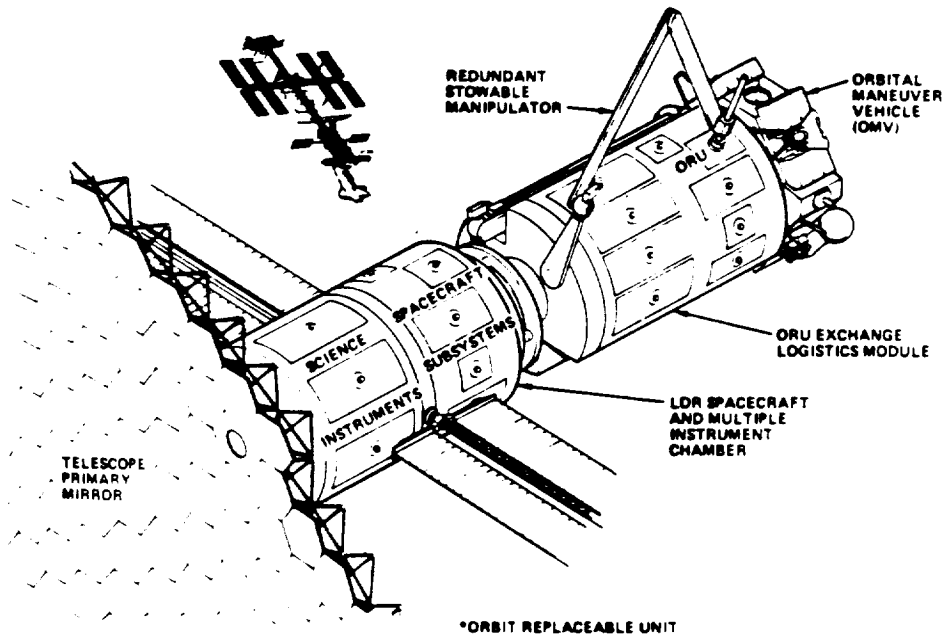
The design philosophy of the scientific instrument should be to introduce the least possible degradation to the image provided by the Cassegrain telescope. Ideally, all of the scientific instruments would be designed with their detector surfaces at the LDR surface. However, there are three basic reasons for optics in the scientific instrument. The first is to correct the coma and astigmatism in the field. LDR has a relatively small field of view (approximately 3 arcminutes). Therefore this should not be a problem. The second reason is to change the system focal ratio (f/10). This will change the angular resolution and the field of view. The third reason is to relay the image to a different location for ease of access.

The scientific instruments will be mounted to the focal plane structure and initialized to tight alignment tolerances using shims and then latched. In order to remove and reinstall a scientific instrument module "simple" latching mechanisms meeting precision tolerances will be required. Due to the stringent temperature control requirements "cool down" before installation may be required.



#### 4.4.13 Mission Analyses

After being launched from the Space Station, the LDR will transfer to a higher altitude for sustained operations, propelling itself, or be transferred by the OMV (Figure 4.4-13). LDR will operate on a self sustaining basis under ground mission control (or possibly some Space Station monitoring) for about two years. Because no science scenario was provided no mission analyses were performed.



ORU\* EXCHANGE LOGISTICS MODULE (OMV-BASED)  
Figure 4.4-13

#### 4.4.14 Development Risks

The preliminary list of development risks is shown in Table 4.4-1. All items except latching mechanisms have been included in the LDR technology plan. Due to the need for refurbishment and replenishment "simple" latching mechanisms will be required. Until further definition this is considered an engineering problem not a technology problem.

TABLE 4.4-1  
TECHNOLOGY RISKS

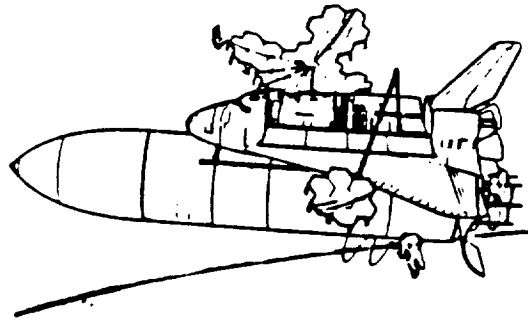
- OFF-AXIS PARABOLIC PRIMARY MIRROR SEGMENTS
- THERMAL SHROUD ("STEP SHIELD")
- CRYO-FLUID STORAGE AND ACTIVE REFRIGERATION SYSTEM FOR SCIENTIFIC INSTRUMENTS AND SECONDARY MIRROR
- SECONDARY MIRROR CHOPPING MECHANISM
- "SIMPLE" LATCHING MECHANISMS
- REACTION STRUCTURE JOINTS
- STRIPPABLE COATING
- RIGID BODY CONTROL MECHANISMS

#### 4.5 CONCEPT 3: SINGLE SHUTTLE/ACC ASSEMBLY

##### 4.5.1 Configuration

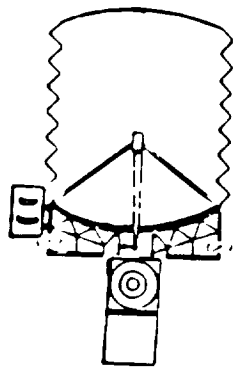
The general purpose External Tank Aft Cargo Carrier (ACC) is suggested as a potential means to transport LDR to orbit. The ACC has a usable volume of 266m<sup>3</sup> (9,000 cubic feet) or 60% of the Orbiter by volume. Concept 3 utilizes this increased volume capability (Figure 4.5-1). Without a free flying platform or Space Station, this LDR concept will require total buildup in one Shuttle launch. The LDR primary mirror segments would be stowed as sets in the ACC. The rest of the LDR observatory (spacecraft, scientific instruments, secondary mirror assembly, shroud, etc.) and support equipment would be stowed in the Orbiter bay. The LDR observatory concept (Figure 4.5-2) is a "true" Cassegrain telescope with hexagonal segments. Chopping would be performed by a fold mirror.

Packing density will limit the size of LDR below the 20 meter requirement. This concept has been sized as a 13 meter aperture. An alternative 20 meter unfilled aperture approach was also investigated in this study. This concept is shown in Figure 4.5-3. The annulus was sized with the same area as a 10 meter filled aperture.



CONCEPT 3: SINGLE SHUTTLE/ACC ASSEMBLY

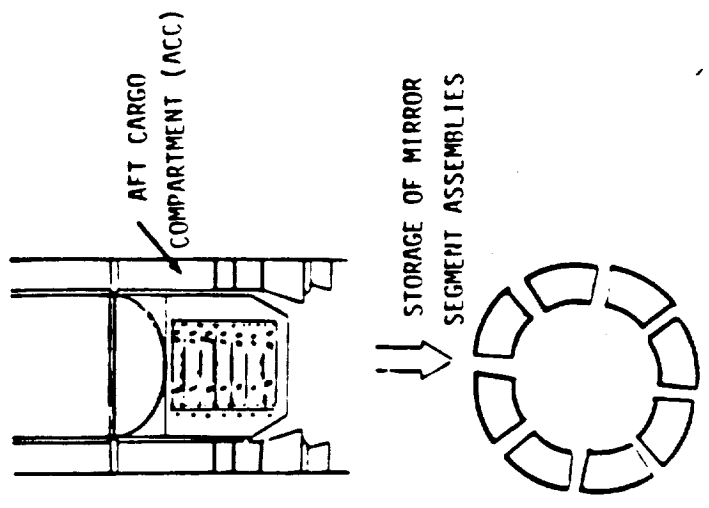
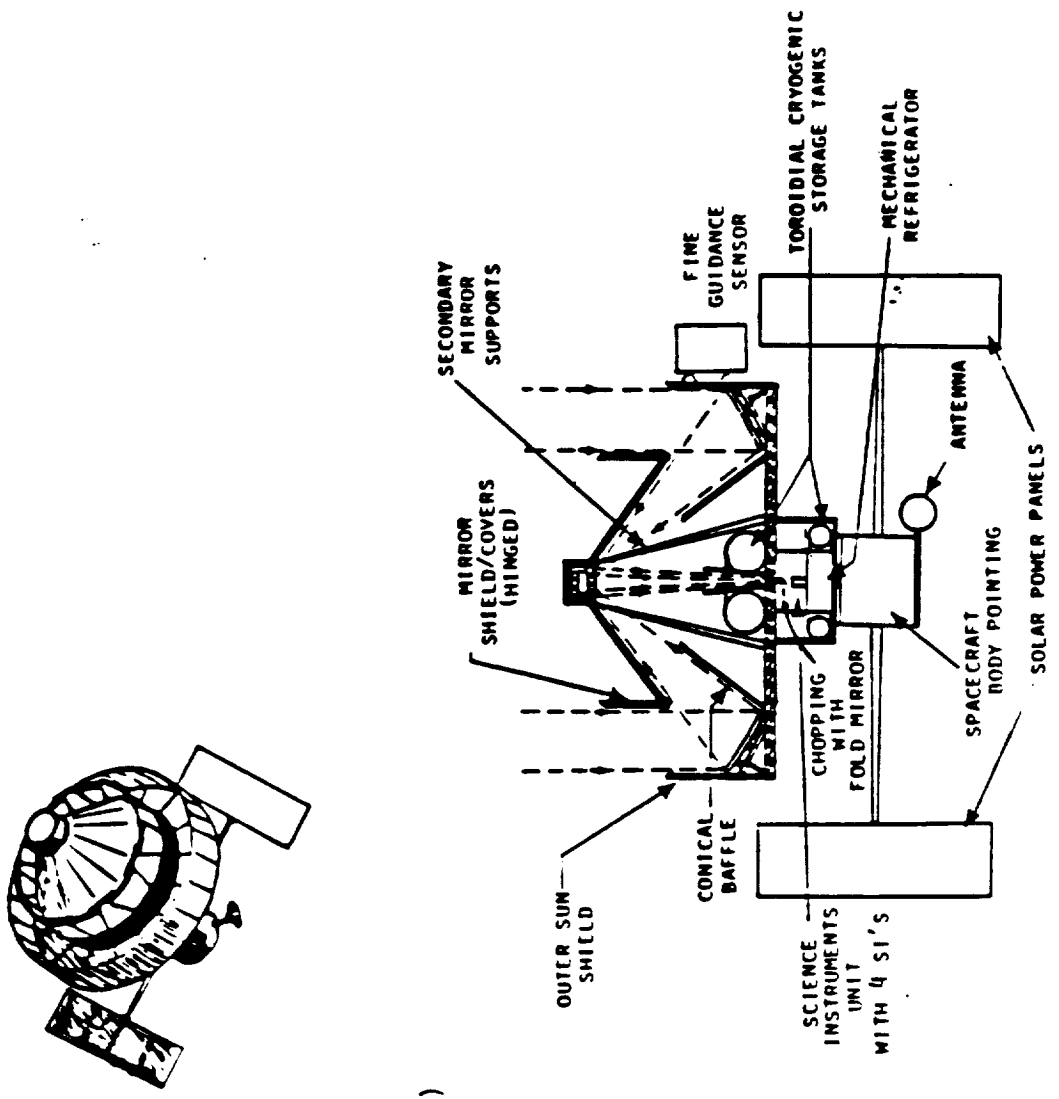
Figure 4.5-1



- CASSEGRAIN
- 4 SIs IN ONE MODULE
- HEXAGONAL SEGMENTS
- FOLD MIRROR CHOPPING
- 13 METERS

LDR OBSERVATORY

Figure 4.5-2



UNFILLED APERTURE CONCEPT

Figure 4.5-3

However, it was eliminated early in the study due to its inability to meet the performance requirement (i.e. low sidelobes).

#### 4.5.2 System And Subsystem Designs

Concept 3 is a smaller version of Concept 1. The primary mirror is glass and will be held uniformly at 200°K. This should enable a passive segmented mirror concept (tilt and piston actuation only) to be implemented. The mirror substrate is assumed to be frit bonded. The aspect ratio (segment diameter/thickness) was set at 20 to 1. This reduces the weight at the expense of the inherent structural rigidity. The mirror is made up of a single annulus of hexagonal segment assemblies. Each segment assembly consists of seven hexagonal segments. The central core mirror is necessary for alignment reference purposes.

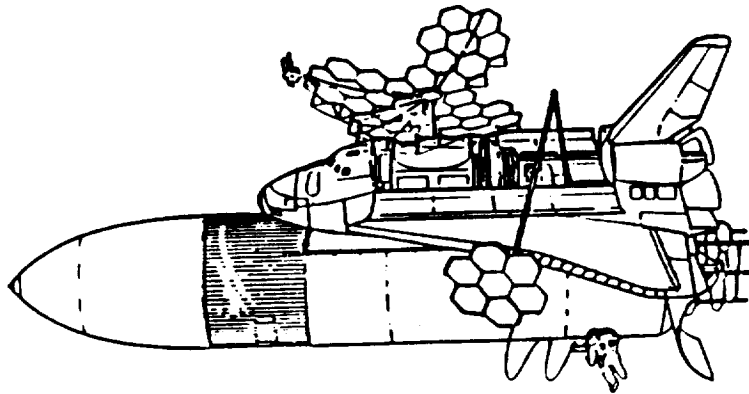
The secondary mirror is fused silica and is metered with six graphite epoxy struts in three triangulated pairs. Six linear actuators are provided for wave front error control. Chopping is performed with the fold mirror. Two fold mirror concepts (rotating and push/pull) were evaluated. In this system, push/pull chopping was chosen due to its smaller modulation noise and implementation advantages. The thermal shroud is the step sunshield in which geometry and surface finishes are used to control the primary mirror uniformity.

#### 4.5.3 Orbital Parameters

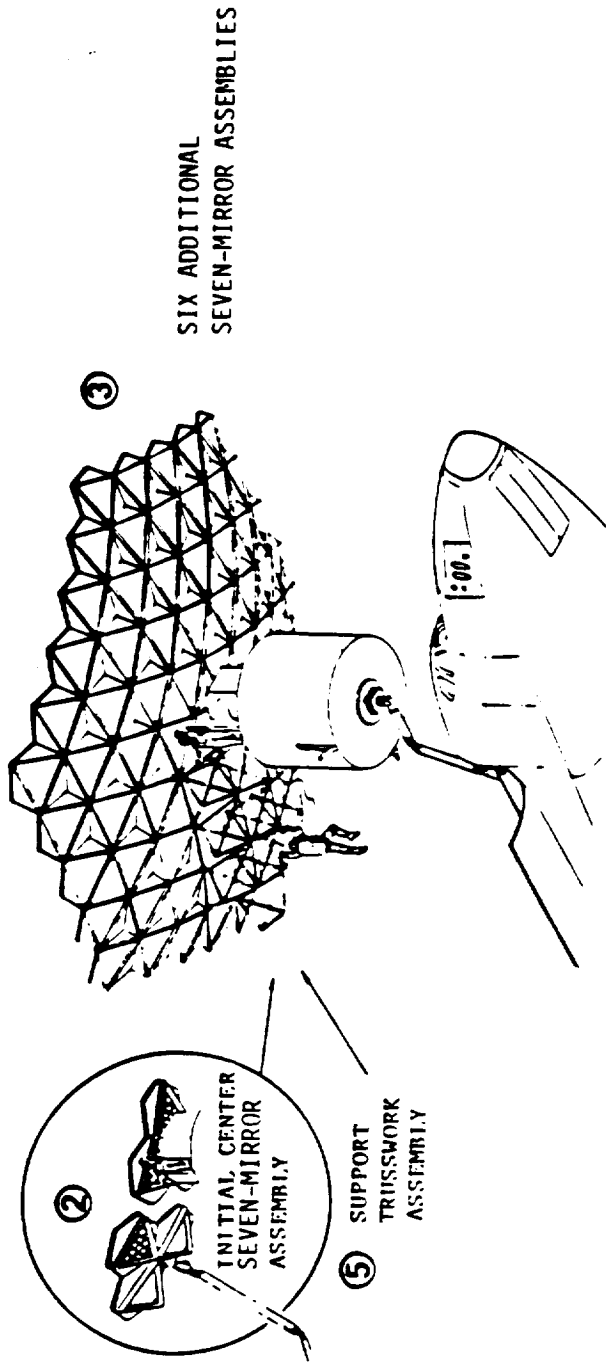
LDR will be assembled in orbit using a Shuttle launch from KSC. For assembly an inclination of 28.5° and an altitude of 300 km has been assumed. The LDR spacecraft would insert LDR into its operational orbit with an inclination of 28.5° and an altitude greater than 600 km. Natural orbit decay to a lower orbit would then occur. Enough propulsion would be provided for a Shuttle revisit in three years.

#### 4.5.4 Assembly Methods And Sequences

The goal is to get the LDR installed in a single Shuttle launch (approximately one week). The first step is to remove the aft end of the LDR observatory from the Orbiter bay using an RMS. This aft end includes the spacecraft, scientific instruments, and cryogenics as an integrated package. The next step is the assembly of the primary mirror. Shown in Figures 4.5-4 and 4.5-5 is the concept for its assembly. The segment assemblies (mirrors with delta support frames) are stowed in the ACC. There are seven segment assemblies each composed of seven hexagonal segments pre-integrated. After mirror removal these seven segment assemblies are colatched using "simple" latching mechanisms. The support trusswork is then installed for rigidization. The final two steps are the installation of the secondary mirror assembly (mirror with metering structure) and the thermal shroud.



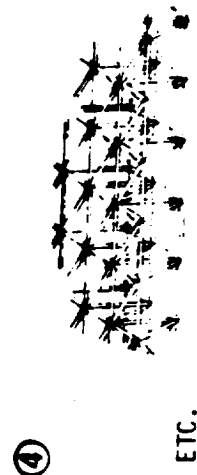
LDR PRIMARY MIRROR SEGMENT ASSEMBLIES IN ACC  
Figure 4.5-4



SHUTTLE DELIVERY

- SEVEN-ELEMENT SEGMENT ASSEMBLIES (IN ACC)
- SUPPORT TRUSSWORK, SPACECRAFT SHROUD, SI'S, ETC. (IN ORBITER BAY)

SUPPORT TRUSSWORK DEPLOYMENT

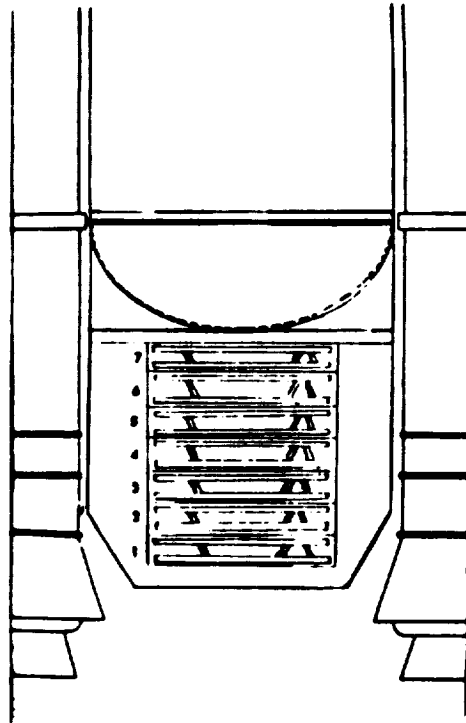


LDR PRIMARY MIRROR ASSEMBLY SEQUENCE IN ORBITER BAY

Figure 4.5-5

#### 4.5.5 Launch Vehicle Integration

In this concept the primary mirror assemblies would be stowed in the ACC (Figure 4.5-6). All other elements of the observatory and support equipment would be stowed in the Orbiter bay.



STOWAGE OF PRIMARY MIRROR ASSEMBLIES IN ACC  
Figure 4.5-6

The ACC has a design weight of 7,585 Kg (16,687 pounds) and 266 cubic meters of usable volume. It consists of a 25-foot diameter by 15-foot long cylinder plus a 5-foot long frustrum of a cone. The cone varies from 25 feet (300 inches) in diameter to 16.67 feet (200 inches) in diameter. The ACC is an assembly of three separate subassemblies. The ACC skirt is attached to the external tank near ring frame by bolts. The Payload Support Structure (PSS) is the general payload carrying structure containing four interlocking beams capable of accommodating a variety of payloads. The shroud protects the payload from thermal and acoustical environment during launch and is jettisoned on the ascent. The ACC payload envelope plus STS Orbiter payload envelope offer about 168 percent of the payload volume of a single STS launch. The payload allocation for this STS/ACC arrangement is approximately 29,000 kg for an equatorial launch. There is no payload weight penalty or advantage in using the ACC.

#### 4.5.6 Space Environmental Factors

The LDR mirrors are sensitive to particulate and gas film deposition; therefore, some protection will be required against the Shuttle reaction control system effluents. A "strippable" coating on the primary mirror and secondary mirror has been suggested as a possible means for minimizing this problem. The coating would be removed after LDR buildup.



#### 4.5.7 Station Keeping

Assembly checkout and launch of the LDR in the single Shuttle concept must be as uncomplicated as possible. Time in assembly orbit will be limited to approximately one week. Handoff to JSC should occur after assembly but before insertion into operational orbit.

#### 4.5.8 Attitude Control and Requirements

The system concept utilizes body pointing about the center of mass for coarse pointing. Two options for fine pointing are suggested. The first utilizes the secondary mirror. The fold mirror is not recommended since chopping is performed here. The second option and the one shown in this concept is body pointing to the fine pointing level. This will require reduction in the level of CMG noise. The sensing concept uses a separate visible telescope. The information from the sensor would be fed directly back to the CMG's if the second option is implemented. In order to cobe-sight this telescope to the LDR line of sight the primary mirror reaction structure is assumed to be the stable reference platform.

#### 4.5.9 Data Handling

Within the proposed science instrument complement, some instruments have the potential for requiring autonomous science data handling and storage. The requirement for high rate data storage and readout is driven by heavy government and commercial interest and is unlikely to be impacted directly by LDR.

#### 4.5.10 Replenishment of Expendables

The total life requirements for LDR are at least 10 years with a goal of 15 years. The large demand for cryogenic cooling over this long period becomes unmanageable in terms of stored cryogenics, and the reliability demands on active closed-cycle mechanical cryogenic refrigeration equipment would be totally unrealistic. Studies show that a "hybrid" system composed of stored cryogen and active closed-cycle mechanical or chemical absorption refrigeration systems are possible and practical over a three year life period. Accordingly, it will be necessary to reservice the cryogenic cooling systems from three to four times over the lifetime of LDR. Two approaches are possible: return LDR to the Shuttle or conduct a robotic controlled service operation (OMV) at the operational orbit position of LDR. The first option is probably preferred since refurbishment will also be required (see Section 4.5.11). At the refurbishment times cryogenics and spacecraft propellants would be replenished.

#### 4.5.11 Refurbishment

The LDR subsystems and science instruments should be designed for on-orbit replacement at the Shuttle. The first step will be to bring back LDR to the Shuttle orbit using the LDR spacecraft. The modules would be designed to interface using "simple" latching mechanisms. This would allow removal of the entire unit and reinstallation of a different unit. For example, this could be a new scientific instrument. Since this approach requires a change in the LDR orbit, careful schedule planning of the Shuttle launch is required.

#### 4.5.12 Typical Instrument Interfaces

The science instrument unit consists of four scientific instruments (SI's) in a single module. The number was "arbitrarily" set but reduced from eight since in a single Shuttle launch concept space in the Orbiter bay will be at a premium. A fold mirror indexes to one of the four instruments. There is no serendipity mode (simultaneous operation). Access would be provided to remove an SI.

The design philosophy of the scientific instrument should be to introduce the least possible degradation to the image provided by the Cassegrain telescope. Ideally, all of the scientific instruments would be designed with their detector surfaces at the LDR image surface. However there are three basic reasons for optics in the scientific instrument. The first is to correct the coma and astigmatism in the field. LDR has a relatively small field of view (approximately 3 arcminutes). Therefore this should not be a problem. The second reason is to change the system focal ratio (f/10). This will change the angular resolution and the field of view. The third reason is to relay the image to a different location for ease of access.

The scientific instruments will be mounted to the focal plane structure and initialized to tight tolerances using shims and then latched. In order to remove and reinstall a scientific instrument, "simple" latching mechanisms meeting precision tolerances will be required. Due to the stringent temperature control requirements "cool down" before installation may be required.

#### 4.5.13 Mission Analyses

Because no science scenario was provided no mission analyses were performed.

#### 4.5.14 Development Risks

The preliminary list of development risks is shown in Table 4.5-1. All items except latching mechanisms have been included in the LDR technology plan. Due to the time limitations in orbit "simple" latching mechanisms will be required. Until further definition this is considered an engineering problem not a technology problem.

TABLE 4.5-1  
TECHNOLOGY RISKS

- OFF-AXIS PARABOLIC PRIMARY MIRROR SEGMENTS
- THERMAL SHROUD ("STEP SHIELD")
- CRYO-FLUID STORAGE AND ACTIVE REFRIGERATION SYSTEM FOR SCIENTIFIC INSTRUMENTS AND SECONDARY MIRROR
- FOLD MIRROR CHOPPING MECHANISM
- "SIMPLE" LATCHING MECHANISMS
- REACTION STRUCTURE JOINTS
- STRIPPABLE COATING
- RIGID BODY CONTROL MECHANISMS

#### 4.6 COST CONSIDERATIONS

Preliminary cost implications of the three selected LDR system concepts were investigated. Costs were considered for four major cost categories: costs to conduct an LDR technology development program; costs for the design and production of the observatory; costs to launch and deploy the observatory; and the costs for orbital re-supply, refurbishment, and changeout.

The top-level cost summary in Table 4.6-1 compares cost estimates in three of the categories for each concept, and their total, less technology development costs.

The costs for developing the technology to space qualify the science instruments is not estimated in this study and the total technology development program costs are therefore incomplete. (Kodak's proposed technology development plan totals about \$70M, but includes no costs for technology initiatives for science instruments).

TABLE 4.6-1  
LDR SYSTEM CONCEPTS  
TOP-LEVEL COST IMPLICATIONS

	<u>CONCEPT 1</u>	<u>CONCEPT 2</u>	<u>CONCEPT 3</u>
TECHNOLOGY DEVELOPMENT	\$ TBD M	\$ TBD M	\$ TBD M
OBSERVATORY DESIGN AND PRODUCTION	\$1067 M	\$1067 M	\$668 M
SYSTEM LAUNCH AND DEPLOYMENT	\$677 M	\$365 M	\$221 M
RESUPPLY REFURBISH EXCHANGE	\$143 M	\$143 M	\$143 M
TOTAL	\$1887 M	\$1575 M	\$1032 M

Costs are shown in millions of 1985 year dollars.

Costs for design and production of Concepts 1 and 2 are essentially the same since the only differences are the shape of the primary mirror segments and the method of packaging the eight Scientific Instruments (SI's). Higher launch and deployment costs for Concept 1, compared to Concept 2, are caused primarily by the need for more STS flights to provide more astronaut labor hours for assembly.

Resupply and refurbishment need to be more fully evaluated for Concept 3. They may be somewhat lower than stated due to fewer scientific instruments and the resulting lower cryo and electronic demands.

Assumptions used in generating these estimates are summarized in Figure 4.6-1. Estimates for customer chargeable costs for the Aft Cargo Carrier (ACC) were based on information obtained from Tom Mobley, Martin-Michoud Operations. The maximum TDRSS data rate was used to establish communication and power subsystem size/cost.

Concepts costed are those shown in Section 3 of this Volume. They have been configured to reflect the inputs of the review team from Progress Review No. 2. Cost reductions or increases among these concepts should, of course, be compared to performance benefits or penalties, shown elsewhere in this report.

- ALL COSTS IN 1985 DOLLARS
- TURN-ON FOR PHASE C/D JANUARY, 1992
- PRIOR TECHNOLOGY DEVELOPMENT PROGRAM HAS BEEN COMPLETED
- GROUND FACILITY FOR DATA NOT INCLUDED
- SPACECRAFT DATA RATE NOT TO EXCEED TDRSS CAPABILITY
- NO ON BOARD DATA PROCESSING
- AN OMV IS AVAILABLE ON A LEASE BASIS
- AN AFT CARGO CARRIER WILL BE AVAILABLE
- SPECIAL FACILITIES NOT INCLUDED
- CONCEPT #1 - 20 M PARABOLIC PRIMARY, MULTIPLE SHUTTLE
- CONCEPT #2 - 20 M PARABOLIC PRIMARY, SPACE STATION
- CONCEPT #3 - 13 M PARABOLIC PRIMARY, SINGLE SHUTTLE/ACC

COST SUMMARY ASSUMPTIONS  
Figure 4.6-1

The elements of the observatory design and production costs are given in Table 4.6-2.

All costs, except those of Component 7 (Spacecraft), were obtained by analysis using the RCA/PRICE computer math model. Model input parameters were based on Kodak, McDonnell Douglas, and NASA experience, as well as industry-wide norms.

The Sunshield is an "accordian" self-erecting design which also makes use of different thermal coatings to control the telescope temperature. Concepts 1 and 2 both incorporate eight Scientific Instruments while Concept 3 uses only four SI's. The cost of the pointing control telescope includes hardware and labor to cobeersight with the telescope and maintain translational reference.

TABLE 4.6-2  
OBSERVATORY DESIGN AND PRODUCTION COSTS

<u>OBSERVATORY DESIGN AND PRODUCTION</u>	<u>COST (K\$, 1985)</u>			<u>COST MODEL INPUTS<sup>(1)</sup> BASIS/RATIONALE</u>
	<u>CONCEPT #1</u>	<u>CONCEPT #2</u>	<u>CONCEPT #3</u>	
1 PRIMARY MIRROR ASSEMBLY	\$294,000	\$294,000	\$74,000	ST MIRROR AND KODAK EXPERIENCE SPACE QUALIFIED MICROINCH ACTUATOR
● PRIMARY MIRROR ASSEMBLY				
● POSITION ACTUATORS, SENSORS, ELECTRONICS				
2 SECONDARY MIRROR ASSEMBLY	86,600	86,600	42,500	KODAK EXPERIENCE, DARPA DEVELOPMENT PROGRAMS
● MIRRORS				
● POSITIONING ACTUATORS/SENSORS/ELECT. AND CHOPPING				
● METERING STRUCTURE (STRUTS AND REACTION)				
● CRYOGENIC TEMPERATURE CONTROL				
3 SUPPORT STRUCTURE	33,800	33,800	41,200 (2)	MDAC EXPERIENCE
4 SUNSHIELD	144,200	144,200	101,000	MDAC EXPERIENCE
5 POINTING CONTROL TELESCOPE/SYSTEM	7,000	7,000	7,000	KODAK EXPERIENCE, DARPA DEVELOPMENT PROGRAMS
6 SCIENTIFIC INSTRUMENT MODULE	278,000	278,000	178,700	PAST NASA EXPERIENCE
● SCIENTIFIC INSTRUMENTS MODULE				
● CRYOGENIC SYSTEM				
● STRUCTURE				
7 SPACECRAFT	\$223,000	\$223,000	\$223,000	FSC
● BASIC MODULE				
● SOLAR PANELS				
● CMG'S				
TOTAL	\$1,066,600	\$1,066,600	\$667,600	

(1) RCA/PRICE MODEL, EXCEPT ITEM 7  
(2) INCLUDES \$25M FOR AUTOMATIC JOINT RIGIDIZATION

Spacecraft costs are based on a detailed estimate for a similar spacecraft, increased by 6.5 million dollars for upgraded gyros, and 19.5 million for increased power capacity. At present, we do not project significant spacecraft cost reductions for the smaller Concept 3 because power usage will not be substantially reduced.

Observatory launch and deployment costs components are presented in Table 4.6-3.

TABLE 4.6-3  
OBSERVATORY LAUNCH AND DEPLOYMENT COSTS

<u>OBSERVATORY LAUNCH AND DEPLOYMENT</u>				
<u>COMPONENT</u>	<u>CONCEPT #1</u>	<u>COST (K\$, 1985)</u>		<u>BASIS/RATIONALE</u>
		<u>CONCEPT #2</u>	<u>CONCEPT #3</u>	
1 SHUTTLE PAYLOAD INTEGRATION	\$ 13,900	\$ 13,900	\$ 8,870	MDAC EXPERIENCE
● SPECIAL PACKAGING				
● LAUNCH SUPPORT EQUIPMENT/SERVICING				
● GROUND TEST EQUIPMENT/TESTING				
2 LAUNCH AND FLIGHT OPERATIONS	640,000	320,000	116,600	\$106,600 PER STS MISSION, \$10,000 PER ACC
3 OBSERVATORY ASSEMBLY CHECKOUT AND TEST	23,100	30,800	95,900	MDAC EXPERIENCE
● ON-ORBIT TOOLS/ASSEMBLY AIDS				
● TEST EQUIPMENT				
● EVA				
TOTAL	\$677,000	\$364,700	\$221,400	

Concepts 1 and 2 each require three STS flights to place the observatory in orbit. The reduced volume and weight of hardware allow Concept 3 (13 m diameter primary) to be placed in orbit with a single Shuttle with an Aft Cargo Carrier (ACC). Although the ACC and associated automatic deployment equipment increase in integration costs over that of a single Shuttle, overall integration costs are still considerably less than those for three Shuttle missions in Concepts 1 and 2.

Launch and deployment costs are substantially higher for Concept 1 because several additional Shuttle flights, each limited to about nine days stay time, will be necessary to bring astronauts to complete the assembly process. The cost of the additional flights for astronaut labor may be reduced if they can be combined with other missions.

The additional per mission costs for ACC capability will depend on whether the ACC is developed as a NASA item, or as a commercial program. The assumed additional cost of \$ 10M per mission is the highest of the range of estimates provided by Martin-Michoud Operations. Since methods are not yet available to estimate the mission chargeable costs (if any) for assistance from the Space Station, no attempt was made to add such costs to the launch and deployment costs of Concept 2.

Space Station assembly, check-out, and test is assumed to require an environmental shroud against contamination, thus making it more expensive than the multiple Shuttle assembly of Concept 1. Additional costs of \$ 15M for automatic deployment fixturing for the ACC and \$ 50M for an aft-mounted manipulator arm make Concept 3 the most expensive assembly choice. The very limited stay time of the Single Shuttle/ACC demands a very high degree of deployment automation.

The resupply, refurbish, and exchange cost elements are shown in Table 4.6-4.

Resupply and SI exchange costs are judged essentially the same for all concepts. Further investigation is needed to determine if Concept 3, which has fewer Scientific Instruments, is significantly less costly.

Resupply includes cost for cryogenics, mechanical refrigeration pump, propellant and module changeouts, plus OMV lease and STS space lease. SI exchange includes OMV lease. It does not, however, include the cost of Scientific Instrument manufacture or refurbishment.

TABLE 4.6-4  
RESUPPLY, REFURBISH, AND EXCHANGE COSTS

RESUPPLY, REFURBISH, EXCHANGE		COST (K\$, 1985)			BASIS/RATIONALE
		CONCEPT #1	CONCEPT #2	CONCEPT #3	
1	RESUPPLY (3-YEAR INTERVALS)	\$141,000	\$141,000	\$141,000	SHUTTLE TRANSPORTATION OMV LEASE
	● CRYOGENS (He, H, N)				
	● REFRIGERATOR PUMP				
	● PROPELLENT				
	● MODULE CHANGE-OUTS				
2	SI EXCHANGE/REFURBISHMENT (2 TIMES)	2,100	2,100	2,100	OMV "TUG" AT FINAL APPROACH
	TOTAL:	\$143,100	\$143,100	\$143,100	

The top five cost elements for each of the concepts are ranked in Table 4.6-5. Numbers in parenthesis represent the cost in millions of dollars of each element. Launch and flight operations for deployment represent the only significant differences between Concepts 1 and 2. The Space Station (Concept 2) reflects cost savings realized by using Space Station facilities and personnel rather than launching additional Shuttles to provide the extended duration facilities and labor required for assembly.

The single Shuttle/ACC (Concept 3) shows launch and flight operations dropping from first to fourth place.

TABLE 4.6-5  
RANKED COST DRIVERS IN EACH CONCEPT

<u>CONCEPT #1</u>	<u>CONCEPT #2</u>
1. LAUNCH & FLIGHT OPERATIONS (640)	1. LAUNCH & FLIGHT OPERATIONS (320)
2. PRIMARY MIRROR ASSEMBLY (294)	2. PRIMARY MIRROR ASSEMBLY (294)
3. SCIENTIFIC INSTRUMENTS (278)	3. SCIENTIFIC INSTRUMENTS (278)
4. SPACECRAFT (223)	4. SPACECRAFT (223)
5. SUNSHIELD (144)	5. SUNSHIELD (144)

CONCEPT #3

1. SPACECRAFT (223)
2. SCIENTIFIC INSTRUMENTS (179)
3. RESUPPLY (141)
4. LAUNCH & FLIGHT OPERATIONS (117)
5. SUNSHIELD (101)

The high cost of actively cooling mirrors was discussed at Technical Progress Review Number 2. There was some thought that the secondary mirror cooling requirement could be relaxed sufficiently to eliminate the need for active cooling. In response to a request from that meeting, an estimate of the potential cost savings of deleting active secondary mirror cooling was generated. A savings of approximately \$38 M was estimated for Concept 1 or 2.

A comparison of primary mirror costs using fused silica and composite materials was conducted in response to interest expressed at the Technical Progress Review No. 2. The cost analysis results are included as Appendix D.4 of this volume.



## 4.7 ANALYSIS TOOLS USED TO GENERATE THE CONCEPTS

Figure 4.7-1 summarizes software programs employed in thermal and optical studies, cost estimating, and design.

### SUMMARY OF ANALYSIS TOOLS USED TO GENERATE THE SYSTEM CONCEPTS

- "NEVADA" COMPUTER PROGRAM (7TH EDITION, 1980 TURNER ASSOC., BREA, CA) AND KODAK CONV PROGRAM
  - RENO SECTION: USED IN THERMAL ANALYSES TO DETERMINE GEOMETRIC VIEW FACTORS ( $F_{1-j}$ ); RADIATION EXCHANGE ( $B_{1-j}$ ), BOTH DIFFUSE AND SPECULAR; SCRIPT - "F" FACTOR ( $B_{1-j} \epsilon_1$ ).
  - KODAK CONV PROGRAM: USED NEVADA OUTPUT TO COMPUTE RADIATION THERMAL TRANSFER CONDUCTANCE BETWEEN NODES (SCRIPT-"F" x AREA)
  - VEGAS SECTION: USED TO COMPUTE DIFFUSE PLUS SPECULAR EXTERNAL HEAT LOADS VERSUS ORBIT POSITION (SOLAR AND SURFACE REFLECTION AND EMISSION).
  - SPLIT SECTION USED TO CONSTRUCT COMPUTER DRAWING OF BOTH CONFIGURATION AND ORBIT GEOMETRY
- SINDA COMPUTER PROGRAM
  - USED FOR DETAILED NODAL TEMPERATURE AND CONTROL POWER ANALYSIS IN ORBIT
  - USED TO SOLVE HEAT BALANCES BETWEEN NODES WITH INPUT CAPACITANCES, CONDUCTANCES (SOLID PLUS RADIATION), BOUNDARY TEMPERATURES, EXTERNAL DIFFUSE PLUS SPECULAR HEAT LOADS, AND OPERATIONAL POWER PROFILES.
- KODAK PROPRIETARY OPTICAL ANALYSIS CODES
  - OPTICAL PHASED ARRAY PROGRAM: USED TO ASSESS EFFECTS OF PANEL ALIGNMENT ERRORS (OF THE SEGMENTED PRIMARY MIRROR) ON THE SYSTEM OPTICAL PERFORMANCE.
  - OPTICAL DESIGN PROGRAM: USED TO ESTABLISH THE FORMULAS FOR THE OPTICAL SYSTEMS OF THE SYSTEM CONCEPTS
- RCA - PRICE
  - USED FOR COMPARATIVE COST ESTIMATING OF SYSTEM CONCEPTS AND SUBSYSTEMS
  - PRICE IS A FAMILY OF PARAMETRIC COST PREDICTING MODELS FOR DEVELOPMENT AND PRODUCTION COSTS FOR PROPOSED ELECTRO-MECHANICAL DEVICES OR SYSTEMS WHILE STILL IN THE CONCEPT STAGE.
- AEROSPACE CORPORATION PAYLOAD MODEL
  - USED FOR COMPARATIVE COST ANALYSIS
- UNIGRAPHICS 3-D COMPUTER AIDED DESIGN SYSTEM (MDAC)

LIST OF ANALYSIS TOOLS  
Figure 4.7-1

## 5.0 CONCLUSIONS AND RECOMMENDATIONS FOR FURTHER STUDY

### 5.1 HIGHLIGHTS OF ANALYSES

From the system analysis and system concept synthesis a number of conclusions can be drawn. This section lists significant findings.

- Of five different optical configurations evaluated in this study, the on-axis Cassegrain (the LDR baseline before the study) was reconfirmed as the best choice. It is the optical form of each of the final three system concepts developed. All of the optical configurations studied have good and bad features, but the on-axis Cassegrain, with its f/0.5 primary mirror enables a small secondary mirror obscuration and compact length. These features coupled with placement of the instruments symmetrically about the optical axis offer potential for good pointing control.
- The largest aperture LDR observatory that can be put into orbit by a single Shuttle is approximately 13 meters - and that requires the use of the launch mode in which the attached External Tank with Aft Cargo Carrier is taken into orbit. At least three Shuttle launches would be needed to lift a 20-meter aperture LDR to orbit and additional Shuttle launches may be required for assembly support. The manned Space Station provides much greater potential for flexibility in assembling LDR in orbit than does the Shuttle alone.
- Primary mirror substrates made of metal will not meet surface quality performance requirements at operational wavelengths as low as 30 micrometers. Glass or glass ceramics should meet the performance requirements utilizing only rigid body motion (piston and tilt) control of the mirror segments. Composite materials (much less technologically mature) have potential in a concept utilizing rigid body motion control with radius control of the mirror segments. Cost favors glass as the leading candidate material.
- Trapezoidal segments are slightly preferred over hexagonal segments for the Primary Mirror. There are two reasons: (1) radial symmetry minimizes the number of different processing tools and (2) more structural options are available. It would be premature to make a segment shape selection.
- The secondary mirror should be made from a high dimensionally stable material, such as fused silica. Adequate metering can be provided by a triple bipod support made from graphite epoxy. Five degrees of rigid body motion control are required on the secondary mirror for wave front control between observations.
- A step sunshield concept with trim heaters on a plate located behind the primary mirror offers the potential to control the primary mirror uniformly over the exclusion angle requirements. To maintain the secondary mirror temperature, active cooling will be required.

- For the scientific instruments the initial cool-down heat loads and the large operational cryogenic heat loads require that a hybrid refrigeration system (comprising both stored cryogenics and active, closed cycle refrigeration machine) be employed. Some proposed LDR scientific instruments may require cooling of the detectors to as low as 0.1°K. Adiabatic demagnetization refrigerators and helium dilution coolers are two candidate approaches.
- Body pointing about the system center of mass is the preferred pointing approach. However, additional fine pointing may be required using a small optical element. Off-set sensing with a separate visible telescope is the preferred fine guidance sensing approach. Two chopping alternatives show promise: (1) neutral point chopping of the secondary mirror and (2) push/pull chopping of a fold mirror. If fine pointing is required it probably should not be implemented by the chopping mirror.
- Contamination control during on-ground build up should be maintained by using clean rooms and packaging. During in-orbit assembly the primary mirror and secondary mirror should be protected by a strippable coating. Some type of collapsible shroud might be needed during Shuttle revisiting for refurbishment and maintenance. Some type of clean room environment might also be needed for Space Station assembly.
- The Space Station will provide a highly useful broad service base for not only assembly of LDR but subsequent checkout, malfunction correction, launch to orbit and module exchange. At approximately three to six year intervals, the LDR could be returned to the Space Station for major refurbishment, overhaul, modifications, and replenishment.
- Lightweight, packageable support structures, capable of being assembled by astronauts, are conceptually feasible for LDR. Dynamic analysis will be required based on more advanced models of LDR to determine accurately the performance adequacy of the concepts.
- Extensive on-orbit deployment automation of LDR structures would result in poor Shuttle packaging density, high risk levels of complexity, and expensive development test programs.

## 5.2 TECHNOLOGY DEVELOPMENT

The primary study objective has been met. Twenty-two technology augmentation needs have been identified that are judged to be beneficial in meeting an LDR schedule requiring technology readiness by year-end 1991. Of these needs, five proposed projects are considered of primary importance.

- Dynamic structural control
- Human factors
- Hybrid cryogenic system for science instruments
- Active primary mirror
- Primary mirror contamination protection

A plan that integrates the 22 individual technology augmentation needs into three programs based on fundamental issues has been created (See Volume II). The programs are:

- Reflector Quality Program
- Pointing and Stability Program
- Detectability Program

In order to achieve a confident-level of technology readiness prior to an LDR program startup, it is recommended that NASA proceed to implement a technology initiative program. The integrated plan in Volume II provides a starting point for LDR program planning and decisions that will need to be made.

### 5.3 RECOMMENDATIONS FOR FURTHER STUDY

The technology initiatives programs are currently assumed to start in FY 1987. In the interim, continued study of LDR issues could provide valuable aid to LDR progress. Some areas we suggest be considered are:

1. Develop a dynamics model of a "point design" LDR, to provide basic guidance to the structural technology development projects. One of the unoptimized system concepts developed in this study could be selected as a departure point.
2. Study the post flight results of experiments aboard the Mission 1 Long Duration Exposure Facility (due to be retrieved in 1987), particularly those concerned with atomic oxygen effects, exposure of composites, debris impacts, and radiation effects.
3. Reassessment by the Science Coordination Group of the baseline requirement for the 75°K difference in temperature of the secondary and primary mirrors is recommended. Cryogenic cooling of the secondary appears necessary under the current requirement, introducing more complexity to the secondary mirror assembly design (which will also have active alignment features and possibly chopping mechanisms). A smaller differential temperature value (a few degrees) could simplify design significantly.
4. The time limitations placed on assembly of LDR from the Shuttle suggests Space Station assembly is an extremely important option. It is recommended that a review study of the requirements LDR imposes on Space Station be undertaken.

APPENDIX A  
GLOSSARY OF TERMS AND ACRONYMS

ACC	Aft Cargo Carrier or Aft Cargo Compartment
ACCESS	Assembly Concept for Construction of Erectable Space Structures
ADR	Adiabatic Demagnetization Refrigerator
AFOSR	Air Force Office of Scientific Research
ARC	Ames Research Center
ASE	Airborne (Aerospace) Support Equipment
BWO	Backward Wave Oscillator
CDR	Critical Design Review
CMG	Control Moment Gyro
CTE	Coefficient of Thermal Expansion
DARPA	Defense Advance Research Projects Agency
DoD	Department of Defense
EASE	Experimental Assembly of Structures in Extravehicular Activity
EVA	Extravehicular Activity
FIR	Far Infrared
FSC	Fairchild Space Company
HPA	Holding and Positioning Aid or Handling and Positioning Adapter
IDR	Interim Design Review
I/F	Interface
IR	Infrared
IR&D	Independent Research and Development
IVA	Intravehicular Activity
JPL	Jet Propulsion Laboratory
LHe	Liquid Helium
LH <sub>2</sub>	Liquid Hydrogen
LN <sub>2</sub>	Liquid Nitrogen
LO	Local Oscillator
MDAC	McDonnell Douglas Astronautics Company
MLI	Multilayer Insulation
MMU	Manned Maneuvering Unit
MPSS	Mission Peculiar Experiment Support Structure
NBP	Normal Boiling Point
NEP	Noise Equivalent Power

NEVADA	Net Energy Verification and Determination Analyzer (Thermal Computer Program)
OPS	Operations
OAST	Office of Aeronautics and Space Technology
OMV	Orbital Maneuvering Vehicle
ORU	Orbit Replaceable Unit
OTV	Orbital Transfer Vehicle
PAM	Payload Assist Module
PDR	Preliminary Design Review
PIDA	Payload Insertion Deployment Aid
PM	Primary Mirror
PSIA	Pounds per square inch absolute
RMS	Remote Manipulating System
RQM	Requirement
SATAN	Simulated Analog Thermal Analysis Network (Thermal Computer Program)
SC or S/C	Spacecraft
SCG	Science Coordination Group
SDI	Space Defense Initiative
SDV	Shuttle Derived Vehicle
SI or S/I	Science Instrument
SINDA	Systems Improved Numerical Differencing Analyzer (Thermal Computer Program)
SIS	Superconductor-Insulator-Superconductor
SIRTF	Space Infrared Telescope Facility
SM	Secondary Mirror
SMM	Submillimeter
SOW	Statement of Work
SRI	Stanford Research Institute
SS	Space Station
STEP	Space Technology Experiments Platform
STS	Space Transportation System
TWTA	Traveling Wave Tube Amplifier
VEM	Viscoelastic Material
WBS	Work Breakdown Structure

## APPENDIX C

### LIST OF REFERENCES

#### LDR BIBLIOGRAPHY

##### CONTRACTUAL DOCUMENTS

<u>No.</u>	<u>Title</u>
1	Statement of Work, No. 2-31229, dated April 3, 1984, Negotiated Contract No. NAS2-11861.
2	LDR System Concept and Technology Definition Study Kickoff Meeting, Briefing Materials, NASA-Ames Research Center, May 3, 1984.

##### GENERAL LDR-RELATED PUBLICATIONS

<u>No.</u>	<u>Title</u>
1	Hollenbach, D., et. al., NASA Conference Publication 2275, "Large Deployable Reflector Science and Technology Workshop, Volume II - Scientific Rationale and Technology Requirements," Asilomar Conference Center, Pacific Grove, CA, June 21-25, 1982.
2	Alff, W. H. et. al., NASA Contractor Report 152402, "Large Deployable Reflector (LDR)," Lockheed Missiles and Space Co., Inc., Palo Alto, CA, 94306, NASA Contract NAS2-10427, July, 1980.
3	Bandermann, L.W., and Alff, W.H., "In-Depth Study of the Effects of Shielding the Primary Mirror of a Large Deployable Reflector Telescope," Lockheed Missiles and Space Co., Inc., Palo Alto, CA, 94056, NASA Contract NAS2-10427, December 15, 1980.
4	Alff, W.H., et. al., "LDR Feasibility Study Update," Lockheed Missiles and Space Co., Inc., 94306, NASA Contract NAS2-11358, June, 1983.
5	Krim, M., et. al., NASA Contractor Report 166493, "Segmented Mirror Technology Assessment Study," Perkin Elmer Corp., Danbury, CT, 06810, NASA Contract NAS2-11104, March, 1983.
6	Anon., "A Technology Development Plan for the Large Deployable Reflector (LDR)," Presented to NASA Office of Aeronautics and Space Technology by Ames Research Center and Jet Propulsion Laboratory, Draft of June, 1982.
7	Kiya, M., "LDR Project Status: Past, Current, and Future Activities," (Briefing Charts), LDR Science and Technology Workshop, June 22, 1982.
8	Hedgepeth, J.M., "Precision Large Deployable Reflectors." Presentation Materials, to Jet Propulsion Laboratory, Astro Research Corporation, December 18, 1981.

## APPENDIX B

### LEGEND OF SYMBOLS, CONSTANTS, AND NUMERICAL VALUES

$\delta_x, \delta_y, \delta_z$	TRANSLATIONAL RIGID BODY MOTIONS
$\tau_x, \tau_y, \tau_z$	ROTATIONAL RIGID BODY MOTIONS
$cc_p, cc_s$	CONIC CONSTANT
$R_p, R_s$	RADIUS OF CURVATURE
$R_{PETZ}$	PETZVAL RADIUS OF CURVATURE
$f^#_p, f^#_s$	MIRROR FOCAL RATIO
$\lambda$	WAVELENGTH
$\widehat{\text{sec}}, \widehat{\text{min}}$	ARCSECONDS, ARCMINUTES
$\alpha$	COEFFICIENT OF THERMAL EXPANSION (CTE)
$\Delta\alpha$	CTE VARIABILITY
$\rho$	DENSITY
$E$	YOUNG'S MODULUS
$\kappa$	THERMAL CONDUCTIVITY
$C_p$	SPECIFIC HEAT
$D$	DIAMETER OR DIFFUSIVITY



<u>No.</u>	<u>Title</u>
9	Hedgepeth, J.M., "Support Structures for Large Infrared Telescope," Astro Research Corporation, Carpinteria, CA, 93013, ARC-TN-1121, 18 May 1983.
10	Hedgepeth, J.M., "Design Concepts for Reflector Antenna Structures," <u>Proc. SPIE</u> , Vol. 383, page 21, Deployable Optical Systems, January 18-19, 1983.
11	Hedgepeth, J.M., "Deployment and Concepts for Modular Assembly of Large Precision Reflectors," Consultant to Advanced Studies Office, Space Science Division, Ames Research Center, 1983(?).
12	Taylor, Thomas C., "LDR Structure in the Aft Cargo Carrier (ACC) - A Conceptual Study," Taylor and Associates, Inc., for Advanced Studies Office, Space Science Division, Ames Research Center, December 5, 1983.
13	Bush, H.G., and Heard, W.L. Jr., NASA Technical Memorandum 81905, "Recent Advances in Structural Technology for Large Deployable and Erectable Spacecraft," October, 1980.
14	Meinel, A.B., and Meinel, M.P., "LDR Configuration Approaches," JPL Contract No. 965017, June, 1982.
15	Meinel, A.B., Meinel, M.P., and Woolf, N.J., "Deployable Reflector Configurations," <u>Proc. SPIE</u> , Vol. 383, page 2, Deployable Optical Systems, January 18-19, 1983.
16	Woolf, N.J., and Ulich, B.L., "Alignment and Phasing of Deployable Telescopes," <u>Proc. SPIE</u> , Vol. 383, page 11, Deployable Optical Systems, December 18-19, 1983.
17	Swanson, P.N., et. al., "Large Deployable Reflector (LDR): A Concept for an Orbiting Submillimeter-Infrared Telescope for the 1990s," <u>Optical Engr.</u> , Vol. 22, No. 6, page 725, November/December 1983.
18	Swanson, P.N., et. al., "Plans for a Large Deployable Reflector for Submillimeter and Infrared Astronomy from Space," <u>Proc. SPIE</u> , Vol. 332, page 151, Advanced Technology Optical Telescopes, 1982.
19	Kiya, M.K., et. al., "A Technology Program for the Development of the Large Deployable Reflector for Space Based Astronomy," Paper 82-1850, Technology for Space Astrophysics Conference: The Next 30 Years, Danbury, CT, October 4-6, 1982.

<u>No.</u>	<u>Title</u>
20	Leidich, C.A., and Pittman, R.B., NASA Conference Publication 2275, "Large Deployable Reflector Science and Technology Workshop, Volume I - Executive Summary and Volume III - Systems and Technology Assessment", Asilomar Conference Center, Pacific Grove, CA June 21-25, 1982.
21	NASA Ames Research Center, "SIRTF-Free Flyer Phase A System Concept Description," PD-1006, 3 May 1984
22	NASA, <u>NASA Space Systems Technology Model</u> , Fifth Issue dated January 1984. NASA Office of Aeronautics and Space Technology, Code RS, Washington, D.C., 20546. Issued under the authority of Stan R. Sadin, Deputy Director, Program Development, OARTS/RS.
23	Steincamp, J.W., Mulqueen, J.A., and Maloney, J.W., Space Station Based Operations and Maintenance Support to Spacecraft, Platforms, and Orbit Transfer Vehicle (OTV), NASA/Marshall Space Flight Center, 35812.
24	NASA, Lyndon B. Johnson Space Center, <u>Satellite Services Catalog, Tools and Equipment</u> , JSC019211, September 1983.
25	NASA, Lyndon B. Johnson Space Center, <u>Satellite Services Handbook, Interface Guidelines</u> , JSC-19212, 23 December 1983
26	NASA, 1985 <u>Long-Range Program Plan</u>

SPECIAL TOPICS

Cryogenics

- | <u>No.</u> | <u>Title</u>   |
|------------|--|
| 1          | Abe, H., and Koga, K., "ESR Measurements at Temperatures Around 0.1K," <u>Japanese Journal of Applied Physics</u> , Vol. 13, No. 7, page 1145, July, 1974.   |
| 2          | Althouse, E.L., "Adiabatic Demagnetization of Ce (PO <sub>3</sub> ) <sub>3</sub> Glass," <u>Cryogenics</u> , Vol. 9, No. 3, page 177, June, 1969.  |
| 3          | Breckenridge, R.W., "Refrigerators for Cooling Spaceborne Sensors," <u>Proc. SPIE</u> , Vol. 245, page 112, Cryogenically Cooled Sensor Technology, 1980.  |
| 4          | Harris, R.E., et. al., "Cryo-Cooler Development for Space Flight Applications," <u>Proc. SPIE</u> , Vol. 280, page 71, Infrared Astronomy - Scientific/Military Thrusts and Instrumentation, 1981.   |
| 5          | Hashimoto, T., et. al., "Estimation of Fundamental Working Efficiency Data of Ferromagnetic Refrigerants in the High Temperature Magnetic Refrigeration," <u>Physica B&amp;C, Part 2</u> , Vol. 108, Issue 1-3, page 1107, August-September, 1981. |
| 6          | Kittel, P., "Magnetic Refrigeration in Space - Practical Considerations," <u>Journal of Energy</u> , Vol. 4, No. 6, page 266, November-December, 1980.   |
| 7          | Kittel, P., "Refrigeration Below 1K in Space," <u>Physica B&amp;C</u> , Vol. 108, Issue 1-3, page 1115, August-September, 1981.  |
| 8          | Lundholm J.G. Jr., "NASA Low and Ultralow Temperature Cryogenic Cooler Systems for Space Missions," <u>ISA Transactions</u> , Vol. 19, No. 1, page 3, 1980.  |
| 9          | Nara, K., et. al., "A Temperature Controller for Experiments Using Adiabatic Demagnetization," <u>Japanese Journal of Applied Physics, Part 1</u> , Vol. 21, No. 7, page 1083, July, 1982.   |
| 10         | Roach, P.R. et. al., "Mechanically Operated Thermal Switches for Use at Ultralow Temperatures," <u>Rev. of Scientific Instruments</u> , Vol. 46, No. 2, page 207, February, 1975.  |
| 11         | Samuelson, G.L. and Ailion, D.C., "Frequency Modulation Method for Performing Adiabatic Demagnetization in the Rotating Reference Frame," <u>Rev. of Scientific Instruments</u> , Vol. 41, No. 5., page 745, May, 1970.                            |

<u>No.</u>	<u>Title</u>
12	Kittel, P., "Temperature Stability Limits for an Isothermal De-Magnetization Refrigerator," <u>Adv. Cryo. Eng.</u> , Vol. 19, page 163 (1984)

### Sensors

<u>No.</u>	<u>Title</u>
1	Buhl, D., "Molecular Astronomy at Submillimeter Wavelengths," <u>Galactic and Extragalactic Infrared Spectroscopy</u> , M.F. Kessler and J.P. Phillips (eds.), page 221, D. Reidel Publishing Company, 1984.
2	Peck, D.D., et. al., "Molecular Astronomy Using Heterodyne Detection at 691 GHz," <u>International Journal of Infrared and Millimeter Waves</u> , Vol. 5, No. 3, page 329, Plenum Publishing Company, 1984.
3	Buhl, D., et. al., "Survey of Submillimeter Heterodyne Receiver Technology for the LDR Program," NASA-Goddard Space Flight Center, 1984(?).
4	Petuchowski, S., "Submillimeter Local Oscillators for Spaceborne Heterodyne Applications," NASA-Goddard Space Flight Center, Revised Outline, April 26, 1984.
5	de Graauw, T., "High Frequency Techniques in Heterodyne Astronomy," <u>Submillimetre Wave Astronomy</u> , page 323, J. E. Beckman and J. P. Phillips (eds), Cambridge University Press, 1982.
6	Encrenaz, P., "The Submillimeter Receiver of the Future," <u>Submillimetre Wave Astronomy</u> , page 315, J. E. Beckman and J. P. Phillips (eds), Cambridge University Press, 1982.
7	Chase, S.T., and Joseph, R.D., "Band-Pass Filters for Submillimetre Astronomy," <u>Submillimetre Wave Astronomy</u> , page 309, J. E. Beckman and J. P. Phillips (eds), Cambridge University Press, 1982.

### Optics and Telescopes

<u>No.</u>	<u>Title</u>
1	Erickson, E.F., and Mathews, S., "Evaluation of Image Quality in a Cassegrain-Type Telescope with an Oscillating Secondary Mirror," NASA TM X-3157, February, 1975.
2	Smith, S.T., "Point Spread Function for a Segmented Mirror System," <u>Proc. SPIE</u> , Vol. 383, page 32, Deployable Optical Systems, January 18-19, 1983.
3	Angel, J.R.P., "New Techniques for Fusion Bonding and Replication for Large Glass Reflectors," <u>Proc. SPIE</u> , Vol. 383, page 52, Deployable Optical Systems, January 18-19, 1983.

<u>No.</u>	<u>Title</u>
4	Leighton, Robert B., "A 10-Meter Telescope for Millimeter and Sub-Millimeter Astronomy," Final Technical Report for NSF Grant AST 73-04908, May 1978.
5	Baars, J.W.M., "Technology of Large Radio Telescopes for Millimeter and Submillimeter Wavelengths," <u>Infrared and Millimeter Waves</u> , Vol. 9, page 241, Academic Press, 1983.
6	Meinel, A.B., Meinel, M.P., Su, Ding-Qiang, and Wang, Ya-Nan, "Four-Mirror Spherical-Primary Submillimeter Telescope Design," Applied Optics, Vol. 23, No. 17, 3020, 1 September 1984.
7	Rodgers, J.M., "Nonstandard Representations of Aspheric Surfaces in a Telescope Design" Applied Optics, Vol. 23, No. 4, 520, 15 February 1984.
8	Korsch Optics Inc., "Highly Corrected Spherical - Primary Telescope Designs Final Report" for George C. Marshall Space Flight Center, October 1984
9	Su, Ding-Qiang and Wang, Ya-Nan, "Some Ideas About Representations of Aspheric Optical Surfaces," Applied Optics, Vol. 24, No. 3, 323, 1 February 1985.

## Chopping

- | <u>No.</u> | <u>Title</u>   |
|------------|--|
| 1          | Allen, D. A., <u>Infrared The New Astronomy</u> , (Keith Reid Ltd., Devon), pages 27-39, (1975).   |
| 2          | Allen, D. A., and Barton, J. R., "A Study of Sky Noise, 1.5 $\mu\text{m}$ -5 $\mu\text{m}$ ," Publ. Astron. Soc. Pac., Vol. <u>93</u> , 381, (1981).   |
| 3          | Apt, J., Goddy, R., and Mertz, L., "Simple Cassegrain Scanning System for Infrared Astronomy," App. Opt., Vol. <u>19</u> (10), 1590, (1980).   |
| 4          | Baum, W. A., in <u>Astronomical Techniques</u> , W. A. Hiltner, ed., The University of Chicago Press, pages 6-13, (1962).  |
| 5          | Fahrbach, U., Haussecker, K., and Lemke, D., "A New Chopper Design for Astronomical Infrared Photometry," Astron. Astrophys., Vol. <u>33</u> , 265, (1974).  |
| 6          | Gautier III, T. N., Hoffmann, W. F., Low, F. J., Reed, M. A., and Rieke, G. H., "Chopping Secondary Mirrors for Infrared Astronomy with the Multiple Mirror Telescope," in <u>Instrumentation in Astronomy III</u> , SPIE 172, 55, (1979). |
| 7          | Jorden, P. R., Long, J. F., MacGregor, A. D., and Selby, M. J., "A New Two-Mirror Focal Plane Chopper for Infrared Astronomy," Astron. Astrophys., Vol. <u>49</u> , 421, (1976).   |
| 8          | Kleinmann, D. E., "The Use of a Large Telescope in the Infrared," in <u>Far Infrared Astronomy</u> , M. Rowan-Robinson, ed. (Pergamon Press, Oxford), page 33, (1976).   |
| 9          | Koornneef, J., and vanOverbeeke, J., "Another Chopper Design for Astronomical Infrared Photometry," Astron. Astrophys., Vol. <u>48</u> , 33, (1976).   |
| 10         | Lemke, D., "Infrared Instrumentation of the Calar Alto Telescopes," Infrared Phys., Vol. <u>17</u> , 487, (1977).  |
| 11         | Low, F. J., and Rieke, G. H., in <u>Methods of Experimental Physics</u> N. Carleton, ed., (Academic, New York), Vol. <u>12</u> , 415-462, (1974).  |
| 12         | Meinel, A. B., and Meinel, M. P., "Aberrations of an IR Chopping Secondary," App. Opt., Vol. <u>23</u> (16), 2675, (1984).   |

## Chopping

- | <u>No.</u> | <u>Title</u>   |
|------------|--|
| 13         | Meinel, A. B., and Meinel, M. P., "Zero-Coma Condition for Decentered and Tilted Secondary Mirror in Cassegrain/Naysmith Configuration," Opt. Eng., Vol. <u>23</u> (6), 801, (1984).     |
| 14         | Milone, E. F., Robb, R. M., Babott, F. M., and Hansen, C. H., "Rapid Alternate Detection System of the Rothney Astrophysical Observatory," App. Opt., Vol. <u>21</u> (16), 2992, (1982). |
| 15         | Myrabo, H. K., "Stellar Chopping Photometry in Auroral Regions," Astron. Astrophys., pages 84, 297, (1980).  |
| 16         | Papoular, P., "The Processing of Infrared Sky Noise by Chopping, Modding and Filtering," Astron. Astrophys., Vol. <u>117</u> , 46, (1983).   |
| 17         | Reich, S. M., "Resonant Devices in Astronomy," Opt. Spectra, page 35, (December, 1977).  |
| 18         | Schneider, C. W., Kucerovsky, Z., and Brannen, E., "High-Precision Optical Switching Modulator," Rev. Sci. Instrum., Vol. <u>53</u> (9), 1376, (1982).                                   |
| 19         | Seki, H., and Itoh, U., "Oscillating Beam Spectrometer," Rev. Sci. Instrum., Vol. 51 (1), 22, (1980).  |

STRUCTURES AND TRANSPORTATION TO ORBIT (MDAC)

<u>No.</u>	<u>Title</u>
1). NASA SP-8013 March 1969	Meteoroid Environment Model 1969 (Near Earth to Lunar Surface)
2). NASA TM82478 1983	Space and Planetary Environment Criteria Guidelines for Use in Space Vehicle Development 1982 Revision (Volume 1)
3). NASA TM86460 Sept. 1984	Natural Environment Design Criteria For the Space Station Definition and Preliminary Design (First Revision)
4). JSC-20001	Orbital Debris Environment for Space Station
5). TOR-269 (4560-40)-2 V.C. Frost Aerospace Corp. 17 August 1964	Aerospace Meteoroid Environment and Penetration Criterion
6). NASA TM-X-74001 March 1977	Structural Stiffness, Strength and Dynamic Characteristics of Large Tetrahedral Space Struss Structures
7). NASA CR 152402 LMSC (ARC) July 1980	Final Report - Large Deployable Reflector
8). ARC-TN-1121 May 1983	Support Structures for Large Infra Red Telescopes
9). NASA TM-81904 October 1980	Deployable and Erectable Concepts for Large Spacecraft
10). NASA CR-172164 April 1983	Fabrication of Slender Struts for Deployable Antennas
11). AIAA 82-4116 Hedgepeth Vol. 20, No. 5, May 1982	Influence of Fabrication Tolerances on the Surface Accuracy of Large Antenna Structures
12). SD-TR-82-106 (U) USAF HQ Space Div. (AFSTC, Det 1)	Space Systems and Technology Workshop II Materials and Structures Panel Proceedings
13). MDAC Presentation to Military Space Systems Technology Workshop III, March 1984	Structural Materials (Status of Today and Tomorrow's Materials Technology)



The Correspondance Between Antenna Theory and Optics

by Joseph J. Charles, Eastman Kodak Company, Rochester, NY 14650

## INTRODUCTION

The objective of this paper is to bridge the gap between the traditional opticians's concepts of optical system performance and the electrical engineer's concepts of antenna performance. In the following discussion, I will show the essential identity of concepts used in both disciplines. While this discussion will be in terms of antennas for microwaves, it applies as well to any other frequencies.

In antenna theory, there is a reciprocity principle which states that the characteristics of the antenna are the same whether it is used as a receiving antenna or as a transmitting antenna. The only major difference between a transmitting antenna and a receiving antenna is the amount of power involved. An analysis of antenna performance may be done in whichever mode of operation is more convenient; the operation in the alternate mode may be deduced from reciprocity.

Both optical system and antenna system performance can be described in terms of the spatial distribution of the illumination in the system's aperture. In both cases, we think of the electromagnetic radiation transmitted by the aperture in three regions: the near field, the Fresnel region, and the Fraunhofer region. Here we are only interested in the far field or the Fraunhofer region. Furthermore, scalar diffraction theory is used wherein the diffracted field is described in terms of one transverse component of the diffracted wave.

Opticians usually use the notation  $U(P)$  to denote the complex amplitude of the optical field as a function of position coordinates  $P$ . The time dependence of the wave is understood. The field  $U$  is one of the components of the electromagnetic field; for example, it can be  $E_x$ , the x-component of the electric field intensity. The electric field intensity is the quantity which stimulates the sensation of vision and produces density in photographic emulsions.

Huygen's principle holds in antenna theory as well as in optics. The properties of conductors and dielectrics familiar to us from dealing with them at visible wavelengths also apply at microwave wavelengths, but of course, consideration must be given to the wavelength dependence of those properties. For example, there are dielectric microwave lenses which have the same shape as optical lenses and which may be designed using the principles of geometrical optics; the index of refraction of the lens medium is defined as usual and is equal to the square root of the dielectric constant.

The Fraunhofer diffraction pattern is described in terms of the spatial distribution in the aperture of some complex function.<sup>1-3</sup> The Fraunhofer diffraction pattern can be obtained by Huygen's principle, i.e., by summing the effects of elemental "sources" in the aperture. In antenna theory, the "sources" may be elemental electrical currents or alternately, they may be elemental

portions of the wavefront of the radiation field such as the electric field intensity. The latter perspective is usually used in optics.

Figure 1 illustrates a simple one-dimensional horn antenna and the coordinate system used. The far-field radiation pattern of an antenna  $E'(s)$  is proportional to the Fourier Transform of the aperture distribution:

$$E'(s) = \int_{-\infty}^{\infty} E\left(\frac{x}{\lambda}\right) \exp(-2\pi jxs/\lambda) dx/\lambda \quad (1)$$

Here  $E\left(\frac{x}{\lambda}\right)$  is the phasor representing the amplitude and phase of the electric field intensity in the antenna aperture.  $E\left(\frac{x}{\lambda}\right)$  is assumed to be zero outside of the aperture in the aperture plane. The variable  $x$  represents the displacement in the plane of the aperture. The variable  $s$  equals  $\sin\theta$ . Notice that the spatial frequency is given by  $\frac{s}{\lambda}$ .

$E'(s)$  is also called the angular spectrum of the aperture distribution. When normalized,  $E'(s)$  becomes characteristic of the antenna.  $|E'(s)|^2$  represents the antenna's power radiation pattern.

Let us consider a few simple examples for the aperture distribution.

Example 1. Uniform Illumination of a Rectangular Aperture of Width  $a$ .

Let

$$E\left(\frac{x}{\lambda}\right) = \begin{cases} 1, & |x| \leq \frac{a}{2} \\ 0, & |x| > \frac{a}{2} \end{cases} \quad (2)$$

This is illustrated in Figure 2a.

The electric field  $E'(s)$  is given by Eq. (1) and results in

$$E'(s) = a \frac{\sin(\pi as/\lambda)}{(\pi as/\lambda)} \quad (3)$$

Hence, the far field diffraction pattern of a uniformly illuminated one-dimensional antenna aperture follows a sinc function behavior just as does a uniformly illuminated single slit in classical optics. The normalized field radiation pattern

$$E_N' = E'(s)/E'(0)$$

is shown in Figure 2b. The intensity or power radiation pattern is given by

$$P(s) = |E'(s)|^2$$

and is shown in Figure 2c. Electrical engineers usually express power  $P$  in units of the decibel which is defined as

$$P_{dB} = 10 \log (P/P_0)$$

where  $P_0$  is some reference power. Here the power  $P(0)$  is used as the reference.

The radiation pattern has zeros every

$$s_{0n} = n\lambda/a, \quad n = 1, 2, 3... .$$

Suppose we wish to know the aperture diameter if we want the first zero to be at 1 arc sec ( $-5 \mu\text{rad}$ ). Therefore

$$a = \lambda/s_{01} = \lambda/\sin\theta_1 = \frac{\lambda}{5} \times 10^6$$

$$a = 0.2 \times 10^6 \lambda .$$

If  $\lambda = 10^{-4}\text{m}$ , then the aperture must be 20m wide.

The central part of the radiation pattern is called the main lobe, whereas the bands containing the secondary maxima are called the sidelobes.

The power at the maximum of the first sidelobe is only 4.7% that of the central maximum, and thus is 13.26 dB below the central maximum.

If the antenna were used as a transmitting antenna, it would transmit most of its power on-axis. It would transmit no power in the directions of the zeros of  $P(s)$ , and it would transmit small fractions of its power into each of its sidelobes. In the receiver mode, the radiation pattern would be interpreted as follows. A source on-axis would be received at full maximum antenna sensitivity. An equally intense source located in the direction of one of the zeros would not be detected at all. Relative to the on-axis source, an equally intense source located in the direction of either first sidelobe maximum would be received with 4.7% of the power; it would be said to be "13.26 dB down".

Beamwidth is used to describe the width of the central maximum between some arbitrarily chosen intensity levels. Common criteria for beamwidth designators are width at half-power, width at -20 dB, or width between the first zeros on each side of the central maximum. From Figure 2c, we see that the half-power (-3 dB) beamwidth is 0.90. Thus,

$$\Delta s = \Delta\theta = \frac{0.90}{\frac{a}{\lambda}} = \frac{0.90}{0.2 \times 10^6} = 4.5 \times 10^{-6} \text{ rad}$$

One-dimensional antenna analysis is useful because many two-dimensional antennas can be described as a product of separable one-dimensional aperture functions as, for example, a uniformly illuminated rectangular antenna.

For non-separable two-dimensional aperture functions, the angular spectrum is given in terms of the two-dimensional Fourier transform of the aperture function:

$$P(l,m) = \int_{-\infty}^{\infty} \int_{-\infty}^{\infty} E\left(\frac{x}{\lambda}, \frac{y}{\lambda}\right) \exp\left[-2\pi j\left(l\frac{x}{\lambda}, m\frac{y}{\lambda}\right)\right] dx dy . \quad (4)$$

Hence, the wave is assumed to be propagating with direction cosines (l,m,n) where  $n = (1-l^2-m^2)^{1/2}$ .

Example 2. Uniformly Illuminated Circular Aperture

Consider a uniformly illuminated circular aperture of radius  $r_0$  wavelengths. The electric field intensity in the aperture is given by:

$$E(r,\phi) = \begin{cases} 1, & r \leq r_0 \\ 0, & r > r_0 \end{cases}$$

The solution to this example, given by Skolnik<sup>1</sup>, is presented here. The electric field intensity a distance R from the aperture is proportional to:

$$E'(R) = \int_0^{2\pi} \int_0^{r_0} E(r,\phi) \exp(-j \frac{2\pi R}{\lambda} r \cos\phi) r dr d\phi \quad (5)$$

Substituting for  $E(r,\phi)$  and redefining  $E'$  to be a function of  $\theta$ , we have

$$E'(\theta) = \int_0^{2\pi} \int_0^{r_0} \exp(-j2\pi \frac{r}{\lambda} \sin\theta \cos\phi) r dr d\phi \quad (6)$$

which integrates to

$$E'(\theta) = 2\pi r_0^2 J_1(\xi) / \xi \quad (7)$$

where

$$\xi = 2\pi \frac{r_0}{\lambda} \sin\theta$$

and  $J_1(\xi)$  is a Bessel function of the first kind of order one. This is the same result obtained in classical optics for Fraunhofer diffraction from a uniformly illuminated circular aperture. The function  $J_1(\xi)/\xi$  is shown in Figure 3a. The power radiation pattern is shown in Figure 3b, and, in decibels, in Figure 3c. The central lobe in each case represents the familiar Airy disk. Note that the first zero occurs at

$$\xi_{01} = 2\pi \frac{r_0}{\lambda} \sin\theta_{01} = 3.83$$

or

$$\sin\theta_{01} = \frac{1.22\lambda}{2r_0} .$$

This is the familiar  $1.22\lambda/D$  of classical optics. In particular, if we wish  $\theta_{01}$  to be about 1 arc sec (5  $\mu$ rad)

$$2r_0 = \frac{1.22\lambda}{5} \times 10^6 = 0.2 \times 10^6 \lambda$$

If  $\lambda = 10^{-4}\text{m}$ , then the antenna must have an aperture diameter of about 20m.

Further analysis of this example is similar to that of Example 1, and will not be repeated here.

### Fraunhofer Diffraction Integral

At this point, it is useful to present the expression for the amplitude  $E'(\theta, \phi, R)$  at a point  $P(R, \theta, \phi)$  in the region of Fraunhofer diffraction of an arbitrary aperture  $A$ . The derivation may be found in standard texts such as those by Silver<sup>5</sup> or Born and Wolf<sup>6</sup>. The amplitude of the diffracted field is

$$E'(P) = \frac{j}{2\lambda R} \exp(-jkR) \int_A E(\xi, \eta) (\cos\theta + \hat{i}_z \cdot \hat{s}) \exp[jk\sin\theta(\xi\cos\theta + \eta\sin\theta)] d\xi d\eta \quad (8)$$

Here we are assuming that the aperture is in the  $xy$ -plane,  $(\xi, \eta)$  are coordinates of a point in the aperture,  $E$  is the aperture illumination function, and  $\hat{i}_z$  and  $\hat{s}$  are unit vectors in the  $z$ -direction and along a ray through the aperture.

### Antenna Gain

The directive gain,  $G_D(\theta, \phi)$ , or directivity, of a directional antenna is the ratio of the power radiated per unit solid angle in a particular direction to the power that would be radiated per unit solid angle in the same direction by a 100% efficient omnidirectional antenna. By reciprocity, the gain of a receiving antenna is the same as it would be in transmitting mode. When a single number is used to describe the directive gain, it usually represents the maximum directive gain. Directive gain is based on the antenna radiation pattern, and does not take into account various antenna losses.

The power gain  $G(\theta, \phi)$  of an antenna is defined as the ratio of the radiation intensity of the antenna to the radiation intensity from a lossless isotropic source with the same input power. Thus

$$G(\theta, \phi) = \frac{P(\theta, \phi)}{P_{\text{Total}}/4\pi} \quad (9)$$

where  $P(\theta, \phi)$  is the power per unit solid angle in the direction specified by  $(\theta, \phi)$ , and  $P_{\text{Total}}$  is the total power. The power gain of an antenna is always less than its directive gain.

It is important to understand clearly what gain is. Since the Poynting vector  $\vec{S}$  is the power passing through a unit area normal to the area, the power per unit solid angle is

$$P(\theta, \phi) = R^2 |\vec{S}| \quad (10)$$

$$= \frac{1}{2} R^2 \left[ \frac{\epsilon}{\mu} \right]^{1/2} |E'|^2 \quad (10a)$$

where  $E'$  is the electric field intensity of the diffracted field. The total power radiated equals the power flow through the aperture which, in turn, is the integral of the normal component of the Poynting vector over the aperture. Thus, the total power is

$$P_{\text{Total}} = \frac{1}{2} \left[ \frac{\epsilon}{\mu} \right]^{1/2} \int_A |E(\xi, \eta)|^2 (\hat{i}_z \cdot \hat{s}) d\xi d\eta \quad (11)$$

Upon substituting Eq. (8) into Eq. (10a) and using Eqs. (10a) and (11) in Eq. (9), the expression for gain becomes

$$G(\theta, \phi) = \frac{\pi}{\lambda^2} \frac{\left| \int_A F(\xi, \eta) (\cos\theta + s_z) \exp [jk \sin\theta (\xi \cos\phi + \eta \sin\phi)] d\xi d\eta \right|^2}{\int_A |F(\xi, \eta)|^2 s_z d\xi d\eta} \quad (12)$$

where  $s_z = \hat{i}_z \cdot \hat{s}$ .

If  $E(\xi, \eta)$  is an aperture function with constant phase over the aperture, the maximum radiation intensity will occur along the z-axis and the power gain is given by

$$G_M = \frac{4\pi}{\lambda^2} \frac{|\iint E(\xi, \eta) d\xi d\eta|^2}{\iint |E(\xi, \eta)|^2 d\xi d\eta} \quad (13)$$

where the integrations are over the antenna aperture. If  $E(\xi, \eta)$  is a constant (uniform antenna illumination), then

$$G_0 = \frac{4\pi}{\lambda^2} \frac{(\iint d\xi d\eta)^2}{\iint d\xi d\eta} \quad (14)$$

$$G_0 = \frac{4\pi}{\lambda^2} A$$

where  $A$  is the area of the aperture. Thus, a 20m diameter circular aperture will have a gain of approximately  $4 \times 10^{11}$  (116 dB) at a  $\lambda$  of  $10^{-4}$ m.

The definition of directive gain does not take into account certain power losses such as ohmic heating, RF heating, or that due to impedance mismatch. These losses are accounted for by the radiation efficiency factor  $\rho_r$  which is the ratio of the power gain to the directive gain of an antenna.

### Strehl Definition

In optics, Strehl definition  $D_S$  is defined as<sup>6,7</sup>

$$D_S = \frac{1}{A} \frac{\left| \int_A P(\xi, \eta) d\xi d\eta \right|^2}{\int_A [P(\xi, \eta)]^2 d\xi d\eta} \quad (15)$$

where

$$P(\xi, \eta) = P(\xi, \eta) \exp[-jW(\xi, \eta)]$$

is the complex pupil function composed of the amplitude transmittance pupil function  $P(\xi, \eta)$  and the wavefront error pupil function  $W(\xi, \eta)$ , and  $A$  is the area of the aperture.

Recognizing that the complex pupil function  $P(\xi, \eta)$  of Eq. (15) is the very same complex amplitude of the electric field intensity  $E(\xi, \eta)$  we have been using all along, we see that the maximum antenna gain is simply

$$G_M = \frac{4\pi A}{\lambda^2} D_S . \quad (16)$$

The maximum gain,  $G_M$ , of any antenna cannot exceed  $G_0$ , the gain of a similar uniformly illuminated antenna. The ratio of  $G_M$  to  $G_0$  is called the aperture efficiency  $\rho_a$  by Skolnik or the gain factor by Silver. From equations (14) and (16), we see that

$$\rho_a = D_S .$$

That is, what electrical engineers call aperture efficiency, optical engineers call Strehl definition. To quote Silver\*, the gain factor... "may be regarded as the efficiency of the aperture in concentrating the available energy into the peak intensity of the beam".

#### Effective Area and Physical Area

The effective area,  $A_e$ , of the aperture may be considered to be the physical area projected onto a plane parallel to the  $xy$  plane multiplied by a gain factor (or Strehl definition). Thus,

$$A_e = AD_S$$

#### Loss of Gain Because of Wavefront Error

The maximum gain of an antenna of area  $A$  which introduces a random uncorrelated wavefront error having a Gaussian distribution with a mean of zero and a (fixed) rms surface error of  $\epsilon$  (measured in the same units as  $\lambda$ ) has been derived by Ruze<sup>6</sup>:

\*See p. 178 of Silver's text which is cited in the references.

$$G = \frac{4\pi A}{\lambda^2} \exp [-(4\pi\epsilon/\lambda)^2] . \quad (17)$$

The maximum value of the gain is reached at

$$\lambda_M = 4\pi\epsilon \quad (18)$$

$$\text{or } \frac{\epsilon}{\lambda} = \frac{1}{4\pi} = \frac{1}{12.6} .$$

The maximum gain at this wavelength is

$$G_{\max} = \frac{A}{4\pi\epsilon^2} e^{-1} \quad (19)$$

thus, at maximum, the gain is reduced from ideal by  $e^{-1}$ , i.e., a factor of 0.37 or 4.3 dB.

Returning to Eq. (17), we see that as  $\epsilon$  approaches zero, the exponential Strehl term approaches unity and the gain approaches the ideal gain of Eq. (14). Furthermore, let us not lose sight of the fact that while the gain of an antenna with an rms surface error of  $\epsilon$  reaches a maximum at a wavelength  $\lambda = 4\pi\epsilon$ , the gain of the ideal antenna ( $\epsilon = 0$ ) has no maximum value, and continues to increase as  $\lambda$  gets smaller, approaching infinity as  $\lambda$  approaches zero.

The Strehl definition is reduced from unity by the random wavefront errors by the same factor as the gain, as originally derived by O'Neill<sup>9</sup> and presented by Swanson, et al<sup>10</sup>:

$$D_{S\epsilon} = \exp [-(4\pi\epsilon/\lambda)^2] \quad (20)$$

Notice particularly the consistency between Ruze's results, Eq. (17), O'Neill's result, Eq. (20), and the relationship between Strehl definition and gain, Eq. (16).

#### Comments on the Paper by Swanson et al

In Figure 1 of their paper, Swanson et al plot the Strehl definition of Eq. (20) and the normalized gain versus the ratio  $\epsilon/\lambda$ . This figure is reproduced here as Figure 4 for convenience. This figure is confusing and can be easily misinterpreted as a result of the use of a normalized gain. The normalized gain, obtained by dividing the gain Eq. (17) by its value at maximum, Eq. (19), is given by:

$$G_N = \left[ \frac{4\pi\epsilon}{\lambda} \right]^2 e \exp [-(4\pi\epsilon/\lambda)^2] . \quad (20)$$

The normalized gain  $G_N$  reaches maximum at  $\lambda = 4\pi\epsilon$  and clearly approaches zero as  $\epsilon$  approaches zero as shown in Swanson's figure. Does this mean one should "design in" a certain amount of wavefront error so the gain maximum occurs at some particular wavelength? How can the "gain" go to zero as  $\epsilon$  goes to zero?

The answer to the last question is that the gain does not go to zero as  $\epsilon$  approaches zero; the gain approaches the ideal gain as we saw earlier. The normalized gain does indeed go to zero as  $\epsilon$  approaches zero, but the problem is



that the normalization factor, Eq. (19), is undefined at  $\epsilon$  equal to zero! We must realize that the wavelength of maximum gain, being  $4\pi\epsilon$ , also goes to zero as  $\epsilon$  goes to zero, as expected! Thus, Figure 4 must be interpreted carefully.

The usual lowest acceptable value of  $D_S$  for a system to be considered diffraction limited is 0.8 which leads to a value of  $\epsilon/\lambda$  equal to 1/26.6. The gain at this point is 0.48  $G_{\max}$ . Swanson et al contend that given free choice of wavelength, the telescope would be operated at the wavelength of maximum gain and that this point, with a Strehl definition of 0.37, would be considered the diffraction limit. However, since Strehl definition equals the ratio of the volume under the surface of the optical transfer function of a given system containing aberrations to that of a similar aberration-free system, it seems untenable to claim that a system with a Strehl definition of 0.37 is diffraction limited.

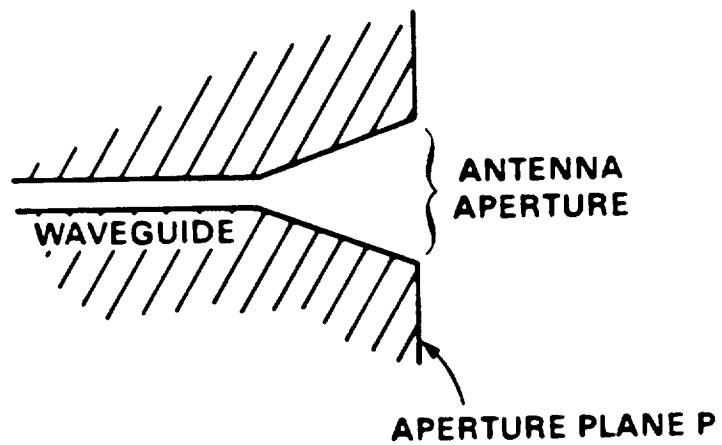
#### Clarification: Effects of Wavefront Error on Unnormalized Gain

Figure 5 shows the ideal gain  $G_0$  and the maximum gain  $G_M$  for an antenna having a 20m diameter circular aperture and an rms wavefront error  $\epsilon$  for various values of  $\lambda_M$  versus wavelength. Neglecting such issues as cost, technical difficulty, development time, etc., it is clearly desirable to have  $\lambda_M$  ( $= 4\pi\epsilon$ ) small enough so there is a tolerably small loss in gain over the operating range of the antenna. From an imaging point of view, the antenna can be considered to be nearly diffraction limited for wavelengths greater than  $2.11 \lambda_M$  since from that point on,  $D_S \geq 0.8$  and the loss in gain from ideal will be less than 1 dB. On the short wavelength side of  $\lambda_M$ , the loss in gain will be accompanied by a severe loss in image quality, particularly resolution. In Figure 5, the difference between the actual gain and ideal gain is the Strehl definition (in decibels).

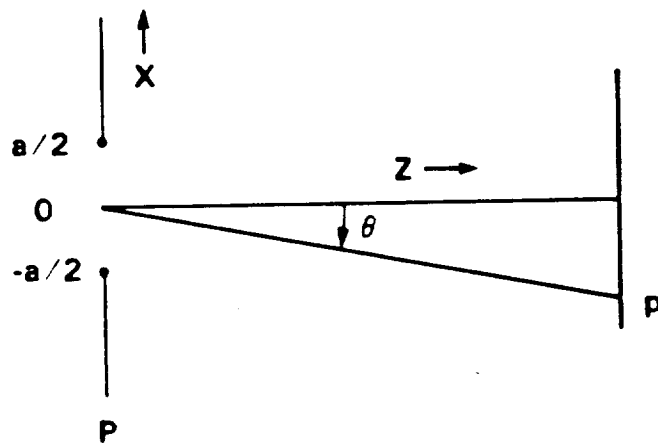
Figure 6 shows the gain curves given by Ruze for several actual radio telescopes and the corresponding ideal gain curves based on their aperture areas. Also shown are the ideal gain curves for three infrared telescope concepts: LDR (20m), SIRT<sup>11</sup> (0.85m), and IRAS<sup>12</sup> (0.60m). The actual antenna gain curves are asymptotic to a line a few decibels below their corresponding ideal curves because of the radiation efficiency factor mentioned earlier. Figure 6 gives some perspective to present LDR aspirations. Note that the gains of the three infrared telescopes follow directly from their aperture areas.

## REFERENCES

1. Skolnik, M.I., Introduction to Radar Systems. McGraw-Hill, New York (1962).
2. Bracewill, R., The Fourier Transform and Its Applications. McGraw-Hill, New York (1965).
3. Steinberg, B.D., Principles of Aperture and Array System Design. John Wiley & sons, New York (1976).
4. Goodman, J.W., Introduction to Fourier Optics. McGraw-Hill, New York (1968).
5. Silver, S., Microwave Antenna Theory and Design. Boston Technical Publisher's Inc. (1964).
6. Born, M. and E. Wolf, Principles of Optics, Fifth Edition, Pergamon Press, New York (1975).
7. Wetherill, W.B., "The Calculation of Image Quality", Applied Optics and Optical Engineering, Volume III, Ed. R.R. Shannon and J.C. Wyant, Academic Press, New York (1980).
8. Ruze, J., "Antenna Tolerance Theory--A Review", Proc. IEEE, Volume 54, No. 4, April, 1966.
9. O'Neill, E.L., Introduction to Statistical Optics. Addison-Wesley, Reading, MA (1963).
10. Swanson, P.N., S. Gulkis, T.B.H. Kulper, and M. Kiya, "Large Deployable Reflector (LDR): A Concept for an Orbiting Submillimeter-Infrared Telescope for the 1990's". Optical Engineering, Volume 22, No. 6, November/December, 1983.
11. McCarthy, S.G., "Shuttle Infrared Telescope Facility". Proceedings SPIE, Vol. 95 (1976).
12. Hedden, R.L., "A Telescope for the Infrared Astronomical Satellite (IRAS)". Proceedings SPIE, Vol. 95 (1976).



(A)

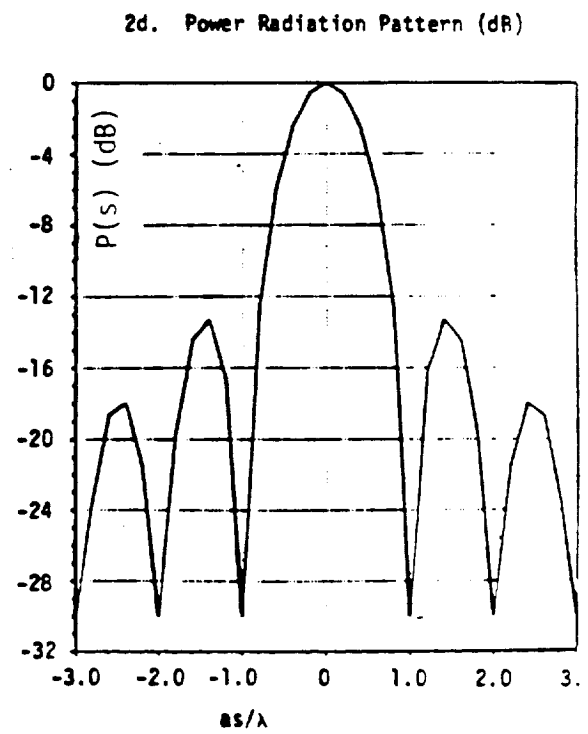
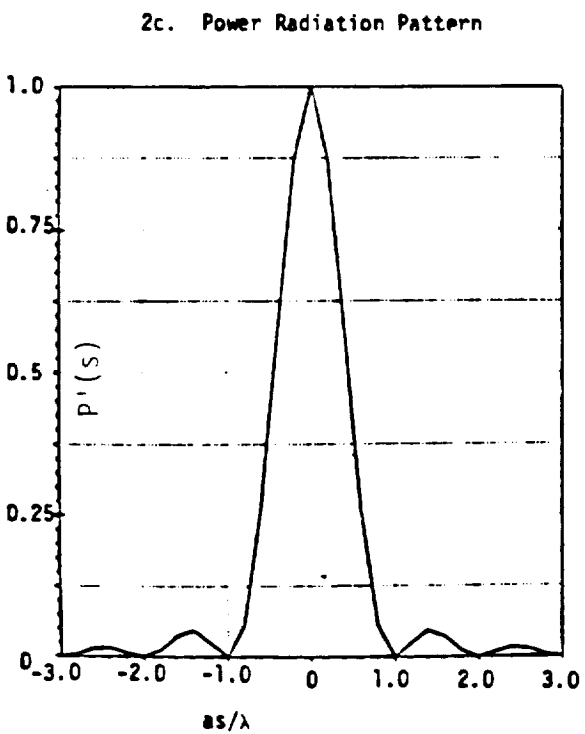
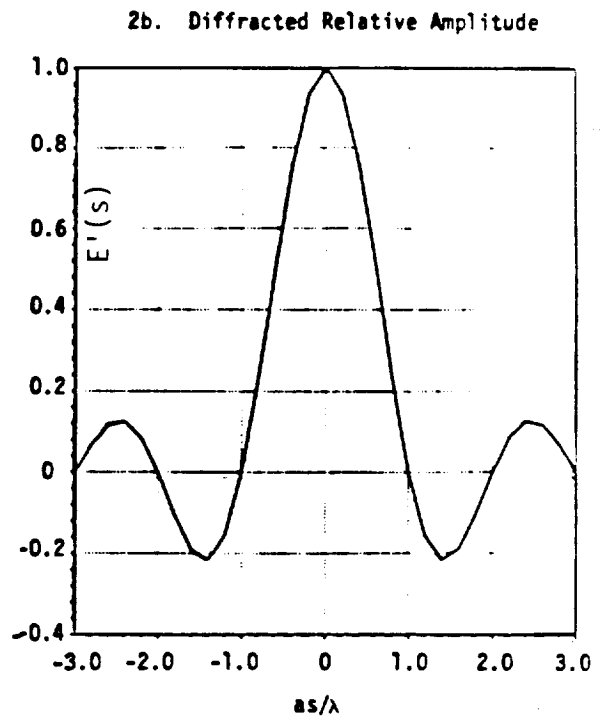
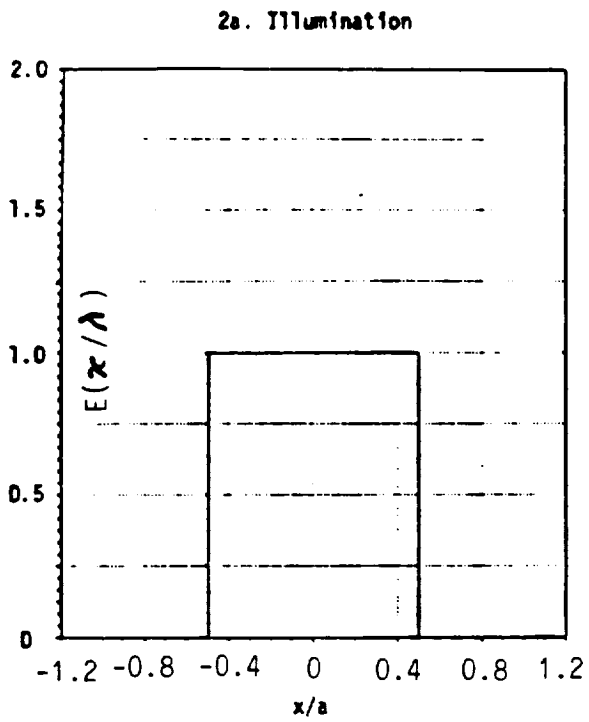


(B)

**A ONE-DIMENSIONAL HORN ANTENNA OF APERTURE WIDTH  $A$ .**

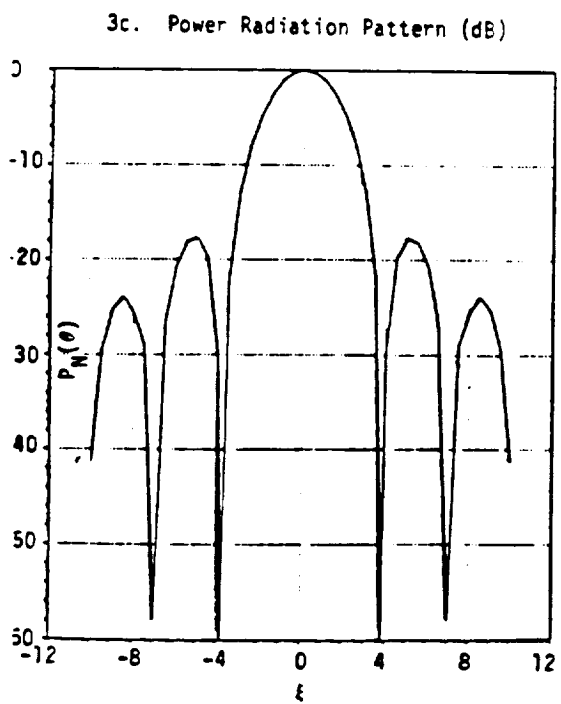
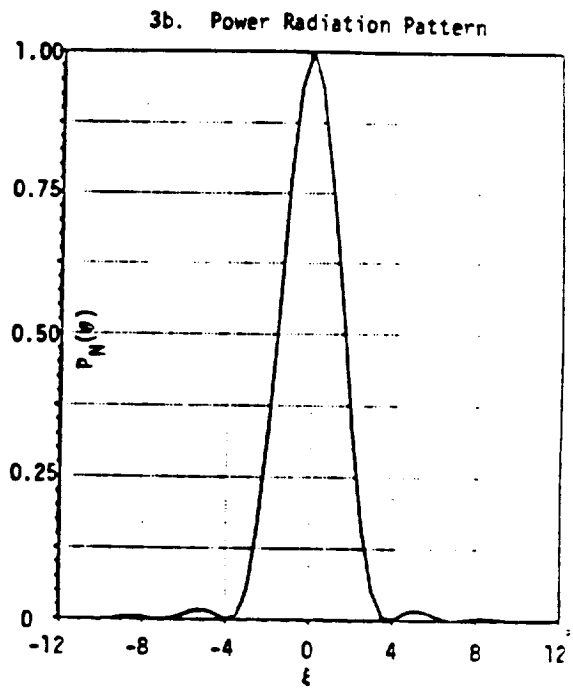
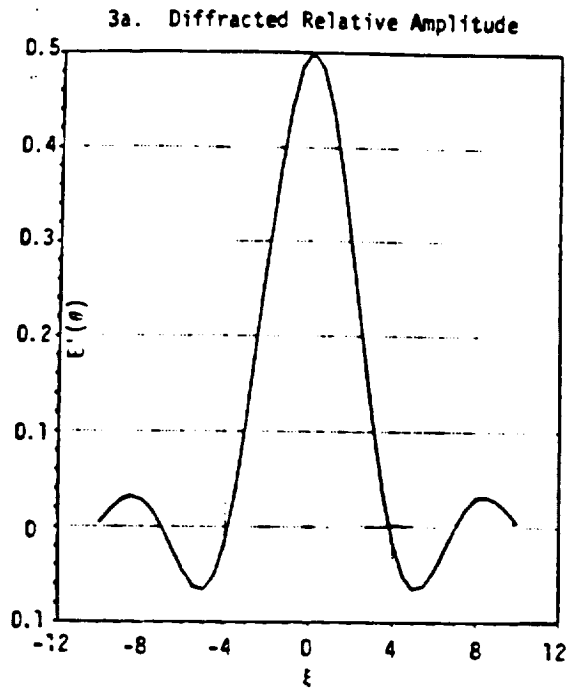
- A) ANTENNA CONFIGURATION**
- B) COORDINATE SYSTEMS**

Figure 1



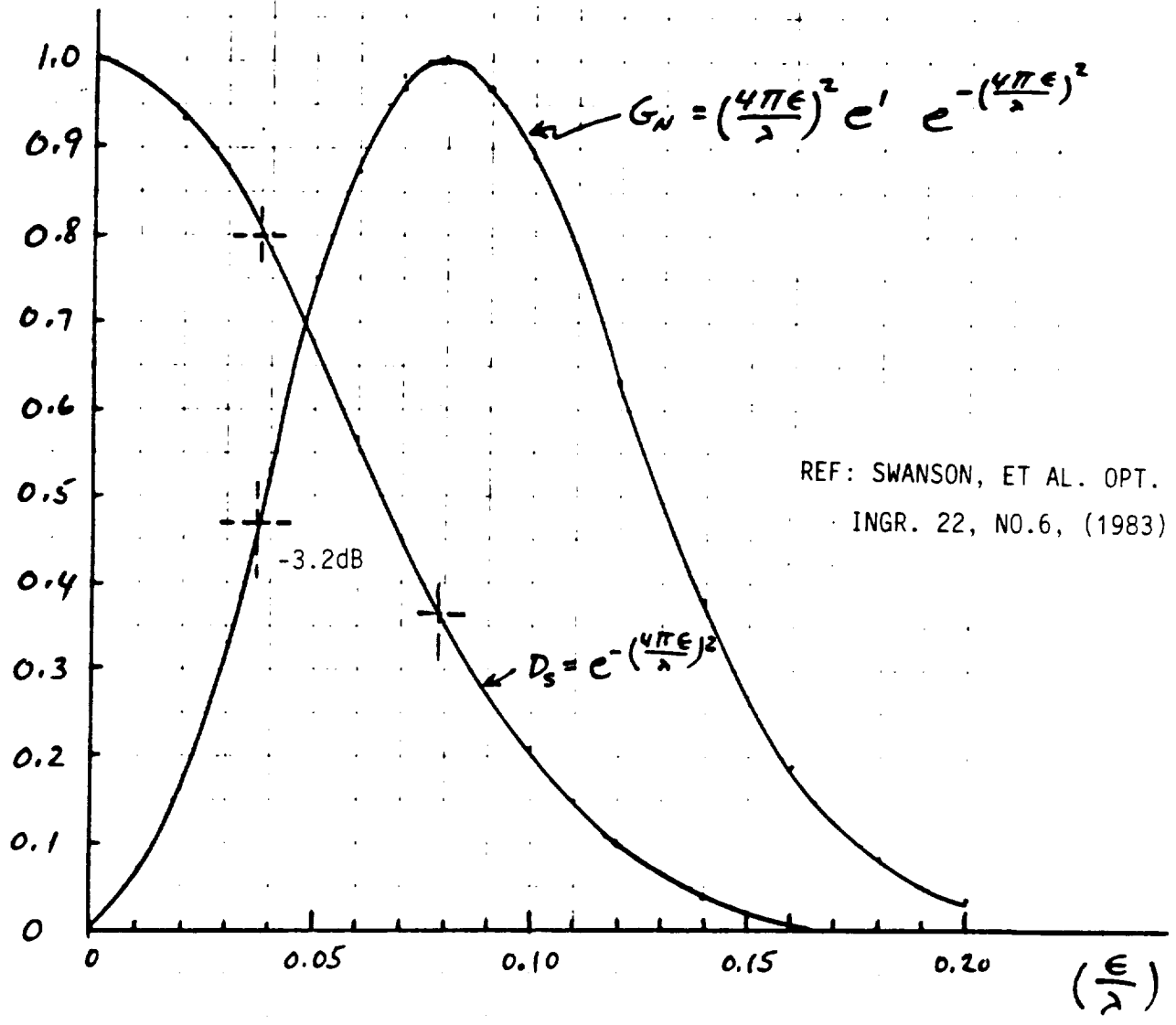
UNIFORMLY ILLUMINATED SLIT APERTURE

Figure 2



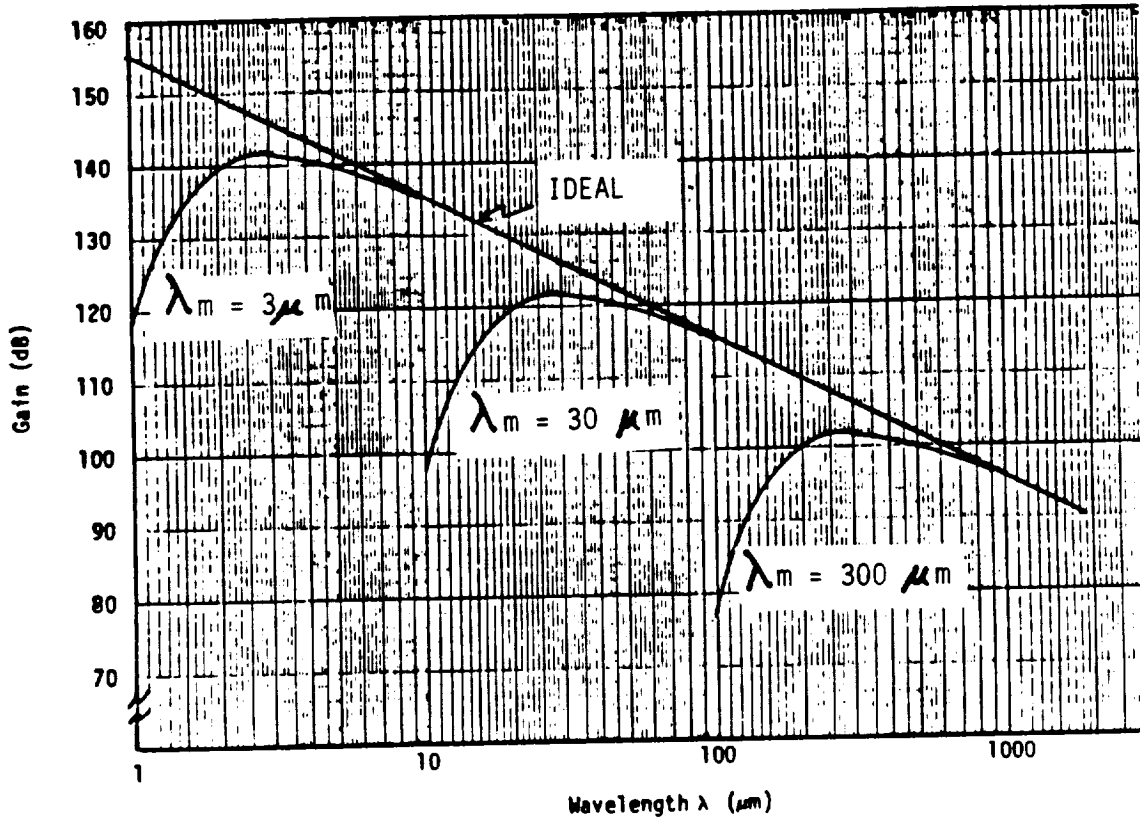
UNIFORMLY ILLUMINATED CIRCULAR APERTURE

Figure 3



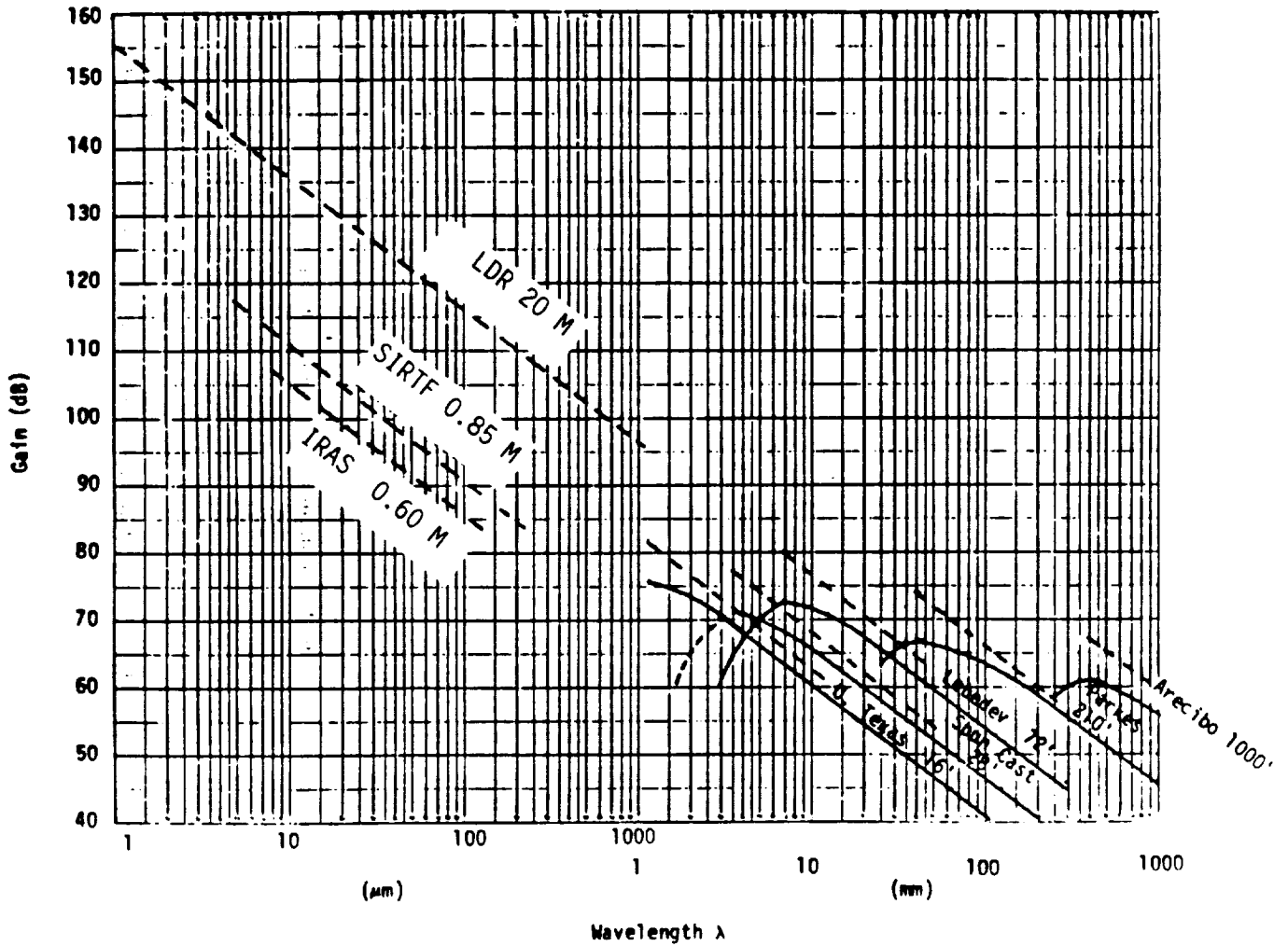
NORMALIZED GAIN AND STREHL DEFINITION VERSUS  $E/\lambda$

Figure 4



INFRARED ANTENNA GAIN

Figure 5



GAINS OF VARIOUS TELESCOPES

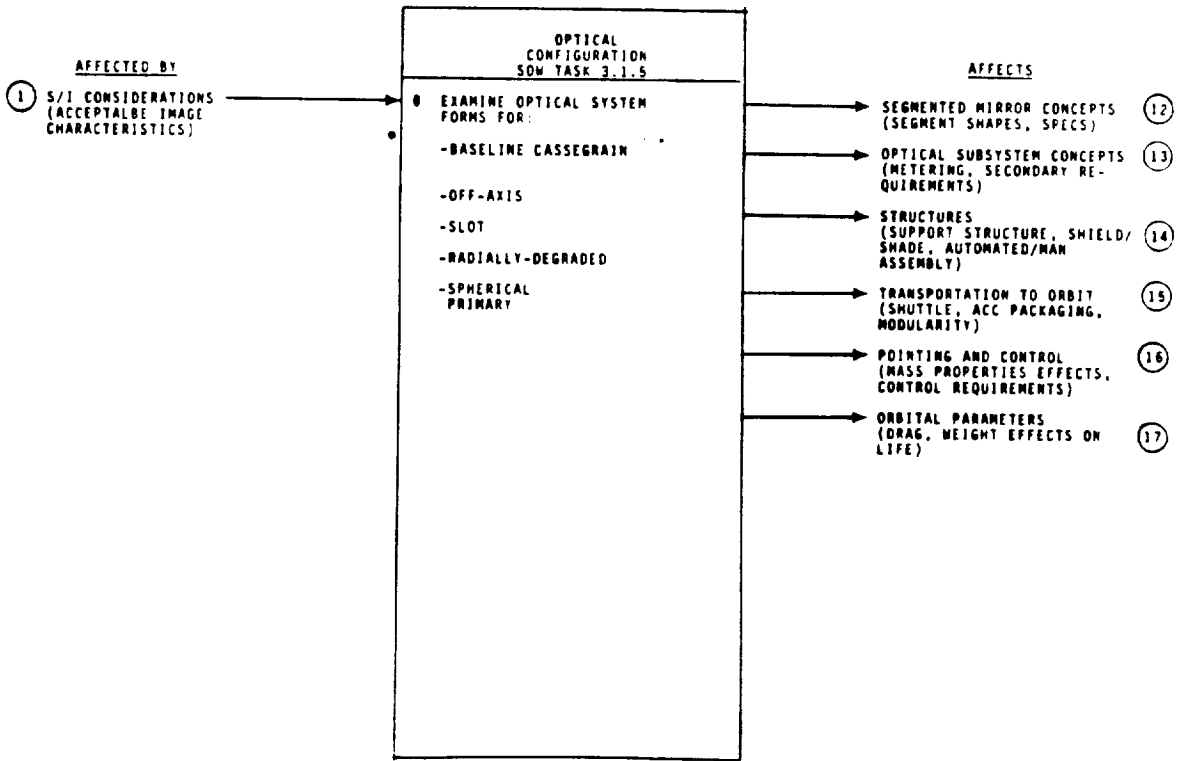
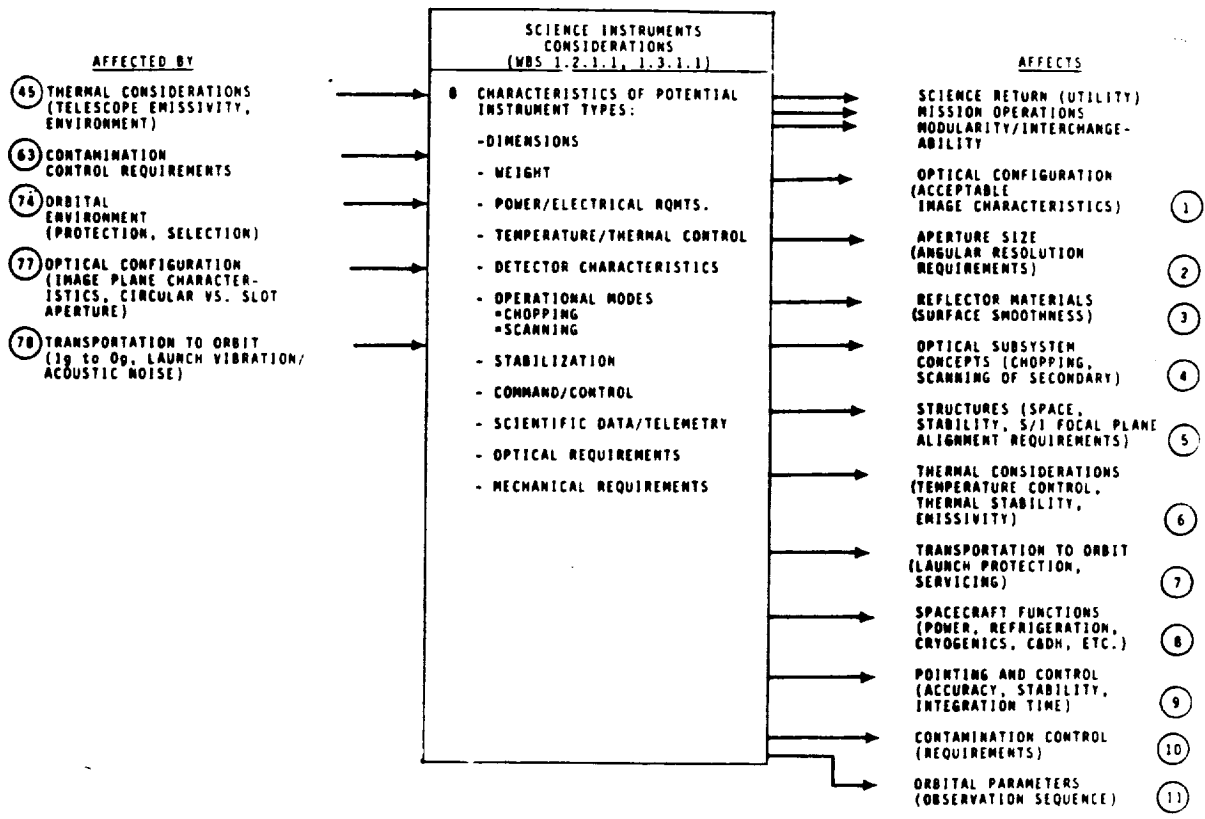
Figure 6

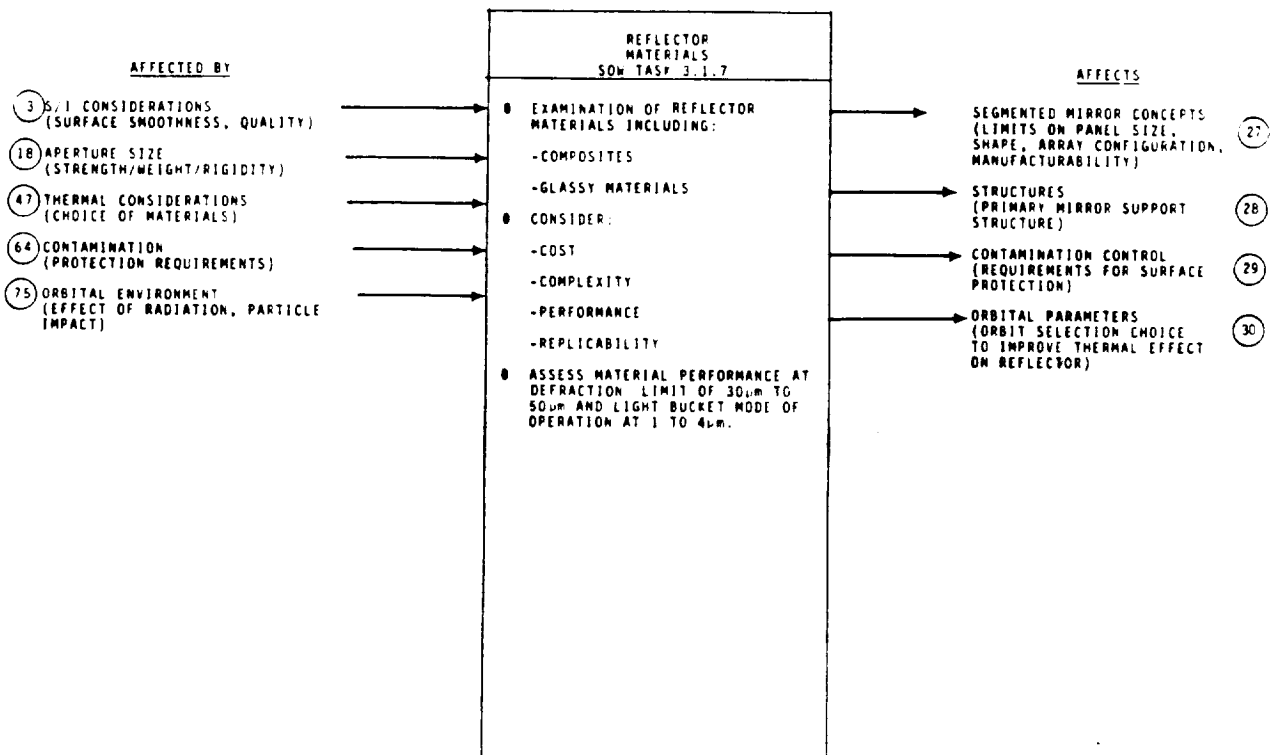
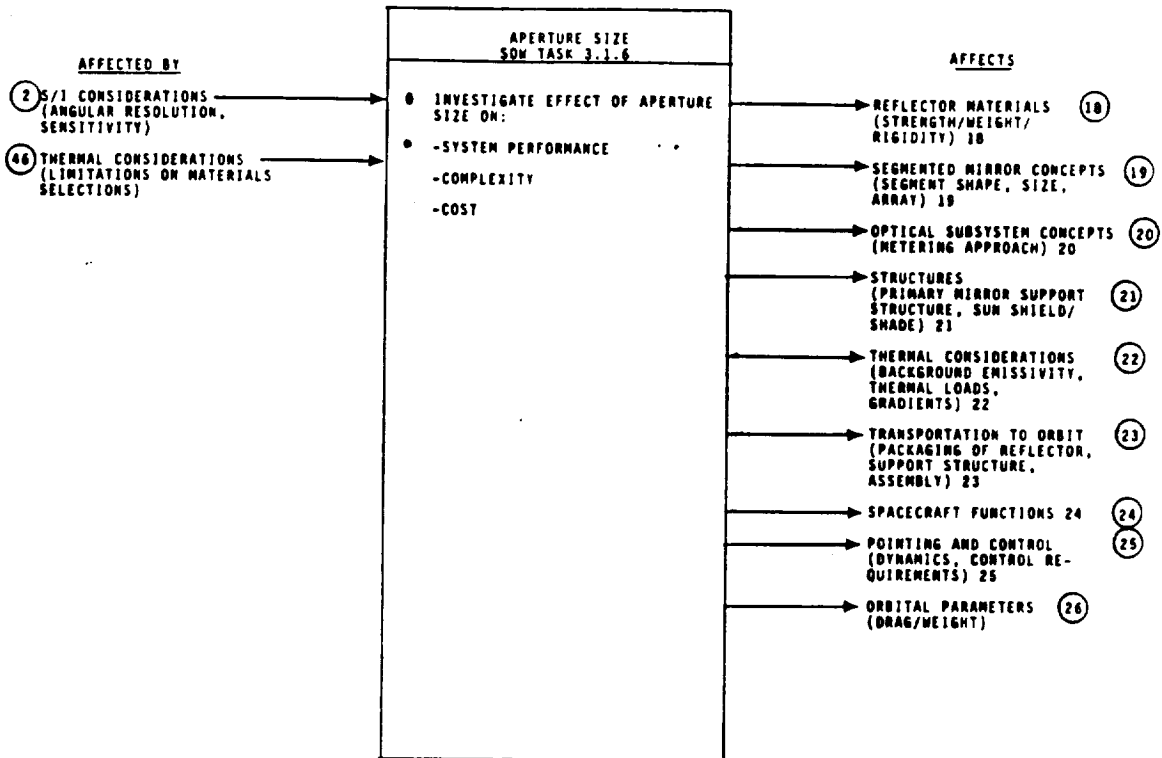


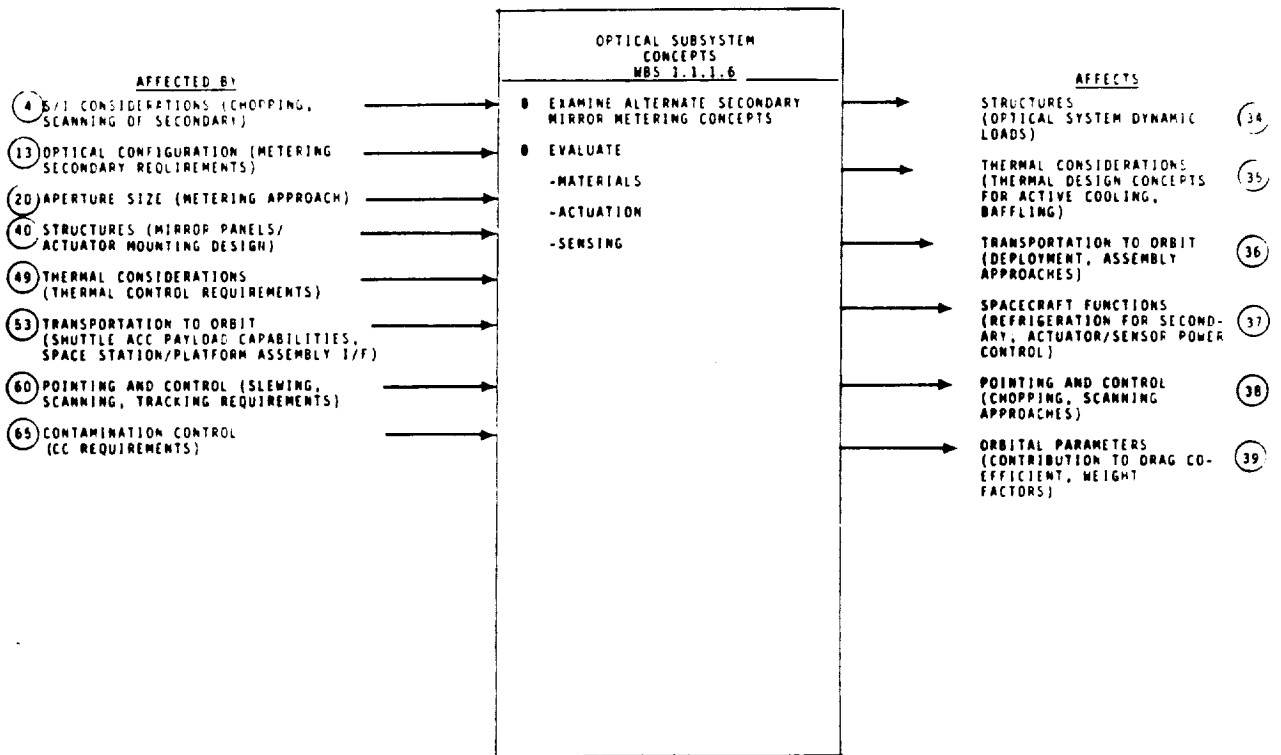
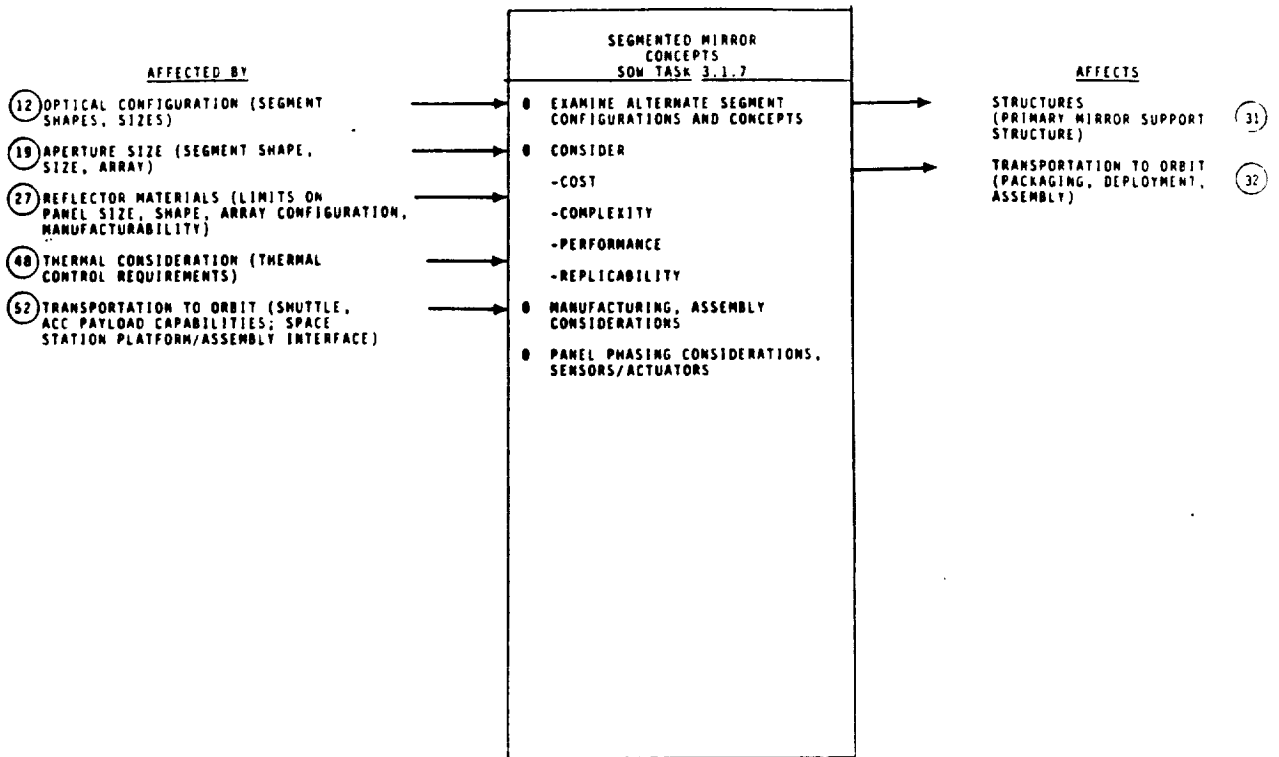
## APPENDIX D2

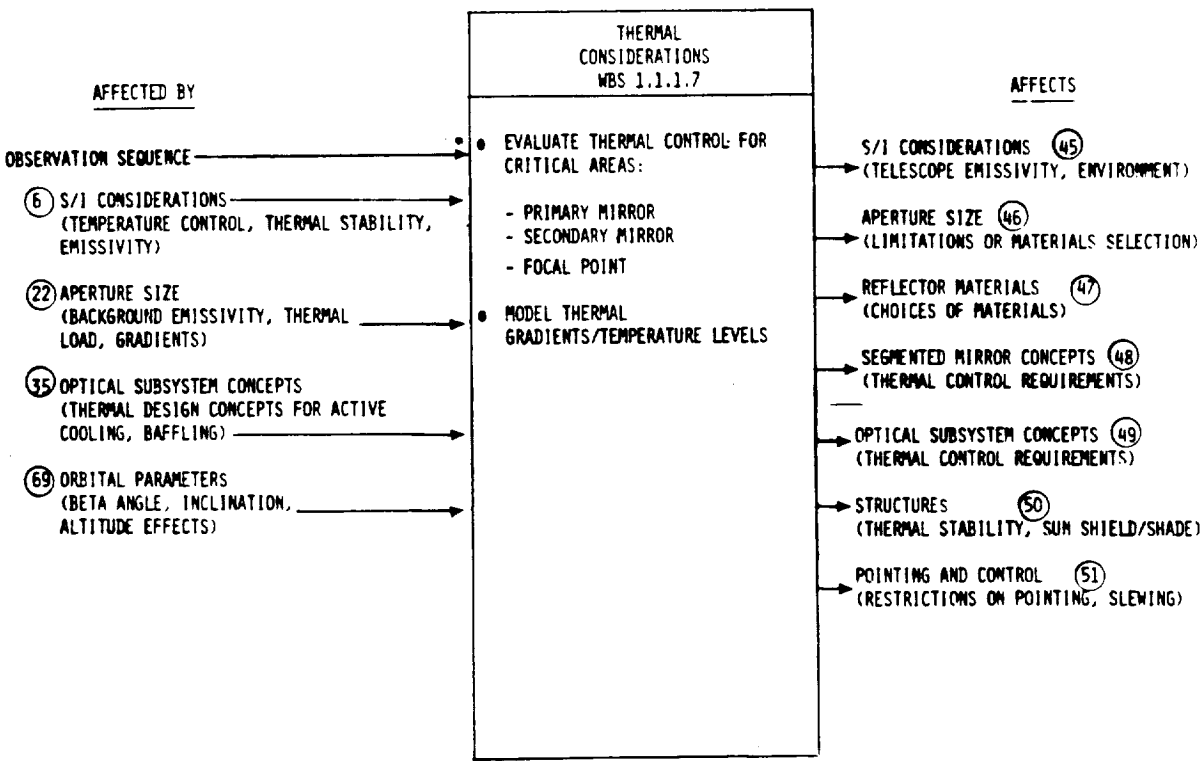
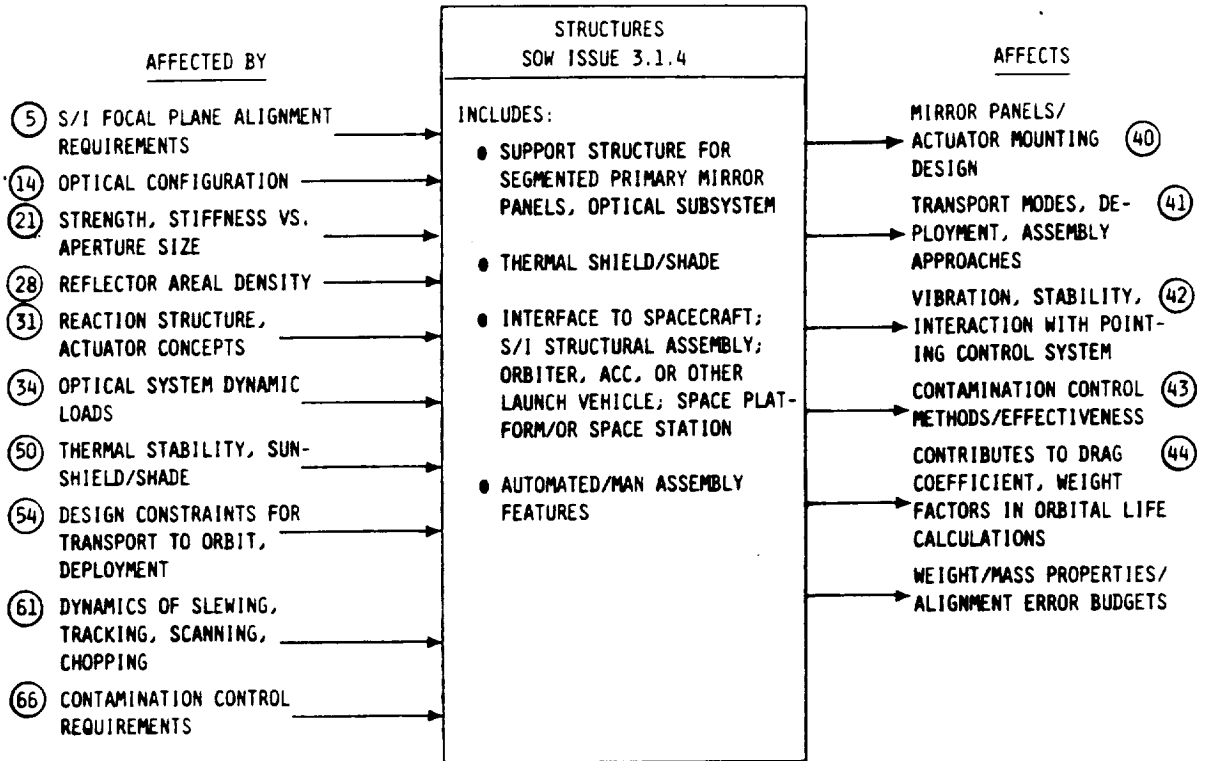
### Issue Interaction Summaries

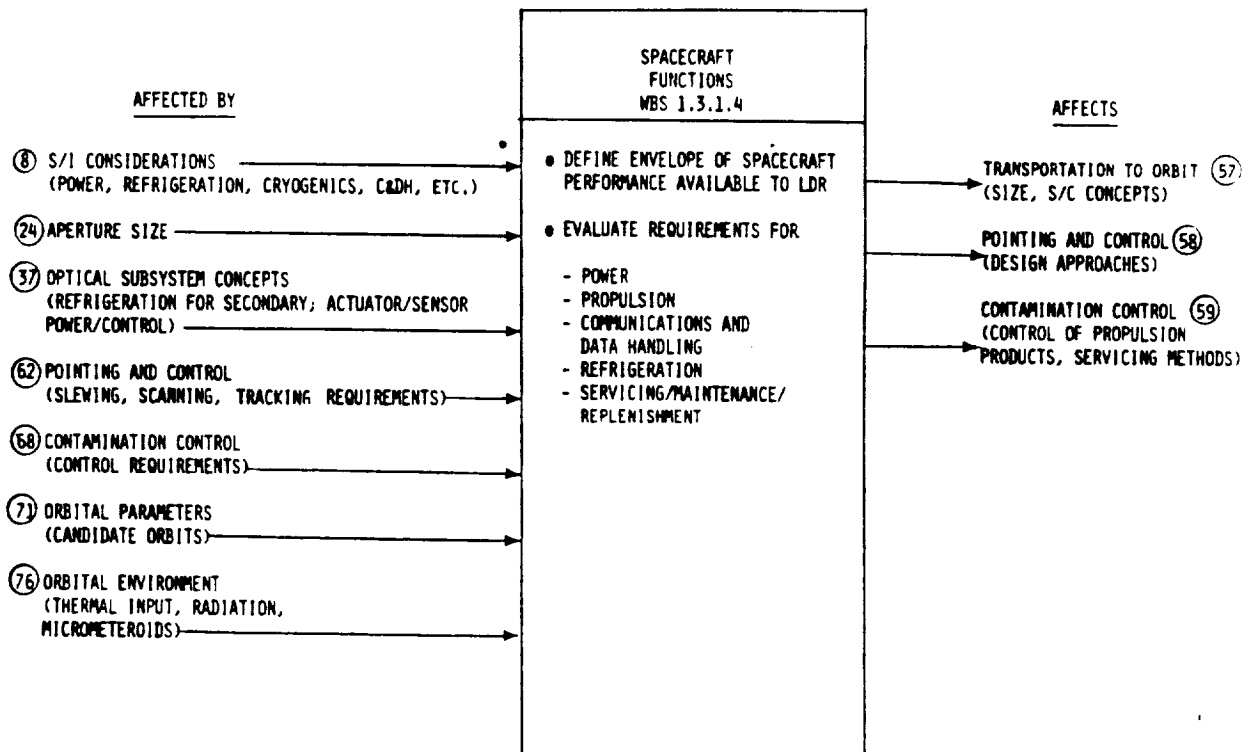
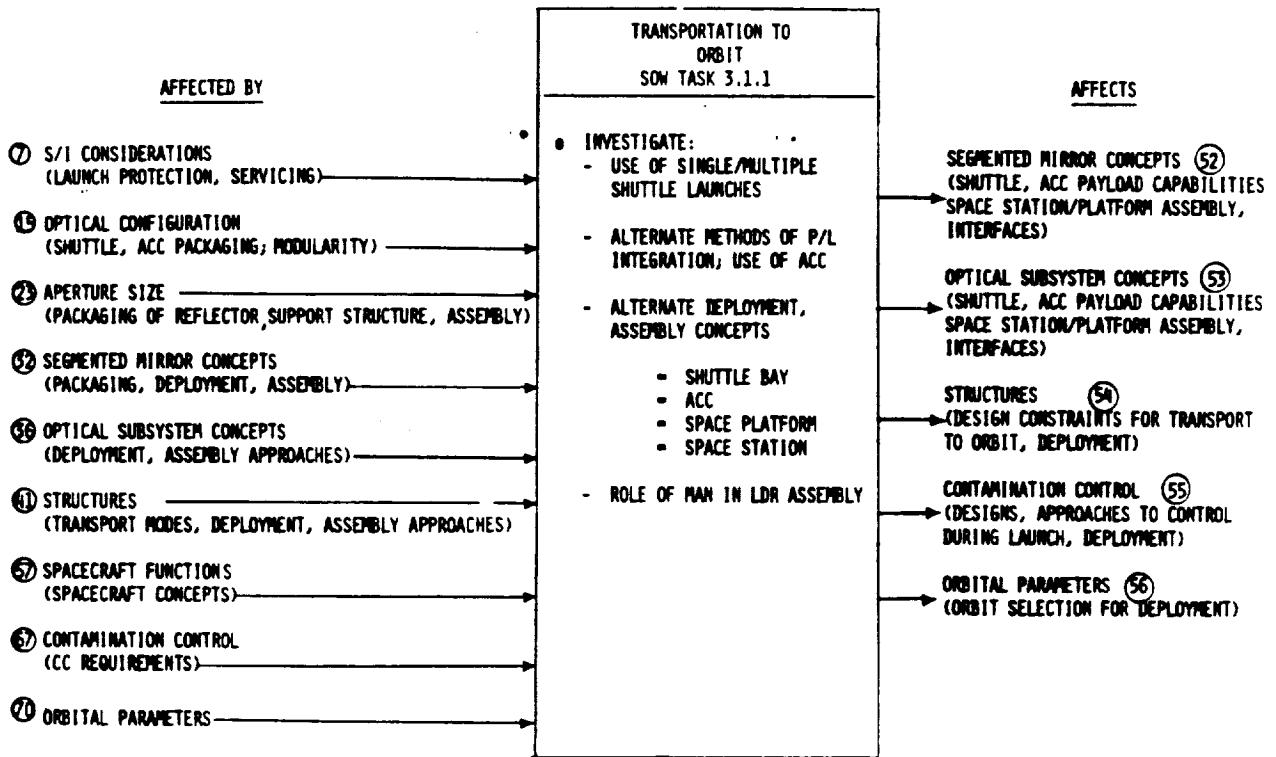
The charts in this Appendix illustrate the interplay of the technical issues addressed in the system analysis phase. They summarize the inputs and outputs of each element of the  $N^2$  matrix shown in Section 2.2.

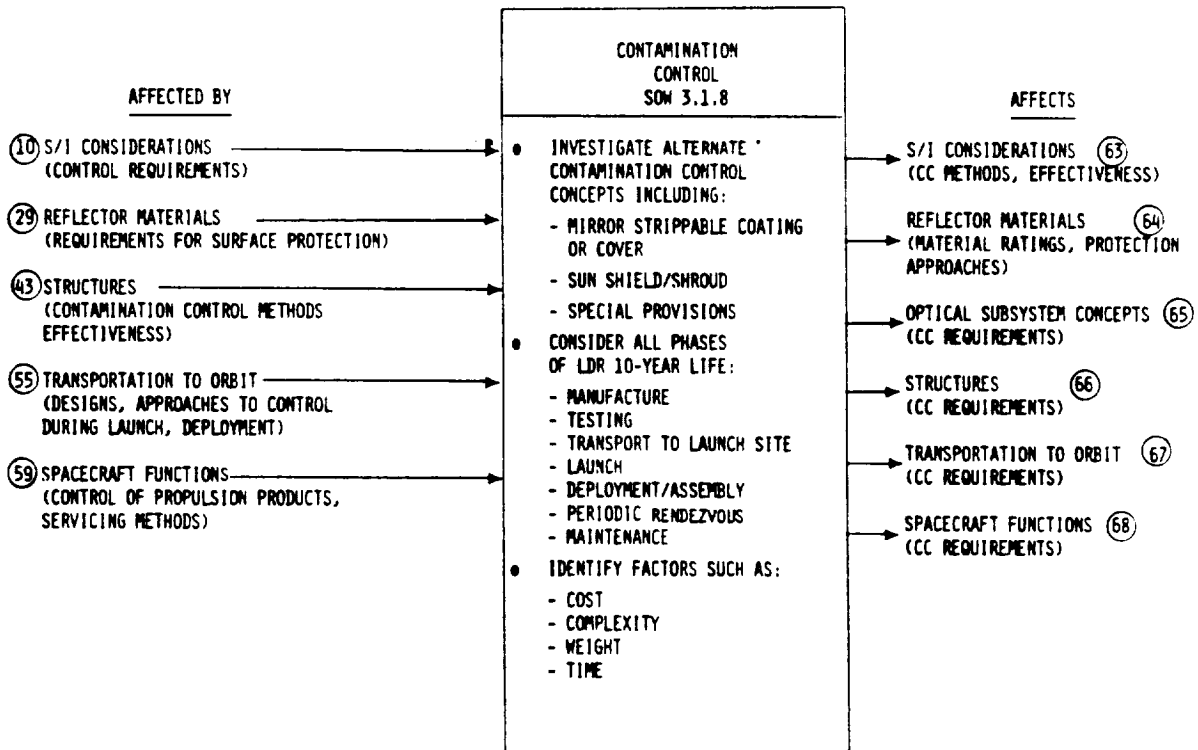
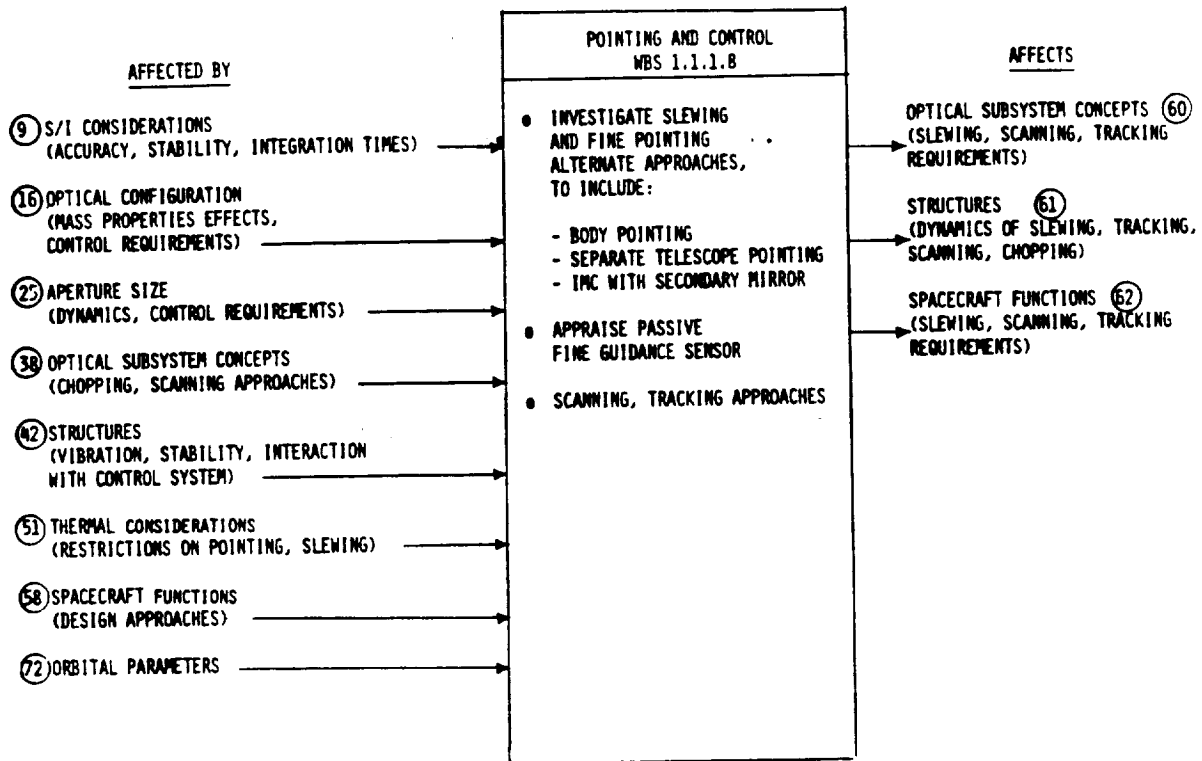


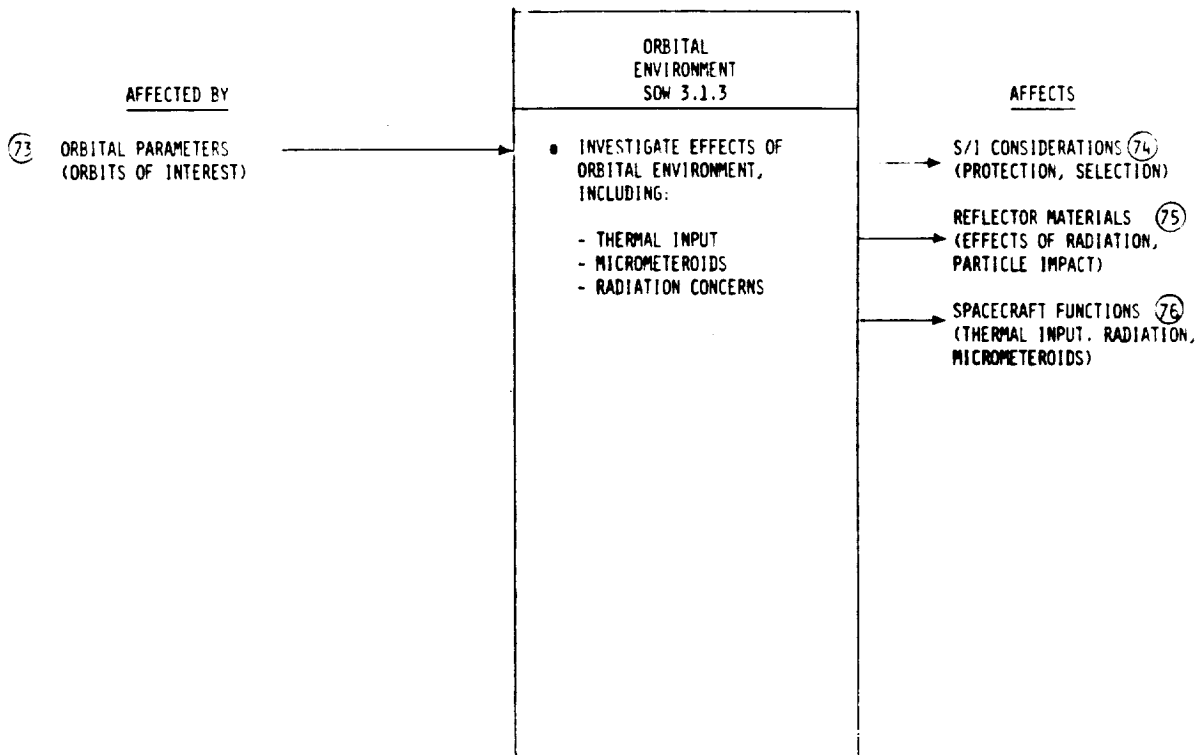
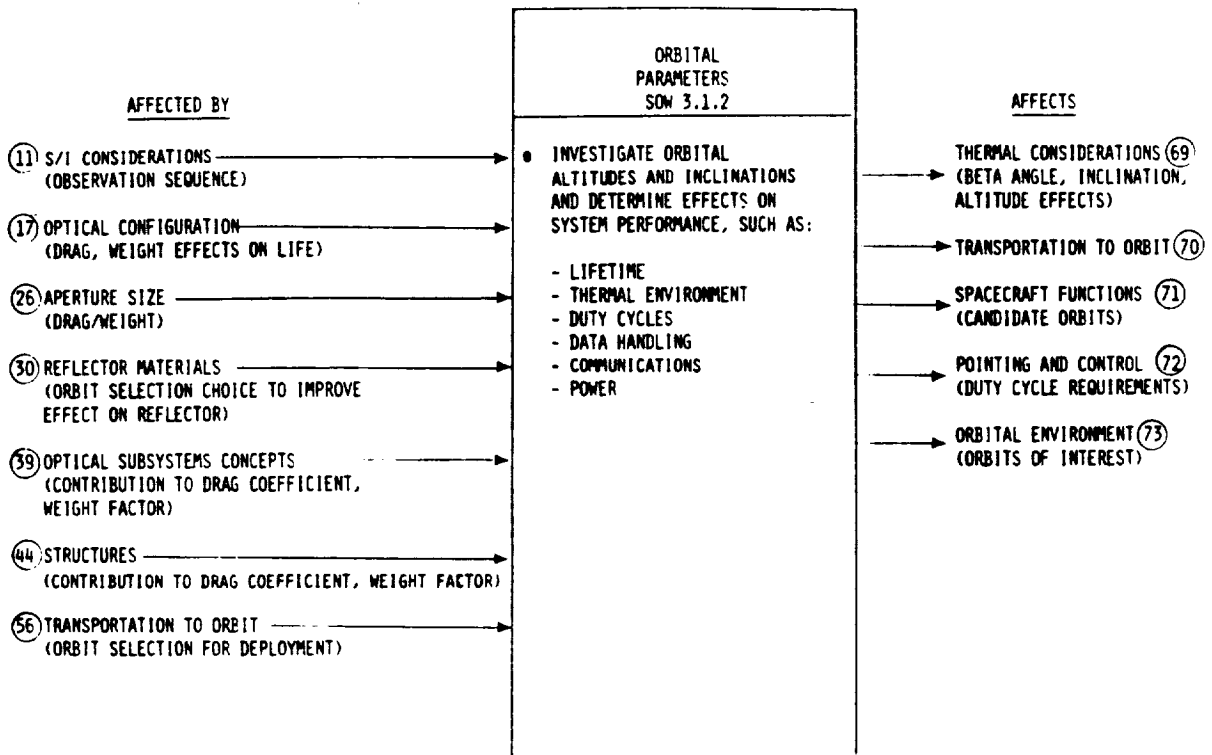














### APPENDIX D3

#### POINTING TRADE STUDY OF OPTICAL CONFIGURATIONS AND POINTING TECHNIQUES

The steps undertaken to develop Table 3.7-5 are listed in order as follows:

1) The energy requirements are based on the moment-of-inertia and torque analysis for a hypothesized mission profile for scan, track, and slew utilizing the different pointing techniques (see section 3.7.3). The magnitudes of the moments-of-inertia and torque profiles were assigned a numerical rating on a scale of 1 to 10, with 1 being the lowest rating, and 10 the highest (see Table D3-1).

Table D3-1

#### ENERGY RATINGS

<u>Rating</u>	<u>Resultant Moment-of-Inertia (<math>10^3 \text{ kg} \cdot \text{m}^2</math>)</u>	<u>Torque (N-M)</u>		
		<u>Scan</u>	<u>Slew</u>	<u>Track</u>
10	<100	<1	<500	<.001
9	100-200	1-10	500-1000	.001-.002
8	200-300	10-20	1K-1.5K	.002-.005
7	300-400	20-30	1.5K-2K	.005-.01
6	400-500	30-40	2K-2.5K	.01-.03
5	500-600	40-50	2.5K-3K	.03-.05
4	600-700			.05-.07
3	700-800			.07-.09
2	800-900			.09-.11
1	>1000	>150	>10K	>.11

Each rating step was further broken down into 10 divisions (i.e.,  $I = 130 \text{ kg} \cdot \text{m}^2$  was given a rating of 9.7, while  $I = 190 \text{ kg} \cdot \text{m}^2$  was given a rating of 9.1).

2) Table D3-2 summarizes the results of step 1 as a function of the contributing parameter. Each column represents the rank of that configuration on an absolute basis as determined from Table D3-1. The row-wise rankings are not completely absolute in the sense that no attempt was made to insure that the rank division steps were equal for each parameter (i.e., an 8 for body pointing in the slew mode was equal in degree of difficulty to an 8 for telescope moment-of-inertia).

Nevertheless, since they are based on magnitude, torque values are absolute within themselves, as are moment-of-inertia values. For each parameter, the telescope technique received the higher rating of the coarse pointing candidates. Overlooking bearing friction, the secondary mirror technique was rated highest for the tracking mode indicating that the tracking mode could possibly best be performed by using the fine pointing technique. Note the contribution of the tertiary mirror technique to moments-of-inertia is insignificant. Therefore, no differentiation between secondary and tertiary pointing was made at this step. The rightmost column is the overall energy rating of the configurations.

3) The telescope moment-of-inertia values were tabulated directly in Table 3.7-5 (the ranks for the techniques in Table 3.7-5 are arrived at by comparing the ranks in Table D3-2). The torque values in Table 3.7-5 were arrived at by averaging the highest rated technique for each of the mission torque profile operations.

4) The alignment, manufacture, and stability and control values for the large optics (primary and secondary mirrors) are tabulated in Table D3-3. A relative rating depicting the degree of difficulty in manufacturing, alignment, or control of different optical parameters was used to arrive at the tabulated ratings for each of the large optics. The average of these values are those tabulated in Table 3.7-5. A similar method was used to rate the system manufacturability of the

TABLE D3-2

ENERGY REQUIREMENTS

Configuration	MOMENT OF INERTIA		TORQUE, SCAN		SLEM		TRACK				
	Telescope		Tele		Tele		Tele				
	Body	w/ or w/o SM	Body	SM	Body	SM	Body	SM			
1. On-axis cass.	2.7	6.1	6.4	8.3	10	6.5	2.5	8.8	5.3	32.3	4
2. Radially deg.	2.7	6.1	6.4	8.3	10	6.5	2.5	8.8	5.3	32.3	4
3. Slot											
a. 12 x 4	7.5	10	8.1	9.6	10	8.5	4.1	10	7.1	39.6	1
b. 12 dia	7.4	9.9	8.3	9.6	10	9	5.4	10	7	39.5	2
c. 20 x 4	4.9	7.4	7.3	8.4	10	7.5	3.9	9	5.3	34	3
4. Off-axis	1	1	5.1	1	9	4.8	1	7.1	0	10.1	6
5. SPH PM	2	5.6	6	8	10	6.2	2	9.6	4.8	31.7	5

D  
3  
3

Conclusions: 1. Telescope pointing requires less energy than body pointing, therefore, coarse pointing choice.

2. Configurations rated in rightmost column.

TABLE D3-3

Configuration	MANUFACTURE			STABILITY/CONTROL			ALIGNMENT		
	PM	SM	Sub-Total	PM	SM	Sub-Total	PM (Cell-to-Cell)	System	Sub-Total
1. On-axis	7	6	6.5	7	9	8	6	9	7.5
2. Rad. Deg.	8	6	7	7	9	8	6	9	7.5
3. Slot									
a. 12 x 4	7	5	6	9	8	8.5	9	8	8.5
b. 12 dia.	6	6	6	8	10	9	7	10	8.5
c. 20 x 4	5	5	5	7	7	7	8	8	8
4. Off-axis	4	5	4.5	5	5	5	2	1	1.5
5. SPH PM	10	4	7	8	4	6	10	4	7

RATING BASIS	Technique		Attitude Control (Leasecraft)	Telescope to ACS Coupling	Sub-Total
	Coarse	Fine			
1. Spherical surface easier (to make, control align; = 10) than asphere (7)	A. Body		9	-	9
2. On-axis asphere (7) easier than off-axis asphere (4)	R. Telescope		9	8	8.5
3. Single asphere (7) easier than compound asphere (4)		Fine	Bearings	Control Mechanisms	
4. Slower (+1) or weaker (+5) easier than faster (-1) or stronger (-5)	C. SM		9	5	7.7
5. Short tripod (+1), long tripod (-1), bipod (-1) vs. tripod	D. TM		Flexures		
6. Large dia. (-1), off-axis (-1)			LAT		

coarse and fine pointing techniques. Alignment and control ratings were assigned to the techniques independently for coarse and fine pointing methods on a relative basis utilizing data on control mechanisms and Table D3-3.

5) Structure weight (mass) values were obtained from the moment-of-inertia studies. Table D3-4 records this data and the rating scheme.

TABLE D3-4  
WEIGHT (MASS) SIEVE  
MASS (kg)

<u>Configuration</u>	<u>Body Pointing</u>	<u>Telescope</u>	<u>Fine Pointing by SM and Body Pointing</u>
1&2 On-axis, rad. deg.	22470	22561	22810
3a Slot 12 x 4	13968	14059	14308
3b Slot 12 dia.	17608	17699	17948
3c Slot 20 x 4	17159	17250	17499
4 Off-axis	23003	23094	23253
5 Sph. PM	22719	22810	23069

<u>Rank</u>	<u>Conf. Mass (kg) x 1000</u>	<u>Tech. Δ Mass (kg)</u>
10	<14	0
9	14-17	100
8	17-20	400
7	20-23	
6		
5		
4		
3		
2		
1		

The coarse and fine pointing techniques are rated independently. The mass of the tertiary mirror structure is insignificant (on a relative basis).

6) Complexity and reliability were evaluated by considering all of the other parameters and arriving at a relative rating.

APPENDIX D4  
MIRROR CONSTRUCTION ALTERNATIVES-  
COST IMPLICATIONS

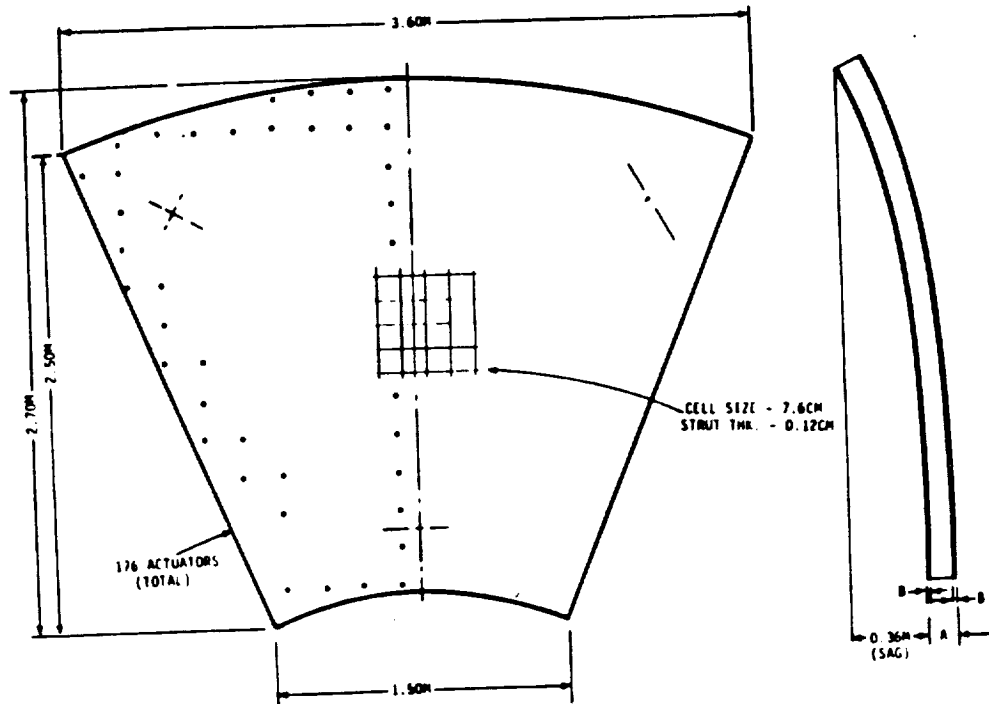
Some participants in Technical Progress Review No. 2 expressed an interest in evaluating the cost differentials between fused silica and composite mirrors. The following section not only compares two materials but also shows active and passive designs for each material.

We have chosen ULE<sup>TM</sup>/frit bonded/fused silica and glass matrix/foamed graphite materials for comparison.

TYPICAL SEGMENT 20.0M MIRROR

ULE™ MIRROR

	FLEXIBLE	PASSIVE
A	3.8CM	10.2CM
B	0.65CM	0.95CM
WT	28.8kg/M <sup>2</sup>	42.7kg/M <sup>2</sup>



A trapezoidal segment, from the inner ring of segments of a 20-meter diameter mirror, was selected as a standard configuration for comparison purposes. Dimensions and area densities, for ULE™ construction, are shown for both active and passive cases. The active case requires 176 actuators and a stable reaction structure (described later) for figure control.

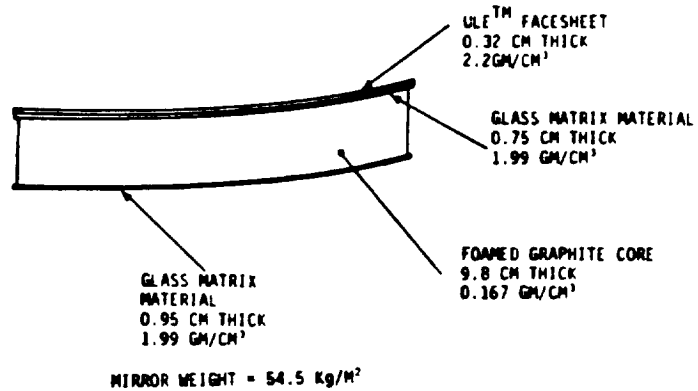
Frit is used to bond the front and rear plates to the core structure. This method of construction is backed by experience, albeit in smaller sizes, and offers lighter weight than more conventional means of ULE™ construction.

The ULE™ material itself offers stability, homogeneity and very low coefficient of thermal expansion. However, material costs are rather high.

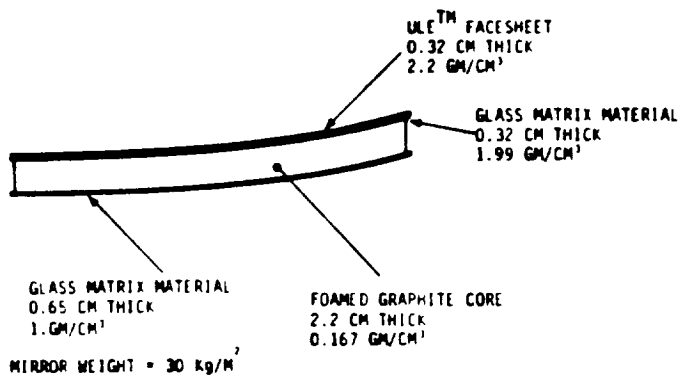


## COMPOSITE MIRROR BLANK

### Passive Design



### Flexible Design

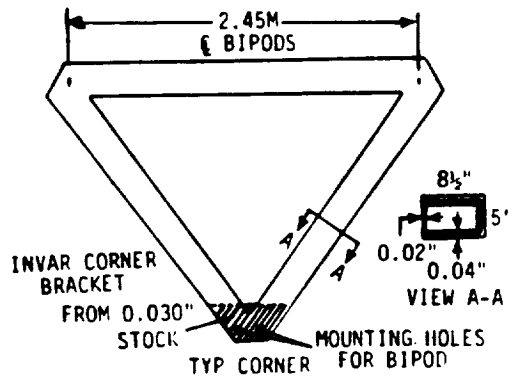


The same trapezoidal section was used to evaluate the composite technology cases. Cross sectional dimensions and materials are shown above. Glass matrix front and back plates are bonded to a low density foamed graphite core after which a thin ULE™ facesheet is bonded to one surface.

Graphite foam offers a very low coefficient of thermal expansion (CTE) which will closely match the low CTE of the glass matrix material. It is also stable and very light weight.

## SEGMENT CONFIGURATIONS

### Delto Frame

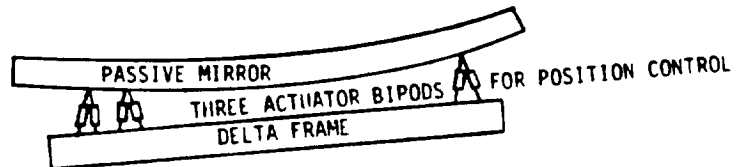


TOTAL WEIGHT = 30 POUNDS  
INVAR WEIGHT = 15 POUNDS  
GR/EP WEIGHT = 15 POUNDS

The delta frame is constructed of graphite-epoxy, for light weight, with Invar brackets at the corners to provide stable mounting points for the bi-pods, while avoiding possible stress concentration problems.

## SEGMENT CONFIGURATIONS

### Passive System



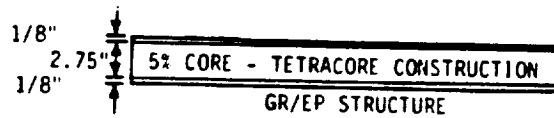
TOTAL AREAL DENSITY  
(INCLUDES MIRROR,  $\Delta$  FRAME,  
ACTUATORS)

GLASS - 50 Kg/M<sup>2</sup>  
GL/GR - 61 Kg/M<sup>2</sup>

The overall configuration for the passive systems is shown above. Six position actuators mounted in three bi-pods provide for rigid body motion of the mirror segment in tilt and piston. Overall density for the ULE™ glass and glass-graphite composite alternatives is estimated.

## SEGMENT CONFIGURATIONS

### Reaction Structure

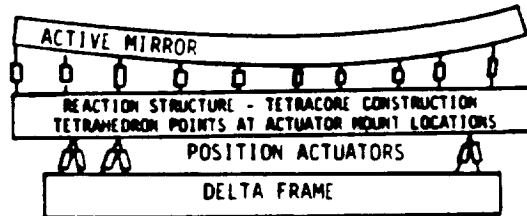


SAME SHAPE AS MIRROR BLANK  
TOTAL WEIGHT = 89 POUNDS (41 Kg)

Active configurations require a stable, rigid, light weight reaction structure to serve as a base for the figure control actuators. The tetracore/ultra-core sandwich construction suggested here consists of polyhedron facets sandwiched between two faceplates. It offers a high stiffness to weight ratio and good attachment accommodation. The 176 figure actuators (per mirror segment) would be attached to the reaction structure at the tetrahedron points.

## SEGMENT CONFIGURATIONS

### Active System



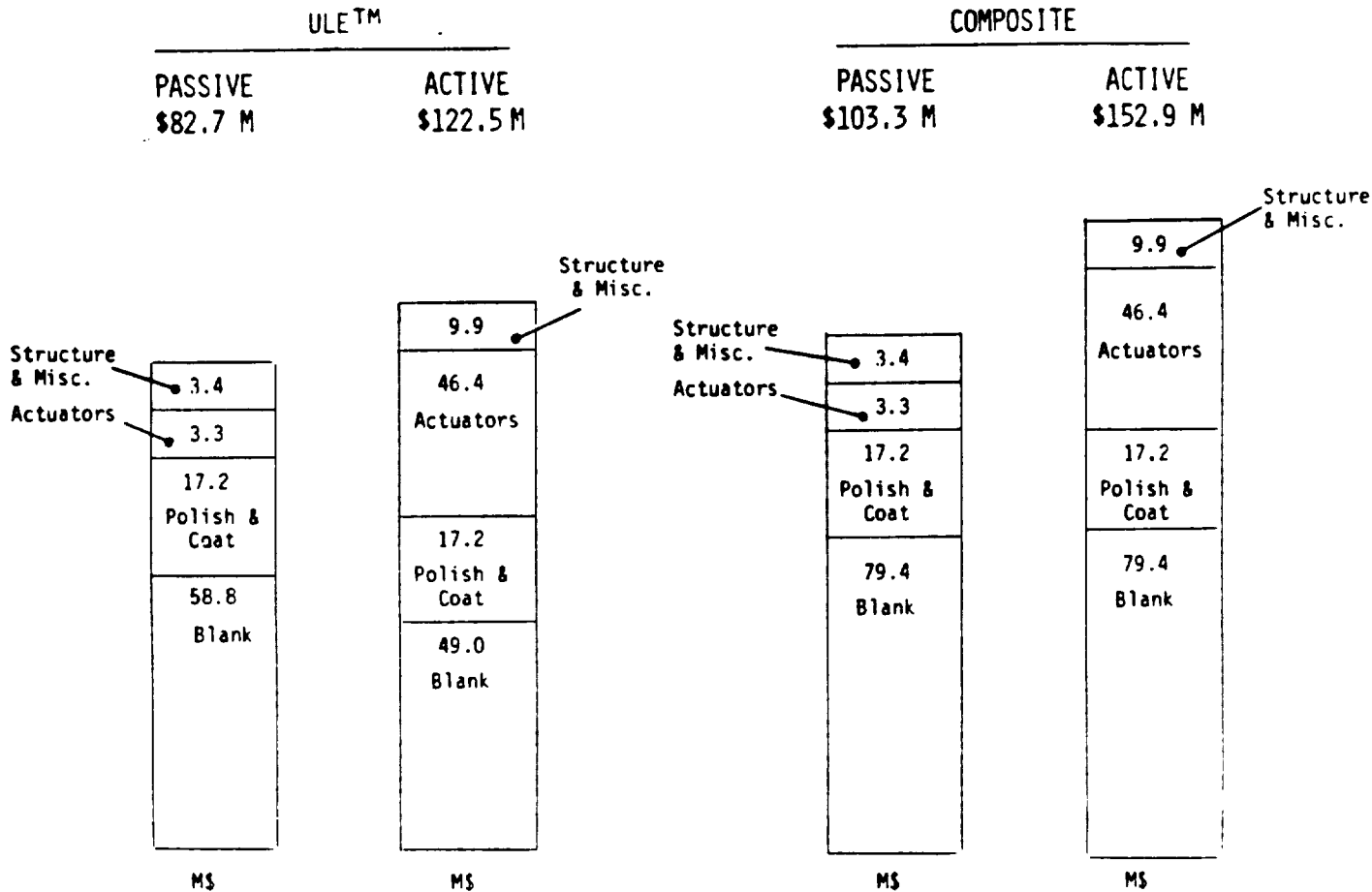
176 FIGURE ACTUATORS  
8" x 8" PATTERN

#### TOTAL AREAL DENSITY

GLASS - 85 Kg/M<sup>2</sup>  
GR/GL - 86 Kg/M<sup>2</sup>

This is the overall configuration for the active systems. Bi-pod mounted actuators provide rigid body motion while additional, reaction structure mounted, actuators provide figure control. There is little difference between the overall areal densities of the glass and glass-matrix configurations, since most of the weight consists of items (actuators, reaction structure, delta frame) common to both configurations.

## MIRROR CONSTRUCTION ALTERNATIVES



18

Overall manufacturing costs for the four configurations are shown here for comparison. The active glass alternative differs from its passive counterpart by a savings in raw (ULE™) material cost due to its thinner blank, offset by somewhat higher costs for structure and much higher costs for actuators.

Similarly, the active composite choice has higher costs for structure and actuators than its passive counterpart. However, in this comparison the cost of the blanks is roughly the same. This is because the cost of the raw material is considered minor compared to overall fabrication and assembly costs.

Either of the composite cases would have to be preceded by a substantial development program not shown in this comparison.

MIRROR CONSTRUCTION ALTERNATIVES  
SOURCES OF INFORMATION

ENERGY RESEARCH AND GENERATION	- ALUMINUM FOAM
BRUSH/WELLMAN	- BERYLLIUM
CORNING	- ULE (3% TiO <sub>2</sub> )
SCHOTT	- ZERODUR
CARBORUNDUM	- HEXALOY
UNITED TECHNOLOGY, RES. CTR.	- GRAPHITE - GLASS
MATERIAL CONCEPTS INC.	- GRAPHITE - MAGNESIUM
UNIVERSITY OF ARIZONA	- GRAPHITE - EPOXY
ATLANTIC RESEARCH CORP.	- ULTRACORE

The above table shows the sources of the information used to select the materials used in these configurations and develop the comparative cost data.

APPENDIX D5  
SPACE STATION RENDEZVOUS (FSC)

I. Drag Area and Ballistic Coefficient

The LDR is a star observer and, therefore, a random inertial pointer and as such, the following relationship is valid based on a cylindrical spacecraft with solar panels:

$$A_{DRAG} = 2/\pi \sin \bar{\phi} \cdot A_{array} + R^2 + L \cdot R$$

Where:  $\bar{\phi}$  = Average sun angle (from orbit normal)

$A_{array}$  = Solar array area

$R$  = Spacecraft radius  
 $L$  = Spacecraft length } cylindrical model

The LDR single mission lifetime is three years, thus, allowing  $\bar{\phi} = 90^\circ$ , and power requirements necessitate  $A_{array} \cong 2700 \text{ ft}^2$ . Thus, as a function of spacecraft effective density we may evaluate  $A_{drag}$  and the ballistic

coefficient,  $W/C_D A_{DRAG} = B$ .

DRAG AREA AND BALLISTIC COEFFICIENT

SPACECRAFT  
EFFECTIVE

DENSITY (lb/ft <sup>3</sup> )	$A_{DRAG}$ (ft <sup>2</sup> )	$(W/C_D A_{DRAG}) = B$ BALLISTIC COEFF. (lb/ft <sup>2</sup> )
1.292	3850	16.18
1.722	3581	17.40*
2.583	3312	18.81

(W = 65,000 KG; C<sub>D</sub> = 2.3)

\*Selected configuration for continued analysis.  
(This is slightly conservative since, with propulsion, the spacecraft weight will be > 65000 kg)



## II. LDR ORBITAL/RENDEZVOUS CONSIDERATIONS

In order for the LDR to leave the Space Station, perform a three year passive mission, and return to the Space Station we may write:

$$\dot{\Omega}_{\text{relative}} \tau_{\oplus} \approx + 360^{\circ} \times N$$

(spacecraft to Space Station)

where:  $N = 1/3, 2/3, 3/3, 4/3$  etc. for a three year mission  
 $\dot{\Omega}$  = relative node rate ( $^{\circ}/\text{day}$ )  
 $\tau_{\oplus}$  = earth's orbital period (365.254 days)

The nodal regression rate for an earth satellite is given as (1st order):

$$\dot{\Omega} = -9.963 \left( \frac{r_0}{r_0+h} \right)^{7/2} \cos i \quad @ \quad \epsilon = \phi$$

( $^{\circ}/\text{day}$ )

satellite altitude  
 earth's radius

$i$  = orbital inclination =  $28.45^{\circ}$   
 $\epsilon$  = orbital eccentricity =  $\phi$

NOTE: We are assuming no plane changing,  $i = \text{const.}$ , since it is velocity/propellant prohibitive.

The solution to the above nodal equations are tabulated below, and graphically in Figure D5-1.

(NODE REPEATS/YEAR) <u>N</u>	--ALTITUDE (km)--	
	LOW	HIGH
1/3	390.057	580.006
2/3	303.344	684.560
3/3	221.417	796.577
4/3	143.825	917.061
5/3	70.176	1047.220
6/3	0.128	1188.529

(420 FT) NOT RECOMMENDED DUE TO AERO HEATING!  
 ( $M \approx 23$  &  $T_{\text{STAG}} = 56,600^{\circ}\text{R}$ )

The  $N = \emptyset$  solution is prohibitive since no fuel utilization is allowed during a three year mission and the altitude solutions below the Space Station are subject to large orbital decay rates.

## III. ORBITAL DECAY RATES

The total LDR life-time (nine years) is a large fraction of the nominal 11 year solar cycle. We may therefore use the following values for 10.7cm solar flux.

SIGMA	$\bar{F}$ 10.7 cm SOLAR FLUX
0 $\sigma$	120.32
+ 2 $\sigma$	203.50 (Nominal)
+ 3 $\sigma$	244.26

The 1977 Jacchia Model atmosphere (Figure D5-2) allows the linking of solar flux, atmospheric density and orbital decay rates.

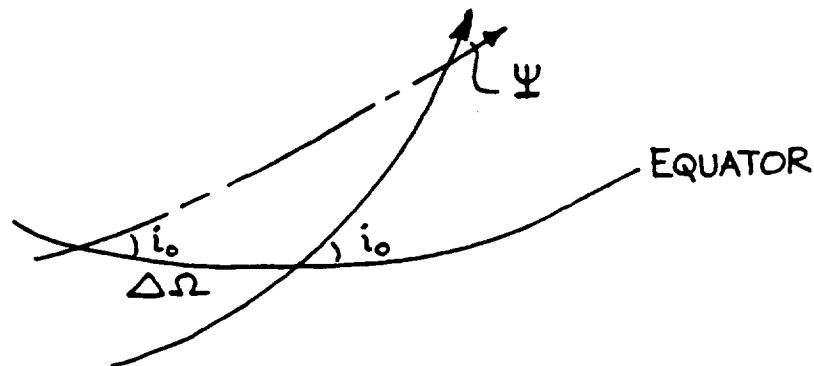
The decay rates at the possible higher altitude orbits are illustrated in Figure D5-3 for a nominal + 2  $\sigma$  solar flux of 200 and a spacecraft ballistic coefficient of 17.4 lb/ft<sup>2</sup>.

#### IV. ALTITUDE/NODAL ERROR SENSITIVITY

The accumulate relative nodal errors for a single three year mission due to an altitude error from a nominal operational altitude are tabulated below.

NOMINAL OPERATIONAL ALTITUDE (km)	$\Delta h$ ERROR (km)	NODAL ERROR (Degrees)
580.006	+ 1	+ 3.563/-3.558
	+ 2	+ 7.126/-7.115
	+ 3	+ 10.692/-10.670
684.560	+ 1	+ 3.329/-3.330
	+ 2	+ 6.655/-6.662
	+ 3	+ 9.979/-9.997

These nodal errors could be corrected by a single burn at an orbital anomaly from the ascending node of slightly less than 90° to produce a node shift at  $\Delta$ inclination =  $\theta$ .



$$\text{i.e., } \sin(\Psi/2) = \sin i_0 \cdot \sin(\Delta\Omega/2)$$

$$\Delta V = V_0 \cdot 2 \cdot \sin(\Psi/2)$$

← orbital velocity

ALTITUDE (km)	$v_0$ (ft/sec)	$\Delta\Omega$ (Degrees)	$\Delta V$ (ft/sec)
580	24832.12	3	619.34
580	24832.12	6	1238.25
580	24832.12	9	1856.31

.. @  $i = 28.45^\circ$

It is possible to conclude from the altitude-nodal error sensitivities and the large velocity requirements for nodal error correction that it is not feasible to correct accumulated nodal errors due to solar flux variability by a single corrective maneuver after a three year mission and that "dwelling" at the end of the mission should be used to eliminate both node and phase errors.

#### V. NODE ERRORS DUE TO EXCURSIONS FROM A +2 $\sigma$ MISSION

Table D5-1 illustrates the three year accumulated node errors for a nominal + 2 $\sigma$  solar flux mission at three selected workable altitudes for dispersions in predicted solar flux of + 1 $\sigma$  and - 2 $\sigma$ . It can be seen from the table that only positive excursions in solar flux from the nominal are workable, i.e., reasonable dwell times or negative nodal errors. Thus, the mission planning must be biased optimistically in terms of anticipated solar flux such that the excursions in solar flux will be positive.

Figure D5-4 illustrates two scenarios at two different operable altitudes for a + 1 $\sigma$  excursion in solar flux from a nominal +2  $\sigma$  value.

In the case of the 684.5 km altitude, simply dwelling approximately 14 days eliminates the accumulated nodal error, and the required mission total  $\Delta V \cong 722.2$  ft/sec.

The lower operational altitude of 580 km would require a 100 day dwell period (thought to be excessive) or 50 days if the dwell altitude was raised to 684.5 km. Thus, we have a trade-off between required  $\Delta V$  and dwell time as illustrated in Figure D5-5.

If 2 1/2 months is taken to be the maximum allowable dwell time after a three year mission the lower bound on  $\Delta V$  is found to be 538 ft/sec.

Thus we have found two workable LDR operational altitudes, 580 km and 684.5 km, and bounded the total  $\Delta V$  requirements as lying between 538 and 722.2 ft/sec for a single three year mission.

## VI. PROPELLANT REQUIREMENTS

The propellant requirements for a three year mission based on the LDR observatory weight of 65,000 kg may be evaluated as;

$$W_{P \text{ TOTAL}} = \frac{P}{\left\{ \frac{1}{(1 - e^{-\Delta V/g_c I_{sp}})} - \frac{1}{r} \right\}^{-1}}$$

where;  $P$  = Payload weight = 65000kg

$\Delta V$  = Required delta velocity

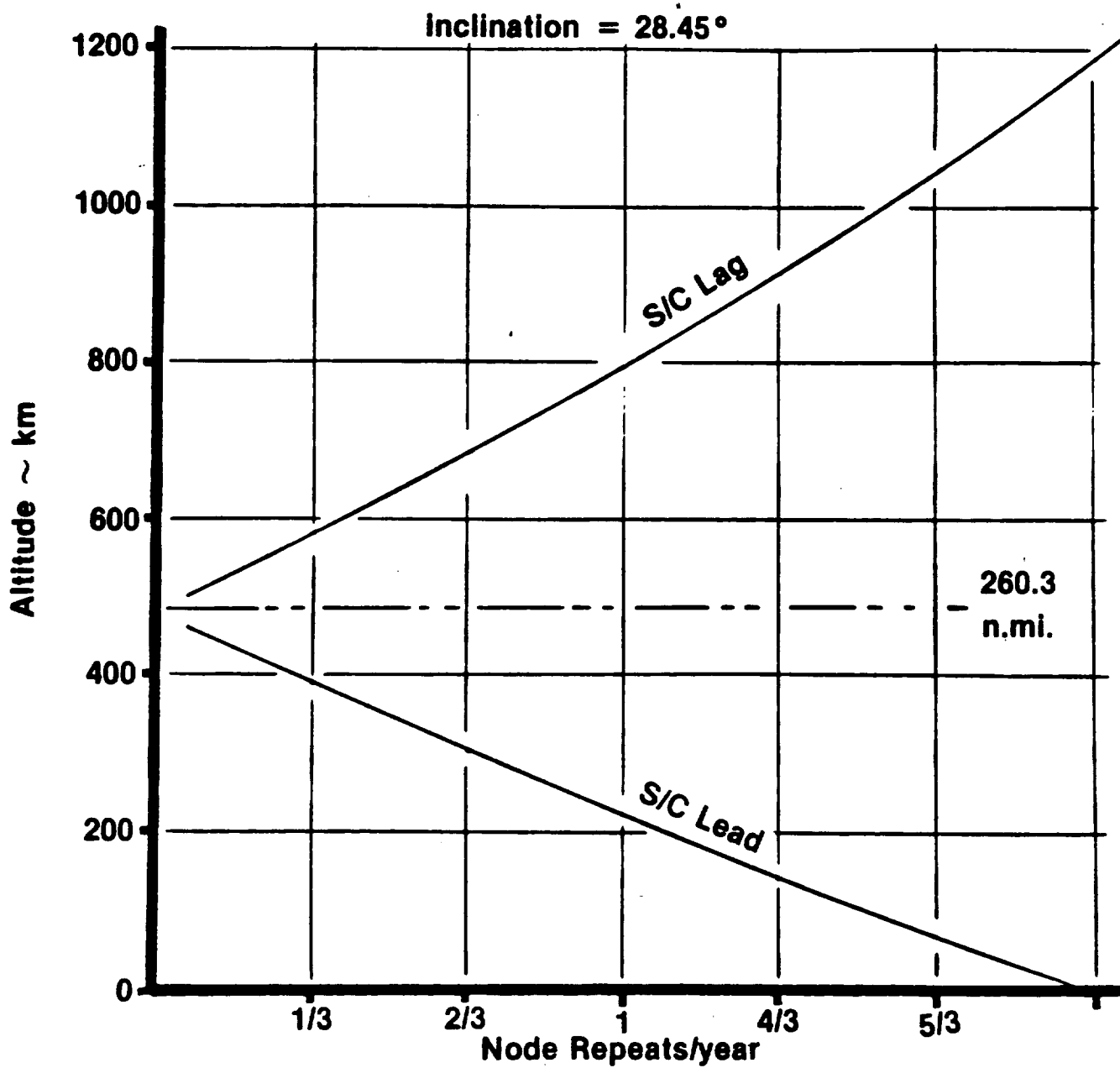
$I_{sp}$  = Propulsion system delivered specific impulse

$r$  = Propulsion system weight efficiency  
(W propellant/W propulsion system)

Figure D5-6 illustrates the LDR propellant requirements for a single three year mission for the range of  $\Delta V$ 's found and reasonable propulsion system weight efficiencies for both monopropellant hydrazine and bi-propellant (storeable) systems.

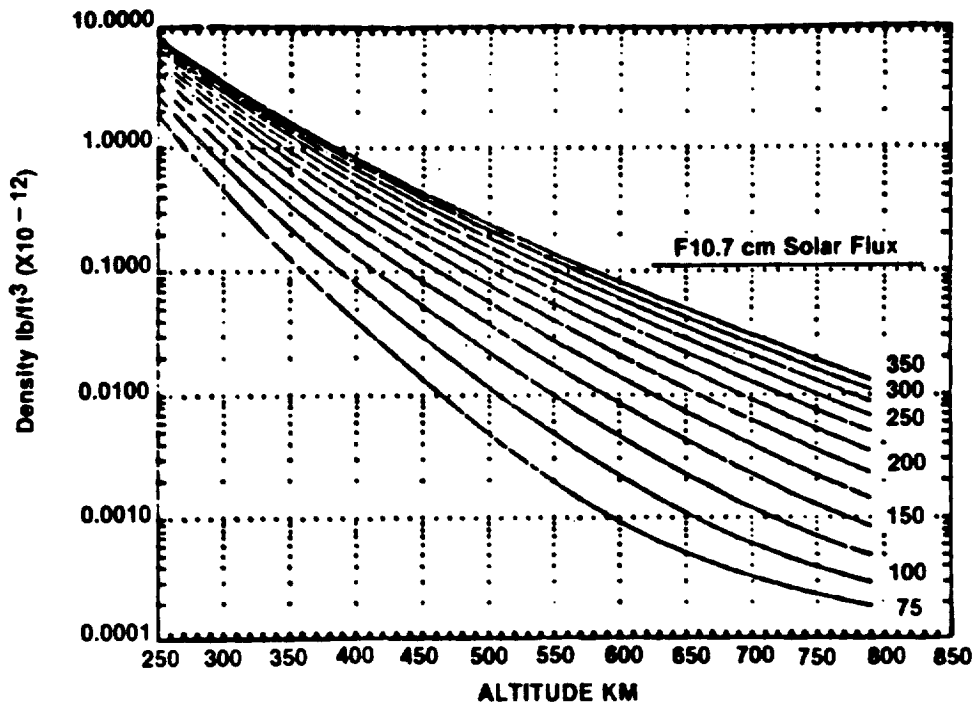
## VII PHASE MAKE-UP

Terminal phase error make-up is illustrated in Table D5-2. Only very short additional dwell times need be considered to eliminate phase errors. (Maximum values are tabulated for  $360^\circ \Delta \phi$  errors). Phase make-up dwelling, of course, incurs additional nodal error ( $\sim -1^\circ$ ) and in practice, at the end of a typical three year mission, knowing both node i phase errors the dwelling maneuver would eliminate both phase and node errors pre-biased for the effects of the Hohmann transfer back to the Space Station such that only minor  $\Delta V$  penalties would be incurred.



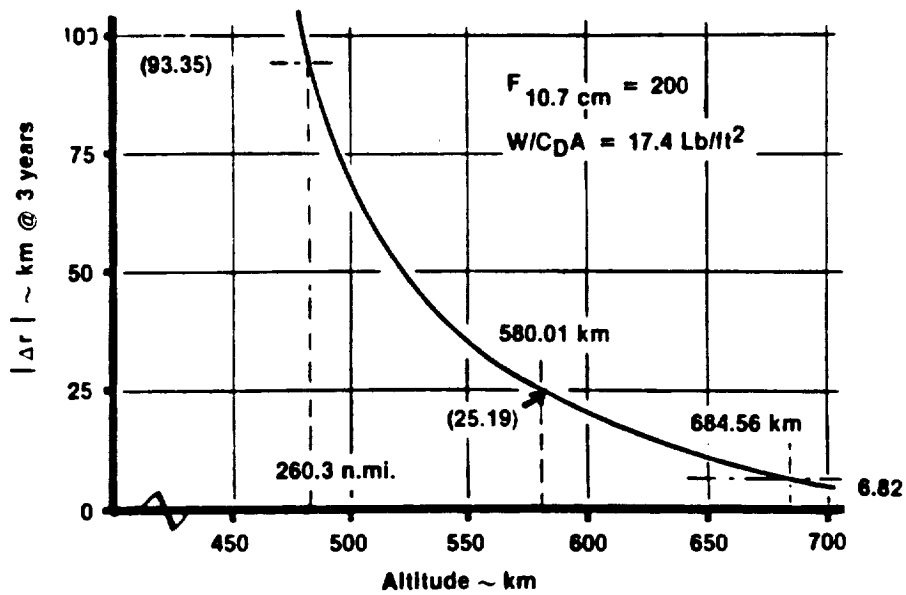
SPACE STATION RENDEZVOUS

Figure D5-1



1977 JACCHIA MODEL ATMOSPHERE

Figure D5-2



ORBITAL DECAY RATES

Figure D5-3

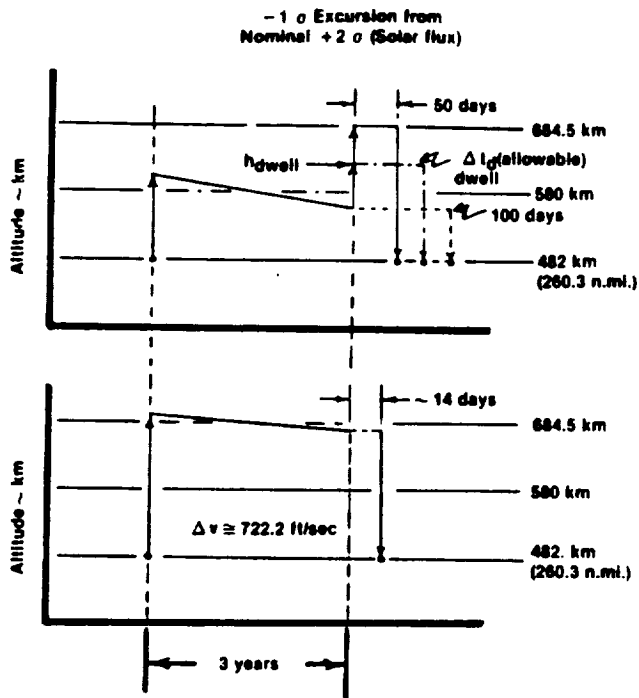
TABLE D5-1

CONCEPT #2

<u>Operational Altitude km (n.mi.)</u>	<u>Relative Node Rate to S.S. (°/day)</u>	<u>Delta Node (°)</u>	
		<u>Excursion from Nom. + 2σ + 1σ</u>	<u>- 2σ</u>
482.08 (260.3)	φ	-98.24 (~ ∞)	+131.16 (~ ∞)
580.01 (313.18)	-.3285	-32.90 (100.15d)	+36.43 (985d)
684.56 (369.63)	-.6571	-9.15 (13.92d)	+9.45 (533.5d)
		▲ Dwell time to make Up Node Error	△ Unworkable Dwell Times

**Conclusion:**

**Must bias nominal orbit such that solar flux excursion is Positive!**



**Preferred Approach:**  
Pre-biased Orbits; Based on "optimistic" Sun  
such that  $\Delta \sigma$  excursion is positive, and relative  
node excursion is negative  
(Allows dwelling @  $h_{dwell}$ )

Figure D5-4

Operational Alt. = 580 km (313.2 n.mi.)  
Inclination = 28.45°  
Single 3 yr. Cycle

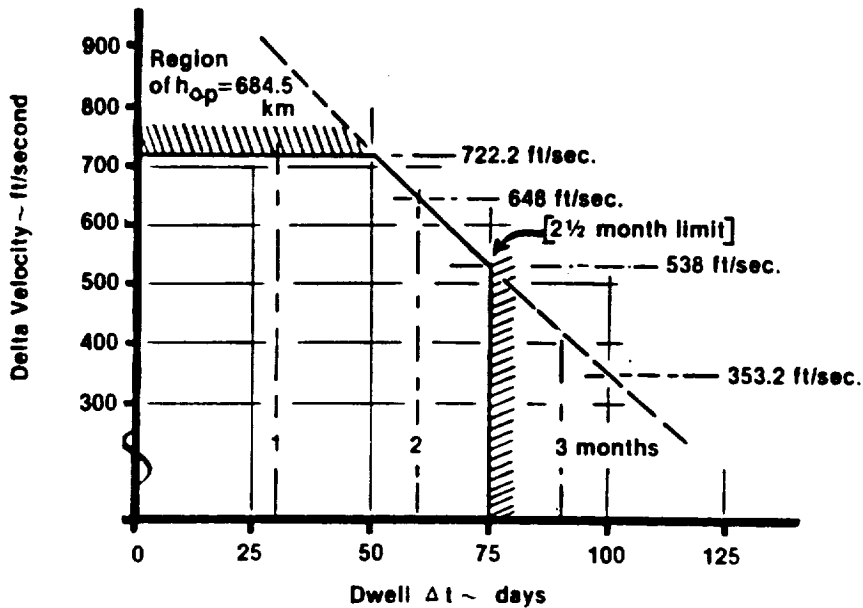


Figure D5-5



Payload Weight = 65,000 Kg  
Single 3 Year Cycle

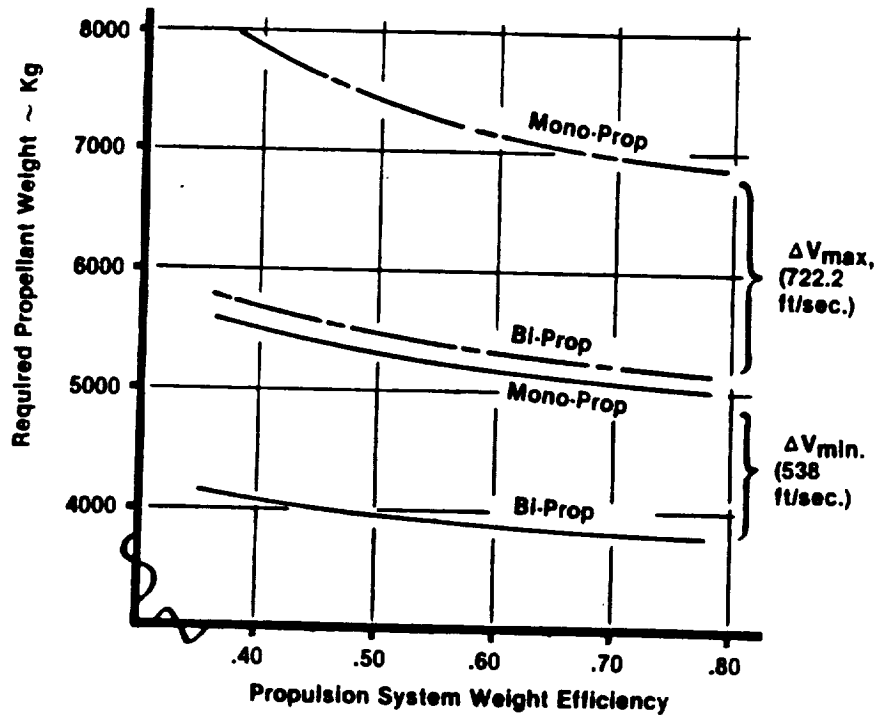


Figure D5-6

TABLE D5-2  
PHASE MAKE-UP

Space Station @ 260.3 n.mi. & 28.45° i  
( $\dot{\theta} = .06366488^\circ/\text{sec}$ ) & ( $T = 94.2435 \text{ min.}$ )

<u>OPERATIONAL</u> <u>Altitude (km)</u>	<u>Node</u> <u>Repeats</u> <u>Per Yr</u>	<u><math>\dot{\theta}_{REL.}</math></u> <u>(°/hr)</u>	<u><math>\Delta t</math> days</u> <u>for 360°</u> <u><math>\Delta \theta_{make-up}</math></u>	<u>Resultant</u> <u><math>\Delta \alpha^\circ</math></u> <u>Error</u>
580.006	1/3	-4.8216	3.11	-1.022
684.560	2/3	-9.7855	1.53	-1.007
796.577	3/3	-14.9038	1.006	-0.992

1. Report No. NASA CR- 177413	2. Government Accession No.	3. Recipient's Catalog No.	
4. Title and Subtitle Large Deployable Reflector (LDR) System Concept and Technology Definition Study, Final Technical Report - Volume I		5. Report Date April 1989	6. Performing Organization Code
		8. Performing Organization Report No.	
7. Author(s) D. L. Agnew and P. A. Jones		10. Work Unit No. 506-62-21	
9. Performing Organization Name and Address Eastman Kodak Company Government Systems Division Research and Engineering Rochester, New York 14650		11. Contract or Grant No. NAS2-11861	
		13. Type of Report and Period Covered Contractor Report	
12. Sponsoring Agency Name and Address National Aeronautics and Space Administration Washington, DC 20546-0001		14. Sponsoring Agency Code	
		15. Supplementary Notes Point of Contact: Technical Monitor, Kenji Nishioka, Code SSS, MS 244-8 Ames Research Center, Moffett Field, CA 94035 (415) 694-6540 or FTS 464-6540	
16. Abstract  A study was conducted to define reasonable and representative LDR system concepts for the purpose of defining a technology development program aimed at providing the requisite technological capability necessary to start LDR development by the end of 1991. This Volume I includes the executive summary for the total study, a report of thirteen system analysis and trades tasks (optical configuration, aperture size, reflector material, segmented mirror, optical subsystem, thermal, pointing and control, transportation to orbit, structures, contamination control, orbital parameters, orbital environment, and spacecraft functions), and descriptions of three selected LDR system concepts. Supporting information is contained in appendices. Volume II (separate) contains technology assessments and the technology development plan.			
17. Key Words (Suggested by Author(s)) Large Deployable Reflector (LDR), Observatory, Spaceborne Telescope, Infrared Astronomy, Submillimeter Astronomy		18. Distribution Statement Unclassified - Unlimited  Subject category: 12	
19. Security Classif. (of this report) Unclassified	20. Security Classif. (of this page) Unclassified	21. No. of Pages 387	22. Price* A17



